ISSN 1007-9327 (print)
ISSN 2219-2840 (online)

# World Journal of *Gastroenterology*

*World J Gastroenterol* 2019 September 21; 25(35): 5220-5402

Published by Baishideng Publishing Group Inc

WJG World Journal of Gastroenterology

Contents

Weekly Volume 25 Number 35 September 21, 2019

*World Journal of Gastroenterology*
**Volume 25 Number 35 September 21, 2019**

# Contents

## ABOUT COVER

Editorial board member of *World Journal of Gastroenterology*, Cesare Tosetti, MD, Doctor, Professor, Department of Primary Care, Health Care Agency of Bologna, Porretta Terme 40046, Bologna, Italy

## AIMS AND SCOPE

The primary aim of *World Journal of Gastroenterology* (*WJG*, *World J Gastroenterol*) is to provide scholars and readers from various fields of gastroenterology and hepatology with a platform to publish high-quality basic and clinical research articles and communicate their research findings online.

*WJG* mainly publishes articles reporting research results and findings obtained in the field of gastroenterology and hepatology and covering a wide range of topics including gastroenterology, hepatology, gastrointestinal endoscopy, gastrointestinal surgery, gastrointestinal oncology, and pediatric gastroenterology.

## INDEXING/ABSTRACTING

The *WJG* is now indexed in Current Contents®/Clinical Medicine, Science Citation Index Expanded (also known as SciSearch®), Journal Citation Reports®, Index Medicus, MEDLINE, PubMed, PubMed Central, and Scopus. The 2019 edition of Journal Citation Report® cites the 2018 impact factor for *WJG* as 3.411 (5-year impact factor: 3.579), ranking *WJG* as 35th among 84 journals in gastroenterology and hepatology (quartile in category Q2). CiteScore (2018): 3.43.

## RESPONSIBLE EDITORS FOR THIS ISSUE

**Responsible Electronic Editor:** *Yu-Jie Ma*

**Proofing Production Department Director:** *Yun-Xiaojian Wu*

**NAME OF JOURNAL**
*World Journal of Gastroenterology*

**ISSN**
ISSN 1007-9327 (print) ISSN 2219-2840 (online)

**LAUNCH DATE**
October 1, 1995

**FREQUENCY**
Weekly

**EDITORS-IN-CHIEF**
Subrata Ghosh, Andrzej S Tarnawski

**EDITORIAL BOARD MEMBERS**
http://www.wjgnet.com/1007-9327/editorialboard.htm

**EDITORIAL OFFICE**
Ze-Mao Gong, Director

**PUBLICATION DATE**
September 21, 2019



**INSTRUCTIONS TO AUTHORS**
https://www.wjgnet.com/bpg/gerinfo/204

**GUIDELINES FOR ETHICS DOCUMENTS**
https://www.wjgnet.com/bpg/GerInfo/287

**GUIDELINES FOR NON-NATIVE SPEAKERS OF ENGLISH**
https://www.wjgnet.com/bpg/gerinfo/240

**PUBLICATION MISCONDUCT**
https://www.wjgnet.com/bpg/gerinfo/208

**ARTICLE PROCESSING CHARGE**
https://www.wjgnet.com/bpg/gerinfo/242

**STEPS FOR SUBMITTING MANUSCRIPTS**
https://www.wjgnet.com/bpg/GerInfo/239

**ONLINE SUBMISSION**
https://www.f6publishing.com

World Journal of Gastroenterology

Submit a Manuscript: https://www.f6publishing.com

*World J Gastroenterol* 2019 September 21; 25(35): 5220-5232

DOI: 10.3748/wjg.v25.i35.5220

ISSN 1007-9327 (print) ISSN 2219-2840 (online)

OPINION REVIEW

# How does *Helicobacter pylori* cause gastric cancer through connexins: An opinion review

Huan Li, Can-Xia Xu, Ren-Jie Gong, Jing-Shu Chi, Peng Liu, Xiao-Ming Liu

**ORCID number:** Huan Li (0000-0001-8568-3151); Can-Xia Xu (0000-0002-6166-6653); Ren-Jie Gong (0000-0001-7001-9522); Jing-Shu Chi (0000-0002-1925-011X); Peng Liu (0000-0001-5844-0277); Xiao-Ming Liu (0000-0002-1811-8758).

**Author contributions:** Li H performed the literature search and wrote the paper; Gong RJ, Chi JS, and Liu P collated and summarized the literature; Liu XM and Xu CX supervised and approved the final version of the review.

**Conflict-of-interest statement:** No author has any potential conflicts of interest to declare.



**Manuscript source**: Invited manuscript

**Received:** April 13, 2019
**Peer-review started:** April 15, 2019
**First decision:** July 22, 2019
**Revised:** August 12, 2019
**Accepted:** August 19, 2019

**Huan Li, Can-Xia Xu, Ren-Jie Gong, Jing-Shu Chi, Peng Liu, Xiao-Ming Liu,** Department of Gastroenterology, the Third Xiangya Hospital of Central South University, Changsha 410013, Hunan Province, China

**Corresponding author:** Xiao-Ming Liu, MD, Chief Doctor, Department of Gastroenterology, the Third Xiangya Hospital of Central South University, No. 138, Tongzipo Street, Changsha 410013, Hunan Province, China. liuxiaoming26@163.com
**Telephone:** +86-731-88618631
**Fax:** +86-731-88618012

## Abstract

*Helicobacter pylori* (*H. pylori*) is a Gram-negative bacterium with a number of virulence factors, such as cytotoxin-associated gene A, vacuolating cytotoxin A, its pathogenicity island, and lipopolysaccharide, which cause gastrointestinal diseases. Connexins function in gap junctional homeostasis, and their downregulation is closely related to gastric carcinogenesis. Investigations into *H. pylori* infection and the fine-tuning of connexins in cells or tissues have been reported in previous studies. Therefore, in this review, the potential mechanisms of *H. pylori*-induced gastric cancer through connexins are summarized in detail.

**Key words:** *Helicobacter pylori*; Connexin; Gap junctional intercellular communications; Gap junction proteins; Gastric cancer; Transcription factors; DNA methylation; Proliferation; Apoptosis



**Core tip:** *Helicobacter pylori* (*H. pylori*) is an independent pathogenic factor for gastric cancer (GC), which is related to some virulence factors of *H. pylori*. It has long been proven that various connexins (Cxs) can regulate the development of GC. Thus, we discuss in detail how *H. pylori* regulates Cxs to cause gastric cancer.

**Citation:** Li H, Xu CX, Gong RJ, Chi JS, Liu P, Liu XM. How does *Helicobacter pylori* cause gastric cancer through connexins: An opinion review. *World J Gastroenterol* 2019; 25(35): 5220-5232
**URL**: https://www.wjgnet.com/1007-9327/full/v25/i35/5220.htm
**DOI**: https://dx.doi.org/10.3748/wjg.v25.i35.5220

**Article in press:** July 22, 2019
**Published online:** September 21, 2019

**P-Reviewer:** Moschovi MA
**S-Editor:** Yan JP
**L-Editor:** Wang TQ
**E-Editor:** Ma YJ

## INTRODUCTION

*Helicobacter pylori* (*H. pylori*) is a Gram-negative and microaerophilic bacterium that colonizes the stomach in nearly 50% of the world's population[1]. *H. pylori* synthesizes many different virulence factors that dysregulate host intracellular signaling mechanisms and contribute to neoplastic transformation[2]. *H. pylori* disrupts the balance between cell proliferation and apoptosis, which is an important driving force for the occurrence and development of gastric cancer (GC) by virulence factors[3]. Of all virulence factors, cytotoxin-associated gene A (CagA), vacuolating cytotoxin A (VacA), and lipopolysaccharide (LPS) are the most important[2,4].

The CagA gene is located downstream of the 40 kb virulence gene cluster, called the Cag pathogenicity island (cagPAI). These genes encode a type IV secretory system, forming a syringe structure that injects CagA protein and peptidoglycan into gastric epithelial cells[5,6]. CagA is an important oncoprotein that plays a critical role in gastric carcinogenesis[7]; one of the mechanisms is that it can induce hypermethylation of tumor suppressor genes[8,9]. CagA is delivered into host gastric epithelial cells, and it may trigger some signal transduction events, such as proliferation and inflammation, leading to a potential risk of GC[10,11]. In addition, intact cagPAI strains may increase the probability of GC[12].

VacA is one of the major virulence factors produced by *H. pylori*, and it is a 140 kDa precursor that produces an 88 kDa toxin after proteolysis[13,14]. The vacA alleles in different *H. pylori* strains can be divided into several families according to their sequence heterogeneity in specific areas that are associated with the biological form of VacA. There are three most extensively studied regions of heterogeneity: The signal or "s" region, the intermediate or "i" region, and the middle or "m" region[15-17]. Previous studies indicated that *H. pylori* strains with s1, i1, and m1 vacA alleles had a higher risk of GC or precancerous lesions than those with s2, i2, and m2 vacA alleles[15,18-24]. VacA-induced gastric epithelial cell death is expected to lead to increased cell proliferation, which may be associated with an increased cancer risk. VacA may disrupt the epithelial cell monolayers[25] and thereby promote the entry of carcinogens into gastric epithelial cells[26].

LPS is an important component of the cell wall of Gram-negative bacteria, for example, *Escherichia coli*[27], *Shigella flexneri*[28], and *Yersinia enterocolitica*[29], among others. Similar to other Gram-negative bacteria, *H. pylori* LPS is composed of three structural domains—lipid A, core oligosaccharide, and O polysaccharides[30,31]. Recently, studies have reported that LPS has close relationships with the development of GC *via* TLR4-dependent pathways[32-36].

Connexins (Cxs), also called gap junction proteins, are the main component of gap junctional intercellular communications that may directly enhance cell cooperation both electrically and metabolically. This intercellular communication plays a crucial role in development and homeostasis[37,38]. Cxs have complex functions in physiological and pathological processes[39,40], and they may influence the proliferation, apoptosis, migration, and invasion of different cells[41-48]. Their regulation is correlated with tumor development, and the evolution of Cxs may inhibit the progression of various cancers[39,40]. Cxs are expressed in a tissue-specific manner. Gastric tissue mainly produces Cx26, Cx32, Cx37, Cx40, Cx43, and Cx45[49-57]. Previous studies have shown that, compared to tissues or cells of the normal gastric mucosa, the expression of Cxs dramatically decreases in GC[58-61]. Therefore, the variations in Cxs can serve as important biomarkers that imply the development of different cancers. Apart from changes in the function and expression of Cxs in cancers, the aberrant cytoplasmic location of Cxs is also linked with various cancers[62-67]. The expression of Cxs in the gastrointestinal tract and liver is presented in Table 1[68-91].

## LITERATURE SEARCH

A scientific literature search was conducted using the PubMed, Web of Science, and Google Scholar databases with the keywords "*Helicobacter pylori*", "Connexin", "Gap junctional intercellular communications", "gap junction proteins", "gastric cancer", "transcription factors", "DNA methylation", "proliferation", "apoptosis", and combinations of the aforementioned.

## HOW TO REGULATE CONNEXINS

Based on previous studies about the relation between *H. pylori* and Cxs, this relation may involve many mechanisms and signaling pathways that are complex and

**Table 1 Connexin expression in the gastrointestinal tract and liver**

| Tissue | Cell type | Cx members | Ref. |
|---|---|---|---|
| Liver | | | |
| | Hepatocytes | Cx32/Cx26 | [161] |
| | Kupffer cells | Cx43/Cx26 | [162-164] |
| | Stellate cells | Cx43/Cx26 | [163-165] |
| | Sinusoidal endothelial cells | Cx43/Cx32/Cx26 | [163,164,166,167] |
| | Portal vein endothelial cells | Cx43/Cx40/Cx37 | [168-170] |
| | Hepatic artery endothelial cells | Cx43/Cx40/37 | [168-170] |
| | Cholangiocytes | Cx43/Cx32 | [171,172] |
| Stomach | | Cx45/Cx43/Cx40/Cx37/Cx32/Cx26 | [49-57,146] |
| | Foveolar cells | Cx32 | [173] |
| Small intestine | | | |
| | Musculus externa cells | Cx43/Cx40 | [51] |
| | Myenteric plexus cells | Cx45/Cx43/Cx40/Cx36 | [51,174,175] |
| | Epithelial cells | Cx43/Cx37/Cx32 | [51,176,177] |
| | Interstitial cells of Cajal | Cx43 | [51,178] |
| Colon | | | |
| | Musculus externa cells | Cx43/Cx40/Cx26 | [51,179] |
| | Myenteric plexus cells | Cx45/Cx43/Cx40/Cx36 | [51,175] |
| | Epithelial cells | Cx43/Cx37/Cx32/Cx26 | [177,180-183] |
| | Muscularis mucosal cells | Cx43 | [51] |
| | Interstitial cells of Cajal | Cx43 | [178] |

profound. *H. pylori* can regulate the expression of key molecules that have an effect on the expression and function of Cxs by its virulence factors. In other words, Cx expression can be regulated in many processes, such as transcription, RNA processing, RNA nucleocytoplasmic transport and localization, mRNA translation, mRNA degradation, and protein activity[68]. Hence, in this review, we mainly discuss possible regulation between *H. pylori* and Cxs during the progression of GC.

## CX32

Cx32, also named gap junction beta-1 protein, was primarily found in the peripheral nervous system[69,70], liver[71,72], gastric tissue[55,73], intestinal system[74], and other biological systems. It is clear that DNA hypermethylation may downregulate the level of the corresponding mRNA and protein[8,75]. A previous study reported that the expression levels of Cx32 and Cx43 mRNA decreased gradually during *H. pylori*-associated gastric carcinogenesis, and this result is associated with the hypermethylation of the promoters of these genes[76]. *H. pylori* infection may upregulate some transcription factors, such as GATA-3[77] and PBX-1[58]. These transcription factors can serve as the determinants in the Cx32 promoter targeting site and thereby inhibit Cx32 expression. However, the authors did not explain which of the virulence factors upregulate these transcription factors. Histone acetylation leads to the opening of chromatin structure, which increases the availability of gene promoters and is generally associated with enhanced transcription of DNA. Histone deacetylases (HDACs) lead to the termination of transcriptional processes *via* counteracting the function of histone acetylation[78]. Several pathogens, including *H. pylori*, manipulate host cell antibacterial responses and evade the immune system by affecting histone acetylation and histone deacetylation status[79]. It has been reported that *H. pylori* infection can decrease histone acetylation levels[80]. Vinken *et al*[81,82] have shown that HDAC inhibitors may elevate Cx32 protein levels in rat hepatocytes; however, the expression levels of Cx26 were downregulated and those of Cx43 were uncertain. Hence, histone acetylation can regulate the expression of Cxs. The p38 mitogen-activated protein kinase (MAPK) signaling pathway can be activated by a variety of extracellular signals. Extracellular signal-regulated kinase (ERK), p38 MAPK, Jun N-terminal kinase (JNK), and ERK5 are members of four subfamilies of MAPK[83,84]. CagA can activate the p38 MAPK signaling pathway[85]. Yamamoto *et al*[86] reported that p38 MAPK was activated during partial hepatectomy, thereby inhibiting

Cx32 expression. The first step for *H. pylori* to invade the gastric mucosa is to escape the host defense mechanism, and then the bacteria adhere to the epithelial surface through cell surface-specific receptors, releasing a large number of pathogenic factors and causing a mucosal inflammation response[87-91]. *H. pylori* infection can regulate the expression level of interleukins. *H. pylori* CagPAI can promote IL-1β production, involving the NOD-like receptor (NLR) family, pyrin domain containing 3 (NLRP3), and its complex, known as the NLRP3 inflammasome[92-94]. A previous study reported that in primary cultured rat hepatocytes, IL-1β causes the disappearance of Cx32, which is related to claudin-2 induction and cell membrane localization[95]. According to previous studies, Cx32 can inhibit proliferation, metastasis, and invasion[73,96-98] and has an antiapoptotic effect in different cancer cells[42,43,99]. Cx32 may regulate the metastasis and proliferation of hepatocellular carcinoma cells through the p53 and Akt pathways[97], also *via* cell cycle arrest and cell cycle regulatory proteins[73]. In other words, downregulated Cx32 may promote cell proliferation, metastasis, and apoptosis. Breaking the balance of these pathological events can promote tumor development. In addition to the changes in Cx32 expression, alterations in Cx32 location are also related to GC development[67]. However, studies about the changes in *H. pylori* and Cx32 localization are scarce.

## CX43

Cx43, also called gap junction alpha-1 protein (GJA1), is expressed in many tissues and organs; it is ubiquitous in gastric tissues[39,50,61]. Cx43-dependent intercellular communication could spread cell death signals between neighboring cells through gap junctions[44,100,101], using some candidate messengers such as $Ca^{2+}$, cAMP, cGMP, and ATP[100,102]. *H. pylori* promoted the expression of GATA3, which can also directly bind to the promoter region of the Cx43 gene, inducing its expression inhibition, and the expression of Cx43 decreased with the progression of gastric mucosal lesions to precancerous lesions[60]. CagPAI-induced IL-1β secretion may inhibit Cx43 expression *via* ERK1/2 and p38 MAPK[93,94,103]. *H. pylori* infection triggers an inflammatory response and promotes the activity of some interleukins, such as IL-1β[92-94], IL-17[104], and IL-22[105,106]. Yu *et al*[103] pointed out that IL-1β can inhibit the level of Cx43 *via* ERK1/2 and p38 MAP kinase in human endometrial stromal cells[103]. Qin *et al*[107] announced that IL-17 can inhibit the expression of CX43 through the AKT signaling pathway, inhibiting the occurrence and development of fungal keratitis. In psoriasis, IL-22 activates the JNK pathway, which will repress the transcriptional activity of the Cx43 gene promoter[108,109]. The inflammation-cancer chain is an important theory in carcinogenesis. Interleukins are important signaling markers of the inflammatory response. The epidermal growth factor family (EGF, EGFR, and HB-EGF) plays a key role in the progression, invasion, and metastasis of GC. The EGF family proteins can be regarded as important biomarkers for GC[110,111], and *H. pylori* infection can promote molecular expression[112,113]. Among the members of the EGF family, Yoshioka *et al*[114] reported that HB-EGF secretion from cardiomyocytes can decrease Cx43 in overexpressing cells and in immediately adjacent cells. We predict that HB-EGF may be seen as a negative regulator of Cx43 in gastric tissue. Moreover, a clinical study showed that HB-EGF enhances resistance to certain cancer drugs during the period of GC treatment[115]. In contrast, Cx43 could enhance chemotherapy sensitivity in human GC[116]. However, the effect of EGF and EGFR on Cx43 expression may be opposite to that of HB-EGF[117-119]. *H. pylori* infection leads to increased reactive oxygen species as well as NADPH oxidase and Jak2/Stat3 activation[120]. The activity of the JAK2/STAT3 signaling pathway has a positive effect on the proliferation and metastasis of carcinoma cells[121,122]. Cell proliferation is a mechanism that contributes to tumorigenesis. Previous studies indicated that Cx43 downregulation promotes carcinogenesis development[60,76,123]. Tang *et al*[124] indicated that JAK2/STAT3 signaling may inhibit Cx43 expression by blocking EGFR activation. Generally, protein phosphorylation may enhance the activity of proteins. Retinoic acid (RA) is an important intermediate metabolite of vitamin A. Among the different RA structures are all-trans RA, 9-cis RA, and 13-cis RA. The absence of RA in normal human development leads to defects in the immune system, embryonic development, vision, brain function, and other systems. In *H. pylori*-infected gastric mucosa, the expression of the gastric RA biosynthetic gene is seriously damaged, which may lead to decreased RA signaling pathways, thus leading to disease progression[125]. However, RA can enhance gap junction intercellular communication by increasing the expression of Cx43[126-128]. A previous study indicated that all-trans RA (ATRA) may inhibit gastric carcinoma tumor growth by targeting GC stem cells[129]; therefore, we predict that it may be mainly due to the effect of ATRA. The LPS-TLR4 signaling

pathway has an important role in LPS-mediated disease. LPS can induce an inflammatory response and upregulate inflammatory mediators, such as inducible nitric oxide synthase, IL-6, and TNF-α, among others, *via* activation of the TLR4/NF-κB signaling pathway[130,131]. Subsequently, the activation of Cx43 may regress by inhibiting caveolin-3[132]. VacA does not affect the mRNA expression of Cx43 and may enhance resistance to the degradation of autophagy, leading to cytoplasmic accumulation of Cx43. VacA can enhance ubiquitinated Cx43 movement to the lysosome for degradation *via* endosomal or autophagic mechanisms, eventually inducing apoptotic cell death *via* glutathione (GSH) and the Rac1/ERK signaling pathway[133]. As a result, the cell membrane is destroyed, which may promote cell proliferation in response to damage repair[134]. However, *H. pylori* disturbs the balance of the proliferation and apoptosis of cells, driving GC development[3].

## CX26

Cx26, also known as gap junction beta-2 protein, plays a role in tumor suppression through the regulation of the cell cycle[135]. It is true that *H. pylori* promotes the DNA promoter methylation of some biomolecules[136-138]. Some studies showed that *H. pylori* may be one of the driving forces to induce the promoter methylation of E-cadherin, mainly induced by CagA[138,139]. Such methylation can downregulate E-cadherin expression, which promotes the localization of Cx26 from the cell membrane to the cytoplasm, thereby inhibiting gap junction communication between endometrial cancer cells[140]. A loss of intercellular Cx26 expression or an increase in Cx26 expression in the cytoplasm has an important role in carcinogenesis and tumor progression[62,64-66]. This finding can be interpreted as the downregulation of Cx26 that inhibits the proliferation and migration of cells and promotes apoptosis[45]. All of these regulations may be drivers of GC development.

## CX37

Cx37, also known as GJA4, like other Cxs proteins, forms connections between cells known as gap junctions. Cx37 can inhibit cell growth both *in vitro* and *in vivo* and inhibits angiogenesis[141,142]. Cx37 may induce cell death and cell cycle arrest and slow down the cell cycle[143,144]. All of those processes may produce a potential inhibitor of the proliferation of cancer cells[144,145]. A clinical study reported that *H. pylori* infection may have a closely related polymorphism of Cx37 (Cx37 C1019T) in GC by altering the frequency of the allele[146]. Further, the Cx37 C1019T polymorphism may promote tumor cell proliferation[145]. Moreover, many diseases are also associated with the Cx37 gene C1019T polymorphism, such as polycystic ovarian syndrome (PCOS)[147] and cardiovascular diseases[148-151], among others.

## CONCLUSION AND PERSPECTIVE

*H. pylori* is a risk factor for GC. *H. pylori* eradication therapy may prevent GC occurrence[152]. In the development of *H. pylori*-induced GC, there are a series of pathological and physiological changes, such as chronic gastritis, atrophic gastritis, intestinal metaplasia, dysplasia, and gastric MALT lymphoma, among others[153-155]. In this long process, there are many interactions of biological signaling pathways. Cxs are important biomarkers that reflect the status of GC. Currently, only a few members of Cxs have been reported to have an association with GC, such as Cx26, Cx32, Cx37, and Cx43. *H. pylori* may regulate those Cxs involved in different signaling pathways, such as DNA promoter methylation[8,75,76], the p38 MAP signaling pathway[85,86], histone acetylation[79-82,156], and the JAK2/STAT3 signaling pathway[120,157]. Further, changes in the expression of Cxs may regulate the proliferation, metastasis, invasion, and apoptosis of cells. For all this, further and deeper studies of the relationship between *H. pylori*-associated GC and Cxs are necessary. The dysregulation of Cxs could cause drug resistance in cancer[116,158-160]. Moreover, improving the expression of intercellular Cxs may be a future therapeutic target for GC.

## ACKNOWLEDGEMENTS

This review was supported by the "New Xiangya Talent Projects" of the Third Xiangya Hospital of Central South University (JY201710).

## REFERENCES


1 **Fontes LES**, Martimbianco ALC, Zanin C, Riera R. N-acetylcysteine as an adjuvant therapy for Helicobacter pylori eradication. *Cochrane Database Syst Rev* 2019; **2**: CD012357 [PMID: 30746681 DOI: 10.1002/14651858.CD012357.pub2]

2 **Wang F**, Meng W, Wang B, Qiao L. Helicobacter pylori-induced gastric inflammation and gastric cancer. *Cancer Lett* 2014; **345**: 196-202 [PMID: 23981572 DOI: 10.1016/j.canlet.2013.08.016]

3 **Crabtree JE**, Court M, Aboshkiwa MA, Jeremy AH, Dixon MF, Robinson PA. Gastric mucosal cytokine and epithelial cell responses to Helicobacter pylori infection in Mongolian gerbils. *J Pathol* 2004; **202**: 197-207 [PMID: 14743502 DOI: 10.1002/path.1498]

4 **Maleki Kakelar H**, Barzegari A, Dehghani J, Hanifian S, Saeedi N, Barar J, Omidi Y. Pathogenicity of Helicobacter pylori in cancer development and impacts of vaccination. *Gastric Cancer* 2019; **22**: 23-36 [PMID: 30145749 DOI: 10.1007/s10120-018-0867-1]

5 **Backert S**, Meyer TF. Type IV secretion systems and their effectors in bacterial pathogenesis. *Curr Opin Microbiol* 2006; **9**: 207-217 [PMID: 16529981 DOI: 10.1016/j.mib.2006.02.008]

6 **Fischer W**, Püls J, Buhrdorf R, Gebert B, Odenbreit S, Haas R. Systematic mutagenesis of the Helicobacter pylori cag pathogenicity island: Essential genes for CagA translocation in host cells and induction of interleukin-8. *Mol Microbiol* 2001; **42**: 1337-1348 [PMID: 11886563 DOI: 10.1046/j.1365-2958.2001.02714.x]

7 **Hatakeyama M**. [H. pylori oncoprotein CagA and gastric cancer]. *Nihon Rinsho* 2012; **70**: 1699-1704 [PMID: 23198548]

8 **Zhang B**, Zhang X, Jin M, Hu L, Zang M, Qiu W, Wang S, Liu B, Liu S, Guo D. CagA increases DNA methylation and decreases PTEN expression in human gastric cancer. *Mol Med Rep* 2019; **19**: 309-319 [PMID: 30431097 DOI: 10.3892/mmr.2018.9654]

9 **Zhang BG**, Hu L, Zang MD, Wang HX, Zhao W, Li JF, Su LP, Shao Z, Zhao X, Zhu ZG, Yan M, Liu B. Helicobacter pylori CagA induces tumor suppressor gene hypermethylation by upregulating DNMT1 via AKT-NFκB pathway in gastric cancer development. *Oncotarget* 2016; **7**: 9788-9800 [PMID: 26848521 DOI: 10.18632/oncotarget.7125]

10 **Yamaoka Y**. Mechanisms of disease: Helicobacter pylori virulence factors. *Nat Rev Gastroenterol Hepatol* 2010; **7**: 629-641 [PMID: 20938460 DOI: 10.1038/nrgastro.2010.154]

11 **Lai YP**, Yang JC, Lin TZ, Lin JT, Wang JT. Helicobacter pylori infection and CagA protein translocation in human primary gastric epithelial cell culture. *Helicobacter* 2006; **11**: 451-459 [PMID: 16961808 DOI: 10.1111/j.1523-5378.2006.00438.x]

12 **Khatoon J**, Prasad KN, Prakash Rai R, Ghoshal UC, Krishnani N. Association of heterogenicity of Helicobacter pylori cag pathogenicity island with peptic ulcer diseases and gastric cancer. *Br J Biomed Sci* 2017; **74**: 121-126 [PMID: 28571523 DOI: 10.1080/09674845.2017.1278887]

13 **Phadnis SH**, Ilver D, Janzon L, Normark S, Westblom TU. Pathological significance and molecular characterization of the vacuolating toxin gene of Helicobacter pylori. *Infect Immun* 1994; **62**: 1557-1565 [PMID: 8168917 DOI: 10.1007/BF01716716]

14 **Cover TL**, Tummuru MK, Cao P, Thompson SA, Blaser MJ. Divergence of genetic sequences for the vacuolating cytotoxin among Helicobacter pylori strains. *J Biol Chem* 1994; **269**: 10566-10573 [PMID: 8144644]

15 **Rhead JL**, Letley DP, Mohammadi M, Hussein N, Mohagheghi MA, Eshagh Hosseini M, Atherton JC. A new Helicobacter pylori vacuolating cytotoxin determinant, the intermediate region, is associated with gastric cancer. *Gastroenterology* 2007; **133**: 926-936 [PMID: 17854597 DOI: 10.1053/j.gastro.2007.06.056]

16 **Atherton JC**, Cao P, Peek RM, Tummuru MK, Blaser MJ, Cover TL. Mosaicism in vacuolating cytotoxin alleles of Helicobacter pylori. Association of specific vacA types with cytotoxin production and peptic ulceration. *J Biol Chem* 1995; **270**: 17771-17777 [PMID: 7629077 DOI: 10.1074/jbc.270.30.17771]

17 **Atherton JC**, Blaser MJ. Coadaptation of Helicobacter pylori and humans: Ancient history, modern implications. *J Clin Invest* 2009; **119**: 2475-2487 [PMID: 19729845 DOI: 10.1172/JCI38605]

18 **Figueiredo C**, Machado JC, Pharoah P, Seruca R, Sousa S, Carvalho R, Capelinha AF, Quint W, Caldas C, van Doorn LJ, Carneiro F, Sobrinho-Simões M. Helicobacter pylori and interleukin 1 genotyping: An opportunity to identify high-risk individuals for gastric carcinoma. *J Natl Cancer Inst* 2002; **94**: 1680-1687 [PMID: 12441323 DOI: 10.1093/jnci/94.22.1680]

19 **Basso D**, Zambon CF, Letley DP, Stranges A, Marchet A, Rhead JL, Schiavon S, Guariso G, Ceroti M, Nitti D, Rugge M, Plebani M, Atherton JC. Clinical relevance of Helicobacter pylori cagA and vacA gene polymorphisms. *Gastroenterology* 2008; **135**: 91-99 [PMID: 18474244 DOI: 10.1053/j.gastro.2008.03.041]

20 **Miehlke S**, Kirsch C, Agha-Amiri K, Günther T, Lehn N, Malfertheiner P, Stolte M, Ehninger G, Bayerdörffer E. The Helicobacter pylori vacA s1, m1 genotype and cagA is associated with gastric carcinoma in Germany. *Int J Cancer* 2000; **87**: 322-327 [PMID: 10897035 DOI: 10.1002/1097-0215(20000801)87:3<322::AID-IJC3>3.3.CO;2-D]

21 **Nogueira C**, Figueiredo C, Carneiro F, Gomes AT, Barreira R, Figueira P, Salgado C, Belo L, Peixoto A, Bravo JC, Bravo LE, Realpe JL, Plaisier AP, Quint WG, Ruiz B, Correa P, van Doorn LJ. Helicobacter pylori genotypes may determine gastric histopathology. *Am J Pathol* 2001; **158**: 647-654 [PMID: 11159201 DOI: 10.1016/s0002-9440(10)64006-0]

22 **Memon AA**, Hussein NR, Miendje Deyi VY, Burette A, Atherton JC. Vacuolating cytotoxin genotypes are strong markers of gastric cancer and duodenal ulcer-associated Helicobacter pylori strains: A matched case-control study. *J Clin Microbiol* 2014; **52**: 2984-2989 [PMID: 24920772 DOI: 10.1128/JCM.00551-14]

23 **Winter JA**, Letley DP, Cook KW, Rhead JL, Zaitoun AA, Ingram RJ, Amilon KR, Croxall NJ, Kaye PV, Robinson K, Atherton JC. A role for the vacuolating cytotoxin, VacA, in colonization and Helicobacter pylori-induced metaplasia in the stomach. *J Infect Dis* 2014; **210**: 954-963 [PMID: 24625807 DOI: 10.1093/infdis/jiu154]

24 **McClain MS**, Beckett AC, Cover TL. Helicobacter pylori Vacuolating Toxin and Gastric Cancer. *Toxins (Basel)* 2017; **9**: pii: E316 [PMID: 29023421 DOI: 10.3390/toxins9100316]

25 **Papini E**, Satin B, Norais N, de Bernard M, Telford JL, Rappuoli R, Montecucco C. Selective increase of the permeability of polarized epithelial cell monolayers by Helicobacter pylori vacuolating toxin. *J Clin Invest* 1998; **102**: 813-820 [PMID: 9710450 DOI: 10.1172/JCI2764]

26 **Abdullah M**, Greenfield LK, Bronte-Tinkew D, Capurro MI, Rizzuti D, Jones NL. VacA promotes CagA

accumulation in gastric epithelial cells during Helicobacter pylori infection. *Sci Rep* 2019; **9**: 38 [PMID: 30631092 DOI: 10.1038/s41598-018-37095-4]

27 **Xing Y**, Zhang Y, Jia L, Xu X. Lipopolysaccharide from Escherichia coli stimulates osteogenic differentiation of human periodontal ligament stem cells through Wnt/β-catenin-induced TAZ elevation. *Mol Oral Microbiol* 2019; 34 [PMID: 30387555 DOI: 10.1111/omi.12249]

28 **Niu C**, Shang N, Liao X, Feng E, Liu X, Wang D, Wang J, Huang P, Hua Y, Zhu L, Wang H. Analysis of Soluble protein complexes in Shigella flexneri reveals the influence of temperature on the amount of lipopolysaccharide. *Mol Cell Proteomics* 2013; **12**: 1250-1258 [PMID: 23378524 DOI: 10.1074/mcp.M112.025270]

29 **Kasperkiewicz K**, Swierzko AS, Bartlomiejczyk MA, Cedzynski M, Noszczynska M, Duda KA, Michalski M, Skurnik M. Interaction of human mannose-binding lectin (MBL) with Yersinia enterocolitica lipopolysaccharide. *Int J Med Microbiol* 2015; **305**: 544-552 [PMID: 26188838 DOI: 10.1016/j.ijmm.2015.07.001]

30 **Lee SJ**, Kim SW, Cho YH, Yoon MS. Anti-inflammatory effect of an Escherichia coli extract in a mouse model of lipopolysaccharide-induced cystitis. *World J Urol* 2006; **24**: 33-38 [PMID: 16389538 DOI: 10.1007/s00345-005-0046-y]

31 **Li H**, Liao T, Debowski AW, Tang H, Nilsson HO, Stubbs KA, Marshall BJ, Benghezal M. Lipopolysaccharide Structure and Biosynthesis in Helicobacter pylori. *Helicobacter* 2016; **21**: 445-461 [PMID: 26934862 DOI: 10.1111/hel.12301]

32 **Li N**, Xu H, Ou Y, Feng Z, Zhang Q, Zhu Q, Cai Z. LPS-induced CXCR7 expression promotes gastric Cancer proliferation and migration via the TLR4/MD-2 pathway. *Diagn Pathol* 2019; **14**: 3 [PMID: 30636642 DOI: 10.1186/s13000-019-0780-x]

33 **Li H**, Xia JQ, Zhu FS, Xi ZH, Pan CY, Gu LM, Tian YZ. LPS promotes the expression of PD-L1 in gastric cancer cells through NF-κB activation. *J Cell Biochem* 2018; **119**: 9997-10004 [PMID: 30145830 DOI: 10.1002/jcb.27329]

34 **Wang F**, Mao Z, Liu D, Yu J, Wang Y, Ye W, Lin D, Zhou N, Xie Y. Overexpression of Tim-3 reduces Helicobacter pylori-associated inflammation through TLR4/NFκB signaling in vitro. *Mol Med Rep* 2017; **15**: 3252-3258 [PMID: 28339054 DOI: 10.3892/mmr.2017.6346]

35 **Chochi K**, Ichikura T, Kinoshita M, Majima T, Shinomiya N, Tsujimoto H, Kawabata T, Sugasawa H, Ono S, Seki S, Mochizuki H. Helicobacter pylori augments growth of gastric cancers via the lipopolysaccharide-toll-like receptor 4 pathway whereas its lipopolysaccharide attenuates antitumor activities of human mononuclear cells. *Clin Cancer Res* 2008; **14**: 2909-2917 [PMID: 18483357 DOI: 10.1158/1078-0432.CCR-07-4467]

36 **Yokota S**, Okabayashi T, Rehli M, Fujii N, Amano K. Helicobacter pylori lipopolysaccharides upregulate toll-like receptor 4 expression and proliferation of gastric epithelial cells via the MEK1/2-ERK1/2 mitogen-activated protein kinase pathway. *Infect Immun* 2010; **78**: 468-476 [PMID: 19858308 DOI: 10.1128/IAI.00903-09]

37 **Vinken M**, Vanhaecke T, Papeleu P, Snykers S, Henkens T, Rogiers V. Connexins and their channels in cell growth and cell death. *Cell Signal* 2006; **18**: 592-600 [PMID: 16183253 DOI: 10.1016/j.cellsig.2005.08.012]

38 **Goodenough DA**, Goliger JA, Paul DL. Connexins, connexons, and intercellular communication. *Annu Rev Biochem* 1996; **65**: 475-502 [PMID: 8811187 DOI: 10.1146/annurev.bi.65.070196.002355]

39 **Xu CX**, Jia Y, Yang WB, Wang F, Shen SR. [Relationship between Helicobacter pylori infection and expression of connexin (Cx) 32 and Cx43 genes in gastric cancer and gastric precancerous lesions]. *Zhonghua Yi Xue Za Zhi* 2008; **88**: 1523-1527 [PMID: 18956631]

40 **Li X**, Zhou Z, Dou K, Wang Y. Connexin evolution ameliorates the risk of various cancers. *Eur Rev Med Pharmacol Sci* 2015; **19**: 1662-1672 [PMID: 26004607]

41 **Xu L**, Chen SW, Qi XY, Li XX, Sun YB. Ginsenoside improves papillary thyroid cancer cell malignancies partially through upregulating connexin 31. *Kaohsiung J Med Sci* 2018; **34**: 313-320 [PMID: 29747774 DOI: 10.1016/j.kjms.2017.12.006]

42 **Lai Y**, Tao L, Zhao Y, Zhang X, Sun X, Wang Q, Xu C. Cx32 inhibits TNFα-induced extrinsic apoptosis with and without EGFR suppression. *Oncol Rep* 2017; **38**: 2885-2892 [PMID: 28901517 DOI: 10.3892/or.2017.5950]

43 **Lai Y**, Fan L, Zhao Y, Ge H, Feng X, Wang Q, Zhang X, Peng Y, Wang X, Tao L. Cx32 suppresses extrinsic apoptosis in human cervical cancer cells via the NFκB signalling pathway. *Int J Oncol* 2017; **51**: 1159-1168 [PMID: 28902345 DOI: 10.3892/ijo.2017.4106]

44 **Radin JN**, González-Rivera C, Frick-Cheng AE, Sheng J, Gaddy JA, Rubin DH, Algood HM, McClain MS, Cover TL. Role of connexin 43 in Helicobacter pylori VacA-induced cell death. *Infect Immun* 2014; **82**: 423-432 [PMID: 24191302 DOI: 10.1128/IAI.00827-13]

45 **Yang J**, Qin GH, Chen JZ. Inhibitory effect of lentivirus targeting interference Cx26 on proliferation and migration of human highly metastatic hepatocellular carcinoma HCCLM3 cells. *Zhongguo Yaolixue Tongbao* 2014; **30**: 937-941 [DOI: 10.3969/j.issn.1001-1978.2014.07.012]

46 **Fong JT**, Kells RM, Gumpert AM, Marzillier JY, Davidson MW, Falk MM. Internalized gap junctions are degraded by autophagy. *Autophagy* 2012; **8**: 794-811 [PMID: 22635056 DOI: 10.4161/auto.19390]

47 **Krutovskikh VA**, Piccoli C, Yamasaki H. Gap junction intercellular communication propagates cell death in cancerous cells. *Oncogene* 2002; **21**: 1989-1999 [PMID: 11960371 DOI: 10.1038/sj.onc.1205187]

48 **Mine T**, Endo C, Kushima R, Kushima W, Kobayashi I, Muraoka H, Taki R, Fujita T. The effects of water extracts of CagA positive or negative Helicobacter pylori on proliferation, apoptosis and connexin formation in acetic acid-induced gastric ulcer of rats. *Aliment Pharmacol Ther* 2000; **14** Suppl 1: 199-204 [PMID: 10807425 DOI: 10.1046/j.1365-2036.2000.014s1199.x]

49 **Liu X**, Furuya T, Li D, Xu J, Cao X, Li Q, Xu J, Xu Z, Sasaki K, Liu X. Connexin 26 expression correlates with less aggressive phenotype of intestinal type-gastric carcinomas. *Int J Mol Med* 2010; **25**: 709-716 [PMID: 20372813 DOI: 10.3892/ijmm_00000395]

50 **Nishitani A**, Hirota S, Nishida T, Isozaki K, Hashimoto K, Nakagomi N, Matsuda H. Differential expression of connexin 43 in gastrointestinal stromal tumours of gastric and small intestinal origin. *J Pathol* 2005; **206**: 377-382 [PMID: 15938003 DOI: 10.1002/path.1799]

51 **Wang YF**, Daniel EE. Gap junctions in gastrointestinal muscle contain multiple connexins. *Am J Physiol Gastrointest Liver Physiol* 2001; **281**: G533-G543 [PMID: 11447034 DOI: 10.1152/ajpgi.2001.281.2.G533]

52 **Iino S**, Asamoto K, Nojyo Y. Heterogeneous distribution of a gap junction protein, connexin43, in the gastroduodenal junction of the guinea pig. *Auton Neurosci* 2001; **93**: 8-13 [PMID: 11695711 DOI:

10.1016/S1566-0702(01)00320-4]
53 **Takahashi N**, Joh T, Yokoyama Y, Seno K, Nomura T, Ohara H, Ueda F, Itoh M. Importance of gap junction in gastric mucosal restitution from acid-induced injury. *J Lab Clin Med* 2000; **136**: 93-99 [PMID: 10945237 DOI: 10.1067/mlc.2000.108158]
54 **Iwata F**, Joh T, Ueda F, Yokoyama Y, Itoh M. Role of gap junctions in inhibiting ischemia-reperfusion injury of rat gastric mucosa. *Am J Physiol* 1998; **275**: G883-G888 [PMID: 9815015 DOI: 10.1152/ajpgi.1998.275.5.G883]
55 **Uchida Y**, Matsuda K, Sasahara K, Kawabata H, Nishioka M. Immunohistochemistry of gap junctions in normal and diseased gastric mucosa of humans. *Gastroenterology* 1995; **109**: 1492-1496 [PMID: 7557130 DOI: 10.1016/0016-5085(95)90635-5]
56 **Jing Y**, Guo S, Zhang X, Sun A, Tao F, Ju H, Qian H. Effects of small interfering RNA interference of connexin 37 on subcutaneous gastric tumours in mice. *Mol Med Rep* 2014; **10**: 2955-2960 [PMID: 25310476 DOI: 10.3892/mmr.2014.2609]
57 **Radebold K**, Horakova E, Gloeckner J, Ortega G, Spray DC, Vieweger H, Siebert K, Manuelidis L, Geibel JP. Gap junctional channels regulate acid secretion in the mammalian gastric gland. *J Membr Biol* 2001; **183**: 147-153 [PMID: 11696856 DOI: 10.1007/s00232-001-0062-9]
58 **Liu XM**, Xu CX, Zhang LF, Huang LH, Hu TZ, Li R, Xia XJ, Xu LY, Luo L, Jiang XX, Li M. PBX1 attributes as a determinant of connexin 32 downregulation in Helicobacter pylori-related gastric carcinogenesis. *World J Gastroenterol* 2017; **23**: 5345-5355 [PMID: 28839434 DOI: 10.3748/wjg.v23.i29.5345]
59 **Zhou L**, Xu C, Hu T, Liu X, Xiao J, Luo L, Jiang X. [Effect of H. pylori on the expression of CCAAT enhancer binding protein α and Cx43 and its role in gastric carcinogenesis]. *Zhong Nan Da Xue Xue Bao Yi Xue Ban* 2016; **41**: 700-706 [PMID: 27592574 DOI: 10.11817/j.issn.1672-7347.2016.07.007]
60 **Liu X**, Cao K, Xu C, Hu T, Zhou L, Cao D, Xiao J, Luo L, Guo Y, Qi Y. GATA-3 augmentation down-regulates Connexin43 in Helicobacter pylori associated gastric carcinogenesis. *Cancer Biol Ther* 2015; **16**: 987-996 [PMID: 25901741 DOI: 10.1080/15384047.2015.1030552]
61 **Tang B**, Peng ZH, Yu PW, Yu G, Qian F. Expression and significance of Cx43 and E-cadherin in gastric cancer and metastatic lymph nodes. *Med Oncol* 2011; **28**: 502-508 [PMID: 20373058 DOI: 10.1007/s12032-010-9492-5]
62 **Jamieson S**, Going JJ, D'Arcy R, George WD. Expression of gap junction proteins connexin 26 and connexin 43 in normal human breast and in breast tumours. *J Pathol* 1998; **184**: 37-43 [PMID: 9582525 DOI: 10.1002/(SICI)1096-9896(199801)184:1<37::AID-PATH966>3.0.CO;2-D]
63 **Mehta PP**, Perez-Stable C, Nadji M, Mian M, Asotra K, Roos BA. Suppression of human prostate cancer cell growth by forced expression of connexin genes. *Dev Genet* 1999; **24**: 91-110 [PMID: 10079514 DOI: 10.1002/(SICI)1520-6408(1999)24:1/2<91::AID-DVG10>3.3.CO;2-R]
64 **Kanczuga-Koda L**, Sulkowski S, Koda M, Sulkowska M. Alterations in connexin26 expression during colorectal carcinogenesis. *Oncology* 2005; **68**: 217-222 [PMID: 16015037 DOI: 10.1159/000086777]
65 **Hong R**, Lim SC. Pathological significance of connexin 26 expression in colorectal adenocarcinoma. *Oncol Rep* 2008; **19**: 913-919 [PMID: 18357375 DOI: 10.3892/or.19.4.913]
66 **Inose T**, Kato H, Kimura H, Faried A, Tanaka N, Sakai M, Sano A, Sohda M, Nakajima M, Fukai Y, Miyazaki T, Masuda N, Fukuchi M, Kuwano H. Correlation between connexin 26 expression and poor prognosis of esophageal squamous cell carcinoma. *Ann Surg Oncol* 2009; **16**: 1704-1710 [PMID: 19326169 DOI: 10.1245/s10434-009-0443-3]
67 **Jee H**, Nam KT, Kwon HJ, Han SU, Kim DY. Altered expression and localization of connexin32 in human and murine gastric carcinogenesis. *Dig Dis Sci* 2011; **56**: 1323-1332 [PMID: 21082351 DOI: 10.1007/s10620-010-1467-z]
68 **Kojima T**, Kokai Y, Chiba H, Yamamoto M, Mochizuki Y, Sawada N. Cx32 but not Cx26 is associated with tight junctions in primary cultures of rat hepatocytes. *Exp Cell Res* 2001; **263**: 193-201 [PMID: 11161718 DOI: 10.1006/excr.2000.5103]
69 **Eugenín EA**, González HE, Sánchez HA, Brañes MC, Sáez JC. Inflammatory conditions induce gap junctional communication between rat Kupffer cells both in vivo and in vitro. *Cell Immunol* 2007; **247**: 103-110 [PMID: 17900549 DOI: 10.1016/j.cellimm.2007.08.001]
70 **Zhang JT**, Nicholson BJ. Sequence and tissue distribution of a second protein of hepatic gap junctions, Cx26, as deduced from its cDNA. *J Cell Biol* 1989; **109**: 3391-3401 [PMID: 2557354 DOI: 10.1083/jcb.109.6.3391]
71 **Fischer R**, Reinehr R, Lu TP, Schönicke A, Warskulat U, Dienes HP, Häussinger D. Intercellular communication via gap junctions in activated rat hepatic stellate cells. *Gastroenterology* 2005; **128**: 433-448 [PMID: 15685554 DOI: 10.1053/j.gastro.2004.11.065]
72 **Lim MC**, Maubach G, Zhuo L. TGF-beta1 down-regulates connexin 43 expression and gap junction intercellular communication in rat hepatic stellate cells. *Eur J Cell Biol* 2009; **88**: 719-730 [PMID: 19781809 DOI: 10.1016/j.ejcb.2009.08.003]
73 **Mitaka T**, Sato F, Mizuguchi T, Yokono T, Mochizuki Y. Reconstruction of hepatic organoid by rat small hepatocytes and hepatic nonparenchymal cells. *Hepatology* 1999; **29**: 111-125 [PMID: 9862857 DOI: 10.1002/hep.510290103]
74 **Maes M**, Crespo Yanguas S, Willebrords J, Cogliati B, Vinken M. Connexin and pannexin signaling in gastrointestinal and liver disease. *Transl Res* 2015; **166**: 332-343 [PMID: 26051630 DOI: 10.1016/j.trsl.2015.05.005]
75 **Hernández-Guerra M**, González-Méndez Y, de Ganzo ZA, Salido E, García-Pagán JC, Abrante B, Malagón AM, Bosch J, Quintero E. Role of gap junctions modulating hepatic vascular tone in cirrhosis. *Liver Int* 2014; **34**: 859-868 [PMID: 24350605 DOI: 10.1111/liv.12446]
76 **Shiojiri N**, Niwa T, Sugiyama Y, Koike T. Preferential expression of connexin37 and connexin40 in the endothelium of the portal veins during mouse liver development. *Cell Tissue Res* 2006; **324**: 547-552 [PMID: 16505993 DOI: 10.1007/s00441-006-0165-9]
77 **Chaytor AT**, Martin PE, Edwards DH, Griffith TM. Gap junctional communication underpins EDHF-type relaxations evoked by ACh in the rat hepatic artery. *Am J Physiol Heart Circ Physiol* 2001; **280**: H2441-H2450 [PMID: 11356596 DOI: 10.1152/ajpheart.2001.280.6.H2441]
78 **Kim EM**, Bae YM, Choi MH, Hong ST. Connexin 43 plays an important role in the transformation of cholangiocytes with Clonochis sinensis excretory-secretory protein and N-nitrosodimethylamine. *PLoS Negl Trop Dis* 2019; **13**: e0006843 [PMID: 30943209 DOI: 10.1371/journal.pntd.0006843]
79 **Bode HP**, Wang L, Cassio D, Leite MF, St-Pierre MV, Hirata K, Okazaki K, Sears ML, Meda P, Nathanson MH, Dufour JF. Expression and regulation of gap junctions in rat cholangiocytes. *Hepatology*

2002; **36**: 631-640 [PMID: 12198655 DOI: 10.1053/jhep.2002.35274]
80 **Jing YM**, Guo SX, Zhang XP, Sun AJ, Tao F, Qian HX. Association between C1019T polymorphism in the connexin 37 gene and Helicobacter pylori infection in patients with gastric cancer. *Asian Pac J Cancer Prev* 2012; **13**: 2363-2367 [PMID: 22901223 DOI: 10.7314/apjcp.2012.13.5.2363]
81 **Fink C**, Hembes T, Brehm R, Weigel R, Heeb C, Pfarrer C, Bergmann M, Kressin M. Specific localisation of gap junction protein connexin 32 in the gastric mucosa of horses. *Histochem Cell Biol* 2006; **125**: 307-313 [PMID: 16205941 DOI: 10.1007/s00418-005-0047-3]
82 **Nakamura K**, Nishii K, Shibata Y. [Networks of pacemaker cells for gastrointestinal motility]. *Nihon Yakurigaku Zasshi* 2004; **123**: 134-140 [PMID: 14993724 DOI: 10.1254/fpj.123.134]
83 **Frinchi M**, Di Liberto V, Turimella S, D'Antoni F, Theis M, Belluardo N, Mudò G. Connexin36 (Cx36) expression and protein detection in the mouse carotid body and myenteric plexus. *Acta Histochem* 2013; **115**: 252-256 [PMID: 22897942 DOI: 10.1016/j.acthis.2012.07.005]
84 **Bracken S**, Byrne G, Kelly J, Jackson J, Feighery C. Altered gene expression in highly purified enterocytes from patients with active coeliac disease. *BMC Genomics* 2008; **9**: 377 [PMID: 18691394 DOI: 10.1186/1471-2164-9-377]
85 **King TJ**, Lampe PD. Mice deficient for the gap junction protein Connexin32 exhibit increased radiation-induced tumorigenesis associated with elevated mitogen-activated protein kinase (p44/Erk1, p42/Erk2) activation. *Carcinogenesis* 2004; **25**: 669-680 [PMID: 14742325 DOI: 10.1093/carcin/bgh071]
86 **Nemeth L**, Maddur S, Puri P. Immunolocalization of the gap junction protein Connexin43 in the interstitial cells of Cajal in the normal and Hirschsprung's disease bowel. *J Pediatr Surg* 2000; **35**: 823-828 [PMID: 10873019 DOI: 10.1053/jpsu.2000.6851]
87 **Mattii L**, Ippolito C, Segnani C, Battolla B, Colucci R, Dolfi A, Bassotti G, Blandizzi C, Bernardini N. Altered expression pattern of molecular factors involved in colonic smooth muscle functions: An immunohistochemical study in patients with diverticular disease. *PLoS One* 2013; **8**: e57023 [PMID: 23437299 DOI: 10.1371/journal.pone.0057023]
88 **Kanczuga-Koda L**, Sulkowski S, Koda M, Skrzydlewska E, Sulkowska M. Connexin 26 correlates with Bcl-xL and Bax proteins expression in colorectal cancer. *World J Gastroenterol* 2005; **11**: 1544-1548 [PMID: 15770735 DOI: 10.3748/wjg.v11.i10.1544]
89 **Ismail R**, Rashid R, Andrabi K, Parray FQ, Besina S, Shah MA, Ul Hussain M. Pathological implications of Cx43 down-regulation in human colon cancer. *Asian Pac J Cancer Prev* 2014; **15**: 2987-2991 [PMID: 24815435 DOI: 10.7314/apjcp.2014.15.7.2987]
90 **Kanczuga-Koda L**, Sulkowski S, Koda M, Sobaniec-Lotowska M, Sulkowska M. Expression of connexins 26, 32 and 43 in the human colon--an immunohistochemical study. *Folia Histochem Cytobiol* 2004; **42**: 203-207 [PMID: 15704645]
91 **Kanady JD**, Munger SJ, Witte MH, Simon AM. Combining Foxc2 and Connexin37 deletions in mice leads to severe defects in lymphatic vascular growth and remodeling. *Dev Biol* 2015; **405**: 33-46 [PMID: 26079578 DOI: 10.1016/j.ydbio.2015.06.004]
92 **Oyamada M**, Oyamada Y, Takamatsu T. Regulation of connexin expression. *Biochim Biophys Acta* 2005; **1719**: 6-23 [PMID: 16359940 DOI: 10.1016/j.bbamem.2005.11.002]
93 **Senderek J**, Hermanns B, Bergmann C, Boroojerdi B, Bajbouj M, Hungs M, Ramaekers VT, Quasthoff S, Karch D, Schröder JM. X-linked dominant Charcot-Marie-Tooth neuropathy: Clinical, electrophysiological, and morphological phenotype in four families with different connexin32 mutations(1). *J Neurol Sci* 1999; **167**: 90-101 [PMID: 10521546 DOI: 10.1016/s0022-510x(99)00146-x]
94 **Nicholson SM**, Ressot C, Gomès D, D'Andrea P, Perea J, Duval N, Bruzzone R. Connexin32 in the Peripheral Nervous System: Functional Analysis of Mutations Associated with X-linked Charcot-Marie-Tooth Syndrome and Implications for the Pathophysiology of the Disease. *Ann N Y Acad Sci* 1999; **883**: 168-185 [PMID: 29086926 DOI: 10.1111/j.1749-6632.1999.tb08580.x]
95 **Nakashima Y**, Ono T, Yamanoi A, El-Assal ON, Kohno H, Nagasue N. Expression of gap junction protein connexin32 in chronic hepatitis, liver cirrhosis, and hepatocellular carcinoma. *J Gastroenterol* 2004; **39**: 763-768 [PMID: 15338370 DOI: 10.1007/s00535-003-1386-2]
96 **Yang J**, Ichikawa A, Tsuchiya T. A novel function of connexin 32: Marked enhancement of liver function in a hepatoma cell line. *Biochem Biophys Res Commun* 2003; **307**: 80-85 [PMID: 12849984 DOI: 10.1016/s0006-291x(03)01117-3]
97 **Jee H**, Lee SH, Park JW, Lee BR, Nam KT, Kim DY. Connexin32 inhibits gastric carcinogenesis through cell cycle arrest and altered expression of p21Cip1 and p27Kip1. *BMB Rep* 2013; **46**: 25-30 [PMID: 23351380 DOI: 10.5483/bmbrep.2013.46.1.078]
98 **Kanczuga-Koda L**, Koda M, Sulkowski S, Wincewicz A, Zalewski B, Sulkowska M. Gradual loss of functional gap junction within progression of colorectal cancer -- a shift from membranous CX32 and CX43 expression to cytoplasmic pattern during colorectal carcinogenesis. *In Vivo* 2010; **24**: 101-107 [PMID: 20133984 DOI: 10.1089/hum.2009.1214]
99 **Hirai A**, Yano T, Nishikawa K, Suzuki K, Asano R, Satoh H, Hagiwara K, Yamasaki H. Down-regulation of connexin 32 gene expression through DNA methylation in a human renal cell carcinoma cell. *Am J Nephrol* 2003; **23**: 172-177 [PMID: 12690227 DOI: 10.1159/000070653]
100 **Wang Y**, Huang LH, Xu CX, Xiao J, Zhou L, Cao D, Liu XM, Qi Y. Connexin 32 and 43 promoter methylation in Helicobacter pylori-associated gastric tumorigenesis. *World J Gastroenterol* 2014; **20**: 11770-11779 [PMID: 25206281 DOI: 10.3748/wjg.v20.i33.11770]
101 **Huang L**, Guo Y, Cao D, Liu X, Zhang L, Cao K, Hu T, Qi Y, Xu C. Effects of Helicobacter pylori on the expression levels of GATA-3 and connexin 32 and the GJIC function in gastric epithelial cells and their association by promoter analysis. *Oncol Lett* 2018; **16**: 1650-1658 [PMID: 30008849 DOI: 10.3892/ol.2018.8796]
102 **Verdin E**, Ott M. 50 years of protein acetylation: From gene regulation to epigenetics, metabolism and beyond. *Nat Rev Mol Cell Biol* 2015; **16**: 258-264 [PMID: 25549891 DOI: 10.1038/nrm3931]
103 **Grabiec AM**, Potempa J. Epigenetic regulation in bacterial infections: Targeting histone deacetylases. *Crit Rev Microbiol* 2018; **44**: 336-350 [PMID: 28971711 DOI: 10.1080/1040841X.2017.1373063]
104 **Ding SZ**, Fischer W, Kaparakis-Liaskos M, Liechti G, Merrell DS, Grant PA, Ferrero RL, Crowe SE, Haas R, Hatakeyama M, Goldberg JB. Helicobacter pylori-induced histone modification, associated gene expression in gastric epithelial cells, and its implication in pathogenesis. *PLoS One* 2010; **5**: e9875 [PMID: 20368982 DOI: 10.1371/journal.pone.0009875]
105 **Vinken M**, Henkens T, Snykers S, Lukaszuk A, Tourwé D, Rogiers V, Vanhaecke T. The novel histone deacetylase inhibitor 4-Me2N-BAVAH differentially affects cell junctions between primary hepatocytes. *Toxicology* 2007; **236**: 92-102 [PMID: 17482745 DOI: 10.1016/j.tox.2007.04.003]

106 **Vinken M**, Henkens T, Vanhaecke T, Papeleu P, Geerts A, Van Rossen E, Chipman JK, Meda P, Rogiers V. Trichostatin a enhances gap junctional intercellular communication in primary cultures of adult rat hepatocytes. *Toxicol Sci* 2006; **91**: 484-492 [PMID: 16531468 DOI: 10.1093/toxsci/kfj152]

107 **Cuadrado A**, Nebreda AR. Mechanisms and functions of p38 MAPK signalling. *Biochem J* 2010; **429**: 403-417 [PMID: 20626350 DOI: 10.1042/BJ20100323]

108 **Zarubin T**, Han J. Activation and signaling of the p38 MAP kinase pathway. *Cell Res* 2005; **15**: 11-18 [PMID: 15686620 DOI: 10.1038/sj.cr.7290257]

109 **Yang M**, Wang L, Gu LJ, Yuan WJ. Helicobacter pylori cytotoxin-associated gene A impairs the filtration barrier function of podocytes via p38 MAPK signaling pathway. *Acta Biochim Pol* 2017; **64**: 471-475 [PMID: 28803254 DOI: 10.18388/abp.2016_1322]

110 **Yamamoto T**, Kojima T, Murata M, Takano K, Go M, Hatakeyama N, Chiba H, Sawada N. p38 MAP-kinase regulates function of gap and tight junctions during regeneration of rat hepatocytes. *J Hepatol* 2005; **42**: 707-718 [PMID: 15826721 DOI: 10.1016/j.jhep.2004.12.033]

111 **Slomiany BL**, Slomiany A. Role of LPS-elicited signaling in triggering gastric mucosal inflammatory responses to H. pylori: Modulatory effect of ghrelin. *Inflammopharmacology* 2017; **25**: 415-429 [PMID: 28516374 DOI: 10.1007/s10787-017-0360-1]

112 **Fallone CA**, Chiba N, van Zanten SV, Fischbach L, Gisbert JP, Hunt RH, Jones NL, Render C, Leontiadis GI, Moayyedi P, Marshall JK. The Toronto Consensus for the Treatment of Helicobacter pylori Infection in Adults. *Gastroenterology* 2016; **151**: 51-69.e14 [PMID: 27102658 DOI: 10.1053/j.gastro.2016.04.006]

113 **Slomiany BL**, Slomiany A. Cytosolic phospholipase A2 activation in Helicobacter pylori lipopolysaccharide-induced interference with gastric mucin synthesis. *IUBMB Life* 2006; **58**: 217-223 [PMID: 16754300 DOI: 10.1080/15216540600732021]

114 **Dhar SK**, Soni RK, Das BK, Mukhopadhyay G. Molecular mechanism of action of major Helicobacter pylori virulence factors. *Mol Cell Biochem* 2003; **253**: 207-215 [PMID: 14619971 DOI: 10.1023/A:1026051530512]

115 **Slomiany BL**, Piotrowski J, Slomiany A. Anti-Helicobacter pylori activities of ebrotidine. A review of biochemical and animal experimental studies and data. *Arzneimittelforschung* 1997; **47**: 475-482 [PMID: 9205747 DOI: 10.1007/BF02974011]

116 **Kameoka S**, Kameyama T, Hayashi T, Sato S, Ohnishi N, Hayashi T, Murata-Kamiya N, Higashi H, Hatakeyama M, Takaoka A. Helicobacter pylori induces IL-1β protein through the inflammasome activation in differentiated macrophagic cells. *Biomed Res* 2016; **37**: 21-27 [PMID: 26912137 DOI: 10.2220/biomedres.37.21]

117 **Semper RP**, Mejías-Luque R, Groß C, Anderl F, Müller A, Vieth M, Busch DH, Prazeres da Costa C, Ruland J, Groß O, Gerhard M. Helicobacter pylori-induced IL-1β secretion in innate immune cells is regulated by the NLRP3 inflammasome and requires the cag pathogenicity island. *J Immunol* 2014; **193**: 3566-3576 [PMID: 25172489 DOI: 10.4049/jimmunol.1400362]

118 **Kim DJ**, Park JH, Franchi L, Backert S, Núñez G. The Cag pathogenicity island and interaction between TLR2/NOD2 and NLRP3 regulate IL-1β production in Helicobacter pylori infected dendritic cells. *Eur J Immunol* 2013; **43**: 2650-2658 [PMID: 23818043 DOI: 10.1002/eji.201243281]

119 **Yamamoto T**, Kojima T, Murata M, Takano K, Go M, Chiba H, Sawada N. IL-1beta regulates expression of Cx32, occludin, and claudin-2 of rat hepatocytes via distinct signal transduction pathways. *Exp Cell Res* 2004; **299**: 427-441 [PMID: 15350541 DOI: 10.1016/j.yexcr.2004.06.011]

120 **Ji YT**, Yang Y, Zheng RS, Zhang WQ, Liu J. Construction of lentiviral vector-mediated Cx32 stably over-expressed Huh7 cell line and its effect on cell proliferation. *Zhongguo Yaolixue Tongbao* 2018; **34**: 284-289 [DOI: 10.3969/j.issn.1001-1978.2018.02.026]

121 **Luo C**, Yuan D, Yao W, Cai J, Zhou S, Zhang Y, Hei Z. Dexmedetomidine protects against apoptosis induced by hypoxia/reoxygenation through the inhibition of gap junctions in NRK-52E cells. *Life Sci* 2015; **122**: 72-77 [PMID: 25529146 DOI: 10.1016/j.lfs.2014.12.009]

122 **Sato H**, Hagiwara H, Ohde Y, Senba H, Virgona N, Yano T. Regulation of renal cell carcinoma cell proliferation, invasion and metastasis by connexin 32 gene. *J Membr Biol* 2007; **216**: 17-21 [PMID: 17565422 DOI: 10.1007/s00232-007-9020-5]

123 **Zhao Y**, Lai Y, Ge H, Guo Y, Feng X, Song J, Wang Q, Fan L, Peng Y, Cao M, Harris AL, Wang X, Tao L. Non-junctional Cx32 mediates anti-apoptotic and pro-tumor effects via epidermal growth factor receptor in human cervical cancer cells. *Cell Death Dis* 2017; **8**: e2773 [PMID: 28492539 DOI: 10.1038/cddis.2017.183]

124 **Decrock E**, De Vuyst E, Vinken M, Van Moorhem M, Vranckx K, Wang N, Van Laeken L, De Bock M, D'Herde K, Lai CP, Rogiers V, Evans WH, Naus CC, Leybaert L. Connexin 43 hemichannels contribute to the propagation of apoptotic cell death in a rat C6 glioma cell model. *Cell Death Differ* 2009; **16**: 151-163 [PMID: 18820645 DOI: 10.1038/cdd.2008.138]

125 **Cusato K**, Zakevicius J, Ripps H. An experimental approach to the study of gap-junction-mediated cell death. *Biol Bull* 2003; **205**: 197-199 [PMID: 14583527 DOI: 10.2307/1543250]

126 **Kalvelyte A**, Imbrasaite A, Bukauskiene A, Verselis VK, Bukauskas FF. Connexins and apoptotic transformation. *Biochem Pharmacol* 2003; **66**: 1661-1672 [PMID: 14555247 DOI: 10.1016/s0006-2952(03)00540-9]

127 **Yu J**, Berga SL, Zou W, Yook DG, Pan JC, Andrade AA, Zhao L, Sidell N, Bagchi IC, Bagchi MK, Taylor RN. IL-1β Inhibits Connexin 43 and Disrupts Decidualization of Human Endometrial Stromal Cells Through ERK1/2 and p38 MAP Kinase. *Endocrinology* 2017; **158**: 4270-4285 [PMID: 28938400 DOI: 10.1210/en.2017-00495]

128 **El-Fakhry AA**, El-Daker MA, Badr RI, El-Nady GM, Mesbah MR, Youssef T, Arafa M, Arafa M, El-Naggar MM. Association of the CagA gene positive Helicobacter pylori and tissue levels of interleukin-17 and interleukin-8 in gastric ulcer patients. *Egypt J Immunol* 2012; **19**: 51-62 [PMID: 23888551]

129 **Shamsdin SA**, Alborzi A, Rasouli M, Ghaderi A, Lankrani KB, Dehghani SM, Pouladfar GR. The importance of TH22 and TC22 cells in the pathogenesis of Helicobacter pylori-associated gastric diseases. *Helicobacter* 2017; 22 [PMID: 27990709 DOI: 10.1111/hel.12367]

130 **Zhuang Y**, Cheng P, Liu XF, Peng LS, Li BS, Wang TT, Chen N, Li WH, Shi Y, Chen W, Pang KC, Zeng M, Mao XH, Yang SM, Guo H, Guo G, Liu T, Zuo QF, Yang HJ, Yang LY, Mao FY, Lv YP, Zou QM. A pro-inflammatory role for Th22 cells in Helicobacter pylori-associated gastritis. *Gut* 2015; **64**: 1368-1378 [PMID: 25134787 DOI: 10.1136/gutjnl-2014-307020]

131 **Qin XH**, Ma X, Fang SF, Zhang ZZ, Lu JM. IL-17 produced by Th17 cells alleviates the severity of fungal keratitis by suppressing CX43 expression in corneal peripheral vascular endothelial cells. *Cell Cycle* 2019; **18**: 274-287 [PMID: 30661459 DOI: 10.1080/15384101.2018.1556059]

132 **Liang J**, Chen P, Li C, Li D, Wang J, Xue R, Zhang S, Ruan J, Zhang X. IL-22 Down-Regulates Cx43 Expression and Decreases Gap Junctional Intercellular Communication by Activating the JNK Pathway in Psoriasis. *J Invest Dermatol* 2019; **139**: 400-411 [PMID: 30171832 DOI: 10.1016/j.jid.2018.07.032]

133 **Yan J**, Thomson JK, Zhao W, Wu X, Gao X, DeMarco D, Kong W, Tong M, Sun J, Bakhos M, Fast VG, Liang Q, Prabhu SD, Ai X. The stress kinase JNK regulates gap junction Cx43 gene expression and promotes atrial fibrillation in the aged heart. *J Mol Cell Cardiol* 2018; **114**: 105-115 [PMID: 29146153 DOI: 10.1016/j.yjmcc.2017.11.006]

134 **Takemura S**, Yashiro M, Sunami T, Tendo M, Hirakawa K. Novel models for human scirrhous gastric carcinoma in vivo. *Cancer Sci* 2004; **95**: 893-900 [PMID: 15546507 DOI: 10.1111/j.1349-7006.2004.tb02199.x]

135 **Chung HW**, Kong HY, Lim JB. Clinical significance and usefulness of soluble heparin binding-epidermal growth factor in gastric cancer. *World J Gastroenterol* 2015; **21**: 2080-2088 [PMID: 25717241 DOI: 10.3748/wjg.v21.i7.2080]

136 **Gunawardhana N**, Jang S, Choi YH, Hong YA, Jeon YE, Kim A, Su H, Kim JH, Yoo YJ, Merrell DS, Kim J, Cha JH. Helicobacter pylori-Induced HB-EGF Upregulates Gastrin Expression via the EGF Receptor, C-Raf, Mek1, and Erk2 in the MAPK Pathway. *Front Cell Infect Microbiol* 2018; **7**: 541 [PMID: 29379775 DOI: 10.3389/fcimb.2017.00541]

137 **Jurkowska G**, Piotrowska-Staworko G, Guzińska-Ustymowicz K, Kemona A, Świdnicka-Siergiejko A, Łaszewicz W, Dąbrowski A. The impact of Helicobacter pylori on EGF, EGF receptor, and the c-erb-B2 expression. *Adv Med Sci* 2014; **59**: 221-226 [PMID: 25051417 DOI: 10.1016/j.advms.2014.01.006]

138 **Yoshioka J**, Prince RN, Huang H, Perkins SB, Cruz FU, MacGillivray C, Lauffenburger DA, Lee RT. Cardiomyocyte hypertrophy and degradation of connexin43 through spatially restricted autocrine/paracrine heparin-binding EGF. *Proc Natl Acad Sci U S A* 2005; **102**: 10622-10627 [PMID: 16020536 DOI: 10.1073/pnas.0501198102]

139 **Kneissl J**, Hartmann A, Pfarr N, Erlmeier F, Lorber T, Keller S, Zwingenberger G, Weichert W, Luber B. Influence of the HER receptor ligand system on sensitivity to cetuximab and trastuzumab in gastric cancer cell lines. *J Cancer Res Clin Oncol* 2017; **143**: 573-600 [PMID: 27933395 DOI: 10.1007/s00432-016-2308-z]

140 **Liu D**, Zhou H, Wu J, Liu W, Li Y, Shi G, Yue X, Sun X, Zhao Y, Hu X, Wang T, Zhang X. Infection by Cx43 adenovirus increased chemotherapy sensitivity in human gastric cancer BGC-823 cells: Not involving in induction of cell apoptosis. *Gene* 2015; **574**: 217-224 [PMID: 26318481 DOI: 10.1016/j.gene.2015.08.052]

141 **Bolamba D**, Floyd AA, McGlone JJ, Lee VH. Epidermal growth factor enhances expression of connexin 43 protein in cultured porcine preantral follicles. *Biol Reprod* 2002; **67**: 154-160 [PMID: 12080012 DOI: 10.1095/biolreprod67.1.154]

142 **Park JH**, Lee MY, Heo JS, Han HJ. A potential role of connexin 43 in epidermal growth factor-induced proliferation of mouse embryonic stem cells: Involvement of Ca2+/PKC, p44/42 and p38 MAPKs pathways. *Cell Prolif* 2008; **41**: 786-802 [PMID: 18823499 DOI: 10.1111/j.1365-2184.2008.00552.x]

143 **Dubé E**, Dufresne J, Chan PT, Cyr DG. Epidermal growth factor regulates connexin 43 in the human epididymis: Role of gap junctions in azoospermia. *Hum Reprod* 2012; **27**: 2285-2296 [PMID: 22611165 DOI: 10.1093/humrep/des164]

144 **Cho SO**, Lim JW, Kim H. Red ginseng extract inhibits the expression of MCP-1 and iNOS in Helicobacter pylori-infected gastric epithelial cells by suppressing the activation of NADPH oxidase and Jak2/Stat3. *J Ethnopharmacol* 2013; **150**: 761-764 [PMID: 24055641 DOI: 10.1016/j.jep.2013.09.013]

145 **Liu K**, Tian T, Zheng Y, Zhou L, Dai C, Wang M, Lin S, Deng Y, Hao Q, Zhai Z, Dai Z. Scutellarin inhibits proliferation and invasion of hepatocellular carcinoma cells via down-regulation of JAK2/STAT3 pathway. *J Cell Mol Med* 2019; **23**: 3040-3044 [PMID: 30697962 DOI: 10.1111/jcmm.14169]

146 **Hou J**, Lv A, Deng Q, Zhang G, Hu X, Cui H. TROP2 promotes the proliferation and metastasis of glioblastoma cells by activating the JAK2/STAT3 signaling pathway. *Oncol Rep* 2019; **41**: 753-764 [PMID: 30431125 DOI: 10.3892/or.2018.6859]

147 **Ai XL**, Chi Q, Qiu Y, Li HY, Li DJ, Wang JX, Wang ZY. Gap junction protein connexin43 deregulation contributes to bladder carcinogenesis via targeting MAPK pathway. *Mol Cell Biochem* 2017; **428**: 109-118 [PMID: 28074341 DOI: 10.1007/s11010-016-2921-9]

148 **Tang Y**, Tong X, Li Y, Jiang G, Yu M, Chen Y, Dong S. JAK2/STAT3 pathway is involved in the protective effects of epidermal growth factor receptor activation against cerebral ischemia/reperfusion injury in rats. *Neurosci Lett* 2018; **662**: 219-226 [PMID: 29061394 DOI: 10.1016/j.neulet.2017.10.037]

149 **Bimczok D**, Kao JY, Zhang M, Cochrun S, Mannon P, Peter S, Wilcox CM, Mönkemüller KE, Harris PR, Grams JM, Stahl RD, Smith PD, Smythies LE. Human gastric epithelial cells contribute to gastric immune regulation by providing retinoic acid to dendritic cells. *Mucosal Immunol* 2015; **8**: 533-544 [PMID: 25249167 DOI: 10.1038/mi.2014.86]

150 **Han X**, Tong XH, Dong SY, Zheng C, Yu BB. [Effects of retinoic acid on the expression of Cx43 and its gap juncion intercellular communication function in testicular cancer cell]. *Sichuan Da Xue Xue Bao Yi Xue Ban* 2013; **44**: 924-927 [PMID: 24490503]

151 **Dong S**, Tong X, Jiang G, Gu Y, Jiao H, Li J. [Expression of connexin 43 and functional modulation of gap junction in neonatal rat astrocytes in vitro]. *Nan Fang Yi Ke Da Xue Xue Bao* 2012; **32**: 1423-1426 [PMID: 23076176]

152 **Tanmahasamut P**, Sidell N. Up-regulation of gap junctional intercellular communication and connexin43 expression by retinoic acid in human endometrial stromal cells. *J Clin Endocrinol Metab* 2005; **90**: 4151-4156 [PMID: 15811935 DOI: 10.1210/jc.2004-0663]

153 **Nguyen PH**, Giraud J, Staedel C, Chambonnier L, Dubus P, Chevret E, Bœuf H, Gauthereau X, Rousseau B, Fevre M, Soubeyran I, Belleannée G, Evrard S, Collet D, Mégraud F, Varon C. All-trans retinoic acid targets gastric cancer stem cells and inhibits patient-derived gastric carcinoma tumor growth. *Oncogene* 2016; **35**: 5619-5628 [PMID: 27157616 DOI: 10.1038/onc.2016.87]

154 **Wu X**, Gao H, Hou Y, Yu J, Sun W, Wang Y, Chen X, Feng Y, Xu QM, Chen X. Dihydronortanshinone, a natural product, alleviates LPS-induced inflammatory response through NF-κB, mitochondrial ROS, and MAPK pathways. *Toxicol Appl Pharmacol* 2018; **355**: 1-8 [PMID: 29906494 DOI: 10.1016/j.taap.2018.06.007]

155 **Liao W**, He X, Yi Z, Xiang W, Ding Y. Chelidonine suppresses LPS-Induced production of inflammatory mediators through the inhibitory of the TLR4/NF-κB signaling pathway in RAW264.7 macrophages. *Biomed Pharmacother* 2018; **107**: 1151-1159 [PMID: 30257328 DOI: 10.1016/j.biopha.2018.08.094]

156 **Liao CK**, Wang SM, Chen YL, Wang HS, Wu JC. Lipopolysaccharide-induced inhibition of connexin43

gap junction communication in astrocytes is mediated by downregulation of caveolin-3. *Int J Biochem Cell Biol* 2010; **42**: 762-770 [PMID: 20093193 DOI: 10.1016/j.biocel.2010.01.016]
157 **Yahiro K**, Akazawa Y, Nakano M, Suzuki H, Hisatune J, Isomoto H, Sap J, Noda M, Moss J, Hirayama T. Helicobacter pylori VacA induces apoptosis by accumulation of connexin 43 in autophagic vesicles via a Rac1/ERK-dependent pathway. *Cell Death Discov* 2015; **1**: 15035 [PMID: 27551466 DOI: 10.1038/cddiscovery.2015.35]
158 **Lin LL**, Huang HC, Ogihara S, Wang JT, Wu MC, McNeil PL, Chen CN, Juan HF. Helicobacter pylori disrupts host cell membranes, initiating a repair response and cell proliferation. *Int J Mol Sci* 2012; **13**: 10176-10192 [PMID: 22949854 DOI: 10.3390/ijms130810176]
159 **Tanaka M**, Grossman HB. Connexin 26 induces growth suppression, apoptosis and increased efficacy of doxorubicin in prostate cancer cells. *Oncol Rep* 2004; **11**: 537-541 [PMID: 14719096 DOI: 10.3892/or.11.2.537]
160 **Yang HJ**, Kim SG, Lim JH, Choi JM, Kim WH, Jung HC. Helicobacter pylori-induced modulation of the promoter methylation of Wnt antagonist genes in gastric carcinogenesis. *Gastric Cancer* 2018; **21**: 237-248 [PMID: 28643146 DOI: 10.1007/s10120-017-0741-6]
161 **Lim JH**, Kim SG, Choi JM, Yang HJ, Kim JS, Jung HC. Helicobacter pylori Is Associated with miR-133a Expression through Promoter Methylation in Gastric Carcinogenesis. *Gut Liver* 2018; **12**: 58-66 [PMID: 28950691 DOI: 10.5009/gnl17263]
162 **Ferrasi AC**, Pinheiro NA, Rabenhorst SH, Caballero OL, Rodrigues MA, de Carvalho F, Leite CV, Ferreira MV, Barros MA, Pardini MI. Helicobacter pylori and EBV in gastric carcinomas: Methylation status and microsatellite instability. *World J Gastroenterol* 2010; **16**: 312-319 [PMID: 20082476 DOI: 10.3748/wjg.v16.i3.312]
163 **Bahnassy AA**, Helal TE, El-Ghazawy IM, Samaan GF, Galal El-Din MM, Abdellateif MS, Desouky E, Zekri AN. The role of E-cadherin and Runx3 in Helicobacter Pylori - Associated gastric carcinoma is achieved through regulating P21waf and P27 expression. *Cancer Genet* 2018; **228-229**: 64-72 [PMID: 30553475 DOI: 10.1016/j.cancergen.2018.08.006]
164 **Nishimura M**, Saito T, Yamasaki H, Kudo R. Suppression of gap junctional intercellular communication via 5' CpG island methylation in promoter region of E-cadherin gene in endometrial cancer cells. *Carcinogenesis* 2003; **24**: 1615-1623 [PMID: 12896902 DOI: 10.1093/carcin/bgg121]
165 **Allagnat F**, Dubuis C, Lambelet M, Le Gal L, Alonso F, Corpataux JM, Déglise S, Haefliger JA. Connexin37 reduces smooth muscle cell proliferation and intimal hyperplasia in a mouse model of carotid artery ligation. *Cardiovasc Res* 2017; **113**: 805-816 [PMID: 28449099 DOI: 10.1093/cvr/cvx079]
166 **Fang JS**, Angelov SN, Simon AM, Burt JM. Cx37 deletion enhances vascular growth and facilitates ischemic limb recovery. *Am J Physiol Heart Circ Physiol* 2011; **301**: H1872-H1881 [PMID: 21856908 DOI: 10.1152/ajpheart.00683.2011]
167 **Jacobsen NL**, Pontifex TK, Li H, Solan JL, Lampe PD, Sorgen PL, Burt JM. Regulation of Cx37 channel and growth-suppressive properties by phosphorylation. *J Cell Sci* 2017; **130**: 3308-3321 [PMID: 28818996 DOI: 10.1242/jcs.202572]
168 **Burt JM**, Nelson TK, Simon AM, Fang JS. Connexin 37 profoundly slows cell cycle progression in rat insulinoma cells. *Am J Physiol Cell Physiol* 2008; **295**: C1103-C1112 [PMID: 18753315 DOI: 10.1152/ajpcell.299.2008]
169 **Morel S**, Burnier L, Roatti A, Chassot A, Roth I, Sutter E, Galan K, Pfenniger A, Chanson M, Kwak BR. Unexpected role for the human Cx37 C1019T polymorphism in tumour cell proliferation. *Carcinogenesis* 2010; **31**: 1922-1931 [PMID: 20705954 DOI: 10.1093/carcin/bgq170]
170 **Guruvaiah P**, Govatati S, Reddy TV, Beeram H, Deenadayal M, Shivaji S, Bhanoori M. Analysis of Connexin37 gene C1019T polymorphism and PCOS susceptibility in South Indian population: Case-control study. *Eur J Obstet Gynecol Reprod Biol* 2016; **196**: 17-20 [PMID: 26656196 DOI: 10.1016/j.ejogrb.2015.11.002]
171 **Tang J**, Li L, Hu LQ, Cai QY, Chen L. Association between 1019C/T polymorphism in the connexin 37 gene and dilated cardiomyopathy. *Minerva Cardioangiol* 2016; **64**: 114-120 [PMID: 25501978]
172 **Zhao L**, Li Y, Wu D, Ma T, Xia SY, Liu Z. Cx37 C1019T polymorphism may contribute to the pathogenesis of coronary heart disease. *Genet Test Mol Biomarkers* 2014; **18**: 497-504 [PMID: 24773516 DOI: 10.1089/gtmb.2014.0034]
173 **Wen D**, Du X, Nie SP, Dong JZ, Ma CS. Association of Connexin37 C1019T with myocardial infarction and coronary artery disease: A meta-analysis. *Exp Gerontol* 2014; **58**: 203-207 [PMID: 24937033 DOI: 10.1016/j.exger.2014.06.011]
174 **Guo S**, Chen W, Yang Y, Yang Z, Cao M. Association between 1019C/T polymorphism in the connexin 37 gene and essential hypertension. *Heart Lung Circ* 2014; **23**: 924-929 [PMID: 24685073 DOI: 10.1016/j.hlc.2014.02.016]
175 **Wu JY**, Lee YC, Graham DY. The eradication of Helicobacter pylori to prevent gastric cancer: A critical appraisal. *Expert Rev Gastroenterol Hepatol* 2019; **13**: 17-24 [PMID: 30791844 DOI: 10.1080/17474124.2019.1542299]
176 **Salar A**. Gastric MALT lymphoma and Helicobacter pylori. *Med Clin (Barc)* 2019; **152**: 65-71 [PMID: 30424932 DOI: 10.1016/j.medcli.2018.09.006]
177 **Akeel M**, Shehata A, Elhafey A, Elmakki E, Aboshouk T, Ageely H, Mahfouz M. Helicobacter pylori vacA, cagA and iceA genotypes in dyspeptic patients from southwestern region, Saudi Arabia: Distribution and association with clinical outcomes and histopathological changes. *BMC Gastroenterol* 2019; **19**: 16 [PMID: 30683054 DOI: 10.1186/s12876-019-0934-z]
178 **Suerbaum S**, Michetti P. Helicobacter pylori infection. *N Engl J Med* 2002; **347**: 1175-1186 [PMID: 12374879 DOI: 10.1056/NEJMra020542]
179 **Byun SW**, Chang YJ, Chung IS, Moss SF, Kim SS. Helicobacter pylori decreases p27 expression through the delta opioid receptor-mediated inhibition of histone acetylation within the p27 promoter. *Cancer Lett* 2012; **326**: 96-104 [PMID: 22867947 DOI: 10.1016/j.canlet.2012.07.032]
180 **Chen B**, Yang L, Chen J, Chen Y, Zhang L, Wang L, Li X, Li Y, Yu H. Inhibition of Connexin43 hemichannels with Gap19 protects cerebral ischemia/reperfusion injury via the JAK2/STAT3 pathway in mice. *Brain Res Bull* 2019; **146**: 124-135 [PMID: 30593877 DOI: 10.1016/j.brainresbull.2018.12.009]
181 **Yeh ES**, Williams CJ, Williams CB, Bonilla IV, Klauber-DeMore N, Phillips SL. Dysregulated connexin 43 in HER2-positive drug resistant breast cancer cells enhances proliferation and migration. *Oncotarget* 2017; **8**: 109358-109369 [PMID: 29312613 DOI: 10.18632/oncotarget.22678]
182 **Arora S**, Heyza JR, Chalfin EC, Ruch RJ, Patrick SM. Gap Junction Intercellular Communication Positively Regulates Cisplatin Toxicity by Inducing DNA Damage through Bystander Signaling. *Cancers*

*(Basel)* 2018; **10**: pii: E368 [PMID: 30279363 DOI: 10.3390/cancers10100368]
183 **Yang Y**, Yao JH, Du QY, Zhou YC, Yao TJ, Wu Q, Liu J, Ou YR. Connexin 32 downregulation is critical for chemoresistance in oxaliplatin-resistant HCC cells associated with EMT. *Cancer Manag Res* 2019; **11**: 5133-5146 [PMID: 31213923 DOI: 10.2147/CMAR.S203656]

World Journal of Gastroenterology

Submit a Manuscript: https://www.f6publishing.com

*World J Gastroenterol* 2019 September 21; 25(35): 5233-5256

DOI: 10.3748/wjg.v25.i35.5233

ISSN 1007-9327 (print) ISSN 2219-2840 (online)

REVIEW

# Colorectal cancer: Parametric evaluation of morphological, functional and molecular tomographic imaging

Pier Paolo Mainenti, Arnaldo Stanzione, Salvatore Guarino, Valeria Romeo, Lorenzo Ugga, Federica Romano, Giovanni Storto, Simone Maurea, Arturo Brunetti

**ORCID number:** Pier Paolo Mainenti (0000-0003-3592-808X); Arnaldo Stanzione (0000-0002-7905-5789); Salvatore Guarino (0000-0003-3978-2567); Valeria Romeo (0000-0002-1603-6396); Lorenzo Ugga (0000-0001-7811-4612); Federica Romano (0000-0003-0685-0201); Giovanni Storto (0000-0002-6168-5598); Simone Maurea (0000-0002-8269-3765); Arturo Brunetti (0000-0001-7057-3494).

**Author contributions:** All authors equally contributed to this paper with conception and design of the study, literature review and analysis, drafting and critical revision and editing, and final approval of the final version.

**Conflict-of-interest statement:** No potential conflicts of interest. No financial support.



**Manuscript source**: Invited manuscript

**Pier Paolo Mainenti,** Institute of Biostructures and Bioimaging of the National Council of Research (CNR), Naples 80145, Italy

**Arnaldo Stanzione, Salvatore Guarino, Valeria Romeo, Lorenzo Ugga, Federica Romano, Simone Maurea, Arturo Brunetti,** University of Naples "Federico II", Department of Advanced Biomedical Sciences, Naples 80131, Italy

**Giovanni Storto,** IRCCS-CROB, Referral Cancer Center of Basilicata, Rionero in Vulture 85028, Italy

**Corresponding author:** Pier Paolo Mainenti, MD, Academic Research, Doctor, Institute of Biostructures and Bioimaging of the National Council of Research (CNR), Naples 80145, Italy. pierpamainenti@hotmail.com
**Telephone:** +39-347-1873089
**Fax:** +39-081-5457081

## Abstract

Colorectal cancer (CRC) represents one of the leading causes of tumor-related deaths worldwide. Among the various tools at physicians' disposal for the diagnostic management of the disease, tomographic imaging (*e.g.*, CT, MRI, and hybrid PET imaging) is considered essential. The qualitative and subjective evaluation of tomographic images is the main approach used to obtain valuable clinical information, although this strategy suffers from both intrinsic and operator-dependent limitations. More recently, advanced imaging techniques have been developed with the aim of overcoming these issues. Such techniques, such as diffusion-weighted MRI and perfusion imaging, were designed for the "*in vivo*" evaluation of specific biological tissue features in order to describe them in terms of quantitative parameters, which could answer questions difficult to address with conventional imaging alone (*e.g.*, questions related to tissue characterization and prognosis). Furthermore, it has been observed that a large amount of numerical and statistical information is buried inside tomographic images, resulting in their invisibility during conventional assessment. This information can be extracted and represented in terms of quantitative parameters through different processes (*e.g.*, texture analysis). Numerous researchers have focused their work on the significance of these quantitative imaging parameters for the management of CRC patients. In this review, we aimed to focus on evidence reported in the academic literature regarding the application of parametric imaging to the diagnosis, staging and prognosis of CRC while discussing future perspectives and present limitations. While the transition from

**Received:** June 18, 2019
**Peer-review started:** June 20, 2019
**First decision:** July 22, 2019
**Revised:** August 6, 2019
**Accepted:** August 24, 2019
**Article in press:** August 24, 2019
**Published online:** September 21, 2019

**P-Reviewer:** Caputo D, Gavriilidis P, Jeong KY, Tchilikidi KY
**S-Editor:** Gong ZM
**L-Editor:** A
**E-Editor:** Ma YJ

purely anatomical to quantitative tomographic imaging appears achievable for CRC diagnostics, some essential milestones, such as scanning and analysis standardization and the definition of robust cut-off values, must be achieved before quantitative tomographic imaging can be incorporated into daily clinical practice.

**Key words:** Colorectal cancer; Computed tomography; Magnetic resonance imaging; Positron emission tomography; Parametric imaging; Perfusion imaging; Diffusion imaging; Texture analysis



**Core tip:** While encouraging progress has been made in the management of colorectal cancer (CRC), it still remains among the malignancies with higher incidence and mortality. Tomographic imaging plays a crucial role in the diagnosis, staging and evaluation of treatment responses in CRC; however, it may also conceal critical information that could guide treatment decisions. The quantitative analysis of computed tomography (CT), magnetic resonance imaging and positron emission tomography/CT images could unveil novel promising biomarkers in the form of numerical parameters. These parameters, if validated in terms of their clinical significance, may contribute to redefining the role of diagnostic imaging and improving CRC management.

**Citation:** Mainenti PP, Stanzione A, Guarino S, Romeo V, Ugga L, Romano F, Storto G, Maurea S, Brunetti A. Colorectal cancer: Parametric evaluation of morphological, functional and molecular tomographic imaging. *World J Gastroenterol* 2019; 25(35): 5233-5256
**URL**: https://www.wjgnet.com/1007-9327/full/v25/i35/5233.htm
**DOI**: https://dx.doi.org/10.3748/wjg.v25.i35.5233

## INTRODUCTION

Colorectal cancer (CRC) is one of the malignancies with the highest incidence in Western countries and is the third most common cancer in both men and women[1]. The TNM staging classification of CRC, based on the depth of tumor invasion (T), lymph node involvement (N) and metastatic spread (M), is strongly associated with the 5-year survival rate[2]. Therefore, the timely identification of CRC represents a critical step to prevent the growth of invasive neoplasms. Similarly, accurate preoperative staging is necessary to differentiate CRCs with a good prognosis from those with a poor prognosis to select the most appropriate treatment and to optimize outcomes.

Currently, various imaging modalities are recommended for the clinical evaluation of patients affected by CRC for diagnosis, characterization (differentiation between mucinous and nonmucinous tumors), staging (depth of tumor spread, extramural vascular invasion, and the presence of malignant lymph nodes and distant metastasis), surgical planning (circumferential resection margin and sphincteric involvement in rectal cancer), the assessment of posttreatment tumor responses and follow-up after therapy[3-5]. Among these, computed tomography (CT), magnetic resonance imaging (MRI) and 18F-fluorodeoxyglucose (18FDG) positron emission tomography (PET) associated with CT (18FDG-PET/CT) or MRI (18FDG-PET/MRI) play a crucial role in the management of CRC. Qualitative evaluation represents the conventional approach to the use of these imaging modalities

The growth of CRC is accompanied by the activation of numerous biological processes, such as neoangiogenesis and anarchic cellular proliferation, and an increase in cellular energy metabolism and glucose consumption. These processes determine neoplastic heterogeneity, which is characterized by a misshapen, irregular and disorganized tissue architecture with areas of high cell density, hypoxia, necrosis, hemorrhage and myxoid changes. Intratumor heterogeneity tends to change over time and to increase as tumors grow, impacting local and distant neoplastic invasion, the delivery of chemotherapeutic agents, cellular resistance to chemotherapy and radiotherapy and, consequently, prognosis[6].

The current state-of-the-art CT, MRI, and hybrid PET scanners offer the possibility to obtain structural, functional and molecular information about these biological

neoplastic processes. Their "*in vivo*" quantitative evaluation can add value to the diagnostic management of CRC in different clinical settings. Parametric analysis (PA) allows the extraction of the numerical data contained in the voxels of each image and information regarding their processing in terms of parametric maps, parameter distributions, and the quantification of spatial complexity and density, signal intensity or activity for CT, MRI or PET, respectively, by using time curves and volumetry[7-9]. PA requires the drawing of a region of interest (ROI) that includes the target tissue for analysis. Depending on the imaging modalities and techniques used, it is possible to obtain different quantitative parameters that are representative of peculiar neoplastic features such as perfusion, structural heterogeneity, cellularity, oxygenation and glucose consumption.

The present review describes the role of imaging PA in patients with CRC by focusing on its technical features, clinical advantages and limitations in advanced quantitative functional and molecular imaging, such as diffusion-weighted MRI (DWI), perfusion imaging (PI), blood oxygenation level-dependent (BOLD) MRI, MR spectroscopy (MRSI) and metabolic imaging as well as advanced quantitative image analysis techniques, such as texture analysis (TA) and volumetry.

## LIMITATIONS OF THE CONVENTIONAL QUALITATIVE ASSESSMENT OF MORPHOLOGICAL IMAGING

The evaluation of images based on morphological features represents the routine clinical approach to CT and MRI. Although this diagnostic approach is recommended in clinical guidelines for the management of CRC, it suffers from several limitations, as shown in Table 1. In particular, the Response Evaluation Criteria in Solid Tumors (RECIST) have been introduced for standardizing the assessment of tumor responses to cytotoxic chemotherapy, and they are mainly based on tumor size measurements[10]. However, it has been observed that RECIST can underestimate both responses to chemotherapy (alone or coupled with antiangiogenic agents) and focal therapies[8,11-13]. Indeed, solid tumors may respond to therapies by developing intratumoral necrotic areas and/or cystic or myxoid degeneration; as a result, the overall size of the neoplasm may be reduced, unchanged or paradoxically increased[12,14,15].

To overcome the above-described limitations, parametric imaging could a useful tool to integrate the information obtained from morphological imaging. PA allows the extraction of numerical data as either quantitative parameters (processed according to a pharmacokinetic model and expressed as an absolute amount with a corresponding unit of measurement) or as semiquantitative parameters (as a ratio of the measured amount and a standard of reference and expressed as pure number). In the following text, for the sake of simplicity, we will use the term quantitative to indicate both quantitative and semiquantitative parameters.

## ADVANCED QUANTITATIVE FUNCTIONAL AND MOLECULAR IMAGING

### *Physiological aspects and technical features*

**DWI with apparent diffusion coefficient maps:** DWI is a functional MR technique that measures the Brownian motion of water molecules in biological tissues, which is restricted by an increase in cellularity and architectural tissue changes[16,17]. Consequently, water diffusion properties are altered in tumors because of the coexistence of dense cellularity, fibrosis, necrosis, neovascularization and hemorrhage. In detail, the increased tissue cellularity observed in the solid part of a tumor reduces the intercellular space and consequently restricts Brownian motion. By using DWI, it is possible to calculate a quantitative measure of water molecule diffusion over time, known as the ADC. The apparent diffusion coefficient (ADC) value is expressed as $10^{-3}$ $mm^2/s$ and can be calculated for each unit volume (voxel) to provide a parametric ADC map. In particular, ADC has been shown to be inversely related to tumor cellularity, and it has been clinically applied to distinguish benign from malignant tumors, to assess tumor grade, to delineate the extent of a tumor, to define the classes of risk that influence the prognosis, and to evaluate and predict tumor treatment responses in CRC patients[18,19] (Figure 1).

**PI based on dynamic contrast enhanced CT or MRI:** Neoangiogenesis, a process induced by the upregulation of vascular growth factors, is a well-known critical aspect of CRC that leads to the development of a new, altered and immature microcirculatory network inside the tumor[20-22]. In particular, neoangiogenesis

**Table 1 Current limitations of qualitative imaging based on morphological features used for the assessment of colorectal cancer**

| Diagnostic task | Limits of qualitative imaging |
|---|---|
| Primary tumor identification | Early stages of CRC hard to detect |
| | Neoplastic and inflammatory tissue not easily differentiable |
| Lymph node involvement | Lymph node size criteria often misleading and insufficient |
| | Shape, border irregularity and structural heterogeneity hard to assess for small lymph nodes |
| Prediction of early responses to chemotherapy and radiation therapy | Not possible with qualitative evaluation alone |
| Evaluation of treatment responses and the detection of recurrent disease | Differentiation of residual or recurrent neoplastic tissue from posttreatment induced fibrosis or necrosis is often challenging |

CRC: Colorectal cancer.

promotes an irregular architectural vascular pattern[23] with areas of low vascular density and regions of high angiogenic activity. Consequently, neoangiogenesis causes structural heterogeneity due to the coexistence of areas of high cell density, necrosis, hemorrhage and myxoid changes within tumoral tissue[24].

The above-described phenomena can be investigated using a functional modality such as PI based on dynamic contrast enhanced (DCE). DCE imaging consists of the acquisition of baseline images before intravenous contrast agent injection, followed by subsequent image acquisition over time[25]. PI is an advanced DCE quantitative technique based on the repeated high frequency acquisition of images, which allows the assessment of changes in signal intensity over time. It can be performed with both CT and MRI scanners. PI allows the assessment of vascularity in biological tissues in terms of tumor vessel features (perfusion, permeability, and density), extracellular-extravascular space composition and plasma volume[25]. In the following text, we will use the terms DCE and PI interchangeably. A broad spectrum of quantitative parameters can be obtained using PI to assess the vascular properties of pathological tissues[22] (Figure 2). A summary of the main PI quantitative parameters used in the assessment of CRC is shown in Table 2[26,27]. There is a growing interest in the role of PI in clinical practice for tumor detection and characterization and the assessment of responses to therapy (especially with respect to antiangiogenic treatment strategies) and prognosis.

**Hybrid Imaging:** 18FDG-PET/CT and 18FDG-PET/MRI are molecular and morphological imaging techniques that couple the metabolic and anatomical assessment of tumor lesions[28]. 18F-FDG is an analog of glucose that is transported into cells through membrane glucose transporter proteins after intravenous administration[29]. Since malignant cells have increased glucose consumption (Figure 3), a preferential accumulation of 18F-FDG occurs in cancer cells compared to normal cells[30]. The uptake of 18F-FDG detected by PET can be quantified using parameters such as the standardized maximum or mean uptake value (SUVmax or SUVmean), the metabolic tumor volume (MTV) or the total lesion glycolysis (TLG). The SUVmax is defined as the uptake value of the pixel with the highest activity inside an ROI divided by the injected dose (which has to be corrected for decay and normalized for the patient's weight or body surface). The SUVmean is the average of all the uptake values of the pixels within an ROI. The MTV is defined as the volume of tumor tissues with pathological FDG uptake and calculated as follows: All the voxels inside a tridimensional ROI with SUV values above a determined threshold are included in the final volume; the threshold may be represented by the absolute value (≥ 2.5 or ≥ 3 or ≥ 3.5) or the percentage (≥ 20% or ≥ 30% or ≥ 40% or ≥ 50%) of the SUVmax. As a result, the MTV incorporates the characteristics of both the volumetric data and the metabolic activity of the tumor. Finally, the TLG is calculated according to the following formula: SUVmean × MTV. 18FDG-PET/CT has played a role in clinical practice in the detection of extrahepatic distant metastasis, the evaluation of tumor responses to therapy and the follow-up of treated patients with rising serum carcinoembryonic antigen levels without detectable disease according to morphological imaging.

While the potential use of non-FDG PET radiotracers in CRC imaging is a current topic of investigation, we refrained from discussing this matter in the present review due to the dearth of clinically oriented evidence available in the current literature.

### *Primary tumor identification, tumor grading and differentiation, and local staging*

While endoscopy is considered the main diagnostic tool for the detection of CRC,

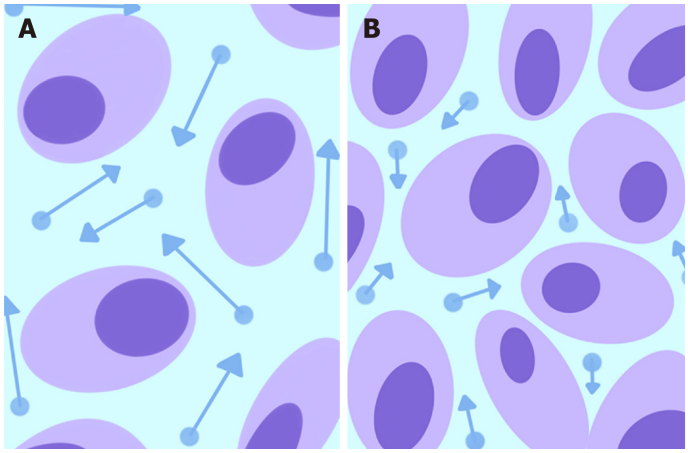


**Figure 1 Schematic representation of water molecule diffusion (dots) in the extracellular space.** Normal tissues (A) show a relatively larger extracellular space with high water diffusion (longer arrow vectors higher ADC values), whereas the increased tissue cellularity in a neoplasm (B) reduces the intercellular space and consequently restricts diffusion (shorter arrow vectors lower ADC values).

imaging has the potential to identify primary tumors. Nevertheless, both malignant and benign abnormalities (*e.g.*, inflammatory bowel disease, complicated diverticulitis, and hyperplasic polyps and adenomas) can present with an increase in bowel wall thickness or as polypoid lesions. When using conventional imaging, differential diagnosis is mainly based on morphological features (*e.g.*, lesion size and longitudinal extension, the evaluation of the transitional zone between pathological and healthy mucosa, the presence of focal or multifocal intestinal involvement, the preservation of mural stratification, and the pattern of mesenteric and lymph node involvement). Although all these characteristics contribute the most to the determination of the correct diagnosis, parametric imaging could increase the overall diagnostic accuracy; moreover, it may be useful for the tumor grading and differentiation and local staging.

**DWI with ADC maps:** ADC values have been investigated as possible quantitative parameters that are useful for differential diagnosis. Kilickesmez *et al*[31] reported that mean ADC values may be used to differentiate recto-sigmoid malignancy from both normal rectum and inflammatory bowel disease-affected tissues. The mean ADC value ($0.97 \times 10^{-3}$ mm$^2$/s) of the recto-sigmoid tumor group was significantly different from those of the healthy control ($1.47 \times 10^{-3}$ mm$^2$/s) and inflammatory bowel disease groups ($1.37 \times 10^{-3}$ mm$^2$/s). A recent metanalysis[32] reported that the ADC values of CRC malignant lesions ranged from $0.97 \times 10^{-3}$ mm$^2$/s to $1.19 \times 10^{-3}$ mm$^2$/s, while those of benign lesions ranged from $1.37 \times 10^{-3}$ mm$^2$/s to $2.69 \times 10^{-3}$ mm$^2$/s.

The ADC value might serve as a potential noninvasive biomarker of CRC tumor aggressiveness. Indeed, Curvo-Semedo *et al*[33] reported significantly lower ADCmean values in poorly differentiated versus well-differentiated RC, as well as in a T3-T4 stage group versus a T1-T2 stage group. Additionally, Tong *et al*[34] showed a negative correlation between ADC values and extramural maximal depth in RC.

**PI:** Quantitative perfusion parameters have been reported as feasible tools that could be used to discriminate between CRC and noncancerous diseases. Goh *et al*[35] reported that the blood volume (BV), blood flow (BF), mean transit time (MTT), and permeability-surface area product (PS) determined based on perfusion CT were significantly different between patients with CRC and diverticulitis. In particular, the CRC group showed significantly higher BV, BF and PS and a shorter MTT compared to the diverticulitis group. These findings are correlated with neoangiogenesis processes associated with CRC growth. Similarly, Shen *et al*[36] showed that transfer constant (Ktrans) values obtained from perfusion MRI were significantly higher in rectal cancer (RC) compared to those in benign abnormalities (0.267 min$^{-1}$ ± 0.07 *vs* 0.118 min$^{-1}$ ± 0.03), indicating that significant angiogenesis and abnormal vasculature enhanced the influx of the contrast agent. Using a 0.156 min$^{-1}$ cut-off value for Ktrans, a sensitivity of 100.0% and a specificity of 93.3% were observed when discriminating RC patients from controls.

Sun *et al*[37] reported that the mean BF and BV obtained from perfusion CT were significantly different among well, moderately, and poorly differentiated tumors (61.17 ± 17.97, 34.8 ± 13.06 and 22.24 ± 9.31 mL/min/100 g, respectively). The same

**Table 2 Main quantitative parameters extracted from perfusion imaging of colorectal cancer**

| Parameter name | Parameter definition | Parameter significance |
|---|---|---|
| Regional blood flow | Blood flow per unit volume or mass of tissue, expressed in mL of blood/min/100 mL tissue | It reflects the rate of the delivery of oxygen and nutrients to a certain tissue |
| Regional blood volume | Volume of capillary blood contained in a certain volume of tissue, expressed in mL blood/100 mL of tissue | It reflects the functional vascular volume |
| Mean transit time | Mean time needed for blood to pass through the capillary network, expressed in seconds | It reflects the time required for the contrast agent bolus to pass through tissue |
| Permeability-surface area product (PS) | Flow of molecules through the capillary membranes in a certain volume of tissue, expressed in mL/min/100 mL tissue | It reflects the vascular leakage rate in the microcirculation |
| Transfer constant (KTrans) | Rate at which the contrast agent transfers from the blood to the interstitium (rate of contrast extraction) | It reflects the balance between capillary permeability and blood flow in a tissue |
| Tissue interstitial volume (Ve) | Volume of extravascular and extracellular contrast agent in a certain tissue, expressed as a percentage | It is a measure of cell density |
| Rate constant (Kep) | Rate at which the contrast agent returns from the extravascular-extracellular space to the vascular compartment: Kep = Ktrans/Ve | It reflects the tissue microcirculation and contrast agent permeability |

working group confirmed these findings, providing further evidence that BF, when determined using perfusion CT images, is associated with tumor grade[38].

**Hybrid imaging:** Due to its utilization of a combination of morphological and molecular information, 18FDG-PET/CT has a high sensitivity for the detection of colorectal lesions. However, unlike determinations based on metabolic information, there is no established consensus regarding the discrimination of benign lesions from premalignant or malignant lesions based on visual appearance alone. A quantitative approach to focal colorectal uptake has been investigated. A few studies have observed that PET quantitative parameters could help to differentiate benign from premalignant or malignant lesions[39], while there have been other studies that have found the opposite[40,41]. Moreover, a quantitative approach may be useful for local staging. Liao *et al*[42] reported that quantitative parameters such as MTV calculated with a 2.5 threshold aided in discriminating the pT1-T2 group from the pT3-T4 group in patients with RC. The MTV2.5 values for the pT1-T2 and pT3-T4 patient groups were 11.6 ± 11.4 and 34.6 ± 21.4, respectively. Using the median value of 28 mL as a cut-off, MTV2.5 provided excellent specificity (92.8%) and a positive predictive value (97.1%) for the T3-T4 group, helping to identify patients who would benefit from preoperative chemoradiation therapy (CRT).

### *Lymph node involvement*

Nodal involvement has an important role in the stratification of risk for CRC patients, and an accurate assessment of this parameter could significantly influence therapeutic management and prognosis. Morphological criteria (size, margins, structural disomogeneity, and clustering) have been used for the detection of pathological lymph node involvement[43-47]; however, this approach is still highly debated.

**DWI with ADC maps:** Quantitative ADC values extracted from DWI have been proposed as tools to differentiate between benign and malignant lymph nodes; however, their role remains unclear in this setting. Heijnen *et al*[48] reported that DWI can facilitate lymph node detection during the primary staging of RC, but although the ADCmean value was higher for benign nodes compared to malignant nodes (1.15 × $10^{-3}$ $mm^2/s$ *vs* 1.04 × $10^{-3}$ $mm^2/s$), the difference was not statistically significant. Lambregts *et al*[49] assessed the performance of ADC measurements for nodal restaging in patients with RC undergoing preoperative CRT. The authors reported that the ADCmean value of malignant lymph nodes after CRT was significantly higher compared to that of benign lymph nodes (1.43 × $10^{-3}$ $mm^2/s$ ± 0.38 *vs* 1.19 × $10^{-3}$ $mm^2/s$ ± 0.27)[49]. This finding was attributed to the induction of posttreatment necrosis, which increases the diffusivity and consequently the ADC value. However, the overlapping of ADC values between benign and malignant nodes resulted in insufficient accuracy when ADC values were used alone for the detection of nodal metastases after CRT.

**PI:** PA of PI could further increase the diagnostic accuracy of conventional imaging

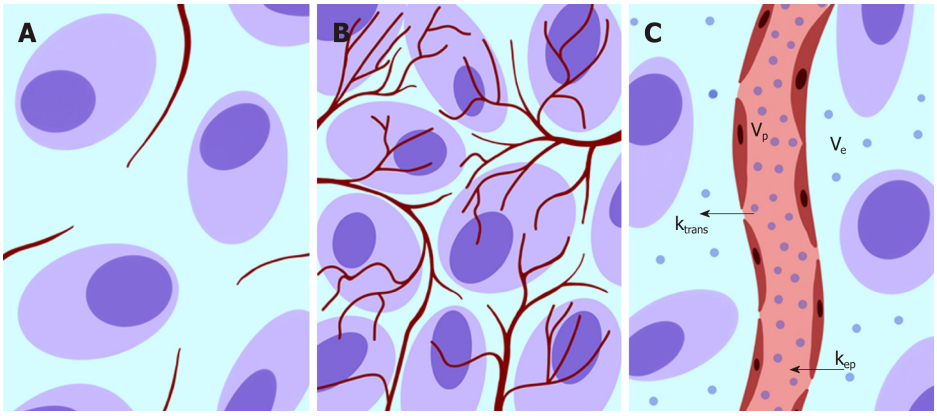


**Figure 2 Schematic representation showing vascularization changes in normal tissue (A) and neoplastic neoangiogenesis (B).** In C, a typical bicompartmental model (extended Toft's model) is depicted with various parameters that can be assessed according to the tissue contrast agent concentration (dots) and the arterial input function data.

for nodal involvement evaluation in RC patients[50-54]. Ambruster *et al*[50] have reported that DCE-MRI quantitative maps increase both the sensitivity (86% *vs* 71%) and specificity (90% *vs* 70%) of conventional MRI for the detection of malignant lymph nodes in locally advanced RC (LARC). Grovik *et al*[51] and Yeo *et al*[52] found that Ktrans values obtained for primary tumors with perfusion MRI were strongly correlated with nodal status in surgical specimens. Yu *et al*[55] reported that metastatic lymph nodes from RC showed significantly higher Ktrans values and tissue interstitial volume (Ve) compared with nonmetastatic lymph nodes during perfusion MRI of lymph nodes with short axis diameters > 5 mm (Ktrans: 0.484 $min^{-1}$ ± 0.198 *vs* 0.218 $min^{-1}$ ± 0.116; Ve: 0.399 ± 0.118 *vs* 0.203 ± 0.096). Conversely, Yang *et al*[54] demonstrated that the Ktrans values were significantly lower in metastatic lymph nodes from RC during perfusion MRI of lymph nodes with short axis diameters < 5 mm. However, when using a Ktrans cut-off value of 0.088 $min^{-1}$ to differentiate between positive and negative lymph nodes, a sensitivity of 60.5% and a specificity of 81.5% were observed.

**Hybrid imaging:** Qualitative evaluation with 18FDG-PET/CT for the assessment of nodal involvement has limited advantages compared to evaluation with CT[56,57], but a quantitative approach might be utilized to overcome this limitation. Tsunoda *et al*[58] compared the diagnostic accuracy of visual analysis and SUVmax evaluation for lymph node metastases using 18FDG-PET/CT in patients with CRC. The sensitivity, specificity and accuracy were 28.6%, 92.9% and 75.0%, respectively, when using a visual approach, while they were 53.1%, 90.6% and 80.1%, respectively, when using a SUVmax cut-off value of 1.5. The mean SUVmax of the malignant lymph nodes (6.3; range: 1.0-33.8) was significantly higher than that of the benign lymph nodes (2.5; range: 1.3-3.3). Similarly, Yu *et al*[59] observed that a quantitative approach based on the use of SUVmax might improve the detection of regional lymph node metastasis when using 18FDG-PET/CT in patients with CRC. A significant difference in SUVmax between metastatic and benign juxtaintestinal lymph nodes was observed. When using a cut-off value for SUVmax of 2.0, the corresponding sensitivity, specificity, PPV and NPV were 91.4%, 87.8%, 69.6% and 97.1%, respectively.

### *Response to treatment: efficacy prediction and the assessment of neoadjuvant CRT in RC*

CRT has become the standard of care for LARC. This treatment is associated with fewer local recurrences and may also result in improved long-term survival. The preoperative noninvasive assessment of CRT response in LARC is crucial for planning the surgical approach. MRI is largely used for the local restaging of LARC after neoadjuvant CRT; however, conventional morphological sequences have intrinsic limitations when used for the differentiation of residual viable tumors from surrounding fibrosis[60,61]. The overall accuracy of local neoplastic restaging using only morphological T2-weighted (T2w) sequences after CRT is reported to be 47-52%[61,62]. CRT induces the necrosis of neoplastic tissue as well as reductions in cellular density and metabolism, increases in the extracellular space and the suppression of neoangiogenesis (Figure 4); these phenomena can be investigated *via* PA of tomographic images.

**DWI with ADC maps:** Several studies[49,63-65] have shown the usefulness of ADC values for the assessment of tumor responses to preoperative CRT, suggesting that the

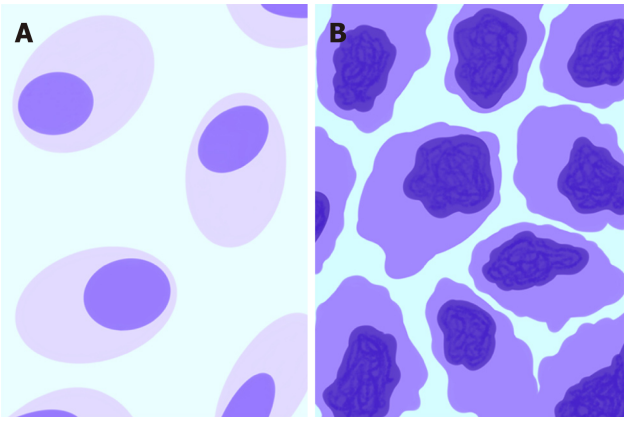


**Figure 3 Schematic representation of morphological and metabolic features of normal tissue (A) compared with those of neoplastic malignant cells (B).** The darker shade of violet represents the higher glucose consumption typical of malignant cells.

increase of ADC values after CRT is associated with a good response to preoperative CRT. The absence of ADC value changes during CRT could be used to identify nonresponding patients[66]. The increase in ADC in neoadjuvant CRT responders may be due to cell death, cellular membrane disruption and decreased cellularity, which contribute to increased water diffusion. Regarding the assessment of post-CRT residual tumors in LARC, Song *et al*[67] reported that the mean ADC after CRT of viable tumors ($0.93 \times 10^{-3}$ mm$^2$/s) differed significantly from that of nonviable tumors ($1.55 \times 10^{-3}$ mm$^2$/s). Moreover, when an ADC value of $1.045 \times 10^{-3}$ mm$^2$/s was used as a cut-off value for distinguishing between viable and nonviable tumors, false positive findings were not observed, resulting in a specificity and positive predictive value of 100%. In the same clinical setting, Grosu *et al*[68] reported that the ADCmean after CRT of viable tumors ($1.02 \times 10^{-3}$ mm$^2$/s) differed significantly from that of scar tissue ($1.77 \times 10^{-3}$ mm$^2$/s). An ADC cut-off value of $1.34 \times 10^{-3}$ mm$^2$/s resulted in a sensitivity, specificity, and accuracy of 93%, 91%, and 92%, respectively. Bassaneze *et al*[69] reported that patients with pathological complete responses (pCRs) to neoadjuvant treatment differed significantly from those with non-pCRs in terms of the absolute value of the post-CRT ADC. The mean post-CRT ADC value was $1.53 \times 10^{-3}$ mm$^2$/s in the pCR patient group and $1.16 \times 10^{-3}$ mm$^2$/s in the non-pCR patient group. All patients with residual tumors in the surgical specimen showed ADC values that were below the cut-off of $1.49 \times 10^{-3}$ mm$^2$/s.

However, conflicting results have been reported regarding the value of pretreatment tumor ADC values for the prediction of CRT response in patients with LARC when using surgical specimens as the standard of reference. Some authors observed significantly lower pretreatment ADC values in good responders compared to nonresponders[70,71]. Conversely, others reported that the pretreatment ADC values were not significantly different between responders and nonresponders[72].

**PI:** Perfusion CT quantitative parameters have been evaluated for the prediction and assessment of the response of LARC to neoadjuvant CRT. Bellomi *et al*[73] reported that the baseline BF and BV were significantly higher and the MTT was significantly lower in responders compared to nonresponders. Conversely, Sahani *et al*[74] and Curvo-Semedo *et al*[75] reported that the baseline BF was significantly higher and the MTT was significantly lower in non-responders compared to responders. Additionally, both groups[73,75] reported a reduction in BF, BV and PS and an increase in MTT after CRT. These perfusion changes are thought to be due to CRT-related fibrosis, which causes the compression of tumor capillaries, a decreased number of arteriovenous shunts, an increased resistance to flow and a reduced volume in the vascular bed[76]. A reduction of 40% or more in BF, BV and permeability was observed in patients with RC who responded to neoadjuvant therapy[22,77].

A few studies have evaluated the usefulness of perfusion MRI quantitative parameters for predicting and assessing responses to preoperative treatment in LARC. Lim *et al*[78] reported that pre-CRT Ktrans values were significantly higher in the downstaged group after CRT than in the non-downstaged group. Tong *et al*[79] reported that patients with pCR had significantly higher Ktrans, Ve and rate constant (Kep) values before CRT than non-pCR patients. In particular, a Ktrans threshold of 0.66 had a sensitivity of 100% for predicting pCR. Gollub *et al*[80] observed that Ktrans was significantly lower for tumors from patients with pCR compared with patients

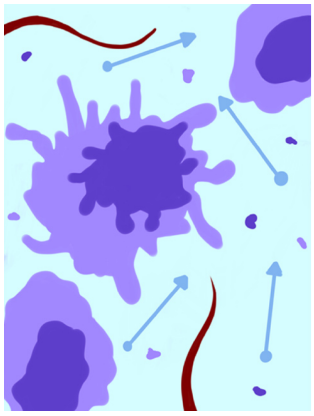

**Figure 4 Schematic representation of neoplastic tissue after treatment.** Cytolysis increases the extracellular space and consequently water diffusion and reduces lesion vascularization and metabolism.

with non-pCR after neoadjuvant chemotherapy; moreover, the posttreatment Ktrans value was correlated with the percentage tumor response and final tumor size according to histopathology. Kim *et al*[64] showed a significant reduction in the Ktrans values in the downstaged group after CRT compared to that in the nondownstaged group. Furthermore, the percentage difference between the pre- and post-CRT Ktrans values in the downstaged group was significantly higher compared to that in the nondownstaged group, suggesting that a large decrease in the Ktrans value after CRT was associated with a good response to CRT. DeVries *et al*[72] investigated the prognostic value of the perfusion index, which is a microcirculatory perfusion MRI parameter representative of both flow and permeability. The perfusion index was significantly increased in patients who failed to respond to CRT.

A final remark should be made regarding the role of PI in the evaluation of the response to antiangiogenic agents. Bevacizumab is an antiangiogenic monoclonal antibody that targets vascular endothelial growth factor (VEGF). This kind of therapeutic agent often suppresses tumor growth in the absence of notable morphological changes and requires a direct "*in vivo*" evaluation of vascularity to reveal therapeutic results. Willett *et al*[81] showed a reduction in BF, BV and PS *via* perfusion CT 12 days after beginning treatment with bevacizumab alone in LARC patients.

In summary, high baseline values and marked post-CRT decreases in perfusion parameters (BF, BV and Ktrans) are predominantly reported in patients with good response. This observation suggests that highly perfused tumors may provide better access for chemotherapy, better oxygenation and higher radiosensitivity compared with poorly perfused tumors. Conversely, the following two neoplastic features may explain a high baseline perfusion parameter in patients who fail to respond to neoadjuvant CRT: (1) The presence of arteriovenous shunts, which is accompanied by a high perfusion rate but a low exchange of nutrients/chemotherapy; and (2) Tissue hypoxia, which induces a high perfusion rate.

**Hybrid imaging:** Several studies have investigated the role of 18FDG-PET/CT in the evaluation of responses to CRT in LARC patients. Lambrecht *et al*[70] observed that changes in SUVmax during (after 10-12 fractions) and 5 wk after CRT with respect to the SUVmax value prior to the beginning of CRT (ΔSUVmax) were significantly correlated with the pathological response to treatment. Janssen *et al*[82] reported that a cut-off value representing a 48% reduction in SUVmax after 2 wk of CRT in patients with LARC resulted in a specificity of 100% and a sensitivity of 64% when differentiating pathological responders from nonresponders. Maffione *et al*[83] performed a systemic review of the early prediction of responses by 18FDG-PET/CT during neoadjuvant CRT in LARC. The percentage decrease in SUVmax showed a high accuracy (mean sensitivity 82%; pooled sensitivity 85%) in terms of the early prediction response when using a mean cut-off of 42%. As a result, the early assessment of nonresponding patients allows the modification of the treatment strategy, especially in terms of timing and the type of surgical approach used. It should be noted that radiation-induced inflammation could cause increased 18FDG uptake, possibly reducing PET specificity[82,84-87]. To overcome this limitation, the use of dual-time 18F-FDG PET has been proposed. This requires two PET scans; the first is conducted 40-60 min after the injection of 18F-FDG (standard time), and the second is conducted 90-270 min after injection (delayed time), thus allowing the evaluation of

18FDG uptake over time. While 18FDG uptake due to inflammation appears to be stable or to decrease over time, neoplastic 18FDG uptake tends to increase[88]. Yoon *et al*[89] compared the accuracy of pre-CRT standard and post-CRT dual-time 18FDG-PET/CT in the prediction of CRT responses in LARC patients. The quantitative dual-time score (defined as the delay index [DI], which is equal to post-SUVmax-early – post-SUVmax-delayed/post-SUVmax-delayed of post-CRT 18FDG-PET/CT) showed significantly better performance with a higher area under the curve value (0.906 *vs* 0.696, $P$ = 0.018) than the standard quantitative score (defined as the response index [RI], which is equal to pre-SUVmax – post-SUVmax/ pre-SUVmax). The DI showed a sensitivity of 86.7%, a specificity of 87%, a PPV of 68.4% and a PNV of 95.2%, suggesting that dual-time post-CRT PET/CT might be the most appropriate diagnostic tool for this specific setting.

### *Responses to treatment: colorectal liver metastases*

Surgical resection remains the only treatment with curative potential for colorectal liver metastases (CRLMs)[89]. In patients who are not suitable candidates for surgery, chemotherapy alone or in combination with local hepatic treatments, such as intrahepatic arterial infusion chemotherapy, transcatheter arterial chemo-embolization (TACE), selective internal radiation therapy (SIRTI), radiofrequency ablation (RFA), laser therapy or cryotherapy, may be performed[90]. Tomographic imaging based on conventional qualitative evaluation contributes mostly to defining the appropriate therapeutic management of CRLMs[91,92]; however, defining tumor biology could allow the improved selection of treatment strategies and, as a result, the more accurate prognostic evaluation of patients[90]. In this setting, PA could provide potentially useful imaging markers for the prediction of treatment response.

**DWI with ADC maps:** ADC values have been proposed for use in assessing the responses of CRLMs to chemotherapy[93,94]. Koh *et al*[93] reported that high mean pretreatment ADC values for CRLMs were associated with poorer responses to chemotherapy (nonresponder: $1.55 \times 10^{-3}$ mm$^2$/s; responder $1.36 \times 10^{-3}$ mm$^2$/s). Indeed, high ADC values are observed in necrotic areas, which typically show poor perfusion and allow only limited local delivery of chemotherapeutic drugs. Cui *et al*[94] found that CRLMs showed significantly decreased mean pretreatment ADC values in responding lesions ($0.95 \times 10^{-3}$ mm$^2$/s ± 0.15) than in nonresponding lesions ($1.18 \times 10^{-3}$ mm$^2$/s ± 0.27). Furthermore, an early increase in ADC values was observed in responding lesions after 3 or 7 d of treatment.

**PI:** Few studies have been performed to assess the utility of quantitative PI parameters as biomarkers for the assessment of CRLM responses to treatment. Using baseline perfusion MRI and follow-up MRI evaluated on the basis of RECIST 1.1 criteria in patients with CRLMs treated with a combination of chemotherapy and bevacizumab, Coenegrachts *et al*[95] found significantly higher Kep values in responders than in nonresponders (responders: 0.09852; nonresponders: 0.07829). Moreover, the Kep values were significantly decreased in responding patients compared to nonresponding patients after 6, 12 and 18 weeks of treatment, suggesting that Kep values may be able to predict early treatment response in CLRMs.

**Hybrid imaging:** Few studies have investigated the possible role of quantitative parameters derived from18FDG-PET/CT in the assessment of CLRM treatment responses. Recently, Nishioka *et al*[96] observed that an SUVmean value cut-off of 3 and morphological CT criteria[10] had similar excellent predictive power for ≤ 10% tumor viability (areas under the curve of 0.916 and 0.882, respectively) compared to that for the degree of tumor shrinkage (area under the curve of 0.69) in patients who underwent PET/CT after chemotherapy and before the surgical resection of CRLMs.

### *CRC prognosis*

Tumor stage at diagnosis is considered the most important prognostic factor for CRC patients[97]. However, other prognostic factors that include biological and molecular information should be taken into account to personalize prognosis[98]. Parameters such as tumor differentiation grade and the presence of lymphangiovascular invasion (LVI)[99] are valuable in the prognostic evaluation of RC patients. Similarly, the plasmatic levels of carcinoembryonic antigen (CEA)[100] are useful for the prognostic assessment of CRLMs.

As a result, detailed information regarding the individual tumor profile of each patient is critical to determine the risk for local and distant recurrence[101]. Measures such as overall survival (OS), progression-free survival (PFS) or recurrence-free survival (RFS) are commonly used for prognostic evaluation. PA has the potential to introduce novel useful biomarkers that could correlate to the biological and genetic prognostic features of CRC and CRLMs or predict OS, PFS and/or RFS.

Consequently, such parameters could be useful in CRC risk stratification and in treatment planning.

**DWI with ADC maps:** The quantitative evaluation of ADC maps derived from DWI could aid in the prediction of patient prognosis[16,18,70]. Curvo-Semedo *et al*[33] reported that ADC values differed significantly between RC tumors with and without mesorectal fascia (MRF) invasion, between N0 and N+ cancers and even among different histological grades. In particular, decreased mean pretreatment ADC values were observed in tumors with MRF involvement, metastatic lymph nodes or poorly differentiated grading. Sun *et al*[102] reported that decreased ADC values were strongly associated with increased T stage and a more aggressive tumor profile. Tong *et al*[34] observed that the extramural maximal depth and the ADC value have a significant negative correlation in the T3 RC spread. Heijmen *et al*[103] reported that low prechemotherapy ADC values in CRLMs predicted poorer outcomes in terms of both PFS and OS.

**PI:** Goh *et al*[104] reported that CRC with low BF at staging according to perfusion CT showed an increased tendency to metastasize and resulted in significantly decreased OS. Particularly, a group of patients who had developed metastatic disease prior to follow up presented a mean baseline BF value of 45.7, while the mean BF value of the disease-free group was 76 mL/min/100 g. Similarly, Hayano *et al*[76] reported that patients with RC with increased BF according to perfusion CT survived significantly longer than those with decreased BF. More recently, two studies reported that Ktrans measured *via* DCE-MRI is correlated with the pathological differentiation of RC; poorly differentiated tumors showed increased Ktrans values[36,105]. Moreover, Ktrans values were significantly higher in lesions with distant metastasis than in lesions without distant metastasis and in the pLVI positive group than in the pLVI negative[105] group.

Finally, perfusion MRI studies conducted on patients with CRLMs treated with bevacizumab are worth mentioning[106-108]. Indeed, Hirashima *et al*[106] observed a significant correlation between a reduction in the Ktrans value 7 days after the start of treatment and a longer time to progression. Subsequently, Kim *et al*[107] confirmed this finding and found that a reduction of 40% in the Ktrans cut-off value could be used to discriminate responders from nonresponders. De Bruyne *et al*[108] found that a decrease in Ktrans of more than 40% after bevacizumab chemotherapy in patients with CRLMs was associated with improved PFS.

**Hybrid imaging:** Avallone *et al*[109] evaluated the prognostic role of early metabolic responses to CRT in patients with LARC. In their study, 18FDG-PET scans were performed before and 12 days after the beginning of CRT. Responders, defined on the basis of a reduction in the SUV mean value ≥ 52% compared to the baseline, showed a 5-year RFS that was significantly higher than that of nonresponders.

Muralidharan *et al*[110] reported that high MTV and TLG values for CRLMs before surgical resection were significantly associated with poorer recurrence-free survival (RFS) and OS, while the SUVmax and SUVmean did not show any significant predictive ability. Lastoria *et al*[111] performed a 18FDG-PET/CT evaluation before and after 1 cycle of FOLFIRI plus bevacizumab treatment in patients with resectable CRLMs. Pathological responses were assessed in patients undergoing resection. For each lesion, a ≤ -50% change in the SUVmax and the TLG compared to baseline was used as a threshold to indicate a significant metabolic response. An early metabolic PET/CT response had a stronger and more independent and statistically significant predictive value for PFS and OS compared to both CT/RECIST and pathological response according to multivariate analysis. Similarly, Lau *et al*[112] investigated the prognostic value of 18FDG-PET/CT before and after preoperative chemotherapy in patients undergoing the liver resection of CRLMs. SUVmax, MTV, and TGV, their changes (DSUVmax, DMTV, DTGV) and their correlation with RFS and OS were evaluated. DSUVmax was the only parameter predictive of RFS and OS according to multivariate analysis. Patients with metabolically responsive tumors had an OS of 86% at 3 years vs 38% for patients with nonresponding lesions. Gulec *et al*[113] investigated the relationship between MTV and TLG and clinical outcomes in patients with unresectable CRLMs undergoing treatment with 90Y resin microspheres. The authors observed that MTV values below 200 cc during pretreatment PET/TC and below 30 cc during posttreatment PET/CT at 4 wk were significantly associated with a longer median survival compared to MTV values above 200 during the pretreatment exam and 30 cc during the posttreatment exam at 4 wk. Similar results were found for TLG values below and above 600 g during the pretreatment exam and below and above 100 g during the posttreatment exam, respectively.

Giacomobono *et al*[114] evaluated the value of SUVmax for stratifying CRC patients

with unexplained CEA increases and FDG uptake at the site of anastomosis after surgical curative resection. Nonspecific FDG uptake at the anastomotic site was the most frequent cause of error because it could be due to both post-CRT/postsurgical fibrosis/scar tissue and disease recurrence. The anastomotic SUVmax was the only significant predictor of tumor recurrence at the site of anastomosis. A decreased OS was reported in patients with a SUVmax greater than 5.7 compared with that in patients with lower values (median survival: 16 mo *vs* 31 mo; $P = 0.002$). Marcus *et al*[115] showed that a decreased MTVtotal and TLGtotal were associated with increased OS in patients with local, loco-regional and/or distant-recurrent biopsy-verified CRC.

## OTHER ADVANCED QUANTITATIVE FUNCTIONAL AND MOLECULAR IMAGING MODALITIES

Blood oxygenation level-dependent (BOLD) MRI and MR spectroscopy (MRSI) represent further advanced imaging modalities available for use with quantitative PA in CRC.

BOLD-MRI is able to assess *in vivo* tissue hypoxia according to blood flow and the paramagnetic properties of deoxyhemoglobin within red blood cells[116]. Endogenous deoxyhemoglobin decreases the transverse relaxation rate (T2*) in blood, which can be quantified by R2* (= 1/T2*)[117,118]. Tumor hypoxia is caused by the inability of the neoplastic vascular system to provide an adequate supply of oxygen to the growing tumor mass. Tumor hypoxia induces the expression of the transcription factor hypoxia inducible factor-1 alpha (HIF-1α), which promotes the adaptation of cancer cells to hypoxia and the development of more aggressive clones less sensitive to radiotherapy and chemotherapy[119] and impacts metastatic spread to favor tumor recurrence and a poor prognosis. Heijmen *et al*[103] investigated the ability of BOLD-MRI to predict outcomes and responses to systemic treatment in patients with CRLMs undergoing MRI before and one week after the beginning of first-line chemotherapy. The authors reported that a low pretreatment T2* value in CRLMs (indicating a higher concentration of deoxyhemoglobin) was a significant predictor for increased OS; however, the T2* value did not significantly change one week after the beginning of treatment, which did not make it a useful predictor of the response to therapy.

MRSI is a noninvasive technique that allows the measurement of metabolites and metabolic processes in normal and pathological tissues[120]. The resonance frequencies of the metabolites are expressed in parts per million (ppm). Tumor tissues are characterized by disordered energy metabolism (an increased lactate concentration due to anaerobic glycolysis and the activation of the creatine/phosphocreatine system), amino acid metabolism (the accumulation of amino acids due to the increased turnover of structural proteins) and choline metabolism (increased levels of choline, which is a marker of cellular membrane turnover related to cell proliferation)[121]. Dzik-Jurasz *et al*[122] demonstrated the presence of choline and lipid peaks in patients with RC. Kim *et al*[120] reported that a choline peak at 3.2 ppm in patients with RC disappeared after radiation therapy and chemotherapy.

Both of these modalities suffer from limited clinical applicability due to their high intrinsic technical complexity; furthermore, there are still insufficient evidence in the literature to define their possible role in CRC clinical management.

## QUANTITATIVE IMAGE ANALYSIS METHODS

### *Texture analysis*

**Physiological aspects and technical features:** As previously stated, tumor heterogeneity is a hallmark of malignancy that is highly related to tumor biology[24,123], and it can be qualitatively and/or quantitatively evaluated by several imaging modalities. TA is a postprocessing imaging technique that allows heterogeneity quantification to evaluate both the distribution and relationships within the information contained in each voxel[123]. The content of this information depends on the imaging modality used (Hounsfield units measure density for CT, signal intensity measures tissue relaxation times for MRI, and standard uptake values measure activity for PET). A broad spectrum of quantitative parameters can be extracted from any diagnostic imaging modality, ranging from first-order parameters (defined on the basis of histogram analysis, which does not account for spatial distribution) to more complex higher-order parameters[124]. Multiple first-order parameters are available, including the mean gray-level intensity (brightness), uniformity (distribution of the gray level), entropy (a measure of irregularity), skewness (a measure of the asymmetry of the pixel histogram distribution) and kurtosis (the magnitude of the

pixel histogram distribution)[125]. The analysis is performed by drawing an ROI in the largest cross-section of the tumor or in tumor subregions and by taking into account the whole tumor volume or delineating the margins in an organ in the absence of a target lesion. Interestingly, TA approaches can also be employed for morphological images (such as unenhanced CT images or T2-weighted MR images), possibly reducing the need for more complex, expensive and time-consuming techniques. Additionally, filtering techniques can be applied to the original images before performing TA to widen the range of available quantitative parameters[126]. Encouraging results have been recently published for TA in the field of oncologic imaging[127,128]. Regarding CRC, the application of TA to CT, MRI and PET/CT images has been investigated and might be useful in different clinical settings for characterization, staging, prognosis and treatment planning.

**Primary tumor identification:** The accurate differentiation of colorectal nonneoplastic (i.e., hyperplasic polyps) and neoplastic lesions (i.e., adenomas and adenocarcinomas) based on computed tomography colonography (CTC) for mucosal colorectal lesions is mandatory for appropriate patient management[129]. The lesion size is correlated with the risk of malignancy, but size alone is not sufficient to discriminate between nonneoplastic and neoplastic lesions for the following reasons: (1) CTC tends to underestimate polyp size[130]; and (2) The overlap in the sizes of benign, premalignant and malignant lesions. Moreover, combination of metabolic and morphological information does not seem to increase the accuracy of CTC[41]. Therefore, TA might improve the diagnostic performance of CTC by introducing additional criteria for evaluation. Song *et al*[131] evaluated the accuracy of the use of CTC texture features in differentiating colorectal lesions. Intensity, gradient (*i.e.*, the degree of the intensity change) and curvature (*i.e.*, the degree that a geometric object deviates from being flat) were calculated for each colorectal polyp lesion. The results showed that the combination of gradient and curvature features significantly improved the performance of CTC in differentiating hyperplasic polyps from neoplastic lesions. The skewness and entropy values calculated on the basis of ADC maps were significantly lower in patients with stage pT1-2 tumors versus those with stage pT3-4 tumors[132]. Kurtosis values obtained on the basis of DWI were significantly higher in high-grade than in low-grade RC[133].

**Lymph node involvement:** The evaluation of the structural heterogeneity of loco-regional lymph nodes by using TA could help predict nodal status in RC to reliably differentiate malignant lymph nodes from benign lymph nodes. In this regard, Cui *et al*[134] reported that the heterogeneity of benign mesorectal nodes calculated by using enhanced CT images was significantly lower than that of malignant nodes when the short-axis diameter was 3–10 mm. However, no difference was observed between benign and malignant lymph nodes less than 3 mm and larger than 10 mm. Liu *et al*[132] reported that entropy values calculated by using ADC maps were significantly higher in pN1-2 than in pN0 RC. Similarly, Zhu *et al*[133] reported significantly higher kurtosis values calculated by using DWI in pN1-2 compared to pN0 RC.

**Response to treatment: Neoadjuvant CRT in RC:** TA of MR images might identify biomarkers able to assess responses to CRT in patients with LARC[125,132,135-137]. Using T2 weighted images, De Cecco *et al*[135] found that pre-neoadjuvant CRT kurtosis was significantly decreased in pCR versus partial-responders or nonresponders. Similarly, using T2 weighted images, Shu *et al*[136] found that TA of a combination of pre- and early-treatment features could distinguish between responders and nonresponders. TA approaches based on advanced sequences such as DCE[137] and ADC maps[132] have also been proposed and have shown promising results.

**CRLMs: early identification and responses to treatment:** Liver colonization by CRC cells is considered to be a multiple step process that progresses from prometastatic hepatic reactions to micrometastases and finally generates macrometastases[138]. The liver prometastatic reaction produces a special microenvironment favoring liver colonization by tumor cells. This reaction begins in the early tumor stage with the release of cytokines and chemokines by hepatic sinusoidal endothelium and Kupffer cells in response to colon cancer soluble factors and circulating cells. Cytokines and chemokines lead to the activation of perisinusoidal stellate cells and portal tract fibroblasts, which deposit extracellular matrix and create stromal support for cancer cells. The early preoperative identification of prometastatic hepatic reactions might facilitate the use of personalized treatment strategies that involve the selection of chemotherapy independently according to local staging[139]. Similarly, the preoperative identification of micrometastases in addition to visible liver metastases might indicate the use of neoadjuvant chemotherapy in CRC patients who are candidates for liver resection[140]. Conventional tomographic imaging is unable to detect liver

prometastatic reactions or occult liver micrometastases. A few studies have tested the ability of TA to detect precocious hepatic alterations on the basis of the fact that the spatial heterogeneity of an apparently disease-free liver may be altered by liver prometastatic reactions and occult liver micrometastases.

Rao *et al*[140] assessed the capability of whole-liver portal phase CT TA to detect structural differences between apparently disease-free liver parenchyma in CRC patients without and with liver metastases. Disease-free liver parenchyma in patients with synchronous liver metastases (Group B) showed entropy values significantly higher and uniformity values significantly lower than those in patients without liver metastases (Group A). Furthermore, the disease-free liver parenchyma in patients who developed metachronous liver metastases within 18 months after primary staging CT (Group C) showed a subtle trend towards increased entropy and decreased uniformity values compared to that in patients in group A, although the difference was not significant. These results produced the following observations: (1) Group B presented greater heterogeneity in the liver parenchymal structure compared to group A due to the possible presence of micrometastases in the apparently disease-free remaining liver tissues or tumor-induced changes in liver perfusion; and (2) Group C may show ongoing tumor-induced, structural and/or hemodynamic changes in the liver parenchyma that precede morphological changes, allowing the identification of patients at risk of developing metachronous hepatic metastases.

Finally, both CT- and MRI-based TA parameters have been explored as feasible tools to predict treatment responses in patients with CRLMs[141,142]. Zhang *et al*[141] evaluated the response to chemotherapy of 193 unresectable liver metastases using dimensional reduction that was observed by the comparison of T2-weighted pretreatment and posttreatment MR images as a reference standard (a cutoff of a 30% decrease in the maximum diameter defined the responders). The authors found that the association of a first-order parameter (variance) and a higher-order parameter (angular second moment) had the ability to predict response, with an AUC of 0.814. Likewise, Ahn *et al*[142] demonstrated that decreased skewness values, obtained from two-dimensional ROIs used to annotate liver metastases on CT portal-phase images, were predictive of responses to chemotherapy (AUC = 0.797).

**Prognosis:** Ng *et al*[143] showed a correlation between the entire primary CRC heterogeneity according to portal venous CT images with the 5-year OS rate. CRC with decreased heterogeneity (decreased entropy, kurtosis and standard deviation of pixel distribution; increased uniformity and skewness) was associated with a decreased 5-year OS.

Miles *et al*[144] assessed the ability of the TA of hepatic portal phase CT images to predict survival in patients with CRC subject to surveillance for at least 24 months after tumor resection. Kaplan-Meier curves showed that increased uniformity was a significant predictor of survival. Finally, Lovinfosse *et al*[145] evaluated the TA of baseline 18FDG-PET/CT in LARC patients and concluded that increased coarseness values may be indicative of worse outcomes.

### *Volumetry*

CT, MRI and PET hybrid imaging allow the "*in vivo*" calculation of neoplastic volume. RC tumor burden is correlated with disease stage and represents an important prognostic feature in terms of the prediction of treatment response, OS and PFS after CRT[146-149]. The tumor volume reduction rate has been reported to be superior to RECIST criteria for the prediction of the pathological responses of RC to neoadjuvant CRT[150].

The determination of tumor volumetry by using morphological CT and MR images requires the delineation of the neoplastic contours, which can be defined visually by manually tracing the presumed lesion boundary in each image containing the neoplasm. The volumes of the lesions are calculated by adding each of the 2D volumes (multiplying the 2D area by image thickness) of the entire lesion. The following considerations can explain the limits of this qualitative visual approach for tumor volumetry measurement: (1) Inflammatory peritumoral reactions can hamper the exact delineation of the interface between the tumor and the surrounding tissues; and (2) The difficulty in distinguishing between therapy-induced fibrosis and the residual viable tumor can also be problematic. A quantitative parametric analysis of images has also been proposed to solve this problem of tumor volumetry measurement.

T2-weighted signal intensity-selected volumetry of post-CRT MRI performed better than visual qualitative T2 volumetry in predicting pCR in patients with LARC[151]. Posttreatment total lesion diffusion (TLD = total DWI tumor volume x mean volumetric ADC) was better correlated than the total DWI tumor volume with histopathological tumor responses after CRT in patients with LARC[152].

## LIMITATIONS AND POTENTIAL EFFECTIVE CLINICAL APPLICATIONS OF PARAMETRIC IMAGING ANALYSIS

### *DWI with ADC maps*

Well-defined cut-off values are needed to use ADC maps in routine clinical practice. The ADC value thresholds used for differentiating normal and pathological tissue, assessing responses to therapy and defining prognosis have not yet been established for CRC. The lack of definite thresholds may be attributed to the following: (1) ADC values depend on the scanner and the acquisition protocol used and the clinical setting; (2) ADC values are subject to measuring errors due to the low spatial resolution of DWI images; and (3) The lack of reproducibility for ADC measurements. ADC values appear to be particularly promising for the prediction and assessment of RC responses to neoadjuvant CRT.

### *Perfusion imaging*

The following general principles concerning angiogenesis and CRC have been established: More poorly perfused tumors usually lead to a poorer outcome; baseline perfusion is significantly higher in responders than in nonresponders to several types of therapies; and an early reduction in vascular parameters after therapy is usually associated with improved patient outcome[22]. The use of PI techniques has not yet been introduced in routine clinical practice, probably due to the numerous different technical approaches required and the complexity of parameter measurement. The following limitations of PI have to be considered: (1) The quantification of contrast agent concentrations is challenging because of the complex relationship between density (CT) or signal (MRI) and the contrast medium concentration, which is dependent on many factors, including the contrast agent dose, rate of injection, time of circulation, machine parameters, and, for MRI, native tissue relaxation rates and imaging sequence; (2) The different models used for the analysis of DCE imaging data and the calculation of quantitative perfusion parameters[153] may influence the measurement of quantitative perfusion parameters[35]; and (3) Tumor ROI analysis with current DCE imaging software platforms utilizes the mean quantitative vascular parameters, which do not reflect the spatial heterogeneity of perfusion[154]. Because of the large variety of potential indicators that could be used as imaging biomarkers, PI still needs further study to be recognized as an effective diagnostic tool in routine clinical practice. Among all the potential clinical applications of DCE imaging for CRC, the assessment and prediction of responses to antiangiogenic agents appears to be the most promising.

### *Hybrid imaging*

18FDG-PET/CT quantitative parameters have added value for routine clinical practice. The following topics may benefit from a quantitative approach: The improvement of the detection of regional lymph node metastases; the prediction and assessment of RC responses to neoadjuvant CRT; the detection of tumor recurrence after surgery in combination with serum CEA levels. There is not enough scientific evidence to recommend the routine use of quantitative 18FDG-PET/CT for the identification and/or local staging of primary CRC because PET has the following limitations: (1) FDG uptake depends on several features, including tumor grade, the type of tumor involvement, histological type (*e.g.*, FDG is limited in the evaluation of mucinous tumors); and (2) Limited spatial resolution, which may cause small lesions to be missed.

### *Texture analysis*

Texture analysis mainly suffers from the following limitations: (1) The biological correlations of TA measurements have not been established definitively; and (2) The image acquisition parameters (for CT: Tube voltage, tube current, collimation; for MRI: features of the sequences) and TA processing (unfiltered or filtered at a fine, medium or coarse scale; TA calculation of single axial sections or whole target volumes; the use of semiautomated and automated systems to delineate tumor regions or volumes) may affect the measurement of TA parameters and may change their biological correlation. TA represents an ongoing topic of investigation, but the clinical effectiveness of the technique still has to be defined in different clinical settings relevant to CRC.

## THE NEXT STEPS: MULTI-PARAMETRIC IMAGING ASSESSMENT, RADIOMICS AND RADIOGENOMICS, AND MACHINE LEARNING

The complexity of tumor biology cannot be described by a single morphological, functional and/or molecular parameter. An integrated approach utilizing noninvasive *in vivo* imaging techniques can be used to accurately represent neoplastic heterogeneity. A more comprehensive multiparametric assessment of tumor biology can be obtained from a single examination combining morphological, functional and/or molecular information by using hybrid devices such as PET/CT or PET/MRI. A few studies have investigated the relationships between functional and molecular parameters in CRC. An inverse relationship between tumor vascularization (expressed as the Kep value) and metabolism (expressed as SUVmax) was observed in CRLMs[155]. CRCs with a low-flow and high-metabolism phenotype were associated with increased levels of hypoxia-inducible factor 1 (HIF-1a), suggesting that flow and metabolism mismatch may represent an adaptative angiogenic response to hypoxia[156]. Highly perfused RC manifested with higher FDG uptake levels than low-perfusion tumors, suggesting that tumor growth is accompanied by an intense inflammatory reaction rather than the development of necrosis[157]. A significant negative correlation between the ADC and SUV values was reported for adenocarcinomas of the rectum, suggesting that the vital cellular burden is associated with increased metabolism[158,159]. The decrease in flow and metabolism (expressed as BF x SUVmax) showed high accuracy in the prediction of histopathological responses to radiation therapy and chemotherapy when using a cutoff value of -75% in patients with RC[159]. Multiparametric quantitative assessment appears to be a promising strategy for CRC management; however, its role in the different clinical settings associated with CRC must still be defined.

Further prospective investigations are needed to evaluate the clinical effectiveness of multiparametric imaging and to propose its routine clinical use in CRC settings.

Radiomics has recently emerged as a promising tool for discovering new imaging biomarkers by extracting and analyzing numerous quantitative image features representative of tumor heterogeneity and phenotype. Radiomics combines the imaging of quantitative biomarkers with clinical reports and laboratory test values in a statistical model (Figure 5). Similarly, radiogenomics evaluates the relationship between radiomics and gene-expression patterns or transcriptomic and/or proteomic data to generate a statistical model. These advanced computational techniques can be applied to any type of clinical image, such as CT, MRI or hybrid PET images, and they can be used in a variety of clinical settings for diagnosis, the prediction of prognosis, and the evaluation of treatment response[160,161]. Although there is still a limited amount of evidence regarding the applications of radiogenomics to CRC, it retains tremendous potential[162]. Indeed, studies conducted using images from different modalities (mainly PET/CT) have investigated the relationship between radiomic data and K-ras gene mutations in CRC patients with encouraging results[163-165]. The K-ras gene mutation is an independent prognostic factor for survival and a negative predictive marker of tumor responses to drugs that target anti-epidermal growth factor receptors (EGFRs). Shin *et al*[163] reported that the frequency of K-ras mutations was higher in polypoid tumors with a larger axial to longitudinal dimension ratio. Using an animal model, Miles *et al*[166] reported that the combined multiparametric assessment of 18F-FDG uptake (expressed as SUVmax), CT texture (expressed as the mean value of tumor pixels with positive values) and perfusion (expressed as BF) has excellent accuracy (90.1%) in the identification of CRCs with K-ras mutations.

The increasing use of quantitative imaging data in clinical practice will require the use of automated and intelligent systems for analyzing a large amount of numerical information. Artificial intelligence and machine learning approaches can be helpful for the evaluation of radiomic and radiogenomic features. Deep learning convolutional neural networks can perform texture analysis and training with large amounts of data to create predictive algorithms.

## CONCLUSION

The interpretation of medical tomographic images can no longer treat images strictly as pictures but instead must use innovative approaches based on numerical analysis. PA allows the extraction and analysis of the large amount of numerical data hidden in tomographic images. This information must be correlated with genetic, histological, clinical, prognostic and/or predictive data. The transition from purely anatomical tomographic imaging to quantitative tomographic imaging can also benefit the

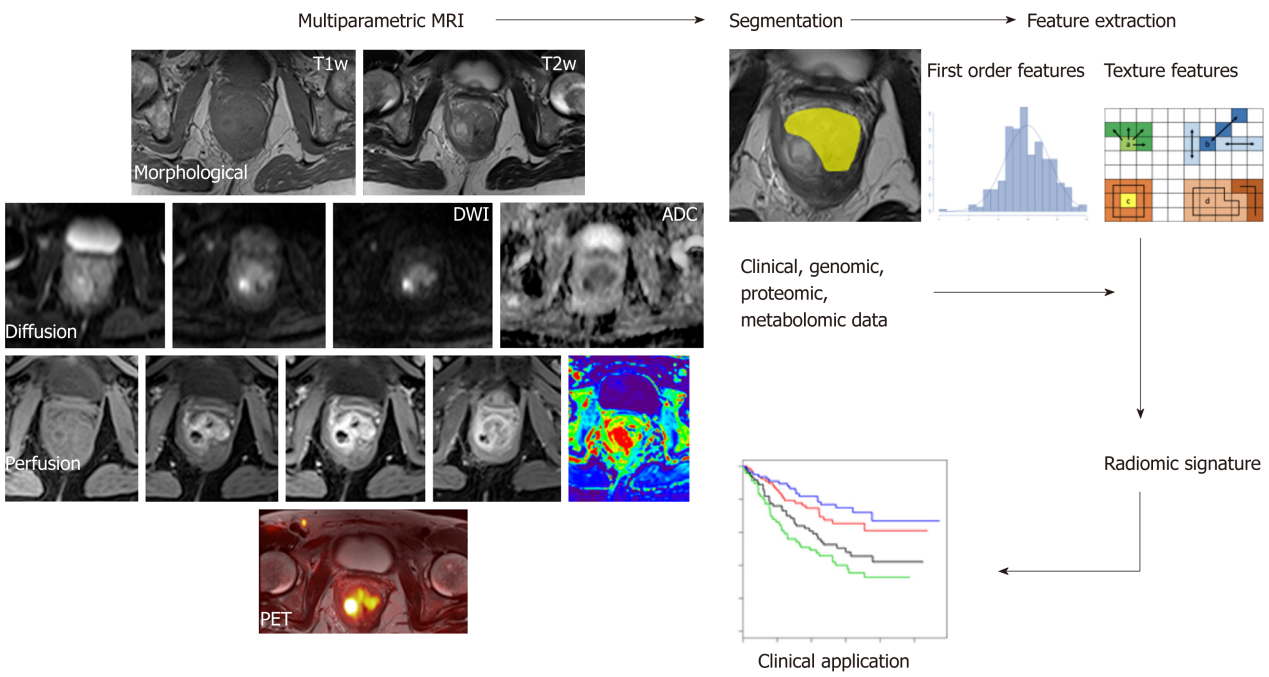


**Figure 5 A typical radiomics workflow consists of several steps.** After image acquisition, segmentation is performed to define the tumor region. From this region, several features are extracted based on the intensity histogram and texture analysis. Finally, these features are assessed for their prognostic power or are linked with the stage or gene expression.

diagnostic management of CRC. However, to be of practical value and to have a real effect on clinical CRC diagnostic management, quantitative imaging approaches require the following: (1) The standardization of technical features to ensure the acquisition of good quality data and the development of robust techniques for analysis to assure reproducibility among different operators, scanners and centers; (2) Well-defined cut-off values for each proposed parameter measure in different clinical settings relevant to CRC; (3) A clear definition of the clinical significance of each numerical parameter as a single measure or a multiparametric combination; and (4) A real added-value when used to determine the known clinical and pathological factors of each new numerical imaging biomarker.

## REFERENCES


1 **Siegel RL**, Miller KD, Jemal A. Cancer statistics, 2019. *CA Cancer J Clin* 2019; **69**: 7-34 [PMID: 30620402 DOI: 10.3322/caac.21551]

2 **Yuan Y**, Li MD, Hu HG, Dong CX, Chen JQ, Li XF, Li JJ, Shen H. Prognostic and survival analysis of 837 Chinese colorectal cancer patients. *World J Gastroenterol* 2013; **19**: 2650-2659 [PMID: 23674872 DOI: 10.3748/wjg.v19.i17.2650]

3 **Labianca R**, Nordlinger B, Beretta GD, Mosconi S, Mandalà M, Cervantes A, Arnold D; ESMO Guidelines Working Group. Early colon cancer: ESMO Clinical Practice Guidelines for diagnosis, treatment and follow-up. *Ann Oncol* 2013; **24** Suppl 6: vi64-vi72 [PMID: 24078664 DOI: 10.1093/annonc/mdt354]

4 **Glynne-Jones R**, Wyrwicz L, Tiret E, Brown G, Rödel C, Cervantes A, Arnold D; ESMO Guidelines Committee. Rectal cancer: ESMO Clinical Practice Guidelines for diagnosis, treatment and follow-up. *Ann Oncol* 2018; **29**: iv263 [PMID: 29741565 DOI: 10.1093/annonc/mdy161]

5 **Van Cutsem E**, Cervantes A, Nordlinger B, Arnold D; ESMO Guidelines Working Group. Metastatic colorectal cancer: ESMO Clinical Practice Guidelines for diagnosis, treatment and follow-up. *Ann Oncol* 2014; **25** Suppl 3: iii1-iii9 [PMID: 25190710 DOI: 10.1093/annonc/mdu260]

6 **Gerlinger M**, Rowan AJ, Horswell S, Math M, Larkin J, Endesfelder D, Gronroos E, Martinez P, Matthews N, Stewart A, Tarpey P, Varela I, Phillimore B, Begum S, McDonald NQ, Butler A, Jones D, Raine K, Latimer C, Santos CR, Nohadani M, Eklund AC, Spencer-Dene B, Clark G, Pickering L, Stamp G, Gore M, Szallasi Z, Downward J, Futreal PA, Swanton C. Intratumor heterogeneity and branched evolution revealed by multiregion sequencing. *N Engl J Med* 2012; **366**: 883-892 [PMID: 22397650 DOI: 10.1056/NEJMoa1113205]

7 **Glüer CC**, Barkmann R, Hahn HK, Majumdar S, Eckstein F, Nickelsen TN, Bolte H, Dicken V, Heller M. [Parametric biomedical imaging--what defines the quality of quantitative radiological approaches?]. *Rofo* 2006; **178**: 1187-1201 [PMID: 17136644 DOI: 10.1055/s-2006-926973]

8 **García-Figueiras R**, Baleato-González S, Padhani AR, Marhuenda A, Luna A, Alcalá L, Carballo-Castro A, Álvarez-Castro A. Advanced imaging of colorectal cancer: From anatomy to molecular imaging. *Insights Imaging* 2016; **7**: 285-309 [PMID: 27136925 DOI: 10.1007/s13244-016-0465-x]

9 **Prezzi D**, Goh V. Rectal Cancer Magnetic Resonance Imaging: Imaging Beyond Morphology. *Clin Oncol*

*(R Coll Radiol)* 2016; **28**: 83-92 [PMID: 26586163 DOI: 10.1016/j.clon.2015.10.010]
10 **Chun YS**, Vauthey JN, Boonsirikamchai P, Maru DM, Kopetz S, Palavecino M, Curley SA, Abdalla EK, Kaur H, Charnsangavej C, Loyer EM. Association of computed tomography morphologic criteria with pathologic response and survival in patients treated with bevacizumab for colorectal liver metastases. *JAMA* 2009; **302**: 2338-2344 [PMID: 19952320 DOI: 10.1001/jama.2009.1755]
11 **Choi H**, Charnsangavej C, Faria SC, Macapinlac HA, Burgess MA, Patel SR, Chen LL, Podoloff DA, Benjamin RS. Correlation of computed tomography and positron emission tomography in patients with metastatic gastrointestinal stromal tumor treated at a single institution with imatinib mesylate: proposal of new computed tomography response criteria. *J Clin Oncol* 2007; **25**: 1753-1759 [PMID: 17470865 DOI: 10.1200/JCO.2006.07.3049]
12 **Lencioni R**, Llovet JM. Modified RECIST (mRECIST) assessment for hepatocellular carcinoma. *Semin Liver Dis* 2010; **30**: 52-60 [PMID: 20175033 DOI: 10.1055/s-0030-1247132]
13 **Rao SX**, Lambregts DM, Schnerr RS, Beckers RC, Maas M, Albarello F, Riedl RG, Dejong CH, Martens MH, Heijnen LA, Backes WH, Beets GL, Zeng MS, Beets-Tan RG. CT texture analysis in colorectal liver metastases: A better way than size and volume measurements to assess response to chemotherapy? *United European Gastroenterol J* 2016; **4**: 257-263 [PMID: 27087955 DOI: 10.1177/2050640615601603]
14 **Shankar S**, Dundamadappa SK, Karam AR, Stay RM, van Sonnenberg E. Imaging of gastrointestinal stromal tumors before and after imatinib mesylate therapy. *Acta Radiol* 2009; **50**: 837-844 [PMID: 19735005 DOI: 10.1080/02841850903059423]
15 **Chung WS**, Park MS, Shin SJ, Baek SE, Kim YE, Choi JY, Kim MJ. Response evaluation in patients with colorectal liver metastases: RECIST version 1.1 versus modified CT criteria. *AJR Am J Roentgenol* 2012; **199**: 809-815 [PMID: 22997372 DOI: 10.2214/AJR.11.7910]
16 **Patterson DM**, Padhani AR, Collins DJ. Technology insight: water diffusion MRI--a potential new biomarker of response to cancer therapy. *Nat Clin Pract Oncol* 2008; **5**: 220-233 [PMID: 18301415 DOI: 10.1038/ncponc1073]
17 **deSouza NM**, Riches SF, Vanas NJ, Morgan VA, Ashley SA, Fisher C, Payne GS, Parker C. Diffusion-weighted magnetic resonance imaging: a potential non-invasive marker of tumour aggressiveness in localized prostate cancer. *Clin Radiol* 2008; **63**: 774-782 [PMID: 18555035 DOI: 10.1016/j.crad.2008.02.001]
18 **Koh DM**, Collins DJ. Diffusion-weighted MRI in the body: applications and challenges in oncology. *AJR Am J Roentgenol* 2007; **188**: 1622-1635 [PMID: 17515386 DOI: 10.2214/AJR.06.1403]
19 **Heijmen L**, Verstappen MC, Ter Voert EE, Punt CJ, Oyen WJ, de Geus-Oei LF, Hermans JJ, Heerschap A, van Laarhoven HW. Tumour response prediction by diffusion-weighted MR imaging: ready for clinical use? *Crit Rev Oncol Hematol* 2012; **83**: 194-207 [PMID: 22269446 DOI: 10.1016/j.critrevonc.2011.12.008]
20 **Rak J**, Mitsuhashi Y, Bayko L, Filmus J, Shirasawa S, Sasazuki T, Kerbel RS. Mutant ras oncogenes upregulate VEGF/VPF expression: implications for induction and inhibition of tumor angiogenesis. *Cancer Res* 1995; **55**: 4575-4580 [PMID: 7553632]
21 **Goh V**, Halligan S, Daley F, Wellsted DM, Guenther T, Bartram CI. Colorectal tumor vascularity: quantitative assessment with multidetector CT--do tumor perfusion measurements reflect angiogenesis? *Radiology* 2008; **249**: 510-517 [PMID: 18812560 DOI: 10.1148/radiol.2492071365]
22 **Goh V**, Glynne-Jones R. Perfusion CT imaging of colorectal cancer. *Br J Radiol* 2014; **87**: 20130811 [PMID: 24434157 DOI: 10.1259/bjr.20130811]
23 **Konerding MA**, Fait E, Gaumann A. 3D microvascular architecture of pre-cancerous lesions and invasive carcinomas of the colon. *Br J Cancer* 2001; **84**: 1354-1362 [PMID: 11355947 DOI: 10.1054/bjoc.2001.1809]
24 **Nelson DA**, Tan TT, Rabson AB, Anderson D, Degenhardt K, White E. Hypoxia and defective apoptosis drive genomic instability and tumorigenesis. *Genes Dev* 2004; **18**: 2095-2107 [PMID: 15314031 DOI: 10.1101/gad.1204904]
25 **O'Connor JP**, Tofts PS, Miles KA, Parkes LM, Thompson G, Jackson A. Dynamic contrast-enhanced imaging techniques: CT and MRI. *Br J Radiol* 2011; **84** Spec No 2: S112-S120 [PMID: 22433822 DOI: 10.1259/bjr/55166688]
26 **Cuenod CA**, Balvay D. Perfusion and vascular permeability: basic concepts and measurement in DCE-CT and DCE-MRI. *Diagn Interv Imaging* 2013; **94**: 1187-1204 [PMID: 24211260 DOI: 10.1016/j.diii.2013.10.010]
27 **Jahng GH**, Li KL, Ostergaard L, Calamante F. Perfusion magnetic resonance imaging: a comprehensive update on principles and techniques. *Korean J Radiol* 2014; **15**: 554-577 [PMID: 25246817 DOI: 10.3348/kjr.2014.15.5.554]
28 **Peller P**, Subramaniam R, Guermazi A, editors. *PET-CT and PET-MRI in Oncology [Internet]*. Berlin, Heidelberg: Springer Berlin Heidelberg; 2012;
29 **Kocael A**, Vatankulu B, Şimşek O, Cengiz M, Kemik A, Kocael P, Halaç M, Sönmezoğlu K, Ulualp K. Comparison of (18)F-fluorodeoxyglucose PET/CT findings with vascular endothelial growth factors and receptors in colorectal cancer. *Tumour Biol* 2016; **37**: 3871-3877 [PMID: 26476536 DOI: 10.1007/s13277-015-4218-0]
30 **Pauwels EK**, Coumou AW, Kostkiewicz M, Kairemo K. [$^{1}$F]fluoro-2-deoxy-d-glucose positron emission tomography/computed tomography imaging in oncology: initial staging and evaluation of cancer therapy. *Med Princ Pract* 2013; **22**: 427-437 [PMID: 23363934 DOI: 10.1159/000346303]
31 **Kilickesmez O**, Atilla S, Soylu A, Tasdelen N, Bayramoglu S, Cimilli T, Gurmen N. Diffusion-weighted imaging of the rectosigmoid colon: preliminary findings. *J Comput Assist Tomogr* 2009; **33**: 863-866 [PMID: 19940651 DOI: 10.1097/RCT.0b013e31819a60f3]
32 **Jia H**, Ma X, Zhao Y, Zhao J, Liu R, Chen Z, Chen J, Huang J, Li Y, Zhang J, Wang F. Meta-analysis of diffusion-weighted magnetic resonance imaging in identification of colorectal cancer. *Int J Clin Exp Med* 2015; **8**: 17333-17342 [PMID: 26770325]
33 **Curvo-Semedo L**, Lambregts DM, Maas M, Beets GL, Caseiro-Alves F, Beets-Tan RG. Diffusion-weighted MRI in rectal cancer: apparent diffusion coefficient as a potential noninvasive marker of tumor aggressiveness. *J Magn Reson Imaging* 2012; **35**: 1365-1371 [PMID: 22271382 DOI: 10.1002/jmri.23589]
34 **Tong T**, Yao Z, Xu L, Cai S, Bi R, Xin C, Gu Y, Peng W. Extramural depth of tumor invasion at thin-section MR in rectal cancer: associating with prognostic factors and ADC value. *J Magn Reson Imaging* 2014; **40**: 738-744 [PMID: 24307597 DOI: 10.1002/jmri.24398]
35 **Goh V**, Halligan S, Taylor SA, Burling D, Bassett P, Bartram CI. Differentiation between diverticulitis and colorectal cancer: quantitative CT perfusion measurements versus morphologic criteria--initial

experience. *Radiology* 2007; **242**: 456-462 [PMID: 17255417 DOI: 10.1148/radiol.2422051670]
36 **Shen FU**, Lu J, Chen L, Wang Z, Chen Y. Diagnostic value of dynamic contrast-enhanced magnetic resonance imaging in rectal cancer and its correlation with tumor differentiation. *Mol Clin Oncol* 2016; **4**: 500-506 [PMID: 27073650 DOI: 10.3892/mco.2016.762]
37 **Sun H**, Xu Y, Yang Q, Wang W. Assessment of tumor grade and angiogenesis in colorectal cancer: whole-volume perfusion CT. *Acad Radiol* 2014; **21**: 750-757 [PMID: 24809317 DOI: 10.1016/j.acra.2014.02.011]
38 **Xu Y**, Sun H, Song A, Yang Q, Lu X, Wang W. Predictive Significance of Tumor Grade Using 256-Slice CT Whole-Tumor Perfusion Imaging in Colorectal Adenocarcinoma. *Acad Radiol* 2015; **22**: 1529-1535 [PMID: 26421473 DOI: 10.1016/j.acra.2015.08.023]
39 **Oh JR**, Min JJ, Song HC, Chong A, Kim GE, Choi C, Seo JH, Bom HS. A stepwise approach using metabolic volume and SUVmax to differentiate malignancy and dysplasia from benign colonic uptakes on 18F-FDG PET/CT. *Clin Nucl Med* 2012; **37**: e134-e140 [PMID: 22614211 DOI: 10.1097/RLU.0b013e318239245d]
40 **van Hoeij FB**, Keijsers RG, Loffeld BC, Dun G, Stadhouders PH, Weusten BL. Incidental colonic focal FDG uptake on PET/CT: can the maximum standardized uptake value (SUVmax) guide us in the timing of colonoscopy? *Eur J Nucl Med Mol Imaging* 2015; **42**: 66-71 [PMID: 25139518 DOI: 10.1007/s00259-014-2887-3]
41 **Mainenti PP**, Salvatore B, D'Antonio D, De Falco T, De Palma GD, D'Armiento FP, Bucci L, Pace L, Salvatore M. PET/CT colonography in patients with colorectal polyps: a feasibility study. *Eur J Nucl Med Mol Imaging* 2007; **34**: 1594-1603 [PMID: 17492447 DOI: 10.1007/s00259-007-0422-5]
42 **Liao CY**, Chen SW, Wu YC, Chen WT, Yen KY, Hsieh TC, Chen PJ, Kao CH. Correlations between 18F-FDG PET/CT parameters and pathological findings in patients with rectal cancer. *Clin Nucl Med* 2014; **39**: e40-e45 [PMID: 24335567 DOI: 10.1097/RLU.0b013e318292f0f6]
43 **Mainenti PP**, Cirillo LC, Camera L, Persico F, Cantalupo T, Pace L, De Palma GD, Persico G, Salvatore M. Accuracy of single phase contrast enhanced multidetector CT colonography in the preoperative staging of colo-rectal cancer. *Eur J Radiol* 2006; **60**: 453-459 [PMID: 16965883 DOI: 10.1016/j.ejrad.2006.08.001]
44 **Filippone A**, Ambrosini R, Fuschi M, Marinelli T, Genovesi D, Bonomo L. Preoperative T and N staging of colorectal cancer: accuracy of contrast-enhanced multi-detector row CT colonography--initial experience. *Radiology* 2004; **231**: 83-90 [PMID: 14990815 DOI: 10.1148/radiol.2311021152]
45 **Kulinna C**, Eibel R, Matzek W, Bonel H, Aust D, Strauss T, Reiser M, Scheidler J. Staging of rectal cancer: diagnostic potential of multiplanar reconstructions with MDCT. *AJR Am J Roentgenol* 2004; **183**: 421-427 [PMID: 15269036 DOI: 10.2214/ajr.183.2.1830421]
46 **Brown G**, Richards CJ, Bourne MW, Newcombe RG, Radcliffe AG, Dallimore NS, Williams GT. Morphologic predictors of lymph node status in rectal cancer with use of high-spatial-resolution MR imaging with histopathologic comparison. *Radiology* 2003; **227**: 371-377 [PMID: 12732695 DOI: 10.1148/radiol.2272011747]
47 **Mainenti PP**, Iodice D, Segreto S, Storto G, Magliulo M, De Palma GD, Salvatore M, Pace L. Colorectal cancer and 18FDG-PET/CT: what about adding the T to the N parameter in loco-regional staging? *World J Gastroenterol* 2011; **17**: 1427-1433 [PMID: 21472100 DOI: 10.3748/wjg.v17.i11.1427]
48 **Heijnen LA**, Lambregts DM, Mondal D, Martens MH, Riedl RG, Beets GL, Beets-Tan RG. Diffusion-weighted MR imaging in primary rectal cancer staging demonstrates but does not characterise lymph nodes. *Eur Radiol* 2013; **23**: 3354-3360 [PMID: 23821022 DOI: 10.1007/s00330-013-2952-5]
49 **Lambregts DM**, Maas M, Riedl RG, Bakers FC, Verwoerd JL, Kessels AG, Lammering G, Boetes C, Beets GL, Beets-Tan RG. Value of ADC measurements for nodal staging after chemoradiation in locally advanced rectal cancer-a per lesion validation study. *Eur Radiol* 2011; **21**: 265-273 [PMID: 20730540 DOI: 10.1007/s00330-010-1937-x]
50 **Armbruster M**, D'Anastasi M, Holzner V, Kreis ME, Dietrich O, Brandlhuber B, Graser A, Brandlhuber M. Improved detection of a tumorous involvement of the mesorectal fascia and locoregional lymph nodes in locally advanced rectal cancer using DCE-MRI. *Int J Colorectal Dis* 2018; **33**: 901-909 [PMID: 29774398 DOI: 10.1007/s00384-018-3083-x]
51 **Grøvik E**, Redalen KR, Storås TH, Negård A, Holmedal SH, Ree AH, Meltzer S, Bjørnerud A, Gjesdal KI. Dynamic multi-echo DCE- and DSC-MRI in rectal cancer: Low primary tumor K<sup>trans</sup> and ΔR2* peak are significantly associated with lymph node metastasis. *J Magn Reson Imaging* 2017; **46**: 194-206 [PMID: 28001320 DOI: 10.1002/jmri.25566]
52 **Yeo DM**, Oh SN, Jung CK, Lee MA, Oh ST, Rha SE, Jung SE, Byun JY, Gall P, Son Y. Correlation of dynamic contrast-enhanced MRI perfusion parameters with angiogenesis and biologic aggressiveness of rectal cancer: Preliminary results. *J Magn Reson Imaging* 2015; **41**: 474-480 [PMID: 24375840 DOI: 10.1002/jmri.24541]
53 **Lollert A**, Junginger T, Schimanski CC, Biesterfeld S, Gockel I, Düber C, Oberholzer K. Rectal cancer: dynamic contrast-enhanced MRI correlates with lymph node status and epidermal growth factor receptor expression. *J Magn Reson Imaging* 2014; **39**: 1436-1442 [PMID: 24127411 DOI: 10.1002/jmri.24301]
54 **Yang X**, Chen Y, Wen Z, Lu B, Shen B, Xiao X, Yu S. Role of Quantitative Dynamic Contrast-Enhanced MRI in Evaluating Regional Lymph Nodes With a Short-Axis Diameter of Less Than 5 mm in Rectal Cancer. *AJR Am J Roentgenol* 2019; **212**: 77-83 [PMID: 30354269 DOI: 10.2214/AJR.18.19866]
55 **Yu XP**, Wen L, Hou J, Wang H, Lu Q. Discrimination of metastatic from non-metastatic mesorectal lymph nodes in rectal cancer using quantitative dynamic contrast-enhanced magnetic resonance imaging. *J Huazhong Univ Sci Technolog Med Sci* 2016; **36**: 594-600 [PMID: 27465339 DOI: 10.1007/s11596-016-1631-6]
56 **Lu YY**, Chen JH, Ding HJ, Chien CR, Lin WY, Kao CH. A systematic review and meta-analysis of pretherapeutic lymph node staging of colorectal cancer by 18F-FDG PET or PET/CT. *Nucl Med Commun* 2012; **33**: 1127-1133 [PMID: 23000829 DOI: 10.1097/MNM.0b013e328357b2d9]
57 **Yi HJ**, Hong KS, Moon N, Chung SS, Lee RA, Kim KH. Reliability of (18)f-fluorodeoxyglucose positron emission tomography/computed tomography in the nodal staging of colorectal cancer patients. *Ann Coloproctol* 2014; **30**: 259-265 [PMID: 25580412 DOI: 10.3393/ac.2014.30.6.259]
58 **Tsunoda Y**, Ito M, Fujii H, Kuwano H, Saito N. Preoperative diagnosis of lymph node metastases of colorectal cancer by FDG-PET/CT. *Jpn J Clin Oncol* 2008; **38**: 347-353 [PMID: 18424814 DOI: 10.1093/jjco/hyn032]
59 **Yu L**, Tian M, Gao X, Wang D, Qin Y, Geng J. The method and efficacy of 18F-fluorodeoxyglucose positron emission tomography/computed tomography for diagnosing the lymphatic metastasis of colorectal

carcinoma. *Acad Radiol* 2012; **19**: 427-433 [PMID: 22265721 DOI: 10.1016/j.acra.2011.12.007]
60 **Maretto I**, Pomerri F, Pucciarelli S, Mescoli C, Belluco E, Burzi S, Rugge M, Muzzio PC, Nitti D. The potential of restaging in the prediction of pathologic response after preoperative chemoradiotherapy for rectal cancer. *Ann Surg Oncol* 2007; **14**: 455-461 [PMID: 17139456 DOI: 10.1245/s10434-006-9269-4]
61 **Chen CC**, Lee RC, Lin JK, Wang LW, Yang SH. How accurate is magnetic resonance imaging in restaging rectal cancer in patients receiving preoperative combined chemoradiotherapy? *Dis Colon Rectum* 2005; **48**: 722-728 [PMID: 15747073 DOI: 10.1007/s10350-004-0851-1]
62 **Kuo LJ**, Chern MC, Tsou MH, Liu MC, Jian JJ, Chen CM, Chung YL, Fang WT. Interpretation of magnetic resonance imaging for locally advanced rectal carcinoma after preoperative chemoradiation therapy. *Dis Colon Rectum* 2005; **48**: 23-28 [PMID: 15690653]
63 **Joye I**, Deroose CM, Vandecaveye V, Haustermans K. The role of diffusion-weighted MRI and (18)F-FDG PET/CT in the prediction of pathologic complete response after radiochemotherapy for rectal cancer: a systematic review. *Radiother Oncol* 2014; **113**: 158-165 [PMID: 25483833 DOI: 10.1016/j.radonc.2014.11.026]
64 **Kim SH**, Lee JM, Gupta SN, Han JK, Choi BI. Dynamic contrast-enhanced MRI to evaluate the therapeutic response to neoadjuvant chemoradiation therapy in locally advanced rectal cancer. *J Magn Reson Imaging* 2014; **40**: 730-737 [PMID: 24307571 DOI: 10.1002/jmri.24387]
65 **Lambrecht M**, Vandecaveye V, De Keyzer F, Roels S, Penninckx F, Van Cutsem E, Filip C, Haustermans K. Value of diffusion-weighted magnetic resonance imaging for prediction and early assessment of response to neoadjuvant radiochemotherapy in rectal cancer: preliminary results. *Int J Radiat Oncol Biol Phys* 2012; **82**: 863-870 [PMID: 21398048 DOI: 10.1016/j.ijrobp.2010.12.063]
66 **Burbach JP**, den Harder AM, Intven M, van Vulpen M, Verkooijen HM, Reerink O. Impact of radiotherapy boost on pathological complete response in patients with locally advanced rectal cancer: a systematic review and meta-analysis. *Radiother Oncol* 2014; **113**: 1-9 [PMID: 25281582 DOI: 10.1016/j.radonc.2014.08.035]
67 **Song I**, Kim SH, Lee SJ, Choi JY, Kim MJ, Rhim H. Value of diffusion-weighted imaging in the detection of viable tumour after neoadjuvant chemoradiation therapy in patients with locally advanced rectal cancer: comparison with T2 weighted and PET/CT imaging. *Br J Radiol* 2012; **85**: 577-586 [PMID: 21343320 DOI: 10.1259/bjr/68424021]
68 **Grosu S**, Schäfer AO, Baumann T, Manegold P, Langer M, Gerstmair A. Differentiating locally recurrent rectal cancer from scar tissue: Value of diffusion-weighted MRI. *Eur J Radiol* 2016; **85**: 1265-1270 [PMID: 27235873 DOI: 10.1016/j.ejrad.2016.04.006]
69 **Bassaneze T**, Gonçalves JE, Faria JF, Palma RT, Waisberg J. Quantitative Aspects of Diffusion-weighted Magnetic Resonance Imaging in Rectal Cancer Response to Neoadjuvant Therapy. *Radiol Oncol* 2017; **51**: 270-276 [PMID: 28959163 DOI: 10.1515/raon-2017-0025]
70 **Lambrecht M**, Deroose C, Roels S, Vandecaveye V, Penninckx F, Sagaert X, van Cutsem E, de Keyzer F, Haustermans K. The use of FDG-PET/CT and diffusion-weighted magnetic resonance imaging for response prediction before, during and after preoperative chemoradiotherapy for rectal cancer. *Acta Oncol* 2010; **49**: 956-963 [PMID: 20586658 DOI: 10.3109/0284186X.2010.498439]
71 **Sun YS**, Zhang XP, Tang L, Ji JF, Gu J, Cai Y, Zhang XY. Locally advanced rectal carcinoma treated with preoperative chemotherapy and radiation therapy: preliminary analysis of diffusion-weighted MR imaging for early detection of tumor histopathologic downstaging. *Radiology* 2010; **254**: 170-178 [PMID: 20019139 DOI: 10.1148/radiol.2541082230]
72 **DeVries AF**, Kremser C, Hein PA, Griebel J, Krezcy A, Ofner D, Pfeiffer KP, Lukas P, Judmaier W. Tumor microcirculation and diffusion predict therapy outcome for primary rectal carcinoma. *Int J Radiat Oncol Biol Phys* 2003; **56**: 958-965 [PMID: 12829130]
73 **Bellomi M**, Petralia G, Sonzogni A, Zampino MG, Rocca A. CT perfusion for the monitoring of neoadjuvant chemotherapy and radiation therapy in rectal carcinoma: initial experience. *Radiology* 2007; **244**: 486-493 [PMID: 17641369 DOI: 10.1148/radiol.2442061189]
74 **Sahani DV**, Kalva SP, Hamberg LM, Hahn PF, Willett CG, Saini S, Mueller PR, Lee TY. Assessing tumor perfusion and treatment response in rectal cancer with multisection CT: initial observations. *Radiology* 2005; **234**: 785-792 [PMID: 15734934 DOI: 10.1148/radiol.2343040286]
75 **Curvo-Semedo L**, Portilha MA, Ruivo C, Borrego M, Leite JS, Caseiro-Alves F. Usefulness of perfusion CT to assess response to neoadjuvant combined chemoradiotherapy in patients with locally advanced rectal cancer. *Acad Radiol* 2012; **19**: 203-213 [PMID: 22130088 DOI: 10.1016/j.acra.2011.10.019]
76 **Hayano K**, Shuto K, Koda K, Yanagawa N, Okazumi S, Matsubara H. Quantitative measurement of blood flow using perfusion CT for assessing clinicopathologic features and prognosis in patients with rectal cancer. *Dis Colon Rectum* 2009; **52**: 1624-1629 [PMID: 19690492 DOI: 10.1007/DCR.0b013e3181afbd79]
77 **Hayano K**, Fujishiro T, Sahani DV, Satoh A, Aoyagi T, Ohira G, Tochigi T, Matsubara H, Shuto K. Computed tomography perfusion imaging as a potential imaging biomarker of colorectal cancer. *World J Gastroenterol* 2014; **20**: 17345-17351 [PMID: 25516645 DOI: 10.3748/wjg.v20.i46.17345]
78 **Lim JS**, Kim D, Baek SE, Myoung S, Choi J, Shin SJ, Kim MJ, Kim NK, Suh J, Kim KW, Keum KC. Perfusion MRI for the prediction of treatment response after preoperative chemoradiotherapy in locally advanced rectal cancer. *Eur Radiol* 2012; **22**: 1693-1700 [PMID: 22427184 DOI: 10.1007/s00330-012-2416-3]
79 **Tong T**, Sun Y, Gollub MJ, Peng W, Cai S, Zhang Z, Gu Y. Dynamic contrast-enhanced MRI: Use in predicting pathological complete response to neoadjuvant chemoradiation in locally advanced rectal cancer. *J Magn Reson Imaging* 2015; **42**: 673-680 [PMID: 25652254 DOI: 10.1002/jmri.24835]
80 **Gollub MJ**, Gultekin DH, Akin O, Do RK, Fuqua JL, Gonen M, Kuk D, Weiser M, Saltz L, Schrag D, Goodman K, Paty P, Guillem J, Nash GM, Temple L, Shia J, Schwartz LH. Dynamic contrast enhanced-MRI for the detection of pathological complete response to neoadjuvant chemotherapy for locally advanced rectal cancer. *Eur Radiol* 2012; **22**: 821-831 [PMID: 22101743 DOI: 10.1007/s00330-011-2321-1]
81 **Willett CG**, Duda DG, di Tomaso E, Boucher Y, Ancukiewicz M, Sahani DV, Lahdenranta J, Chung DC, Fischman AJ, Lauwers GY, Shellito P, Czito BG, Wong TZ, Paulson E, Poleski M, Vujaskovic Z, Bentley R, Chen HX, Clark JW, Jain RK. Efficacy, safety, and biomarkers of neoadjuvant bevacizumab, radiation therapy, and fluorouracil in rectal cancer: a multidisciplinary phase II study. *J Clin Oncol* 2009; **27**: 3020-3026 [PMID: 19470921 DOI: 10.1200/JCO.2008.21.1771]
82 **Janssen MH**, Öllers MC, van Stiphout RG, Riedl RG, van den Bogaard J, Buijsen J, Lambin P, Lammering G. PET-based treatment response evaluation in rectal cancer: prediction and validation. *Int J*

*Radiat Oncol Biol Phys* 2012; **82**: 871-876 [PMID: 21377810 DOI: 10.1016/j.ijrobp.2010.11.038]
83 **Maffione AM**, Chondrogiannis S, Capirci C, Galeotti F, Fornasiero A, Crepaldi G, Grassetto G, Rampin L, Marzola MC, Rubello D. Early prediction of response by ¹F-FDG PET/CT during preoperative therapy in locally advanced rectal cancer: a systematic review. *Eur J Surg Oncol* 2014; **40**: 1186-1194 [PMID: 25060221 DOI: 10.1016/j.ejso.2014.06.005]
84 **Rosenberg R**, Herrmann K, Gertler R, Künzli B, Essler M, Lordick F, Becker K, Schuster T, Geinitz H, Maak M, Schwaiger M, Siewert JR, Krause B. The predictive value of metabolic response to preoperative radiochemotherapy in locally advanced rectal cancer measured by PET/CT. *Int J Colorectal Dis* 2009; **24**: 191-200 [PMID: 19050900 DOI: 10.1007/s00384-008-0616-8]
85 **Vecchio FM**, Valentini V, Minsky BD, Padula GD, Venkatraman ES, Balducci M, Micciché F, Ricci R, Morganti AG, Gambacorta MA, Maurizi F, Coco C. The relationship of pathologic tumor regression grade (TRG) and outcomes after preoperative therapy in rectal cancer. *Int J Radiat Oncol Biol Phys* 2005; **62**: 752-760 [PMID: 15936556 DOI: 10.1016/j.ijrobp.2004.11.017]
86 **Dworak O**, Keilholz L, Hoffmann A. Pathological features of rectal cancer after preoperative radiochemotherapy. *Int J Colorectal Dis* 1997; **12**: 19-23 [PMID: 9112145]
87 **Haberkorn U**, Strauss LG, Dimitrakopoulou A, Engenhart R, Oberdorfer F, Ostertag H, Romahn J, van Kaick G. PET studies of fluorodeoxyglucose metabolism in patients with recurrent colorectal tumors receiving radiotherapy. *J Nucl Med* 1991; **32**: 1485-1490 [PMID: 1714497]
88 **Schillaci O**. Use of dual-point fluorodeoxyglucose imaging to enhance sensitivity and specificity. *Semin Nucl Med* 2012; **42**: 267-280 [PMID: 22681676 DOI: 10.1053/j.semnuclmed.2012.02.003]
89 **Yoon HJ**, Kim SK, Kim TS, Im HJ, Lee ES, Kim HC, Park JW, Chang HJ, Choi HS, Kim DY, Oh JH. New application of dual point 18F-FDG PET/CT in the evaluation of neoadjuvant chemoradiation response of locally advanced rectal cancer. *Clin Nucl Med* 2013; **38**: 7-12 [PMID: 23242038 DOI: 10.1097/RLU.0b013e3182639a58]
90 **Chow FC**, Chok KS. Colorectal liver metastases: An update on multidisciplinary approach. *World J Hepatol* 2019; **11**: 150-172 [PMID: 30820266 DOI: 10.4254/wjh.v11.i2.150]
91 **Mainenti PP**, Mancini M, Mainolfi C, Camera L, Maurea S, Manchia A, Tanga M, Persico F, Addeo P, D'Antonio D, Speranza A, Bucci L, Persico G, Pace L, Salvatore M. Detection of colo-rectal liver metastases: prospective comparison of contrast enhanced US, multidetector CT, PET/CT, and 1.5 Tesla MR with extracellular and reticulo-endothelial cell specific contrast agents. *Abdom Imaging* 2010; **35**: 511-521 [PMID: 19562412 DOI: 10.1007/s00261-009-9555-2]
92 **Mainenti PP**, Romano F, Pizzuti L, Segreto S, Storto G, Mannelli L, Imbriaco M, Camera L, Maurea S. Non-invasive diagnostic imaging of colorectal liver metastases. *World J Radiol* 2015; **7**: 157-169 [PMID: 26217455 DOI: 10.4329/wjr.v7.i7.157]
93 **Koh DM**, Scurr E, Collins D, Kanber B, Norman A, Leach MO, Husband JE. Predicting response of colorectal hepatic metastasis: value of pretreatment apparent diffusion coefficients. *AJR Am J Roentgenol* 2007; **188**: 1001-1008 [PMID: 17377036 DOI: 10.2214/AJR.06.0601]
94 **Cui Y**, Zhang XP, Sun YS, Tang L, Shen L. Apparent diffusion coefficient: potential imaging biomarker for prediction and early detection of response to chemotherapy in hepatic metastases. *Radiology* 2008; **248**: 894-900 [PMID: 18710982 DOI: 10.1148/radiol.2483071407]
95 **Coenegrachts K**, Bols A, Haspeslagh M, Rigauts H. Prediction and monitoring of treatment effect using T1-weighted dynamic contrast-enhanced magnetic resonance imaging in colorectal liver metastases: potential of whole tumour ROI and selective ROI analysis. *Eur J Radiol* 2012; **81**: 3870-3876 [PMID: 22944331 DOI: 10.1016/j.ejrad.2012.07.022]
96 **Nishioka Y**, Yoshioka R, Gonoi W, Sugawara T, Yoshida S, Hashimoto M, Shindoh J. Fluorine-18-fluorodeoxyglucose positron emission tomography as an objective substitute for CT morphologic response criteria in patients undergoing chemotherapy for colorectal liver metastases. *Abdom Radiol (NY)* 2018; **43**: 1152-1158 [PMID: 28815337 DOI: 10.1007/s00261-017-1287-0]
97 **Brenner H**, Kloor M, Pox CP. Colorectal cancer. *Lancet* 2014; **383**: 1490-1502 [PMID: 24225001 DOI: 10.1016/S0140-6736(13)61649-9]
98 **Mahar AL**, Compton C, Halabi S, Hess KR, Weiser MR, Groome PA. Personalizing prognosis in colorectal cancer: A systematic review of the quality and nature of clinical prognostic tools for survival outcomes. *J Surg Oncol* 2017; **116**: 969-982 [PMID: 28767139 DOI: 10.1002/jso.24774]
99 **Du CZ**, Xue WC, Cai Y, Li M, Gu J. Lymphovascular invasion in rectal cancer following neoadjuvant radiotherapy: a retrospective cohort study. *World J Gastroenterol* 2009; **15**: 3793-3798 [PMID: 19673022 DOI: 10.3748/wjg.15.3793]
100 **Huh JW**, Oh BR, Kim HR, Kim YJ. Preoperative carcinoembryonic antigen level as an independent prognostic factor in potentially curative colon cancer. *J Surg Oncol* 2010; **101**: 396-400 [PMID: 20119979 DOI: 10.1002/jso.21495]
101 **Kremser C**, Judmaier W, Hein P, Griebel J, Lukas P, de Vries A. Preliminary results on the influence of chemoradiation on apparent diffusion coefficients of primary rectal carcinoma measured by magnetic resonance imaging. *Strahlenther Onkol* 2003; **179**: 641-649 [PMID: 14628131 DOI: 10.1007/s00066-003-1045-9]
102 **Sun Y**, Tong T, Cai S, Bi R, Xin C, Gu Y. Apparent Diffusion Coefficient (ADC) value: a potential imaging biomarker that reflects the biological features of rectal cancer. *PLoS One* 2014; **9**: e109371 [PMID: 25303288 DOI: 10.1371/journal.pone.0109371]
103 **Heijmen L**, ter Voert EE, Oyen WJ, Punt CJ, van Spronsen DJ, Heerschap A, de Geus-Oei LF, van Laarhoven HW. Multimodality imaging to predict response to systemic treatment in patients with advanced colorectal cancer. *PLoS One* 2015; **10**: e0120823 [PMID: 25831053 DOI: 10.1371/journal.pone.0120823]
104 **Goh V**, Halligan S, Wellsted DM, Bartram CI. Can perfusion CT assessment of primary colorectal adenocarcinoma blood flow at staging predict for subsequent metastatic disease? A pilot study. *Eur Radiol* 2009; **19**: 79-89 [PMID: 18704434 DOI: 10.1007/s00330-008-1128-1]
105 **Yu J**, Xu Q, Huang DY, Song JC, Li Y, Xu LL, Shi HB. Prognostic aspects of dynamic contrast-enhanced magnetic resonance imaging in synchronous distant metastatic rectal cancer. *Eur Radiol* 2017; **27**: 1840-1847 [PMID: 27595835 DOI: 10.1007/s00330-016-4532-y]
106 **Hirashima Y**, Yamada Y, Tateishi U, Kato K, Miyake M, Horita Y, Akiyoshi K, Takashima A, Okita N, Takahari D, Nakajima T, Hamaguchi T, Shimada Y, Shirao K. Pharmacokinetic parameters from 3-Tesla DCE-MRI as surrogate biomarkers of antitumor effects of bevacizumab plus FOLFIRI in colorectal cancer with liver metastasis. *Int J Cancer* 2012; **130**: 2359-2365 [PMID: 21780098 DOI: 10.1002/ijc.26282]
107 **Kim YE**, Joo B, Park MS, Shin SJ, Ahn JB, Kim MJ. Dynamic Contrast-Enhanced Magnetic Resonance

Imaging as a Surrogate Biomarker for Bevacizumab in Colorectal Cancer Liver Metastasis: A Single-Arm, Exploratory Trial. *Cancer Res Treat* 2016; **48**: 1210-1221 [PMID: 26987390 DOI: 10.4143/crt.2015.374]
108 **De Bruyne S**, Van Damme N, Smeets P, Ferdinande L, Ceelen W, Mertens J, Van de Wiele C, Troisi R, Libbrecht L, Laurent S, Geboes K, Peeters M. Value of DCE-MRI and FDG-PET/CT in the prediction of response to preoperative chemotherapy with bevacizumab for colorectal liver metastases. *Br J Cancer* 2012; **106**: 1926-1933 [PMID: 22596235 DOI: 10.1038/bjc.2012.184]
109 **Avallone A**, Aloj L, Caracò C, Delrio P, Pecori B, Tatangelo F, Scott N, Casaretti R, Di Gennaro F, Montano M, Silvestro L, Budillon A, Lastoria S. Early FDG PET response assessment of preoperative radiochemotherapy in locally advanced rectal cancer: correlation with long-term outcome. *Eur J Nucl Med Mol Imaging* 2012; **39**: 1848-1857 [PMID: 23053320 DOI: 10.1007/s00259-012-2229-2]
110 **Muralidharan V**, Kwok M, Lee ST, Lau L, Scott AM, Christophi C. Prognostic ability of 18F-FDG PET/CT in the assessment of colorectal liver metastases. *J Nucl Med* 2012; **53**: 1345-1351 [PMID: 22797376 DOI: 10.2967/jnumed.112.102749]
111 **Lastoria S**, Piccirillo MC, Caracò C, Nasti G, Aloj L, Arrichiello C, de Lutio di Castelguidone E, Tatangelo F, Ottaiano A, Iaffaioli RV, Izzo F, Romano G, Giordano P, Signoriello S, Gallo C, Perrone F. Early PET/CT scan is more effective than RECIST in predicting outcome of patients with liver metastases from colorectal cancer treated with preoperative chemotherapy plus bevacizumab. *J Nucl Med* 2013; **54**: 2062-2069 [PMID: 24136935 DOI: 10.2967/jnumed.113.119909]
112 **Lau LF**, Williams DS, Lee ST, Scott AM, Christophi C, Muralidharan V. Metabolic response to preoperative chemotherapy predicts prognosis for patients undergoing surgical resection of colorectal cancer metastatic to the liver. *Ann Surg Oncol* 2014; **21**: 2420-2428 [PMID: 24595797 DOI: 10.1245/s10434-014-3590-0]
113 **Gulec SA**, Suthar RR, Barot TC, Pennington K. The prognostic value of functional tumor volume and total lesion glycolysis in patients with colorectal cancer liver metastases undergoing 90Y selective internal radiation therapy plus chemotherapy. *Eur J Nucl Med Mol Imaging* 2011; **38**: 1289-1295 [PMID: 21461737 DOI: 10.1007/s00259-011-1758-4]
114 **Giacomobono S**, Gallicchio R, Capacchione D, Nardelli A, Gattozzi D, Lettini G, Molinari L, Mainenti P, Cammarota A, Storto G. F-18 FDG PET/CT in the assessment of patients with unexplained CEA rise after surgical curative resection for colorectal cancer. *Int J Colorectal Dis* 2013; **28**: 1699-1705 [PMID: 23846517 DOI: 10.1007/s00384-013-1747-0]
115 **Marcus C**, Wray R, Taghipour M, Marashdeh W, Ahn SJ, Mena E, Subramaniam RM. JOURNAL CLUB: Value of Quantitative FDG PET/CT Volumetric Biomarkers in Recurrent Colorectal Cancer Patient Survival. *AJR Am J Roentgenol* 2016; **207**: 257-265 [PMID: 27447341 DOI: 10.2214/AJR.15.15806]
116 **Ogawa S**, Lee TM, Nayak AS, Glynn P. Oxygenation-sensitive contrast in magnetic resonance image of rodent brain at high magnetic fields. *Magn Reson Med* 1990; **14**: 68-78 [PMID: 2161986]
117 **Gonçalves MR**, Johnson SP, Ramasawmy R, Pedley RB, Lythgoe MF, Walker-Samuel S. Decomposition of spontaneous fluctuations in tumour oxygenation using BOLD MRI and independent component analysis. *Br J Cancer* 2015; **113**: 1168-1177 [PMID: 26484634 DOI: 10.1038/bjc.2015.270]
118 **Chavhan GB**, Babyn PS, Thomas B, Shroff MM, Haacke EM. Principles, techniques, and applications of T2*-based MR imaging and its special applications. *Radiographics* 2009; **29**: 1433-1449 [PMID: 19755604 DOI: 10.1148/rg.295095034]
119 **Padhani AR**, Krohn KA, Lewis JS, Alber M. Imaging oxygenation of human tumours. *Eur Radiol* 2007; **17**: 861-872 [PMID: 17043737 DOI: 10.1007/s00330-006-0431-y]
120 **Kim MJ**, Lee SJ, Lee JH, Kim SH, Chun HK, Kim SH, Lim HK, Yun SH. Detection of rectal cancer and response to concurrent chemoradiotherapy by proton magnetic resonance spectroscopy. *Magn Reson Imaging* 2012; **30**: 848-853 [PMID: 22503087 DOI: 10.1016/j.mri.2012.02.013]
121 **Wang H**, Wang L, Zhang H, Deng P, Chen J, Zhou B, Hu J, Zou J, Lu W, Xiang P, Wu T, Shao X, Li Y, Zhou Z, Zhao YL. $^{1}$H NMR-based metabolic profiling of human rectal cancer tissue. *Mol Cancer* 2013; **12**: 121 [PMID: 24138801 DOI: 10.1186/1476-4598-12-121]
122 **Dzik-Jurasz AS**, Murphy PS, George M, Prock T, Collins DJ, Swift I, Leach MO, Rowland IJ. Human rectal adenocarcinoma: demonstration of 1H-MR spectra in vivo at 1.5 T. *Magn Reson Med* 2002; **47**: 809-811 [PMID: 11948744 DOI: 10.1002/mrm.10108]
123 **Ganeshan B**, Miles KA. Quantifying tumour heterogeneity with CT. *Cancer Imaging* 2013; **13**: 140-149 [PMID: 23545171 DOI: 10.1102/1470-7330.2013.0015]
124 **Lubner MG**, Smith AD, Sandrasegaran K, Sahani DV, Pickhardt PJ. CT Texture Analysis: Definitions, Applications, Biologic Correlates, and Challenges. *Radiographics* 2017; **37**: 1483-1503 [PMID: 28898189 DOI: 10.1148/rg.2017170056]
125 **Aker M**, Ganeshan B, Afaq A, Wan S, Groves AM, Arulampalam T. Magnetic Resonance Texture Analysis in Identifying Complete Pathological Response to Neoadjuvant Treatment in Locally Advanced Rectal Cancer. *Dis Colon Rectum* 2019; **62**: 163-170 [PMID: 30451764 DOI: 10.1097/DCR.0000000000001224]
126 **Gillies RJ**, Kinahan PE, Hricak H. Radiomics: Images Are More than Pictures, They Are Data. *Radiology* 2016; **278**: 563-577 [PMID: 26579733 DOI: 10.1148/radiol.2015151169]
127 **Stanzione A**, Cuocolo R, Cocozza S, Romeo V, Persico F, Fusco F, Longo N, Brunetti A, Imbriaco M. Detection of Extraprostatic Extension of Cancer on Biparametric MRI Combining Texture Analysis and Machine Learning: Preliminary Results. *Acad Radiol* 2019 [PMID: 30655050 DOI: 10.1016/j.acra.2018.12.025]
128 **Romeo V**, Maurea S, Cuocolo R, Petretta M, Mainenti PP, Verde F, Coppola M, Dell'Aversana S, Brunetti A. Characterization of Adrenal Lesions on Unenhanced MRI Using Texture Analysis: A Machine-Learning Approach. *J Magn Reson Imaging* 2018; **48**: 198-204 [PMID: 29341325 DOI: 10.1002/jmri.25954]
129 **Mainenti PP**, Romano M, Imbriaco M, Camera L, Pace L, D'Antonio D, Bucci L, Galloro G, Salvatore M. Added value of CT colonography after a positive conventional colonoscopy: impact on treatment strategy. *Abdom Imaging* 2005; **30**: 42-47 [PMID: 15647869 DOI: 10.1007/s00261-004-0246-8]
130 **Summers RM**. Polyp size measurement at CT colonography: what do we know and what do we need to know? *Radiology* 2010; **255**: 707-720 [PMID: 20501711 DOI: 10.1148/radiol.10090877]
131 **Song B**, Zhang G, Lu H, Wang H, Zhu W, J Pickhardt P, Liang Z. Volumetric texture features from higher-order images for diagnosis of colon lesions via CT colonography. *Int J Comput Assist Radiol Surg* 2014; **9**: 1021-1031 [PMID: 24696313 DOI: 10.1007/s11548-014-0991-2]
132 **Liu L**, Liu Y, Xu L, Li Z, Lv H, Dong N, Li W, Yang Z, Wang Z, Jin E. Application of texture analysis

based on apparent diffusion coefficient maps in discriminating different stages of rectal cancer. *J Magn Reson Imaging* 2017; **45**: 1798-1808 [PMID: 27654307 DOI: 10.1002/jmri.25460]

133 **Zhu L**, Pan Z, Ma Q, Yang W, Shi H, Fu C, Yan X, Du L, Yan F, Zhang H. Diffusion Kurtosis Imaging Study of Rectal Adenocarcinoma Associated with Histopathologic Prognostic Factors: Preliminary Findings. *Radiology* 2017; **284**: 66-76 [PMID: 27929929 DOI: 10.1148/radiol.2016160094]

134 **Cui C**, Cai H, Liu L, Li L, Tian H, Li L. Quantitative analysis and prediction of regional lymph node status in rectal cancer based on computed tomography imaging. *Eur Radiol* 2011; **21**: 2318-2325 [PMID: 21713526 DOI: 10.1007/s00330-011-2182-7]

135 **De Cecco CN**, Ciolina M, Caruso D, Rengo M, Ganeshan B, Meinel FG, Musio D, De Felice F, Tombolini V, Laghi A. Performance of diffusion-weighted imaging, perfusion imaging, and texture analysis in predicting tumoral response to neoadjuvant chemoradiotherapy in rectal cancer patients studied with 3T MR: initial experience. *Abdom Radiol (NY)* 2016; **41**: 1728-1735 [PMID: 27056748 DOI: 10.1007/s00261-016-0733-8]

136 **Shu Z**, Fang S, Ye Q, Mao D, Cao H, Pang P, Gong X. Prediction of efficacy of neoadjuvant chemoradiotherapy for rectal cancer: the value of texture analysis of magnetic resonance images. *Abdom Radiol (NY)* 2019 [PMID: 30852633 DOI: 10.1007/s00261-019-01971-y]

137 **Palmisano A**, Esposito A, Rancoita PMV, Di Chiara A, Passoni P, Slim N, Campolongo M, Albarello L, Fiorino C, Rosati R, Del Maschio A, De Cobelli F. Could perfusion heterogeneity at dynamic contrast-enhanced MRI be used to predict rectal cancer sensitivity to chemoradiotherapy? *Clin Radiol* 2018; **73**: 911.e1-911.e7 [PMID: 30029837 DOI: 10.1016/j.crad.2018.06.007]

138 **Vidal-Vanaclocha F**. The liver prometastatic reaction of cancer patients: implications for microenvironment-dependent colon cancer gene regulation. *Cancer Microenviron* 2011; **4**: 163-180 [PMID: 21870094 DOI: 10.1007/s12307-011-0084-5]

139 **Wakai T**, Shirai Y, Sakata J, Kameyama H, Nogami H, Iiai T, Ajioka Y, Hatakeyama K. Histologic evaluation of intrahepatic micrometastases in patients treated with or without neoadjuvant chemotherapy for colorectal carcinoma liver metastasis. *Int J Clin Exp Pathol* 2012; **5**: 308-314 [PMID: 22670174]

140 **Rao SX**, Lambregts DM, Schnerr RS, van Ommen W, van Nijnatten TJ, Martens MH, Heijnen LA, Backes WH, Verhoef C, Zeng MS, Beets GL, Beets-Tan RG. Whole-liver CT texture analysis in colorectal cancer: Does the presence of liver metastases affect the texture of the remaining liver? *United European Gastroenterol J* 2014; **2**: 530-538 [PMID: 25452849 DOI: 10.1177/2050640614552463]

141 **Zhang H**, Li W, Hu F, Sun Y, Hu T, Tong T. MR texture analysis: potential imaging biomarker for predicting the chemotherapeutic response of patients with colorectal liver metastases. *Abdom Radiol (NY)* 2019; **44**: 65-71 [PMID: 29967982 DOI: 10.1007/s00261-018-1682-1]

142 **Ahn SJ**, Kim JH, Park SJ, Han JK. Prediction of the therapeutic response after FOLFOX and FOLFIRI treatment for patients with liver metastasis from colorectal cancer using computerized CT texture analysis. *Eur J Radiol* 2016; **85**: 1867-1874 [PMID: 27666629 DOI: 10.1016/j.ejrad.2016.08.014]

143 **Ng F**, Ganeshan B, Kozarski R, Miles KA, Goh V. Assessment of primary colorectal cancer heterogeneity by using whole-tumor texture analysis: contrast-enhanced CT texture as a biomarker of 5-year survival. *Radiology* 2013; **266**: 177-184 [PMID: 23151829 DOI: 10.1148/radiol.12120254]

144 **Miles KA**, Ganeshan B, Griffiths MR, Young RC, Chatwin CR. Colorectal cancer: texture analysis of portal phase hepatic CT images as a potential marker of survival. *Radiology* 2009; **250**: 444-452 [PMID: 19164695 DOI: 10.1148/radiol.2502071879]

145 **Lovinfosse P**, Polus M, Van Daele D, Martinive P, Daenen F, Hatt M, Visvikis D, Koopmansch B, Lambert F, Coimbra C, Seidel L, Albert A, Delvenne P, Hustinx R. FDG PET/CT radiomics for predicting the outcome of locally advanced rectal cancer. *Eur J Nucl Med Mol Imaging* 2018; **45**: 365-375 [PMID: 29046927 DOI: 10.1007/s00259-017-3855-5]

146 **Martens MH**, van Heeswijk MM, van den Broek JJ, Rao SX, Vandecaveye V, Vliegen RA, Schreurs WH, Beets GL, Lambregts DM, Beets-Tan RG. Prospective, Multicenter Validation Study of Magnetic Resonance Volumetry for Response Assessment After Preoperative Chemoradiation in Rectal Cancer: Can the Results in the Literature be Reproduced? *Int J Radiat Oncol Biol Phys* 2015; **93**: 1005-1014 [PMID: 26581139 DOI: 10.1016/j.ijrobp.2015.09.008]

147 **Neri E**, Guidi E, Pancrazi F, Castagna M, Castelluccio E, Balestri R, Buccianti P, Masi L, Falcone A, Manfredi B, Faggioni L, Bartolozzi C. MRI tumor volume reduction rate vs tumor regression grade in the pre-operative re-staging of locally advanced rectal cancer after chemo-radiotherapy. *Eur J Radiol* 2015; **84**: 2438-2443 [PMID: 26462793 DOI: 10.1016/j.ejrad.2015.08.008]

148 **Atasoy G**, Arslan NC, Elibol FD, Sagol O, Obuz F, Sokmen S. Magnetic resonance-based pelvimetry and tumor volumetry can predict surgical difficulty and oncologic outcome in locally advanced mid-low rectal cancer. *Surg Today* 2018; **48**: 1040-1051 [PMID: 29961173 DOI: 10.1007/s00595-018-1690-3]

149 **Okuno T**, Kawai K, Koyama K, Takahashi M, Ishihara S, Momose T, Morikawa T, Fukayama M, Watanabe T. Value of FDG-PET/CT Volumetry After Chemoradiotherapy in Rectal Cancer. *Dis Colon Rectum* 2018; **61**: 320-327 [PMID: 29360680 DOI: 10.1097/DCR.0000000000000959]

150 **Pomerri F**, Pucciarelli S, Gennaro G, Maretto I, Nitti D, Muzzio PC. Comparison between CT volume measurement and histopathological assessment of response to neoadjuvant therapy in rectal cancer. *Eur J Radiol* 2012; **81**: 3918-3924 [PMID: 22902408 DOI: 10.1016/j.ejrad.2012.04.038]

151 **Kim S**, Han K, Seo N, Kim HJ, Kim MJ, Koom WS, Ahn JB, Lim JS. T2-weighted signal intensity-selected volumetry for prediction of pathological complete response after preoperative chemoradiotherapy in locally advanced rectal cancer. *Eur Radiol* 2018; **28**: 5231-5240 [PMID: 29858637 DOI: 10.1007/s00330-018-5520-1]

152 **Gollub MJ**, Hotker AM, Woo KM, Mazaheri Y, Gonen M. Quantitating whole lesion tumor biology in rectal cancer MRI: taking a lesson from FDG-PET tumor metrics. *Abdom Radiol (NY)* 2018; **43**: 1575-1582 [PMID: 29159523 DOI: 10.1007/s00261-017-1389-8]

153 **Koh TS**, Ng QS, Thng CH, Kwek JW, Kozarski R, Goh V. Primary colorectal cancer: use of kinetic modeling of dynamic contrast-enhanced CT data to predict clinical outcome. *Radiology* 2013; **267**: 145-154 [PMID: 23297334 DOI: 10.1148/radiol.12120186]

154 **Hakimé A**, Peddi H, Hines-Peralta AU, Wilcox CJ, Kruskal J, Lin S, de Baere T, Raptopoulos VD, Goldberg SN. CT perfusion for determination of pharmacologically mediated blood flow changes in an animal tumor model. *Radiology* 2007; **243**: 712-719 [PMID: 17517930 DOI: 10.1148/radiol.2433052048]

155 **van Laarhoven HW**, de Geus-Oei LF, Wiering B, Lok J, Rijpkema M, Kaanders JH, Krabbe PF, Ruers T, Punt CJ, van der Kogel AJ, Oyen WJ, Heerschap A. Gadopentetate dimeglumine and FDG uptake in liver metastases of colorectal carcinoma as determined with MR imaging and PET. *Radiology* 2005; **237**: 181-188 [PMID: 16183932 DOI: 10.1148/radiol.2371041397]

156 **Goh V**, Engledow A, Rodriguez-Justo M, Shastry M, Peck J, Blackman G, Endozo R, Taylor S, Halligan S, Ell P, Groves AM. The flow-metabolic phenotype of primary colorectal cancer: assessment by integrated 18F-FDG PET/perfusion CT with histopathologic correlation. *J Nucl Med* 2012; **53**: 687-692 [PMID: 22454485 DOI: 10.2967/jnumed.111.098525]

157 **Janssen MH**, Aerts HJ, Buijsen J, Lambin P, Lammering G, Öllers MC. Repeated positron emission tomography-computed tomography and perfusion-computed tomography imaging in rectal cancer: fluorodeoxyglucose uptake corresponds with tumor perfusion. *Int J Radiat Oncol Biol Phys* 2012; **82**: 849-855 [PMID: 21392896 DOI: 10.1016/j.ijrobp.2010.10.029]

158 **Gu J**, Khong PL, Wang S, Chan Q, Wu EX, Law W, Liu RK, Zhang J. Dynamic contrast-enhanced MRI of primary rectal cancer: quantitative correlation with positron emission tomography/computed tomography. *J Magn Reson Imaging* 2011; **33**: 340-347 [PMID: 21274975 DOI: 10.1002/jmri.22405]

159 **Fischer MA**, Vrugt B, Alkadhi H, Hahnloser D, Hany TF, Veit-Haibach P. Integrated ¹F-FDG PET/perfusion CT for the monitoring of neoadjuvant chemoradiotherapy in rectal carcinoma: correlation with histopathology. *Eur J Nucl Med Mol Imaging* 2014; **41**: 1563-1573 [PMID: 24760269 DOI: 10.1007/s00259-014-2752-4]

160 **Wu J**, Tha KK, Xing L, Li R. Radiomics and radiogenomics for precision radiotherapy. *J Radiat Res* 2018; **59**: i25-i31 [PMID: 29385618 DOI: 10.1093/jrr/rrx102]

161 **García-Figueiras R**, Baleato-González S, Padhani AR, Luna-Alcalá A, Marhuenda A, Vilanova JC, Osorio-Vázquez I, Martínez-de-Alegría A, Gómez-Caamaño A. Advanced Imaging Techniques in Evaluation of Colorectal Cancer. *Radiographics* 2018; **38**: 740-765 [PMID: 29676964 DOI: 10.1148/rg.2018170044]

162 **Horvat N**, Veeraraghavan H, Pelossof RA, Fernandes MC, Arora A, Khan M, Marco M, Cheng CT, Gonen M, Golia Pernicka JS, Gollub MJ, Garcia-Aguillar J, Petkovska I. Radiogenomics of rectal adenocarcinoma in the era of precision medicine: A pilot study of associations between qualitative and quantitative MRI imaging features and genetic mutations. *Eur J Radiol* 2019; **113**: 174-181 [PMID: 30927944 DOI: 10.1016/j.ejrad.2019.02.022]

163 **Shin YR**, Kim KA, Im S, Hwang SS, Kim K. Prediction of KRAS Mutation in Rectal Cancer Using MRI. *Anticancer Res* 2016; **36**: 4799-4804 [PMID: 27630331 DOI: 10.21873/anticanres.11039]

164 **Mao W**, Zhou J, Zhang H, Qiu L, Tan H, Hu Y, Shi H. Relationship between KRAS mutations and dual time point <sup>18</sup>F-FDG PET/CT imaging in colorectal liver metastases. *Abdom Radiol (NY)* 2019; **44**: 2059-2066 [PMID: 30143816 DOI: 10.1007/s00261-018-1740-8]

165 **Chen SW**, Chiang HC, Chen WT, Hsieh TC, Yen KY, Chiang SF, Kao CH. Correlation between PET/CT parameters and KRAS expression in colorectal cancer. *Clin Nucl Med* 2014; **39**: 685-689 [PMID: 24978328 DOI: 10.1097/RLU.0000000000000481]

166 **Miles KA**, Ganeshan B, Rodriguez-Justo M, Goh VJ, Ziauddin Z, Engledow A, Meagher M, Endozo R, Taylor SA, Halligan S, Ell PJ, Groves AM. Multifunctional imaging signature for V-KI-RAS2 Kirsten rat sarcoma viral oncogene homolog (KRAS) mutations in colorectal cancer. *J Nucl Med* 2014; **55**: 386-391 [PMID: 24516257 DOI: 10.2967/jnumed.113.120485]

World Journal of Gastroenterology

Submit a Manuscript: https://www.f6publishing.com

*World J Gastroenterol* 2019 September 21; 25(35): 5257-5265

DOI: 10.3748/wjg.v25.i35.5257

ISSN 1007-9327 (print) ISSN 2219-2840 (online)

MINIREVIEWS

# Sarcopenia and cognitive impairment in liver cirrhosis: A viewpoint on the clinical impact of minimal hepatic encephalopathy

Silvia Nardelli, Stefania Gioia, Jessica Faccioli, Oliviero Riggio, Lorenzo Ridola

**ORCID number:** Silvia Nardelli (0000-0002-7038-9539); Stefania Gioia (0000-0002-3940-4390); Jessica Faccioli (0000-0001-6960-9701); Oliviero Riggio (0000-0000-2241-3223); Lorenzo Ridola (0000-0002-8596-2609).

**Author contributions:** Nardelli S and Ridola L drafted the article; Nardelli S, Riggio O and Ridola L contributed to critical revision of the article for important intellectual content; Gioia S and Faccioli J contributed to acquisition of data; Ridola L contributed to conception and design; Riggio O and Ridola L contributed to final approval of the article.

**Conflict-of-interest statement:** There are no conflicts of interest arising from this work.



**Manuscript source**: Invited manuscript

**Received:** July 2, 2019
**Peer-review started:** July 2, 2019
**First decision:** August 2, 2019

**Silvia Nardelli, Stefania Gioia, Jessica Faccioli, Oliviero Riggio, Lorenzo Ridola,** Department of Translational and Precision Medicine, "Sapienza" University of Rome, Rome 00185, Italy

**Corresponding author:** Lorenzo Ridola, MD, PhD, Doctor, Department of Translational and Precision Medicine, "Sapienza" University of Rome, viale dell'Università 37, Rome 00185, Italy. lorenzo.ridola@uniroma1.it
**Telephone:** +39-773-6556155
**Fax:** +39-773-6556155

## Abstract

Minimal hepatic encephalopathy (MHE) represents the mildest type of hepatic encephalopathy (HE). MHE is considered as a preclinical stage of HE and is part of a wide spectrum of typical neurocognitive alterations characteristic of patients with liver cirrhosis, particularly involving the areas of attention, alertness, response inhibition, and executive functions. MHE can be detected by testing the patients' psychometric performance, attention, working memory, psychomotor speed, and visuospatial ability, as well as by means of electrophysiological and other functional brain measures. MHE is very frequent, affecting from 20% up to 80% of patients tested, depending of the diagnostic tools used. Although subclinical, MHE is considered to be clinically relevant. In fact, MHE has been related to the patients' falls, fitness to drive, and working ability. As a consequence, MHE affects the patients and caregivers lives by altering their quality of life and even their socioeconomic status. Recently sarcopenia, a very common condition in patients with advanced liver disease, has been shown to be strictly related to both minimal and overt HE. Aim of this review is to summarize the most recently published evidences about the emerging relationship between sarcopenia and cognitive impairment in cirrhotic patients and provide suggestions for future research.

**Key words:** Minimal hepatic encephalopathy; Cognitive impairment; Sarcopenia; Muscle alterations; Cirrhosis



**Core tip:** Minimal hepatic encephalopathy (MHE) represents the mildest type of hepatic encephalopathy, is very frequent, affecting from 20% up to 80% of patients tested, depending of the diagnostic tools used and has been related to the patients' falls, fitness to drive, and working ability. As a consequence, MHE affects the patients and caregivers lives by altering their quality of life and even their socioeconomic status. Sarcopenia has

**Revised:** August 8, 2019
**Accepted:** August 24, 2019
**Article in press:** August 2, 2019
**Published online:** September 21, 2019

**P-Reviewer:** Li LJ, Lv Y, Shi YJ
**S-Editor:** Yan JP
**L-Editor:** A
**E-Editor:** Ma YJ

been recently proposed as a risk factor for both minimal and overt Hepatic Encephalopathy. Aim of this review is to summarize the most recently published evidences about the emerging relationship between sarcopenia and cognitive impairment.

**Citation:** Nardelli S, Gioia S, Faccioli J, Riggio O, Ridola L. Sarcopenia and cognitive impairment in liver cirrhosis: A viewpoint on the clinical impact of minimal hepatic encephalopathy. *World J Gastroenterol* 2019; 25(35): 5257-5265
**URL**: https://www.wjgnet.com/1007-9327/full/v25/i35/5257.htm
**DOI**: https://dx.doi.org/10.3748/wjg.v25.i35.5257

## THE BURDEN OF MINIMAL HEPATIC ENCEPHALOPATHY IN LIVER CIRRHOSIS

Hepatic encephalopathy (HE) is a complex neurological syndrome caused by liver failure and shunting of the portal blood into the systemic circulation. HE produces a wide and complex spectrum of nonspecific neurological and psychiatric manifestations[1]. In its milder expression, the so called minimal HE (MHE)[2,3], the manifestations are subclinical and detectable only by means of psychometric testing as well as electrophysiological and other functional brain measures[4,5]. Depending on the population studied and the diagnostic tool used, MHE ranges between 20% and 80% and thus, may be considered as the most complication of liver cirrhosis[6-11]. Although subclinical, MHE involves the areas of attention, alertness, response inhibition, and executive functions as well as the working memory, psychomotor speed, and visuospatial ability[12-15].

Depending on the population studied and the diagnostic tool used, MHE can be detected in 20%-80% of patients with cirrhosis, MHE is considered as a pre-clinical stage of HE and is part of a wide spectrum of typical neurocognitive alterations in liver cirrhosis, particularly involving the areas of attention, alertness, response inhibition, and executive functions. Although these typical characteristics of MHE reduce the safety and quality of life of patients with cirrhosis together with their caregivers, they are difficult to detect from the clinical point of view. The optimal diagnostic criteria for MHE remain controversial, also because an essential condition for MHE diagnosis is the correct standardization of the tests used by age, education and also employment of the patient. To overcome the difficulties in the execution of complex psychometric batteries, which may require specialist staff for their administration, are time and money consuming, other techniques have been proposed, such as the critical flicker frequency, the smooth pursuit eye movement, and the use of cognitive evoked potentials. Computerized psychometric tests, including the scan test and the inhibitory control test (ICT), which may be more specific and repeatable, have also been proposed. An electroencephalogram is also useful for detecting conditions MHE, especially if a spectral analysis is carried out. A comprehensive summary on the clinical manifestations and diagnosis of MHE has been recently published by our group[12,16].

Low quality of life, falls, sleep disorders, erectile dysfunction in males, impairment in fitness to drive and car accident incidence have been found to be more frequent in patients with MHE than in those without. Moreover, MHE by reducing the patients' working capacity, may affect their socioeconomic status[16,17]. Finally, MHE is a clear risk factor for the development of overt HE and for its recurrence, leading to frequent hospitalization of the patients. In summary, MHE, despite subclinical is a burden for the patients and their caregivers, which results in the use of more health care resource than other manifestations of liver disease[6,18-21]. Recently, a strong statistical correlation between muscle alterations, sarcopenia and myosteatosis, and MHE was found[22-25]. A first consequence of this observation is that muscle alterations should be investigated in all patients with cirrhosis and cognitive impairment.

## PREVALENCE AND CAUSE OF SARCOPENIA IN LIVER CIRRHOSIS

In cirrhotic patients, sarcopenia has been assessed by different techniques such as anthropometry (Triceps-Skinfold-Thickness or Mid-Arm-Muscle-Circumference), the

bioelectrical impedance analysis and the dual-energy X-ray. The functional consequence of sarcopenia is estimable by the Hand Grip or other more composite tests such the six-minute walk test[26-30]. Moreover, some evidences showed that patients with cirrhosis may develop simultaneously loss of skeletal muscle and gain of intermuscular and intramuscular fat, denominated 'myosteatosis'[31].

The gold standard to quantify muscle mass is to date represented by the computed tomography (CT) and magnetic resonance image (MRI) analysis[32-34]. The CT scan, by using muscle attenuation, is indirectly able to measure muscle fat infiltration and to add informations not only on quantity but also on the quality of muscle tissue[31,35]. MRI is able to quantify the muscle mass and the fat free muscle mass[36]. These diagnostic tools are certainly limited by cost, radiation exposure and logistic concerns[37]. Nevertheless, a CT or MR scan is often performed in cirrhotic patient for clinical reasons, such as the suspicion of hepatocellular carcinoma or portal vein thrombosis. In these patients, sarcopenia can be easily assessed by validated softwares such as SliceOmatic V4.2 software (Tomovision, Montreal, Quebec, Canada), which enables specific tissue demarcation by using previously reported Hounsfield unit (HU) thresholds[38], as shown in Figure 1. Skeletal muscle is identified and quantified by HU thresholds of -29 to +150 as previously described[34] and with these specific HU thresholds, measurements of the SMI are not influenced by the presence of ascites. Cross-sectional areas ($cm^2$) were automatically computed by summing tissue pixels and multiplying by pixel surface area. Muscle cross-sectional area was normalized for stature ($cm^2/m^2$) to obtain the L3 Skeletal Muscle Index (L3 SMI). Sarcopenia was defined according to previously validated cutoff values in cirrhotic patients: L3 SMI: < 39 $cm^2/m^2$ for females and < 50 $cm^2/m^2$ for males[26]. The following HU thresholds were used for adipose tissues: -190 to -30 for subcutaneous and intermuscular adipose tissue[39], and -150 to -50 for visceral adipose tissue[40].

Since muscle attenuation indirectly measures fat infiltration in muscles, mean muscle attenuation in HU was reported for the entire muscle area from the same image used to calculate L3 SMI. To define myosteatosis, we used cutoff values that have been previously associated with mortality: < 41 HU in patients with a body mass index (BMI) up to 24.9, and < 33 in those with a BMI ≥ 25[27,31].

Using these cut off, sarcopenia, with a prevalence ranging between 65 and 90%, has to be considered a very common condition in patients with advanced liver disease[41]. The severity and prevalence of sarcopenia correlates with Child-Pugh's Class[42] and, when added to model for end-stage liver disease (MELD) score, sarcopenia has been shown to improve the prediction of the patients' survival[22,23]. Sarcopenia contributes to fatigue, limits exercise tolerance and may have a heavy burden on performance status and activities of daily living[24]. Multiple factors are involved in sarcopenia development. In liver disease dietary intake may be inadequate to the energy expenditure; nutrient absorption compromised and substrate utilization impaired[25]. Moreover, malabsorption, altered metabolism, hormonal factors, hyperammonemia, may also play a role.

## SARCOPENIA AND HE

In Addition to the prognostic impact[32,43,44], sarcopenia is related to several complications of cirrhosis[45-49], including overt HE[22-24,38,50]. The pathophysiological background supporting the relationship between muscle depletion and HE origins from the involvement of muscle tissue in ammonia metabolism and trafficking (Figure 2). Ammonia plays a central role in the pathogenesis of cognitive impairment of cirrhosis. Its concentrations is increased because of the inability of the impaired liver in removing ammonia through urea synthesis due to liver failure and porto-systemic shunts. Skeletal muscle may plays a compensatory role in ammonia clearance[49,50] through glutamine-synthase, which metabolize ammonia into glutamine. Consequently, a muscle depletion may favor the ammonia accumulation. Furthermore, any catabolic increases the glutamine release from muscle. Glutamine metabolism in the small intestine and the kidney to glutamic acid and ammonia, may contribute to the appearance of ammonia in portal circulation where, due to liver failure and the shunts may lead the whole-body ammonia availability[49,51]. Moreover, on the other hand, ammonia impairs muscle protein synthesis in part through the up regulation of myostatin production[52], that is upregulated because skeletal muscle removes large quantities of ammonia from the circulation[53]. Finally, the mitochondrial dysfunction increases reactive oxygen species bringing to autophagy and muscle damage. Therefore, hyperammonemia may be considered the trigger of a vicious circle: By one side the occurrence of hyperammonemia is a consequence of sarcopenia due to the inability of the depleted muscle to metabolize ammonia, on the

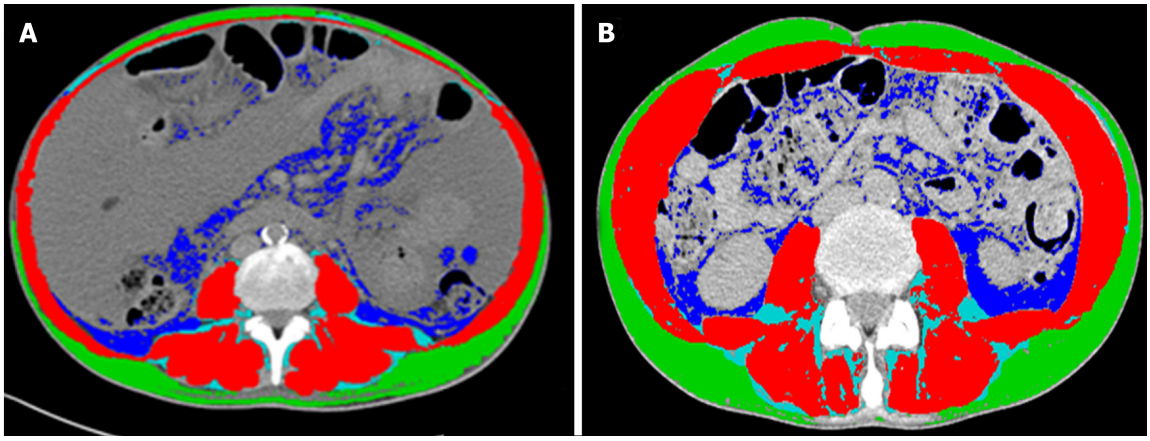


**Figure 1 Computed tomography images used for the muscularity assessment of patients with cirrhosis.** Comparison of two cirrhotic patients with (A) and without (B) sarcopenia. Muscle mass is highlighted in red, intra and intermuscular fat in light blue, subcutaneous fat in green and visceral fat in blue.

other side, the increase in ammonia concentrations, through the above processes, induces further muscle wasting.

The studies in which the possible association between muscle alterations and MHE was evaluated are summarized in Table 1. In the first one[47], conducted on 300 hospitalized cirrhotic patients, muscle depletion was evaluated with anthropometry, muscle function with handgrip strength and minimal HE with psychometric tests. At multivariate analysis, muscle depletion was significantly and independently associated with MHE. In another study MHE was found to be higher in patients with sarcopenia than in those without and sarcopenia was an independent predictor of MHE at multivariate analysis[54]. In a further study, a multivariate analysis showed that the time needed to perform number connection test A (one of the tests used to detect MHE) was independently correlated to age, Child Pugh class, malnutrition and diabetes[55]. None of the above studies used the CT scan to determine muscle quantity and quality. This limitation was recently filled by a prospective study which used CT scan for the quantitative estimation of sarcopenia and myosteatosis and the Phychometric Hepatic Encephalopathy Score (PHES) for the estimation of the cognitive impairment in order to investigate the link between muscle quantitative alteration and MHE. In this study both myosteatosis and sarcopenia were strongly related to presence of MHE as well as to the development of overt HE during the follow-up[46]. In particular, a direct correlation was found between the muscle quantity estimated by the SMI and the psychometric performance estimated by the PHES (more muscle = better psychometric performance) while SMI was inversely correlated to ammonia levels. These correlations support the possibility that a reduced muscle mass (and muscle quality) is able at least to contribute to higher ammonia levels and to the cognitive impairment observable in cirrhotic patients. A further evidence on the importance of muscle alteration on both ammonia level and HE is provided by a recently published paper on the modification of muscle mass and the evolution of HE after a transjugular intrahepatic portosystemic shunt (TIPS)[56,57]. TIPS can ameliorate the muscle mass, at least in some patients. In this setting we described that the patients with a muscle wasting amelioration after TIPS placement obtained an improvement of MHE and a lower number of episodes of overt HE in the follow up supporting a causal relationship between muscle alterations and cognitive impairment. Ammonia was also reduced in the patients with muscle mass amelioration and a significant correlation between muscle and ammonia modifications after TIPS was observed. The last study, recently published by Tapper *et al*[58] evaluated the cognitive impairment with the ICT, a computerized test previously validated on cirrhotic patients. In this study, hand grip correlated strongly with skeletal muscle area and mildly with ICT performance.

## HYPOTHESIS AND FUTURE RESEARCH

Given the above background, a possible hypothetical point of view is that at least some of the clinical effects attributed until now to the presence of MHE may be partially or totally explained by the contemporary presence of sarcopenia. The falls, which have been shown to be more frequent in the cirrhotic patients with MHE could be due to sarcopenia and to their functional consequences. The same could be

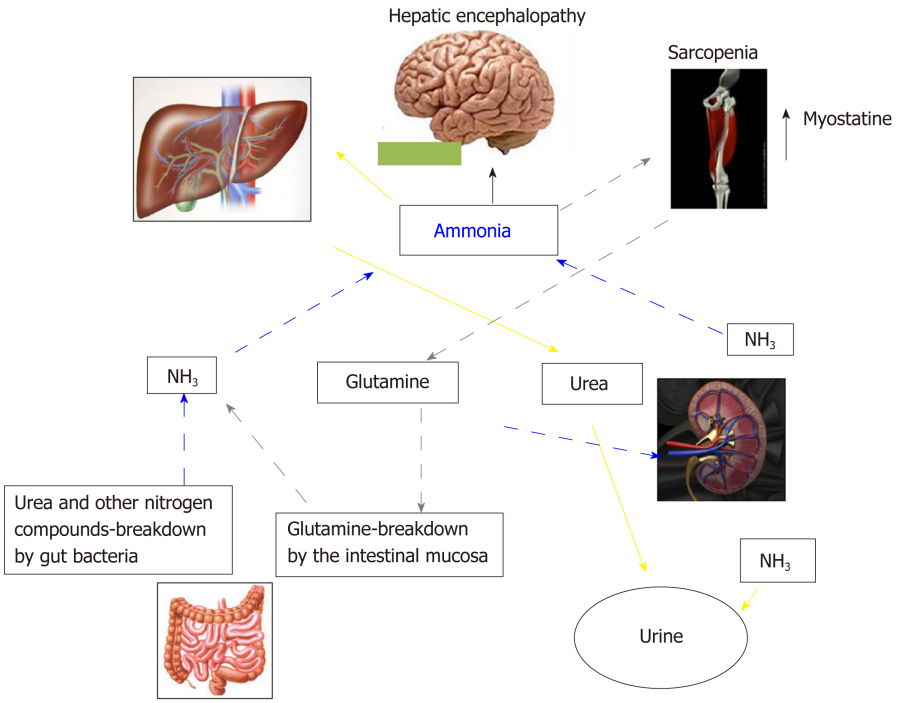


**Figure 2 Inter-organ ammonia metabolism showing sites of ammonia generation and disposal.** Yellow arrows indicate the ammonia removed by the urea-cycle and disposed in urine. Grey pointed arrows indicate ammonia disposed as glutamine in muscle, which is then broken down in the small intestine to ammonia. This pattern of ammonia disposal does not lead to a net ammonia removal. Ammonia may be also produced by glutamine breakdown in the kidney and by urea and other nitrogen compounds breakdown in the large intestine (blue dashed arrows).

hypothesized for the reduced driven capacity and car accidents. Even the reduced working capacity could be considered as an outcome of muscle alterations. This hypothesis should be supported by studies in which the contemporary assessment of the quantity, quality and functionality of the muscle mass are coupled with the assessment of the cognitive impairment. Multivariate analysis should be used to distinguish, at least statistically, the relative role of these two components, which are expected to covariate. This point of view, which must be supported by adequate observations could open a new perspective on the evaluation of the patients' risk.

Moreover, recent studies showed an improvement of the nutritional assessment after physical exercise in patients with cirrhosis[59-61], but no study investigated the modifications of cognitive impairment after physical activity. Thus, the management of cirrhotic patients could be also seen from a new perspective. In fact, the amelioration of nutritional status may be a possible goal to decrease the prevalence of MHE and its clinical consequences.

**Table 1 Studies evaluating the relationship between muscle alterations and minimal hepatic encephalopathy in cirrhosis**

| First author (year) | Number of patients | Methods to identify sarcopenia and/or myosteatosis | Tests to detect minimal hepatic encephalopathy | Results |
|---|---|---|---|---|
| Merli *et al*[23], (2013) | 300 hospitalized cirrhotics | Anthropometric measurements (MAMC) and hand grip strenghth | PHES battery (NCT-A, NCT-B, LT, SDT, LTT): 5 paper pencil tests | MHE prevalence was higher in pts with malnutrition compared to those without (49% *vs* 30%, $P < 0.001$). At multivariate analysis, only protein malnutrition (OR 2.15, 95%CI: 1.1-4.1, $P = 00.02$) and hyponatremia (OR 4.6, 95%CI: 1.9-9, $P = 00.01$) were independent predictors of MHE. Venous blood ammonia levels resulted significantly higher in patients with *vs* those without muscle depletion (85 ± 64 *vs* 61 ± 46 μg/dL, $P = 0.025$) and in patients with *vs* those without a decreased muscle strength (81 ± 62 μg/dL *vs* 63 ± 45 μg/dL, $P = 0.047$) |
| Hanai *et al*[56], (2017) | 120 cirrhotic patients | Bioelectrical impedance analysis and hand grip strenght | NCT-A, NCT-B, DST, BDT | The prevalence of MHE was higher in patients with sarcopenia than in those without sarcopenia ($P = 0.01$). In the multivariate analysis, serum BCAA levels (OR = 2.98, 95%CI: 1.08-8.34, $P = 0.03$) and sarcopenia (OR 3.31, 95%CI: 1.19-9.42, $P = 0.02$) were found to be associated with MHE. Ammonia levels were similar in sarcopenic and non-sarcopenic patients |
| Kalaitzakis *et al*[57], (2007) | 128 cirrhotic patients | BMI, weight loss, MAMC and triceps skinfold | NCT-A, NCT-B | Multivariate analysis showed that the time needed to perform number connection test was independently associated to age, the Child–Pugh score, diabetes and malnutrition ($P < 0.05$). Plasma ammonium ion was also related to BMI ($r = 0.26$, $P = 0.006$) and to muscle mass expressed as mid-arm muscle circumference ($r = 0.28$, $P = 0.003$) but not to fat mass expressed as triceps skin-fold thickness ($r = 0.02$, NS) |
| Nardelli *et al*[22], (2019) | 89 cirrhotic patients | CT scan to evaluate sarcopenia and myosteatosis | PHES battery (NCT-A, NCT-B, LT, SDT, LTT): 5 paper pencil tests | Both myosteatosis (62.5% *vs* 12.5%, $P < 0.001$) and sarcopenia (84% *vs* 31%, $P < 0.001$) were more frequent in patients with MHE. At multivariate analysis, the variables independently associated to the presence of MHE were: sarcopenia, previous overt HE and myosteatosis. Venous ammonia was significantly higher in patients with sarcopenia (62.6 ± 17.7 μg/dL *vs* 41.4 ± 16.1 μg/dL, $P < 0.001$) and in patients with myosteatosis (65.2 ± 19.2 μg/dL *vs* 46.7 ± 17.1 μg/dL, $P < 0.001$) and inversely correlated to both parameters |

| | | | | |
|---|---|---|---|---|
| Gioia *et al*[25], (2019) | 27 cirrhotic patients submitted to TIPS | CT scan to evaluate sarcopenia and myosteatosis before and after TIPS | PHES battery (NCT-A, NCT-B, LT, SDT, LTT): 5 paper pencil tests | PHES and ammonia significantly improved in the patients with amelioration in Skeletal Muscle Index (SMI) > 10% ($n$ = 16) and not in those without ($n$ = 11) (PHES: -1.6 ± 2 *vs* -4.8 ± 2.1, $P$ = 0.0005; ammonia: 48.5 ± 28.7 μg/dL *vs* 96 ± 31.5 μg/dL, $P$ = 0.0004). Moreover, the prevalence of minimal HE (12.5% *vs* 73%, $P$ = 0.001) was significantly reduced in patients with muscle improvement |
| Tapper *et al*[58], (2019) | 106 cirrhotic patients | Anthropometric measurements (MAMA), hand grip strenght and CT scan to evaluate muscle assesment | ICT | Hand grip correlated strongly with skeletal muscle area (correlation coefficient 0.64, $P$ < 0.001) and mildly with ICT performance (0.34, $P$ = 0.002) |

MHE: Minimal hepatic encephalopathy; HE: Hepatic encephalopathy; NCT-A: Number connection test part A; NCT-B: Number connection test part B; LTT: Line tracing test; SDT: Symbol digit test; ICT: Inhibitory control test; TIPS: Transjugular intrahepatic portosystemic shunt; PHES: Phychometric Hepatic Encephalopathy Score; CT: Computed tomography; NS: Not significant; BMI: Body mass index.

## REFERENCES


1 **Vilstrup H**, Amodio P, Bajaj J, Cordoba J, Ferenci P, Mullen KD, Weissenborn K, Wong P. Hepatic encephalopathy in chronic liver disease: 2014 Practice Guideline by the American Association for the Study of Liver Diseases and the European Association for the Study of the Liver. *Hepatology* 2014; **60**: 715-735 [PMID: 25042402 DOI: 10.1002/hep.27210]

2 **Gitlin N**, Lewis DC, Hinkley L. The diagnosis and prevalence of subclinical hepatic encephalopathy in apparently healthy, ambulant, non-shunted patients with cirrhosis. *J Hepatol* 1986; **3**: 75-82 [PMID: 3745889 DOI: 10.1016/S0168-8278(86)80149-0]

3 **Lockwood AH**. "What's in a name?" Improving the care of cirrhotics. *J Hepatol* 2000; **32**: 859-861 [PMID: 10845675 DOI: 10.1016/S0168-8278(00)80257-3]

4 **Amodio P**, Montagnese S, Gatta A, Morgan MY. Characteristics of minimal hepatic encephalopathy. *Metab Brain Dis* 2004; **19**: 253-267 [PMID: 15554421 DOI: 10.1023/B:MEBR.0000043975.01841.de]

5 **McCrea M**, Cordoba J, Vessey G, Blei AT, Randolph C. Neuropsychological characterization and detection of subclinical hepatic encephalopathy. *Arch Neurol* 1996; **53**: 758-763 [PMID: 8759982 DOI: 10.1001/archneur.1996.00550080076015]

6 **Bajaj JS**, Wade JB, Gibson DP, Heuman DM, Thacker LR, Sterling RK, Stravitz RT, Luketic V, Fuchs M, White MB, Bell DE, Gilles H, Morton K, Noble N, Puri P, Sanyal AJ. The multi-dimensional burden of cirrhosis and hepatic encephalopathy on patients and caregivers. *Am J Gastroenterol* 2011; **106**: 1646-1653 [PMID: 21556040 DOI: 10.1038/ajg.2011.157]

7 **Groeneweg M**, Moerland W, Quero JC, Hop WC, Krabbe PF, Schalm SW. Screening of subclinical hepatic encephalopathy. *J Hepatol* 2000; **32**: 748-753 [PMID: 10845661 DOI: 10.1016/S0168-8278(00)80243-3]

8 **Saxena N**, Bhatia M, Joshi YK, Garg PK, Tandon RK. Auditory P300 event-related potentials and number connection test for evaluation of subclinical hepatic encephalopathy in patients with cirrhosis of the liver: A follow-up study. *J Gastroenterol Hepatol* 2001; **16**: 322-327 [PMID: 11339425 DOI: 10.1046/j.1440-1746.2001.02388.x]

9 **Schomerus H**, Hamster W. Quality of life in cirrhotics with minimal hepatic encephalopathy. *Metab Brain Dis* 2001; **16**: 37-41 [PMID: 11726087 DOI: 10.1023/A:1011610427843]

10 **Sharma P**, Sharma BC, Puri V, Sarin SK. Critical flicker frequency: Diagnostic tool for minimal hepatic encephalopathy. *J Hepatol* 2007; **47**: 67-73 [PMID: 17459511 DOI: 10.1016/j.jhep.2007.02.022]

11 **Bajaj JS**. Management options for minimal hepatic encephalopathy. *Expert Rev Gastroenterol Hepatol* 2008; **2**: 785-790 [PMID: 19090738 DOI: 10.1586/17474124.2.6.785]

12 **Ridola L**, Cardinale V, Riggio O. The burden of minimal hepatic encephalopathy: From diagnosis to therapeutic strategies. *Ann Gastroenterol* 2018; **31**: 151-164 [PMID: 29507462 DOI: 10.20524/aog.2018.0232]

13 **Bajaj JS**, Saeian K, Verber MD, Hischke D, Hoffmann RG, Franco J, Varma RR, Rao SM. Inhibitory control test is a simple method to diagnose minimal hepatic encephalopathy and predict development of overt hepatic encephalopathy. *Am J Gastroenterol* 2007; **102**: 754-760 [PMID: 17222319 DOI: 10.1111/j.1572-0241.2007.01048.x]

14 **Ford JM**, Gray M, Whitfield SL, Turken AU, Glover G, Faustman WO, Mathalon DH. Acquiring and inhibiting prepotent responses in schizophrenia: Event-related brain potentials and functional magnetic resonance imaging. *Arch Gen Psychiatry* 2004; **61**: 119-129 [PMID: 14757588 DOI: 10.1001/archpsyc.61.2.119]

15 **Schiff S**, Vallesi A, Mapelli D, Orsato R, Pellegrini A, Umiltà C, Gatta A, Amodio P. Impairment of response inhibition precedes motor alteration in the early stage of liver cirrhosis: A behavioral and electrophysiological study. *Metab Brain Dis* 2005; **20**: 381-392 [PMID: 16382348 DOI: 10.1007/s11011-005-7922-4]

16 **Ridola L**, Nardelli S, Gioia S, Riggio O. Quality of life in patients with minimal hepatic encephalopathy. *World J Gastroenterol* 2018; **24**: 5446-5453 [PMID: 30622374 DOI: 10.3748/wjg.v24.i48.5446]

17 **Bajaj JS**, Riggio O, Allampati S, Prakash R, Gioia S, Onori E, Piazza N, Noble NA, White MB, Mullen

KD. Cognitive dysfunction is associated with poor socioeconomic status in patients with cirrhosis: An international multicenter study. *Clin Gastroenterol Hepatol* 2013; **11**: 1511-1516 [PMID: 23707462 DOI: 10.1016/j.cgh.2013.05.010]

18 **Rakoski MO**, McCammon RJ, Piette JD, Iwashyna TJ, Marrero JA, Lok AS, Langa KM, Volk ML. Burden of cirrhosis on older Americans and their families: Analysis of the health and retirement study. *Hepatology* 2012; **55**: 184-191 [PMID: 21858847 DOI: 10.1002/hep.24616]

19 **Kappus MR**, Bajaj JS. Covert hepatic encephalopathy: Not as minimal as you might think. *Clin Gastroenterol Hepatol* 2012; **10**: 1208-1219 [PMID: 22728384 DOI: 10.1016/j.cgh.2012.05.026]

20 **Bajaj JS**, Hafeezullah M, Hoffmann RG, Varma RR, Franco J, Binion DG, Hammeke TA, Saeian K. Navigation skill impairment: Another dimension of the driving difficulties in minimal hepatic encephalopathy. *Hepatology* 2008; **47**: 596-604 [PMID: 18000989 DOI: 10.1002/hep.22032]

21 **Prasad S**, Dhiman RK, Duseja A, Chawla YK, Sharma A, Agarwal R. Lactulose improves cognitive functions and health-related quality of life in patients with cirrhosis who have minimal hepatic encephalopathy. *Hepatology* 2007; **45**: 549-559 [PMID: 17326150 DOI: 10.1002/hep.21533]

22 **Nardelli S**, Lattanzi B, Merli M, Farcomeni A, Gioia S, Ridola L, Riggio O. Muscle Alterations Are Associated With Minimal and Overt Hepatic Encephalopathy in Patients With Liver Cirrhosis. *Hepatology* 2019 [PMID: 31038758 DOI: 10.1002/hep.30692]

23 **Merli M**, Giusto M, Lucidi C, Giannelli V, Pentassuglio I, Di Gregorio V, Lattanzi B, Riggio O. Muscle depletion increases the risk of overt and minimal hepatic encephalopathy: Results of a prospective study. *Metab Brain Dis* 2013; **28**: 281-284 [PMID: 23224378 DOI: 10.1007/s11011-012-9365-z]

24 **Nardelli S**, Lattanzi B, Torrisi S, Greco F, Farcomeni A, Gioia S, Merli M, Riggio O. Sarcopenia Is Risk Factor for Development of Hepatic Encephalopathy After Transjugular Intrahepatic Portosystemic Shunt Placement. *Clin Gastroenterol Hepatol* 2017; **15**: 934-936 [PMID: 27816756 DOI: 10.1016/j.cgh.2016.10.028]

25 **Gioia S**, Merli M, Nardelli S, Lattanzi B, Pitocchi F, Ridola L, Riggio O. The modification of quantity and quality of muscle mass improves the cognitive impairment after TIPS. *Liver Int* 2019; **39**: 871-877 [PMID: 30667572 DOI: 10.1111/liv.14050]

26 **Carey EJ**, Lai JC, Wang CW, Dasarathy S, Lobach I, Montano-Loza AJ, Dunn MA; Fitness, Life Enhancement, and Exercise in Liver Transplantation Consortium. A multicenter study to define sarcopenia in patients with end-stage liver disease. *Liver Transpl* 2017; **23**: 625-633 [PMID: 28240805 DOI: 10.1002/lt.24750]

27 **Martin L**, Birdsell L, Macdonald N, Reiman T, Clandinin MT, McCargar LJ, Murphy R, Ghosh S, Sawyer MB, Baracos VE. Cancer cachexia in the age of obesity: Skeletal muscle depletion is a powerful prognostic factor, independent of body mass index. *J Clin Oncol* 2013; **31**: 1539-1547 [PMID: 23530101 DOI: 10.1200/JCO.2012.45.2722]

28 **Giusto M**, Lattanzi B, Albanese C, Galtieri A, Farcomeni A, Giannelli V, Lucidi C, Di Martino M, Catalano C, Merli M. Sarcopenia in liver cirrhosis: The role of computed tomography scan for the assessment of muscle mass compared with dual-energy X-ray absorptiometry and anthropometry. *Eur J Gastroenterol Hepatol* 2015; **27**: 328-334 [PMID: 25569567 DOI: 10.1097/MEG.0000000000000274]

29 **Dazzani F**, Micati M, Caraceni P, Drago GM, Domenicali M, Pacilli P, Tomassetti V, Gelonesi E, Trevisani F, Bernardi M. Transthoracic electrical bioimpedance: A non-invasive technique for the evaluation of the haemodynamic alterations in patients with liver cirrhosis. *Dig Liver Dis* 2005; **37**: 786-792 [PMID: 16027054 DOI: 10.1016/j.dld.2005.05.008]

30 **Bhanji RA**, Narayanan P, Allen AM, Malhi H, Watt KD. Sarcopenia in hiding: The risk and consequence of underestimating muscle dysfunction in nonalcoholic steatohepatitis. *Hepatology* 2017; **66**: 2055-2065 [PMID: 28777879 DOI: 10.1002/hep.29420]

31 **Montano-Loza AJ**, Angulo P, Meza-Junco J, Prado CM, Sawyer MB, Beaumont C, Esfandiari N, Ma M, Baracos VE. Sarcopenic obesity and myosteatosis are associated with higher mortality in patients with cirrhosis. *J Cachexia Sarcopenia Muscle* 2016; **7**: 126-135 [PMID: 27493866 DOI: 10.1002/jcsm.12039]

32 **Montano-Loza AJ**, Meza-Junco J, Prado CM, Lieffers JR, Baracos VE, Bain VG, Sawyer MB. Muscle wasting is associated with mortality in patients with cirrhosis. *Clin Gastroenterol Hepatol* 2012; **10**: 166-173, 173.e1 [PMID: 21893129 DOI: 10.1016/j.cgh.2011.08.028]

33 **Shen W**, Punyanitya M, Wang Z, Gallagher D, St-Onge MP, Albu J, Heymsfield SB, Heshka S. Total body skeletal muscle and adipose tissue volumes: Estimation from a single abdominal cross-sectional image. *J Appl Physiol (1985)* 2004; **97**: 2333-2338 [PMID: 15310748 DOI: 10.1152/japplphysiol.00744.2004]

34 **Mitsiopoulos N**, Baumgartner RN, Heymsfield SB, Lyons W, Gallagher D, Ross R. Cadaver validation of skeletal muscle measurement by magnetic resonance imaging and computerized tomography. *J Appl Physiol (1985)* 1998; **85**: 115-122 [PMID: 9655763 DOI: 10.1152/jappl.1998.85.1.115]

35 **Cruz-Jentoft AJ**, Baeyens JP, Bauer JM, Boirie Y, Cederholm T, Landi F, Martin FC, Michel JP, Rolland Y, Schneider SM, Topinková E, Vandewoude M, Zamboni M; European Working Group on Sarcopenia in Older People. Sarcopenia: European consensus on definition and diagnosis: Report of the European Working Group on Sarcopenia in Older People. *Age Ageing* 2010; **39**: 412-423 [PMID: 20392703 DOI: 10.1093/ageing/afq034]

36 **Praktiknjo M**, Book M, Luetkens J, Pohlmann A, Meyer C, Thomas D, Jansen C, Feist A, Chang J, Grimm J, Lehmann J, Strassburg CP, Abraldes JG, Kukuk G, Trebicka J. Fat-free muscle mass in magnetic resonance imaging predicts acute-on-chronic liver failure and survival in decompensated cirrhosis. *Hepatology* 2018; **67**: 1014-1026 [PMID: 29059469 DOI: 10.1002/hep.29602]

37 **Dasarathy S**, Merli M. Sarcopenia from mechanism to diagnosis and treatment in liver disease. *J Hepatol* 2016; **65**: 1232-1244 [PMID: 27515775 DOI: 10.1016/j.jhep.2016.07.040]

38 **Bhanji RA**, Moctezuma-Velazquez C, Duarte-Rojo A, Ebadi M, Ghosh S, Rose C, Montano-Loza AJ. Myosteatosis and sarcopenia are associated with hepatic encephalopathy in patients with cirrhosis. *Hepatol Int* 2018; **12**: 377-386 [PMID: 29881992 DOI: 10.1007/s12072-018-9875-9]

39 **Kvist H**, Sjöström L, Tylén U. Adipose tissue volume determinations in women by computed tomography: Technical considerations. *Int J Obes* 1986; **10**: 53-67 [PMID: 3710689 DOI: 10.1159/000180330]

40 **Vehmas T**, Kairemo KJ, Taavitsainen MJ. Measuring visceral adipose tissue content from contrast enhanced computed tomography. *Int J Obes Relat Metab Disord* 1996; **20**: 570-573 [PMID: 8782734 DOI: 10.1006/hbeh.1996.0022]

41 **Merli M**, Giusto M, Gentili F, Novelli G, Ferretti G, Riggio O, Corradini SG, Siciliano M, Farcomeni A, Attili AF, Berloco P, Rossi M. Nutritional status: Its influence on the outcome of patients undergoing liver transplantation. *Liver Int* 2010; **30**: 208-214 [PMID: 19840246 DOI: 10.1111/j.1478-3231.2009.02135.x]

42 **Kim G**, Kang SH, Kim MY, Baik SK. Prognostic value of sarcopenia in patients with liver cirrhosis: A systematic review and meta-analysis. *PLoS One* 2017; **12**: e0186990 [PMID: 29065187 DOI: 10.1371/journal.pone.0186990]

43 **Montano-Loza AJ**, Duarte-Rojo A, Meza-Junco J, Baracos VE, Sawyer MB, Pang JX, Beaumont C, Esfandiari N, Myers RP. Inclusion of Sarcopenia Within MELD (MELD-Sarcopenia) and the Prediction of Mortality in Patients With Cirrhosis. *Clin Transl Gastroenterol* 2015; **6**: e102 [PMID: 26181291 DOI: 10.1038/ctg.2015.31]

44 **Kang SH**, Jeong WK, Baik SK, Cha SH, Kim MY. Impact of sarcopenia on prognostic value of cirrhosis: Going beyond the hepatic venous pressure gradient and MELD score. *J Cachexia Sarcopenia Muscle* 2018; **9**: 860-870 [PMID: 30371017 DOI: 10.1002/jcsm.12333]

45 **Musumeci G**. Sarcopenia and exercise "The State of the Art". *J Funct Morphol Kinesiol* 2017; **2**: 40 [DOI: 10.3390/jfmk2040040]

46 **European Association for the Study of the Liver**. EASL Clinical Practice Guidelines on nutrition in chronic liver disease. *J Hepatol* 2019; **70**: 172-193 [PMID: 30144956 DOI: 10.1016/j.jhep.2018.06.024]

47 **Hanai T**, Shiraki M, Nishimura K, Ohnishi S, Imai K, Suetsugu A, Takai K, Shimizu M, Moriwaki H. Sarcopenia impairs prognosis of patients with liver cirrhosis. *Nutrition* 2015; **31**: 193-199 [PMID: 25441595 DOI: 10.1016/j.nut.2014.07.005]

48 **Durand F**, Buyse S, Francoz C, Laouénan C, Bruno O, Belghiti J, Moreau R, Vilgrain V, Valla D. Prognostic value of muscle atrophy in cirrhosis using psoas muscle thickness on computed tomography. *J Hepatol* 2014; **60**: 1151-1157 [PMID: 24607622 DOI: 10.1016/j.jhep.2014.02.026]

49 **Eslamparast T**, Montano-Loza AJ, Raman M, Tandon P. Sarcopenic obesity in cirrhosis-The confluence of 2 prognostic titans. *Liver Int* 2018; **38**: 1706-1717 [PMID: 29738109 DOI: 10.1111/liv.13876]

50 **Lattanzi B**, D'Ambrosio D, Merli M. Hepatic Encephalopathy and Sarcopenia: Two Faces of the Same Metabolic Alteration. *J Clin Exp Hepatol* 2019; **9**: 125-130 [PMID: 30765945 DOI: 10.1016/j.jceh.2018.04.007]

51 **Olde Damink SW**, Jalan R, Redhead DN, Hayes PC, Deutz NE, Soeters PB. Interorgan ammonia and amino acid metabolism in metabolically stable patients with cirrhosis and a TIPSS. *Hepatology* 2002; **36**: 1163-1171 [PMID: 12395326 DOI: 10.1053/jhep.2002.36497]

52 **Ganda OP**, Ruderman NB. Muscle nitrogen metabolism in chronic hepatic insufficiency. *Metabolism* 1976; **25**: 427-435 [PMID: 1263837 DOI: 10.1016/0026-0495(76)90075-5]

53 **Wright G**, Noiret L, Olde Damink SW, Jalan R. Interorgan ammonia metabolism in liver failure: The basis of current and future therapies. *Liver Int* 2011; **31**: 163-175 [PMID: 20673233 DOI: 10.1111/j.1478-3231.2010.02302.x]

54 **Dasarathy S**. Myostatin and beyond in cirrhosis: All roads lead to sarcopenia. *J Cachexia Sarcopenia Muscle* 2017; **8**: 864-869 [PMID: 29168629 DOI: 10.1002/jcsm.12262]

55 **Qiu J**, Tsien C, Thapalaya S, Narayanan A, Weihl CC, Ching JK, Eghtesad B, Singh K, Fu X, Dubyak G, McDonald C, Almasan A, Hazen SL, Naga Prasad SV, Dasarathy S. Hyperammonemia-mediated autophagy in skeletal muscle contributes to sarcopenia of cirrhosis. *Am J Physiol Endocrinol Metab* 2012; **303**: E983-E993 [PMID: 22895779 DOI: 10.1152/ajpendo.00183.2012]

56 **Hanai T**, Shiraki M, Watanabe S, Kochi T, Imai K, Suetsugu A, Takai K, Moriwaki H, Shimizu M. Sarcopenia predicts minimal hepatic encephalopathy in patients with liver cirrhosis. *Hepatol Res* 2017; **47**: 1359-1367 [PMID: 28199774 DOI: 10.1111/hepr.12873]

57 **Kalaitzakis E**, Olsson R, Henfridsson P, Hugosson I, Bengtsson M, Jalan R, Björnsson E. Malnutrition and diabetes mellitus are related to hepatic encephalopathy in patients with liver cirrhosis. *Liver Int* 2007; **27**: 1194-1201 [PMID: 17919230 DOI: 10.1111/j.1478-3231.2007.01562.x]

58 **Tapper EB**, Derstine B, Baki J, Su GL. Bedside Measures of Frailty and Cognitive Function Correlate with Sarcopenia in Patients with Cirrhosis. *Dig Dis Sci* 2019 [PMID: 31292783 DOI: 10.1007/s10620-019-05713-4]

59 **Zenith L**, Meena N, Ramadi A, Yavari M, Harvey A, Carbonneau M, Ma M, Abraldes JG, Paterson I, Haykowsky MJ, Tandon P. Eight weeks of exercise training increases aerobic capacity and muscle mass and reduces fatigue in patients with cirrhosis. *Clin Gastroenterol Hepatol* 2014; **12**: 1920-1926.e2 [PMID: 24768811 DOI: 10.1016/j.cgh.2014.04.016]

60 **Duarte-Rojo A**, Ruiz-Margáin A, Montaño-Loza AJ, Macías-Rodríguez RU, Ferrando A, Kim WR. Exercise and physical activity for patients with end-stage liver disease: Improving functional status and sarcopenia while on the transplant waiting list. *Liver Transpl* 2018; **24**: 122-139 [PMID: 29024353 DOI: 10.1002/lt.24958]

61 **Reuter B**, Shaw J, Hanson J, Tate V, Acharya C, Bajaj JS. Nutritional Assessment in Inpatients with Cirrhosis can be Improved after Training and is Associated with Lower Readmissions. *Liver Transpl* 2019 [PMID: 31301208 DOI: 10.1002/lt.25602]

World Journal of Gastroenterology

Submit a Manuscript: https://www.f6publishing.com

*World J Gastroenterol* 2019 September 21; 25(35): 5266-5282

DOI: 10.3748/wjg.v25.i35.5266

ISSN 1007-9327 (print) ISSN 2219-2840 (online)

ORIGINAL ARTICLE

Basic Study

# Significance of tumor-infiltrating immunocytes for predicting prognosis of hepatitis B virus-related hepatocellular carcinoma

Qi-Feng Chen, Wang Li, Pei-Hong Wu, Lu-Jun Shen, Zi-Lin Huang

**ORCID number:** Qi-Feng Chen (0000-0001-8998-3450); Wang Li (0000-0002-4293-8182); Pei-Hong Wu (0000-0001-8008-1872); Lu-Jun Shen (0000-0002-7936-0206); Zi-Lin Huang (0000-0002-1643-1994).

**Author contributions:** Chen QF, Huang ZL, and Li W contributed to study conceptualization; Chen LJ contributed to the methodology; Wu PH provided software; Chen QF, Wu PH, and Huang ZL performed the validation; Chen QF, Wu PH, Huang ZL, and Shen LJ analyzed the data; Chen QF and Li W prepared the original draft; Chen QF, Wu PH, Huang ZL, and Shen LJ reviewed and edited the manuscript; Chen QF contributed to data visualization; Huang ZL supervised the study.

**Supported by** the National Natural Science Foundation of China, No. 81801804.

**Conflict-of-interest statement:** The authors deny any conflict of interest.

**Data sharing statement:** The data used in this manuscript are accessible through https://portal.gdc.cancer.gov/.

**ARRIVE guidelines statement:** The ARRIVE guidelines have been adopted.



**Qi-Feng Chen, Wang Li, Pei-Hong Wu, Lu-Jun Shen, Zi-Lin Huang,** Department of Medical Imaging and Interventional Radiology, Sun Yat-sen University Cancer Center; State Key Laboratory of Oncology in South China; Collaborative Innovation Center for Cancer Medicine, Guangzhou 510060, Guangdong Province, China

**Corresponding author:** Zi-Lin Huang, MD, Professor, Department of Medical Imaging and Interventional Radiology, Sun Yat-sen University Cancer Center; 651 Dongfeng Road East, Yuexiu District, Guangzhou 510060, Guangdong Province, China. huangzl@sysucc.org.cn.
**Telephone:** +86-20-87343272
**Fax:** +86-20-87343392

## Abstract

### *BACKGROUND*

Hepatitis B virus (HBV) has been recognized as a leading cause of hepatocellular carcinoma (HCC). Numerous reports suggest that immune infiltration can predict the prognosis of HCC. Nonetheless, no creditable markers for prognosis of HBV-related HCC have been established by systematically assessing the immune-related markers based on tumor transcriptomes.

### *AIM*

To establish an immune-related marker based on the cell compositions of immune infiltrate obtained based on tumor transcriptomes, so as to enhance the prediction accuracy of HBV-related HCC prognosis.

### *METHODS*

RNA expression patterns as well as the relevant clinical data of HCC patients were obtained from The Cancer Genome Atlas. Twenty-two immunocyte fraction types were estimated by cell type identification by estimating relative subsets of RNA transcripts. Subsequently, the least absolute shrinkage and selection operator (LASSO) Cox regression model was employed to construct an immunoscore based on the immunocyte fraction types. Afterwards, the receiver operating characteristic (ROC) curve, Kaplan-Meier, and multivariate Cox analyses were performed. Additionally, a nomogram for prognosis that integrated the immunoscore as well as the clinical features was established. Meanwhile, the correlation of immunoscore with immune genes was also detected, and gene set enrichment analysis (GSEA) of the immunoscore was conducted.

### *RESULTS*

A total of 22 immunocyte fraction types were predicted and compared among the

**Manuscript source**: Unsolicited manuscript

**Received:** April 22, 2019
**Peer-review started:** April 22, 2019
**First decision:** June 10, 2019
**Revised:** July 18, 2019
**Accepted:** August 7, 2019
**Article in press:** June 10, 2019
**Published online:** September 21, 2019

**P-Reviewer:** Kai K, El-Bendary M
**S-Editor:** Ma RY
**L-Editor:** Wang TQ
**E-Editor:** Ma YJ

tumor as well as non-tumor samples. An immunoscore was constructed through adopting the LASSO model, which contained eight immunocyte fraction types. Meanwhile, the areas under the ROC curves for the immunoscore biomarker prognostic model were 0.971, 0.912, and 0.975 for 1-, 3-, and 5-year overall survival (OS), respectively. Difference in OS between the high-immunoscore group and the low-immunoscore group was statistically significant [hazard ratio (HR) = 66.007, 95% confidence interval (CI): 8.361-521.105; $P < 0.0001$]. Moreover, multivariable analysis showed that the immunoscore was an independent factor for predicting the prognosis (HR = 2.997, 95%CI: 1.737-5.170). A nomogram was established, and the C-index was 0.757 (95%CI: 0.648-0.866). The immunoscore showed a significant negative correlation with the expression of PD-1 ($P = 0.024$), PD-L1 ($P = 0.026$), PD-L2 ($P = 0.029$), and CD27 ($P = 0.033$). Eight pathways were confirmed by GSEA.

### *CONCLUSION*

The established immunoscore can potentially serve as a candidate marker to estimate the OS for HBV-related HCC cases.

**Key words:** Immune risk score; Hepatitis B virus; Hepatocellular carcinoma; Prognostic signature; Cell type identification by estimating relative subsets of RNA transcripts



**Core tip:** Hepatitis B virus (HBV) infection is epidemiologically related to hepatocellular carcinoma (HCC) development. Immune cells have been recognized to play crucial roles in the prognosis of various types of cancers, including HCC. The immune signature for HBV-related HCC remains unknown. In this study, we explored the proportions of immunocytes, and constructed a robust immune signature to predict the prognosis. These results might contribute to risk stratification and facilitate individualized clinical approach for HBV-related HCC.

**Citation:** Chen QF, Li W, Wu PH, Shen LJ, Huang ZL. Significance of tumor-infiltrating immunocytes for predicting prognosis of hepatitis B virus-related hepatocellular carcinoma. *World J Gastroenterol* 2019; 25(35): 5266-5282
**URL**: https://www.wjgnet.com/1007-9327/full/v25/i35/5266.htm
**DOI**: https://dx.doi.org/10.3748/wjg.v25.i35.5266

## INTRODUCTION

Although the screening, diagnostic, and therapeutic techniques for hepatocellular carcinoma (HCC) have progressed, it remains a major cause of cancer-related death worldwide, with dismal clinical outcomes[1]. Hepatitis viruses have been epidemiologically related to HCC development[2,3], of which hepatitis B virus (HBV) has been recognized as a major factor for HCC in Asian countries[4]. Typically, HBV infection is more prevalent in Eastern Asia, such as China, where over two-thirds of patients are detected[5].

Although the etiological link between HBV and HCC has been well established, the effect of immunocytes on tumor-related microenvironment remains largely unclear. The tumor-infiltrating lymphocytes can serve as prognostic factors for HCC, and are a research hotspot[6,7]. Nonetheless, the non-lymphocyte immunocytes have also been recognized to play crucial roles in prognosis of various types of cancers[8]. Therefore, it is critical to comprehensively predict the immune-related prognosis.

The traditional approaches to measure immune infiltrate in tumors, like immunohistochemistry (IHC) and flow cytometry, cannot thoroughly evaluate the immune functions of various types of cells or effectively distinguish closely related cell populations, since few immune markers can be simultaneously detected using the existing technology. In recent years, the algorithm cell type identification by estimating relative subsets of RNA transcripts (CIBERSORT), known as the metagene means, is recognized as the method with the highest accuracy. Typically, CIBERSORT can accurately estimate 22 human immunocyte phenotypes[9].

This study explored the proportions of immunocytes by appropriately selecting

HBV-related HCC cases, so as to identify candidate immune biomarkers using The Cancer Genome Atlas data. The least absolute shrinkage and selection operator (LASSO) algorithm was employed to determine key immunocytes. Thereafter, a HCC immunoscore system was formulated, aiming to establish an immune-related marker that could be used to predict the survival of HBV-related HCC patients.

## MATERIALS AND METHODS

### Patient datasets and processing

Data were downloaded from the TCGA database. The data transfer tool of the Genomic Data Commons applications was employed to download gene expression profiles as well as clinical information of HCC patients (https://tcga-data.nci.nih.gov/). HCC patients with seroprevalence of hepatitis B surface antigen (HBsAg) were included. Among them, 58 patients were HBV-related, but patients with CIBERSORT $P \geq 0.05$ were excluded ($n = 5$), leaving 53 HCC cases in the final cohort for analysis. The flow chart for this analysis is shown in Figure 1. A total of 53 HBV-related HCC cases were enrolled for comprehensive integrated and functional analyses. The mRNA expression in HCC samples was derived from the Illumina HiSeq RNASeq platform and normalized based on TCGA. All data were publicly available and open access. Hence, approval from the ethics committee was not required. All data were processed in accordance with the guidelines from data access policy as well as the NIH TCGA human subject protection (http://cancergenome.nih.gov/publications/publicationguidelines).

### Immunocyte type fraction estimation

The CIBERSORT method was used to quantify immunocyte fractions[9], which could sensitively and specifically distinguish 22 phenotypes of human hematopoietic cells. Pornpimol *et al*[10,11] had used the deconvolution method through the CIBERSORT tool, with the threshold set at $P < 0.05$; their results suggested that CIBERSORT could accurately predict the immunocyte population fractions. Hence, only those possessing the CIBERSORT $P < 0.05$ were deemed as eligible in subsequent analysis. Moreover, the immunocyte proportions were separately estimated for 76 samples. For all samples, each estimate of immunocyte type fractions added up to be 1.

### Immunoscore signature construction

The optimal threshold for each immunocyte fraction was generated using the survminer package. Then, the value of immunocyte fraction was assigned as 0 or 1; specifically, the value 0 was given to the cell type fraction below the corresponding threshold, otherwise the value 1 was assigned. The correlation of each immunocyte expression with the overall survival (OS) of patients was calculated using the univariate Cox model. Then, the immunocytes were screened, followed by verification through LASSO regression using "glmnet" package in R project. Finally, an immunoscore was constructed based on immunocytes by linearly combining the multiplication of regression model (β) by expression level as follows: Immunoscore = $\beta 1 \times$ immunocyte 1 expression level + $\beta 2 \times$ immunocyte 2 expression level + ⋯⋯ + $\beta n \times$ immunocyte n expression level. In addition, the time dependent receiver operating characteristic (ROC) curves were employed to evaluate the accuracy of prognosis prediction in five years, which was achieved by the comparisons of sensitivity as well as specificity in predicting the survival using the immunoscore.

### Confirmation of the immunoscore signature

The patients were distributed based on the immunoscore and their survival information. Furthermore, all cases were classified into a high- or low-risk group according to the immunoscore threshold. In addition, related Kaplan-Meier survival curves for patients with high or low predicted risk were plotted. Thereafter, univariate as well as multivariate Cox proportional hazard regression analyses were performed. We developed a nomogram with "rms" package in R project. The prognosis prediction accuracy of the nomogram was verified for discrimination and calibration. Each test was two-sided, and a difference of $P < 0.05$ was deemed statistically significant. The R (version 3.4.1; R Foundation) software was adopted for all analyses.

### Functional analysis of the prognostic immunoscore

Inhibitory checkpoint molecules can be potentially used in numerous cancer types, which are thereby recognized as the immunotherapy targets for cancer. The correlations of the immunoscore with corresponding genes were further investigated. In addition, the correlation of the immunoscore with the determined immune markers

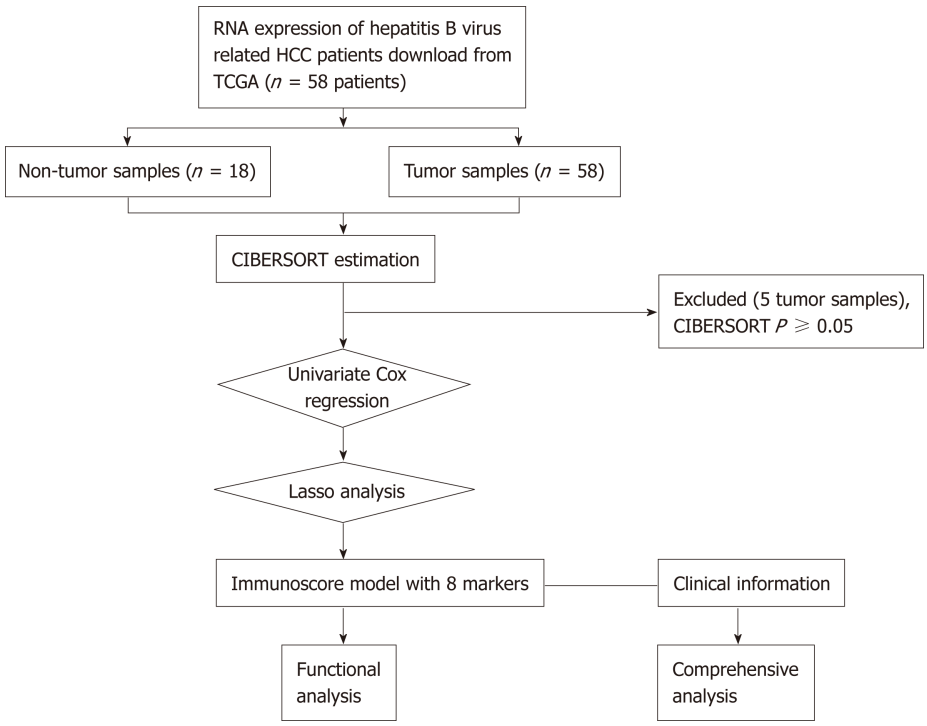


**Figure 1 General design of this study.**

was analyzed through Pearson's correlation analysis based on their expression levels. The mechanisms underlying "Molecular Signatures Database" for the c2.cp.kegg.v6.2.symbols were investigated according to gene set enrichment analysis (GSEA)[12] with JAVA procedure (http://software.broadinstitute.org/gsea/index.jsp). The random sample permutation number was deemed at 1000 and a significant level was $P < 0.05$.

## RESULTS

### *Patient characteristics and composition of immunocytes*

Detailed patient characteristics are listed in Table 1. The immunocyte compositions of cancer and normal tissues were analyzed. Figure 2A summarizes immunocyte composition in the entire cohort. Resting CD4 memory T cells ranked the first, accounting for 25% on average; while CD4 naive T cells and gamma delta T cells were not detected. Heatmap summarizing the distribution of immunocytes was also plotted (Figure 2B). Various immunocyte subpopulation fractions showed a low to moderate correlation (Figure 2C). Relative to para-carcinoma tissues, higher proportions of regulatory T cells as well as resting dendritic cells could be detected in cancer tissues, along with lower proportions of plasma cells, resting NK cells, M2 macrophages, and neutrophils (Figure 2D, $P < 0.05$).

### *Immunoscore derivation*

Table 2 displays the thresholds of all cell types. Figure 3A presents the forest plot of the correlation of 18 immunocyte subsets with OS. Through the LASSO algorithm (Figure 3B and C ), eight types of immunocytes (including plasma cells, naive B cells, CD4 memory resting T cells, M1 macrophages, activated NK cells, resting dendritic cells, M2 macrophages, and neutrophils) were selected to build the prognostic immunoscore model. The immunoscore was calculated according to the formula: (2.764 × fraction level of naive B cells) - (0.371 × fraction level of plasma cells) + (1.694 × fraction level of resting CD4 memory T cells) + (21.45 × fraction level of activated NK cells) + (1.669 × fraction level of M1 macrophages) - (1.649 × fraction level of M2 macrophages) + (0.504 × fraction level of resting dendritic cells) + (3.647 × fraction level of neutrophils). Moreover, the immunoscore prognosis performance, as the continuous variable, was also studied within the cohort through time-dependent ROC analysis. The areas under the curves of the immunoscore biomarker prognostic model were 0.971, 0.912, and 0.975 for 1-, 3-, and 5-year OS, respectively (Figure 3D).

**Table 1 Baseline patient characteristics**

| Variable | | Number (*n*) | Percent (%) |
|---|---|---|---|
| Age | 60.1 ± 15.4 | 53 | 100 |
| Gender | | | |
| Male | | 31 | 58.5 |
| Female | | 22 | 41.5 |
| Race | | | |
| White | | 33 | 62.3 |
| Others | | 20 | 37.7 |
| Grade | | | |
| I | | 18 | 34.0 |
| II | | 16 | 30.2 |
| III | | 14 | 26.4 |
| IV | | 5 | 9.4 |
| Stage | | | |
| I | | 5 | 9.4 |
| II | | 25 | 47.2 |
| III | | 22 | 41.5 |
| IV | | 1 | 1.9 |

Grade: Neoplasm histologic grade; Stage: TNM stage.

### *Confirmation of the immunoscore*

The patients were distributed based on the immunoscore and their survival information (Figure 4A). Subsequently, the patients were classified into high *vs* low immunoscore groups according to the threshold (36.47) acquired using survminer package. The Kaplan-Meier curves for both groups are presented in Figure 4B. The patients with a high immunoscore were associated with worse OS than those with a low immunoscore [hazard ratio (HR) = 66.007, 95% confidence interval (CI): 8.361-521.105; $P < 0.0001$]. The HR of the immunoscore was 2.010 (95%CI: 1.487-2.716) based on the univariate Cox proportional hazard regression model, and similar results were obtained from the multivariate Cox proportional hazard regression model (HR = 2.997, 95%CI: 1.737-5.170) after adjustment for clinical covariables (Table 3).

Additionally, a prognostic nomogram incorporating the above prognostic factors for visualization and prediction was built to identify a composite factor to predict the prognosis for HCC cases (Table 3). Notably, the nomogram was constituted by six factors (Figure 5A), with a C-index of 0.757 (95%CI: 0.648-0.866). Meanwhile, the 1-, 3-, and 5-year calibration curves of the recurrence probability were consistent between predicted values by the nomogram and measured values (Figure 5B-D).

### *Functional analysis of the prognostic immunoscore*

Gene expression profiles were examined for exploring the potential immunoscore model-related biological phenotypes. First, the correlation of the immunoscore with the screened immune-related gene expression was particularly emphasized. Figure 6 displays the significant negative correlations of the immunoscore with programmed death (PD)-1 ($P = 0.024$), PD-L1 ($P = 0.026$), PD-L2 ($P = 0.029$), and CD27 ($P = 0.033$) expression. Second, GSEA was performed for illustrating the biological roles for the prepared immunoscore model (Supplemental Table 1). The highly expressed genes showed significant enrichment in pathways including glycosaminoglycan chondroitin sulfate biosynthesis, proximal tubule bicarbonate reclamation, focal adhesion, autoimmune thyroid disease, the Notch signaling pathway, basal transcription factors, DNA replication, and homologous recombination (Figure 7).

## DISCUSSION

The CIBERSORT was utilized for the quantification of composition of 22 immunocytes for HBV-related HCC. Furthermore, the immunoscore was developed, which was based on eight immunocyte fractions and served as a new tool to predict the prognosis of HBV-related HCC survival. The prognostic significance of the immunoscore signature was confirmed by the time-dependent ROC curve, Kaplan-

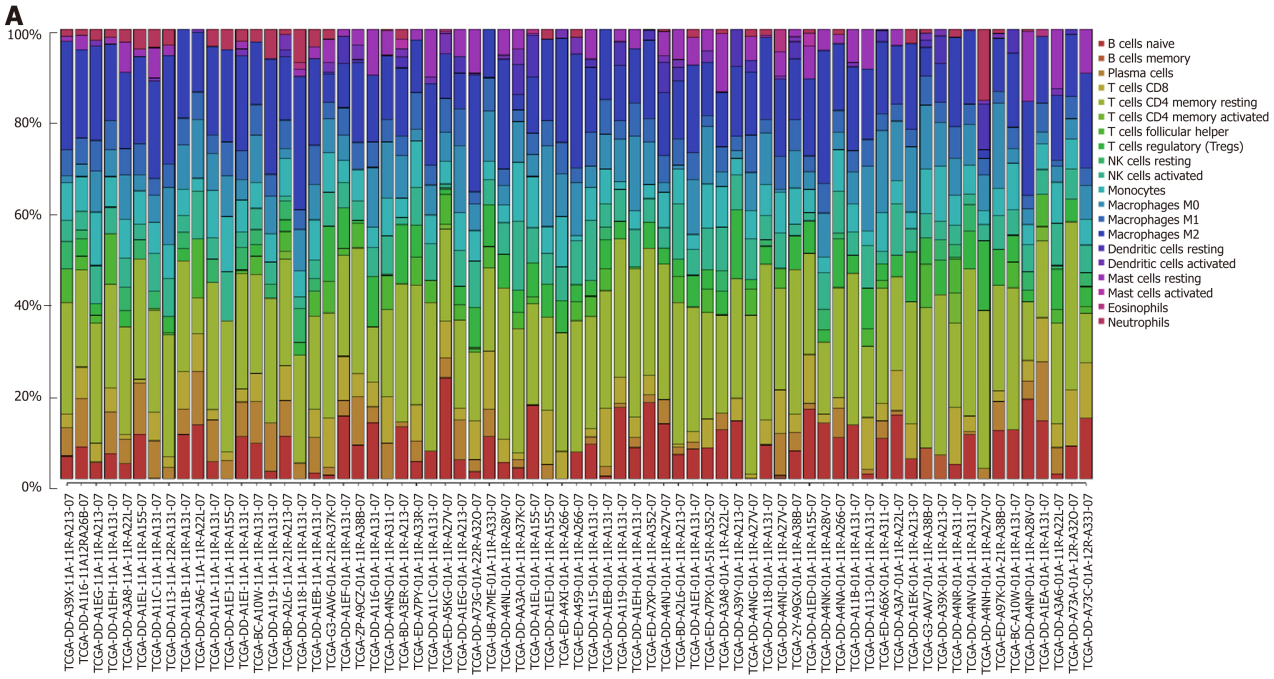
A
100%
80%
60%
40%
20%
0%
B cells naive
B cells memory
Plasma cells
T cells CD8
T cells CD4 memory resting
T cells CD4 memory activated
T cells follicular helper
T cells regulatory (Tregs)
NK cells resting
NK cells activated
Monocytes
Macrophages M0
Macrophages M1
Macrophages M2
Dendritic cells resting
Dendritic cells activated
Mast cells resting
Mast cells activated
Eosinophils
Neutrophils

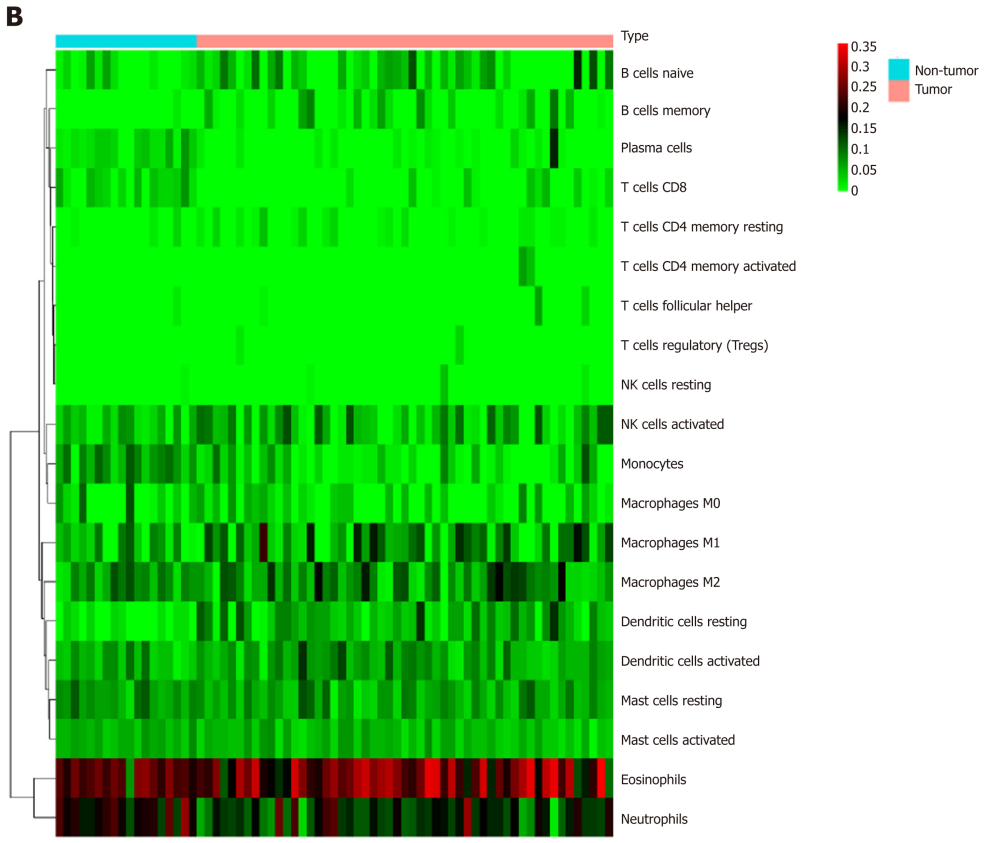
B
Type
B cells naive
B cells memory
Plasma cells
T cells CD8
T cells CD4 memory resting
T cells CD4 memory activated
T cells follicular helper
T cells regulatory (Tregs)
NK cells resting
NK cells activated
Monocytes
Macrophages M0
Macrophages M1
Macrophages M2
Dendritic cells resting
Dendritic cells activated
Mast cells resting
Mast cells activated
Eosinophils
Neutrophils
0.35
0.3
0.25
0.2
0.15
0.1
0.05
0
Non-tumor
Tumor

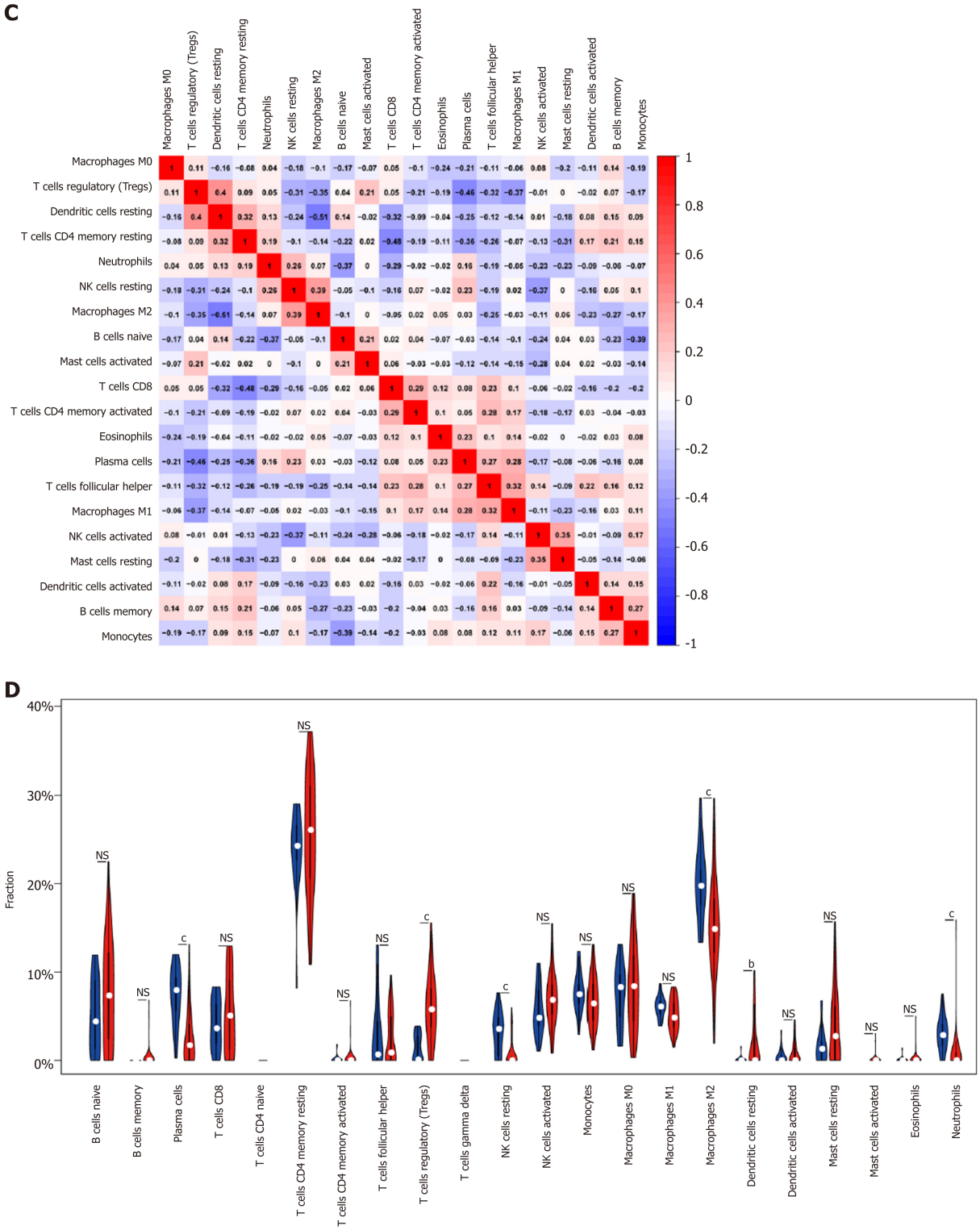


**Figure 2 Immune infiltrate landscape for hepatitis B virus-related hepatocellular carcinoma.** A: Immune infiltrate composition in each sample. B: Heatmap showing the 20 fractions of immunocytes, where the horizontal axis displays samples that were classified as two leading clusters; C: Correlation matrix for the 20 immunocyte proportions as well as the immunocyte lytic activity. Variables were sorted according to the mean linkage clustering; D: Violin plot showing differential expression of 20 immunocytes. $^{b}P < 0.01$, $^{c}P < 0.001$. NS: Not significant.

Meier, and Cox regression analyses. The results suggested that the established immunoscore system displayed favorable accuracy for estimating OS of HBV-related HCC by nomogram analysis. Further functional analysis uncovered several immune checkpoints and pathways that played crucial roles in the immunoscore system during the progression of HCC.

There are few available immunoscore-based models for the prognosis of HCC. In 2015, Sun *et al*[13] confirmed that center tumor CD8+ T cells could predict the prognosis

**Table 2 Thresholds for immunocyte fractions**

| Cell type | Cut-off value |
|---|---|
| B cells naive | 0.107 |
| B cells memory | 0 |
| Plasma cells | 0.010 |
| T cells CD8 | 0.020 |
| T cells CD4 memory resting | 0.157 |
| T cells CD4 memory activated | 0 |
| T cells follicular helper | 0.054 |
| T cells regulatory | 0.108 |
| NK cells resting | 0.002 |
| NK cells activated | 0.035 |
| Monocytes | 0.082 |
| Macrophages M0 | 0.067 |
| Macrophages M1 | 0.030 |
| Macrophages M2 | 0.131 |
| Dendritic cells resting | 0.039 |
| Dendritic cells activated | 0.002 |
| Mast cells resting | 0.074 |
| Mast cells activated | 0 |
| Eosinophils | 0 |
| Neutrophils | 0.013 |

for HCC patients, and were a valuable marker for predicting patient survival and tumor recurrence. However, only CD3+ and CD8+ T cells were measured by IHC in their research. Similarly, in 2016, Gabrielson *et al*[14] concluded that immunoscore as well as PD-L1 expression could be used as valuable markers to predict the prognosis for HCC patients undergoing resection of primary tumor. However, regarding etiology of HCC, only 16.9% (11/65) of cases suffered from HBV infection in their study. In 2016, Petrizzo demonstrated that immunoscore was a meaningful marker to predict the prognosis for HCC patients undergoing resection for primary tumor[15]. However, 65 HCC patients with unknown virus condition were reviewed in that study, and IHC was only performed with anti-CD3, CD8, and PD-L1 monoclonal antibodies. In 2017, Yao *et al*[16] conducted a cohort study by recruiting 92 consecutive HBV-HCC patients, and concluded that the immunoscore classification showed close relation to patient outcome. However, only CD3+, CD8+, and CD45RO+ T cells were measured by IHC in that study.

The current study was superior to previous studies examining the prognosis value of immunoscore for HCC in several aspects. First, assessing CD3+ and CD8+ lymphocytes alone could not comprehensively represent local immune status. Prior research was limited by its narrow view of immunological reaction due to technical limitations, and immunocytes were evaluated through IHC based on a single surface marker, which was ineffective for distinguishing the tightly correlated cell types, since numerous marker proteins would be expressed among various types of cells. Technically, IHC is limited to existing phenotypic markers, and may lead to inconsistent findings in clinical studies. However, using transcriptomic data for computationally describing tumor microenvironment can serve as a promising tool to overcome the technical limitations related to IHC, and can be more readily employed for the further characterization of 22 different immune populations than IHC. Second, homogeneity in the case cohort was largely enhanced through pre-analysis case selection. Viral and non-viral HCC were suggested to be associated with different prognoses, and different treatment strategies were recommended; therefore, they must be distinctively analyzed to develop the models for prognosis[17-20]. In contrast to previous studies that combined viral and non-viral related HCC, the current study was conducted in HBV-positive patients only. Third, in terms of the methodology, LASSO penalized regression could increase the accuracy of bioinformatic analysis, and allowed for simultaneous analysis of each independent variable to select the most valuable parameters[21]. Therefore, such approach would show much higher accuracy than stepwise regression of the multivariate Cox model[22]. Fourth, an easy-to-use nomogram model based on Cox analysis was constructed in our meticulously chosen

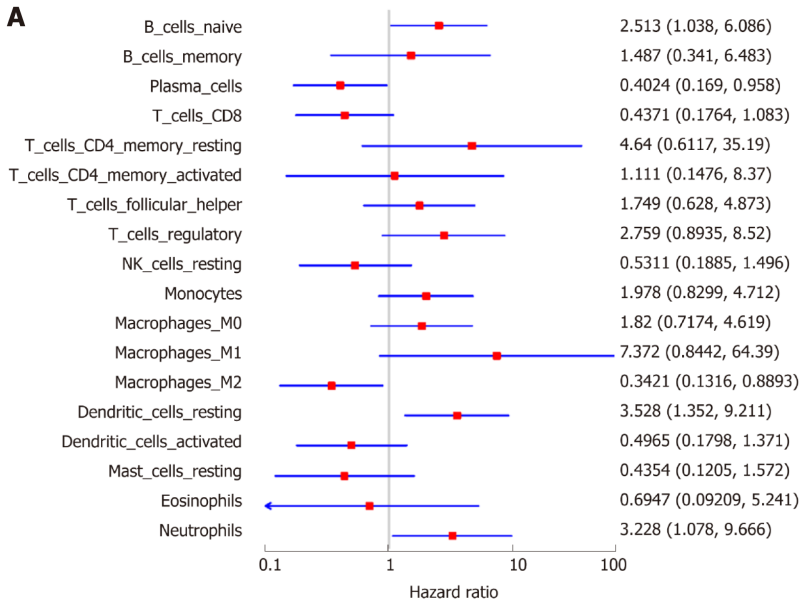
A
B_cells_naive
B_cells_memory
Plasma_cells
T_cells_CD8
T_cells_CD4_memory_resting
T_cells_CD4_memory_activated
T_cells_follicular_helper
T_cells_regulatory
NK_cells_resting
Monocytes
Macrophages_M0
Macrophages_M1
Macrophages_M2
Dendritic_cells_resting
Dendritic_cells_activated
Mast_cells_resting
Eosinophils
Neutrophils
2.513 (1.038, 6.086)
1.487 (0.341, 6.483)
0.4024 (0.169, 0.958)
0.4371 (0.1764, 1.083)
4.64 (0.6117, 35.19)
1.111 (0.1476, 8.37)
1.749 (0.628, 4.873)
2.759 (0.8935, 8.52)
0.5311 (0.1885, 1.496)
1.978 (0.8299, 4.712)
1.82 (0.7174, 4.619)
7.372 (0.8442, 64.39)
0.3421 (0.1316, 0.8893)
3.528 (1.352, 9.211)
0.4965 (0.1798, 1.371)
0.4354 (0.1205, 1.572)
0.6947 (0.09209, 5.241)
3.228 (1.078, 9.666)
0.1
1
10
100
Hazard ratio

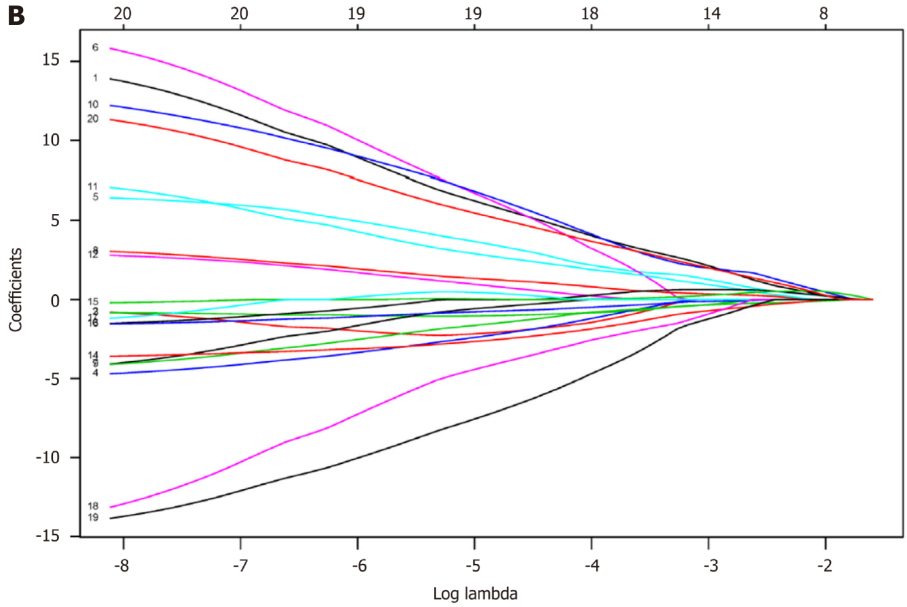
B
20
20
19
19
18
14
8
Coefficients
Log lambda

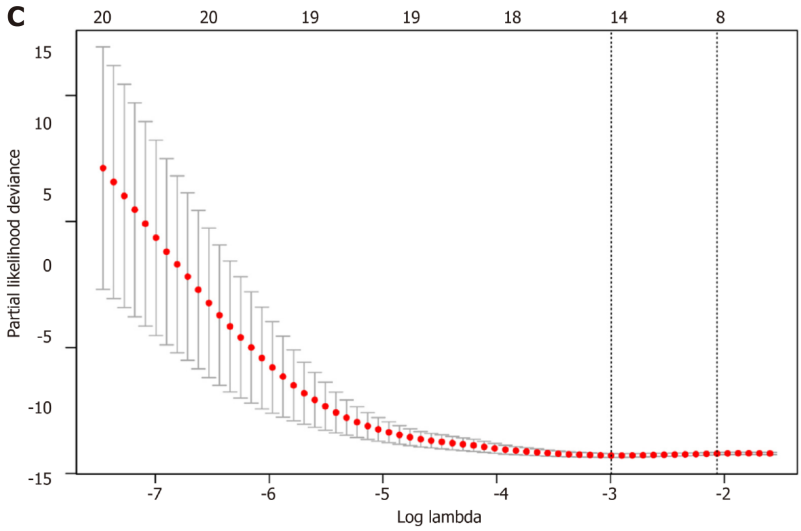
C
20
20
19
19
18
14
8
Partial likelihood deviance
Log lambda

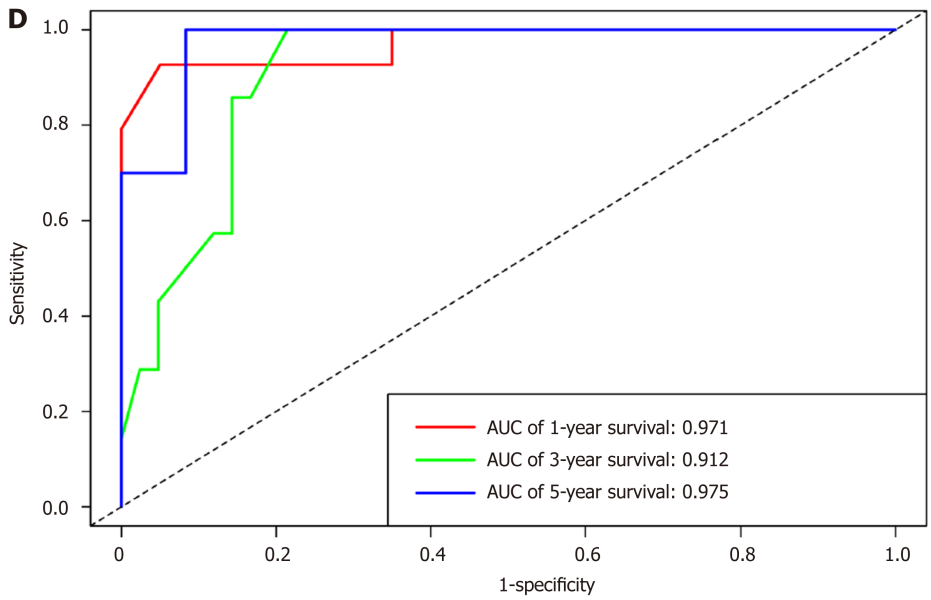


**Figure 3 Immunoscore model construction.** A: Forest plots presenting the relationships of various immunocyte subpopulations with overall survival, in which the unadjusted hazard ratios as well as the corresponding 95% confidence intervals are displayed; B: Coefficient profiles of 20 immunocyte type fractions using the least absolute shrinkage and selection operator (LASSO); C: 10-fold cross-validation to select parameters for LASSO model, which can determine the cell type numbers adopted for LASSO model; D: Immunoscore determined using the time dependent receiver operating characteristic curves. For the 1-, 3-, and 5-year OS, the AUCs for the immunoscore were 0.971, 0.912, and 0.975, respectively. [a]$P < 0.05$. LASSO: Least absolute shrinkage and selection operator; AUC: Areas under the curve.

patient cohort with clinicopathological characteristics that might facilitate individualized prediction of patients.

Immune checkpoint inhibitors have shown significant therapeutic responses to tumors. Clinical trials of antibodies targeting the immune checkpoint inhibitors to treat advanced HCC are ongoing[23]. Our results showed that the immunoscore was negatively correlated with PD-1, PD-L1, PD-L2, and CD27 (Figure 6). There are two ligands for PD-1 receptor, namely, PD-L1 and PD-L2[24,25]. Our previous studies found that excessive PD-1-positive intratumoral lymphocytes could predict the cytokine-induced killer cell survival benefits for HCC patients[26], and serum soluble PD-1 and PD-L1 can independently predict the prognosis for HCC patients in distinct ways[27]. CD27 is a cytokine that facilitates naive T cell expansion specific to antigen, which is of vital importance to generate T cell memory[28]. Moreover, pathway enrichment analysis suggested that such immunocytes could affect HCC genesis as well as progression by eight pathways whose biological functions have been previously reported in HCC. Most of these pathways are canonical and crucial, which participate in HCC genesis as well as progression.

This study had several limitations. First, information, such as acute infection, immune system diseases, as well as anti-inflammatory drugs, could not be obtained since this study was conducted based on the publicly available datasets, and this could potentially result in error or bias. Second, each case was retrospectively chosen, so an underlying bias may exist related to the imbalanced clinicopathological characteristics with treatment heterogeneity. Third, all data were downloaded from Western countries to establish the models, so the findings should be cautiously applied to the Asian population. Finally, further large-sample research is needed for external validation of our results.

In summary, this study uncovered the immunocyte signature in HBV-related HCC. The proposed immunoscore model may comprehensively provide the required clinical data to improve the personalized treatment for HBV-related HCC cases.

**Table 3 Cox regression analysis for overall survival-related clinicopathological features**

| Parameter | Univariate analysis | | Multivariate analysis | |
|---|---|---|---|---|
| | HR (95%CI) | *P*-value | HR (95%CI) | *P*-value |
| Risk_score | 2.010 (1.487-2.716) | < 0.001 | 2.997 (1.737-5.170) | < 0.001 |
| Age | 1.022 (0.985-1.060) | 0.255 | 1.091 (1.024-1.162) | 0.007 |
| Gender (*vs* male) | 1.001 (0.404-2.479) | 0.999 | 0.727 (0.215-2.459) | 0.608 |
| Race (*vs* white) | 1.369 (0.470-3.992) | 0.565 | 0.905 (0.195-4.208) | 0.899 |
| Grade (*vs* I/II) | 1.800 (0.743-4.359) | 0.193 | 0.987 (0.327-2.975) | 0.981 |
| Stage (*vs* I/II) | 2.161 (0.865-5.400) | 0.099 | 10.182 (2.251-46.058) | 0.003 |

Grade: Neoplasm histologic grade; Stage: TNM stage; HR: Hazard ratio; CI: Confidence interval.

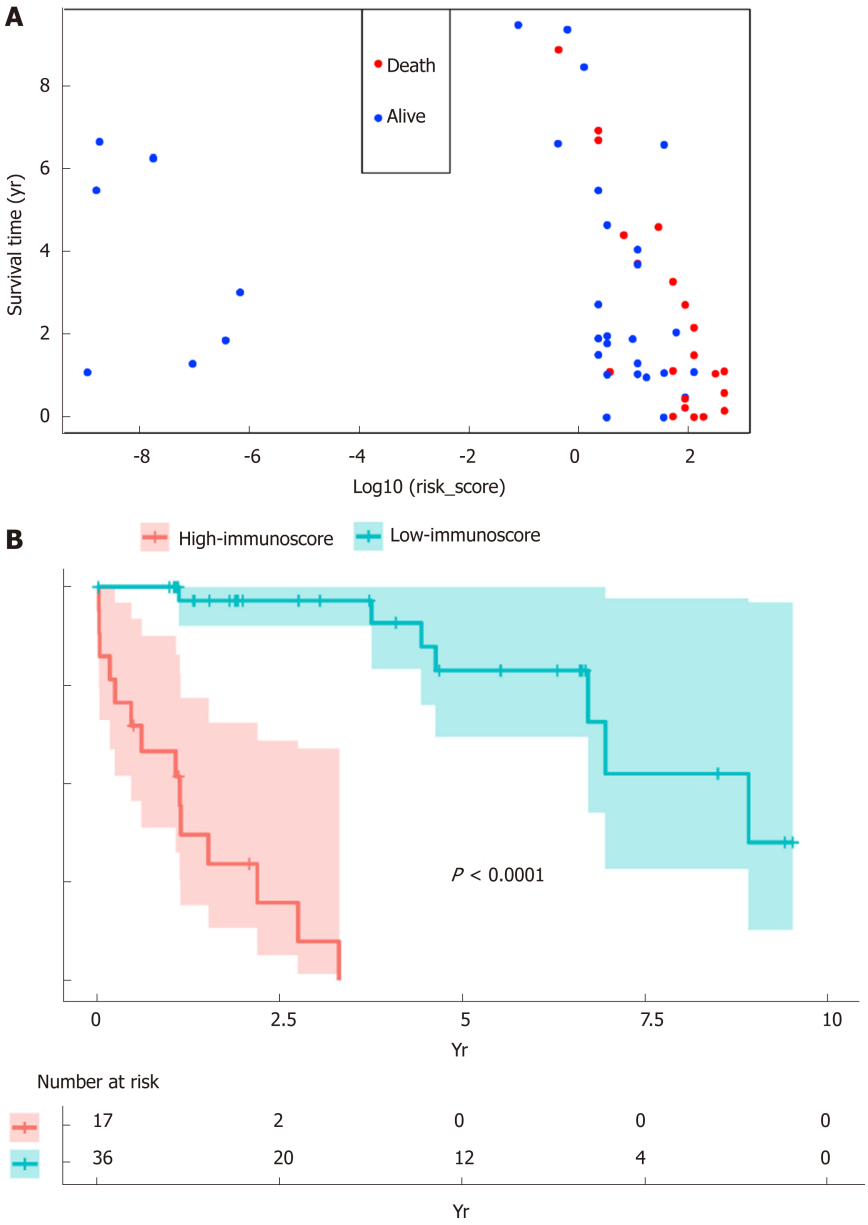


**Figure 4 Verification of the immunoscore signature to predict the prognosis for hepatitis B virus-related hepatocellular carcinoma.** A: The vital status and overall survival were distributed based on the immunoscore; B: Kaplan-Meier curve regarding the overall survival of high- *vs* low- immunoscore groups.

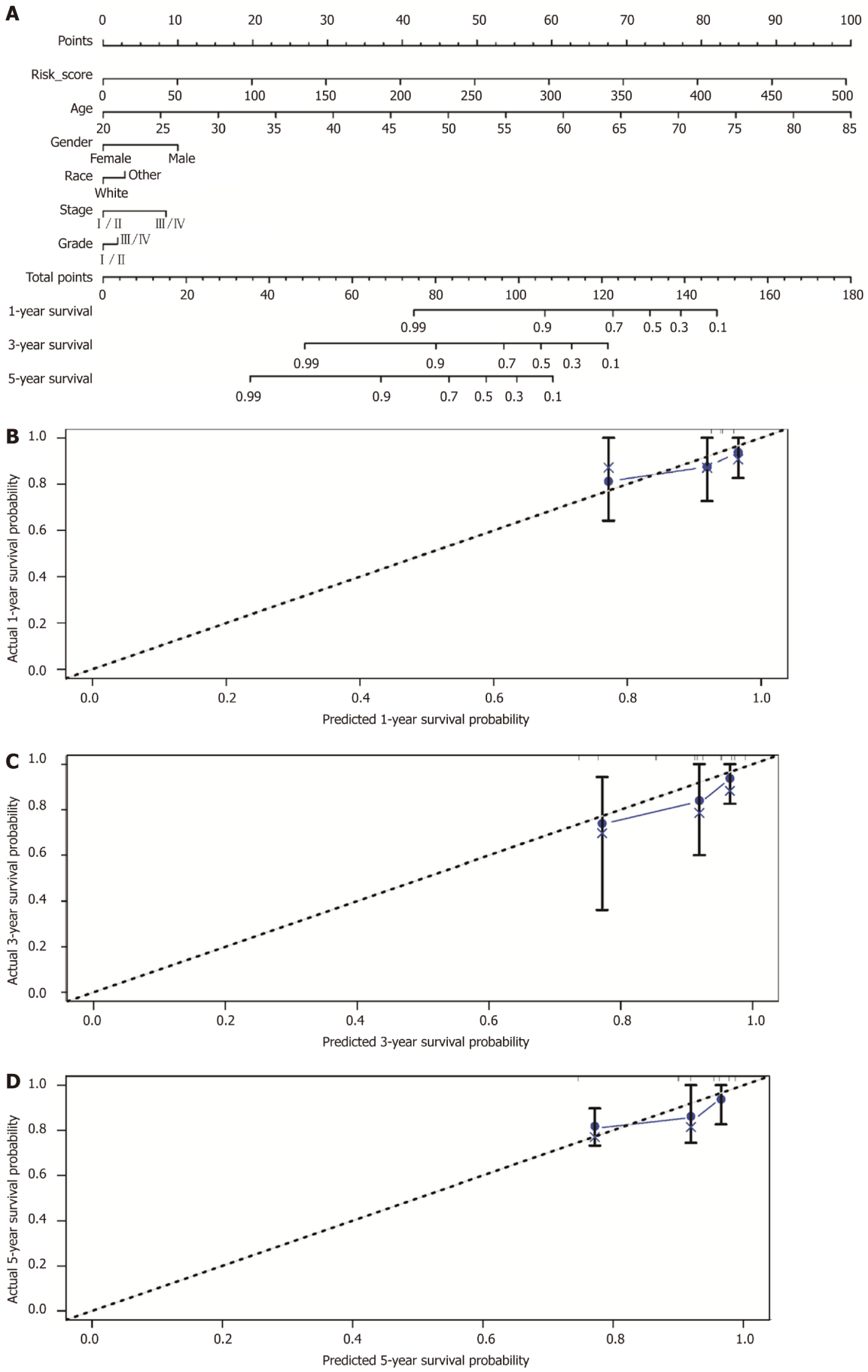


**Figure 5 Construction of the nomogram.** A: Nomogram to predict the 1-, 3-, and 5-year overall survival of hepatitis B virus-related hepatocellular carcinoma patients based on the immunoscore and clinicopathological parameters; Calibration curves for predicting patient survival at 1 (B), 3 (C), and 5 (D) years.

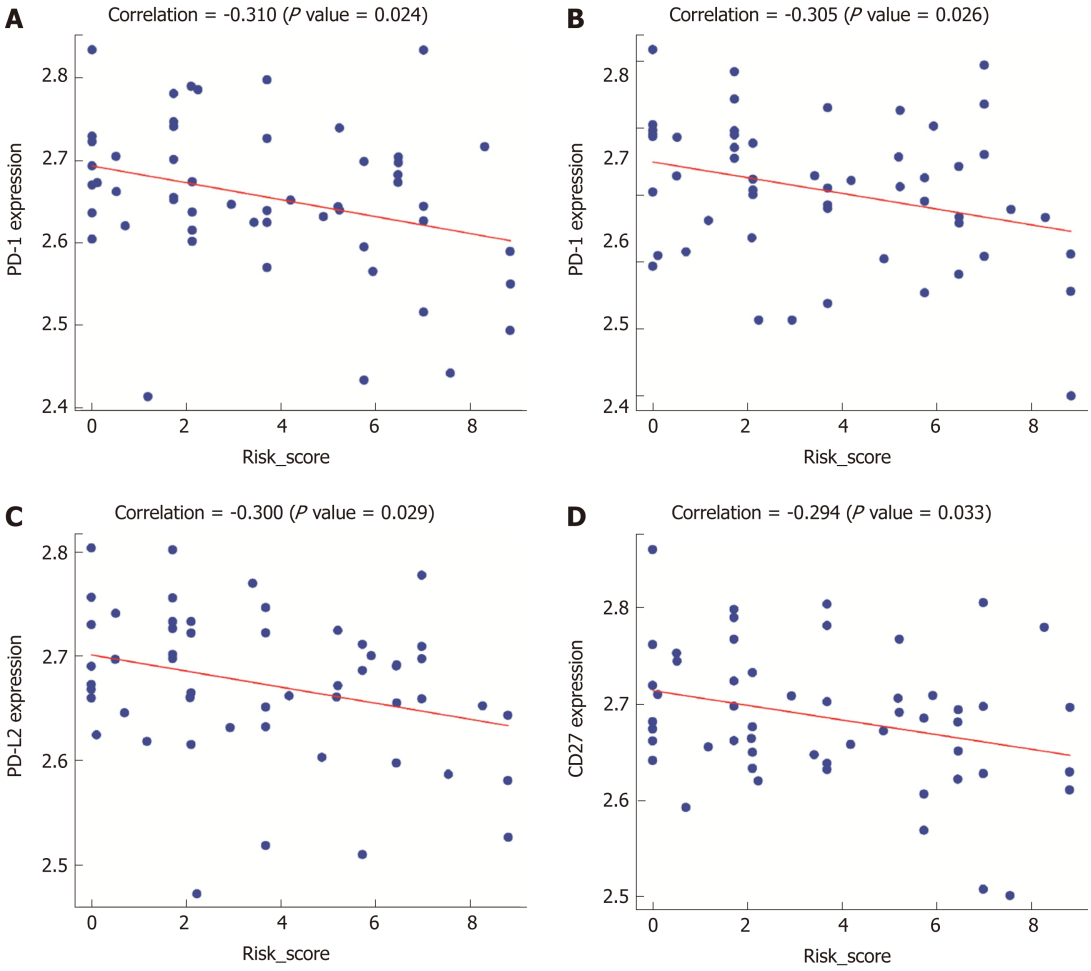


**Figure 6 Scatter plots describing the relationship of immunoscore with the expression of immune checkpoint regulators, including PD-1 (A), PD-L1 (B), PD-L2 (C), and CD27 (D).**

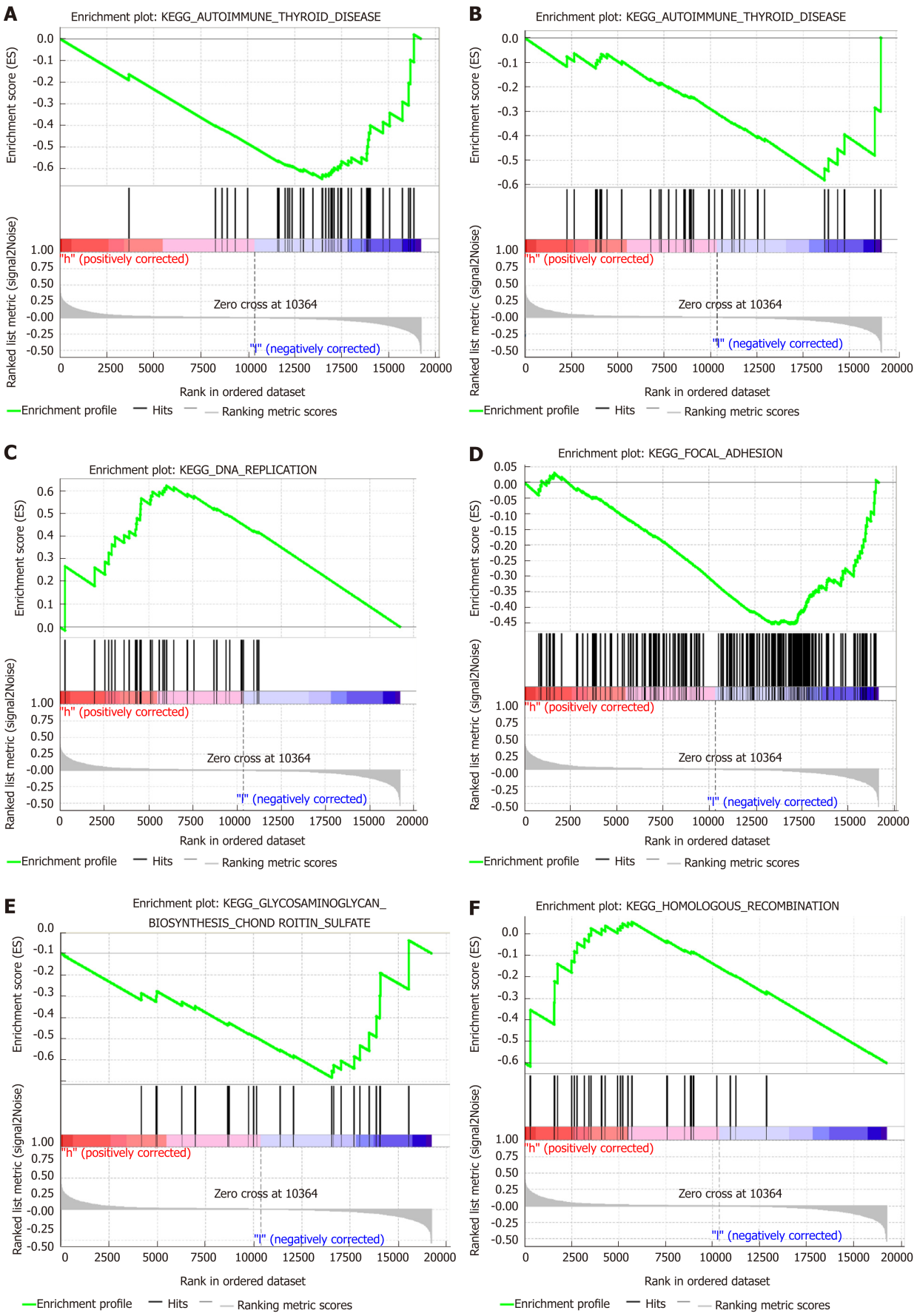
A
Enrichment plot: KEGG_AUTOIMMUNE_THYROID_DISEASE
B
Enrichment plot: KEGG_AUTOIMMUNE_THYROID_DISEASE
C
Enrichment plot: KEGG_DNA_REPLICATION
D
Enrichment plot: KEGG_FOCAL_ADHESION
E
Enrichment plot: KEGG_GLYCOSAMINOGLYCAN_BIOSYNTHESIS_CHOND ROITIN_SULFATE
F
Enrichment plot: KEGG_HOMOLOGOUS_RECOMBINATION
Enrichment score (ES)
Ranked list metric (signal2Noise)
"h" (positively corrected)
"l" (negatively corrected)
Zero cross at 10364
Rank in ordered dataset
Enrichment profile
Hits
Ranking metric scores

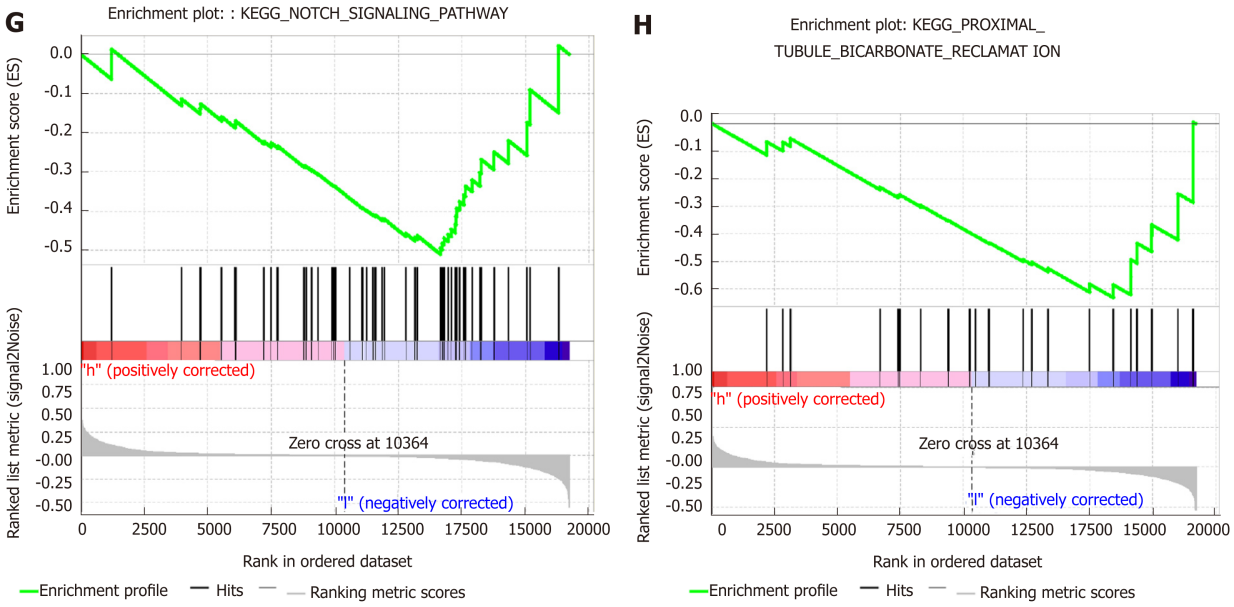


**Figure 7 Gene set enrichment analysis delineating the biological pathways related to the immunoscore values using the "c2.cp.kegg.v6.2.symbols" gene sets.**

## ARTICLE HIGHLIGHTS

### *Research background*

Hepatocellular carcinoma (HCC) is a common subtype of liver cancer, which has become a serious health threat worldwide. Hepatitis B virus (HBV) has been identified as a leading cause of HCC. Increasing evidence indicates that cancer immune infiltration is associated with clinical outcomes. However, no credible prognosis signature for HBV-associated HCC has been constructed through systemically assessing bulk tumor transcriptomic immune landscape.

### *Research motivation*

Tumor-infiltrating immunocytes represent a vital prognosis clue in HBV-associated HCC patients. In this study, a new immune model for HBV-associated HCC cases was developed through systematically assessing the bulk tumor transcriptomic immune landscape.

### *Research objectives*

The current research aimed to establish a prognosis-related immune signature based on bulk tumor transcriptome-derived immune infiltrate compositions, thus improving the prognosis prediction accuracy for HBV-associated HCC.

### *Research methods*

The fractions of 22 immunocyte types extracted based on public datasets were predicated using the cell type identification by estimating relative subsets of RNA transcripts (CIBERSORT) algorithm. Furthermore, an immunoscore was calculated based on immunocyte type fractions by the least absolute shrinkage and selection operator (LASSO) model.

### *Research results*

The immunoscore constituted by eight immunocyte type fractions was constructed by adopting the LASSO model, which displayed a high sensitivity and specificity for overall survival (OS), and the areas under the curves for the 1-year, 3-year, and 5-year OS were 0.971, 0.912, and 0.975, respectively. Difference in OS between the low-immunoscore and high-immunoscore groups was statistically significant. Additionally, a nomogram was established to expand the applied range of the model, which included the immunoscore as well as other clinical characteristics. The related pathways were enriched through gene set enrichment analysis.

### *Research conclusions*

The established immunoscore showed high prognosis prediction accuracy for patients with HBV-associated HCC, which may facilitate the risk stratification and provide valuable clinical suggestions for individual cases.

### *Research perspectives*

Findings of this study suggested that the tumor-infiltrating immunocytes could be used as promising biomarkers to predict the prognosis for HBV-associated HCC patients. This forms the framework for identification of efficient prognosis predictors and molecular biomarkers for HCC patients in the future.

## REFERENCES


1 **Chen QF**, Jia ZY, Yang ZQ, Fan WL, Shi HB. Transarterial Chemoembolization Monotherapy *vs* Combined Transarterial Chemoembolization-Microwave Ablation Therapy for Hepatocellular Carcinoma Tumors ≤ 5 cm: A Propensity Analysis at a Single Center. *Cardiovasc Intervent Radiol* 2017; **40**: 1748-1755 [PMID: 28681222 DOI: 10.1007/s00270-017-1736-8]

2 **Zhou HY**, Luo Y, Chen WD, Gong GZ. Hepatitis B virus mutation may play a role in hepatocellular carcinoma recurrence: A systematic review and meta-regression analysis. *J Gastroenterol Hepatol* 2015; **30**: 977-983 [PMID: 25689418 DOI: 10.1111/jgh.12917]

3 **Tang A**, Hallouch O, Chernyak V, Kamaya A, Sirlin CB. Epidemiology of hepatocellular carcinoma: target population for surveillance and diagnosis. *Abdom Radiol (NY)* 2018; **43**: 13-25 [PMID: 28647765 DOI: 10.1007/s00261-017-1209-1]

4 **El-Serag HB**. Epidemiology of viral hepatitis and hepatocellular carcinoma. *Gastroenterology* 2012; **142**: 1264-1273 [PMID: 22537432 DOI: 10.1053/j.gastro.2011.12.061]

5 **de Martel C**, Maucort-Boulch D, Plummer M, Franceschi S. World-wide relative contribution of hepatitis B and C viruses in hepatocellular carcinoma. *Hepatology* 2015; **62**: 1190-1200 [PMID: 26146815 DOI: 10.1002/hep.27969]

6 **Jang JE**, Hajdu CH, Liot C, Miller G, Dustin ML, Bar-Sagi D. Crosstalk between Regulatory T Cells and Tumor-Associated Dendritic Cells Negates Anti-tumor Immunity in Pancreatic Cancer. *Cell Rep* 2017; **20**: 558-571 [PMID: 28723561 DOI: 10.1016/j.celrep.2017.06.062]

7 **Wang TT**, Zhao YL, Peng LS, Chen N, Chen W, Lv YP, Mao FY, Zhang JY, Cheng P, Teng YS, Fu XL, Yu PW, Guo G, Luo P, Zhuang Y, Zou QM. Tumour-activated neutrophils in gastric cancer foster immune suppression and disease progression through GM-CSF-PD-L1 pathway. *Gut* 2017; **66**: 1900-1911 [PMID: 28274999 DOI: 10.1136/gutjnl-2016-313075]

8 **Fridman WH**, Pagès F, Sautès-Fridman C, Galon J. The immune contexture in human tumours: impact on clinical outcome. *Nat Rev Cancer* 2012; **12**: 298-306 [PMID: 22419253 DOI: 10.1038/nrc3245]

9 **Newman AM**, Liu CL, Green MR, Gentles AJ, Feng W, Xu Y, Hoang CD, Diehn M, Alizadeh AA. Robust enumeration of cell subsets from tissue expression profiles. *Nat Methods* 2015; **12**: 453-457 [PMID: 25822800 DOI: 10.1038/nmeth.3337]

10 **Charoentong P**, Finotello F, Angelova M, Mayer C, Efremova M, Rieder D, Hackl H, Trajanoski Z. Pan-cancer Immunogenomic Analyses Reveal Genotype-Immunophenotype Relationships and Predictors of Response to Checkpoint Blockade. *Cell Rep* 2017; **18**: 248-262 [PMID: 28052254 DOI: 10.1016/j.celrep.2016.12.019]

11 **Ali HR**, Chlon L, Pharoah PD, Markowetz F, Caldas C. Patterns of Immune Infiltration in Breast Cancer and Their Clinical Implications: A Gene-Expression-Based Retrospective Study. *PLoS Med* 2016; **13**: e1002194 [PMID: 27959923 DOI: 10.1371/journal.pmed.1002194]

12 **Subramanian A**, Tamayo P, Mootha VK, Mukherjee S, Ebert BL, Gillette MA, Paulovich A, Pomeroy SL, Golub TR, Lander ES, Mesirov JP. Gene set enrichment analysis: a knowledge-based approach for interpreting genome-wide expression profiles. *Proc Natl Acad Sci USA* 2005; **102**: 15545-15550 [PMID: 16199517 DOI: 10.1073/pnas.0506580102]

13 **Sun C**, Xu J, Song J, Liu C, Wang J, Weng C, Sun H, Wei H, Xiao W, Sun R, Tian Z. The predictive value of centre tumour CD8 T cells in patients with hepatocellular carcinoma: comparison with Immunoscore. *Oncotarget* 2015; **6**: 35602-35615 [PMID: 26415232 DOI: 10.18632/oncotarget.5801]

14 **Gabrielson A**, Wu Y, Wang H, Jiang J, Kallakury B, Gatalica Z, Reddy S, Kleiner D, Fishbein T, Johnson L, Island E, Satoskar R, Banovac F, Jha R, Kachhela J, Feng P, Zhang T, Tesfaye A, Prins P, Loffredo C, Marshall J, Weiner L, Atkins M, He AR. Intratumoral CD3 and CD8 T-cell Densities Associated with Relapse-Free Survival in HCC. *Cancer Immunol Res* 2016; **4**: 419-430 [PMID: 26968206 DOI: 10.1158/2326-6066.CIR-15-0110]

15 **Petrizzo A**, Buonaguro L. Application of the Immunoscore as prognostic tool for hepatocellular carcinoma. *J Immunother Cancer* 2016; **4**: 71 [PMID: 27879973 DOI: 10.1186/s40425-016-0182-5]

16 **Yao Q**, Bao X, Xue R, Liu H, Liu H, Li J, Dong J, Duan Z, Ren M, Zhao J, Song Q, Yu H, Zhu Y, Lu J, Meng Q. Prognostic value of immunoscore to identify mortality outcomes in adults with HBV-related primary hepatocellular carcinoma. *Medicine (Baltimore)* 2017; **96**: e6735 [PMID: 28445292 DOI: 10.1097/MD.0000000000006735]

17 **Hosaka T**, Suzuki F, Kobayashi M, Seko Y, Kawamura Y, Sezaki H, Akuta N, Suzuki Y, Saitoh S, Arase Y, Ikeda K, Kobayashi M, Kumada H. Long-term entecavir treatment reduces hepatocellular carcinoma incidence in patients with hepatitis B virus infection. *Hepatology* 2013; **58**: 98-107 [PMID: 23213040 DOI: 10.1002/hep.26180]

18 **Ogawa E**, Furusyo N, Nomura H, Dohmen K, Higashi N, Takahashi K, Kawano A, Azuma K, Satoh T, Nakamuta M, Koyanagi T, Kato M, Shimoda S, Kajiwara E, Hayashi J; Kyushu University Liver Disease Study (KULDS) Group. Short-term risk of hepatocellular carcinoma after hepatitis C virus eradication following direct-acting anti-viral treatment. *Aliment Pharmacol Ther* 2018; **47**: 104-113 [PMID: 29035002 DOI: 10.1111/apt.14380]

19 **Liu GM**, Huang XY, Shen SL, Hu WJ, Peng BG. Adjuvant antiviral therapy for hepatitis B virus-related hepatocellular carcinoma after curative treatment: A systematic review and meta-analysis. *Hepatol Res* 2016; **46**: 100-110 [PMID: 26331530 DOI: 10.1111/hepr.12584]

20 **Shinn BJ**, Martin A, Coben RM, Conn MI, Prieto J, Kroop H, DiMarino AJ, Hann HW. Persistent risk for new, subsequent new and recurrent hepatocellular carcinoma despite successful anti-hepatitis B virus therapy and tumor ablation: The need for hepatitis B virus cure. *World J Hepatol* 2019; **11**: 65-73 [PMID: 30705719 DOI: 10.4254/wjh.v11.i1.65]

21 **Friedman J**, Hastie T, Tibshirani R. Regularization Paths for Generalized Linear Models *via* Coordinate Descent. *J Stat Softw* 2010; **33**: 1-22 [PMID: 20808728 DOI: 10.18637/jss.v033.i01]

22 **McNeish DM**. Using Lasso for Predictor Selection and to Assuage Overfitting: A Method Long Overlooked in Behavioral Sciences. *Multivariate Behav Res* 2015; **50**: 471-484 [PMID: 26610247 DOI: 10.1080/00273171.2015.1036965]

23 **Kudo M**. Immune Checkpoint Inhibition in Hepatocellular Carcinoma: Basics and Ongoing Clinical Trials. *Oncology* 2017; **92**: 50-62 [PMID: 28147363 DOI: 10.1159/000451016]

24 **Syn NL**, Teng MWL, Mok TSK, Soo RA. De-novo and acquired resistance to immune checkpoint targeting. *Lancet Oncol* 2017; **18**: e731-e741 [PMID: 29208439 DOI: 10.1016/S1470-2045(17)30607-1]

25 **Philips GK**, Atkins M. Therapeutic uses of anti-PD-1 and anti-PD-L1 antibodies. *Int Immunol* 2015; **27**: 39-46 [PMID: 25323844 DOI: 10.1093/intimm/dxu095]

26 **Chang B**, Shen L, Wang K, Jin J, Huang T, Chen Q, Li W, Wu P. High number of PD-1 positive intratumoural lymphocytes predicts survival benefit of cytokine-induced killer cells for hepatocellular carcinoma patients. *Liver Int* 2018; **38**: 1449-1458 [PMID: 29356308 DOI: 10.1111/liv.13697]
27 **Chang B**, Huang T, Wei H, Shen L, Zhu D, He W, Chen Q, Zhang H, Li Y, Huang R, Li W, Wu P. The correlation and prognostic value of serum levels of soluble programmed death protein 1 (sPD-1) and soluble programmed death-ligand 1 (sPD-L1) in patients with hepatocellular carcinoma. *Cancer Immunol Immunother* 2019; **68**: 353-363 [PMID: 30506460 DOI: 10.1007/s00262-018-2271-4]
28 **Hendriks J**, Gravestein LA, Tesselaar K, van Lier RA, Schumacher TN, Borst J. CD27 is required for generation and long-term maintenance of T cell immunity. *Nat Immunol* 2000; **1**: 433-440 [PMID: 11062504 DOI: 10.1038/80877]

World Journal of Gastroenterology

Submit a Manuscript: https://www.f6publishing.com

*World J Gastroenterol* 2019 September 21; 25(35): 5283-5299

DOI: 10.3748/wjg.v25.i35.5283

ISSN 1007-9327 (print) ISSN 2219-2840 (online)

ORIGINAL ARTICLE

Basic Study

# Long non-coding RNA highly up-regulated in liver cancer promotes exosome secretion

Shun-Qi Cao, Hong Zheng, Bao-Cun Sun, Zheng-Lu Wang, Tao Liu, Dong-Hui Guo, Zhong-Yang Shen

**ORCID number:** Shun-Qi Cao (0000-0002-4248-474X); Hong Zheng (0000-0002-4677-7945); Bao-Cun Sun (0000-0002-6478-1366); Zheng-Lu Wang (0000-0003-0922-7706); Tao Liu (0000-0002-1042-3168); Dong-Hui Guo (0000-0001-5077-2664); Zhong-Yang Shen (0000-0002-0837-1805).

**Author contributions:** Cao SQ, Zheng H, Sun BC, Wang ZL, and Liu T performed the research, analysed the data, and wrote and revised the manuscript; Shen ZY designed the study and participated in the revision of the article; all authors have read and approved the final manuscript.

**Supported by** Tianjin Clinical Research Center for Organ Transplantation Project, No. 15ZXLCSY00070; and The Non-profit Central Research Institute Fund of Chinese Academy of Medical Sciences, No. 2018PT32021.

**Institutional review board statement:** The study was reviewed and approved by the Tianjin First Central Hospital Medical Ethics Committee.

**Conflict-of-interest statement:** The authors declare no potential conflict of interest in this paper.



**Shun-Qi Cao, Dong-Hui Guo,** Tianjin First Central Hospital Clinic Institute, Tianjin Medical University, Tianjin 300070, China

**Hong Zheng, Zhong-Yang Shen,** Department of Organ Transplantation, Tianjin First Central Hospital, Tianjin 300192, China

**Bao-Cun Sun,** Department of Pathology, Tianjin Medical University, Tianjin 300070, China

**Zheng-Lu Wang,** Department of Pathology, Tianjin First Central Hospital, Tianjin 300192, China

**Tao Liu,** NHC Key Laboratory of Critical Care Medicine, Tianjin First Central Hospital, Tianjin 300192, China

**Corresponding author:** Zhong-Yang Shen, MD, PhD, Professor, Department of Organ Transplantation, Tianjin First Central Hospital, No. 24, Fukang Road, Nankai District, Tianjin 300192, China. shen_zhongyang@126.com
**Telephone:** +86-22-2362698
**Fax:** +86-22-2362698

## Abstract

### *BACKGROUND*

Highly upregulated in liver cancer (*HULC*) is a long non-coding RNA (lncRNA) which has recently been identified as a key regulator in hepatocellular carcinoma (HCC) progression. However, its role in the secretion of exosomes from HCC cells remains unknown.

### *AIM*

To explore the mechanism by which *HULC* promotes the secretion of exosomes from HCC cells.

### *METHODS*

Serum and liver tissue samples were collected from 30 patients with HCC who had not received chemotherapy, radiotherapy, or immunotherapy before surgery. *HULC* expression in serum exosomes and liver cancer tissues of patients was measured, and compared with the data obtained from healthy controls and tumor adjacent tissues. The effect of *HULC* upregulation in HCC cell lines and the relationship between *HULC* and other RNAs were studied using qPCR and dual-luciferase reporter assays. Nanoparticle tracking analysis was performed to detect the quantity of exosomes.

**Manuscript source**: Unsolicited manuscript

**Received:** April 26, 2019
**Peer-review started:** April 26, 2019
**First decision:** May 24, 2019
**Revised:** June 7, 2019
**Accepted:** July 19, 2019
**Article in press:** May 24, 2019
**Published online:** September 21, 2019

**P-Reviewer:** Bramhall C, Hoyos S, Ocker M, Yu J
**S-Editor:** Ma YJ
**L-Editor:** Wang TQ
**E-Editor:** Ma YJ

***RESULTS***
*HULC* expression in serum exosomes of patients with HCC was higher than that in serum exosomes of healthy controls, and *HULC* levels were higher in liver cancer tissues than in tumor adjacent tissues. The expression of *HULC* in serum exosomes and liver cancer tissues correlated with the tumor-node-metastasis (TNM) classification, and *HULC* expression in tissues correlated with that in serum exosomes. Upregulation of *HULC* promoted HCC cell growth and invasion and repressed apoptosis. Notably, it also facilitated the secretion of exosomes from HCC cells. Moreover, qPCR assays showed that *HULC* repressed *microRNA-372-3p* (*miR-372-3p*) expression. We also identified *Rab11a* as a downstream target of *miR-372-3p*. Dual-luciferase reporter assays suggested that *miR-372-3p* could directly bind both *HULC* and *Rab11a*.

***CONCLUSION***
Our findings illustrate the importance of the *HULC*/*miR-372-3p*/*Rab11a* axis in HCC and provide new insights into the molecular mechanism regulating the secretion of exosomes from HCC cells.

**Key words:** Long non-coding RNA; Exosomes; Hepatocellular carcinoma; *miR-372-3p*; *Rab11a*



**Core tip:** We found that (1) *HULC* expression was higher in serum exosomes of patients with HCC than in those of healthy controls, and higher in liver cancer tissues than in tumor adjacent tissues; (2) *HULC* expression in serum exosomes and liver cancer tissues were correlated with the TNM classification, and *HULC* expression in tissues was correlated with that in serum exosomes; (3) Increased *HULC* expression was associated with increased proliferation and invasion and reduced apoptosis of HCC cells; and (4) *HULC* repressed *miR-372-3p* expression, and *miR-372-3p* could directly bind both *HULC* and *Rab11a*. Furthermore, the *HULC*/ *miR-372-3p* /*Rab11a* axis promoted the secretion of exosomes from HCC cells.

**Citation:** Cao SQ, Zheng H, Sun BC, Wang ZL, Liu T, Guo DH, Shen ZY. Long non-coding RNA highly up-regulated in liver cancer promotes exosome secretion. *World J Gastroenterol* 2019; 25(35): 5283-5299
**URL**: https://www.wjgnet.com/1007-9327/full/v25/i35/5283.htm
**DOI**: https://dx.doi.org/10.3748/wjg.v25.i35.5283

## INTRODUCTION

Hepatocellular carcinoma (HCC) is a malignant tumor with high mortality, and more than 700000 patients with HCC die every year worldwide. Tumor invasion, metastasis, and recurrence are the main causes of death in these patients[1]. Despite advances in the understanding of the molecular mechanisms underlying HCC and improved therapeutic methods to treat this disease, the 5-year overall survival (OS) for patients with HCC is still unsatisfactory[2].

Long noncoding RNAs (lncRNAs) are transcribed RNAs that regulate gene expression through various mechanisms. LncRNAs exert vital roles in many processes such as transcriptional control, posttranscriptional regulation, and epigenetic regulation[3]. In recent years, it has been demonstrated that several lncRNAs play an important role in the progression of HCC[4]. One of these lncRNAs is *HULC*, located on chromosome 6p24.3, which was found to be highly expressed in HCC tissue by Panzitt in 2007[5]. *HULC* transcription produces an RNA of approximately 500 nt that is located in the cytoplasm and participates in the development of HCC[6]; it acts as a competitive endogenous RNA (ceRNA), which regulates mRNA through competitive miRNA sharing. For example, *HULC*, in combination with *miR-15a*, inhibits *PTEN* expression and participates in autophagy to promote the progression of HCC[7]. *Via* sequestrating *miR-124*, *HULC* participates in endothelial cell angiogenesis[8]. However, the mechanism of *HULC*-mediated invasion and metastasis of HCC remains unclear.

In recent years, exosomes have become a research hotspot, and they have been

found to be closely related to tumor progression[9]. Exosomes are membranous structures derived from cells that play various roles in normal physiology[10]. In cancer, exosomes have been shown to contribute to essential cancer-related processes such as sustaining the proliferative signalling, evading growth suppression, resisting cell death, enabling replicative immortality, inducing angiogenesis, promoting genome instability and mutations, increasing tumor-promoting inflammation, and especially activating invasion and metastasis. In the tumor, exosomes participate in basic cancer-related processes such as promoting cancer cell proliferation, reducing apoptosis, achieving replication immortality, inducing angiogenesis, promoting genomic instability and mutations, increasing tumors and promoting inflammation, and especially activating tumors. For example, exosomal *miR-335* could be a novel therapeutic strategy for HCC[11]. Tumor-derived exosomes could elicit tumor suppression in murine HCC models and humans *in vivo*[12]. Additionally, exosomes are frequently released by tumor cells and may facilitate the communication between the primary tumor and its local microenvironment[13]. The link between *HULC* and exosomes in tumor genesis and development has not been clarified to date.

In this study, we investigated the expression of *HULC* in serum-derived exosomes and hepatic tissues, analysed the correlation between *HULC* expression and other RNAs, and demonstrated the mechanism of action of *HULC* in HCC. Increased *HULC* expression was associated with increased proliferation and invasion, and reduced apoptosis of HCC cells. *HULC* was found to function as a ceRNA of *miR-372-3p*, which, in turn, inhibits the expression of *Rab11a*. Rab proteins are key regulators of intracellular membrane trafficking, and Rab11a has been reported to promote exosome secretion[14,15]. Thus, *HULC* induces exosome secretion and contributes to tumor growth and metastasis.

## MATERIALS AND METHODS

### Subjects

Serum samples and tissues ($n$ = 30) and paired adjacent liver tissues ($n$ = 30) were obtained from patients with HCC who underwent surgery at the Tianjin First Central Hospital (China) from January to August 2017. Normal human serum was taken from patients undergoing a physical examination at the Tianjin First Central Hospital (China). All our patients had hepatitis B virus associated cancer with cirrhosis. The average age of the patients was 53.9 ± 16.2 years. Patient clinical data are shown in Table 1. Tumor differentiation and TNM stage were assessed based on the WHO grading system. Each HCC case was confirmed by histopathological diagnosis. Blood samples from the patients were taken one week before surgery. Tissue samples were taken from the resected HCC tissues and tumor-adjacent liver tissues (histopathological diagnosis confirmed that the tumor had not invaded the adjacent tissues). The serum and tissue samples were immediately stored at -80 °C before use. This study was approved by the Tianjin First Central Hospital Medical Ethics Committee, and all patients provided written informed consent for the use of their samples for clinical research.

The inclusion criteria were: (1) Patients with complete clinical data; and (2) Patients had not received chemotherapy, radiotherapy, or immunotherapy before surgery. The exclusion criteria were: (1) Lack of clinical data; (2) Area of necrosis in the tumor tissue > 60%; and (3) Presence of additional malignant tumors.

### Cell culture

Human HCC cell lines (HepG2 and SMMC7721) and a normal hepatic cell line (LO2) were purchased from the Institute of Biochemistry and Cell Biology of the Chinese Academy of Sciences (Shanghai, China). Cells were cultured in DMEM or RPMI-1640 (GIBCO, Grand Island, NY, United States) containing 10% foetal bovine serum (FBS; BioWest, Nuaille, France), and 1% bivalent antibiotics (Hyclone, South Logan, UT, United States). Cells were incubated at 37 °C with 5% $CO_2$.

### Exosome extract

Exosomes were isolated from HCC cells as follows. Exosome-depleted FBS was obtained by ultracentrifugation at 110000 $g$ (CP80MX; HITACHI, Japan) for 16 h and used for culturing HCC cells. HCC cell culture medium supernatants were collected after incubation for 48 h, and then centrifuged at 10000 $g$ for 40 min to remove HCC cell debris. Supernatants were filtrated through a 0.22 μm-pore filter (Millipore). The ExoQuick solution (EXOTC10A-1, System Biosciences, Mountain View, United States) was added to the filtered solution at a 1:5 ratio. The mixed solution was stored at 4 °C for 12 h, and then centrifuged at 1500 $g$ for 30 min. The supernatants were discarded,

**Table 1 Relationship between expression of long non-coding RNA highly up-regulated in liver cancer and clinicopathological factors in patients with hepatocellular carcinoma**

| Clinicopathological factor | Number of patients (*n* = 30) | *HULC* in serum exosomes | | $X^2$ | *P*-value | *HULC in* HCC tissue | | $X^2$ | *P*-value |
|---|---|---|---|---|---|---|---|---|---|
| | | High | Low | | | High | Low | | |
| Age (yr) | | | | 0.391 | 0.532 | | | 0.382 | 0.497 |
| ≤ 55 | 18 | 11 | 7 | | | 12 | 8 | | |
| > 55 | 12 | 7 | 5 | | | 5 | 5 | | |
| sex | | | | 0.370 | 0.492 | | | 0.365 | 0.592 |
| Female | 21 | 11 | 7 | | | 13 | 8 | | |
| Male | 9 | 6 | 6 | | | 4 | 5 | | |
| **Tumor size (cm)** | | | | 2.323 | 0.124 | | | 2.225 | 0.126 |
| ≤ 5 | 10 | 4 | 6 | | | 5 | 5 | | |
| > 5 | 20 | 11 | 9 | | | 10 | 10 | | |
| **Tumor differentiation** | | | | 2.224 | 0.115 | | | 2.356 | 0.098 |
| Well/moderate | 21 | 12 | 9 | | | 11 | 8 | | |
| Poor | 9 | 5 | 4 | | | 6 | 5 | | |
| **Clinical stage (TNM)** | | | | 4.812 | 0.032 | | | 4.924 | 0.026 |
| I-II | 10 | 5 | 5 | | | 4 | 6 | | |
| III-IV | 20 | 11 | 9 | | | 12 | 8 | | |

*HULC*: Highly upregulated in liver cancer; HCC: Hepatocellular carcinoma; TNM: Tumor-node-metastasis.

and the precipitate (containing the exosomes) was dissolved in phosphate buffered saline (PBS).

Exosomes were isolated from patients' serum as follows. The serum was filtrated through a 0.22 μm-pore filter (Millipore). The ExoQuick solution (EXOQ5A-1, System Biosciences, Mountain View, United States) was added to the filtered solution at a 1:4 ratio. The mixed solution was stored at 4 °C for 12 h, and then centrifuged at 1500 *g* for 30 min. The supernatants were discarded, and the precipitate (containing the exosomes) was dissolved in PBS.

### Transfection

*HULC* (*HULC* over-expression plasmid), *HULC*-NC (*HULC* over-expression normal control plasmid), *HULC*-siRNA (*HULC* low-expression plasmid), *HULC*-siRNA-NC (*HULC* low-expression control plasmid), miRNA-*372-3p* (miRNA-*372-3p* over-expression plasmid), miRNA-*372-3p* inhibitor, WT-*HULC* (*HULC* wild type luciferase reporter plasmid), MUT-*HULC* (*HULC* mutant luciferase reporter plasmid), WT-*Rab11a* (*Rab11a* wild type luciferase reporter plasmid), and MUT-*Rab11a* (*Rab11a* mutant luciferase reporter plasmids) (Genechem, Shanghai, China) were used for transfection experiments. HepG2 and SMMC7721 cells were seeded in 6-well plates and transfected with *HULC* inhibitors or plasmids causing *HULC* overexpression, using Lipofectamine 3000 (Invitrogen, Carlsbad, CA, USA) according to the manufacturer's instructions. The transfected cells were incubated for 48 h before analysis.

### Western blot analysis

Protein samples were collected from cells or exosomes in RIPA lysis buffer (Solarbio, Beijing, China). The processed protein samples were separated by 10% SDS–polyacrylamide gel electrophoresis (SDS-PAGE), transferred to 0.22 μm PVDF membranes (Millipore), and incubated with primary antibodies against CD63, TSG101, Rab11a, and GAPDH (Abcam, Cambridge, MA, United States) at 4 °C. The secondary antibody was goat anti-rabbit antibody (Abcam, Cambridge, MA, United States) and incubation was performed at 24 °C. Chemiluminescence reagent (Millipore) was used to detect the proteins.

### Nanoparticle tracking analysis (NTA)

NTA with a ZetaView PMX (Particle Metrix, Dusseldorf, Germany) was used to measure concentration, mean particle size, and distribution of exosomes. Exosomes were resuspended in 0.05 × PBS (filtered through a 0.22 μm-pore filter) and added to the instrument. The same parameters were used for size and concentration

measurements. Data were analysed using the software ZetaView 8.02.28 and Microsoft Excel 2016 (Microsoft, Seattle, WA, United States).

### Transmission electron microscopy

The purified exosomes were fixed with 1% glutaraldehyde in PBS. A drop of the suspension (approximately 20 μL) was pipetted onto formvar/carbon-coated grids and stained with aqueous phosphotungstic acid for 1 min. The morphology of isolated exosomes was identified using a transmission electron microscope (HT7800, Hitachi, Japan).

### Quantitative PCR

Total RNA was extracted from HCC tissues and cells using Trizol reagent (Invitrogen, Carlsbad, CA, United States) and total RNA was extracted from exosomes using the SeraMir Exosome RNA Purification Kit (System Biosciences, Mountain View, United States) following the manufacturer's instructions. After determining the concentration, degree, and purity of RNA, cDNA was synthesised using a reverse transcription kit (Takara Biotechnology, Japan) and PCR was performed with a commercial kit (Takara Biotechnology). With GAPDH and U6 as references, the expression levels of HULC, miRNA-372-3p, and Rab11a were calculated using relative quantitative analysis. The relative standard curve method ($2^{-CT}$) was used to determine the relative RNA expression in cells and -CT was used to determine the relative RNA expression in HCC tissues and serum exosomes. The primers used for quantitative PCR (qPCR) are shown in Table 2.

### Dual-luciferase reporter assay

*HULC* could specifically bind to *miR-372-3p*, acting as a "microRNA sponge"[16,17]. At the same time, *miR-372-3p* was predicted to regulate *Rab11a* expression using TargetScan (http://www.targetscan.org/) and starBase (http://starbase.sysu.edu.cn/). *HULC* and *Rab11a* 3′-UTR double luciferase recombinant plasmids (Genechem, Shanghai, China) were constructed and transfected into HCC cells. Luciferase assays were performed using a luciferase reporter assay kit (Genecopoeia) according to the manufacturer's recommendations. Before detection, HCC cells were washed 2-3 times with PBS, and 150 μL of fresh passive cell lysate was added into each well (24-well plates) to lyse the cells. The supernatant was centrifuged at 13000 *g* for 1 min, and 20 μL of the supernatant was transferred to 96-well plates. Then, 100 μL of LAR II was added to detect the firefly luciferase activity. The Stop&Glo reagent (100 mL) was used to detect the fluorescence of the *Renilla* luciferase. Luciferase was measured using a microplate reader, with 1-2 s delay and 5-10 s readings for measurement. The final luciferase activity is expressed as the ratio of luciferase activity of firefly/luciferase activity of *Renilla*.

### Cell counting kit-8 (CCK8)

Cells (50000 cells per well) were cultured overnight in a 96-well plate. At 0, 24, 36, 48, and 72 h, respectively, 100 μL of CCK8 solution (BOSTER, Wuhan, China) was added. The assay was performed according to the manufacturer's recommendations. A microplate reader (Bio Tek Synergy2, United States) was used to measure the absorbance at 450 nm.

### Transwell assay

Cells were seeded in the upper chamber of Matrigel-coated Transwells (BD Bioscience, CA, United States). Serum-free medium was added to the upper chamber, and medium with 10% FBS was added into the lower chamber. Cells were incubated for 24 h; the non-migrating or non-invading cells were removed, and the remaining cells (on the bottom of the filters) were fixed using methanol and stained with crystal violet. Five random fields were chosen and counted per well using a microscope (×100), (Olympus, Tokyo, Japan).

### TUNEL assay

Apoptosis was detected using TUNEL assay. Cells were fixed using 4% paraformaldehyde for 30 min, and the assay was carried out using a TUNEL kit (Roche, Basel, Switzerland) according to the manufacturers' recommendations. Nuclei were stained with DAPI. Apoptotic cells with green nuclear staining were observed. Five random fields were chosen and counted per well by using a microscope (×100). The number of apoptotic cells was counted, and the apoptotic rate (%) was calculated as (apoptotic cell count/total cell number) × 100%.

### Statistical analysis

The SPSS statistical software version 20.0 was used for statistical analyses. The data,

**Table 2 Primers used for quantitative PCR**

| Gene | Primer sequence |
|---|---|
| *HULC* | Forward: 5′-GCAAGCCAGGAAGAGTCGTC-3' |
| | Reverse: 5′-GCTGTGCTTAGTTTATTGCCAGG-3' |
| *GAPDH* | Forward: 5'-GTCAACGGATTTGGTCTGTATT-3' |
| | Reverse: 5'-AGTCTTCTGGGTGGCAGTGAT-3' |
| miRNA-*372-3p* | Forward: 5'-CAACAGAAGGCTCGAGCAACCTGCGGAGAAGATAC-3' |
| | Reverse: 5'-TTCTGATCAGGATCCCATTACAGCCAGACGCTGTAAG-3' |
| *U6* | Forward: 5'-GCGCGTCGTGAAGCGTTC-3' |
| | Reverse: 5'-GTGCAGGGTCCGAGGT-3' |
| *Rab11a* | Forward: 5'-ACATCAGCATATTATCGTGGAGC-3' |
| | Reverse: 5'-GGAACTGCCCTGAGATGACG-3' |

*HULC*: Highly upregulated in liver cancer.

expressed as the mean ± SD, were analysed using one-way ANOVA. Count data, expressed as percentages (%), were analysed using the $\chi^2$ tests. *P*-values < 0.05 were considered statistically significant.

## RESULTS

### *Exosome extraction from HCC cells and serum of patients with HCC*

Exosomes were successfully extracted from the serum of patients with HCC and HCC cell medium (Figure 1). First, we examined the shape and size of the exosomes isolated from HCC serum (Figure 1A) and the culture medium of HepG2 or SMMC7721 cells (Figure 1B) by transmission electron microscopy. The exosomes were homogeneous in shape and size, and the vesicles had the characteristic appearance of exosomes with a membrane-capsulated spherical shape. The median size of the vesicles, calculated by NTA, was 110.2 nm and 106.9 nm in HCC serum (Figure 1C) and the culture medium of HepG2 or SMMC7721 cells (Figure 1D), respectively, similar to the reported size of exosomes (30–120 nm)[18]. Additionally, Western blot assays showed that the TSG101 and CD63 exosome markers were part of the exosome cargo (Figure 1E, 1F), confirming that the isolated vesicles were indeed exosomes.

### *HULC is upregulated in liver cancer serum-derived exosomes, hepatic tissues, and HCC cells*

The baseline characteristics of the 30 patients (9 men and 21 women) enrolled in this study are summarised in Table 1. The average age was 53.9 ± 16.2 years. The expression of *HULC* in the serum exosomes of patients with HCC was higher than that in exosomes from healthy subjects ($P < 0.05$; Figure 2A). *HULC* levels in liver cancer tissues were higher than those in adjacent tissues ($P < 0.05$; Figure 2B). The expression of *HULC* in tissues correlated with that in exosomes ($r = 0.633$, $P < 0.05$; Figure 2C). Additionally, the expression of *HULC* in serum exosomes correlated with the TNM stage of the patients ($P < 0.05$; Table 1). Finally, *HULC* was upregulated in HepG2 and SMMC7721 cells (Figure 3A).

### *HULC induces HCC cell proliferation and invasion and inhibits apoptosis*

After transfection of *HULC* over-expression and inhibiting plasmids into HCC cells, the expression of *HULC* changed significantly (Figure 3B, 3C). To explore the role of *HULC* in HCC cells, we performed CCK8 assays. We observed that *HULC* upregulation was associated with the growth of HepG2 and SMMC7721 cells (Figure 4A). Next, TUNEL assays showed that apoptosis was significantly inhibited by *HULC* (Figure 4B, 4C). Finally, we tested the effect of HULC on the invasion capabilities of HCC cells using Transwell assays, which showed that HULC induced the invasion of HCC cells (Figure 4D, 4E). These results suggest that *HULC* remarkably promoted HCC development.

### *HULC reduces the expression of miR-372-3p by sponging it*

The relationship between lncRNA *HULC* and *miR-372-3p* has been reported in many studies[16,17]. Therefore, we identified the binding sites between *miR-372-3p* and *HULC* (Figure 5A). To confirm the direct interaction between *miR-372-3p* and *HULC*, we

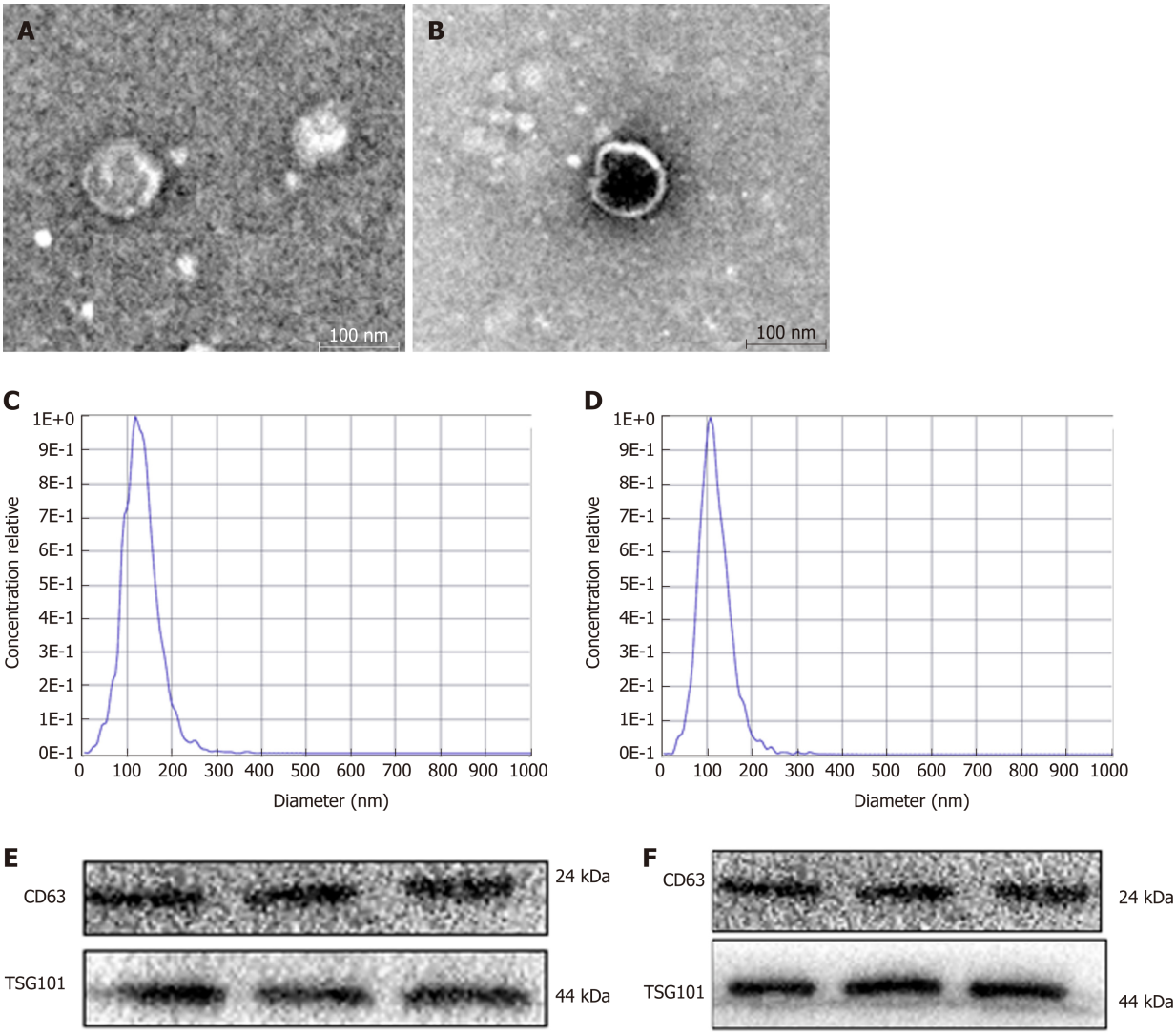


**Figure 1 Identification of the exosomes.** A: Transmission electronc microscopy (TEM) of exosomes extracted from the serum of patients with hepatocellular carcinoma (HCC); B: TEM of exosomes isolated from HCC cell medium; C: Western blot analysis of exosomal markers (CD63 and TSG101) in HCC serum; D: Western blot analysis of exosomal markers (CD63 and TSG101) in HCC cell medium; E: Nanoparticle tracking analysis (NTA) for detection of exosomes extracted from the HCC serum; F: NTA detection of exosomes extracted from HCC cell medium.

generated luciferase reporter plasmids with the wild type or mutated *HULC* sequence (Figure 5A). A decreased reporter activity was observed when wild type *HULC* and *miR-372-3p* mimics were co-transfected into HCC cells (Figure 5B). To investigate whether *miR-372-3p* is regulated by *HULC in vitro*, we overexpressed *HULC* in HepG2 and SMMC7721 cells and measured *miR-372-3p* expression (Figure 5C). We found that *miR-372-3p* levels decreased after *HULC* upregulation (Figure 5C), indicating a negative correlation between *miR-372-3p* and *HULC*. These results showed that *miR-372-3p* is a direct target of *HULC* in HCC cells.

### *Rab11a is a direct target of miR-372-3p in HCC cells*

Next, we used bioinformatic analyses to predict the downstream target of *miR-372-3p*. We identified *Rab11a* as a putative target of *miR-372-3p*. To validate the interaction between *miR-372-3p* and *Rab11a*, we performed luciferase reporter assays using plasmids with wild type *Rab11a* and mutated *Rab11a* (Figure 5D, 5E). Co-transfection of the luciferase reporter plasmid containing wild type *Rab11a* and *miR-372-3p* inhibitors in HCC cells led to increased luciferase activity (Figure 5E). Additionally, *miR-372-3p* inhibitors increased Rab11a expression (Figure 5F).

### *HULC acts via the miR-372-3p /Rab11a axis*

To further confirm whether *HULC* can regulate the secretion of exosomes *via* the *miR-372-3p*/Rab11a axis, *HULC*-siRNA and *miR-372-3p*-siRNA were co-transfected into HCC cells. We found that the expression of Rab11a was inhibited by *HULC* silencing, whereas *miR-372-3p* downregulation rescued Rab11a expression (Figure 6). Western

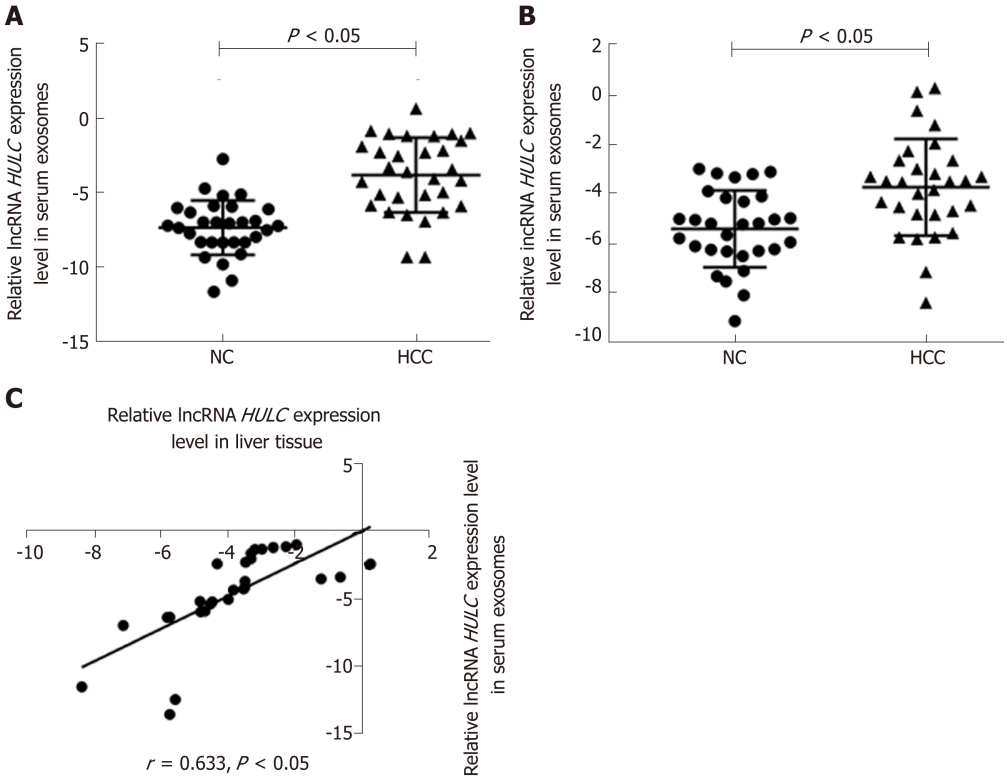


**Figure 2 Detection of long non-coding RNA highly up-regulated in liver cancer in hepatocellular carcinoma.** A: Expression of *HULC* in the serum exosomes of patients with HCC; B: Expression of *HULC* in liver cancer tissues; C: Correlation between *HULC* expression in HCC serum exosomes and tissue. Error bars stand for the mean ± SD of at least triplicate experiments. *HULC*: Highly upregulated in liver cancer; HCC: Hepatocellular carcinoma.

blot assays showed similar results (Figure 6). These findings indicate that *HULC* can promote the secretion of exosomes by decreasing *miR-372-3p* and increasing Rab11a expression.

### *Increased HULC and Rab11a and decreased miR-372-3p promote secretion of exosomes from HCC cells*

NTA was used to detect the expression of exosomes in the following groups. The number of exosomes from HepG2 and SMMC7721 cells in the *HULC* group was higher than that in the *HULC*-NC or NC group. However, there was no significant difference between the *HULC*-NC and NC groups (Figure 7A).

The number of exosomes from HepG2 and SMMC7721 cells in the *miR-372-3p-siRNA* group was higher than that in the *miR-372-3p-siRNA*-NC or NC groups. However, there was no significant difference between the *miR-372-3p*-NC and NC groups (Figure 7B).

The number of exosomes from HepG2 and SMMC7721 cells in the *Rab11a* group was higher than that in the *Rab11a*-NC or NC groups. However, there was no significant difference between the *Rab11a*-NC and NC groups (Figure 7C).

## DISCUSSION

Many studies have reported that lncRNAs participate in various cellular processes and have key functions in cancer epigenetics. Specifically, some lncRNAs are associated with recurrence, metastasis, and prognosis of various cancers, such as HCC, gastric cancer, and breast cancer[19-22]. LncRNA *HULC* is one of them, playing an important role in the development of liver tumors. *HULC* is highly expressed in HCC and is involved in the regulation of tumorigenesis and development[5]. Phosphorylation of the cAMP response element binding protein (CREB) activates the transcription of HULC[16]. Du *et al*[23] found that the mechanism for hepatitis B virus X protein (HBx)-activated *HULC* to promote the proliferation of HCC cells is closely related to downregulation of p18. *HULC* mediates abnormal lipid metabolism in HCC cells by sequestering *miR-9*[24]. *HULC* is also expressed in gastric cancer[25], pancreatic cancer[26], and other cancers.

Our clinical data showed that *HULC* expression is increased in HCC tissues

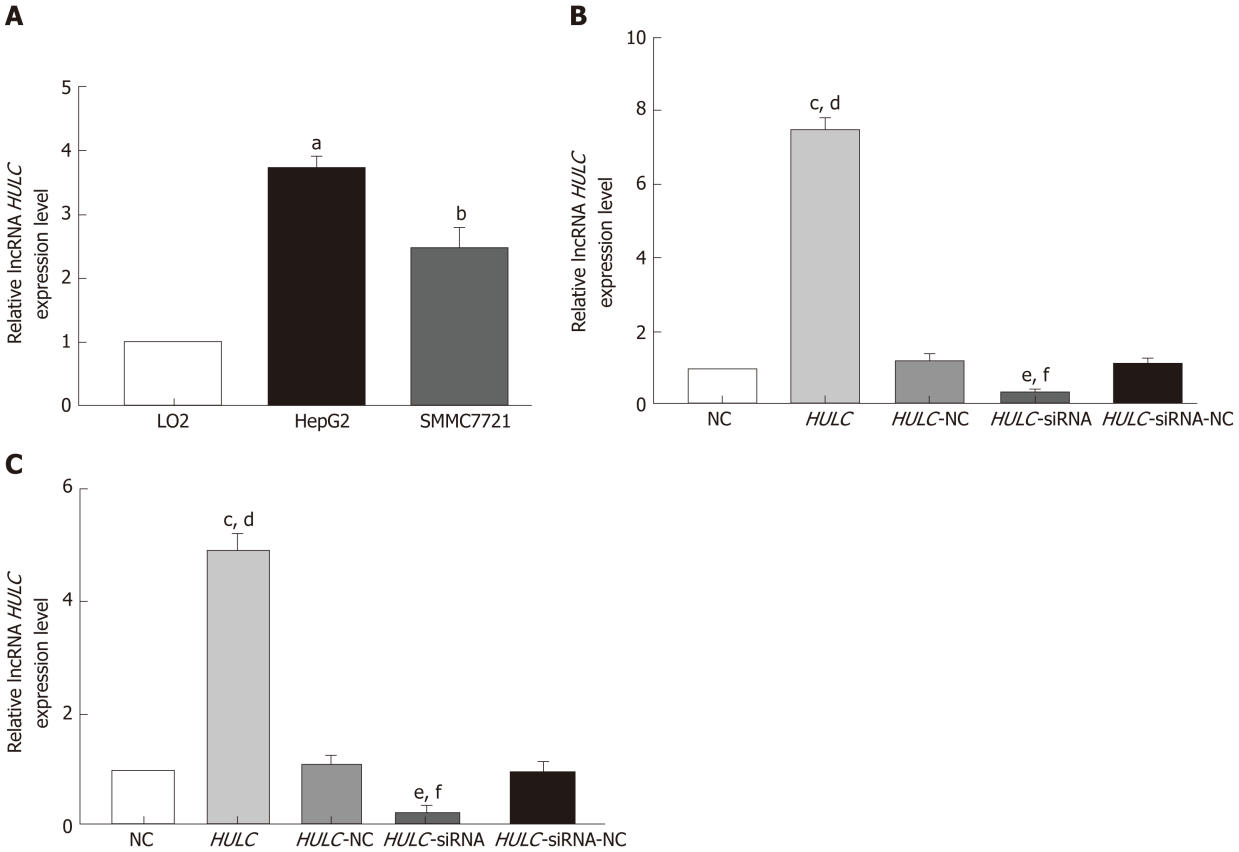


**Figure 3 Detection of long non-coding RNA highly up-regulated in liver cancer in hepatocellular carcinoma cells.** A:Expression of *HULC* in HepG2, SMMC7721, and LO2 cells; B: Expression of *HULC* in HepG2 transfected with *HULC* inhibitors or plasmids causing *HULC* overexpression; C: Expression of *HULC* in SMMC7721 transfected with *HULC* inhibitors or plasmids causing *HULC* overexpression. Error bars stand for the mean ± SD of at least triplicate experiments. $^{a}P < 0.05$ *vs* LO2 group; $^{b}P < 0.05$ *vs* LO2 group; $^{c}P < 0.01$ *vs* NC group; $^{d}P < 0.01$ *vs* *HULC*-NC group; $^{e}P < 0.05$ *vs* NC group; $^{f}P < 0.05$ *vs* *HULC*-siRNA-NC group. *HULC*: Highly upregulated in liver cancer; NC: Normal control group; *HULC*: *HULC* over-expression plasmid group; *HULC*-NC: *HULC* over-expression normal control plasmid group; *HULC*-siRNA: *HULC* low-expression plasmid group; *HULC*-siRNA-NC: *HULC* low-expression control plasmid group.

compared with adjacent liver tissues. Moreover, we found that *HULC* expression was higher in the exosomes derived from the serum of patients with HCC than in those derived from the serum of healthy controls. Notably, *HULC* expression in HCC tissues and serum exosomes was significantly related to HCC clinical stage. Therefore, *HULC* can be used as a potential biomarker candidate in HCC. Although *HULC* has been shown to participate in neoplasm invasion and metastasis, the underlying mechanism remains unclear. In recent years, the relation between exosomes and tumor progression has become evident[27]. However, the role of *HULC* in this process has not been demonstrated.

Exosomes play a key role in HCC progression[13]. Exosome-mediated miRNAs regulate TAK1 expression and lead to deterioration of HCC[28]. In addition, lncRNA *H19* in exosomes derived from CD90+ HCC cells influence tumor microenvironment balance by accelerating angiogenesis[29]. Exosome-mediated lysyl oxidase-like 4 (LOXL4) activation promotes tumor metastasis by modulating the *FAK/SRC* pathway in HCC[30]. Several studies have confirmed that lncRNAs in blood-circulating exosomes can be used as diagnostic markers for cancers: *LINC00152*[31] and *ZFAS1*[32] in gastric cancer, *MALAT-1*[33] in lung cancer, *BCAR4*[34] and *CRNDE-h*[35] in colon cancer, and *HOTAIR*[36] in laryngeal squamous cell carcinoma.

In this study, we showed that the expression of *HULC* in exosomes from HCC serum and in HCC tissues were higher than that in the control group, and that there was a linear correlation between them. Therefore, *HULC* in exosomes from the blood of patients with HCC can be used as a diagnostic marker. We showed that the expression of *HULC* in exosomes correlated with TNM stage and therefore, with the progression of HCC. These findings are in agreement with previous studies[5,37].

We also investigated the relationship between *HULC* and exosome secretion. Bioinformatic analyses suggest that *HULC* mediated the secretion of exosomes from HCC cells *via* the *miR-372-3p/Rab11a* axis. Rab11a is a key regulatory protein that induces exosome secretion. In addition, we found that the number of exosomes from HCC cell lines overexpressing *HULC* was higher than that of control groups,

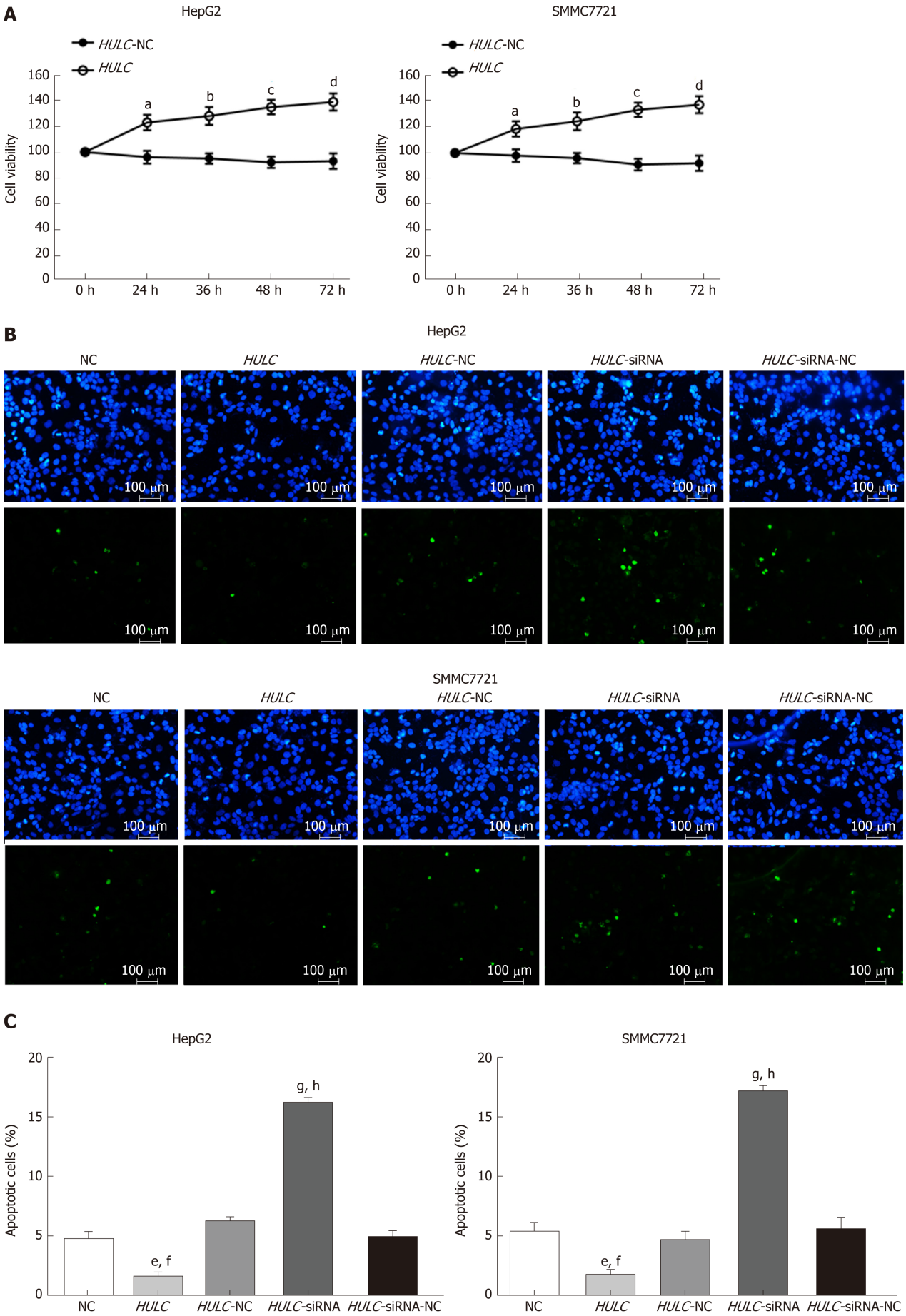
A
HepG2
SMMC7721
HULC-NC
HULC
Cell viability
0 h
24 h
36 h
48 h
72 h
a
b
c
d
B
HepG2
SMMC7721
NC
HULC
HULC-NC
HULC-siRNA
HULC-siRNA-NC
100 μm
C
Apoptotic cells (%)
e, f
g, h

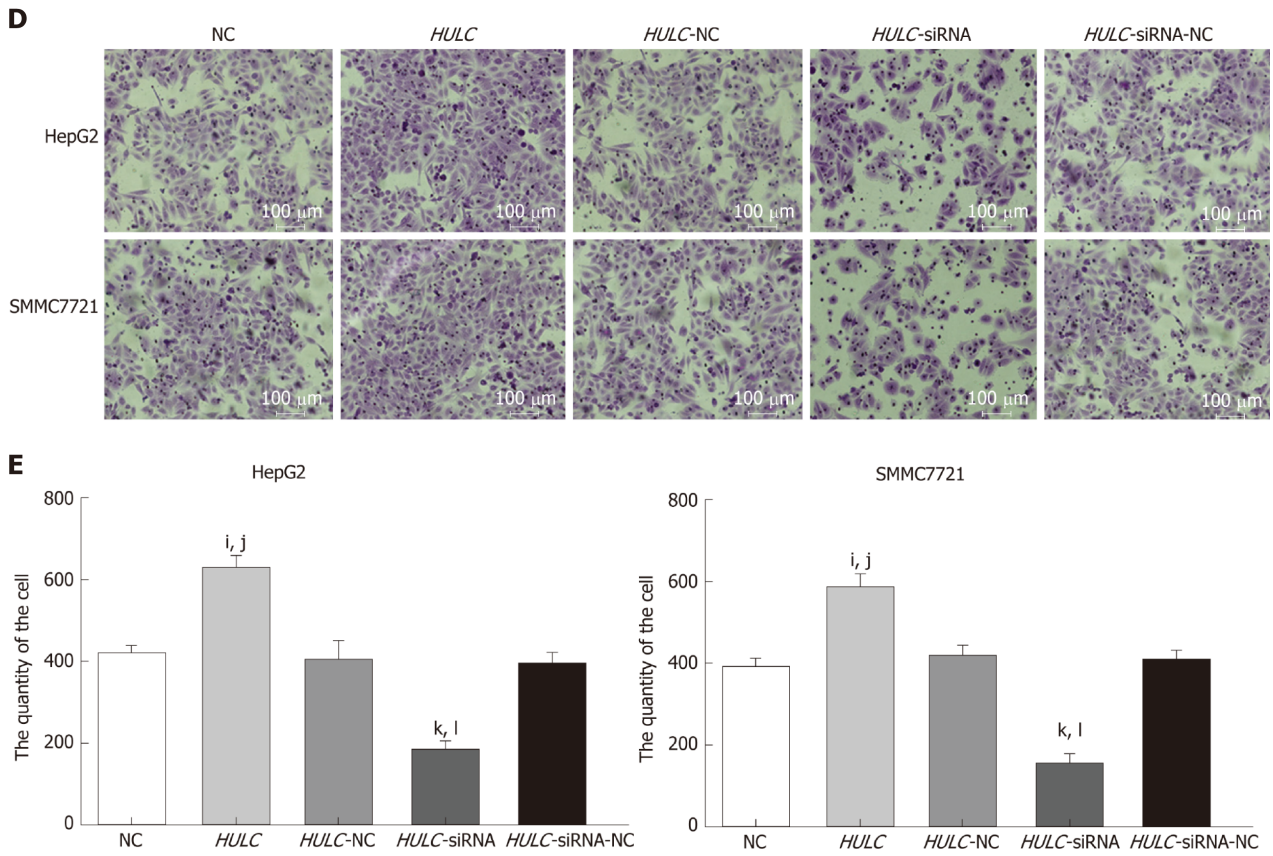


**Figure 4 Long non-coding RNA highly up-regulated in liver cancer induces hepatocellular carcinoma cell proliferation and invasion and inhibits apoptosis *in vitro*.** A: Proliferation of hepatocellular carcinoma (HCC) cells transfected with *HULC* inhibitors or plasmids causing *HULC* overexpression; B: Apoptotic pictures of HCC cells (×100). The blue fluorescence is DAPI nuclear staining and green fluorescence is the apoptotic cell. The index of apoptosis is the number of apoptotic cells/total number of visual field × 100%; C: Column chart of index of apoptosis in different groups; D: Effect of *HULC* on invasion of HCC cells evaluated bTranswell assay (×100); E: Column chart of number of invasive HCC cells in different groups. Error bars stand for the mean ± SD of at least triplicate experiments. $^{a}P < 0.05$ *vs* *HULC*-NC 24 h group; $^{b}P < 0.05$ *vs* *HULC*-NC 36 h group; $^{c}P < 0.05$ *vs* *HULC*-NC 48 h group; $^{d}P < 0.05$ *vs* *HULC*-NC 72 h group; $^{e}P < 0.05$ *vs* NC group; $^{f}P < 0.05$ *vs* *HULC*-NC group; $^{g}P < 0.01$ *vs* NC group; $^{h}P < 0.01$ *vs* *HULC*-siRNA-NC group; $^{i}P < 0.05$ *vs* NC group; $^{j}P < 0.05$ *vs* *HULC*-NC group; $^{k}P < 0.05$ *vs* NC group; $^{l}P < 0.05$ *vs* *HULC*-siRNA-NC group. *HULC*: Highly upregulated in liver cancer; NC: Normal control group; *HULC*: *HULC* over-expression plasmid group; *HULC*-NC: *HULC* over-expression normal control plasmid group; *HULC*-siRNA: *HULC* low-expression plasmid group; *HULC*-siRNA-NC: *HULC* low-expression control plasmid group.

indicating that *HULC* promotes exosome secretion.

Many studies have reported that lncRNAs act as sponges of miRNAs and inhibit their function[38]. For example, *HULC* mediates abnormal lipid metabolism in HCC cells by sequestering *miR-9*[24]. Here, we observed a negative correlation between *HULC* and *miR-372-3p*. A previous report showed that low *miR-372-3p* expression correlates with a poor prognosis and tumor metastasis in HCC[39]. Our results showed that when *HULC* was upregulated in HCC cells, *miR-372-3p* was repressed. Dual-luciferase reporter assays confirmed that *HULC* directly interacted with *miR-372-3p*. In addition, decreased levels of *miR-372-3p* promoted the secretion of exosomes from HCC cells.

Rab11a is a member of the subfamily of the Rab small molecule GTPases and is a key regulatory protein that induces exosome secretion[14,15]. Rab11a plays an important role in the regulation of endosome recycling and is highly expressed in many tumors, such as esophageal adenocarcinoma[40] and skin cancer[41]. In addition, the Rab11 family-interacting protein 4 is involved in the metastasis of HCC[42]. In our study, we found that *Rab11a* is a downstream target of *miR-372-3p* and that it promotes the secretion of exosomes from HCC cells. Collectively, our results suggest that *HULC* negatively interferes with *miR-372-3p*-mediated inhibition of Rab11a, leading to secretion of exosomes in HCC.

In conclusion, we demonstrated that *HULC* enhances the secretion of exosomes by sponging *miR-372-3p* which in turn targets *Rab11a*. Our findings provide novel insights into the mechanism of action of *HULC* in HCC. We plan to continue investigating the precise mechanisms through which Rab11a and exosomes regulate HCC development. Whether *HULC* targets other miRNAs to promote exosome secretion also warrants additional research. In addition, we need to further explore the relationship between silencing of *HULC* and angiogenesis, epidermal

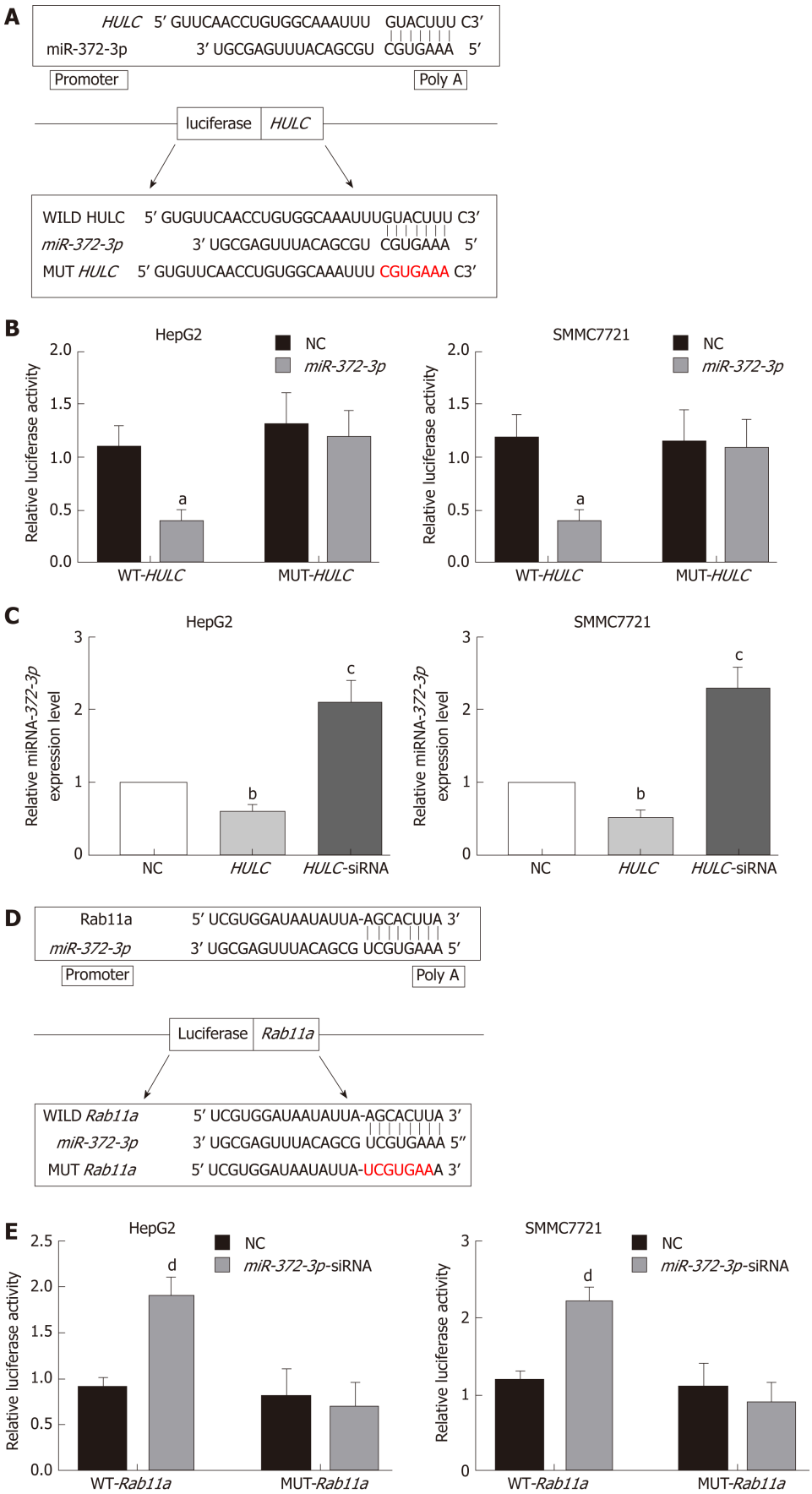
A
HULC 5′ GUUCAACCUGUGGCAAAUUU GUACUUU C3′
miR-372-3p 3′ UGCGAGUUUACAGCGU CGUGAAA 5′
Promoter
Poly A
luciferase HULC
WILD HULC 5′ GUGUUCAACCUGUGGCAAAUUUGUACUUU C3′
miR-372-3p 3′ UGCGAGUUUACAGCGU CGUGAAA 5′
MUT HULC 5′ GUGUUCAACCUGUGGCAAAUUU CGUGAAA C3′
B
HepG2
SMMC7721
NC
miR-372-3p
Relative luciferase activity
WT-HULC
MUT-HULC
C
Relative miRNA-372-3p expression level
NC
HULC
HULC-siRNA
D
Rab11a 5′ UCGUGGAUAAUAUUA-AGCACUUA 3′
miR-372-3p 3′ UGCGAGUUUACAGCG UCGUGAAA 5′
Promoter
Poly A
Luciferase Rab11a
WILD Rab11a 5′ UCGUGGAUAAUAUUA-AGCACUUA 3′
miR-372-3p 3′ UGCGAGUUUACAGCG UCGUGAAA 5″
MUT Rab11a 5′ UCGUGGAUAAUAUUA-UCGUGAAA 3′
E
miR-372-3p-siRNA
WT-Rab11a
MUT-Rab11a

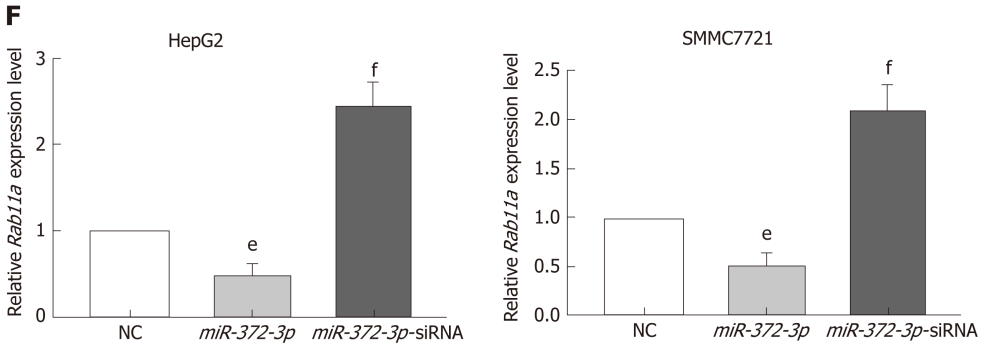


**Figure 5 Long non-coding RNA highly up-regulated in liver cancer mediates secretion of exosomes from hepatocellular carcinoma cells *via miR-372-3p /Rab11a*.** A: Sequence of binding sites between *HULC* and *miR-372-3p*; B: Dual-luciferase reporter assay for *miR-372-3p* and *HULC*; C: Relative expression of *miR-372-3p* after HCC cells were transfected with *HULC* inhibitors or plasmids causing *HULC* overexpression; D: Sequence of binding sites with *Rab11a* and *miR-372-3p*; E: Dual-luciferase reporter assay for miR-*372-3p* and *Rab11a*; F: Relative expression of *Rab11a* after HCC cells were transfected with *miR-372-3p*-siRNA or plasmids causing *miR-372-3p* overexpression. Error bars stand for the mean ± SD of at least triplicate experiments. [a]$P < 0.05$ *vs* WT-*HULC*-NC group; [b]$P < 0.05$ *vs* NC group; [c]$P < 0.01$ *vs* NC group; [d]$P < 0.05$ *vs* WT-*Rab11a* -NC group; [e]$P < 0.05$ *vs* NC group; [f]$P < 0.01$ *vs* NC group. *HULC*: Highly upregulated in liver cancer; NC: Normal control group; *HULC*: *HULC* over-expression plasmid group; *HULC*-siRNA: *HULC* low-expression plasmid group; *miRNA-372-3p*: *miRNA-372-3p* over-expression plasmid group; *miR-372-3p*-siRNA: *miR-372-3p* low-expression plasmid group; WT-*HULC*: *HULC* wild type luciferase reporter plasmid group; MUT-*HULC*: *HULC* mutant luciferase reporter plasmids group; WT-*Rab11a*: *Rab11a* wild type luciferase reporter plasmid group; MUT-*Rab11a*: *Rab11a* mutant luciferase reporter plasmids group.

mesenchymal transition, and lipid metabolism in HCC. Furthermore, the relationship between silencing of *HULC* and survival and prognosis of patients with HCC needs to be elucidated.

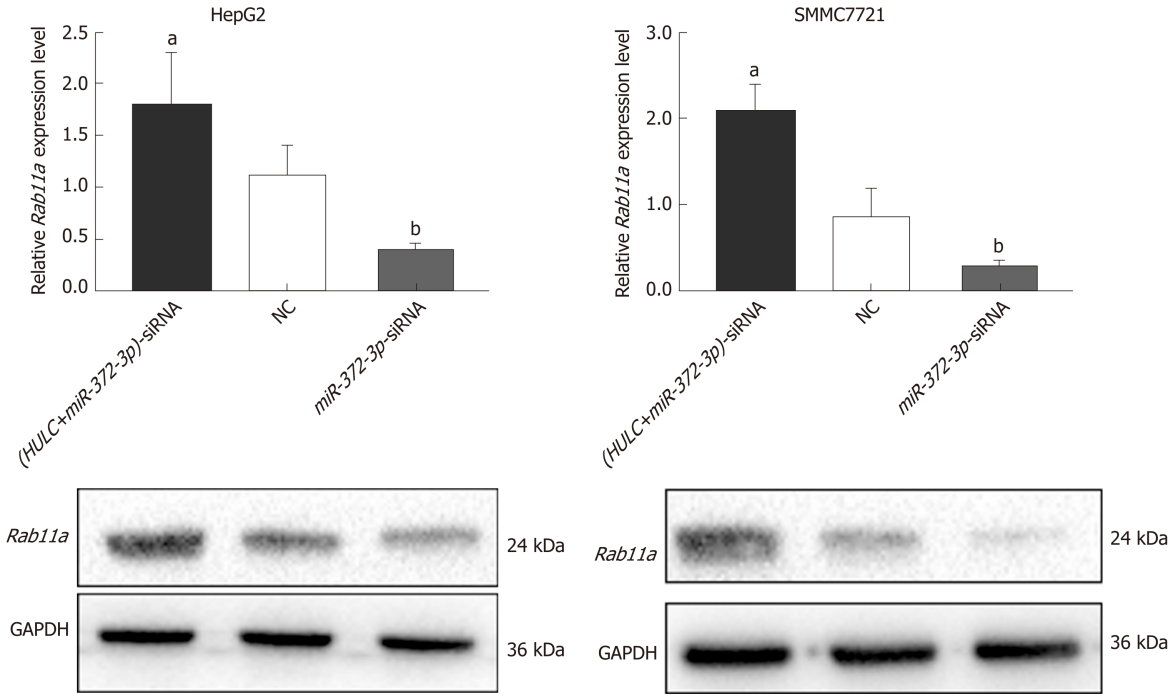


**Figure 6 Expression of Rab11a in hepatocellular carcinoma cells transfected with highly up-regulated in liver cancer-siRNA and *miR-372-3p*-siRNA.** Silencing *HULC* inhibited Rab11a expression, while silencing *HULC* and *miR-372-3p* increased Rab11a expression *in vitro*. Error bars stand for the mean ± SD of at least triplicate experiments. [a]$P < 0.05$ *vs* NC group; [b]$P < 0.05$ *vs* NC group. *HULC*: Highly upregulated in liver cancer; NC: Normal control group; *HULC*-siRNA: *HULC* low-expression plasmid group; *miR-372-3p*-siRNA: *miR-372-3p* low-expression plasmid group.

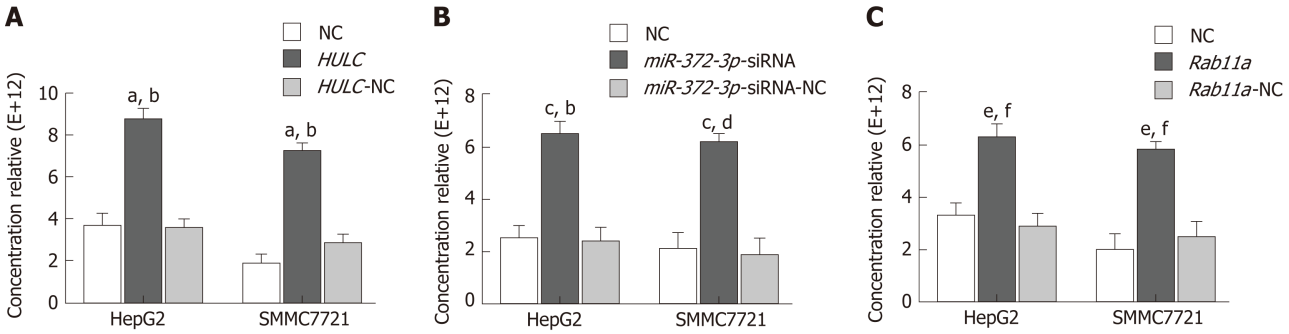


**Figure 7 Increased long non-coding RNA highly up-regulated in liver cancer and *Rab11a* and decreased *miR-372-3p* promote the secretion of exosomes from hepatocellular carcinoma cells.** A: Quantification of exosomes after transfecting *HULC* over-expression plasmid into HCC cells; B: Quantification of exosomes after transfecting *miR-372-3p* low-expression plasmid into HCC cells; C: Quantification of exosomes after transfecting *Rab11a* over-expression plasmid into HCC cells. Error bars stand for the mean ± SD of at least triplicate experiments. [a]$P < 0.01$ *vs* NC group; [b]$P < 0.01$ *vs* *HULC*-NC group; [c]$P < 0.01$ *vs* NC group; [d]$P < 0.01$ *vs* miRNA-*372-3p*-siRNA-NC group; [e]$P < 0.01$ *vs* NC group; [f]$P < 0.01$ *vs* *Rab11a-NC* group. *HULC*: Highly upregulated in liver cancer; *HULC*: *HULC* over-expression group; *HULC*-NC: *HULC* (over-expression plasmid normal control group); NC: Normal control; *miR-372-3p*-siRNA: *miR-372-3p* low-expression group; *miR-372-3p*-siRNA-NC: *miR-372-3p* low-expression plasmid normal control group; *Rab11a*: *Rab11a* over-expression group; *Rab11a-NC*: *Rab11a* over-expression plasmid normal control group.

## ARTICLE HIGHLIGHTS

### *Research background*

Long non-coding RNA highly up-regulated in liver cancer (lncRNA *HULC*) is highly expressed in hepatocellular carcinoma (HCC), and involved in the development and regulation of tumorigenesis. The relationship between *HULC* and exosomes has not yet been reported. Studying the mechanism of exosome secretion is helpful to reveal the pathogenesis of HCC.

### *Research motivation*

Although *HULC* has long been known to play important roles in HCC, its function and regulatory mechanism are unclear. Since exosomes participate in the progression of HCC, they have been actively studied. We are interested in exploring whether *HULC* regulates exosome secretion and is involved in the occurrence and development of hepatocellular carcinoma. This study will provide novel insights into the mechanism of action of *HULC* in HCC.

### Research objectives
The main objective of the study was to explore the molecular mechanism of *HULC* to regulate exosome secretion and and provide novel insights into the mechanism of action of *HULC* in HCC.

### Research methods
We collected samples from serum and tissues of 30 patients with HCC. We measured *HULC* expression in the serum exosomes and liver cancer tissues of patients, and compared the data to those obtained from controls. We further explored the effect of *HULC* upregulation in HCC cell lines and studied the relationship between *HULC* and other RNAs using qPCR and dual-luciferase reporter assays. NTA was used to detect the quantity of exosomes.

### Research results
*HULC* expression in serum exosomes of patients with HCC was higher than that in serum exosomes of healthy controls, and *HULC* levels were higher in liver cancer tissues than in adjacent tissues. The expression of *HULC* in serum exosomes and liver cancer tissues correlated with the tumor-node-metastasis (TNM) classification and *HULC* expression in tissues correlated with that in serum exosomes. *HULC* promoted HCC cell growth and invasion and repressed apoptosis. Additionly, it also facilitated the secretion of exosomes from HCC cells. Moreover, qPCR assays show that *HULC* repressed *microRNA-372-3p* (*miR-372-3p*) expression. We also identified Rab11a as a downstream target of *miR-372-3p*. Dual-luciferase reporter assays suggest that *miR-372-3p* could directly bind both *HULC* and Rab11a.

### Research conclusions
*HULC* regulates Rab11a to promote secretion of exosomes by competitive *miR-372-3p* sharing, and this finding provides new insights into the molecular mechanism to regulate the secretion of exosomes from HCC cells.

### Research perspectives
We aim to further explore the potential of serum exosome *HULC* as a sensitive preoperative marker for HCC and the role of *HULC* in the staging and prognosis evaluation of HCC.

## ACKNOWLEDGEMENTS

We thank NHC Key Laboratory of Critical Care Medicine for allowing this work to be performed there.

## REFERENCES

1 **Global Burden of Disease Liver Cancer Collaboration**; Akinyemiju T, Abera S, Ahmed M, Alam N, Alemayohu MA, Allen C, Al-Raddadi R, Alvis-Guzman N, Amoako Y, Artaman A, Ayele TA, Barac A, Bensenor I, Berhane A, Bhutta Z, Castillo-Rivas J, Chitheer A, Choi JY, Cowie B, Dandona L, Dandona R, Dey S, Dicker D, Phuc H, Ekwueme DU, Zaki MS, Fischer F, Fürst T, Hancock J, Hay SI, Hotez P, Jee SH, Kasaeian A, Khader Y, Khang YH, Kumar A, Kutz M, Larson H, Lopez A, Lunevicius R, Malekzadeh R, McAlinden C, Meier T, Mendoza W, Mokdad A, Moradi-Lakeh M, Nagel G, Nguyen Q, Nguyen G, Ogbo F, Patton G, Pereira DM, Pourmalek F, Qorbani M, Radfar A, Roshandel G, Salomon JA, Sanabria J, Sartorius B, Satpathy M, Sawhney M, Sepanlou S, Shackelford K, Shore H, Sun J, Mengistu DT, Topór-Mądry R, Tran B, Ukwaja KN, Vlassov V, Vollset SE, Vos T, Wakayo T, Weiderpass E, Werdecker A, Yonemoto N, Younis M, Yu C, Zaidi Z, Zhu L, Murray CJL, Naghavi M, Fitzmaurice C. The Burden of Primary Liver Cancer and Underlying Etiologies From 1990 to 2015 at the Global, Regional, and National Level: Results From the Global Burden of Disease Study 2015. *JAMA Oncol* 2017; **3**: 1683-1691 [PMID: 28983565 DOI: 10.1001/jamaoncol.2017.3055]

2 **Hung AK**, Guy J. Hepatocellular carcinoma in the elderly: Meta-analysis and systematic literature review. *World J Gastroenterol* 2015; **21**: 12197-12210 [PMID: 26576104 DOI: 10.3748/wjg.v21.i42.12197]

3 **Furuno M**, Pang KC, Ninomiya N, Fukuda S, Frith MC, Bult C, Kai C, Kawai J, Carninci P, Hayashizaki Y, Mattick JS, Suzuki H. Clusters of internally primed transcripts reveal novel long noncoding RNAs. *PLoS Genet* 2006; **2**: e37 [PMID: 16683026 DOI: 10.1371/journal.pgen.0020037]

4 **Balas MM**, Johnson AM. Exploring the mechanisms behind long noncoding RNAs and cancer. *Noncoding RNA Res* 2018; **3**: 108-117 [PMID: 30175284 DOI: 10.1016/j.ncrna.2018.03.001]

5 **Panzitt K**, Tschernatsch MM, Guelly C, Moustafa T, Stradner M, Strohmaier HM, Buck CR, Denk H, Schroeder R, Trauner M, Zatloukal K. Characterization of HULC, a novel gene with striking up-regulation in hepatocellular carcinoma, as noncoding RNA. *Gastroenterology* 2007; **132**: 330-342 [PMID: 17241883 DOI: 10.1053/j.gastro.2006.08.026]

6 **Hämmerle M**, Gutschner T, Uckelmann H, Ozgur S, Fiskin E, Gross M, Skawran B, Geffers R, Longerich T, Breuhahn K, Schirmacher P, Stoecklin G, Diederichs S. Posttranscriptional destabilization of the liver-specific long noncoding RNA HULC by the IGF2 mRNA-binding protein 1 (IGF2BP1). *Hepatology* 2013; **58**: 1703-1712 [PMID: 23728852 DOI: 10.1002/hep.26537]

7 **Xin X**, Wu M, Meng Q, Wang C, Lu Y, Yang Y, Li X, Zheng Q, Pu H, Gui X, Li T, Li J, Jia S, Lu D. Long noncoding RNA HULC accelerates liver cancer by inhibiting PTEN via autophagy cooperation to miR15a. *Mol Cancer* 2018; **17**: 94 [PMID: 29895332 DOI: 10.1186/s12943-018-0843-8]

8 **Yin D**, Li Y, Fu C, Feng Y. Pro-Angiogenic Role of LncRNA HULC in Microvascular Endothelial Cells via Sequestrating miR-124. *Cell Physiol Biochem* 2018; **50**: 2188-2202 [PMID: 30415256 DOI: 10.1159/000495060]

9 **Hu C**, Chen M, Jiang R, Guo Y, Wu M, Zhang X. Exosome-related tumor microenvironment. *J Cancer* 2018; **9**: 3084-3092 [PMID: 30210631 DOI: 10.7150/jca.26422]

10 **Colombo M**, Moita C, van Niel G, Kowal J, Vigneron J, Benaroch P, Manel N, Moita LF, Théry C, Raposo G. Analysis of ESCRT functions in exosome biogenesis, composition and secretion highlights the heterogeneity of extracellular vesicles. *J Cell Sci* 2013; **126**: 5553-5565 [PMID: 24105262 DOI: 10.1242/jcs.128868]

11 **Wang F**, Li L, Piontek K, Sakaguchi M, Selaru FM. Exosome miR-335 as a novel therapeutic strategy in hepatocellular carcinoma. *Hepatology* 2018; **67**: 940-954 [PMID: 29023935 DOI: 10.1002/hep.29586]

12 **Rao Q**, Zuo B, Lu Z, Gao X, You A, Wu C, Du Z, Yin H. Tumor-derived exosomes elicit tumor suppression in murine hepatocellular carcinoma models and humans in vitro. *Hepatology* 2016; **64**: 456-472 [PMID: 26990897 DOI: 10.1002/hep.28549]

13 **Raposo G**, Stoorvogel W. Extracellular vesicles: exosomes, microvesicles, and friends. *J Cell Biol* 2013; **200**: 373-383 [PMID: 23420871 DOI: 10.1083/jcb.201211138]

14 **Koles K**, Nunnari J, Korkut C, Barria R, Brewer C, Li Y, Leszyk J, Zhang B, Budnik V. Mechanism of evenness interrupted (Evi)-exosome release at synaptic boutons. *J Biol Chem* 2012; **287**: 16820-16834 [PMID: 22437826 DOI: 10.1074/jbc.M112.342667]

15 **Savina A**, Vidal M, Colombo MI. The exosome pathway in K562 cells is regulated by Rab11. *J Cell Sci* 2002; **115**: 2505-2515 [PMID: 12045221]

16 **Wang J**, Liu X, Wu H, Ni P, Gu Z, Qiao Y, Chen N, Sun F, Fan Q. CREB up-regulates long non-coding RNA, HULC expression through interaction with microRNA-372 in liver cancer. *Nucleic Acids Res* 2010; **38**: 5366-5383 [PMID: 20423907 DOI: 10.1093/nar/gkq285]

17 **Wang WT**, Ye H, Wei PP, Han BW, He B, Chen ZH, Chen YQ. LncRNAs H19 and HULC, activated by oxidative stress, promote cell migration and invasion in cholangiocarcinoma through a ceRNA manner. *J Hematol Oncol* 2016; **9**: 117 [PMID: 27809873 DOI: 10.1186/s13045-016-0348-0]

18 **Colombo M**, Raposo G, Théry C. Biogenesis, secretion, and intercellular interactions of exosomes and other extracellular vesicles. *Annu Rev Cell Dev Biol* 2014; **30**: 255-289 [PMID: 25288114 DOI: 10.1146/annurev-cellbio-101512-122326]

19 **Huo X**, Han S, Wu G, Latchoumanin O, Zhou G, Hebbard L, George J, Qiao L. Dysregulated long noncoding RNAs (lncRNAs) in hepatocellular carcinoma: implications for tumorigenesis, disease progression, and liver cancer stem cells. *Mol Cancer* 2017; **16**: 165 [PMID: 29061150 DOI: 10.1186/s12943-017-0734-4]

20 **Sun M**, Nie F, Wang Y, Zhang Z, Hou J, He D, Xie M, Xu L, De W, Wang Z, Wang J. LncRNA HOXA11-AS Promotes Proliferation and Invasion of Gastric Cancer by Scaffolding the Chromatin Modification Factors PRC2, LSD1, and DNMT1. *Cancer Res* 2016; **76**: 6299-6310 [PMID: 27651312 DOI: 10.1158/0008-5472.CAN-16-0356]

21 **Li Z**, Xu L, Liu Y, Fu S, Tu J, Hu Y, Xiong Q. LncRNA MALAT1 promotes relapse of breast cancer patients with postoperative fever. *Am J Transl Res* 2018; **10**: 3186-3197 [PMID: 30416660]

22 **Matsuoka T**, Yashiro M. Biomarkers of gastric cancer: Current topics and future perspective. *World J Gastroenterol* 2018; **24**: 2818-2832 [PMID: 30018477 DOI: 10.3748/wjg.v24.i26.2818]

23 **Du Y**, Kong G, You X, Zhang S, Zhang T, Gao Y, Ye L, Zhang X. Elevation of highly up-regulated in liver cancer (HULC) by hepatitis B virus X protein promotes hepatoma cell proliferation via down-regulating p18. *J Biol Chem* 2012; **287**: 26302-26311 [PMID: 22685290 DOI: 10.1074/jbc.M112.342113]

24 **Cui M**, Xiao Z, Wang Y, Zheng M, Song T, Cai X, Sun B, Ye L, Zhang X. Long noncoding RNA HULC modulates abnormal lipid metabolism in hepatoma cells through an miR-9-mediated RXRA signaling pathway. *Cancer Res* 2015; **75**: 846-857 [PMID: 25592151 DOI: 10.1158/0008-5472.CAN-14-1192]

25 **Zhao Y**, Guo Q, Chen J, Hu J, Wang S, Sun Y. Role of long non-coding RNA HULC in cell proliferation, apoptosis and tumor metastasis of gastric cancer: a clinical and in vitro investigation. *Oncol Rep* 2014; **31**: 358-364 [PMID: 24247585 DOI: 10.3892/or.2013.2850]

26 **Peng W**, Gao W, Feng J. Long noncoding RNA HULC is a novel biomarker of poor prognosis in patients with pancreatic cancer. *Med Oncol* 2014; **31**: 346 [PMID: 25412939 DOI: 10.1007/s12032-014-0346-4]

27 **Ruivo CF**, Adem B, Silva M, Melo SA. The Biology of Cancer Exosomes: Insights and New Perspectives. *Cancer Res* 2017; **77**: 6480-6488 [PMID: 29162616 DOI: 10.1158/0008-5472.CAN-17-0994]

28 **Kogure T**, Lin WL, Yan IK, Braconi C, Patel T. Intercellular nanovesicle-mediated microRNA transfer: a mechanism of environmental modulation of hepatocellular cancer cell growth. *Hepatology* 2011; **54**: 1237-1248 [PMID: 21721029 DOI: 10.1002/hep.24504]

29 **Conigliaro A**, Costa V, Lo Dico A, Saieva L, Buccheri S, Dieli F, Manno M, Raccosta S, Mancone C, Tripodi M, De Leo G, Alessandro R. CD90+ liver cancer cells modulate endothelial cell phenotype through the release of exosomes containing H19 lncRNA. *Mol Cancer* 2015; **14**: 155 [PMID: 26272696 DOI: 10.1186/s12943-015-0426-x]

30 **Li R**, Wang Y, Zhang X, Feng M, Ma J, Li J, Yang X, Fang F, Xia Q, Zhang Z, Shang M, Jiang S. Exosome-mediated secretion of LOXL4 promotes hepatocellular carcinoma cell invasion and metastasis. *Mol Cancer* 2019; **18**: 18 [PMID: 30704479 DOI: 10.1186/s12943-019-0948-8]

31 **Li Q**, Shao Y, Zhang X, Zheng T, Miao M, Qin L, Wang B, Ye G, Xiao B, Guo J. Plasma long noncoding RNA protected by exosomes as a potential stable biomarker for gastric cancer. *Tumour Biol* 2015; **36**: 2007-2012 [PMID: 25391424 DOI: 10.1007/s13277-014-2807-y]

32 **Pan L**, Liang W, Fu M, Huang ZH, Li X, Zhang W, Zhang P, Qian H, Jiang PC, Xu WR, Zhang X. Exosomes-mediated transfer of long noncoding RNA ZFAS1 promotes gastric cancer progression. *J Cancer Res Clin Oncol* 2017; **143**: 991-1004 [PMID: 28285404 DOI: 10.1007/s00432-017-2361-2]

33 **Zhang R**, Xia Y, Wang Z, Zheng J, Chen Y, Li X, Wang Y, Ming H. Serum long non coding RNA MALAT-1 protected by exosomes is up-regulated and promotes cell proliferation and migration in non-small cell lung cancer. *Biochem Biophys Res Commun* 2017; **490**: 406-414 [PMID: 28623135 DOI: 10.1016/j.bbrc.2017.06.055]

34 **Dong L**, Lin W, Qi P, Xu MD, Wu X, Ni S, Huang D, Weng WW, Tan C, Sheng W, Zhou X, Du X. Circulating Long RNAs in Serum Extracellular Vesicles: Their Characterization and Potential Application as Biomarkers for Diagnosis of Colorectal Cancer. *Cancer Epidemiol Biomarkers Prev* 2016; **25**: 1158-1166 [PMID: 27197301 DOI: 10.1158/1055-9965.EPI-16-0006]

35 **Liu T**, Zhang X, Gao S, Jing F, Yang Y, Du L, Zheng G, Li P, Li C, Wang C. Exosomal long noncoding RNA CRNDE-h as a novel serum-based biomarker for diagnosis and prognosis of colorectal cancer. *Oncotarget* 2016; **7**: 85551-85563 [PMID: 27888803 DOI: 10.18632/oncotarget.13465]

36 **Wang J**, Zhou Y, Lu J, Sun Y, Xiao H, Liu M, Tian L. Combined detection of serum exosomal miR-21 and HOTAIR as diagnostic and prognostic biomarkers for laryngeal squamous cell carcinoma. *Med Oncol*

2014; **31**: 148 [PMID: 25099764 DOI: 10.1007/s12032-014-0148-8]
37 **Xie H**, Ma H, Zhou D. Plasma HULC as a promising novel biomarker for the detection of hepatocellular carcinoma. *Biomed Res Int* 2013; **2013**: 136106 [PMID: 23762823 DOI: 10.1155/2013/136106]
38 **Salmena L**, Poliseno L, Tay Y, Kats L, Pandolfi PP. A ceRNA hypothesis: the Rosetta Stone of a hidden RNA language? *Cell* 2011; **146**: 353-358 [PMID: 21802130 DOI: 10.1016/j.cell.2011.07.014]
39 **Wu G**, Wang Y, Lu X, He H, Liu H, Meng X, Xia S, Zheng K, Liu B. Low mir-372 expression correlates with poor prognosis and tumor metastasis in hepatocellular carcinoma. *BMC Cancer* 2015; **15**: 182 [PMID: 25880458 DOI: 10.1186/s12885-015-1214-0]
40 **Goldenring JR**, Ray GS, Lee JR. Rab11 in dysplasia of Barrett's epithelia. *Yale J Biol Med* 1999; **72**: 113-120 [PMID: 10780572]
41 **Gebhardt C**, Breitenbach U, Richter KH, Fürstenberger G, Mauch C, Angel P, Hess J. c-Fos-dependent induction of the small ras-related GTPase Rab11a in skin carcinogenesis. *Am J Pathol* 2005; **167**: 243-253 [PMID: 15972968 DOI: 10.1016/S0002-9440(10)62969-0]
42 **Hu F**, Deng X, Yang X, Jin H, Gu D, Lv X, Wang C, Zhang Y, Huo X, Shen Q, Luo Q, Zhao F, Ge T, Zhao F, Chu W, Shu H, Yao M, Fan J, Qin W. Hypoxia upregulates Rab11-family interacting protein 4 through HIF-1α to promote the metastasis of hepatocellular carcinoma. *Oncogene* 2015; **34**: 6007-6017 [PMID: 25745995 DOI: 10.1038/onc.2015.49]

World Journal of Gastroenterology

Submit a Manuscript: https://www.f6publishing.com

*World J Gastroenterol* 2019 September 21; 25(35): 5300-5309

DOI: 10.3748/wjg.v25.i35.5300

ISSN 1007-9327 (print) ISSN 2219-2840 (online)

ORIGINAL ARTICLE

Basic Study

# Circular RNA PIP5K1A promotes colon cancer development through inhibiting miR-1273a

Qu Zhang, Chi Zhang, Jian-Xin Ma, Hui Ren, Yu Sun, Jiao-Zhen Xu

**ORCID number:** Qu Zhang (0000-0002-9295-4690); Chi Zhang (0000-0002-2639-7179); Jian-Xin Ma (0000-0003-2117-706X); Hui Ren (0000-0001-6806-0948); Yu Sun (0000-0001-6328-4766); Jiao-Zhen Xu (0000-0001-7157-1968).

**Author contributions:** Zhang Q performed the majority of experiments; Ma JX analyzed the data; Zhang C and Sun Y performed the molecular investigations; Xu JZ designed and coordinated the research; Ren H wrote the paper.

**Supported by** the National Natural Science Foundation of China, No. 81703028; and Hubei Cancer Hospital, No. 20162017B01.

**Institutional review board statement:** This study was reviewed and approved by the Hubei Cancer Hospital Ethics Committee.

**Conflict-of-interest statement:** The authors declare no conflict of interest.

**Data sharing statement:** No additional data are available.



**Qu Zhang, Jiao-Zhen Xu,** Department of Radiotherapy Center, Hubei Cancer Hospital, Wuhan 430079, Hubei Province, China

**Chi Zhang,** Department of Radiation Oncology, The First Affiliated Hospital of Nanjing Medical University/Jiangsu Province Hospital, Nanjing 210029, Jiangsu Province, China

**Jian-Xin Ma,** Department of Oncology, Lianyungang Municipal Oriental Hospital, Lianyungang 222042, Jiangsu Province, China

**Hui Ren,** Department of Chest Medicine, Hubei Cancer Hospital, Wuhan 430079, Hubei Province, China

**Yu Sun,** Department of Radiation Oncology, Wanbei Coal-Electricity Group General Hospital, Suzhou 234000, Anhui Province, China

**Corresponding author:** Jiao-Zhen Xu, MSc, Attending Doctor, Department of Radiotherapy Center, Hubei Cancer Hospital, No. 116 Zhuodaoquan South Road, Hongshan District, Wuhan 430079, Hubei Province, China. fuposhuic51@163.com
**Telephone:** +86-27-190077000
**Fax:** +86-27-6003200

## Abstract

### *BACKGROUND*

Circular RNAs (circRNAs) are considered to be highly stable due to the closed structure, which are predominately correlated with the development and progression of a wide variety of cancers. Colon cancer is one of the most common malignancies worldwide. A recent study demonstrated the upregulated expression of circPIP5K1A in non-small cell lung cancer. However, few studies have investigated the relationship between circ_0014130 level and colon cancer. Therefore, elucidating the underlying mechanisms of circPIP5K1A's role may help with the identification of novel diagnostic and therapeutic targets for colon cancer.

### *AIM*

To investigate the status of circPIP5K1A in colon cancers and its effects on the modulation of cancer development.

### *METHODS*

The expression level of circPIP5K1A in tissue and serum samples from colon cancer patients, as well as human colonic cancer cell lines was detected by real-time quantitative reverse transcription-polymerase chain reaction. Following the

**Manuscript source**: Unsolicited manuscript

**Received:** May 16, 2019
**Peer-review started:** May 16, 2019
**First decision:** June 16, 2019
**Revised:** July 11, 2019
**Accepted:** July 19, 2019
**Article in press:** July 19, 2019
**Published online:** September 21, 2019

**P-Reviewer:** Bordonaro M, Christodoulou DK
**S-Editor:** Yan JP
**L-Editor:** Filipodia
**E-Editor:** Ma YJ

transfection of specifically synthesized small interfering RNA (siRNA) into colon cell lines, we used Hoechst staining assay to measure the ratio of cell death in the absence of circPIP5K1A. Moreover, we also used the Transwell assay to assess the migratory function of colon cells overexpressing circPIP5K1A. Additionally, we employed a series of bioinformatics prediction programs to predict the potential of circPIP5K1A-targeted miRNAs and mRNAs. The miR-1273a vector was constructed, and then transfected with or without circPIP5K1A vector into colon cancer cells. Afterwards, the expression of activator protein 1 (AP-1), interferon regulating factor 4 (IRF-4), caudal type homeobox 2 (CDX-2), and zinc finger of the cerebellum 1 (Zic-1) was detected by western blotting.

*RESULTS*

CircPIP5K1A was significantly upregulated in colon cancer tissue relative to their adjacent normal tissues. Knockdown of circPIP5K1A in colon cancer cells impaired cell viability and suppressed cell invasion and migration, while enforced expression of circPIP5K1A exhibited the opposite effects on cell migration. Bioinformatics prediction program predicted that the association of circPIP5K1A with miR-1273a, as well as AP-1, IRF-4, CDX-2, and Zic-1. Subsequent studies showed that overexpression of circPIP5K1A augmented the expression of AP-1 but attenuated the expression of IRF-4, CDX-2, and Zic-1. Reciprocally, overexpression of miR-1273a abrogated the oncogenic function of circPIP5K1A in colon cancers.

*CONCLUSION*

Overall, our data demonstrate the oncogenic role of circPIP5K1A-miR-1273a axis in regulation of colon cancer development, which provides a novel insights into colon cancer pathogenesis.

**Key words:** Circular RNA PIP5K1A; miR-1273a; Cell death; Cell migration; Colon cancer



**Core tip:** We found that circular RNA PIP5K1A (circPIP5K1A) was selectively upregulated in colon cancer. Through sponging miR-1273a, circPIP5K1A promoted cell survival and enhanced the invasive and migratory functions of colon cancer cells, eventually exacerbating malignant transformation.

**Citation:** Zhang Q, Zhang C, Ma JX, Ren H, Sun Y, Xu JZ. Circular RNA PIP5K1A promotes colon cancer development through inhibiting miR-1273a. *World J Gastroenterol* 2019; 25(35): 5300-5309
**URL**: https://www.wjgnet.com/1007-9327/full/v25/i35/5300.htm
**DOI**: https://dx.doi.org/10.3748/wjg.v25.i35.5300

## INTRODUCTION

As the third most common malignant disease, colon cancer is the leading cause of mortality worldwide[1]. To date, conventional and effective therapeutic methods for colon cancer include surgery, adjuvant radiation therapy or chemotherapy, and molecular targeted therapy[2]. Despite the extensive improvements in diagnosis and treatments, poor survival and unsatisfactory prognosis remain an issue due to delayed diagnosis and adverse drug effects[2]. Therefore, investigation of novel diagnostic and therapeutic methods, as well as the underlying molecular mechanisms of colon cancer is required.

Accumulating studies have shown that the roles of noncoding RNAs such as circular RNAs (circRNAs) and microRNAs (miRNAs) are predominately correlated with the development and progression of a wide variety of cancers[3]. CircRNAs, one class of noncoding RNA with covalent closed loops, are widely spread in eukaryotes and are mainly formed by back-splicing without 3'- and 5'-ends[4]. CircRNAs are considered to be highly stable due to the closed structure, which has garnered interest from scholars in determining whether they can be used as novel biomarkers in many

diseases[5]. Several studies have identified many possible functions of circRNAs[6] including miRNA sponges[7], regulating gene transcription and splicing[8], and forming RNA-protein complexes[9]. It is widely acknowledged that some circRNAs may participate in disease progression by interfering with miRNA, thereby influencing target gene expression[10]. Remarkably, the prevalence of high-throughput sequencing technologies make diverse bioinformatics analyses available, and more studies have revealed dysregulated expression of circRNAs in many cancers including laryngeal cancer[11], hepatocellular carcinoma[12], gastric cancer[13], gliomas[14], and esophageal cancer[15]. A previous study demonstrated that circ_001988 is downregulated in colon cancer, and may be a novel diagnostic biomarker in colon cancer[16]. Another study showed that circ_000984 induces cell growth and metastasis in colon cancer[17]. A recent study demonstrated the upregulated expression of circ_0014130 in non-small cell lung cancer[18]. However, few studies have investigated the relationship between circ_0014130 level and colon cancer. Based on the circBase database (http://www.circbase.org/), hsa_circ_0014130 is located at chr1:151206672-151212515, and the corresponding gene symbol is PIP5K1A. Thus, we denoted hsa_circ_0014130 as circPIP5K1A.

Here we found that circPIP5K1A was selectively upregulated in cancerous tissues from patients with colon cancer, which in turn suppressed cell death and augmented cancer cell invasion and migration. Through sponging miR-1273a, circPIP5K1A augmented the expression of factor activator protein 1 (AP-1), but attenuated the expression of interferon regulating factor 4 (IRF-4), caudal type homeobox 2 (CDX-2), and zinc finger of the cerebellum 1 (Zic-1), which are crucial for tumorigenesis.

## MATERIALS AND METHODS

### *Clinical sample collection*

This study obtained ethical approval from the ethics committee of Hubei Cancer Hospital (Hubei Sheng, China). Twenty paired tumor samples and adjacent normal samples were collected from colon cancer patients in our hospital. The specimens were confirmed by hematoxylin and eosin staining and stored in RNAlater. Written informed consent was obtained from all participants.

### *Cell culture*

Human keratinocyte line HaCaT, normal human colon epithelial cell line HCoEpiC, human colon cancer cell lines HCT-116, SW620, SW480, and COLO320DM, as well as human gastric cancer cell line HGC-27, human esophageal cancer cell line TE-10, human lung cancer cell line A549, and human hepatoma cell line HepG2 were obtained from Obio Technology Co., Ltd (Shanghai, China). The cells were maintained in Dulbecco's Modified Eagle Medium (DMEM) (Gibco, Carlsbad, CA, United States) containing 10% fetal bovine serum (FBS; Gibco) with standard incubation conditions (5% $CO_2$ and 37 °C).

### *Cell transfection*

The synthesis of three small interfering RNAs (siRNAs) and relative si-NC for circPIP5K1A, as well as the construction of overexpressing circPIP5K1A vector and overexpressing miR-1273a vector were performed by Biosyntech Co., Ltd (Suzhou, China). The siRNA or overexpressing vector was transfected into COLO320DM cells by Lipofectamine 2000 (Invitrogen, Gaithersburg, MD, United States). Silence or overexpression effect was detected by real-time quantitative polymerase chain reaction (RT-qPCR) 48 h after transfection. The most effective siRNA was used for subsequent experiments.

### *RT-qPCR and RNase R treatment*

Total RNA was obtained by Trizol (Invitrogen) according to the manufacturer's instructions. RNA concentration and purity were measured using a UV spectrophotometer (BD, Franklin Lakes, NJ, United States), and RNA with A260/A280 ratios of 1.8-2.0 was considered high-quality RNA without protein and DNA contamination. Then high-quality RNA was reverse transcribed into complementary DNA with a Reverse Transcription Kit (TaKaRa, Dalian, China). PCR amplification was performed by a SYBR Premix Ex Taq TM II (Takara). The primers sequences are listed in Table 1. The PCR program was: 95 °C for 3 min, 40 cycles of 95 °C for 10 s and 59 °C for 20 s, using the ABI Stepone plus Real-time PCR system (Applied Biosystems, Foster City, CA, United States). Glyceraldehyde-3-phosphate dehydrogenase (GAPDH) and U6 served as the internal control for measuring circPIP5K1A and PIP5K1A levels. Data were analyzed with $2^{-\Delta\Delta Ct}$ method. To identify the cyclic structure of circPIP5K1A, RNA was treated with or without RNase R at 37

°C for 15 min, purified by phenol–chloroform extraction, and then subjected to RT-qPCR.

### Predicting potential molecules bound to circPIP5K1A

The potential miRNAs and mRNAs bound to the promoter regions of circPIP5K1A were predicted, and then the potential miRNAs and mRNAs bound to circPIP5K1A sequence were further predicted using RegRNA2.0 (http://www.regrna.mbc.nctu.edu.tw/).

### Cell apoptosis assay

Hoechst staining kit (Beyotime Institute of Biotechnology, Shanghai, China) was used to evaluate cell apoptosis. Cells treated with circPIP5K1A siRNA were collected and fixed in 4% paraformaldehyde, followed by staining with Hoechst 33258 as manufacturer's instructions. The apoptotic cells were calculated by fluorescence microscope.

### Cell migration assay

Transwell inserts (Corning, New York, NY, United States) were used to detect cell migration ability. First, the cells transfected with circPIP5K1A siRNA or overexpressing circPIP5K1A vector were plated onto the upper chamber containing serum-free medium. Meanwhile, DMEM with 10% FBS was added to the bottom chamber for 48 h. Next, the cells in the bottom chamber insert were treated with 4,6-diamidino-2-phenylindole for 5 min. The number of migrated cells was calculated with an inverted microscope (Olympus, Tokyo, Japan).

### Western blotting

COLO320DM cells were transfected with overexpressing circPIP5K1A vector, overexpressing miR-1273a vector, or the combination of overexpressing circPIP5K1A vector and overexpressing miR-1273a vector. The cells with various treatments were collected, and then lysed by RIPA lysis buffer (Gibco) supplemented with phenylmethanesulfonyl fluoride (1 mM; Sigma, St. Louis, MO, United States). Protein was extracted by centrifugation and detected by the BCA kit (Shanghai Sangon Biotech Co., Ltd, China). The protein sample was separated on an SDS-PAGE gel, and electrotransferred to polyvinylidene fluoride membranes, followed by blocking in 5% nonfat milk for 1 h. Next, the membrane was probed with primary antibodies for transcription factor AP-1, IRF-4, CDX-2, Zic1, or GAPDH (1:1000; Abcam, Cambridge, MA, United States), followed by incubation with secondary antibody (1:1000; Beyotime) for 2 h at room temperature, respectively. Finally, enhanced chemiluminescence (Millipore, Burlington, MA, United States) was used to detect the protein levels.

### Statistical analysis

Statistical analysis was conducted using SPSS Statistics software 22.0 (Chicago, IL, United States). Data are presented as mean ± standard deviation (SD) and analyzed by one-way analysis of variance followed by Dunnett's post-hoc *t*-test. $^{a}P < 0.05$ was considered statistically significant.

## RESULTS

### CircPIP5K1A is selectively upregulated in colon cancer

To assess the status of circPIP5K1A in colon cancer development, we employed the RT-qPCR assay to detect the mRNA level of CircPIP5K1A in clinical samples. As shown in Figure 1A, circPIP5K1A was markedly upregulated in colon cancer tissues relative to their adjacent normal tissues. Similar results were detected in in several human cancer cell lines including SW480, SW620, HCT-116, COLO320DM, HGC-27, TE-10, HepG2, and A549M, while the mRNA level of circPIP5K1A in normal cell line HCoEpiC and HaCaT was undetectable (Figure 1B). Moreover, we also found that cell over-confluence led to conspicuously inhibited circPIP5K1A expression (Figure 1C), which suggested that circPIP5K1A was involved in colon cancer development.

### CircPIP5K1A knockdown induces cell death

To investigate the role of circPIP5K1A in colon cancer progression, we transfected circPIP5K1A-targeted siRNA1, 2, and 3 into COLO320DM cells, which expressed the highest level of circPIP5K1A among the cancer cell lines. Our data revealed that the expression of circPIP5K1A was dramatically suppressed in the cells transfected with circPIP5K1A-targeted siRNA compared with cells transfected with scrambled siRNA. Moreover, the downregulation of circPIP5K1A by siRNA was resistant to RNase R

**Table 1 Primer sequences used for RT-qPCR and siRNA**

| RNA | Primers sequences |
|---|---|
| circPIP5K1A | F: 5'-AGATTCCCTAACCTCAACCAGA-3' |
| | R: 5'-CGAATGTTCTTGCCACCTGC-3' |
| PIP5K1A | F: 5'-CCTCATGCAAGATTTCTACGTGG-3' |
| | R: 5'-GGCCGGATACCAAATAGCTCC-3' |
| GAPDH | F: 5'-AGAAGGCTGGGGCTCATTTG-3' |
| | R: 5'-AGGGGCCATCCACAGTCTTC-3' |
| U6 | F: 5'-AGGGGCCATCCACAGTCTTC-3' |
| | R: 5'-AACGCTTCACGAATTTGCGT-3' |
| circ-PIP5K1A siRNA-1 | 5'-UUCUUCUAAGGGAUUGGAGUU-3' |
| circ-PIP5K1A siRNA-2 | 5'-UUCUAAGGGAUUGGAGUUGGU-3' |
| circ-PIP5K1A siRNA-3 | 5'-UAAGGGAUUGGAGUUGGUCUU-3' |
| Relative si-NC | 5'-AAUUCUCCGAACGUGUCACGU-3' |

digestion ($^{b}P < 0.01$, Figure 2A). Conversely, circPIP5K1A-targeted siRNA hardly affected the endogenous expression of PIP5K1A (Figure 2B), which confirmed the specificity of circPIP5K1A-targeted siRNA. Notably, we found that the absence of circPIP5K1A resulted in obviously increased cell death compared with cells transfected with scrambled siRNA (Figure 2C).

### *CircPIP5K1A increases cancer cell invasion and migration*

To determine whether circPIP5K1A can regulate cancer migration, we utilized the Transwell assay, and found that enforced expression of circPIP5K1A significantly augmented cell invasion and migration relative to mock-transfected cells. Reciprocally, silencing of endogenous circPIP5K1A exhibited opposite effects on cell migration (Figure 3). Taken together, our data demonstrate that upregulation of circPIP5K1A promotes cell viability and migration.

### *CircPIP5K1A and miR-1273a act antagonistically on the modulation of oncogene expression*

To investigate the molecular function of circPIP5K1A in colon cancer development, we used RegRNA to predict circPIP5K1A-associated RNAs. The highest score of RNAs were miR-1273a as well as traditional mRNAs such as AP-1, IRF-4, CDX-2, and Zic-1 (Figure 4A). Further study revealed that overexpression of circPIP5K1A significantly upregulated both the mRNA and protein level of AP-1, while attenuating the expression of IRF-4, CDX-2, and Zic-1 (Figure 4B and C). Conversely, overexpression of miR-1273a obviously alleviated circPIP5K1A-mediated suppression of IRF-4, CDX-2 and Zic-1 expression (Figure 4B and C).

## DISCUSSION

Our present study showed that circPIP5K1A was significantly upregulated in colon cancer tissue and cell lines. Silencing of circPIP5K1A in COLO320DM cells induced cell death and suppressed cell migration. Moreover, bioinformatics predicted that circPIP5K1A could bind to miR-1273a as well as AP-1, IRF-4, CDX-2, and Zic-1. Overexpression of circPIP5K1A augmented AP-1 expression but attenuated the expression of IRF-4, CDX-2, and Zic-1, while overexpression of miR-1273a inhibited the oncogenic role of circPIP5K1A in the progression of colon cancer development.

Accumulating studies have identified circRNAs as novel biomarkers in cancer diagnosis due to the differential expression between normal and tumor tissues. For example, hsa_circ_0000520 level is increased in gastric cancer tissues and cells, which is negatively related to TNM stage, indicating that circ_0000520 may be a novel biomarker in gastric cancer[19]. Circ_0001649 is reportedly negatively correlated with colorectal cancer pathological differentiation, and is considered a new biomarker for the diagnosis of colorectal cancer[20]. A recent study reported the upregulation of hsa_circ_0014130 (circPIP5K1A) in non-small cell lung cancer, and it is considered a potential biomarker in non-small cell lung cancer[18]. In this study, we found that circPIP5K1A was selectively upregulated in colon cancer tissues and cells. It is well known that circRNAs are involved in various cellular biological processes and exert important regulatory roles in the progression of multiple cancers. A previous study

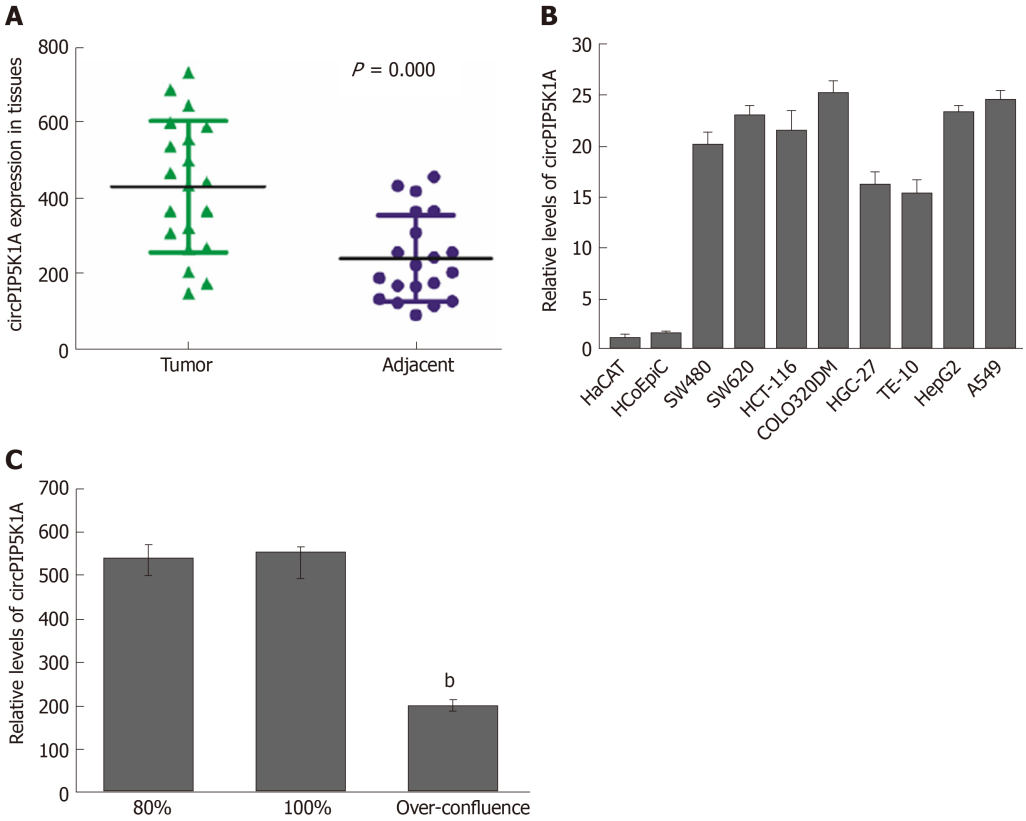


**Figure 1 Expression of circPIP5K1A in colon cancer.** A: RT-qPCR detection of circPIP5K1A expression in tumors and their adjacent normal tissues; B: The mRNA level of circPIP5K1A in various normal and cancer cell lines; C: The circPIP5K1A level in COLO320DM cells with different degrees of confluence. [a]$P < 0.01$ *vs* 80% or 100% group. Values are mean ± SD. circPIP5K1A: Circular RNA PIP5K1A.

demonstrated that hsa_circ_0001649 exerted tumor-suppressive effects by inducing cell apoptosis, as well as inhibiting cell proliferation and migration in cholangiocarcinoma cells[21]. In addition, it has been reported that the downregulation of circARHGAP26 inhibits cell proliferation and promotes cells apoptosis, indicating that circARHGAP26 may have tumor-promoting effects[22]. Here, we found that circPIP5K1A elicited stimulatory effects on cell proliferation and migration. These findings suggest that circPIP5K1A might contribute to the development of colon cancer.

Similarly to long non-coding RNA, the main role of circRNAs is to decrease miRNA abundance by sponging miRNA in the cytoplasm, and then affecting the expression of related genes. For example, hsa_circ_001564 knockdown suppresses osteosarcoma progression by acting as an miRNA sponge[23]. In this study, miR-1273a, AP-1, IRF-4, CDX-2, and Zic-1 were predicted to bind to circPIP5K1A. AP-1, encoding transcription factor AP-1, plays a pivotal role in tumorigenesis[24]. In cancers, AP-1 activity is increased, and inhibiting AP-1 activity can block cell proliferation and invasion[24]. A previous study reported that inhibition of AP-1 signaling may be a therapeutic target for colon cancer[25]. IRF-4, as a member of the interferon regulating factor family of transcription factors, is considered to be an oncogene in lymphoid malignancy and multiple myeloma[26]. Notably, recent studies have demonstrated that IRF-4 is a tumor suppressor in breast cancer[27] and lung cancer[28]. The homeodomain transcription factor CDX-2 has been investigated in colon cancer by many studies, which have suggested that CDX-2 loss is associated with the poor prognosis of colon cancer[29-32]. Zic-1 is a member of zinc finger of the cerebellum family, which encodes zinc-finger transcription factors[33]. In colorectal cancer, Zic-1 is downregulated and considered a tumor inhibitor[34]. Consistent with these studies, circPIP5K1A overexpression clearly upregulated the expression of AP-1, as well as downregulated the expression of IRF-4, CDX-2, and Zic-1. Notably, miR-1273a overexpression rescued the effects of circPIP5K1A on the expression of AP-1, IRF-4, CDX-2, and Zic-1 in colon cancer cells. Thus, we speculate that miR-1273a may inhibit the regulatory role of circPIP5K1A in colon cancer cells. However, the relationship between circPIP5K1A and miR-1273a should be investigated in further studies. In conclusion, our data demonstrate that circPIP5K1A is selectively increased in colon cancer and exerts oncogenic effects on tumorigenesis, which may be regulated by miR-1273a.

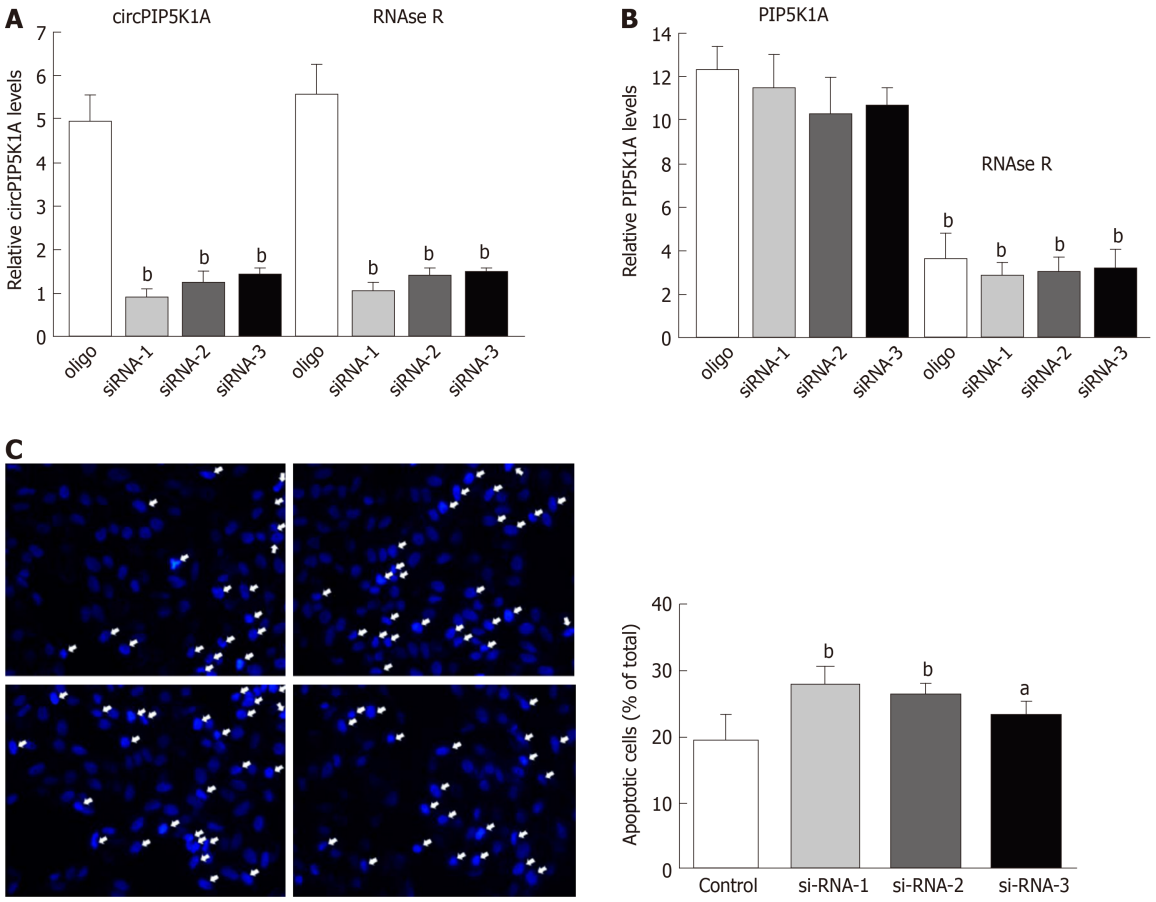


**Figure 2 Silencing of circPIP5K1A promotes cell death.** A: RT-qPCR detection of circular RNA PIP5K1A expression in COLO320DM cells transfected with siRNA1, siRNA2, or siRNA3 in the absence or presence of RNase R; B: RT-qPCR detection of PIP5K1A mRNA level in COLO320DM cells transfected with siRNA1, 2, and 3 in presence or absence of RNase R; C: Cell death rate in COLO320DM cells transfected with siRNA1, 2, or 3 by Hoechst staining. $^{a}P < 0.05$, $^{b}P < 0.01$ *vs* oligo or control group. Values are mean ± SD. circPIP5K1A: Circular RNA PIP5K1A; siRNA: Small interfering RNAs.

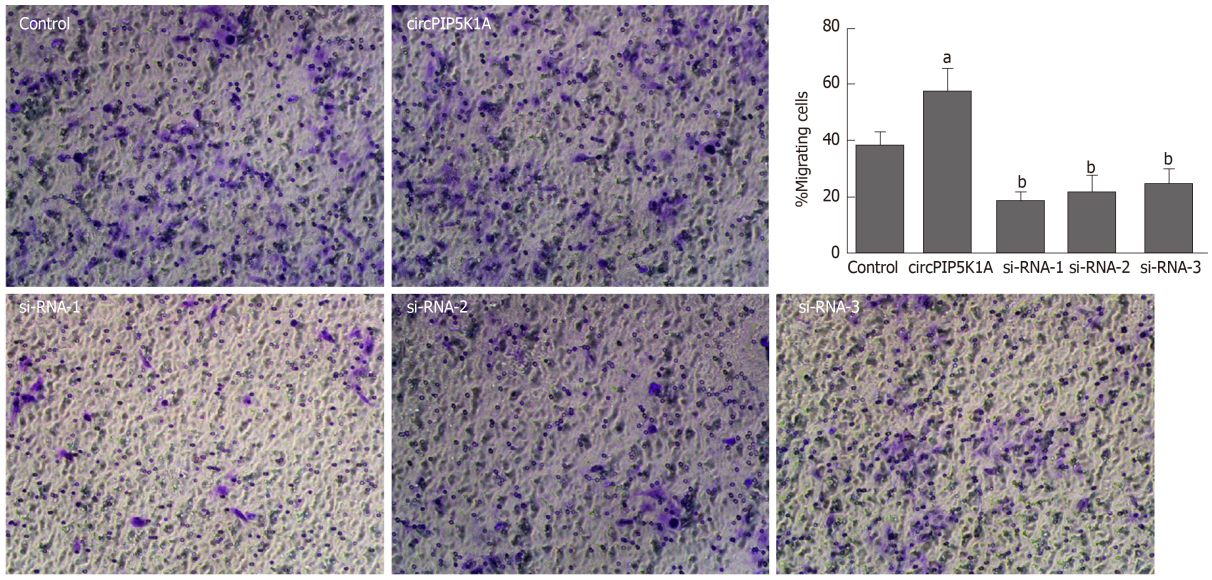


**Figure 3 Role of circPIP5K1A in the modulation of cell migration.** The migratory function of COLO320DM cells transfected with circPIP5K1A vector or siRNA1, siRNA2, or siRNA3 was measured by the Transwell assay. $^{a}P < 0.05$, $^{b}P < 0.01$ *vs* control group. Values are mean ± SD. circPIP5K1A: Circular RNA PIP5K1A; siRNA: Small interfering RNAs.

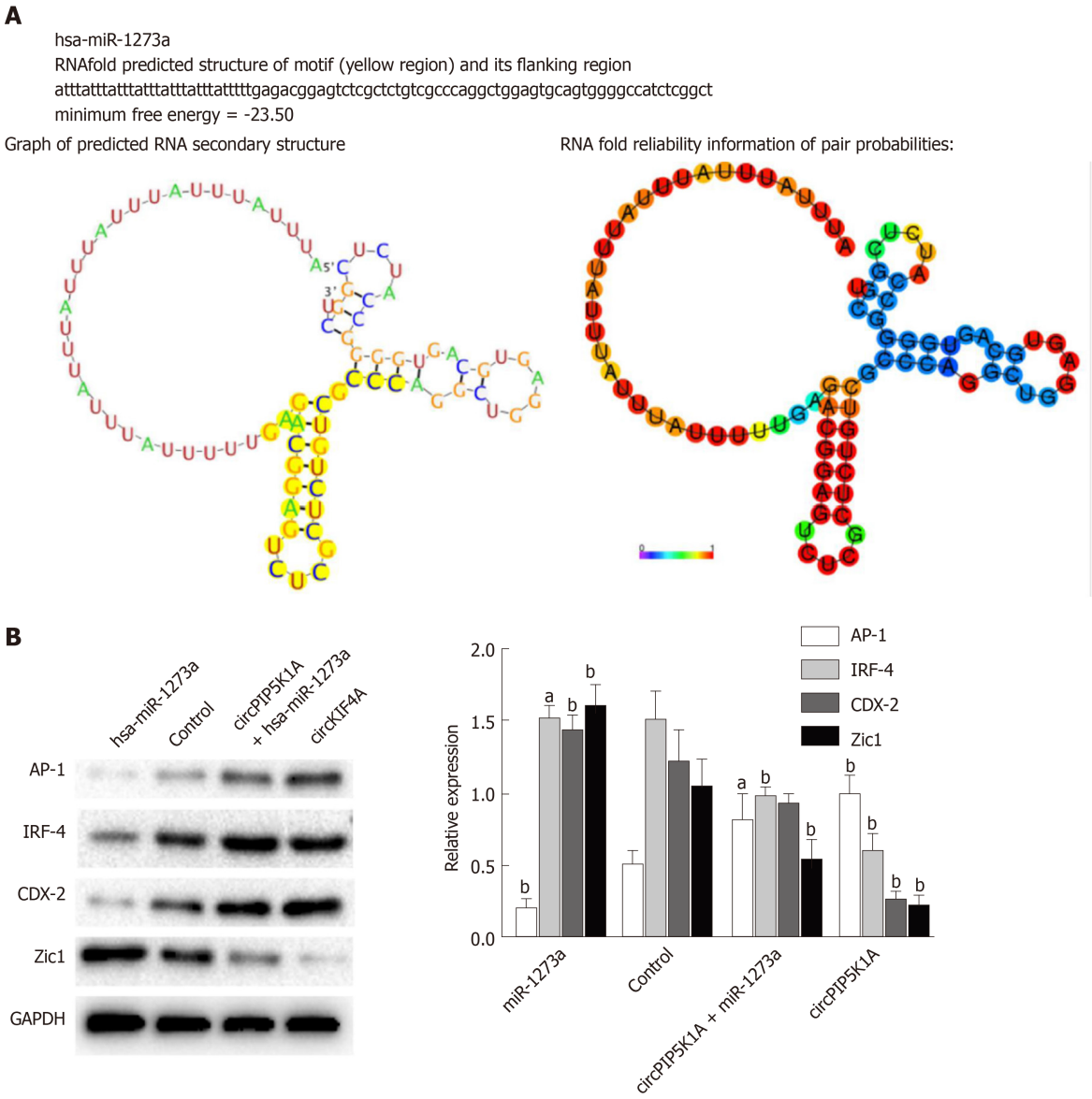


**Figure 4 Effect of miR-1273a overexpression on circPIP5K1A upregulation.** A: Binding site of miR-1273a and circPIP5K1A; B: Expression of AP-1, IRF-4, CDX-2, and Zic-1 in COLO320DM cells transfected with circPIP5K1A vector, miR-1273a vector, or co-transfection of circPIP5K1A vector and overexpressing miR-1273a vector, respectively, by western blotting. $^{a}P < 0.05$, $^{b}P < 0.01$ *vs* control group; $^{c}P < 0.05$, $^{d}P < 0.01$ *vs* circPIP5K1A group. Values are mean ± SD. circPIP5K1A: Circular RNA PIP5K1A; AP-1: Activator protein 1; IRF-4: Interferon regulating factor 4; CDX-2: Caudal type homeobox 2; Zic-1: Zinc finger of the cerebellum 1.

## ARTICLE HIGHLIGHTS

### *Research background*

Circular RNAs (circRNAs) are considered to be highly stable due to their closed structure, which are predominately correlated with the development and progression of a wide variety of cancers. A recent study demonstrated the upregulated expression of circPIP5K1A in non-small cell lung cancer. However, few studies have investigated the relationship between circ_0014130 level and colon cancer. Therefore, elucidating the underlying mechanisms of circPIP5K1A's role may help identify novel diagnostic and therapeutic targets for colon cancer.

### *Research motivation*

It is necessary to explore whether circPIP5K1A regulates miR-1273a to affect cell death, cell invasion, and migration in colon cancer. Recent studies have demonstrated that circPIP5K1A exerts an oncogenic role in non-small cell lung cancer, which made it a good lead for further studies regarding the mechanism of circPIP5K1A regulation during colon cancer development.

### *Research objectives*

In this study, we evaluated the expression level of circPIP5K1A in clinical tumor samples and colon cancer cells, and then investigated the effects of circPIP5K1A on colon cell apoptosis and migration *in vitro* by gain- and loss-of–function approaches. Moreover, we explored whether

circPIP5K1A promotes colon cancer development through sponging miR-1273a. Our study provides significant insights into the mechanism of circPIP5K1A during colon cancer development that may contribute to the future design of more effective therapies.

### Research methods

First, circPIP5K1A level was detected in colon cancer tissue and cell lines by RT-qPCR assay. Then gene transfection or silencing experiments were conducted to construct stably expressed or depleted circPIP5K1A cell lines to complete subsequent functional studies. A series of in vitro experiments, such as cell apoptosis assay and Transwell assays, were performed to explore the effects of circPIP5K1A on cell apoptosis, invasion and migration. The potential miRNAs and mRNAs bound to the promoter regions of circPIP5K1A were predicted, and then the potential miRNAs and mRNAs bound to circPIP5K1A sequence were further predicted using RegRNA2.0. MiR-1273a vector was constructed, and then transfected with or without circPIP5K1A vector into colon cancer cells. Then the expression of AP-1, IRF-4, CDX-2, and Zic-1 was detected by western blotting.

### Research results

CircPIP5K1A was significantly upregulated in colon cancer tissue relative to their adjacent normal tissues. The results of in vitro experiments showed a positive role of circPIP5K1A in the proliferation, invasion, and migration of colon cancer cells. Bioinformatics prediction program predicted that the association of circPIP5K1A with miR-1273a, as well as AP-1, IRF-4, CDX-2, and Zic-1. Further study revealed that the overexpression of circPIP5K1A significantly upregulated both the mRNA and protein level of AP-1, while attenuating the expression of IRF-4, CDX-2, and Zic-1. Conversely, overexpression of miR-1273a clearly alleviated the circPIP5K1A-mediated suppression of IRF-4, CDX-2 and Zic-1 expression.

### Research conclusions

In conclusion, circPIP5K1A is selectively increased in colon cancer, and circPIP5K1A plays a positive role in colon cancer cell proliferation, invasion, and migration. In addition, overexpression of circPIP5K1A augmented AP-1 expression but attenuated the expression of IRF-4, CDX-2, and Zic-1, while overexpression of miR-1273a inhibited the oncogenic role of circPIP5K1A in progression of colon cancer development.

### Research perspectives

Our study illuminates the role and molecular mechanism of circPIP5K1A in the regulation of colon cancer development, and demonstrates the oncogenic role of the circPIP5K1A-miR-1273a axis in regulating colon cancer development. The findings of this study provide novel insights into colon cancer pathogenesis.

## REFERENCES


1 **Siegel RL**, Miller KD, Jemal A. Cancer statistics, 2019. *CA Cancer J Clin* 2019; **69**: 7-34 [PMID: 30620402 DOI: 10.3322/caac.21551]

2 **Muro K**. Systemic chemotherapy for metastatic colorectal cancer -Japanese Society for Cancer of the Colon and Rectum (JSCCR) Guidelines 2016 for treatment of colorectal cancer. *Nihon Shokakibyo Gakkai Zasshi* 2017; **114**: 1217-1223 [PMID: 28679979 DOI: 10.11405/nisshoshi.114.1217]

3 **Zhang Z**, Xie Q, He D, Ling Y, Li Y, Li J, Zhang H. Circular RNA: New star, new hope in cancer. *BMC Cancer* 2018; **18**: 834 [PMID: 30126353 DOI: 10.1186/s12885-018-4689-7]

4 **Guo JU**, Agarwal V, Guo H, Bartel DP. Expanded identification and characterization of mammalian circular RNAs. *Genome Biol* 2014; **15**: 409 [PMID: 25070500 DOI: 10.1186/s13059-014-0409-z]

5 **Meng S**, Zhou H, Feng Z, Xu Z, Tang Y, Li P, Wu M. CircRNA: Functions and properties of a novel potential biomarker for cancer. *Mol Cancer* 2017; **16**: 94 [PMID: 28535767 DOI: 10.1186/s12943-017-0663-2]

6 **Chen LL**. The biogenesis and emerging roles of circular RNAs. *Nat Rev Mol Cell Biol* 2016; **17**: 205-211 [PMID: 26908011 DOI: 10.1038/nrm.2015.32]

7 **Memczak S**, Jens M, Elefsinioti A, Torti F, Krueger J, Rybak A, Maier L, Mackowiak SD, Gregersen LH, Munschauer M, Loewer A, Ziebold U, Landthaler M, Kocks C, le Noble F, Rajewsky N. Circular RNAs are a large class of animal RNAs with regulatory potency. *Nature* 2013; **495**: 333-338 [PMID: 23446348 DOI: 10.1038/nature11928]

8 **Zhang Y**, Zhang XO, Chen T, Xiang JF, Yin QF, Xing YH, Zhu S, Yang L, Chen LL. Circular intronic long noncoding RNAs. *Mol Cell* 2013; **51**: 792-806 [PMID: 24035497 DOI: 10.1016/j.molcel.2013.08.017]

9 **Jeck WR**, Sorrentino JA, Wang K, Slevin MK, Burd CE, Liu J, Marzluff WF, Sharpless NE. Circular RNAs are abundant, conserved, and associated with ALU repeats. *RNA* 2013; **19**: 141-157 [PMID: 23249747 DOI: 10.1261/rna.035667.112]

10 **Wang Y**, Mo Y, Gong Z, Yang X, Yang M, Zhang S, Xiong F, Xiang B, Zhou M, Liao Q, Zhang W, Li X, Li X, Li Y, Li G, Zeng Z, Xiong W. Circular RNAs in human cancer. *Mol Cancer* 2017; **16**: 25 [PMID: 28143578 DOI: 10.1186/s12943-017-0598-7]

11 **Xuan L**, Qu L, Zhou H, Wang P, Yu H, Wu T, Wang X, Li Q, Tian L, Liu M, Sun Y. Circular RNA: A novel biomarker for progressive laryngeal cancer. *Am J Transl Res* 2016; **8**: 932-939 [PMID: 27158380 DOI: 10.3892/mmr.2016.5048]

12 **Hu J**, Li P, Song Y, Ge YX, Meng XM, Huang C, Li J, Xu T. Progress and prospects of circular RNAs in Hepatocellular carcinoma: Novel insights into their function. *J Cell Physiol* 2018; **233**: 4408-4422 [PMID: 28833094 DOI: 10.1002/jcp.26154]

13 **Shao Y**, Li J, Lu R, Li T, Yang Y, Xiao B, Guo J. Global circular RNA expression profile of human gastric cancer and its clinical significance. *Cancer Med* 2017; **6**: 1173-1180 [PMID: 28544609 DOI:

10.1002/cam4.1055]
14 **Song X**, Zhang N, Han P, Moon BS, Lai RK, Wang K, Lu W. Circular RNA profile in gliomas revealed by identification tool UROBORUS. *Nucleic Acids Res* 2016; **44**: e87 [PMID: 26873924 DOI: 10.1093/nar/gkw075]
15 **Su H**, Lin F, Deng X, Shen L, Fang Y, Fei Z, Zhao L, Zhang X, Pan H, Xie D, Jin X, Xie C. Profiling and bioinformatics analyses reveal differential circular RNA expression in radioresistant esophageal cancer cells. *J Transl Med* 2016; **14**: 225 [PMID: 27465405 DOI: 10.1186/s12967-016-0977-7]
16 **Wang X**, Zhang Y, Huang L, Zhang J, Pan F, Li B, Yan Y, Jia B, Liu H, Li S, Zheng W. Decreased expression of hsa_circ_001988 in colorectal cancer and its clinical significances. *Int J Clin Exp Pathol* 2015; **8**: 16020-16025 [PMID: 26884878]
17 **Xu XW**, Zheng BA, Hu ZM, Qian ZY, Huang CJ, Liu XQ, Wu WD. Circular RNA hsa_circ_000984 promotes colon cancer growth and metastasis by sponging miR-106b. *Oncotarget* 2017; **8**: 91674-91683 [PMID: 29207676 DOI: 10.18632/oncotarget.21748]
18 **Zhang S**, Zeng X, Ding T, Guo L, Li Y, Ou S, Yuan H. Microarray profile of circular RNAs identifies hsa_circ_0014130 as a new circular RNA biomarker in non-small cell lung cancer. *Sci Rep* 2018; **8**: 2878 [PMID: 29440731 DOI: 10.1038/s41598-018-21300-5]
19 **Sun H**, Tang W, Rong D, Jin H, Fu K, Zhang W, Liu Z, Cao H, Cao X. Hsa_circ_0000520, a potential new circular RNA biomarker, is involved in gastric carcinoma. *Cancer Biomark* 2018; **21**: 299-306 [PMID: 29103021 DOI: 10.3233/CBM-170379]
20 **Ji W**, Qiu C, Wang M, Mao N, Wu S, Dai Y. Hsa_circ_0001649: A circular RNA and potential novel biomarker for colorectal cancer. *Biochem Biophys Res Commun* 2018; **497**: 122-126 [PMID: 29421663 DOI: 10.1016/j.bbrc.2018.02.036]
21 **Xu Y**, Yao Y, Zhong X, Leng K, Qin W, Qu L, Cui Y, Jiang X. Downregulated circular RNA hsa_circ_0001649 regulates proliferation, migration and invasion in cholangiocarcinoma cells. *Biochem Biophys Res Commun* 2018; **496**: 455-461 [PMID: 29337065 DOI: 10.1016/j.bbrc.2018.01.077]
22 **Wangxia LV**, Fang Y, Liu Y, Zhao Y, Shi Z, Zhong H. Circular RNA ARHGAP26 is over-expressed and its downregulation inhibits cell proliferation and promotes cell apoptosis in gastric cancer cells. *Saudi J Gastroenterol* 2019; **25**: 119-125 [PMID: 30719998 DOI: 10.4103/sjg.SJG_283_18]
23 **Song YZ**, Li JF. Circular RNA hsa_circ_0001564 regulates osteosarcoma proliferation and apoptosis by acting miRNA sponge. *Biochem Biophys Res Commun* 2018; **495**: 2369-2375 [PMID: 29229385 DOI: 10.1016/j.bbrc.2017.12.050]
24 **Matthews CP**, Colburn NH, Young MR. AP-1 a target for cancer prevention. *Curr Cancer Drug Targets* 2007; **7**: 317-324 [PMID: 17979626 DOI: 10.2174/156800907780809723]
25 **Vaiopoulos AG**, Papachroni KK, Papavassiliou AG. Colon carcinogenesis: Learning from NF-kappaB and AP-1. *Int J Biochem Cell Biol* 2010; **42**: 1061-1065 [PMID: 20348011 DOI: 10.1016/j.biocel.2010.03.018]
26 **Gualco G**, Weiss LM, Bacchi CE. MUM1/IRF4: A Review. *Appl Immunohistochem Mol Morphol* 2010; **18**: 301-310 [PMID: 20182347 DOI: 10.1097/PAI.0b013e3181cf1126]
27 **Heimes AS**, Madjar K, Edlund K, Battista MJ, Almstedt K, Gebhard S, Foersch S, Rahnenführer J, Brenner W, Hasenburg A, Hengstler JG, Schmidt M. Prognostic significance of interferon regulating factor 4 (IRF4) in node-negative breast cancer. *J Cancer Res Clin Oncol* 2017; **143**: 1123-1131 [PMID: 28251349 DOI: 10.1007/s00432-017-2377-7]
28 **Wu YY**, Hwang YT, Perng WC, Chian CF, Ho CL, Lee SC, Chang H, Terng HJ, Chao TY. CPEB4 and IRF4 expression in peripheral mononuclear cells are potential prognostic factors for advanced lung cancer. *J Formos Med Assoc* 2017; **116**: 114-122 [PMID: 27113098 DOI: 10.1016/j.jfma.2016.01.009]
29 **Mallo GV**, Soubeyran P, Lissitzky JC, André F, Farnarier C, Marvaldi J, Dagorn JC, Iovanna JL. Expression of the Cdx1 and Cdx2 homeotic genes leads to reduced malignancy in colon cancer-derived cells. *J Biol Chem* 1998; **273**: 14030-14036 [PMID: 9593754 DOI: 10.1074/jbc.273.22.14030]
30 **Hinoi T**, Loda M, Fearon ER. Silencing of CDX2 expression in colon cancer via a dominant repression pathway. *J Biol Chem* 2003; **278**: 44608-44616 [PMID: 12947088 DOI: 10.1074/jbc.M307435200]
31 **Hinkel I**, Duluc I, Martin E, Guenot D, Freund JN, Gross I. Cdx2 controls expression of the protocadherin Mucdhl, an inhibitor of growth and β-catenin activity in colon cancer cells. *Gastroenterology* 2012; **142**: 875-885.e3 [PMID: 22202456 DOI: 10.1053/j.gastro.2011.12.037]
32 **Olsen J**, Eiholm S, Kirkeby LT, Espersen ML, Jess P, Gögenür I, Olsen J, Troelsen JT. CDX2 downregulation is associated with poor differentiation and MMR deficiency in colon cancer. *Exp Mol Pathol* 2016; **100**: 59-66 [PMID: 26551082 DOI: 10.1016/j.yexmp.2015.11.009]
33 **Ali RG**, Bellchambers HM, Arkell RM. Zinc fingers of the cerebellum (Zic): Transcription factors and co-factors. *Int J Biochem Cell Biol* 2012; **44**: 2065-2068 [PMID: 22964024 DOI: 10.1016/j.biocel.2012.08.012]
34 **Gan L**, Chen S, Zhong J, Wang X, Lam EK, Liu X, Zhang J, Zhou T, Yu J, Si J, Wang L, Jin H. ZIC1 is downregulated through promoter hypermethylation, and functions as a tumor suppressor gene in colorectal cancer. *PLoS One* 2011; **6**: e16916 [PMID: 21347233 DOI: 10.1371/journal.pone.0016916]

World Journal of Gastroenterology

Submit a Manuscript: https://www.f6publishing.com

*World J Gastroenterol* 2019 September 21; 25(35): 5310-5322

DOI: 10.3748/wjg.v25.i35.5310

ISSN 1007-9327 (print) ISSN 2219-2840 (online)

ORIGINAL ARTICLE

Basic Study

# LncRNA-ATB promotes autophagy by activating Yes-associated protein and inducing autophagy-related protein 5 expression in hepatocellular carcinoma

Chuan-Zhuo Wang, Guang-Xin Yan, De-Shuo Dong, He Xin, Zhao-Yu Liu

**ORCID number:** Chuan-Zhuo Wang (0000-0002-2859-6403); Guang-Xin Yan (0000-0002-6686-451X); De-Shuo Dong (0000-0002-0142-015X); He Xin (0000-0001-9478-5803); Zhao-Yu Liu (0000-0001-8789-7479).

**Author contributions:** Wang CZ and Liu ZY conceived the study and participated in its design; Wang CZ, Yan GX, and Dong DS performed the experiments; Xin H performed the statistical analysis.

**Institutional review board statement:** The human subject research performed in this study was approved by the Clinical Research Ethics Committee of the Hospital of China Medical University.

**Conflict-of-interest statement:** The authors declare no conflicts of interest regarding the publication of this paper.

**Data sharing statement:** No additional data are available.



**Chuan-Zhuo Wang, Guang-Xin Yan, De-Shuo Dong, He Xin, Zhao-Yu Liu,** Department of Radiology, Shengjing Hospital of China Medical University, Shenyang 110004, Liaoning Province, China

**Corresponding author:** Zhao-Yu Liu, MD, Academic Research, Professor, Chairman, Department of Radiology, Shengjing Hospital of China Medical University, No. 36, Sanhao Street, Heping District, Shenyang 110004, Liaoning Province, China. liuzy@sj-hospital.org
**Telephone:** +86-18940251226
**Fax:** +86-24-23901480

## Abstract

### *BACKGROUND*

Long non-coding RNAs (lncRNAs) play important roles in many diseases, including hepatocellular carcinoma (HCC). Autophagy is a metabolic pathway that facilitates cancer cell survival in response to stress. The relationship between autophagy and the lncRNA-activated by transforming growth factor beta (lncRNA-ATB) in HCC remains unknown.

### *AIM*

To explore the influence of lncRNA-ATB in regulating autophagy in HCC cells and the underlying mechanism.

### *METHODS*

In the present study, we evaluated lncRNA-ATB expression in tumor and adjacent non-tumor tissues from 72 HCC cases by real-time PCR. We evaluated the role of lncRNA-ATB in the proliferation and clonogenicity of HCC cells *in vitro*. The effect of lncRNA-ATB on autophagy was determined using a LC3-GFP reporter and transmission electron microscopy. Furthermore, the mechanism by which lncRNA-ATB regulates autophagy was explored by immunofluorescence staining, RNA immunoprecipitation (RIP), and Western blot.

### *RESULTS*

The expression of lncRNA-ATB was higher in HCC tissues than in normal liver tissues, and lncRNA-ATB expression was positively correlated with tumor size, TNM stage, and poorer survival of patients with HCC. Moreover, ectopic overexpression of lncRNA-ATB promoted cell proliferation and clonogenicnity of HCC cells *in vitro*. LncRNA-ATB promoted autophagy by activating Yes-associated protein (YAP). Moreover, lncRNA-ATB interacted with autophagy-

**Manuscript source**: Unsolicited manuscript

**Received:** May 24, 2019
**Peer-review started:** May 27, 2019
**First decision:** July 21, 2019
**Revised:** July 30, 2019
**Accepted:** August 7, 2019
**Article in press:** August 7, 2019
**Published online:** September 21, 2019

**P-Reviewer:** Kimkong I
**S-Editor:** Ma RY
**L-Editor:** Wang TQ
**E-Editor:** Ma YJ

related protein 5 (ATG5) mRNA and increased ATG5 expression.

***CONCLUSION***
LncRNA-ATB regulates autophagy by activating YAP and increasing ATG5 expression. Our data demonstrate a novel function for lncRNA-ATB in autophagy and suggest that lncRNA-ATB plays an important role in HCC.

**Key words:** LncRNA-ATB; Autophagy; Yes-associated protein; Autophagy-related protein 5; Hepatocellular carcinoma



**Core tip:** In the present study, we identified the relationship between lncRNA-activated by transforming growth factor beta (lncRNA-ATB) and autophagy in hepatocellular carcinoma (HCC). We demonstrated that lncRNA-ATB promoted autophagic flux in HCC cells. We found that lncRNA-ATB regulated autophagy by activating Yes-associated protein and increasing autophagy-related protein 5 expression. Our findings provide a novel link between lncRNA-ATB and autophagy, and suggest that lncRNA-ATB may be a potential therapeutic target in the treatment of HCC.

**Citation:** Wang CZ, Yan GX, Dong DS, Xin H, Liu ZY. LncRNA-ATB promotes autophagy by activating Yes-associated protein and inducing autophagy-related protein 5 expression in hepatocellular carcinoma. *World J Gastroenterol* 2019; 25(35): 5310-5322
**URL**: https://www.wjgnet.com/1007-9327/full/v25/i35/5310.htm
**DOI**: https://dx.doi.org/10.3748/wjg.v25.i35.5310

## INTRODUCTION

Hepatocellular carcinoma (HCC) is the second leading cause of cancer-related mortality among males, and is the fifth most common cancer worldwide[1,2]. Although therapy for HCC has seen significant improvement in recent years, clinical outcome prognosis remains poor for patients with HCC. A large number of aberrantly expressed genes influence the progression of HCC, but the molecular mechanisms governing HCC malignancy are still not entirely clear, and the potential connection between long non-coding RNAs (lncRNAs) and autophagy remains to be fully elucidated. There is an important and unmet need to elucidate molecular mechanisms of autophagy, and to capitalize on that knowledge to develop autophagy-related methods as therapeutic strategies for treatment of HCC.

LncRNAs are a class of RNA transcripts that are longer than 200 nucleotides and exhibit limited protein-coding capacity[3]. LncRNAs regulate many aspects of cancer progression and can influence different malignant behaviors, including cancer cell proliferation, apoptosis, metastasis, glycolysis, and angiogenesis[4,5]. LncRNA-activated by transforming growth factor beta (lncRNA-ATB) is a lncRNA transcript regulated by transforming growth factor beta signaling; it mediates induction of epithelial-mesenchymal transition (EMT) downstream of transforming growth factor beta signaling by competitively binding to members of the miR-200 family[6]. Recently, up-regulation of lncRNA-ATB was reported in a variety of human cancers, and was found to influence a multitude of cellular functions in cancer cells[7]. Emerging reports have identified the role of lncRNAs in regulating autophagy[8], but the involvement of lncRNA-ATB in autophagy in HCC is not entirely clear.

Autophagy is an evolutionarily conserved catabolic process that regulates the coordinated lysosomal degradation of cellular components and damaged organelles. Autophagy can support cell survival and maintenance of homeostasis in response to different forms of stress, such as hypoxia, or deprivation of nutrients and energy[9]. Additionally, autophagy can promote the invasion and migration of HCC cells[10,11]. Nevertheless, whether and how autophagy facilitates cancer progression remains controversial[12]. Based on the cytoprotective properties of autophagy in cancer cells, most research into autophagy has focused on exploring the value of autophagy-targeted therapy[13]. There are currently more than 50 randomized controlled trials evaluating the effects of autophagy as relates to cancer therapy. However, the molecular mechanism of autophagy and the exploitation of autophagy as a

therapeutic strategy in HCC remain understudied.

In the present study, we evaluated the relationship between lncRNA-ATB and autophagy in HCC. We demonstrated that lncRNA-ATB promotes autophagic flux in HCC cells. We found that lncRNA-ATB regulates autophagy by activating Yes-associated protein (YAP) and increasing autophagy-related protein 5 (ATG5) expression. Our findings provide a novel link between lncRNA-ATB and autophagy, and suggest that lncRNA-ATB may be a potential therapeutic target in the treatment of HCC.

## MATERIALS AND METHODS

### Patients and tissue samples

Seventy-two HCC tissue samples and adjacent non-tumor tissue samples were obtained from the Cancer Hospital of China Medical University (Shenyang, China). All patients on this study provided informed consent. The human subject research performed in this study was approved by the Clinical Research Ethics Committee of the Hospital of China Medical University. Fresh patient tissue samples were frozen in liquid nitrogen and were immediately stored at -80 °C. The clinical characteristics of the 72 patients with HCC are provided in Table 1.

### Cell culture

The human HCC cell lines SMMC-7721 and HepG2 were obtained from the Type Culture Collection of the Chinese Academy of Sciences (Shanghai, China). HCC cells were cultured in RPMI 1640 medium (BioWhittaker, Walkersville, MD, United States) supplemented with 10% fetal bovine serum (FBS; HyClone, Logan, UT, United States) and 1% penicillin/streptomycin in a humidified atmosphere containing 5% $CO_2$ at 37 °C.

### Cell transfection

DNA vectors were transfected into cells using the Lipofectamine 3000 reagent (Invitrogen, CA, United States), according to the manufacturer's instructions. Briefly, pcDNA3.1 or pcDNA3.1-lncRNA-ATB (Genechem, Shanghai, China) was introduced into cells when cell growth reached approximately 80% confluence. Cells were collected 48 h after transfection. Small interfering RNAs (siRNA) targeting YAP were synthesized by Sigma (Shanghai, China) and the sequences used are as follows: YAP siRNA#1: 5′-GACAUCUUCUGGUCAGAGATT-3′ and YAP siRNA#2: 5′-GGUGAUACUAUCAACCAAATT-3′.

### Cell proliferation assay

Proliferation of HCC cells was measured using a Cell Counting Kit-8 (CCK-8, Dojindo, Japan). First, cells transfected with pcDNA3.1-lncRNA-ATB or pcDNA3.1 were seeded at a density of 3000 cells/well into 96-well plates. Cells were cultured at 37 °C for 0, 24, 48, and 72 h. At these indicated time points, 20 μL of CCK8 solution was added to each well. Plates were then incubated at 37 °C for 2 h. Absorbance was measured at 490 nm using a microplate reader. Data are presented as the mean of three independent experiments.

### Colony formation assay

For colony formation assays, cells transfected with pcDNA3.1-lncRNA-ATB or pcDNA3.1 were plated in 6-well plates and cultured at 37 °C in growth medium containing 10% FBS. After 14 d, colonies were fixed with 4% polyoxymethylene for 10 min and then stained with 0.1% crystal violet solution for 10 min. Colonies were observed using an Olympus microscope (Tokyo, Japan), and the number of colonies was recorded.

### Western blot analysis

Protein lysates were prepared from cells using RIPA buffer supplemented with a protease inhibitor cocktail (Roche, China). Protein lysates were separated by SDS-PAGE and then transferred to PVDF membranes (Sigma, United States). Membranes were then incubated with specific antibodies. Protein expression was assessed using ECL chemiluminescent reagents. The primary antibodies used are as follows: antibodies against ATG5, LC3, and β-actin were purchased from Cell Signaling Technology (United States) and those against phospho-PI3K (Tyr458), PI3K, phospho-AKT (Ser473), AKT, phospho-mTOR (Ser2248), mTOR, phospho-YAP (S127), and YAP were purchased from Abcam (United Kingdom).

**Table 1 Correlation between lncRNA-ATB expression and clinicopathological parameters in patients with hepatocellular carcinoma**

| Clinical feature | *n* | LncRNA-ATB | | *P*-value |
|---|---|---|---|---|
| | | High expression (*n* = 36) | Low expressio -n (*n* = 36) | |
| Gender | | | | 0.096 |
| Male | 41 | 17 | 24 | |
| Female | 31 | 19 | 12 | |
| Age (yr) | | | | 0.617 |
| ≤ 60 | 48 | 23 | 25 | |
| > 60 | 24 | 13 | 11 | |
| HBsAg | | | | 0.306 |
| Negative | 50 | 27 | 23 | |
| Postive | 22 | 9 | 13 | |
| AFP (ng/mL) | | | | 0.216 |
| ≤ 400 | 25 | 15 | 10 | |
| > 400 | 47 | 21 | 26 | |
| Tumor size | | | | 0.032* |
| ≤ 5cm | 41 | 16 | 25 | |
| > 5cm | 31 | 20 | 11 | |
| TNM stage | | | | 0.017* |
| I + II | 30 | 10 | 20 | |
| III + IV | 42 | 26 | 16 | |
| Differentiation | | | | 0.465 |
| Well/moderate | 45 | 21 | 24 | |
| Poor | 27 | 15 | 12 | |

The median expression level of lncRNA-ATB was used as the cutoff. Pearson's chi-square tests were used for analysis. *$P < 0.05$. LncRNA-ATB: LncRNA-activated by transforming growth factor beta.

### *Immunofluorescence staining*

For immunofluorescence, cells were fixed with 4% paraformaldehyde (Sigma-Aldrich, United States) for 30 min at room temperature. Cells were then permeabilized with 0.4% Triton X-100 for 5 min at room temperature, and then blocked in 5% bovine serum albumin at 37 °C for 25 min. Next, cells were incubated with primary antibodies at 4 °C overnight. Following overnight incubation, cells were incubated with specific secondary antibodies for 1 h at 37 °C, and were then washed with PBS three times. After a final wash, nuclei were stained with DAPI for 3 min at room temperature. Immunofluorescence was observed and evaluated using a confocal microscope (Olympus, United States).

### *Transmission electron microscopy (TEM)*

HCC cell samples were processed and autophagosomes were visualized by TEM as described previously[14]. In brief, samples were fixed with 2.5% glutaraldehyde in 0.1 mol/L cacodylate buffer for 4 h and underwent post-fixation with 1% $OsO_4$ in 0.1 mol/L cacodylate buffer for 2 h. Next, samples were dehydrated, embedded in resin-propylene oxide, and sectioned using a Leica UFC6 ultra-thin microtome at 80 nm thickness. Finally, images were captured using a Hitachi Model H-7650 transmission electron microscope.

### *RNA isolation and real time-PCR*

Isolation of total RNA, cDNA reverse transcription, and quantitative real-time PCR were performed as previously described[10]. The PCR amplification primers used are as follows: LncRNA-ATB forward, 5′-CTTCACCAGCACCCAGAGA-3′ and reverse, 5′-AAGACAGAAAAACAGTTCCGAGTC-3′; GAPDH forward, 5′-AAAGATGTG CTTCGAGATGTGT-3′ and reverse, 5′-CACTTTGTCAGTTACCAACGTCA-3′; ATG3 forward 5′-GACCCCGGTCCTCAAGGAA-3′ and reverse, 5′-TGTAGCCCA TTGCCATGTTGG-3′; ATG5 forward, AAAGATGTGCTTCGAGATGTGT-3′ and

reverse, 5′-CACTTTGTCAGTTACCAACGTCA-3′; ATG7 forward 5′-CAGTTTGCCC CTTTTAGTAGTGC-3′ and reverse, 5′-CCAGCCGATACTCGTTCAGC-3′; ATG10 forward 5′-AGACCATCAAAGGACTGTTCTGA-3′ and reverse, 5′-GGGTAGATGC TCCTAGATGTGAC-3′; ATG12 forward 5′-CTGCTGGCGACACCAAGAAA-3′ and reverse, 5′-CGTGTTCGCTCTACTGCCC-3′; ATG16L forward 5′-AAGAAAC GTGGGGAGTT AGC-3′ and reverse, 5′-AGAGACAGAGCGTCTCCCAA -3′.

### RNA immunoprecipitation (RIP)

HepG2 and SMMC-7721 cells were co-transfected with pcDNA3.1-MS2, pcDNA3.1-ATB-MS2, pcDNA3.1-ATB-MS2-mut (ATG5), and pMS2-GFP. The plasmids were synthesized by Genechem (Shanghai, China). After transfection for 48 h, cells were cultured to use in experiments for RIP. RIP was performed using a GFP antibody and the Magna RIPTM RNA-Binding protein, according to the manufacturer's instructions.

### Statistical analysis

All of data analyses were performed using SPSS software (version 17.0, SPSS). Data are presented as the mean ± SD. Significant differences between groups were analyzed using the Student's *t*-test. Chi-square tests were performed to determine the relationship between lncRNA-ATB and clinicopathological characteristics. Pearson's correlation analysis was used to evaluate correlations in expression between two genes. Kaplan-Meier survival analysis was used to evaluate overall survival, and the log-rank test was used to determine differences in survival between groups. Differences were considered to be statistically significant at $^{a}P < 0.05$ and $^{b}P < 0.01$.

## RESULTS

### LncRNA-ATB is highly expressed in HCC and is predictive of poor prognosis

We evaluated expression profiles of lncRNA-ATB in HCC samples by measuring lncRNA-ATB levels in 72 pairs of HCC and adjacent non-tumor tissues by qRT-PCR. LncRNA-ATB was expressed at higher levels in HCC tissues than in non-tumor tissue (Figure 1A). High expression of lncRNA-ATB was associated with larger tumor size and advanced TNM stage. The expression of lncRNA-ATB in patients with HCC tumors larger than 5 cm was significantly higher than in patients with tumor size smaller than 5 cm (Figure 1B). LncRNA-ATB was significantly higher in HCC patients with advanced TNM stage (III/IV) than in patients with local TNM stage (I/II) (Figure 1C). We stratified the 72 patients into a high lncRNA-ATB group and a low lncRNA-ATB group, based on the median expression of lncRNA-ATB. We then examined the relationship between lncRNA-ATB expression and prognosis in patients with HCC. Kaplan-Meier survival analysis revealed that patients with higher lncRNA-ATB expression had a poorer prognosis (Figure 1D). These results indicated that lncRNA-ATB is overexpressed in HCC compared to normal tissues, and that higher lncRNA-ATB expression predicts poor survival for patients with HCC.

### Overexpression of lncRNA-ATB promotes HCC cell proliferation and clonogenicity

To explore the function of lncRNA-ATB in HCC cells, we established lncRNA-ATB overexpressing cell lines by transfecting SMMC-7721 and HepG2 cells with pcDNA3.1-ATB. At 48 h post-transfection, lncRNA-ATB expression was about 29-fold and 34-fold higher than that in cells transfected with negative control (pcDNA3.1), respectively (Figure 2A). Overexpression of lncRNA-ATB significantly promoted HCC cell proliferation, as indicated by the CCK-8 proliferation assay (Figure 2B). *In vitro* colony formation assays demonstrated that overexpression of lncRNA-ATB increased the number of colonies formed by both SMMC-7721 and HepG2 cells (Figure 2C). These results show that lncRNA-ATB has an oncogenic capacity to facilitate the proliferation and clonogenicity of HCC cells.

### LncRNA-ATB promotes autophagic flux in HCC cells

To determine the biological effect of lncRNA-ATB on autophagy, we evaluated the effects of lncRNA-ATB overexpression on autophagy in HCC cells. Overexpression of lncRNA-ATB increased the accumulation of LC3-II, which is generally considered to be a marker of autophagosome formation. Furthermore, we used bafilomycin A1, an inhibitor of the fusion of autophagosomes and lysosomes, to examine autophagic flux by evaluating changes in the degradation of LC3-II. Accumulation of LC3-II was significantly increased in HCC cells treated with bafilomycin A1, after transfection with pcDNA3.1-lncRNA-ATB (Figure 3A and B), indicating that lncRNA-ATB induces autophagic flux. By using a LC3-GFP reporter, the abundance of LC3 puncta was measured, and HCC cells transfected with pcDNA3.1-lncRNA-ATB exhibited similar

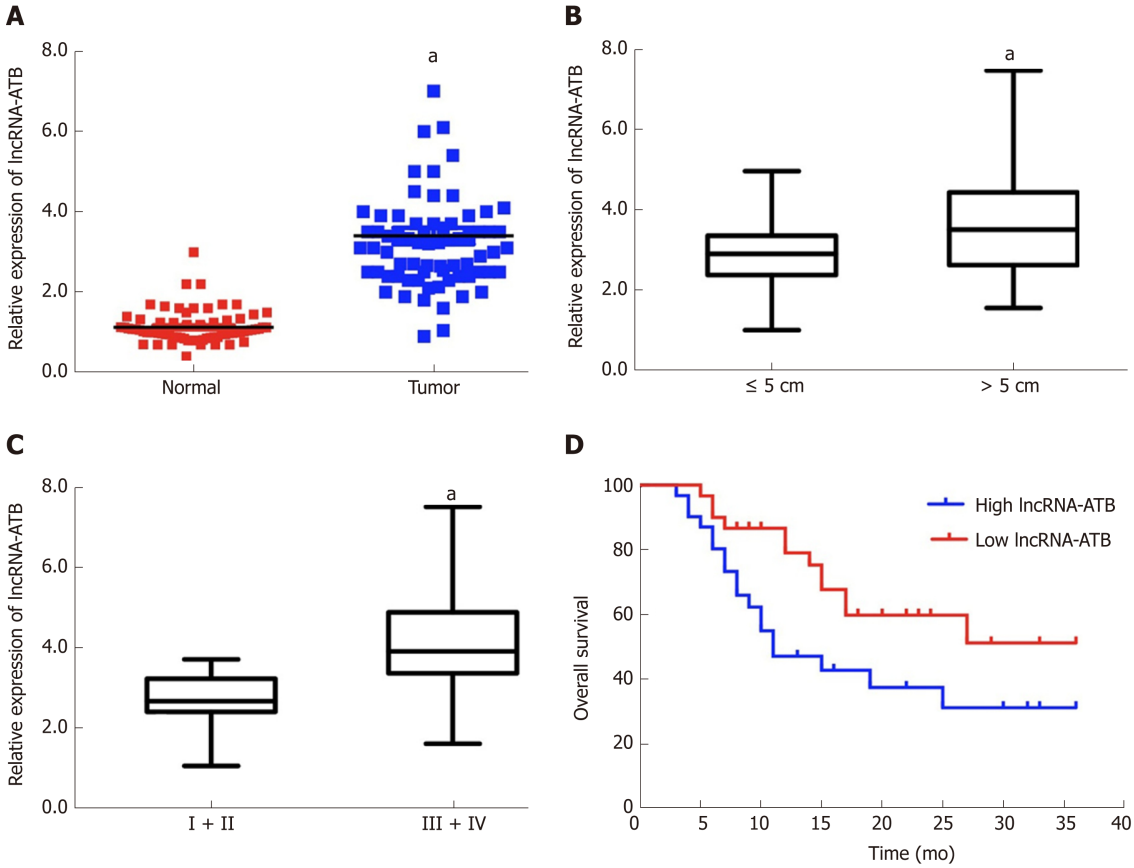


**Figure 1 LncRNA-ATB is significantly up-regulated in human hepatocellular carcinoma tissues and predicts a poor prognosis.** A: Relative expression levels of lncRNA-activated by transforming growth factor beta (lncRNA-ATB) in hepatocellular carcinoma (HCC) tissues and adjacent normal tissues; B: Relative expression levels of lncRNA-ATB in HCC patients with larger tumor sizes (> 5 cm) and smaller tumor sizes (≤ 5 cm); C: Relative expression levels of lncRNA-ATB in HCC patients with early stage (I/II) and advanced stage (III/IV) disease; D: Kaplan-Meier analysis of overall survival in 72 HCC patients according to median lncRNA-ATB expression. The log-rank test was used to calculate the *P*-value. Data are expressed as the mean ± SD of three independent experiments. Statistical significance is indicated at $^{a}P < 0.05$. HCC: Hepatocellular carcinoma; LncRNA-ATB: LncRNA-activated by transforming growth factor beta.

LC3 puncta accumulation to cells treated with rapamycin (Figure 3C and D). TEM analysis detected autophagosomes and autolysosomes in HCC cells overexpressing lncRNA-ATB, and fewer were observed in negative control cells (Figure 3E and F). These results indicate that lncRNA-ATB promotes autophagic flux and autolysosome formation.

### *LncRNA-ATB promotes autophagy by modulating YAP activation*

YAP is a key coactivator of the Hippo pathway, and has been demonstrated to promote cancer cell survival by enhancing autophagic flux[15]. Moreover, a growing number of studies have found that lncRNAs are able to regulate Hippo-YAP signaling in cancer cells. We therefore hypothesized that lncRNA-ATB promotes autophagy by activating YAP. To explore this, we measured YAP expression in HCC cells overexpressing lncRNA-ATB, and found that overexpression of lncRNA-ATB did not change the expression of total YAP protein, but decreased p-YAP expression in SMMC-7721 and HepG2 cells (Figure 4A and B). In addition, consistent with the decrease in p-YAP, overexpression of lncRNA-ATB induced YAP translocation from the cytoplasm to the nucleus, as indicated by immunofluorescence (Figure 4C and D). These data demonstrate that lncRNA-ATB induces nuclear translocation of YAP. To determine whether lncRNA-ATB promotes autophagy by activating YAP, we inhibited YAP expression with siRNA. YAP expression was significantly decreased by si-YAP1, as demonstrated by Western blot analysis (Figure 4E and F). Consistently, we found that YAP knockdown partially attenuated lncRNA-ATB-induced activation of autophagy in HCC cells (Figure 4G and H). These results reveal that lncRNA-ATB promotes autophagy in HCC cells by modulating YAP activation.

### *LncRNA-ATB influences autophagy by targeting ATG5 expression*

Autophagy is a dynamic, continuous, and tightly coordinated metabolic process that is regulated by a series of autophagy-related genes (ATGs). ATG proteins are essential

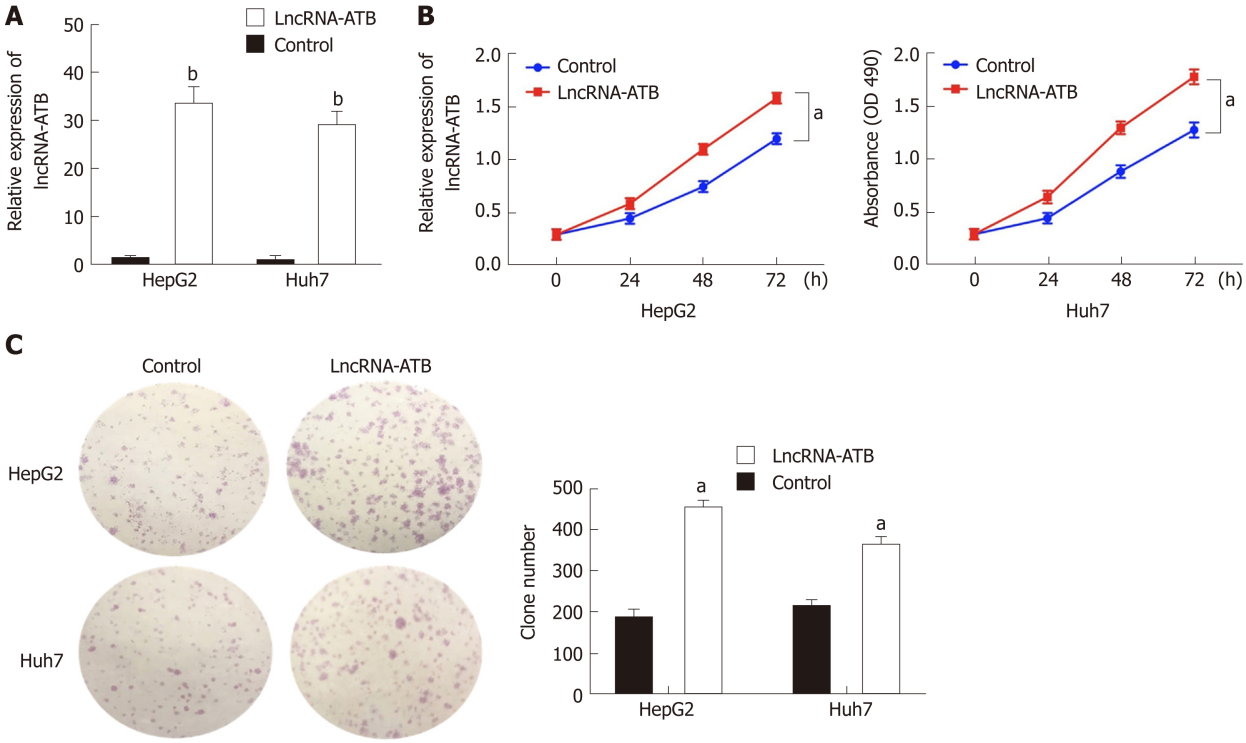


**Figure 2 Overexpression of lncRNA-ATB promotes the proliferation of hepatocellular carcinoma cells *in vitro*.** A: LncRNA-activated by transforming growth factor beta (lncRNA-ATB) expression was determined by real-time PCR in hepatocellular carcinoma (HCC) cells transfected with pcDNA3.1-lncRNA-ATB; B: CCK-8 assays were performed to determine the proliferation of HCC cell lines (SMMC-7721 and HepG2) transfected with pcDNA3.1-lncRNA-ATB; C: Colony formation assays were performed to measure the proliferation of HCC cells transfected pcDNA3.1-lncRNA-ATB. Data are expressed as the mean ± SD of three independent experiments. Statistical significance is indicated at $^{a}P < 0.05$ or $^{b}P < 0.01$. HCC: Hepatocellular carcinoma; LncRNA-ATB: LncRNA-activated by transforming growth factor beta.

for the formation of the autophagosome, and are crucial for delivery of autophagic cargo to fuse with the lysosome[16]. To determine which ATG genes are involved in regulation of autophagy by lncRNA-ATB, we used real-time PCR to evaluate the expression of ATG genes in HCC cells following overexpression of lncRNA-ATB. ATG5 mRNA expression was significantly up-regulated by lncRNA-ATB overexpression (Figure 5A and B). In addition, Western blot analysis confirmed that ATG5 protein expression was increased by lncRNA-ATB overexpression (Figure 5C and D). Next, we explored the mechanism by which lncRNA-ATB regulates ATG5. LncRNAs can interact with mRNAs to increase mRNA stability, which promotes gene expression[6,17]. We used BLAST to find potential binding sites between lncRNA-ATB and the ATG5 mRNA, and identified several regions of high complementarity. We used RIP to investigate direct interactions of lncRNA-ATB and ATG5 mRNA, and found that LncRNA-ATB was significantly enriched for ATG5 mRNA compared to the empty vector or to lncRNA-ATB with mutated binding sites (Figure 5E and F). We then determined the expression correlation between ATG5 and lncRNA-ATB in HCC tissue. These demonstrate that lncRNA-ATB interacts with ATG5 mRNA and regulates autophagy by increasing ATG5 expression.

### *Nuclear localization of YAP and ATG5 expression are correlated positively with lncRNA-ATB expression*

We examined YAP expression in 72 HCC tissues by immunohistochemistry. We found that 62.5% (45/72) of HCC samples showed stronger YAP staining than adjacent non-tumor tissues (Figure 6A). YAP localization showed stronger nuclear staining in HCC tissues than in normal tissues. We then evaluated ATG5 expression by real-time PCR and found that ATG5 expression was significantly higher in HCC tissues compared with adjacent normal tissues (Figure 6B). Additionally, we determined the correlation between the expression of lncRNA-ATB and ATG5, and found that ATG5 mRNA expression was positively correlated with lncRNA-ATB expression (Figure 6C).

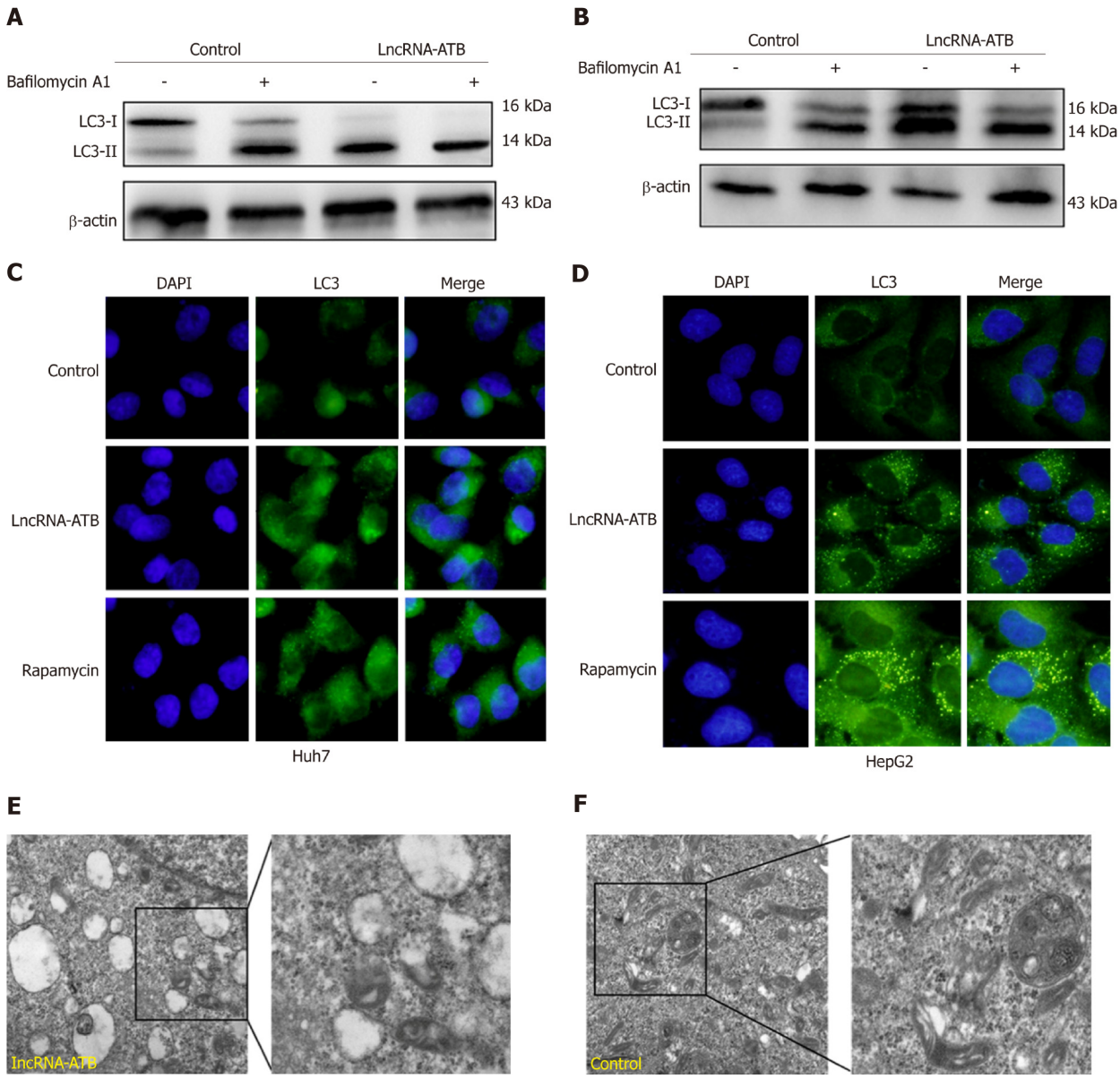


**Figure 3 LncRNA-ATB promotes autophagy in hepatocellular carcinoma cells.** A and B: Hepatocellular carcinoma (HCC) cells transfected with pcDNA3.1-lncRNA-ATB were subjected to Western blot analysis to detect LC3-II/LC3-I expression, with and without bafilomycin A1 treatment (20 μmol/L for 6 h); C and D: Immunofluorescence of LC3 puncta (green) was measured in HCC cells transfected with pcDNA3.1-lncRNA-ATB or treated with rapamycin; E and F: Electron microscopy identified highly visible autophagosomes and autolysosomes in HCC cells overexpressing lncRNA-ATB compared to negative control cells. HCC: Hepatocellular carcinoma; LncRNA-ATB: LncRNA-activated by transforming growth factor beta.

## DISCUSSION

LncRNAs play vital roles in tumor progression[18], and more and more lncRNAs are being shown to influence tumor cells biology[19]. In the present study, we found that lncRNA-ATB is expressed at high levels in HCC tissues. We report that elevated expression of lncRNA-ATB associates with increased tumor size and higher TNM stage, suggesting that lncRNA-ATB may serve as a prognostic biomarker to identify those HCC patients who are at higher risk of disease progression. In previous studies, lncRNA-ATB was found to be overexpressed in various tumors of the digestive system, such as gastric cancer, colorectal cancer, and pancreatic cancer[20-22]. In gastric cancer, Iguchi *et al*[21] found that expression of lncRNA-ATB significantly correlates with postoperative overall survival of patients with GC, and induced EMT in GC cells. They reported that lncRNA-ATB expression is correlated to tumor size, depth of tumor invasion, and TNM stage in colorectal tumors. In functional experiments, lncRNA-ATB was found to influence multiple biological processes of cancer cells. LncRNA-ATB promotes cell viability, migration, and invasion in T24 cells by regulating miR-126 as a molecular sponge[23]. Here we report that lncRNA-ATB overexpression promotes proliferation of HCC cells. These data suggest that lncRNA-

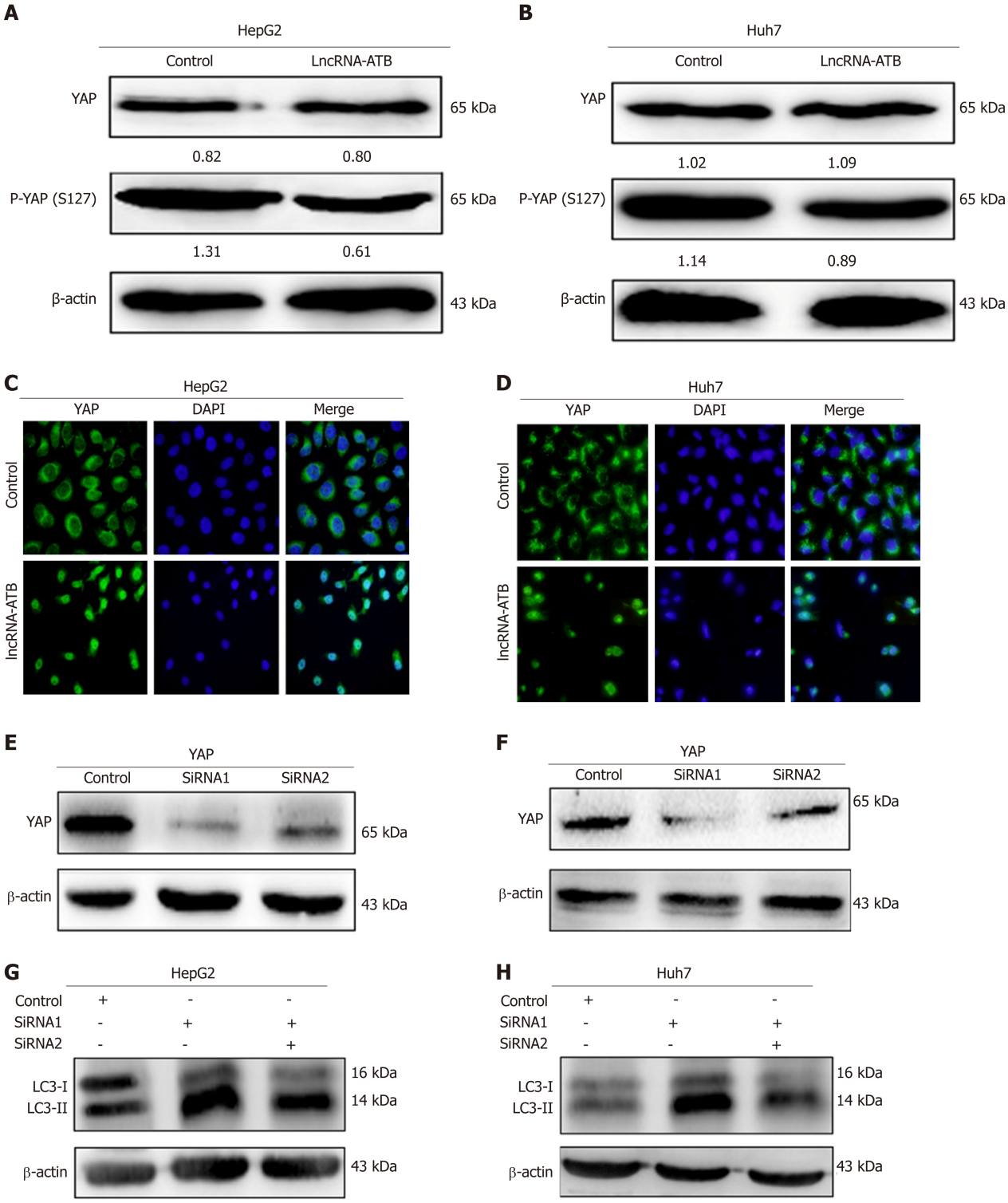


**Figure 4 LncRNA-ATB promotes autophagy through modulation of Yes-associated protein activation.** A and B: The protein levels of total Yes-associated protein (YAP) and p-YAP in hepatocellular carcinoma (HCC) cells transfected with pcDNA3.1-lncRNA-ATB were measured by Western blot; C and D: The nuclear localization of YAP was detected in transfected HCC cells by immunofluorescence; E and F: Knockdown of YAP in HCC cells transfected with si-YAP (si-YAP 1# and si-YAP 2#) was measured using Western blot; G and H: HCC cells were co-transfected with pcDNA3.1-lncRNA-ATB and si-YAP, and the protein levels of LC3 were determined by Western blot. Yes-associated protein: YAP; HCC: Hepatocellular carcinoma; LncRNA-ATB: LncRNA-activated by transforming growth factor beta.

ATB plays an oncogenic role in HCC progression.

Autophagy can be considered a kind of metabolic reprogramming pathway, and is a topic of increasing relevance to cancer research. The role of autophagy as an anti-tumor or tumor-promoting pathway is context dependent[24], and emerging studies have indicated that autophagy can facilitate survival of tumor cells in response to stress[9,25]. Reports have also demonstrated that non-coding RNAs can act as regulators in the autophagy pathway[8]. In our current study, we analyzed the potential link

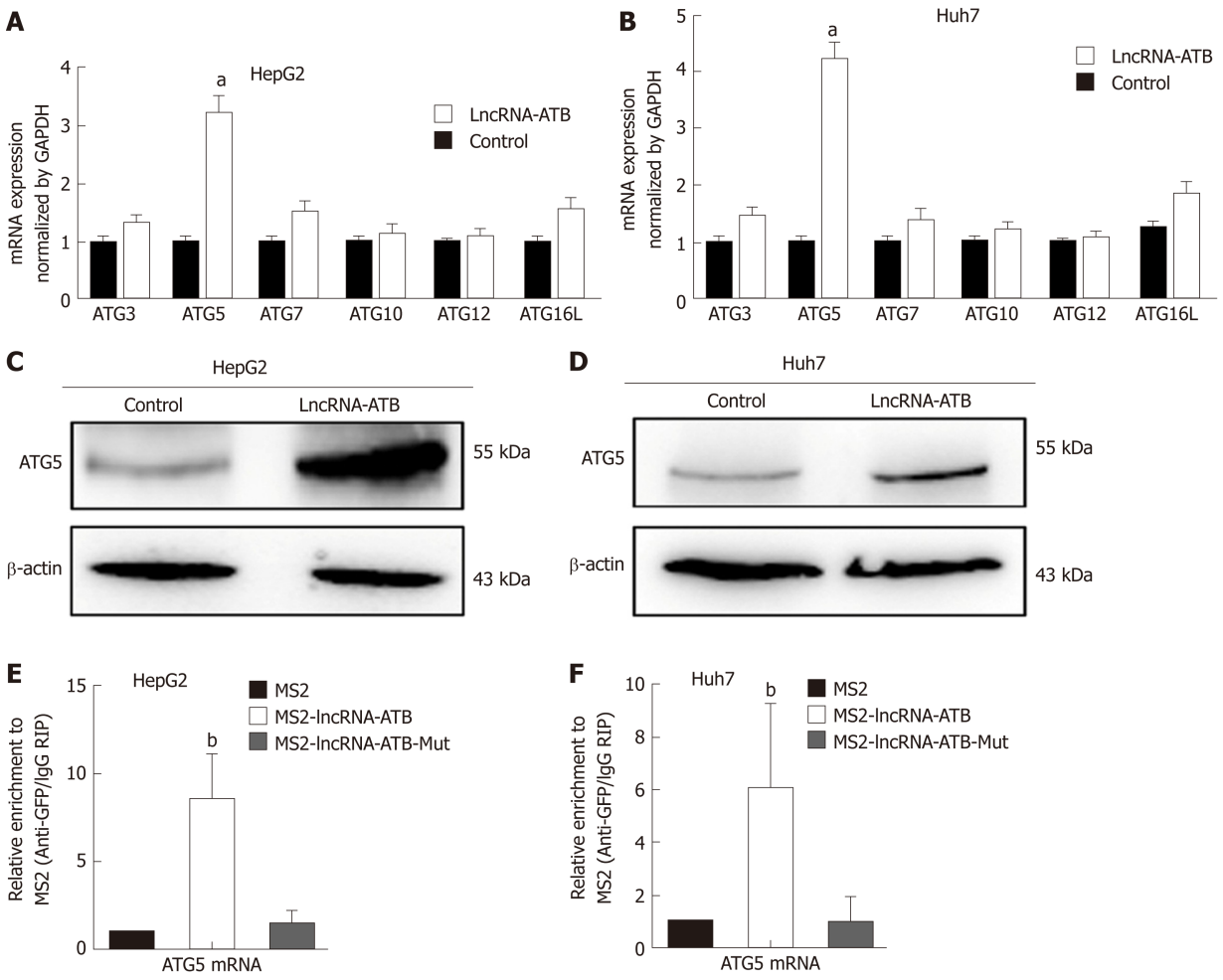


**Figure 5 LncRNA-ATB induces autophagy by regulating autophagy-related protein 5 expression.** A and B: The mRNA expression of autophagy-related genes involved in autophagy was examined by real-time PCR in hepatocellular carcinoma (HCC) cells transfected with lncRNA-ATB; C and D: The protein levels of ATG5 were analyzed in HCC cells transfected with lncRNA-ATB by Western blot; E and F: RIP-derived RNA was evaluated by real-time PCR. Data are expressed as the mean ± SD of three independent experiments. Statistical significance is indicated at $^{a}P < 0.05$ or $^{b}P < 0.01$. ATG3: Autophagy-related protein 3; ATG5: Autophagy-related protein 5; ATG7: Autophagy-related protein 7; ATG10: Autophagy-related protein 10; ATG12: Autophagy-related protein 12; ATG16L: Autophagy-related protein 16L; HCC: Hepatocellular carcinoma; RIP: RNA immunoprecipitation; LncRNA-ATB: LncRNA-activated by transforming growth factor beta.

between lncRNA-ATB and autophagy. We identified enrichment of autophagy signatures in the gene expression data from SMMC-7721 cells engineered to overexpress lncRNA-ATB. We investigated the influence of lncRNA-ATB on autophagy in HCC cells, and found that overexpression of lncRNA-ATB significantly promoted autophagy flux in HCC cells. The Hippo-YAP pathway regulates autophagy and promotes cancer cell survival during nutrient deprivation[15]. Moreover, lncRNAs play a vital role in activating YAP signaling[26,27]. Therefore, we explored whether lncRNA-ATB induces autophagy by regulating YAP. We found that lncRNA-ATB overexpression decreased p-YAP expression and induced the nuclear translocation of YAP. Rescue experiments showed that lncRNA-ATB promotes autophagy by modulating YAP activation. Our previous study found Hippo-YAP signaling plays an essential role in liver cancer development. Our present data suggest that YAP activation acts as a mediator between lncRNA-ATB expression and autophagy.

Autophagy is a dynamic and continuous process that is regulated by a series of ATG proteins. Yoshinori Ohsumi's laboratory identified the core ATGs that are essential for formation of the autophagosome and delivery of autophagic cargo to the lysosome[28]. In addition, lncRNAs have been shown to coordinate autophagy by influencing the expression and post-transcriptional regulation of ATG genes[8]. For example, lncRNA PVT1 activates autophagy in glioma vascular endothelial cells by upregulating the expression of ATG7 and beclin1[29]. In our study, we found that lncRNA-ATB increases ATG5 expression by interacting with ATG5 mRNA. ATG5 is part of the ATG12-ATG5–ATG16L1 complex, and it enhances ATG3-mediated conjugation of ATG8 family proteins, resulting in phagophore elongation[30]. Previous

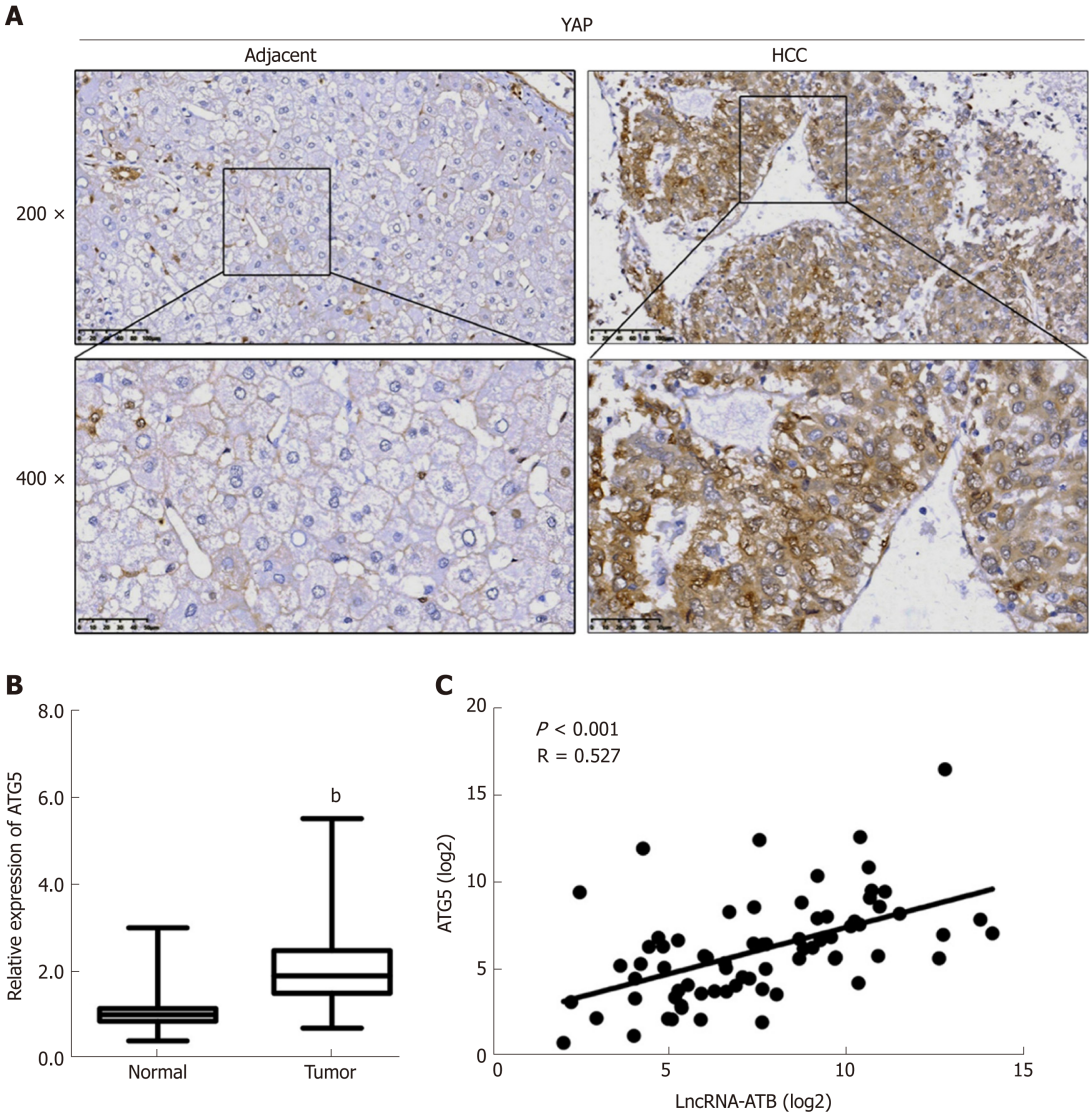


**Figure 6 Yes-associated protein nuclear localization and autophagy-related protein 5 expression are positively correlated with lncRNA-ATB expression.** A: Representative immunostaining for Yes-associated protein (YAP) in hepatocellular carcinoma (HCC) and adjacent normal tissues (magnification: ×200 or ×400); B: The expression levels of autophagy-related protein 5 (ATG5) in 72 pairs of HCC tumor and adjacent normal tissues were evaluated by real-time PCR; C: Pearson's correlation analysis of the relationship between expression of lncRNA-ATB and ATG5 ($r$ = 0.527, $P$ < 0.001). Statistical significance is indicated at $^{b}P$ < 0.01. YAP: Yes-associated protein; ATG5: Autophagy-related protein 5; HCC: Hepatocellular carcinoma; LncRNA-ATB: LncRNA-activated by transforming growth factor beta.

studies have also found that lncRNA HNF1A-AS1 functions as an oncogene and promotes autophagy by regulating ATG5. Our results indicate that lncRNA-ATB promotes autophagy by regulating ATG5 expression.

In summary, our study elucidates the role of lncRNA-ATB in regulating autophagy in HCC. We report that lncRNA-ATB is often overexpressed in HCC tissues and acts as an oncogene to facilitate the progression of HCC. Our data show that lncRNA-ATB promotes autophagy by modulating YAP activation. Additionally, we report that lncRNA-ATB interacts with ATG5 mRNA and influences autophagy by increasing the expression of ATG5. Our study provides novel insights into the molecular mechanisms by which lncRNA-ATB regulates autophagy in HCC cells.

## ARTICLE HIGHLIGHTS

### *Research background*

Long non-coding RNAs (lncRNAs) play a vital role in the progression of hepatocellular carcinoma (HCC). Autophagy is a dynamic metabolic process that supports cancer cell survival in response to stress. The relationship between autophagy and the lncRNA-activated by transforming growth factor beta (lncRNA-ATB) in HCC remains unknown.

### *Research motivation*

A large number of aberrantly expressed genes influence the progression of HCC, but the molecular mechanisms governing HCC malignancy are still not entirely clear, and the potential connection between lncRNAs and autophagy remains to be fully elucidated. There is an important and unmet need to elucidate the molecular mechanisms of autophagy, and to capitalize on that knowledge to develop autophagy-related methods as therapeutic strategies for treatment of HCC.

### Research objectives
To explore the influence of lncRNA-ATB in regulating autophagy in HCC cells and the underlying mechanism.

### Research methods
We compared the expression of lncRNA-ATB in 72 HCC tissues and adjacent non-tumor tissues by real-time PCR. The role of lncRNA-ATB in cell proliferation and colony formation was evaluated *in vitro*. The effect of lncRNA-ATB on autophagy was determined using a LC3-GFP reporter and transmission electron microscopy. Furthermore, the mechanism by which lncRNA-ATB regulates autophagy was explored by immunofluorescence staining, RNA immunoprecipitation, and Western blot.

### Research results
We found that lncRNA-ATB was up-regulated in HCC and lncRNA-ATB expression positively correlated with tumor size, TNM stage, and poor survival of HCC patients. Overexpression of lncRNA-ATB promoted cell proliferation and colony formation *in vitro*. LncRNA-ATB promoted autophagy by activating Yes-associated protein (YAP). Moreover, lncRNA-ATB interacted with autophagy-related protein 5 (ATG5) mRNA and increased ATG5 expression.

### Research conclusions
Our study reveals that lncRNA-ATB regulates autophagy by activating YAP and increasing ATG5 expression. These results provide new insights into the role of lncRNA-ATB in autophagy in HCC.

### Research perspectives
Our findings provide a novel link between lncRNA-ATB and autophagy, and suggest that lncRNA-ATB may be a potential therapeutic target in the treatment of HCC.

## REFERENCES


1 **Ingle PV**, Samsudin SZ, Chan PQ, Ng MK, Heng LX, Yap SC, Chai AS, Wong AS. Development and novel therapeutics in hepatocellular carcinoma: a review. *Ther Clin Risk Manag* 2016; **12**: 445-455 [PMID: 27042086 DOI: 10.2147/TCRM.S92377]

2 **Torre LA**, Siegel RL, Ward EM, Jemal A. Global Cancer Incidence and Mortality Rates and Trends--An Update. *Cancer Epidemiol Biomarkers Prev* 2016; **25**: 16-27 [PMID: 26667886 DOI: 10.1158/1055-9965.EPI-15-0578]

3 **Evans JR**, Feng FY, Chinnaiyan AM. The bright side of dark matter: lncRNAs in cancer. *J Clin Invest* 2016; **126**: 2775-2782 [PMID: 27479746 DOI: 10.1172/JCI84421]

4 **Beermann J**, Piccoli MT, Viereck J, Thum T. Non-coding RNAs in Development and Disease: Background, Mechanisms, and Therapeutic Approaches. *Physiol Rev* 2016; **96**: 1297-1325 [PMID: 27535639 DOI: 10.1152/physrev.00041.2015]

5 **Prensner JR**, Chinnaiyan AM. The emergence of lncRNAs in cancer biology. *Cancer Discov* 2011; **1**: 391-407 [PMID: 22096659 DOI: 10.1158/2159-8290.CD-11-0209]

6 **Yuan JH**, Yang F, Wang F, Ma JZ, Guo YJ, Tao QF, Liu F, Pan W, Wang TT, Zhou CC, Wang SB, Wang YZ, Yang Y, Yang N, Zhou WP, Yang GS, Sun SH. A long noncoding RNA activated by transforming growth factor beta promotes the invasion-metastasis cascade in hepatocellular carcinoma. *Cancer Cell* 2014; **25**: 666-681 [PMID: 24768205 DOI: 10.1016/j.ccr.2014.03.010]

7 **Xiao H**, Zhang F, Zou Y, Li J, Liu Y, Huang W. The Function and Mechanism of Long Non-coding RNA-ATB in Cancers. *Front Physiol* 2018; **9**: 321 [PMID: 29692736 DOI: 10.3389/fphys.2018.00321]

8 **Sun T**. Long noncoding RNAs act as regulators of autophagy in cancer. *Pharmacol Res* 2018; **129**: 151-155 [PMID: 29133213 DOI: 10.1016/j.phrs.2017.11.009]

9 **Rybstein MD**, Bravo-San Pedro JM, Kroemer G, Galluzzi L. The autophagic network and cancer. *Nat Cell Biol* 2018; **20**: 243-251 [PMID: 29476153 DOI: 10.1038/s41556-018-0042-2]

10 **Fan Q**, Yang L, Zhang X, Ma Y, Li Y, Dong L, Zong Z, Hua X, Su D, Li H, Liu J. Autophagy promotes metastasis and glycolysis by upregulating MCT1 expression and Wnt/β-catenin signaling pathway activation in hepatocellular carcinoma cells. *J Exp Clin Cancer Res* 2018; **37**: 9 [PMID: 29351758 DOI: 10.1186/s13046-018-0673-y]

11 **Li J**, Yang B, Zhou Q, Wu Y, Shang D, Guo Y, Song Z, Zheng Q, Xiong J. Autophagy promotes hepatocellular carcinoma cell invasion through activation of epithelial-mesenchymal transition. *Carcinogenesis* 2013; **34**: 1343-1351 [PMID: 23430956 DOI: 10.1093/carcin/bgt063]

12 **Morel E**, Mehrpour M, Botti J, Dupont N, Hamaï A, Nascimbeni AC, Codogno P. Autophagy: A Druggable Process. *Annu Rev Pharmacol Toxicol* 2017; **57**: 375-398 [PMID: 28061686 DOI: 10.1146/annurev-pharmtox-010716-104936]

13 **Levy JMM**, Towers CG, Thorburn A. Targeting autophagy in cancer. *Nat Rev Cancer* 2017; **17**: 528-542 [PMID: 28751651 DOI: 10.1038/nrc.2017.53]

14 **Yang L**, Zhang X, Li H, Liu J. The long noncoding RNA HOTAIR activates autophagy by upregulating ATG3 and ATG7 in hepatocellular carcinoma. *Mol Biosyst* 2016; **12**: 2605-2612 [PMID: 27301338 DOI: 10.1039/c6mb00114a]

15 **Song Q**, Mao B, Cheng J, Gao Y, Jiang K, Chen J, Yuan Z, Meng S. YAP enhances autophagic flux to

promote breast cancer cell survival in response to nutrient deprivation. *PLoS One* 2015; **10**: e0120790 [PMID: 25811979 DOI: 10.1371/journal.pone.0120790]

16 **Klionsky DJ**, Baehrecke EH, Brumell JH, Chu CT, Codogno P, Cuervo AM, Debnath J, Deretic V, Elazar Z, Eskelinen EL, Finkbeiner S, Fueyo-Margareto J, Gewirtz D, Jäättelä M, Kroemer G, Levine B, Melia TJ, Mizushima N, Rubinsztein DC, Simonsen A, Thorburn A, Thumm M, Tooze SA. A comprehensive glossary of autophagy-related molecules and processes (2nd edition). *Autophagy* 2011; **7**: 1273-1294 [PMID: 21997368 DOI: 10.4161/auto.7.11.17661]

17 **Yoon JH**, Abdelmohsen K, Srikantan S, Yang X, Martindale JL, De S, Huarte M, Zhan M, Becker KG, Gorospe M. LincRNA-p21 suppresses target mRNA translation. *Mol Cell* 2012; **47**: 648-655 [PMID: 22841487 DOI: 10.1016/j.molcel.2012.06.027]

18 **Schmitt AM**, Chang HY. Long Noncoding RNAs in Cancer Pathways. *Cancer Cell* 2016; **29**: 452-463 [PMID: 27070700 DOI: 10.1016/j.ccell.2016.03.010]

19 **Yan X**, Hu Z, Feng Y, Hu X, Yuan J, Zhao SD, Zhang Y, Yang L, Shan W, He Q, Fan L, Kandalaft LE, Tanyi JL, Li C, Yuan CX, Zhang D, Yuan H, Hua K, Lu Y, Katsaros D, Huang Q, Montone K, Fan Y, Coukos G, Boyd J, Sood AK, Rebbeck T, Mills GB, Dang CV, Zhang L. Comprehensive Genomic Characterization of Long Non-coding RNAs across Human Cancers. *Cancer Cell* 2015; **28**: 529-540 [PMID: 26461095 DOI: 10.1016/j.ccell.2015.09.006]

20 **Lei K**, Liang X, Gao Y, Xu B, Xu Y, Li Y, Tao Y, Shi W, Liu J. Lnc-ATB contributes to gastric cancer growth through a MiR-141-3p/TGFβ2 feedback loop. *Biochem Biophys Res Commun* 2017; **484**: 514-521 [PMID: 28115163 DOI: 10.1016/j.bbrc.2017.01.094]

21 **Iguchi T**, Uchi R, Nambara S, Saito T, Komatsu H, Hirata H, Ueda M, Sakimura S, Takano Y, Kurashige J, Shinden Y, Eguchi H, Sugimachi K, Maehara Y, Mimori K. A long noncoding RNA, lncRNA-ATB, is involved in the progression and prognosis of colorectal cancer. *Anticancer Res* 2015; **35**: 1385-1388 [PMID: 25750289]

22 **Qu S**, Yang X, Song W, Sun W, Li X, Wang J, Zhong Y, Shang R, Ruan B, Zhang Z, Zhang X, Li H. Downregulation of lncRNA-ATB correlates with clinical progression and unfavorable prognosis in pancreatic cancer. *Tumour Biol* 2016; **37**: 3933-3938 [PMID: 26482611 DOI: 10.1007/s13277-015-4252-y]

23 **Zhai X**, Xu W. Long Noncoding RNA ATB Promotes Proliferation, Migration, and Invasion in Bladder Cancer by Suppressing MicroRNA-126. *Oncol Res* 2018; **26**: 1063-1072 [PMID: 29321082 DOI: 10.3727/096504018X15152072098476]

24 **Kreuzaler P**, Watson CJ. Killing a cancer: what are the alternatives? *Nat Rev Cancer* 2012; **12**: 411-424 [PMID: 22576162 DOI: 10.1038/nrc3264]

25 **Edinger AL**, Thompson CB. Defective autophagy leads to cancer. *Cancer Cell* 2003; **4**: 422-424 [PMID: 14706333 DOI: 10.1016/S1535-6108(03)00306-4]

26 **Zhuo W**, Kang Y. Lnc-ing ROR1-HER3 and Hippo signalling in metastasis. *Nat Cell Biol* 2017; **19**: 81-83 [PMID: 28139652 DOI: 10.1038/ncb3467]

27 **Yang C**, Wu K, Wang S, Wei G. Long non-coding RNA XIST promotes osteosarcoma progression by targeting YAP *via* miR-195-5p. *J Cell Biochem* 2018; **119**: 5646-5656 [PMID: 29384226 DOI: 10.1002/jcb.26743]

28 **Tsukada M**, Ohsumi Y. Isolation and characterization of autophagy-defective mutants of Saccharomyces cerevisiae. *FEBS Lett* 1993; **333**: 169-174 [PMID: 8224160 DOI: 10.1016/0014-5793(93)80398-e]

29 **Ma Y**, Wang P, Xue Y, Qu C, Zheng J, Liu X, Ma J, Liu Y. PVT1 affects growth of glioma microvascular endothelial cells by negatively regulating miR-186. *Tumour Biol* 2017; **39**: 1010428317694326 [PMID: 28351322 DOI: 10.1177/1010428317694326]

30 **Dikic I**, Elazar Z. Mechanism and medical implications of mammalian autophagy. *Nat Rev Mol Cell Biol* 2018; **19**: 349-364 [PMID: 29618831 DOI: 10.1038/s41580-018-0003-4]

World Journal of Gastroenterology

Submit a Manuscript: https://www.f6publishing.com

*World J Gastroenterol* 2019 September 21; 25(35): 5323-5333

DOI: 10.3748/wjg.v25.i35.5323

ISSN 1007-9327 (print) ISSN 2219-2840 (online)

ORIGINAL ARTICLE

Case Control Study

# Liver stiffness and serum markers for excluding high-risk varices in patients who do not meet Baveno VI criteria

Hong Zhou, Jun Long, Han Hu, Cai-Yun Tian, Shi-De Lin

**ORCID number:** Hong Zhou (0000-0002-5580-6744); Jun Long (0000-0001-7595-3840); Han Hu (0000-0001-7604-4008); Cai-Yun Tian (0000-0002-6847-4400); Shi-De Lin (0000-0001-8803-4069).

**Author contributions:** Zhou H and Long J contributed equally to this work; Zhou H, Long J, Hu H, Tian CY, and Lin SD performed the research; Zhou H and Lin SD wrote the manuscript; Long J and Lin SD performed the biostatistics analysis; Hu H, Tian CY, and Lin SD analyzed the data; all authors discussed the results and commented on the manuscript.

**Supported by** the National Natural Science Foundation of China, No. 81860114.

**Institutional review board statement:** This study was approved by the Institutional Review Board of Affiliated Hospital of Zunyi Medical University, Guizhou Province, China.

**Informed consent statement:** All patients were informed in writing of the use of their data for clinical research purposes and accepted.

**Conflict-of-interest statement:** The authors declare that they have no conflicts of interest in this study.

**STROBE statement:** The authors have read the STROBE Statement-checklist of items, and the manuscript was prepared and revised according to the STROBE Statement-checklist of items.

**Open-Access:** This article is an

**Hong Zhou, Jun Long, Han Hu, Cai-Yun Tian, Shi-De Lin,** Department of Infectious Diseases, Affiliated Hospital of Zunyi Medical University, Zunyi 563003, Guizhou Province, China

**Hong Zhou,** Department of Infectious Diseases, Suining Central Hospital, Suining 629000, Sichuan Province, China

**Corresponding author:** Shi-De Lin, MD, Occupational Physician, Professor, Department of Infectious Diseases, Affiliated Hospital of Zunyi Medical University, 201 Dalian Street, Zunyi 563003, Guizhou Province, China. linshide6@zmu.edu.cn
**Telephone:** +86-851-28609183
**Fax:** +86-851-28609183

## Abstract

### *BACKGROUND*

The Baveno VI criteria for predicting esophageal varices, *i.e.*, liver stiffness measurement (LSM) < 20 kPa and platelet (PLT) count > 150 × $10^9$/L, identify patients who can safely avoid gastroscopy screening. However, they require further refinement.

### *AIM*

To evaluate the utility of LSM and serum markers of liver fibrosis in ruling out high-risk varices (HRV) in patients who do not meet Baveno VI criteria.

### *METHODS*

Data from 132 patients with hepatitis B virus (HBV)-related compensated liver cirrhosis who did not meet the Baveno VI criteria were retrospectively reviewed. MedCalc 15.8 was used to calculate receiver operating characteristic (ROC) curves, and the accuracy of LSM, PLT count, aspartate aminotransferase (AST)-to-PLT ratio index, Fibrosis-4, and the Lok index in predicting HRV were evaluated according to the area under each ROC curve (AUROC). The utility of LSM, PLT, and serum markers of liver fibrosis stratified by alanine transaminase (ALT) and total bilirubin (TBil) levels was evaluated for ruling out HRV.

### *RESULTS*

In all patients who did not meet the Baveno VI criteria, the independent risk factors for HRV were LSM and ALT. Only the AUROC of Lok index was above 0.7 for predicting HRV, and at a cutoff value of 0.4531 it could further spare 24.2% of gastroscopies without missing HRVs. The prevalence of HRV was significantly lower in patients with ALT or TBil ≥ 2 upper limit of normal (ULN) (14.3%) than in patients with both ALT and TBil < 2 ULN (34.1%) ($P$ = 0.018). In

**Manuscript source**: Unsolicited manuscript

**Received:** May 29, 2019
**Peer-review started:** May 30, 2019
**First decision:** July 21, 2019
**Revised:** July 30, 2019
**Accepted:** August 24, 2019
**Article in press:** July 21, 2019
**Published online:** September 21, 2019

**P-Reviewer:** El-Karaksy H, Fouad YM, Thomopoulos K
**S-Editor:** Yan JP
**L-Editor:** Wang TQ
**E-Editor:** Ma YJ

the 41 patients with ALT and TBil < 2 ULN, LSM had an AUROC for predicting HRV of 0.821. LSM < 20.6 kPa spared 39.0% of gastroscopies without missing HRVs. In the 91 patients with ALT or TBiL ≥ 2 ULN, the Lok index and PLT had AUROCs of 0.814 and 0.741, respectively. Lok index ≤ 0.5596 or PLT > 100 × $10^9$/L further spared 39.6% and 43.9% of gastroscopies, respectively, without missing HRVs.

*CONCLUSION*

In HBV-related compensated cirrhosis patients who do not meet Baveno VI criteria, the LSM, PLT, or Lok index cutoff stratified by ALT and TBil accurately identifies more patients without HRV.

**Key words:** Baveno VI; Esophageal varices; Liver cirrhosis; Liver stiffness measurement; Serum markers of liver fibrosis



**Core tip:** In patients with hepatitis B virus (HBV)-related compensated cirrhosis who did not meet the Baveno VI criteria, the prevalence of high-risk varices among patients with alanine transaminase (ALT) or total bilirubin (TBil) ≥ 2 upper limit of normal (ULN) was significantly lower compared to patients with ALT and TBil < 2 ULN. In the 41 patients with ALT and TBil < 2 ULN, liver stiffness measurement (LSM) < 20.6 kPa spared 39.0% of gastroscopies without missing high-risk varices (HRVs). In the 91 patients with ALT or TBiL ≥ 2 ULN, Lok index ≤ 0.5596 or platelet (PLT) > 100 × $10^9$/L further spared 39.6% and 43.9% of gastroscopies, respectively, without missing HRVs.

**Citation:** Zhou H, Long J, Hu H, Tian CY, Lin SD. Liver stiffness and serum markers for excluding high-risk varices in patients who do not meet Baveno VI criteria. *World J Gastroenterol* 2019; 25(35): 5323-5333
**URL**: https://www.wjgnet.com/1007-9327/full/v25/i35/5323.htm
**DOI**: https://dx.doi.org/10.3748/wjg.v25.i35.5323

## INTRODUCTION

About 30% of cases of liver cirrhosis worldwide result from chronic hepatitis B virus (HBV) infection[1]. Esophageal varices (EV) and esophagogastric variceal bleeding (EVB) are major complications among patients with liver cirrhosis and are associated with high morbidity and mortality[2]. Six-week mortality rates range between 15% and 25% in patients with EVB[3,4]. High-risk varices (HRV) are medium or large EV or small EV with red wale signs. Prophylactic therapy with beta-blockers or elastic band ligation benefits patients with HRV and is the standard of care in patients with cirrhosis to identify those with HRV[5,6].

Gastroscopy is the gold standard for diagnosing EV and assessing bleeding risk[7]. However, gastroscopy is an invasive and expensive procedure with associated risks[6]. In the last 10 years, evidence has accumulated regarding the usefulness of non-invasive methods for stratifying EV risk in patients with compensated advanced chronic liver disease[8]. The 2015 Baveno VI consensus workshop recommended that patients with liver stiffness measurement (LSM) < 20 kPa and platelet (PLT) count > 150 × $10^9$/L could safely avoid gastroscopy screening[3,4]. These criteria were verified in several clinical studies and can safely spare 20%-30% of liver cirrhosis patients from undergoing gastroscopy[9,10]. The American Association for the Study of Liver Disease recently recommended using the Baveno VI criteria to stratify EV risk in patients with liver cirrhosis[3]. However, up to 40% of gastroscopies are still unnecessary[11]. It is therefore imperative to finding a new strategy to identify more patients without HRV.

Several studies reported that adjusting the LSM and PLT thresholds could spare more patients from undergoing gastroscopy. The expanded Baveno VI criteria (PLT > 110 × $10^9$/L and LSM < 25 kPa) further spare 19% of gastroscopies compared to the original Baveno VI criteria, with a risk of missing 1.6% of HRV cases[12]. Jangouk *et al*[9] recently reported a 12% increase in spared gastroscopies (with no additional HRV cases missed) by expanding the Baveno VI criteria to include a Model for End-Stage

Liver Disease (MELD) score of 6. Using cutoff values of LSM ≤ 25 kPa and PLT ≥ 100 × $10^9$/L, Ding *et al*[13] found that 21% of gastroscopies were spared. However, these criteria have not been confirmed.

Because liver inflammation can significantly increase LSM, it is recommended that the interpretation of LSM is based on the levels of alanine transaminase (ALT) and total bilirubin (TBil)[14,15]. Clinically, most patients with HBV-related liver cirrhosis have concomitant liver inflammation. However, it remains unknown whether adjusting the LSM and PLT cutoffs according to ALT and TBiL levels would increase the number of spared gastroscopies among patients who do not meet the Baveno VI criteria.

Serum markers of liver fibrosis such as PLT count, aspartate aminotransferase (AST)-to-PLT ratio index (APRI), Fibrosis-4 (FIB-4), and the Lok index are useful in predicting severe liver fibrosis or cirrhosis[16-18], EV risk, and variceal bleeding risk in patients with HBV infection[19]. It remains unknown whether these serum markers of liver fibrosis can identify patients without HRV among those who do not meet the Baveno VI criteria. In this study, we aimed to evaluate the utilities of LSM, PLT count, APRI, FIB-4, and the Lok index stratified by ALT and TBil levels for ruling out HRV in patients with HBV-related compensated cirrhosis who did not meet the Baveno VI criteria.

## MATERIALS AND METHODS

### Study population

From September 2016 to June 2018, we applied the Baveno VI criteria to patients with compensated liver cirrhosis who were admitted to the Affiliated Hospital of Zunyi Medical University and Suining Central Hospital. All the patients with compensated liver cirrhosis who did not meet the Baveno VI criteria underwent gastroscopy screening during this period. We retrospectively reviewed records of 183 hospitalized patients with HBV-related compensated liver cirrhosis who underwent a FibroScan procedure and gastroscopy within 6 months and had complete clinical, laboratory, and imaging data. A total of 132 patients were included in the study. The remaining 51 were excluded from the study because they had the following concomitant conditions: 19, alcoholic liver disease; 15, hepatocellular carcinoma; 6, invalid LSM; 4, human immunodeficiency virus infection; 3, cardiovascular disease; 3, splenectomy; and 1, primary biliary cholangitis.

### Diagnostic criteria for HBV-related compensated liver cirrhosis

The diagnosis of cirrhosis was based on previous liver biopsy findings or a composite of clinical signs and findings provided by laboratory tests, gastroscopy, radiologic imaging, and FibroScan procedures. Decompensated liver cirrhosis was defined as the presence of one of the following: New onset of hepatic encephalopathy, EVB, or ascites[2].

Two professionally trained operators performed each transient elastography (TE) measurement using a FibroScan device (Echosens, Paris, France). The M probe was used in all measurements. Only cases with 10 valid measurements obtained with a success rate ≥ 60% and an interquartile range-to-median ratio ≤ 30% were considered valid. The median valid LSM value is expressed in kPa.

### Grading criteria for EV

Gastroscopy procedures were performed by two experienced endoscopists who were unaware of the LSM results. EV stage was classified as none (no veins above the esophageal mucosal surface; F0), small (minimally elevated veins above the esophageal mucosal surface; F1), medium (large tortuous veins occupying < 1/3 of the lumen; F2), or large (large coil-shaped veins occupying ≥ 1/3 of the lumen; F3). HRV was defined as F2/F3 EV or F1 EV with red wale signs[20].

### Candidate predictor variables

Laboratory parameters included white blood cell (WBC) count, PLT count, ALT, AST, gamma-glutamyl transpeptidase (GGT), TBil, albumin (ALB), globulin (GLB), prothrombin (PT), prothrombin time activity (PTA), international normalized ratio (INR), HBV DNA, serum sodium ($Na^+$), blood urea nitrogen (BUN), creatinine (Cr), and alpha-fetoprotein (AFP). For patients with multiple laboratory parameter measurements, we used the results obtained nearest in time to the TE procedure.

The serum markers of liver fibrosis were calculated according to the following formulas: APRI = [AST/upper limit of normal (ULN)] × 100/PLT; FIB-4 = (age × AST)/(PLT × square root of ALT); Lok index = exp (log odds)/[1 + exp(log odds)], log odds = -5.56 - 0.0089 × PLT + 1.26 × (AST/ALT) + 5.27 × INR. The following formula

was used for calculating the MELD scores: MELD score = 3.8 × ln[TBil (mg/dL)] + 11.2 × ln(INR) + 9.6 × ln[Cr (mg/dL)] + 6.4 × (constant for liver disease etiology: 0 if cholestatic or alcoholic, otherwise 1).

### Ethics statement

The protocol conformed to the provisions of the Declaration of Helsinki and was approved by the Human Ethical Committee of the Affiliated Hospital of Zunyi Medical University and Suining Central Hospital. All patients were informed in writing regarding the potential use of their data for clinical research purposes, and all accepted.

### Statistical analysis

Statistical analyses were performed using SPSS 19.0 (SPSS, Chicago, IL, USA) and MedCalc® 15.8 (MedCalc Software BVBA, Ostend, Belgium). Patient characteristics were compared between patients with and without HRV, using $\chi^2$ tests for categorical variables, *t*-tests for variables with normal distributions, and Mann–Whitney U tests for variables with non-normal distributions. Logistic regression analysis was used for univariate and multivariate analyses. MedCalc 15.8 was used to calculate receiver operating characteristic (ROC) curves, and the accuracy of each diagnostic criterion was evaluated according to the area under each ROC curve (AUROC). Given that the aim of this study was to identify patients without HRV, we defined the cutoff values of LSM, PLT, MELD score, and serum markers of liver fibrosis based on the values corresponding to a negative predictive value (NPV) of 100%. The main results calculated were sensitivity, specificity, positive predictive value (PPV), and positive likelihood ratio (PLR) as well as the number of unnecessary gastroscopy procedures. Since we set the cutoff values based on an NPV of 100%, we did not calculate the negative likelihood ratio (NLR). $P < 0.05$ was considered statistically significant.

## RESULTS

### Patient characteristics and HRV prevalence

Among the 132 patients enrolled in the study, 59 (44.7%) had EV. Among them, 32 (24.2%) had small EV without red wale signs and 27 (20.5%) had HRV (medium or large EV). Regarding Child-Pugh class, 95 and 37 patients had classes A and B, respectively. Of the 132 patients, 99 (26 with HRV) did not meet the Baveno VI criteria due to having both LSM ≥ 20 kPa and PLT ≤ 150 × $10^9$/L; 11 (1 with HRV) due to having only LSM ≥ 20 kPa; and 22 (0 with HRV) due to having only PLT ≤ 150 × $10^9$/L. As shown in Table 1, PT, INR, LSM, and MELD score were significantly higher in patients with HRV than in those without, whereas ALT, AST, GGT, PLT, PTA, and HBV DNA levels were significantly lower.

### Independent risk factors for HRV and performance of LSM and serum markers of liver fibrosis for ruling out HRV

As shown in Table 2, the risk factors for HRV in patients who did not meet the Baveno VI criteria included PT, PLT, ALT, GGT, LSM, and MELD score. Independent risk factors for HRV were LSM and ALT. We then explored whether adjusting the LSM and PLT cutoff values and using serum markers of liver fibrosis could exclude more patients without HRV among those who did not meet the Baveno VI criteria. As shown in Table 3, the Lok index had an AUROC of 0.753 [95% confidence interval (CI): 0.671-0.824]. The AUROCs of LSM, APRI, FIB-4, and MELD score were all < 0.7. The Lok index cutoff value of 0.4531 could further spare 32/132 (24.2%) of gastroscopies without missing HRVs. Although PLT had an AUROC of 0.712 (95%CI: 0.627-0.787), PLT > 151 × $10^9$/L could only spare 10/132 (7.6%) of gastroscopies without missing HRVs. The AUROC of LSM was 0.637 (95%CI: 0.548-0.718), and LSM < 20.9 kPa could spare 31/132 (23.5%) of gastroscopies without missing HRVs.

If the expanded Baveno VI criteria (LSM < 25 kPa with a PLT count > 110 × $10^9$/L) were applied to patients who did not meet the Baveno VI criteria, they only spared 8 (6.1%) gastroscopies without missing HRVs. In our study, only 7 patients had an MELD score of 6, and a stepwise strategy using PLT > 150 × $10^9$/L and MELD = 6 only led to 7/132 (5.3%) additional patients avoiding gastroscopies without missing HRVs. Using cutoff values of LSM ≤ 25 kPa and PLT ≥ 100 × $10^9$/L, as suggested by Ding *et al*[13], only led to 16/132 (12.1%) more patients avoiding gastroscopies without missing HRVs.

### Effects of ALT and TBil on LSM in patients who did not meet the Baveno VI criteria

LSM in patients with ALT < 2 ULN (26.77 ± 12.08 kPa) was significantly lower than

**Table 1 Biochemical characteristics of patients with hepatitis B virus-related liver cirrhosis with and without high-risk varices**

| Variable | Without high-risk varices (*n* = 105) | With high-risk varices (*n* = 27) | *P*-value |
|---|---|---|---|
| Age | 46.32 ± 11.83 | 46.74 ± 11.17 | 0.869[1] |
| Male | 88 (83.81) | 25 (92.59) | 0.246[2] |
| BMI (kg/m$^2$) | 24.6 ± 3.53 | 23.8 ± 2.96 | 0.912[1] |
| HBeAg: Positive | 59 (56.19) | 11 (40.74) | 0.151[2] |
| HBV DNA (log 10, copies/mL) | 6.27 ± 1.43 | 5.08 ± 1.46 | 0.002[1] |
| $Na^+$ (mmol/L) | 137.56 ± 13.80 | 139.12 ± 3.07 | 0.560[1] |
| ALT (U/L) | 177.0 (64.0-318.0) | 54.0 (33.0-92.0) | 0.000[3] |
| AST (U/L) | 144.0 (55.5-266.5) | 60.0 (37.0-136.9) | 0.001[3] |
| GGT (U/L) | 105.0 (68.4-198.0) | 60.0 (35.0-93.0) | 0.000[3] |
| TBil (μmol/L) | 24.4 (16.75-37.5) | 27.8 (15.5-48.2) | 0.676[3] |
| ALB (g/L) | 37.35 ± 5.74 | 36.07 ± 5.74 | 0.305[1] |
| GLB (g/L) | 31.4 (28.55-35.65) | 34.6 (28.6-39.1) | 0.101[3] |
| AFP (ng/mL) | 16.47 (6.66-74.73) | 13.6 (7.00-30.1) | 0.422[3] |
| BUN (mmol/L) | 4.64 ± 1.28 | 4.71 ± 1.29 | 0.801[1] |
| Cr (μmol/L) | 73.0 (62.0-80.5) | 73.0 (69.0-90.0) | 0.277[3] |
| PT (s) | 13.0 (11.8-14.4) | 15.4 (12.5-16.3) | 0.002[3] |
| INR | 1.08 (0.98-1.17) | 1.23 (1.04-1.38) | 0.003[3] |
| PTA (%) | 85.05 ± 21.33 | 74.52 ± 20.25 | 0.022[1] |
| WBC ($10^9$/L) | 4.21 (3.28-5.34) | 3.64 (2.68-4.50) | 0.052[3] |
| PLT ($10^9$/L) | 98.35 ± 46.49 | 67.00 ± 28.29 | 0.000[1] |
| LSM (kPa) | 28.93 ± 12.41 | 35.42 ± 14.44 | 0.021[1] |
| Child-Pugh score | 5.00 (5.00-7.00) | 6.00 (5.00-7.00) | 0.508[3] |
| MELD | 8.83 (7.50-11.76) | 11.33 (8.81-13.18) | 0.025[3] |

Data are presented as the mean ± SD, or median (interquartile range).
[1]*t*-test results;
[2]Chi square test results;
[3]Mann–Whitney *U* test results.
$P < 0.05$ was statistically significant. AFP: Alpha-fetoprotein; ALB: Albumin; ALT: Alanine aminotransferase; AST: Aspartate aminotransferase; BMI: Body mass index; BUN: Urea nitrogen; Cr: Creatinine; GGT: Glutamine transpeptidase; GLB: Globulin; HBeAg: Hepatitis B e-antigen; HBV DNA: Hepatitis B virus DNA; INR: International normalized ratio; LSM: Liver stiffness measurement; MELD: Model for End-Stage Liver Disease; $Na^+$: Sodium; PLT: Platelet; PT: Prothrombin time; PTA: Prothrombin activity; TBil: Total bilirubin; WBC: White blood cell.

that in patients with ALT ≥ 2 ULN (32.59 ± 13.25 kPa) ($P$ = 0.011). The mean LSM value in patients with TBil < 2 ULN (26.40 ± 8.66 kPa) was also significantly lower than that in patients with TBil ≥ 2 ULN (38.80 ± 16.77 kPa) ($P$ = 0.000). The LSM in patients with both ALT and TBil < 2 ULN (23.66 ± 8.44 kPa) was significantly lower than that in patients with ALT or TBil ≥ 2 ULN (33.23 ± 13.71 kPa) ($P$ = 0.000).

### *LSM and serum markers of liver fibrosis for ruling out HRV in patients with ALT and TBil < 2 ULN*

To explore the possibility of increasing the number of patients spared gastroscopy by adjusting the cutoff values of LSM and PLT according to ALT and TBil levels, we divided them into patients with ALT and TBil < 2 ULN ($n$ = 41) and patients with ALT or TBil ≥ 2 ULN ($n$ = 91). Among the 41 patients with both ALT and TBIL < 2 ULN, 14 (34.1%) had HRV. As shown in Table 4, LSM had an AUROC of 0.821 (95%CI: 0.670-0.923, $P$ < 0.0001). At a cutoff value of 20.6 kPa, LSM further spared 16/41 (39.0%) of gastroscopies without missing HRVs. PLT, Lok index, MELD score, APRI, FiB-4, and PLT had no predictive value for HRV.

### *LSM and serum markers of liver fibrosis for ruling out HRV in patients with ALT or TBil ≥ 2 ULN*

Among the 91 patients with ALT or TBil ≥ 2 ULN, the prevalence of HRV (13/91, 14.3%) was significantly lower than that among patients with ALT and TBil < 2 ULN (14/41, 34.1%, $P$ < 0.05). As shown in Table 5, only the AUROC of the Lok index for identifying HRV was > 0.800. The AUROC of LSM was significantly reduced to 0.672, which was lower than those for the Lok index (0.814), PLT (0.741), and MELD score (0.735).

Using a Lok index cutoff ≤ 0.5596 could spare 36/91 (39.6%) of gastroscopies

**Table 2 Univariate and multivariate analyses of risk factors associated with high-risk varices in patients who did not meet the 2015 Baveno VI criteria**

| Variable | Univariate analysis | | | | Multivariate analysis | | | |
|---|---|---|---|---|---|---|---|---|
| | β | OR | 95%CI | *P*-value | β | OR | 95%CI | *P*-value |
| PT | 0.289 | 1.335 | 1.117-1.595 | 0.001 | | | | |
| PLT | -0.025 | 0.975 | 0.960-0.990 | 0.001 | | | | |
| ALT | -0.008 | 0.992 | 0.987-0.997 | 0.003 | -0.007 | 0.993 | 0.987-0.999 | 0.029 |
| GGT | -0.013 | 0.987 | 0.979-0.996 | 0.003 | | | | |
| LSM | 0.035 | 1.035 | 1.004-1.068 | 0.025 | 0.077 | 1.080 | 1.030-1.132 | 0.001 |
| MELD | 0.091 | 1.096 | 1.002-1.198 | 0.045 | | | | |

ALT: Alanine aminotransferase; CI: Confidence interval; GGT: Glutamine transpeptidase; LSM: Liver stiffness measurement; MELD: Model for End-Stage Liver Disease; OR: Odds ratio; PLT: Platelet; PT: Prothrombin time. $P < 0.05$ was statistically significant.

without missing HRVs. Using PLT > 100 × $10^9$/L could spare 40/91 (43.9%) of gastroscopies without missing HRVs. An MELD score ≤ 7 could only spare 10/91 (11.0%) of gastroscopies without missing HRVs. These results suggested that the Lok index and PLT performed satisfactorily in identifying patients without HRV among patients with ALT or TBil ≥ 2 ULN.

## DISCUSSION

Although many studies have validated the accuracy of the Baveno VI criteria for ruling out HRV[9,21-23], studies have also found that the criteria are conservative and need to be refined to accurately identify more patients without HRV[10,24,25]. In this study, we focused on patients with HBV-related compensated liver cirrhosis who did not meet the 2015 Baveno VI criteria because the prevalence of HRV is relatively high in this population and the possible HRV risk factors may be different from those for patients who fulfill the 2015 Baveno VI criteria[3,26]. We found that only 20.5% of the patients had HRV. Moreover, among the 91 patients with ALT or TBil ≥ 2 ULN, only 14.3% had HRV. Thus, our results demonstrated that many unnecessary gastroscopies are conducted in patients with HBV-related compensated liver cirrhosis despite excluding patients at low risk for EV using the 2015 Baveno VI criteria, especially among patients with ALT or TBil ≥ 2 ULN.

Although LSM was still one of the independent factors associated with HRV, it only had an AUROC of 0.637 for predicting HRV among patients who did not meet the Baveno VI criteria. This result indicated that LSM was not a good predictor of HRV in the overall cohort of patients who did not meet the Baveno VI criteria.

We also found that ALT was independently negatively associated with HRV, because most patients in our study had concomitant liver inflammation. Previous studies showed that LSM can be elevated by liver inflammation and cholestasis[27,28]. Our results suggested that concomitant liver inflammation might be an important factor that interfered with the predictive accuracy of LSM in patients with HBV-related compensated liver cirrhosis who did not meet the Baveno VI criteria.

It was previously unknown whether adjusting the LSM cutoff value according to ALT and TBil levels could improve its utility for predicting HRV among patients with compensated liver cirrhosis and obvious liver inflammation. We found that LSM could accurately identify patients with HRV in those with ALT and TBil < 2 ULN. By slightly increasing the LSM cutoff to 20.6 kPa, LSM further spared 16/41 (39.0%) of gastroscopies without missing HRVs. PLT, Lok index, MELD score, APRI, FiB-4, and PLT had no value for predicting HRV. However, in the patients with ALT or TBil ≥ 2 ULN, LSM had no HRV predictive value.

Previous studies have found that serum markers of liver fibrosis have moderate value for predicting liver cirrhosis in patients with HBV infection[29,30]. However, there is disagreement on the performance of serum markers of liver fibrosis in EV or HRV prediction[8,19,31]. In this study, we found that APRI and FIB-4 could not predict HRV. We also found that PLT and the Lok index performed better in predicting HRV in patients with ALT or TBil ≥ 2 ULN compared with ALT and TBil < 2 ULN. As previous studies found that the Lok index could better predict liver fibrosis in patients with a slightly higher ALT level compared with a normal ALT level[16,32], it is

**Table 3 Performance of liver stiffness measurement and serum markers of liver fibrosis in predicting high-risk varices in patients who did not meet the 2015 Baveno VI criteria**

| Variable | AUROC (95%CI) | *P*-value | Cutoffvalue | Se (%) | Sp (%) | PPV (%) | PLR | Spared gastroscopies, *n* = 132, (%) |
|---|---|---|---|---|---|---|---|---|
| LSM | 0.637 (0.548-0.718) | 0.0141 | 20.9 | 100 | 29.52 | 26.7 | 1.42 | 31/132 (23.5) |
| PLT | 0.712 (0.627-0.787) | < 0.0001 | 151.0 | 100 | 9.52 | 22.1 | 1.11 | 10/132 (7.6) |
| Lok index | 0.753 (0.671-0.824) | < 0.0001 | 0.4531 | 100 | 30.48 | 27.0 | 1.44 | 32/132 (24.2) |
| MELD | 0.644 (0.556-0.726) | 0.0122 | 6.0 | 100 | 6.67 | 21.6 | 1.07 | 7/132 (5.3) |
| APRI | 0.586 (0.497-0.671) | 0.1453 | | | | | | |
| FIB-4 | 0.585 (0.496-0.670) | 0.1281 | | | | | | |

APRI: Aspartate aminotransferase-to-platelet ratio index; AUROC: Area under the receiver operating characteristic curve; CI: Confidence interval; MELD: Model for End-Stage Liver Disease; PLT: Platelet; PLR: Positive likelihood ratio; PPV: Positive predictive value; Se: Sensitivity; Sp: Specificity. $P < 0.05$ was statistically significant.

reasonable that the Lok index performed better in predicting HRV in patients with ALT or TBil ≥ 2 ULN. However, it is difficult to explain the different performances of PLT in patients with ALT or TBil ≥ 2 ULN *vs* < 2 ULN. The different prevalence rates of HRV in these two groups may be a possible explanation, as the prevalence in the patients with ALT and TBil < 2 ULN (34.1%) was significantly higher compared to that in patients with ALT or TBil ≥ 2 ULN (14.3%). Indeed, previous studies reported that the utility of serum markers of liver fibrosis in predicting EV or HRV is greatly affected by the prevalence[29,33,34]. Because patients with ALT or TBil ≥ 2 ULN had obvious liver inflammation, which could elevate LSM, they were difficult to fulfill the Baveno VI criteria, and as a result, the prevalence rate of HRV in patients with ALT or TBil ≥ 2 ULN was lower than that in patients with ALT and TBil < 2 ULN.

Our study had several limitations. First, it was a two-center, retrospective study based on LSM assessed and gastroscopies performed by different operators, although all were experienced. Second, because we only included the patients with HBV-related compensated liver cirrhosis who did not meet the Baveno VI criteria, the number of patients in this study was small, and the cutoff values were not tested in a validation cohort. Further studies are required to verify our findings.

In conclusion, our study found that in patients with HBV-related compensated cirrhosis who did not meet the Baveno VI criteria, using the cutoff value of LSM, PLT, or the Lok index stratified by ALT and TBil levels accurately identified more patients without HRV. An algorithm-based screening process for HRV in patients with HBV-related compensated liver cirrhosis is shown in Figure 1.

**Table 4 Performance of liver stiffness measurement and serum markers of liver fibrosis in predicting high-risk varices in patients with alanine aminotransferase and total bilirubin < 2 upper limit of normal**

| Variable | AUROC (95%CI) | *P* -value | Cutoffvalue | Se (%) | Sp (%) | PPV (%) | PLR | Spared gastroscopies, *n* = 41, (%) |
|---|---|---|---|---|---|---|---|---|
| LSM | 0.821 (0.670-0.923) | < 0.0001 | 20.60 | 100 | 66.7 | 60.9 | 3.00 | 16/41 (39.0) |
| PLT | 0.628 (0.464-0.774) | 0.1928 | | | | | | |
| Lok index | 0.638 (0.473-0.782) | 0.1407 | | | | | | |
| MELD | 0.644 (0.479-0.787) | 0.1449 | | | | | | |
| APRI | 0.569 (0.405- 0.722) | 0.4667 | | | | | | |
| FIB-4 | 0.608 (0.444-0.757) | 0.2474 | | | | | | |

APRI: Aspartate aminotransferase-to-platelet ratio index; AUROC: Area under the receiver operating characteristic curve; CI: Confidence interval; MELD: Model for End-Stage Liver Disease; PLT: Platelet; PLR: Positive likelihood ratio; PPV: Positive predictive value; Se: Sensitivity; Sp: Specificity. $P < 0.05$ was statistically significant.

**Table 5 Performance of liver stiffness measurement and serum markers of liver fibrosis in predicting high-risk varices in patients with alanine aminotransferase or total bilirubin ≥ 2 upper limit of normal**

| Variable | AUROC (95%CI) | *P*-value | Cutoffvalue | Se (%) | Sp( %) | PPV (%) | PLR | Spared gastroscopies, *n* = 91, (%) |
|---|---|---|---|---|---|---|---|---|
| LSM | 0.672 (0.565-0.766) | 0.0508 | | | | | | |
| PLT | 0.741 (0.639-0.827) | < 0.0001 | 100.0 | 100 | 51.28 | 25.5 | 2.05 | 40/91 (43.9) |
| Lok index | 0.814 (0.718-0.888) | < 0.0001 | 0.5596 | 100 | 47.44 | 24.1 | 1.90 | 36/91 (39.6) |
| MELD | 0.735 (0.632-0.822) | 0.0003 | 7.0 | 100 | 12.82 | 16.0 | 1.15 | 10/91 (11.0) |
| APRI | 0.532 (0.424-0.637) | 0.7256 | | | | | | |
| FIB-4 | 0.576 (0.468-0.679) | 0.3329 | | | | | | |

APRI: Aspartate aminotransferase-to-platelet ratio index; AUROC: Area under the receiver operating characteristic curve; CI: Confidence interval; MELD: Model for End-Stage Liver Disease; PLT: Platelet; PLR: Positive likelihood ratio; PPV: Positive predictive value; Se: Sensitivity; Sp: Specificity. $P < 0.05$ was statistically significant.

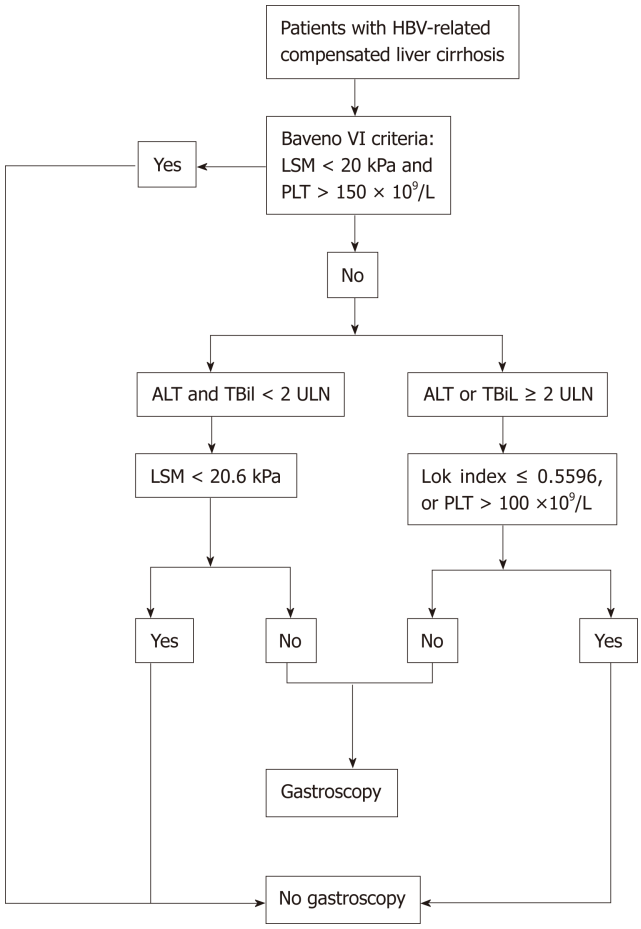


**Figure 1 Algorithm-based screening process for high-risk varices in patients with HBV-related compensated liver cirrhosis.** ALT: Alanine aminotransferase; HBV: Hepatitis B virus; LSM: Liver stiffness measurement; PLT: Platelet; TBil: Total bilirubin; ULN: Upper limit of normal.

## ARTICLE HIGHLIGHTS

### *Research background*

The 2015 Baveno VI consensus workshop recommended that patients with liver stiffness measurement (LSM) < 20 kPa and platelet (PLT) count >150 × $10^9$/L could safely avoid gastroscopy screening. However, studies have also found that such criteria are conservative and need to be refined to accurately identify more patients without high-risk varices (HRV).

### *Research motivation*

It is recommended that the interpretation of LSM is based on the levels of alanine transaminase (ALT) and total bilirubin (TBil), but it remains unknown whether the LSM, PLT and serum markers of liver fibrosis stratified by ALT and TBil levels can identify more patients without HRV among those who do not meet the Baveno VI criteria.

### *Research objectives*

To evaluate the utility of LSM and serum markers of liver fibrosis in ruling out high-risk varices (HRV) in patients who do not meet Baveno VI criteria.

### *Research methods*

Data from 132 patients with hepatitis B virus (HBV)-related compensated liver cirrhosis who did not meet the Baveno VI criteria were retrospectively reviewed. The accuracy of LSM, PLT count, aspartate aminotransferase (AST)-to-PLT ratio index, Fibrosis-4, and the Lok index in predicting HRV was evaluated. The utility of LSM, PLT, and serum markers of liver fibrosis stratified by ALT and TBil levels was evaluated for ruling out HRV.

### *Research results*

The prevalence of HRV was significantly lower in patients with ALT or TBil ≥ 2 upper limit of normal (ULN) (14.3%) than in patients with both ALT and TBil < 2 ULN (34.1%) ($P$ = 0.018). In the 41 patients with ALT and TBil < 2 ULN, LSM < 20.6 kPa spared 39.0% of gastroscopies without missing HRVs. In the 91 patients with ALT or TBiL ≥ 2 ULN, Lok index ≤ 0.5596 or PLT > 100 × $10^9$/L further spared 39.6% and 43.9% of gastroscopies, respectively, without missing HRVs.

### Research conclusions

In HBV-related compensated cirrhosis patients who do not meet Baveno VI criteria, the LSM, PLT, or Lok index cutoff stratified by ALT and TBil accurately identified more patients without HRV.

### Research perspectives

Our study found that in patients with HBV-related compensated cirrhosis who did not meet the Baveno VI criteria, using the cutoff value of LSM, PLT or the Lok index stratified by ALT and TBil levels accurately identified more patients without HRV.

## REFERENCES


1 **Terrault NA**, Lok ASF, McMahon BJ, Chang KM, Hwang JP, Jonas MM, Brown RS, Bzowej NH, Wong JB. Update on prevention, diagnosis, and treatment of chronic hepatitis B: AASLD 2018 hepatitis B guidance. *Hepatology* 2018; **67**: 1560-1599 [PMID: 29405329 DOI: 10.1002/hep.29800]

2 **European Association for the Study of the Liver**. EASL Clinical Practice Guidelines for the management of patients with decompensated cirrhosis. *J Hepatol* 2018; **69**: 406-460 [PMID: 29653741 DOI: 10.1016/j.jhep.2018.03.024]

3 **Garcia-Tsao G**, Abraldes JG, Berzigotti A, Bosch J. Portal hypertensive bleeding in cirrhosis: Risk stratification, diagnosis, and management: 2016 practice guidance by the American Association for the study of liver diseases. *Hepatology* 2017; **65**: 310-335 [PMID: 27786365 DOI: 10.1002/hep.28906]

4 **de Franchis R**; Baveno VI Faculty. Expanding consensus in portal hypertension: Report of the Baveno VI Consensus Workshop: Stratifying risk and individualizing care for portal hypertension. *J Hepatol* 2015; **63**: 743-752 [PMID: 26047908 DOI: 10.1016/j.jhep.2015.05.022]

5 **Fukui H**, Saito H, Ueno Y, Uto H, Obara K, Sakaida I, Shibuya A, Seike M, Nagoshi S, Segawa M, Tsubouchi H, Moriwaki H, Kato A, Hashimoto E, Michitaka K, Murawaki T, Sugano K, Watanabe M, Shimosegawa T. Evidence-based clinical practice guidelines for liver cirrhosis 2015. *J Gastroenterol* 2016; **51**: 629-650 [PMID: 27246107 DOI: 10.1007/s00535-016-1216-y]

6 **Garcia-Tsao G**, Sanyal AJ, Grace ND, Carey W; Practice Guidelines Committee of the American Association for the Study of Liver Diseases; Practice Parameters Committee of the American College of Gastroenterology. Prevention and management of gastroesophageal varices and variceal hemorrhage in cirrhosis. *Hepatology* 2007; **46**: 922-938 [PMID: 17879356 DOI: 10.1002/hep.21907]

7 **de Franchis R**; Baveno V Faculty. Revising consensus in portal hypertension: Report of the Baveno V consensus workshop on methodology of diagnosis and therapy in portal hypertension. *J Hepatol* 2010; **53**: 762-768 [PMID: 20638742 DOI: 10.1016/j.jhep.2010.06.004]

8 **Sebastiani G**, Tempesta D, Fattovich G, Castera L, Halfon P, Bourliere M, Noventa F, Angeli P, Saggioro A, Alberti A. Prediction of oesophageal varices in hepatic cirrhosis by simple serum non-invasive markers: Results of a multicenter, large-scale study. *J Hepatol* 2010; **53**: 630-638 [PMID: 20615567 DOI: 10.1016/j.jhep.2010.04.019]

9 **Jangouk P**, Turco L, De Oliveira A, Schepis F, Villa E, Garcia-Tsao G. Validating, deconstructing and refining Baveno criteria for ruling out high-risk varices in patients with compensated cirrhosis. *Liver Int* 2017; **37**: 1177-1183 [PMID: 28160373 DOI: 10.1111/liv.13379]

10 **Sousa M**, Fernandes S, Proença L, Silva AP, Leite S, Silva J, Ponte A, Rodrigues J, Silva JC, Carvalho J. The Baveno VI criteria for predicting esophageal varices: Validation in real life practice. *Rev Esp Enferm Dig* 2017; **109**: 704-707 [PMID: 28776387 DOI: 10.17235/reed.2017.5052/2017]

11 **Silva MJ**, Bernardes C, Pinto J, Loureiro R, Duarte P, Mendes M, Calinas F. Baveno VI Recommendation on Avoidance of Screening Endoscopy in Cirrhotic Patients: Are We There Yet? *GE Port J Gastroenterol* 2017; **24**: 79-83 [PMID: 28848787 DOI: 10.1159/000452693]

12 **Augustin S**, Pons M, Maurice JB, Bureau C, Stefanescu H, Ney M, Blasco H, Procopet B, Tsochatzis E, Westbrook RH, Bosch J, Berzigotti A, Abraldes JG, Genescà J. Expanding the Baveno VI criteria for the screening of varices in patients with compensated advanced chronic liver disease. *Hepatology* 2017; **66**: 1980-1988 [PMID: 28696510 DOI: 10.1002/hep.29363]

13 **Ding NS**, Nguyen T, Iser DM, Hong T, Flanagan E, Wong A, Luiz L, Tan JY, Fulforth J, Holmes J, Ryan M, Bell SJ, Desmond PV, Roberts SK, Lubel J, Kemp W, Thompson AJ. Liver stiffness plus platelet count can be used to exclude high-risk oesophageal varices. *Liver Int* 2016; **36**: 240-245 [PMID: 26212020 DOI: 10.1111/liv.12916]

14 **Shiha G**, Ibrahim A, Helmy A, Sarin SK, Omata M, Kumar A, Bernstien D, Maruyama H, Saraswat V, Chawla Y, Hamid S, Abbas Z, Bedossa P, Sakhuja P, Elmahatab M, Lim SG, Lesmana L, Sollano J, Jia JD, Abbas B, Omar A, Sharma B, Payawal D, Abdallah A, Serwah A, Hamed A, Elsayed A, AbdelMaqsod A, Hassanein T, Ihab A, GHaziuan H, Zein N, Kumar M. Asian-Pacific Association for the Study of the Liver (APASL) consensus guidelines on invasive and non-invasive assessment of hepatic fibrosis: A 2016 update. *Hepatol Int* 2017; **11**: 1-30 [PMID: 27714681 DOI: 10.1007/s12072-016-9760-3]

15 **Singh S**, Muir AJ, Dieterich DT, Falck-Ytter YT. American Gastroenterological Association Institute Technical Review on the Role of Elastography in Chronic Liver Diseases. *Gastroenterology* 2017; **152**: 1544-1577 [PMID: 28442120 DOI: 10.1053/j.gastro.2017.03.016]

16 **Dong M**, Wu J, Yu X, Li J, Yang S, Qi X, Mao R, Zhang Y, Yu J, Zhu H, Yang F, Qin Y, Zhang J. Validation and comparison of seventeen noninvasive models for evaluating liver fibrosis in Chinese hepatitis B patients. *Liver Int* 2018; **38**: 1562-1570 [PMID: 29314613 DOI: 10.1111/liv.13688]

17 **Lok AS**, Ghany MG, Goodman ZD, Wright EC, Everson GT, Sterling RK, Everhart JE, Lindsay KL, Bonkovsky HL, Di Bisceglie AM, Lee WM, Morgan TR, Dienstag JL, Morishima C. Predicting cirrhosis in patients with hepatitis C based on standard laboratory tests: Results of the HALT-C cohort. *Hepatology* 2005; **42**: 282-292 [PMID: 15986415 DOI: 10.1002/hep.20772]

18 **Ma J**, Jiang Y, Gong G. Evaluation of seven noninvasive models in staging liver fibrosis in patients with chronic hepatitis B virus infection. *Eur J Gastroenterol Hepatol* 2013; **25**: 428-434 [PMID: 23358121 DOI: 10.1097/MEG.0b013e32835cb5dd]

19 **Rockey DC**, Elliott A, Lyles T. Prediction of esophageal varices and variceal hemorrhage in patients with acute upper gastrointestinal bleeding. *J Investig Med* 2016; **64**: 745-751 [PMID: 26912006 DOI: 10.1136/jim-2015-000047]

20 **Beppu K**, Inokuchi K, Koyanagi N, Nakayama S, Sakata H, Kitano S, Kobayashi M. Prediction of variceal hemorrhage by esophageal endoscopy. *Gastrointest Endosc* 1981; **27**: 213-218 [PMID: 6975734 DOI: 10.1016/s0016-5107(81)73224-3]

21 **Marot A**, Trépo E, Doerig C, Schoepfer A, Moreno C, Deltenre P. Liver stiffness and platelet count for identifying patients with compensated liver disease at low risk of variceal bleeding. *Liver Int* 2017; **37**: 707-716 [PMID: 27862856 DOI: 10.1111/liv.13318]

22 **Stafylidou M**, Paschos P, Katsoula A, Malandris K, Ioakim K, Bekiari E, Haidich AB, Akriviadis E, Tsapas A. Performance of Baveno VI and Expanded Baveno VI Criteria for Excluding High-Risk Varices in Patients With Chronic Liver Diseases: A Systematic Review and Meta-analysis. *Clin Gastroenterol Hepatol* 2019; **17**: 1744-1755. e11 [PMID: 31077823 DOI: 10.1016/j.cgh.2019.04.062]

23 **Augustin S**, Pons M, Genesca J. Validating the Baveno VI recommendations for screening varices. *J Hepatol* 2017; **66**: 459-460 [PMID: 27826055 DOI: 10.1016/j.jhep.2016.09.027]

24 **Colecchia A**, Ravaioli F, Marasco G, Colli A, Dajti E, Di Biase AR, Bacchi Reggiani ML, Berzigotti A, Pinzani M, Festi D. A combined model based on spleen stiffness measurement and Baveno VI criteria to rule out high-risk varices in advanced chronic liver disease. *J Hepatol* 2018; **69**: 308-317 [PMID: 29729368 DOI: 10.1016/j.jhep.2018.04.023]

25 **Moctezuma Velázquez C**, Abraldes JG. Non-invasive diagnosis of esophageal varices after Baveno VI. *Turk J Gastroenterol* 2017; **28**: 159-165 [PMID: 28492370 DOI: 10.5152/tjg.2017.16744]

26 **Maurice JB**, Brodkin E, Arnold F, Navaratnam A, Paine H, Khawar S, Dhar A, Patch D, O'Beirne J, Mookerjee R, Pinzani M, Tsochatzis E, Westbrook RH. Validation of the Baveno VI criteria to identify low risk cirrhotic patients not requiring endoscopic surveillance for varices. *J Hepatol* 2016; **65**: 899-905 [PMID: 27388923 DOI: 10.1016/j.jhep.2016.06.021]

27 **Wong GL**, Wong VW, Choi PC, Chan AW, Chim AM, Yiu KK, Chan FK, Sung JJ, Chan HL. Increased liver stiffness measurement by transient elastography in severe acute exacerbation of chronic hepatitis B. *J Gastroenterol Hepatol* 2009; **24**: 1002-1007 [PMID: 19457152 DOI: 10.1111/j.1440-1746.2009.05779.x]

28 **Millonig G**, Reimann FM, Friedrich S, Fonouni H, Mehrabi A, Büchler MW, Seitz HK, Mueller S. Extrahepatic cholestasis increases liver stiffness (FibroScan) irrespective of fibrosis. *Hepatology* 2008; **48**: 1718-1723 [PMID: 18836992 DOI: 10.1002/hep.22577]

29 **Leung JC**, Loong TC, Pang J, Wei JL, Wong VW. Invasive and non-invasive assessment of portal hypertension. *Hepatol Int* 2018; **12**: 44-55 [PMID: 28361299 DOI: 10.1007/s12072-017-9795-0]

30 **Tan YW**, Zhou XB, Ye Y, He C, Ge GH. Diagnostic value of FIB-4, aspartate aminotransferase-to-platelet ratio index and liver stiffness measurement in hepatitis B virus-infected patients with persistently normal alanine aminotransferase. *World J Gastroenterol* 2017; **23**: 5746-5754 [PMID: 28883700 DOI: 10.3748/wjg.v23.i31.5746]

31 **Wang L**, Feng Y, Ma X, Wang G, Wu H, Xie X, Zhang C, Zhu Q. Diagnostic efficacy of noninvasive liver fibrosis indexes in predicting portal hypertension in patients with cirrhosis. *PLoS One* 2017; **12**: e0182969 [PMID: 28820885 DOI: 10.1371/journal.pone.0182969]

32 **Dong XQ**, Wu Z, Zhao H, Wang GQ; China HepB-Related Fibrosis Assessment Research Group. Evaluation and comparison of thirty noninvasive models for diagnosing liver fibrosis in chinese hepatitis B patients. *J Viral Hepat* 2019; **26**: 297-307 [PMID: 30380170 DOI: 10.1111/jvh.13031]

33 **Paternostro R**, Reiberger T, Bucsics T. Elastography-based screening for esophageal varices in patients with advanced chronic liver disease. *World J Gastroenterol* 2019; **25**: 308-329 [PMID: 30686900 DOI: 10.3748/wjg.v25.i3.308]

34 **Calès P**, Buisson F, Ravaioli F, Berger A, Carboni C, Marasco G, Festi D. How to clarify the Baveno VI criteria for ruling out varices needing treatment by noninvasive tests. *Liver Int* 2019; **39**: 49-53 [PMID: 30129700 DOI: 10.1111/liv.13945]

World Journal of Gastroenterology

Submit a Manuscript: https://www.f6publishing.com

*World J Gastroenterol* 2019 September 21; 25(35): 5334-5343

DOI: 10.3748/wjg.v25.i35.5334

ISSN 1007-9327 (print) ISSN 2219-2840 (online)

ORIGINAL ARTICLE

Retrospective Study

# Pathological response measured using virtual microscopic slides for gastric cancer patients who underwent neoadjuvant chemotherapy

Sadayuki Kawai, Tadakazu Shimoda, Takashi Nakajima, Masanori Terashima, Katsuhiro Omae, Nozomu Machida, Hirofumi Yasui

**ORCID number:** Sadayuki Kawai (0000-0001-6815-6261); Tadakazu Shimoda (0000-0001-7018-1677); Takashi Nakajima (0000-0003-4136-5383); Masanori Terashima (0000-0002-2967-8267); Katsuhiro Omae (0000-0001-6722-3311); Nozomu Machida (0000-0003-0160-7085); Hirofumi Yasui (0000-0002-7176-8354).

**Author contributions:** All authors helped to perform the research: Kawai S manuscript writing, performing procedures, experiments, and data analysis; Shimoda T manuscript writing, drafting the conception and design of this work, and performing experiments; Nakajima T performing experiments; Terashima M contributing to writing the manuscript; Omae K data analysis and statistical review; Machida N and Yasui H contributing to writing the manuscript, and drafting the conception and design of this work.

**Institutional review board statement:** This study was reviewed and approved by the Institutional Review Committee of Shizuoka Cancer Center.

**Informed consent statement:** Patients were not required to give informed consent to the study because the analysis used anonymous clinical data that had been obtained after each patient had agreed to treatment by providing written informed consent.

**Sadayuki Kawai, Hirofumi Yasui,** Division of Gastrointestinal Oncology, Shizuoka Cancer Center, Sunto-gun 411-8777, Shizuoka, Japan

**Tadakazu Shimoda, Takashi Nakajima,** Division of Pathology, Shizuoka Cancer Center, Sunto-gun 411-8777, Shizuoka, Japan

**Masanori Terashima,** Division of Gastric Surgery, Shizuoka Cancer Center, Nagaizumi 411-0932, Shizuoka, Japan

**Katsuhiro Omae,** Clinical Research Center, Shizuoka Cancer Center, Sunto-gun 411-8777, Shizuoka, Japan

**Nozomu Machida,** Department of Gastrointestinal Oncology, Shizuoka Cancer Center, Sunto-gun 411-8777, Shizuoka, Japan

**Corresponding author:** Sadayuki Kawai, MD, PhD, Doctor, Division of Gastrointestinal Oncology, Shizuoka Cancer Center, 1007 Shimonagakubo, Nagaizumi, Sunto-gun 411-8777, Shizuoka, Japan. sadayuki-kawai@i.shizuoka-pho.jp
**Telephone:** +81-55-9895222
**Fax:** +81-55-9895634

## Abstract

### *BACKGROUND*

Although pathological response is a common endpoint used to assess the efficacy of neoadjuvant chemotherapy (NAC) for gastric cancer, the problem of a low rate of concordance from evaluations among pathologists remains unresolved. Moreover, there is no globally accepted consensus regarding the optimal evaluation. A previous study based on a clinical trial suggested that pathological response measured using digitally captured virtual microscopic slides predicted patients' survival well. However, the pathological concordance rate of this approach and its usefulness in clinical practice were unknown.

### *AIM*

To investigate the prognostic utility of pathological response measured using digital microscopic slides in clinical practice.

### *METHODS*

We retrospectively evaluated pathological specimens of gastric cancer patients who underwent NAC followed by surgery and achieved R0 resection between March 2009 and May 2015. Residual tumor area and primary tumor beds were

**Conflict-of-interest statement:** All authors declare no conflicts of interest related to this article.

**Data sharing statement:** No additional data are available.



**Manuscript source**: Unsolicited manuscript

**Received:** May 8, 2019
**Peer-review started:** May 8, 2019
**First decision:** July 22, 2019
**Revised:** August 8, 2019
**Accepted:** August 19, 2019
**Article in press:** August 19, 2019
**Published online:** September 21, 2019

**P-Reviewer:** Park WS
**S-Editor:** Tang JZ
**L-Editor:** A
**E-Editor:** Ma YJ

measured in one captured image slide, which contained the largest diameter of the resected specimens. We classified patients with < 10% residual tumor relative to the primary tumorous area as responders, and the rest as non-responders; we then compared overall survival (OS) and relapse-free survival (RFS) between these two groups. Next, we compared the prognostic utility of this method using conventional Japanese criteria.

***RESULTS***

Fifty-four patients were evaluated. The concordance rate between two evaluators was 96.2%. Median RFS of 25 responders and 29 non-responders was not reached (NR) *vs* 18.2 mo [hazard ratio (HR) = 0.35, $P$ = 0.023], and median OS was NR *vs* 40.7 mo (HR = 0.3, $P$ = 0.016), respectively. This prognostic value was statistically significant even after adjustment for age, eastern cooperative oncology group performance status, macroscopic type, reason for NAC, and T- and N-classification (HR = 0.23, $P$ = 0.018). This result was also observed even in subgroup analyses for different macroscopic types (Borrmann type 4/non-type 4) and histological types (differentiated/undifferentiated). Moreover, the adjusted HR for OS between responders and non-responders was lower in this method than that in the conventional histological evaluation of Japanese Classification of Gastric Carcinoma criteria (0.23 *vs* 0.39, respectively).

***CONCLUSION***

The measurement of pathological response using digitally captured virtual microscopic slides may be useful in clinical practice.

**Key words:** Stomach neoplasm; Neoadjuvant therapy; Drug therapy; Pathology; Prognostic factor



**Core tips:** Although pathological response is commonly evaluated to assess the efficacy of neoadjuvant chemotherapy for gastric cancer in clinical practice, the results evaluated by pathologists are sometimes discordant. A previous study suggested that pathological evaluation using digital virtual microscopic slides might be useful. However, the application of this approach to clinical practice was not investigated. We thus assessed the utility of this method in clinical practice and the concordance rate between evaluators, and compared the usefulness of this method with conventional histological evaluation using Japanese Classification of Gastric Carcinoma criteria.

**Citation:** Kawai S, Shimoda T, Nakajima T, Terashima M, Omae K, Machida N, Yasui H. Pathological response measured using virtual microscopic slides for gastric cancer patients who underwent neoadjuvant chemotherapy. *World J Gastroenterol* 2019; 25(35): 5334-5343
**URL**: https://www.wjgnet.com/1007-9327/full/v25/i35/5334.htm
**DOI**: https://dx.doi.org/10.3748/wjg.v25.i35.5334

## INTRODUCTION

Gastric cancer is common, being the third leading cause of cancer-related death globally. Its incidence was estimated to be 1033701 new cases and 782685 deaths due to it occurred in 2018[1]. Of these, 49% were from East Asia, including China, Japan, and South Korea. Although standard treatments for locally advanced gastric cancer differ from one country to the next, surgery has a key role for curative treatment. Despite the application of multimodal treatments, the relapse rate is still high, resulting in a poor prognosis. Type 4 tumor, large type 3 tumor, and extended nodal metastasis, such as bulky lymph nodes or positive para-aortic lymph nodes, in particular were associated with high recurrence rates, even if curative resection was achieved[2,3]. To improve survival, several perioperative treatment strategies have been investigated. Whereas neoadjuvant chemotherapy (NAC) is considered as a standard therapy in the Western world, it is still exploratory and normally investigated in clinical trials in Japan[4-6].

Although progression-free survival (PFS) or overall survival (OS) is often used as

an endpoint in clinical trials of gastric cancer treated with NAC followed by surgery, a long period is required to confirm these outcomes. As an alternative, the response rate based on the Response Evaluation Criteria in Solid Tumor (RECIST) guidelines is one of the short-term endpoints[7], but is not applicable to gastric cancer without measurable lesions. Moreover, there has been some debate about its prognostic utility[8].

Pathological response, which is commonly used for a surrogate marker for PFS and OS after surgery globally, is evaluated microscopically in resected specimens of the stomach and estimated based on the percentage of the residual tumor area relative to the primary tumor bed. Although many clinical trials have used pathological response as an endpoint, no globally accepted consensus has been reached regarding the optimal cut-off percentage to classify individuals as responders. Various definitions regarding the cut-off percentage, such as 10%[9,10], 40%[11], 50%[12], and 67%[13], were used in previous clinical trials. Moreover, this subjective evaluation by pathologists was shown to have limited reproducibility.

Nakamura *et al*[14] retrospectively evaluated pathological specimens digitally captured on virtual microscopic slides from four clinical trials of NAC for gastric cancer (JCOG0001[6], JCOG0002[2], JCOG0210[4], and JCOG0405[5]), and concluded that pathological response using a 10% cut-off on virtual microscopic slides was the best prognostic marker in this method for patients who achieved R0 resection, rather than a cut-off of 33%, 50%, or 67%. However, this study included only patients with type 4 tumor, large type 3 tumor, or extended nodal metastasis. In clinical practice, gastric cancer patients with esophageal or other organic invasion sometimes receive NAC before surgery to avoid an extended operation. Moreover, this study did not report the rate of concordance between pathologists and did not compare the prognostic utility of this cut-off with the histological evaluation criteria of the 14th Japanese Classification of Gastric Carcinoma (JCGC)[15] generally used in Japanese clinical practice. Kurokawa *et al*[8] reported that the OS of patients who achieved a histological response of JCGC of grade 1b, 2, or 3 was significantly longer than that of those who did not.

Here, we examine whether the 10% cut-off for pathological response evaluated using virtual microscopic slides is useful as a prognostic marker even in clinical practice and compare the usefulness of this approach with conventional JCGC criteria.

## MATERIALS AND METHODS

### Study population

Sixty-one patients with gastric or esophagogastric junction adenocarcinoma who received NAC followed by surgery at Shizuoka Cancer Center between March 2009 and May 2015 were retrospectively identified from medical records. Of these, seven patients in whom R0 resection was not achieved were excluded. This study was approved by the Institutional Review Committee of Shizuoka Cancer Center (Shizuoka, Japan) and met the standards set forth in the Declaration of Helsinki.

### Pathological diagnosis

Histological evaluations of JCGC criteria were performed as described previously[15] and were classified into five categories according to the proportion of the residual tumor relative to the primary tumorous area: grade 3, no viable tumor cells remain; grade 2, viable tumor cells remain in less than one-third of the primary tumorous area; grade 1b, viable tumor cells remain in more than one-third but less than two-thirds of the tumorous area; grade 1a, viable tumor cells occupy more than two-thirds of the tumorous area; and grade 0, no evidence of a treatment effect. The primary tumor area was defined by microscopic findings such as necrosis, foamy macrophage accumulation, and interstitial fibrosis below the submucosal layer.

Pathological evaluation of a therapeutic effect using digitally captured virtual microscopic slides was performed by the same method as previously reported by Nakamura *et al*[14]. Briefly, hematoxylin-eosin-stained pathological specimens including the largest tumor diameter were digitally captured on a virtual microscopic slide. The largest tumor diameter was determined by macroscopic findings and by reference to preoperative imaging findings. The square measures of residual tumor and primary tumorous area were calculated using software for virtual microscopic diagnosis (NanoZoomer Virtual Microscopy System, Hamamatsu Photonics). If tumor cells were sparsely distributed in the specimen, for example, when the density of tumor cells was less than 10%, the square measure multiplied by 0.1 was added to the sum of the residual tumor area. Pathological response was calculated as the percentage of the residual tumor area relative to the primary tumorous area. A

representative example a virtual microscopic slide and pathological diagnosis is shown in Figure 1. Histological type (differentiated or undifferentiated) and TNM staging were assigned according to the 14th JCGC. Pathological specimens were prepared and evaluated using JCGC criteria by pathologists of Shizuoka Cancer Center. Two authors (SK and TS) captured the hematoxylin-eosin-stained pathological slides including the largest tumor diameter in digital microscopic images and independently evaluated them. If the opinions of the two authors differed, they discussed the case in order to reach a consensus.

### Statistical analysis

Based on the 10% cut-off evaluated using virtual microscopic slides, patients were classified into a responder group, in which the residual tumor area was less than 10%, and a non-responder group comprising the rest. OS was defined as the time from the date of operation to the date of death from any cause. Relapse-free survival (RFS) was defined as the time from the date of operation to the date of confirming recurrence or death from any cause, whichever came first. Survival rates were estimated using the Kaplan–Meier method. The hazard ratio (HR) of responders to non-responders in OS was calculated by Cox regression analysis. HRs adjusted by the multivariate stratified Cox model were also estimated, including age, eastern cooperative oncology group performance status (ECOG PS), macroscopic type, reason for NAC, T-classification, and N-classification as covariates. All statistical tests were two-sided, and $P < 0.05$ was considered significant. Statistical analyses were performed using EZR software (Saitama Medical Center, Jichi Medical University, Saitama, Japan)[16].

## RESULTS

The clinicopathological characteristics of the 54 eligible patients in this study are shown in Table 1. The median age of the patients was 64 years (range 19–83) and all of them had ECOG PS of 0 to 1. Half of the patients had histologically undifferentiated-type adenocarcinoma and 18.5% had type 4 tumors. Ninety percent of patients received a platinum doublet regimen and the remaining 10% received a triplet regimen as NAC. The main reasons for NAC were as follows: 53% of patients had extended nodal metastasis; 13% had large type 3 tumor; 17% had type 4 tumor; and 17% had other reasons, including esophageal or other organ invasion, or solitary liver metastasis. Follow-up was performed until May 2016. The median follow-up time was 37.7 mo.

Twenty-five (46.3%) patients were classified into the responder group and 29 (53.7%) into the non-responder group. The concordance rate between two evaluators was 96.2%. Eighteen patients died within the observational period and among them, 16 (88.9%) died of recurrent gastric cancer. The survival curves of responders and non-responders are shown in Figure 2. Median RFS of responders and non-responders was not reached (NR) and 18.2 mo, respectively [HR = 0.35, 95% confidence interval (CI): 0.14–0.86, $P = 0.023$]. Median OS (mOS) was NR and 40.7 mo, respectively (HR = 0.30, 95%CI: 0.10–0.84, $P = 0.016$). Even after adjustment for age, ECOG PS, macroscopic type, reason for NAC, T-stage, and N-stage, the OS of responders was significantly better than that of non-responders (HR = 0.23, 95%CI: 0.07–0.78, $P = 0.018$). There were no other statistically significant prognostic factors in the clinicopathological background (Table 2). This tendency was also observed in subgroup analyses for macroscopic types (type 4/non-type 4) and histological types (differentiated/undifferentiated) shown in Figure 3.

Next, to compare the prognostic utility of the 10% cut-off evaluated using virtual microscopic slides with that of conventional JCGC criteria, the adjusted HR of each cut-off was calculated. Histological evaluations according to the JCGC criteria revealed that the numbers of patients who had grades 0, 1a, 1b, 2, and 3 were 4 (7.4%), 13 (24.0%), 11 (20.3%), 22 (40.7%), and 4 (7.4%), respectively. When using the 10% cut-off on virtual microscopic slides, the adjusted HR for RFS was 0.29 (95%CI: 0.10-0.82, $P = 0.019$) and that for OS was 0.23 (95%CI: 0.07-0.78, $P = 0.018$). These HRs were the lowest upon comparing the HRs for each cut-off according to the JCGC criteria (Table 3). Moreover, in this study, there was no statistically significant difference in OS of the two groups according to each cut-off of the JCGC criteria.

## DISCUSSION

The prognostic utility of pathological response, especially pathological complete response (pCR), has been indicated in many studies[13,17-19]. However, patients who

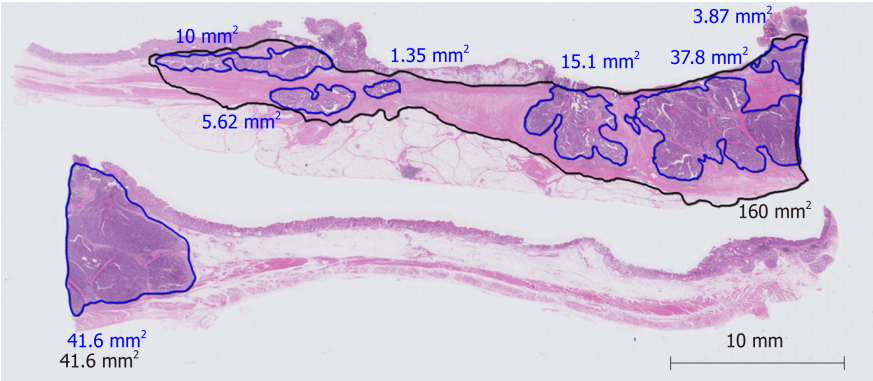


**Figure 1 An example of a virtual microscopic slide and pathological diagnosis of the residual tumor area and primary tumorous bed.** The areas enclosed by a red line and a black line are the residual tumor area and the primary tumorous bed, respectively. Their square measures were automatically calculated by the software of the virtual microscopic system.

achieve pCR are rare. Indeed, in this study, only 7.4% of patients achieved pCR. Therefore, a more common endpoint is needed. Nakamura *et al*[14] suggested that a 10% cut-off evaluated using virtual microscopic slides could be the global standard cut-off of residual tumor. Our analysis supports that result and indicates that this approach may be applicable to clinical practice. Our results suggest that the method may be useful for a prognostic marker regardless of the reason for undergoing NAC, which has not been examined in clinical trials but is sometimes considered in clinical practice, including esophageal or adjacent organ invasion, or a metastatic lesion.

In addition, in this study, we compared the prognostic utility of this method with that of using the conventional JCGC criteria. Kurokawa *et al*[8] reported the prognostic utility of JCGC criteria and demonstrated that histological responders who achieved a response of grade 1b or more had significantly longer survival than non-responders. Compared with this, in our study, the HRs of PFS and OS were the lowest when responders were defined as patients who achieved a response of grade 2 or more. This difference appeared to be caused by the differences in the patients included in each study. The study by Kurokawa *et al*[8] also included patients who underwent R1 or R2 resection. Although our data were limited to patients who underwent R0 resection, the HRs for RFS and OS with the 10% cut-off evaluated using virtual microscopic slides were lower than those for the other cut-offs according to the JCGC criteria. Therefore, our method might at least be as useful as the JCGC criteria. We consider that it would be worthwhile confirming this result in future prospective studies.

The advantage of histological evaluation with virtual microscopic slides compared with conventional histological evaluation is its objectivity. Smyth *et al*[20] reported that there was poor inter-observer agreement of pathological response independently evaluated by two pathologists (kappa = 0.64) in the Medical Research Council Adjuvant Gastric Infusional Chemotherapy trial. Therefore, to improve the rate of concordance among pathologists and standardize pathological evaluations, more objective and simpler methods were needed. Our method used only stained pathological specimens of the largest tumor diameter and its concordance rate was high (96.2%). Thus, we consider that this approach is more applicable for evaluating pathological response.

Evaluating the area of type 4 tumors is sometimes difficult. Although Nakamura *et al*[14] reported that a 10% cut-off evaluated using virtual microscopic slides in type 4 tumors was less useful than that in non-type 4 tumors, our results suggest that this cut-off s useful in both of these groups. This discrepancy appears to be caused by the small sample size of our study ($n$ = 10) and the subjectivity of the evaluation for the area in which tumor cells were sparsely distributed. Further improvement of the evaluation method is thus needed.

Our study had some limitations. First, the analysis was performed in a single center and the sample size was relatively small. To evaluate the application of the cut-off widely in clinical practice and to examine the concordance rate of pathological response precisely, a multi-center study is desirable. Second, patients included in this analysis were those seen from March 2009 until May 2015. However, in 2011, trastuzumab was approved for HER2-positive gastric cancer in Japan. mOS of patients with recurrence after surgery might thus have been prolonged after 2011. Third, this analysis was limited to patients who underwent R0 resection. Therefore, to evaluate whether the cut-off is useful for patients who have undergone R1 or R2 resection,

**Table 1 Clinicopathological characteristics of the patients**

| Background | *n* (%) | Background | *n* (%) |
|---|---|---|---|
| Age | Median 64 | M-classification | |
| | Range 39–77 | | |
| < 65 yr | 28 (51.9) | 0 | 51 (94.4) |
| ≥ 65 yr | 26 (48.1) | 1 | 3 (5.6) |
| Gender | | Tumor histology | |
| Male | 40 (74.1) | Differentiated | 26 (48.1) |
| Female | 14 (25.9) | Undifferentiated | 28 (51.9) |
| ECOG PS | | Reason for NAC | |
| 0 | 46 (85.2) | Clinical SE or T4b | 14 (25.9) |
| 1 | 8 (14.8) | Extended LN | 24 (44.4) |
| Tumor type | | Large type 3 | 5 (9.3) |
| Non-type 4 | 44 (81.5) | Type 4 | 4 (7.4) |
| Type 4 | 10 (18.5) | Others | 7 (13.0) |
| Primary site | | HER2 overexpression | |
| Stomach | 51 (94.4) | Negative or unknown | 48 (88.9) |
| Esophagogastric junction | 3 (5.6) | Positive | 6 (11.1) |
| T-classification | | NAC regimen | |
| 1 | 1 (1.9) | SP or SOX (+ trastuzumab) | 49 (90.7) |
| 2 | 2 (3.7) | DCS | 5 (9.3) |
| 3 | 13 (24.1) | Adjuvant treatment | |
| 4 | 38 (70.4) | S-1 | 52 (96.3) |
| N-classification | | Others or no treatment | 2 (3.7) |
| 0 | 6 (11.1) | Participant of clinical trials | |
| 1 | 10 (18.5) | Yes | 17 (31.5) |
| 2 | 22 (40.7) | No | 37 (68.5) |
| 3 | 15 (27.8) | | |
| Not evaluable | 1 (1.9) | | |

NAC: Neoadjuvant chemotherapy; LN: Lymph node; SP: S-1 + cisplatin; SOX: S-1 + oxaliplatin; DCS: Docetaxel + cisplatin + S-1; ECOG PS: Eastern cooperative oncology group performance status.

further studies will be needed. Fourth, this was a retrospective study. It could thus have been influenced by confounding factors such as demographic factors or patient comorbidities.

In conclusion, a 10% cut-off of pathological response evaluated using virtual microscopic slides might be a useful prognostic marker for gastric cancer patients who have undergone NAC followed by R0 resection. The utility of this method needs to be evaluated in further prospective studies.

**Table 2 Prognostic analysis according to patients' characteristics**

| Background | | HR (95%CI) | *P* value |
|---|---|---|---|
| Age | ≥ 65 yr | 0.57 (0.21–1.51) | 0.26 |
| Gender | Male | 1.09 (0.38–3.07) | 0.87 |
| ECOG PS | 0 | 0.37 (0.04–2.84) | 0.34 |
| Macroscopic type | Type 4 | 1.51 (0.53–4.25) | 0.43 |
| Primary site | Stomach | 0.27 (0.05–1.24) | 0.09 |
| Tumor histology | Undifferentiated | 1.14 (0.44–2.90) | 0.78 |
| T-classification | ≥ 4a | 4.73 (0.62–35.7) | 0.13 |
| N-classification | ≥ 3a | 1.63 (0.57–4.61) | 0.35 |
| M-classification | 1 | 0.96 (0.22–4.19) | 0.95 |
| HER2 | Positive | < 0.001 (0–infinity) | 0.14 |
| Main reason for NAC | Extended LN | 1 (reference) | |
| | Large type 3 | 1.22 (0.32–4.70) | 0.76 |
| | Type 4 | 1.49 (0.48–4.60) | 0.48 |
| | Others | 0.62 (0.13–3.02) | 0.58 |
| NAC regimen | SP or SOX | 1.85 (0.24–14.2) | 0.55 |
| Adjuvant treatment | Yes | 0.43 (0.05–3.39) | 0.42 |
| Participant of clinical trials | Yes | 0.79 (0.29–2.14) | 0.65 |

NAC: Neoadjuvant chemotherapy; LN: Lymph node; SP: S-1 + cisplatin; SOX: S-1 + oxaliplatin; DCS: Docetaxel + cisplatin + S-1; HR: Hazard ratio; CI: Confidence interval; ECOG PS: Eastern cooperative oncology group performance status.

**Table 3 Comparison of prognostic utility of 10% cut-off evaluated using virtual microscopic slides with JCGC criteria**

| Histological criteria of JCGC | RFS | | OS | |
|---|---|---|---|---|
| | HR (95%CI) | *P* value | HR (95%CI) | *P* value |
| Grade 0 *vs* 1a–3 | 0.52 (0.15–1.80) | 0.304 | 2.27 (0.27–19.0) | 0.449 |
| Grade 0–1a *vs* 1b–3 | 0.63 (0.26–1.55) | 0.321 | 0.72 (0.26–1.95) | 0.52 |
| Grade 0–1b *vs* 2–3 | 0.33 (0.12–0.87) | 0.026 | 0.39 (0.13–1.15) | 0.089 |
| Grade 0–2 *vs* 3 | 0.69 (0.08–5.34) | 0.722 | 0.62 (0.07–5.34) | 0.665 |
| Our method | | | | |
| Responder *vs* non-responder | 0.29 (0.10–0.82) | 0.019 | 0.23 (0.07–0.78) | 0.018 |

NAC: Neoadjuvant chemotherapy; HR: Hazard ratio; JCGC: Japanese Classification of Gastric Carcinoma; CI: Confidence interval; RFS: Relapse-free survival; OS: Overall survival.

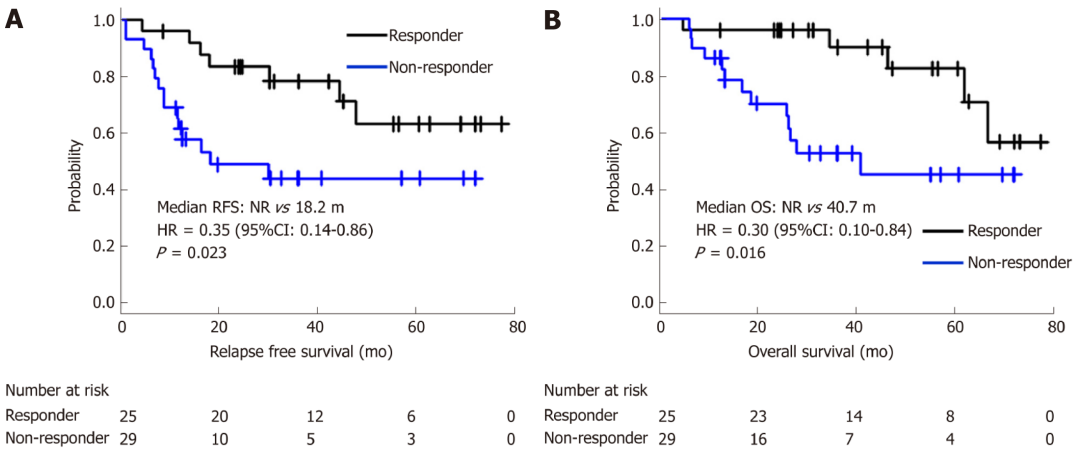


**Figure 2 Survival curves of responders and non-responders classified according to pathological response of 10% cut-off evaluated using virtual microscopic slides.** A: Relapse-free survival; B: Overall survival. HR: Hazard ratio; CI: Confidence interval; NR: Not reached; RFS: Relapse-free survival; OS: Overall survival.

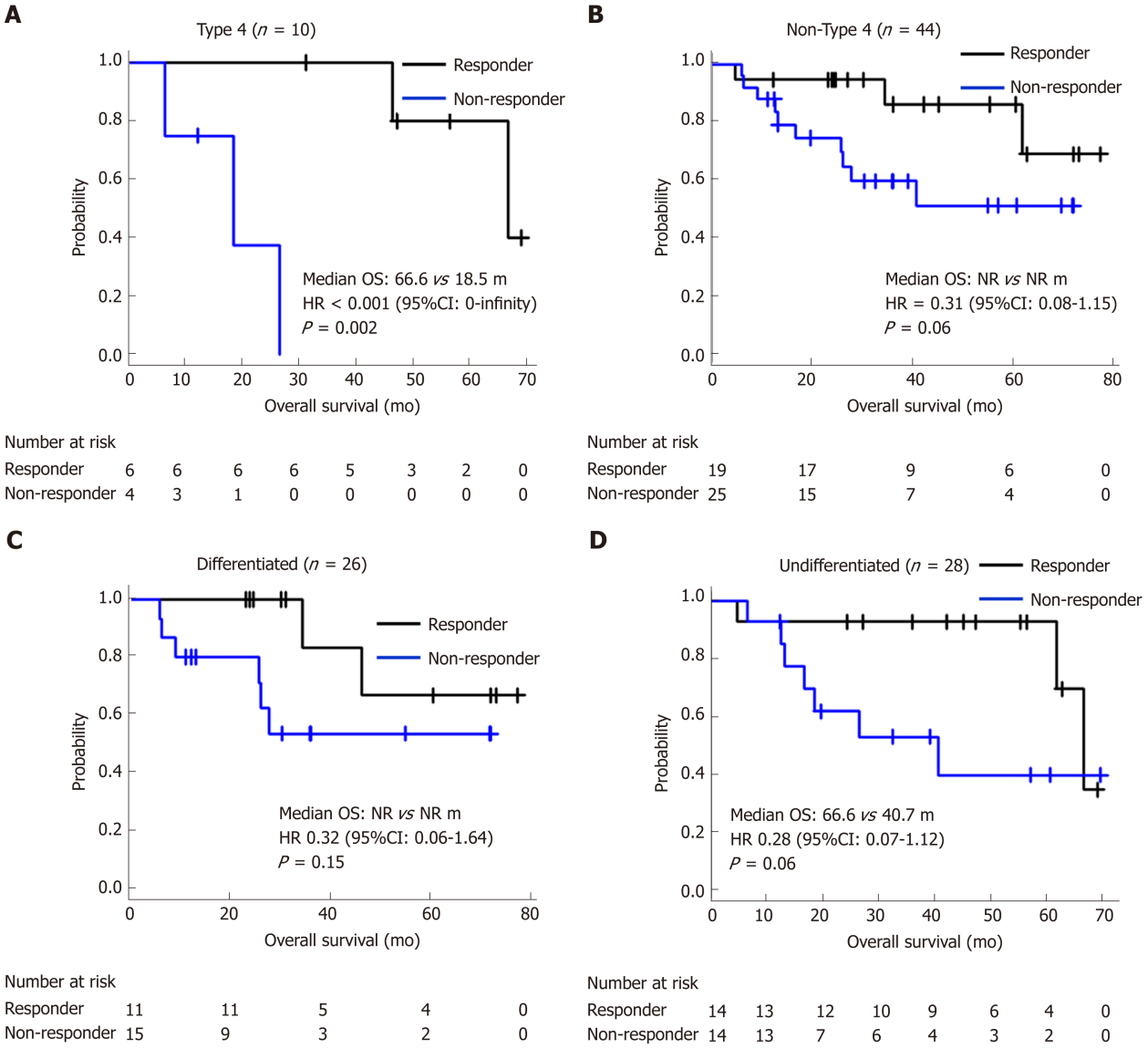


**Figure 3 Subgroup analyses of survival of responders and non-responders classified according to pathological response of 10% cut-off evaluated using virtual microscopic slides.** A: Macroscopic type 4; B: Non-type 4; C: Histologically differentiated; D: Undifferentiated. OS: Overall survival; HR: Hazard ratio; CI: Confidence interval; NR: Not reached.

## ARTICLE HIGHLIGHTS

### Research background
Although pathological response is a common endpoint used to assess the efficacy of neoadjuvant chemotherapy (NAC) for gastric cancer, the problem of a low rate of concordance from evaluations among pathologists remains unresolved. Moreover, there is no globally accepted consensus regarding the optimal evaluation.

### Research motivation
Pathological response is commonly used for a surrogate marker for progression-free survival and overall survival (OS) after surgery. However, no globally accepted consensus has been reached regarding the optimal cut-off, and the reproducibility between pathologists was limited.

### Research objectives
To examine the clinical utility of 10% cut-off for pathological response evaluated using virtual microscopic slides as a prognostic marker.

### Research methods
We retrospectively evaluated pathological specimens of gastric cancer patients who underwent NAC followed by surgery and achieved R0 resection between March 2009 and May 2015. Residual tumor area and primary tumor beds were measured in one captured image slide. We classified patients with < 10% residual tumor relative to the primary tumorous area as responders, and the rest as non-responders; we then compared OS and relapse-free survival (RFS) between these two groups.

### Research results
Fifty-four patients were evaluated. The concordance rate between two evaluators was 96.2%. Median RFS of 25 responders and 29 non-responders was not reached (NR) *vs* 18.2 mo [hazard ratio (HR) = 0.35, $P$ = 0.023], and median OS was NR *vs* 40.7 mo (HR = 0.3, $P$ = 0.016), respectively. This result was also observed even in subgroup analyses for different macroscopic types (Borrmann type 4/non-type 4) and histological types (differentiated/undifferentiated).

### Research conclusions
The measurement of pathological response using digitally captured virtual microscopic slides may be useful in clinical practice because of its objectivity and its high concordance rate. We consider that this approach is more applicable for evaluating pathological response.

### Research perspectives
Out results indicated that the measurement of pathological response using digitally captured virtual microscopic slides might be as useful as conventional criteria. However, further studies is needed to evaluate the utility of the method especially for patients who have undergone R1 or R2 resection, and type 4 tumor.

## REFERENCES


1 **Bray F**, Ferlay J, Soerjomataram I, Siegel RL, Torre LA, Jemal A. Global cancer statistics 2018: GLOBOCAN estimates of incidence and mortality worldwide for 36 cancers in 185 countries. *CA Cancer J Clin* 2018; **68**: 394-424 [PMID: 30207593 DOI: 10.3322/caac.21492]

2 **Kinoshita T**, Sasako M, Sano T, Katai H, Furukawa H, Tsuburaya A, Miyashiro I, Kaji M, Ninomiya M. Phase II trial of S-1 for neoadjuvant chemotherapy against scirrhous gastric cancer (JCOG 0002). *Gastric Cancer* 2009; **12**: 37-42 [PMID: 19390930 DOI: 10.1007/s10120-008-0496-1]

3 **Keighley MR**, Moore J, Roginski C, Powell J, Thompson H. Incidence and prognosis of N4 node involvement in gastric cancer. *Br J Surg* 1984; **71**: 863-866 [PMID: 6208963 DOI: 10.1002/bjs.1800711121]

4 **Iwasaki Y**, Sasako M, Yamamoto S, Nakamura K, Sano T, Katai H, Tsujinaka T, Nashimoto A, Fukushima N, Tsuburaya A; Gastric Cancer Surgical Study Group of Japan Clinical Oncology Group. Phase II study of preoperative chemotherapy with S-1 and cisplatin followed by gastrectomy for clinically resectable type 4 and large type 3 gastric cancers (JCOG0210). *J Surg Oncol* 2013; **107**: 741-745 [PMID: 23400787 DOI: 10.1002/jso.23301]

5 **Tsuburaya A**, Mizusawa J, Tanaka Y, Fukushima N, Nashimoto A, Sasako M; Stomach Cancer Study Group of the Japan Clinical Oncology Group. Neoadjuvant chemotherapy with S-1 and cisplatin followed by D2 gastrectomy with para-aortic lymph node dissection for gastric cancer with extensive lymph node metastasis. *Br J Surg* 2014; **101**: 653-660 [PMID: 24668391 DOI: 10.1002/bjs.9484]

6 **Yoshikawa T**, Sasako M, Yamamoto S, Sano T, Imamura H, Fujitani K, Oshita H, Ito S, Kawashima Y, Fukushima N. Phase II study of neoadjuvant chemotherapy and extended surgery for locally advanced gastric cancer. *Br J Surg* 2009; **96**: 1015-1022 [PMID: 19644974 DOI: 10.1002/bjs.6665]

7 **Eisenhauer EA**, Therasse P, Bogaerts J, Schwartz LH, Sargent D, Ford R, Dancey J, Arbuck S, Gwyther S, Mooney M, Rubinstein L, Shankar L, Dodd L, Kaplan R, Lacombe D, Verweij J. New response evaluation criteria in solid tumours: revised RECIST guideline (version 1.1). *Eur J Cancer* 2009; **45**: 228-247 [PMID: 19097774 DOI: 10.1016/j.ejca.2008.10.026]

8 **Kurokawa Y**, Shibata T, Sasako M, Sano T, Tsuburaya A, Iwasaki Y, Fukuda H. Validity of response assessment criteria in neoadjuvant chemotherapy for gastric cancer (JCOG0507-A). *Gastric Cancer* 2014; **17**: 514-521 [PMID: 23999869 DOI: 10.1007/s10120-013-0294-2]

9 **Reim D**, Gertler R, Novotny A, Becker K, zum Büschenfelde CM, Ebert M, Dobritz M, Langer R, Hoefler H, Friess H, Schumacher C. Adenocarcinomas of the esophagogastric junction are more likely to respond

to preoperative chemotherapy than distal gastric cancer. *Ann Surg Oncol* 2012; **19**: 2108-2118 [PMID: 22130620 DOI: 10.1245/s10434-011-2147-8]

10 **Valenti V**, Hernandez-Lizoaín JL, Beorlegui MC, Diaz-Gozalez JA, Regueira FM, Rodriguez JJ, Viudez A, Sola I, Cienfuegos JA. Morbidity, mortality, and pathological response in patients with gastric cancer preoperatively treated with chemotherapy or chemoradiotherapy. *J Surg Oncol* 2011; **104**: 124-129 [PMID: 21509785 DOI: 10.1002/jso.21947]

11 **Brenner B**, Shah MA, Karpeh MS, Gonen M, Brennan MF, Coit DG, Klimstra DS, Tang LH, Kelsen DP. A phase II trial of neoadjuvant cisplatin-fluorouracil followed by postoperative intraperitoneal floxuridine-leucovorin in patients with locally advanced gastric cancer. *Ann Oncol* 2006; **17**: 1404-1411 [PMID: 16788003 DOI: 10.1093/annonc/mdl133]

12 **Ferri LE**, Ades S, Alcindor T, Chasen M, Marcus V, Hickeson M, Artho G, Thirlwell MP. Perioperative docetaxel, cisplatin, and 5-fluorouracil (DCF) for locally advanced esophageal and gastric adenocarcinoma: a multicenter phase II trial. *Ann Oncol* 2012; **23**: 1512-1517 [PMID: 22039085 DOI: 10.1093/annonc/mdr465]

13 **Jia Y**, Dong B, Tang L, Liu Y, Du H, Yuan P, Wu A, Ji J. Apoptosis index correlates with chemotherapy efficacy and predicts the survival of patients with gastric cancer. *Tumour Biol* 2012; **33**: 1151-1158 [PMID: 22383294 DOI: 10.1007/s13277-012-0357-8]

14 **Nakamura K**, Kuwata T, Shimoda T, Mizusawa J, Katayama H, Kushima R, Taniguchi H, Sano T, Sasako M, Fukuda H. Determination of the optimal cutoff percentage of residual tumors to define the pathological response rate for gastric cancer treated with preoperative therapy (JCOG1004-A). *Gastric Cancer* 2015; **18**: 597-604 [PMID: 24968818 DOI: 10.1007/s10120-014-0401-z]

15 **Japanese Gastric Cancer Association**. Japanese classification of gastric carcinoma: 3rd English edition. *Gastric Cancer* 2011; **14**: 101-112 [PMID: 21573743 DOI: 10.1007/s10120-011-0041-5]

16 **Kanda Y**. Investigation of the freely available easy-to-use software 'EZR' for medical statistics. *Bone Marrow Transplant* 2013; **48**: 452-458 [PMID: 23208313 DOI: 10.1038/bmt.2012.244]

17 **Becker K**, Mueller JD, Schulmacher C, Ott K, Fink U, Busch R, Böttcher K, Siewert JR, Höfler H. Histomorphology and grading of regression in gastric carcinoma treated with neoadjuvant chemotherapy. *Cancer* 2003; **98**: 1521-1530 [PMID: 14508841 DOI: 10.1002/cncr.11660]

18 **Becker K**, Langer R, Reim D, Novotny A, Meyer zum Buschenfelde C, Engel J, Friess H, Hofler H. Significance of histopathological tumor regression after neoadjuvant chemotherapy in gastric adenocarcinomas: a summary of 480 cases. *Ann Surg* 2011; **253**: 934-939 [PMID: 21490451 DOI: 10.1097/SLA.0b013e318216f449]

19 **Ajani JA**, Mansfield PF, Crane CH, Wu TT, Lunagomez S, Lynch PM, Janjan N, Feig B, Faust J, Yao JC, Nivers R, Morris J, Pisters PW. Paclitaxel-based chemoradiotherapy in localized gastric carcinoma: degree of pathologic response and not clinical parameters dictated patient outcome. *J Clin Oncol* 2005; **23**: 1237-1244 [PMID: 15718321 DOI: 10.1200/JCO.2005.01.305]

20 **Smyth EC**, Fassan M, Cunningham D, Allum WH, Okines AF, Lampis A, Hahne JC, Rugge M, Peckitt C, Nankivell M, Langley R, Ghidini M, Braconi C, Wotherspoon A, Grabsch HI, Valeri N. Effect of Pathologic Tumor Response and Nodal Status on Survival in the Medical Research Council Adjuvant Gastric Infusional Chemotherapy Trial. *J Clin Oncol* 2016; **34**: 2721-2727 [PMID: 27298411 DOI: 10.1200/JCO.2015.65.7692]

World Journal of Gastroenterology

Submit a Manuscript: https://www.f6publishing.com

*World J Gastroenterol* 2019 September 21; 25(35): 5344-5355

DOI: 10.3748/wjg.v25.i35.5344

ISSN 1007-9327 (print) ISSN 2219-2840 (online)

ORIGINAL ARTICLE

Retrospective Study

# Feasibility of endoscopic treatment and predictors of lymph node metastasis in early gastric cancer

Yu-Ning Chu, Ya-Nan Yu, Xue Jing, Tao Mao, Yun-Qing Chen, Xiao-Bin Zhou, Wen Song, Xian-Zhi Zhao, Zi-Bin Tian

**ORCID number:** Yu-Ning Chu (0000-0001-7047-2327); Ya-Nan Yu (0000-0002-7530-1647); Xue Jing (0000-0002-9636-9296); Tao Mao (0000-0002-5294-5474); Yun-Qing Chen (0000-0001-9964-2537); Xiao-bin Zhou (0000-0001-7445-7466); Wen Song (0000-0002-8410-6974); Xian-Zhi Zhao (0000-0001-8107-0905); Zi-Bin Tian (0000-0002-3211-2934).

**Author contributions:** Chu YN, Tian ZB, and Mao T contributed to study conception and design; Chu YN, Son W, Zhao XZ, and Chen YQ collected the data; Chu YN, Jing X, Zhou XB, and Yu YN analyzed and interpreted the data; Zhou XB reviewed the statistical methods and analysis; Chu YN wrote the manuscript; Tian ZB, Jing X, and Yu YN made the critical revision of the article.

**Supported by** the National Natural Science Foundation of China, No. 81502025; and the China Postdoctoral Science Foundation, No. 2018M632631.

**Institutional review board statement:** This study was approved by the Institutional Review Board of the Ethics Committee of the Affiliated Hospital of Qingdao University.

**Informed consent statement:** Patients were not required to give informed consent to the study because the analysis used anonymous clinical data that were obtained after each patient agreed to treatment by written consent.

**Yu-Ning Chu, Ya-Nan Yu, Xue Jing, Tao Mao, Xian-Zhi Zhao, Zi-Bin Tian,** Department of Gastroenterology, the Affiliated Hospital of Qingdao University, Qingdao 266003, Shandong Province, China

**Yun-Qing Chen,** Department of Pathology, the Affiliated Hospital of Qingdao University, Qingdao 266003, Shandong Province, China

**Xiao-Bin Zhou,** Department of Epidemiology and Health Statistics, School of Public Health, Qingdao University, Qingdao 266021, Shandong Province, China

**Wen Song,** Endoscopy Center, the Affiliated Hospital of Qingdao University, Qingdao 266003, Shandong Province, China

**Corresponding author:** Zi-Bin Tian, MD, Director, Professor, Department of Gastroenterology, the Affiliated Hospital of Qingdao University, No. 16, Jiangsu Road, Qingdao 266003, Shandong Province, China. tianzbsun@163.com
**Telephone:** +86-532-82911302
**Fax:** +86-532-82911302

## Abstract

### *BACKGROUND*

Endoscopic submucosal dissection (ESD) has been routinely performed in applicable early gastric cancer (EGC) patients as an alternative to conventional surgical operations that involve lymph node dissection. The indications for ESD have been recently expanded to include larger, ulcerated, and undifferentiated mucosal lesions, and differentiated lesions with slight submucosal invasion. The risk of lymph node metastasis (LNM) is the most important consideration when deciding on a treatment strategy for EGC. Despite the advantages over surgical procedures, lymph nodes cannot be removed by ESD. In addition, whether patients who meet the expanded indications for ESD can be managed safely remains controversial.

### *AIM*

To determine whether the ESD indications are applicable to Chinese patients and to investigate the predictors of LNM in EGC.

### *METHODS*

We retrospectively analyzed 12552 patients who underwent surgery for gastric cancer between June 2007 and December 2018 at the Affiliated Hospital of Qingdao University. A total of 1262 (10.1%) EGC patients were eligible for

**Conflict-of-interest statement:** All authors declare no conflicts of interest related to this article.

**Data sharing statement:** No additional data are available.



**Manuscript source**: Unsolicited manuscript

**Received:** July 12, 2019
**Peer-review started:** July 15, 2019
**First decision:** August 18, 2019
**Revised:** August 28, 2019
**Accepted:** September 9, 2019
**Article in press:** September 9, 2019
**Published online:** September 21, 2019

**P-Reviewer:** Draganov PV, Friedel D
**S-Editor:** Tang JZ
**L-Editor:** Wang TQ
**E-Editor:** Ma YJ

inclusion in this study. Data on the patients' clinical, endoscopic, and histopathological characteristics were collected. The absolute and expanded indications for ESD were validated by regrouping the enrolled patients and determining the positive LNM results in each subgroup. Predictors of LNM in patients were evaluated by univariate and multivariate analyses.

*RESULTS*

LNM was observed in 182 (14.4%) patients. No LNM was detected in the patients who met the absolute indications (0/90). LNM occurred in 4/311 (1.3%) patients who met the expanded indications. According to univariate analysis, LNM was significantly associated with positive tumor marker status, medium (20-30 mm) and large (>30 mm) lesion sizes, excavated macroscopic-type tumors, ulcer presence, submucosal invasion (SM1 and SM2), poor differentiation, lymphovascular invasion (LVI), perineural invasion, and diffuse and mixed Lauren's types. Multivariate analysis demonstrated SM1 invasion (odds ration [OR] = 2.285, $P = 0.03$), SM2 invasion (OR = 3.230, $P < 0.001$), LVI (OR = 15.702, $P < 0.001$), mucinous adenocarcinoma (OR = 2.823, $P = 0.015$), and large lesion size (OR = 1.900, $P = 0.006$) to be independent risk factors.

*CONCLUSION*

The absolute indications for ESD are reasonable, and the feasibility of expanding the indications for ESD requires further investigation. The predictors of LNM include invasion depth, LVI, mucinous adenocarcinoma, and lesion size.

**Key words:** Early gastric cancer; Lymph node metastasis; Predictors; Endoscopic submucosal dissection; Expanded indications



**Core tip:** We aimed to re-evaluate and verify the current indications and guidelines for endoscopic treatment and to analyze the clinicopathological predictors of lymph node metastasis in early gastric cancer (EGC), which have been inconsistently identified across studies. To the best of our knowledge, this study involves the largest number of EGC patients in China, and is the first study to perform statistical analyses on certain clinical features, such as drinking, smoking, obesity, family history of tumors, and tumor markers.

**Citation:** Chu YN, Yu YN, Jing X, Mao T, Chen YQ, Zhou XB, Song W, Zhao XZ, Tian ZB. Feasibility of endoscopic treatment and predictors of lymph node metastasis in early gastric cancer. *World J Gastroenterol* 2019; 25(35): 5344-5355
**URL**: https://www.wjgnet.com/1007-9327/full/v25/i35/5344.htm
**DOI**: https://dx.doi.org/10.3748/wjg.v25.i35.5344

## INTRODUCTION

Gastric cancer is currently the fifth most common cancer and the third leading cause of cancer-related death worldwide[1]. Early gastric cancer (EGC) is defined as a tumor that is confined to the mucosa and submucosa of the stomach, irrespective of regional lymph node metastasis (LNM)[2]. Several studies have reported a frequency of LNM ranging from 5%-10% among EGC patients undergoing radical surgery[3], suggesting that over 90% of surgeries could potentially be avoided if curative endoscopic resection (ER) is accurately predicted based on the histopathology of an endoscopic-resected specimen.

Endoscopic submucosal dissection (ESD) has notable advantages over conventional surgical resection, as it causes less trauma, minor bleeding, and fewer postoperative complications[4]. The absolute indications for ESD for curative resection in EGC that were proposed by the Japanese Gastric Cancer Association (JGCA) initially include nonulcerated, well-differentiated mucosal lesions ≤ 2 cm in diameter[5]. The absolute indications for ESD, however, are so strict that unnecessary surgeries may be performed. Subsequently, the expanded indications for ESD, which include larger, ulcerated, and undifferentiated mucosal lesions as well as differentiated lesions with

slight submucosal invasion, were proposed. A recent meta-analysis involving 12 studies revealed that the incidence of LNM was only 0.2% among patients who met the absolute indications, compared with an LNM incidence of 0.7% among patients who met the expanded indications[6]. Furthermore, several studies have shown that LNM is closely related to an unsatisfactory prognosis in EGC[7-10].

To date, universal preoperative examination methods, such as gastroscopy, endoscopic ultrasonography, computed tomography, and X rays, fail to provide adequate data on the lesion and regional lymph node status before surgery or ER[11]. However, evaluating the risk of LNM is critical for determining the best course of management for EGC patients[12]. Unfortunately, the risk factors that have been identified in different studies are diverse, and controversy still exists regarding the expanded indications for ESD. Therefore, in this study, which involved a relatively large number of EGC patients, we aimed to reevaluate and verify the current guidelines for endoscopic treatment of EGC in a Chinese population and to investigate the predictors of EGC with LNM.

## MATERIALS AND METHODS

### Patients

We retrospectively reviewed all patients who were diagnosed with gastric cancer and underwent gastrectomy with lymphadenectomy between June 2007 and December 2018 at the Affiliated Hospital of Qingdao University. This study was performed in accordance with the Declaration of Helsinki (2000) of the World Medical Association. Our study was also approved by the Institutional Review Board of the Ethics Committee of the Affiliated Hospital of Qingdao University (QYFY WZLL 2019-04-04). In all, 12552 patients were reviewed. Patients were excluded if they had: (1) Advanced-stage gastric cancer ($n$ = 11099); (2) Intestinal metaplasia or intraepithelial neoplasia ($n$ = 72); (3) Metastatic gastric cancer or multiple carcinomas ($n$ = 38); (4) Lymphoma ($n$ = 28); (5) Gastric stump carcinoma ($n$ = 36); and (6) Other life-threatening diseases ($n$ = 17). Ultimately, 1262 EGC patients were enrolled in this study.

### Data collection

The included patients underwent gastrectomy with lymph node dissection. All operations were performed according to the 4th edition of the JGCA treatment guidelines[5]. The specimens were serially sectioned into 3-mm-thick slices, and two experienced pathologists individually examined the histological slides immediately after resection. The diagnostic criterion for LNM is the presence of cancerous tissue inside the lymph node capsule, as shown in Figures 1 and 2. We collected the clinical data, endoscopic features, and pathological characteristics of all enrolled patients. These data included age, sex, incidence of hypertension, heart disease and diabetes mellitus, drinking and smoking history, body mass index (BMI), family history, carcinoembryonic antigen (CEA) level, tumor location, lesion size, macroscopic type, depth of invasion, number of tumors, presence of ulcers, tumor differentiation, Lauren type, presence of lymphovascular invasion (LVI), perineural invasion, and LNM.

Based on the distribution of gastric glands, we classified the tumor locations as cardia, fundus/corpora, or angle/antrum. According to the Paris endoscopic classification, the macroscopic features of EGC were divided into the following five subtypes: Type 0-I (protruded), type 0-IIa (superficial elevated), type 0-IIb (flat), type 0-IIc (superficial depressed), and type 0-III (excavated)[13]. Tumors were also graded as small (≤ 20 mm), medium (20-30 mm), and large (≥ 30 mm) to further analyze the indications for ESD. For invasion depth, submucosal lesions were classified into two groups: SM1 (≤ 500 μm depth of invasion) and SM2 (> 500 μm depth of invasion). In accordance with the JGCA, when multiple lesions were present, the tumor with the most advanced T category (or the largest lesion when the T stages were identical) was classified[2].

### Statistical analysis

Statistical analyses were conducted with SPSS software (SPSS, version 23.0, Chicago, IL, United States). Continuous variables, such as age and BMI, were translated into categorical variables. For age, we calculated the mean value (59.25 years) of the patients and set 60 years as the cut-off value. According to the criteria for obesity, the enrolled patients were divided into a nonobesity group (BMI < 28) and an obesity group (BMI ≥ 28). Differences among categorical variables associated with predictors and LNM were assessed using a chi-square test or Fisher's exact test, and variables

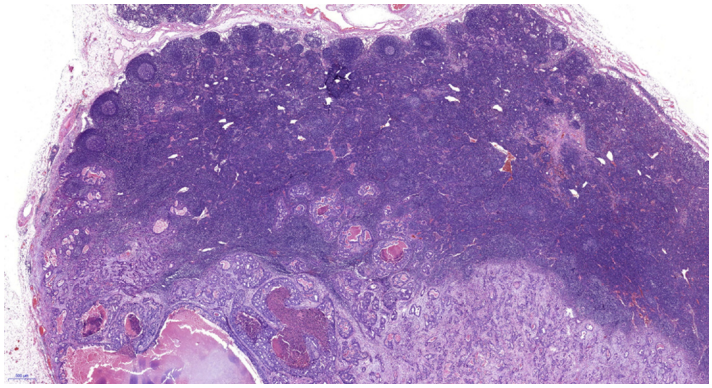

**Figure 1 Pathological image of lymph node metastasis (20×).**

that were significant in the univariate analysis were subsequently entered into a multivariate logistic regression model for analysis of independent risk factors for LNM in EGC. The association between variables and LNM was described by an odds ratio (OR) and a 95% confidence interval (CI). $P < 0.05$ (two-sided) was considered statistically significant.

The statistical methods and analyses of this study were reviewed by professor Xiao-Bin Zhou from the Department of Health Statistics, Qingdao University.

## RESULTS

### Clinical characteristics

We assessed 12552 patients who underwent radical gastrectomy with lymph node dissection. A total of 1262 (10.1%) eligible EGC patients with LNM ($n$ = 182) and without LNM ($n$ = 1080) were included in this study. The sex distribution was 899 (71.2%) males and 363 (28.8%) females (ratio: 2.48:1), with an average age of 59.25 years (range, 24-90 years). Data on the clinical characteristics are shown in Table 1. Patients with a CEA value that exceeded the normal level were more likely to have LNM, and this association was statistically significant ($P$ = 0.007). However, other clinical parameters, such as age, sex, underlying diseases, lifestyle habits, family history, and *Helicobacter pylori* (*H. pylori*) infection, failed to reach statistical significance.

### Positive LNM results in EGC according to indications for ESD

According to further analysis, no LNM metastasis was observed in patients who met the absolute indications for ESD (0/90). However, LNM occurred in a few patients (4/311) who met the following expanded indications for ESD: (1) Differentiated mucosal tumors, ≤ 30 mm in size, without LVI, and with ulceration (3/86 cases, 3.5%); (2) Differentiated mucosal tumors, without ulcer and LVI, and of any size (1/32 cases, 3.1%); (3) Undifferentiated mucosal tumors without ulcer and LVI, and ≤ 20 mm in size (0/110 cases, 0%); and (4) Differentiated tumors with SM1 invasion, no LVI, and ≤ 30 mm in size (0/83 cases, 0%). As shown in Table 2, patients who met the surgical indications had a higher risk of LNM ($P < 0.001$). Table 3 contains more details on the frequency of LNM among EGC patients who met the indications for ESD.

### Comparison of endoscopic features

The endoscopic features are shown in Table 4. More EGCs were in the angle/antrum of the stomach ($n$ = 928, 73.5%) than in the cardia ($n$ = 46, 3.6%) and in the fundus/corpora ($n$ = 288, 22.8%). Forty-two (3.3%) patients had multifocal lesions. The univariate analysis revealed that the location and number of tumors were not significantly associated with LNM. Regarding tumor size, LNM occurred significantly more frequently in patients with medium ($P$ = 0.016) or large ($P$ = 0.000) tumors than in patients with small tumors. With regard to macroscopic features, type IIc ($n$ = 486, 38.5%) occurred most frequently among the five subtypes, but type III ($n$ = 481, 38.1%) occurred more frequently in patients with LNM ($P$ = 0.001). Ulcerative lesions also occurred more frequently in patients with LNM ($P$ = 0.013).

### Analysis of histopathological characteristics

Among the 1262 EGC patients, 182 (14.4%) had LNM according to the pathological diagnostic criteria, including 123 (67.6%) with stage N1, 39 (21.4%) with stage N2, and

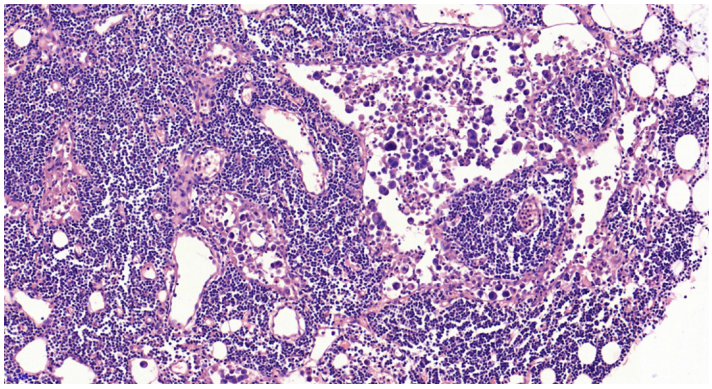

**Figure 2 Pathological image of lymph node metastasis (200×).**

20 (11.0%) with stage N3 LNM according to the 8th edition of the American Joint Committee on Cancer (AJCC) Staging Manual. The mean number of metastatic lymph nodes was 2.8 (range, 1-17). Regarding lesion depth, 596 (47.2%) patients had tumors limited to the mucosal (M) layer, whereas 245 had SM1 (superficial submucosal) tumors (19.4%), and 421 had SM2 (deep submucosal) tumors (33.4%). The percentages of lymph node positivity were 5.2%, 19.6%, and 24.5% for M, SM1, and SM2, respectively. In terms of tumor differentiation, the undifferentiated type ($n$ = 807, 63.9%) was the major histologic type of EGC based on the JGCA criteria and was significantly more likely to occur in patients with LNM than the differentiated type ($n$ = 455, 36.1%) ($P$ 0.001). Regarding cell histology, the patients with mucinous adenocarcinoma had a higher risk of LNM than patients with other histologic lesion types ($P$ = 0.019). Based on the Lauren classification, LNM was observed more frequently in diffuse-type (DT) and mixed-type (MT) tumors ($P$ = 0.003) than in intestinal-type (IT) tumors. Moreover, LNM was found significantly more frequently in patients with LVI ($P$ 0.001) and perineural invasion ($P$ 0.001) than in the patient subgroup without invasion. Additional detailed histopathologic features of the enrolled patients are summarized in Table 5.

### *Univariate analysis*

The univariate analysis results showed that 10 out of the 20 factors were significantly associated with a higher risk of LNM. The risk factors included high CEA levels, medium and large lesion sizes, excavated macroscopic type, presence of ulcers, deep submucosal invasion (SM1 and SM2), poor differentiation, LVI, mucinous adenocarcinoma, perineural invasion, and diffuse and mixed Lauren classifications.

### *Multivariate logistic regression analysis of lymph node metastasis*

Based on stepwise multivariate analysis, the significant independent risk factors for LNM in EGC were SM1 invasion (OR = 2.285, $P$ = 0.030), SM2 invasion (OR = 3.230, $P$ < 0.001), LVI (OR = 15.702, $P$ < 0.001), pathological pattern of mucinous adenocarcinoma (OR = 2.823, $P$ = 0.015), and lesion size over 30 mm (OR = 1.900, $P$ = 0.006). The independent risk factors are listed in Table 6.

## DISCUSSION

Following the introduction of the expanded indications for ESD, many studies have reevaluated the risk of LNM in EGC. A meta-analysis involving 9798 EGC patients showed that among the expanded indications for ESD, the inclusion of mucosal differentiated lesions of any size that were not ulcerated and of differentiated mucosal lesions < 30 mm that were ulcerated can be justified with a minimally increased risk. Nonetheless, the reasonableness of expanding the indications for ESD to include undifferentiated lesions smaller than 20 mm and differentiated lesions with slight submucosal invasion still requires careful investigation[6]. Our study demonstrated that the rate of LNM for patients who met the expanded indications for ESD was 4/311 (1.3%). No LNM occurred in patients who met the absolute indications. Similarly, reassessment of the expanded indications in Korea also showed an LNM rate of 2.4% among patients who met the expanded indications[14], which is inconsistent with the results of a large dataset from Japan that revealed no LNM in patients who met the expanded indications[15]. It is difficult to identify the reasons for this difference. A probable interpretation is that the existing indications are still not

**Table 1 Lymph node metastasis risk according to clinical parameters**

| | Total (*n* = 1262), *n* (%) | LNM negative (*n* = 1080), *n* (%) | LNM positive (*n* = 182), *n* (%) | Univariate OR (95%CI) | *P*-value |
|---|---|---|---|---|---|
| Age (yr) | | | | | 0.090 |
| ≤ 60 | 628 (49.8) | 548 (50.7) | 80 (44.0) | 1 | |
| > 60 | 634 (50.2) | 532 (49.3) | 102 (56.0) | 1.313 (0.960, 1.800) | |
| Sex | | | | | 0.239 |
| Male | 899 (71.2) | 776 (71.9) | 123 (67.6) | 1 | |
| Female | 363 (28.8) | 304 (28.1) | 59 (32.4) | 0.817 (0.580, 1.150) | |
| Hypertension | | | | | 0.554 |
| Absence | 958 (75.9) | 823 (76.2) | 135 (74.2) | 1 | |
| Presence | 304 (24.1) | 257 (23.8) | 47 (25.8) | 1.115 (0.78, 1.60) | |
| Heart disease | | | | | 0.449 |
| Absence | 1146 (90.8) | 978 (90.4) | 168 (92.3) | 1 | |
| Presence | 116 (9.2) | 102 (9.6) | 14 (7.7) | 0.799 (0.446, 1.430) | |
| Diabetes mellitus | | | | | 0.933 |
| Absence | 1142 (90.5) | 977 (90.5) | 165 (90.7) | 1 | |
| Presence | 120 (9.5) | 103 (9.5) | 17 (9.3) | 0.977 (0.570, 1.675) | |
| BMI | | | | | 0.086 |
| ≤ 28 | 1134 (89.9) | 964 (89.3) | 170 (93.4) | 1 | |
| > 28 | 128 (10.1) | 116 (10.7) | 12 (6.6) | 0.587 (0.317, 1.086) | |
| Drinking | | | | | 0.104 |
| Absence | 827 (65.6) | 698 (64.7) | 129 (70.9) | 1 | |
| Presence | 434 (34.4) | 381 (35.3) | 53 (29.1) | 0.753 (0.534, 1.061) | |
| Smoking | | | | | 0.138 |
| Absence | 692 (54.8) | 583 (54.0) | 109 (59.9) | 1 | |
| Presence | 570 (45.2) | 497 (46.0) | 73 (40.1) | 0.786 (0.571, 1.082) | |
| Family history | | | | | 0.872 |
| Absence | 1011 (80.1) | 866 (80.2) | 145 (79.7) | 1 | |
| Presence | 251 (19.9) | 214 (19.8) | 37 (20.3) | 1.033 (0.699, 1.526) | |
| *H. pylori* infection | | | | | 0.225 |
| Negative | 634 (50.2) | 535 (49.5) | 99 (54.4) | 1 | |
| Positive | 628 (49.8) | 545 (50.5) | 83(45.6) | 0.823 (0.601, 1.128) | |
| CEA | | | | | 0.007 |
| Negative | 960 (76.1) | 836 (77.4) | 124 (68.1) | 1 | |
| Positive | 302 (23.9) | 244 (22.6) | 58 (31.9) | 1.603 (1.137, 2.258) | |

LNM: Lymph node metastasis; OR: Odds ratio; CI: Confidence interval; BMI: Body mass index; *H. pylori*: *Helicobacter pylori*; CEA: Carcinoembryonic antigen.

sufficiently comprehensive. The JGCA added invasion depth, ulceration, tumor size, differentiation, and LVI to its criteria for ESD. Based on our results, it is necessary to take the cellular histology of tumors into consideration when deciding upon the ESD indications. If ESD is performed in a more selective subgroup, the risk of LNM will likely be reduced. Therefore, predictive factors may be used to optimize the ESD criteria.

In line with other relevant studies, our study also concluded that deeper invasion significantly increased LNM risk. Additionally, the measurement of the width of the infiltration could be a useful additional parameter in the indications for supplemental gastrectomy after ESD. Therefore, a detailed measurement of invasion depth is truly necessary during the pathological evaluation of endoscopic-resected specimens[16]. Regarding lesion size, we found that larger tumor size was a significant predictor of regional LNM in our patients with EGC, which is similar to the conclusions of many other investigators[7,9,17-19]. However, the cut-off values varied among these studies, which increased the difficulty in determining a uniform standard. Two possible explanations can be identified: First, this parameter is a continuous variable, and the cut-off values are inconsistent in different studies; alternatively, the study subjects are diverse and included individuals with signet ring cell EGC, undifferentiated-type

**Table 2 Lymph node metastasis in early gastric cancer according to therapeutic indications**

| | LNM (%) | 95%CI | *P*-value |
|---|---|---|---|
| Absolute indications for ESD | 0/90 (0.0) | 0%-4.1% | < 0.001 |
| Expanded indications for ESD | 4/311 (1.3) | 0.35%-3.29% | |
| Surgical indications | 178/861 (20.7) | 17.75%-23.94% | |

LNM: Lymph node metastasis; CI: Confidence interval; ESD: Endoscopic submucosal dissection.

EGC, and mixed type EGC among others, which may also account for the difference.

In the latest gastric cancer treatment guidelines (2014 ver. 4), the JGCA noted that endoscopic dissection should be defined as noncurative if mucinous adenocarcinoma is found in the submucosal layer, regardless of whether the mucinous cells are believed to be derived from a differentiated or undifferentiated-type tumor. We conclude that the histological pattern of mucinous adenocarcinoma is an independent risk factor for LNM based on multivariate analysis, which provided powerful evidence to support this statement. With regard to signet ring cell carcinoma in EGC, it has been reported that the LNM rate of signet ring cell-type tumors is lower than that of other undifferentiated-type carcinomas and is equivalent to that of differentiated-type carcinomas[20], which is in line with our results. This suggests that ESD is more feasible for signet ring cell carcinoma compared with other early undifferentiated-type gastric carcinomas. However, the cellular histology of signet ring cell carcinoma is an important factor for LNM in EGC[21]. Huh *et al*[22] also stated that EGC with a mixed signet ring cell histology exhibited more aggressive behavior than pure tubular adenocarcinoma or pure signet ring cell carcinoma. Hence, a more accurate application of the classification of signet ring cell carcinoma could improve the ESD criteria.

In a previous study that focused on the prognosis of different types of gastric cancer as classified by the Lauren classification, patients with MT carcinomas were found to be significantly more likely to have LNM than patients with IT and DT carcinomas, which was also confirmed in our study. A possible explanation of this difference is that patients with MT tumors always exhibit severe characteristics, including larger lesion sizes and a higher frequency of spread into local lymphatic and venous vessels or regional lymph nodes[23]. In various clinical and pathological studies, LVI has been reported to be the strongest risk factor for nodal metastasis in EGC[24], and we confirmed this finding by showing that LVI predicted a high risk of LNM in EGC. However, unlike other risk factors that can be observed by endoscopic investigation and other auxiliary examinations, LVI is difficult to detect before the ER specimen is obtained. However, based on the criteria for local treatment, the presence of LVI commonly requires additional extended surgery, which is clinically significant. As shown in Table 3, every histopathological factor included in this study was significantly associated with LNM, which indicates that all of these factors are vitally important for performing an accurate pathological analysis after gastroscopic examination.

Researchers have previously concluded that the overall 3-year survival rate was higher in patients without LNM and that patients with LNM had a higher rate of tumor recurrence[25]. Several factors are associated with an increased rate of LNM. The risk factors varied in some relevant studies, but LVI, submucosal invasion, histological type, and tumor size were found to be significantly related to LNM in almost every study. Consistent with other studies[7,18,26], our study demonstrated that age, sex, tumor location, macroscopic type, presence of ulcers, tumor differentiation, Lauren type, and *H. pylori* infection were not independent risk factors for LNM, although some of these factors were statistically significant in the univariate analysis. Specifically, we analyzed other clinical features, such as drinking and smoking history, obesity, family history of tumors, and the levels of the tumor marker CEA, which is an innovative aspect of this study. In recent years, biomarkers have begun to play an increasingly important role in the detection and management of patients with gastrointestinal malignancies[27]. Serum CEA is considered a complementary test, although it is insufficient to diagnose EGC and LNM. In this study, a higher than normal CEA value was found to be statistically significant in univariate analysis, which attaches great importance to its preoperative detection. However, inconsistencies were found among the test items of the included patients, which made it difficult to perform an analysis of other less common tumor markers. Buckland *et al*[28] reported that nicotine and alcohol played an important role in the development of gastric cancer, and therefore, we further analyzed the relationships between drinking

**Table 3 Lymph node metastasis in early gastric cancer according to the endoscopic submucosal dissection indications**

| | LNM negative | LNM positive | LNM rate (%) | 95%CI | *P*-value |
|---|---|---|---|---|---|
| Ab ($n$ = 90) | 90 | 0 | 0.0 | 0%-4.1% | 0.021 |
| Ex1 ($n$ = 86) | 83 | 3 | 3.5 | 0.75%-10.56% | |
| Ex2 ($n$ = 32) | 31 | 1 | 3.1 | 0.08%-17.91% | |
| Ex3 ($n$ = 110) | 110 | 0 | 0 | 0%-3.35% | |
| Ex4 ($n$ = 83) | 83 | 0 | 0 | 0%-4.44% | |

Ex1: Differentiated mucosal tumors, ≤ 30 mm in size, without lymphovascular invasion (LVI), and with ulceration. Ex2: Differentiated mucosal tumors, without ulcer and LVI, and of any size. Ex3: Undifferentiated mucosal tumors without ulcer and LVI, and ≤ 20 mm in size. Ex4: Differentiated tumors with SM1 invasion, no LVI, and ≤ 30 mm in size. LNM: Lymph node metastasis; CI: Confidence interval; Ab: Absolute indications for endoscopic submucosal dissection; Ex: Expanded indications for endoscopic submucosal dissection.

and smoking with LNM. Despite the lack of significant association between the occurrence of LNM and these lifestyle habits in this study, we cannot ignore these factors because the clinical data collected in retrospective studies may be incomplete. Although this research, to the best of our knowledge, involved the largest number of EGC patients in China, the limitation that it was a retrospective study at a single institution should still be noted. Therefore, a well-designed multicentric prospective study is needed.

In conclusion, the absolute indications for ESD can be applied to Chinese patients, while the feasibility of expanding these indications requires further investigation. The predictive factors for LNM included submucosal invasion depth, LVI, mucinous adenocarcinoma, and large lesion size. Taking the histology of tumors into consideration when deciding upon the ESD indications is therefore of great necessity.

**Table 4 Lymph node metastasis risk according to endoscopic features**

| | Total (*n* = 1262), *n* (%) | LNM negative (*n* = 1080), *n* (%) | LNM positive (*n* = 182), *n* (%) | Univariate OR (95%CI) | *P*-value |
|---|---|---|---|---|---|
| Location | | | | | 0.462 |
| Cardia | 46 (3.6) | 40 (3.7) | 6 (3.3) | 1 | |
| Fundus/corpora | 288 (22.8) | 240 (22.2) | 48 (26.4) | 1.333 (0.535, 3.320) | 0.537 |
| Angle/antrum | 928 (73.5) | 800 (74.1) | 128 (70.3) | 1.067 (0.443, 2.567) | 0.885 |
| Lesion size | | | | | < 0.001 |
| Small (≤ 20 mm) | 761 (60.3) | 680 (63.0) | 81 (44.5) | 1 | |
| Middle (20-30 mm) | 285 (22.6) | 239 (22.1) | 46 (25.3) | 1.616 (1.093, 2.388) | 0.016 |
| Large (> 30 mm) | 216 (17.1) | 161 (14.9) | 55 (30.2) | 2.868 (1.955, 4.207) | < 0.001 |
| Macroscopic type | | | | | 0.001 |
| 0-I(Protruded) | 86 (6.8) | 71 (6.6) | 15 (8.2) | 1.712 (0.823, 3.564) | 0.147 |
| 0-IIa (Elevated) | 36 (2.9) | 35 (3.2) | 1 (0.5) | 0.232 (0.030, 1.788) | 0.128 |
| 0-IIb (Flat) | 173 (13.7) | 154 (14.3) | 19 (10.4) | 1 | |
| 0-IIc (Depressed) | 486 (38.5) | 432 (40) | 54 (29.7) | 1.013 (0.582, 1.763) | 0.963 |
| 0-III (Excavated) | 481 (38.1) | 388 (35.9) | 93 (51.1) | 1.943 (1.146, 3.293) | 0.012 |
| Number of tumors | | | | | 0.191 |
| Single | 1220 (96.7) | 1044 (96.7) | 176 (96.7) | 1 | |
| Multitude | 42 (3.3) | 36 (3.3) | 6 (3.3) | 1.724 (0.641, 4.635) | |
| Ulcer | | | | | 0.013 |
| Absence | 558 (44.2) | 493 (45.6) | 65 (35.7) | 1 | |
| Presence | 704 (55.8) | 587 (54.4) | 117 (64.3) | 1.512 (1.091, 2.094) | |

LNM: Lymph node metastasis; OR: Odds ratio; CI: Confidence interval.

**Table 5 Lymph node metastasis risk according to histopathological characteristics**

| | Total (*n* = 1262), *n* (%) | LNM negative (*n* = 1080), *n* (%) | LNM positive (*n* = 182), *n* (%) | Univariate OR (95%CI) | *P*-value |
|---|---|---|---|---|---|
| Invasion depth | | | | | < 0.001 |
| M | 596 (47.2) | 565 (52.3) | 31 (17.0) | 1 | |
| SM1 | 245 (19.4) | 197 (18.2) | 48 (26.4) | 4.441 (2.748, 7.176) | < 0.001 |
| SM2 | 421 (33.4) | 318 (29.4) | 103 (56.6) | 5.903 (3.862, 9.024) | < 0.001 |
| Differentiation | | | | | < 0.001 |
| Differentiated | 455 (36.1) | 412 (38.1) | 43 (23.6) | 1 | |
| Undifferentiated | 807 (63.9) | 668 (61.9) | 139 (76.4) | 1.994 (1.386, 2.867) | |
| Histology | | | | | 0.019 |
| Pap/Tub/Por | 1004 (79.6) | 866 (80.2) | 138 (75.8) | 1 | |
| Sig | 223 (17.7) | 190 (17.6) | 33 (18.1) | 1.090 (0.723, 1.644) | 0.681 |
| Muc | 35 (2.8) | 24 (2.2) | 11 (6.1) | 2.876 (1.378, 6.004) | 0.005 |
| LVI | | | | | < 0.001 |
| Absence | 1104 (87.5) | 1021 (94.5) | 83 (45.6) | 1 | |
| Presence | 158 (12.5) | 59 (5.5) | 99 (54.4) | 20.641 (13.942, 30.559) | |
| Perineural invasion | | | | | < 0.001 |
| Absence | 1181 (93.6) | 1026 (95) | 155 (85.2) | 1 | |
| Presence | 81 (6.4) | 54 (5.0) | 27 (14.8) | 3.310 (2.024, 5.413) | |
| Lauren's type | | | | | 0.003 |
| Intestinal type | 500 (39.6) | 448 (41.5) | 52 (28.6) | 1 | |
| Diffuse type | 399 (31.6) | 335 (31.0) | 64 (35.2) | 1.646 (1.112, 2.437) | 0.013 |
| Mixed type | 363 (28.8) | 297 (27.5) | 66 (36.3) | 1.915 (1.294, 2.833) | 0.001 |

SM1: Tumor invading the superficial (< 0.5 mm in depth) submucosa. SM2: Tumor invading the deep (> 0.5 mm in depth) submucosa. LNM: Lymph node metastasis; OR: Odds ratio; CI: Confidence interval; M: Tumor confined within the mucosal layer; Pap: Papillary adenocarcinoma; Tub: Tubular adenocarcinoma; Por: Poorly differentiated adenocarcinoma; Sig: Signet ring cell carcinoma; Muc: Mucinous adenocarcinoma; LVI: Lymph-vascular

invasion.

**Table 6 Multivariate logistic regression analysis of lymph node metastasis in early gastric cancer**

| Factor | OR (95%CI) | *P*-value |
|---|---|---|
| Lesion size | | 0.025 |
| Middle lesion size (20-30 mm) | 1.230 (0.774, 1.955) | 0.380 |
| Large lesion size (>30 mm) | 1.900 (1.197, 3.015) | 0.006 |
| Histology | | 0.049 |
| Sig | 1.146 (0.698, 1.881) | 0.590 |
| Muc | 2.823 (1.225, 6.505) | 0.015 |
| LVI | 15.702 (10.405, 23.695) | < 0.001 |
| Invasion depth | | < 0.001 |
| SM1 | 2.285 (1.317, 3.965) | 0.003 |
| SM2 | 3.230 (2.006, 5.201) | < 0.001 |

SM1: Invading the superficial (<0.5 mm in depth) submucosa. SM2: Invading the deep (> 0.5 mm in depth) submucosa. LNM: Lymph node metastasis; OR: Odds ratio; CI: Confidence interval; LVI: Lymph-vascular invasion; Sig: Signet ring cell carcinoma; Muc: Mucinous adenocarcinoma.

## ARTICLE HIGHLIGHTS

### *Research background*

The indications for endoscopic submucosal dissection (ESD) have been recently expanded to include larger, ulcerated, and undifferentiated mucosal lesions, and differentiated lesions with slight submucosal invasion. Despite the advantages over surgical procedures, lymph nodes cannot be removed by ESD. However, the risk of lymph node metastasis (LNM) is the most important consideration when deciding on a treatment strategy for early gastric cancer (EGC).

### *Research motivation*

Evaluating the risk of LNM is critical for determining the best course of management for EGC patients. Unfortunately, the risk factors that have been identified in different studies are diverse, and whether patients who met the expanded indications for ESD can be managed safely remains controversial.

### *Research objectives*

We aimed to determine whether the ESD indications are applicable to Chinese patients and to investigate the predictors of LNM in EGC. After working hard on this topic, we have re-evaluated and verified the current indications and guidelines for endoscopic treatment and analyzed the clinicopathological predictors of LNM, which provides strong evidence and reference to future research.

### *Research methods*

We retrospectively analyzed 12552 patients who underwent surgery for gastric cancer between June 2007 and December 2018 at the Affiliated Hospital of Qingdao University. A total of 1262 (10.1%) EGC patients were eligible for inclusion in this study. Data on the patients' clinical, endoscopic, and histopathological characteristics were collected. The absolute and expanded indications for ESD were validated by regrouping the enrolled patients and determining the positive LNM results in each subgroup. Predictors of LNM in patients were evaluated by univariate and multivariate analyses. Specifically, we analyzed other clinical features, such as drinking and smoking history, obesity, family history of tumors, and the levels of the tumor marker carcinoembryonic antigen (CEA), which is an innovative aspect of this study.

### *Research results*

LNM was observed in 182 (14.4%) patients. No LNM was detected in the patients who met the absolute indications (0/90). LNM occurred in 4/311 (1.3%) patients who met the expanded indications. According to univariate analysis, LNM was significantly associated with positive tumor marker status, medium (20-30 mm) and large (>30 mm) lesion sizes, excavated macroscopic-type tumors, ulcer presence, submucosal invasion (SM1 and SM2), poor differentiation, lymphovascular invasion (LVI), perineural invasion, and diffuse and mixed Lauren's types. Multivariate analysis demonstrated SM1 invasion (OR = 2.285, $P$ = 0.03), SM2 invasion (OR = 3.230, $P$ < 0.001), LVI (OR = 15.702, $P$ < 0.001), mucinous adenocarcinoma (OR = 2.823, $P$ = 0.015), and large lesion size (OR = 1.900, $P$ = 0.006) to be independent risk factors. Also, the results of this research affirmed the feasibility of the absolute indications for ESD. However, whether it is reasonable to expand the indications remains to be further discussed.

### Research conclusions

The absolute indications for ESD can be applied to Chinese patients, while the feasibility of expanding these indications requires further investigation. The predictive factors for LNM included submucosal invasion depth, LVI, mucinous adenocarcinoma, and large lesion size. This study provides clinicians with important reference when evaluating the risk of LNM and determining the best course of management for EGC patients.

### Research perspectives

Besides invasion depth, LVI, and lesion size, taking the histology of tumors into consideration when deciding upon the ESD indications is vitally important. In addition, preoperative detection of tumor markers is of great necessity. The direction of the future research is to further optimize the ESD indications by analyzing the predictive factors for LNM in EGC. A well-designed multicentric prospective study is the best method for the future research.

## REFERENCES


1 **Balakrishnan M**, George R, Sharma A, Graham DY. Changing Trends in Stomach Cancer Throughout the World. *Curr Gastroenterol Rep* 2017; **19**: 36 [PMID: 28730504 DOI: 10.1007/s11894-017-0575-8]

2 **Japanese Gastric Cancer Association**. Japanese classification of gastric carcinoma: 3rd English edition. *Gastric Cancer* 2011; **14**: 101-112 [PMID: 21573743 DOI: 10.1007/s10120-011-0041-5]

3 **Abdelfatah MM**, Barakat M, Othman MO, Grimm IS, Uedo N. The incidence of lymph node metastasis in submucosal early gastric cancer according to the expanded criteria: a systematic review. *Surg Endosc* 2019; **33**: 26-32 [PMID: 30298447 DOI: 10.1007/s00464-018-6451-2]

4 **Isomoto H**, Shikuwa S, Yamaguchi N, Fukuda E, Ikeda K, Nishiyama H, Ohnita K, Mizuta Y, Shiozawa J, Kohno S. Endoscopic submucosal dissection for early gastric cancer: a large-scale feasibility study. *Gut* 2009; **58**: 331-336 [PMID: 19001058 DOI: 10.1136/gut.2008.165381]

5 **Japanese Gastric Cancer Association**. Japanese gastric cancer treatment guidelines 2014 (ver. 4). *Gastric Cancer* 2017; **20**: 1-19 [PMID: 27342689 DOI: 10.1007/s10120-016-0622-4]

6 **Abdelfatah MM**, Barakat M, Lee H, Kim JJ, Uedo N, Grimm I, Othman MO. The incidence of lymph node metastasis in early gastric cancer according to the expanded criteria in comparison with the absolute criteria of the Japanese Gastric Cancer Association: a systematic review of the literature and meta-analysis. *Gastrointest Endosc* 2018; **87**: 338-347 [PMID: 28966062 DOI: 10.1016/j.gie.2017.09.025]

7 **Wang Z**, Zhang X, Hu J, Zeng W, Liang J, Zhou H, Zhou Z. Predictive factors for lymph node metastasis in early gastric cancer with signet ring cell histology and their impact on the surgical strategy: analysis of single institutional experience. *J Surg Res* 2014; **191**: 130-133 [PMID: 24768142 DOI: 10.1016/j.jss.2014.03.065]

8 **Ahmad R**, Setia N, Schmidt BH, Hong TS, Wo JY, Kwak EL, Rattner DW, Lauwers GY, Mullen JT. Predictors of Lymph Node Metastasis in Western Early Gastric Cancer. *J Gastrointest Surg* 2016; **20**: 531-538 [PMID: 26385006 DOI: 10.1007/s11605-015-2945-6]

9 **Kunisaki C**, Takahashi M, Nagahori Y, Fukushima T, Makino H, Takagawa R, Kosaka T, Ono HA, Akiyama H, Moriwaki Y, Nakano A. Risk factors for lymph node metastasis in histologically poorly differentiated type early gastric cancer. *Endoscopy* 2009; **41**: 498-503 [PMID: 19533552 DOI: 10.1055/s-0029-1214758]

10 **Suzuki H**, Oda I, Abe S, Sekiguchi M, Mori G, Nonaka S, Yoshinaga S, Saito Y. High rate of 5-year survival among patients with early gastric cancer undergoing curative endoscopic submucosal dissection. *Gastric Cancer* 2016; **19**: 198-205 [PMID: 25616808 DOI: 10.1007/s10120-015-0469-0]

11 **Zhang Y**, Liu Y, Zhang J, Wu X, Ji X, Fu T, Li Z, Wu Q, Bu Z, Ji J. Construction and external validation of a nomogram that predicts lymph node metastasis in early gastric cancer patients using preoperative parameters. *Chin J Cancer Res* 2018; **30**: 623-632 [PMID: 30700931 DOI: 10.21147/j.issn.1000-9604.2018.06.07]

12 **Wang H**, Zhang H, Wang C, Fang Y, Wang X, Chen W, Liu F, Shen K, Qin X, Shen Z, Sun Y. Expanded endoscopic therapy criteria should be cautiously used in intramucosal gastric cancer. *Chin J Cancer Res* 2016; **28**: 348-354 [PMID: 27478320 DOI: 10.21147/j.issn.1000-9604.2016.03.09]

13 The Paris endoscopic classification of superficial neoplastic lesions: esophagus, stomach, and colon: November 30 to December 1, 2002. *Gastrointest Endosc* 2003; **58**: S3-43 [PMID: 14652541 DOI: 10.1016/S0016-5107(03)02159-X]

14 **Kang HJ**, Kim DH, Jeon TY, Lee SH, Shin N, Chae SH, Kim GH, Song GA, Kim DH, Srivastava A, Park DY, Lauwers GY. Lymph node metastasis from intestinal-type early gastric cancer: experience in a single institution and reassessment of the extended criteria for endoscopic submucosal dissection. *Gastrointest Endosc* 2010; **72**: 508-515 [PMID: 20554277 DOI: 10.1016/j.gie.2010.03.1077]

15 **Gotoda T**, Yanagisawa A, Sasako M, Ono H, Nakanishi Y, Shimoda T, Kato Y. Incidence of lymph node metastasis from early gastric cancer: estimation with a large number of cases at two large centers. *Gastric Cancer* 2000; **3**: 219-225 [PMID: 11984739 DOI: 10.1007/PL00011720]

16 **Zhao B**, Zhang J, Zhang J, Luo R, Wang Z, Xu H, Huang B. Risk Factors Associated with Lymph Node Metastasis for Early Gastric Cancer Patients Who Underwent Non-curative Endoscopic Resection: a Systematic Review and Meta-analysis. *J Gastrointest Surg* 2019; **23**: 1318-1328 [PMID: 30187319 DOI: 10.1007/s11605-018-3924-5]

17 **Lee JH**, Choi IJ, Han HS, Kim YW, Ryu KW, Yoon HM, Eom BW, Kim CG, Lee JY, Cho SJ, Kim YI, Nam BH, Kook MC. Risk of lymph node metastasis in differentiated type mucosal early gastric cancer mixed with minor undifferentiated type histology. *Ann Surg Oncol* 2015; **22**: 1813-1819 [PMID: 25344305 DOI: 10.1245/s10434-014-4167-7]

18 **Fang WL**, Huang KH, Lan YT, Chen MH, Chao Y, Lo SS, Wu CW, Shyr YM, Li AF. The Risk Factors of Lymph Node Metastasis in Early Gastric Cancer. *Pathol Oncol Res* 2015; **21**: 941-946 [PMID: 25749755 DOI: 10.1007/s12253-015-9920-0]

19 **Du MZ**, Gan WJ, Yu J, Liu W, Zhan SH, Huang S, Huang RP, Guo LC, Huang Q. Risk factors of lymph node metastasis in 734 early gastric carcinoma radical resections in a Chinese population. *J Dig Dis* 2018; **19**: 586-595 [PMID: 30207084 DOI: 10.1111/1751-2980.12670]

**Kook MC**. Risk Factors for Lymph Node Metastasis in Undifferentiated-Type Gastric Carcinoma. *Clin*

20 *Endosc* 2019; **52**: 15-20 [PMID: 30677790 DOI: 10.5946/ce.2018.193]
21 **Kim YH**, Park JH, Park CK, Kim JH, Lee SK, Lee YC, Noh SH, Kim H. Histologic purity of signet ring cell carcinoma is a favorable risk factor for lymph node metastasis in poorly cohesive, submucosa-invasive early gastric carcinoma. *Gastric Cancer* 2017; **20**: 583-590 [PMID: 27663439 DOI: 10.1007/s10120-016-0645-x]
22 **Huh CW**, Jung DH, Kim JH, Lee YC, Kim H, Kim H, Yoon SO, Youn YH, Park H, Lee SI, Choi SH, Cheong JH, Noh SH. Signet ring cell mixed histology may show more aggressive behavior than other histologies in early gastric cancer. *J Surg Oncol* 2013; **107**: 124-129 [PMID: 22991272 DOI: 10.1002/jso.23261]
23 **Zheng HC**, Li XH, Hara T, Masuda S, Yang XH, Guan YF, Takano Y. Mixed-type gastric carcinomas exhibit more aggressive features and indicate the histogenesis of carcinomas. *Virchows Arch* 2008; **452**: 525-534 [PMID: 18266006 DOI: 10.1007/s00428-007-0572-7]
24 **Ono H**, Yao K, Fujishiro M, Oda I, Nimura S, Yahagi N, Iishi H, Oka M, Ajioka Y, Ichinose M, Matsui T. Guidelines for endoscopic submucosal dissection and endoscopic mucosal resection for early gastric cancer. *Dig Endosc* 2016; **28**: 3-15 [PMID: 26234303 DOI: 10.1111/den.12518]
25 **Li X**, Liu S, Yan J, Peng L, Chen M, Yang J, Zhang G. The Characteristics, Prognosis, and Risk Factors of Lymph Node Metastasis in Early Gastric Cancer. *Gastroenterol Res Pract* 2018; **2018**: 6945743 [PMID: 29853864 DOI: 10.1155/2018/6945743]
26 **Haruta H**, Hosoya Y, Sakuma K, Shibusawa H, Satoh K, Yamamoto H, Tanaka A, Niki T, Sugano K, Yasuda Y. Clinicopathological study of lymph-node metastasis in 1,389 patients with early gastric cancer: assessment of indications for endoscopic resection. *J Dig Dis* 2008; **9**: 213-218 [PMID: 18959593 DOI: 10.1111/j.1751-2980.2008.00349.x]
27 **Duffy MJ**, Lamerz R, Haglund C, Nicolini A, Kalousová M, Holubec L, Sturgeon C. Tumor markers in colorectal cancer, gastric cancer and gastrointestinal stromal cancers: European group on tumor markers 2014 guidelines update. *Int J Cancer* 2014; **134**: 2513-2522 [PMID: 23852704 DOI: 10.1002/ijc.28384]
28 **Buckland G**, Travier N, Huerta JM, Bueno-de-Mesquita HB, Siersema PD, Skeie G, Weiderpass E, Engeset D, Ericson U, Ohlsson B, Agudo A, Romieu I, Ferrari P, Freisling H, Colorado-Yohar S, Li K, Kaaks R, Pala V, Cross AJ, Riboli E, Trichopoulou A, Lagiou P, Bamia C, Boutron-Ruault MC, Fagherazzi G, Dartois L, May AM, Peeters PH, Panico S, Johansson M, Wallner B, Palli D, Key TJ, Khaw KT, Ardanaz E, Overvad K, Tjønneland A, Dorronsoro M, Sánchez MJ, Quirós JR, Naccarati A, Tumino R, Boeing H, Gonzalez CA. Healthy lifestyle index and risk of gastric adenocarcinoma in the EPIC cohort study. *Int J Cancer* 2015; **137**: 598-606 [PMID: 25557932 DOI: 10.1002/ijc.29411]

World Journal of Gastroenterology

Submit a Manuscript: https://www.f6publishing.com

*World J Gastroenterol* 2019 September 21; 25(35): 5356-5375

DOI: 10.3748/wjg.v25.i35.5356

ISSN 1007-9327 (print) ISSN 2219-2840 (online)

SYSTEMATIC REVIEWS

# *De novo* malignancies after liver transplantation: The effect of immunosuppression-personal data and review of literature

Tommaso Maria Manzia, Roberta Angelico, Carlo Gazia, Ilaria Lenci, Martina Milana, Oludamilola T Ademoyero, Domiziana Pedini, Luca Toti, Marco Spada, Giuseppe Tisone, Leonardo Baiocchi

**ORCID number:** Tommaso Maria Manzia (0000-0002-4636-3478); Roberta Angelico (0000-0002-3439-7750); Carlo Gazia (0000-0002-3543-4170); Ilaria Lenci (0000-0001-5704-9890); Martina Milana (0000-0003-2027-0481); Oludamilola T Ademoyero (0000-0003-3706-4828); Domiziana Pedini (0000-0001-9035-0984); Luca Toti (0000-0001-8407-5939); Marco Spada (0000-0003-0796-6847); Giuseppe Tisone (0000-0001-8860-5909); Leonardo Baiocchi (0000-0003-3672-4505).

**Author contributions:** Manzia TM and Angelico R contributed equally to the work, paper conception and design and critical revision; Gazia C, Lenci I, Milana M, Ademoyero OT, Pedini D and Toti L contributed to acquisition of data, analysis and interpretation, drafting of manuscript and critical revision; Spada M, Tisone G and Baiocchi L contributed to study conception and critical revision.

**Conflict-of-interest statement:** The authors declare they have no conflicts of interest to disclose.

**PRISMA 2009 Checklist statement:** Authors read the PRISMA 2009 Checklist and the manuscript was prepared and revised according to the PRISMA 2009.



**Tommaso Maria Manzia, Carlo Gazia, Luca Toti, Giuseppe Tisone,** HPB and Transplant Unit, Department of Surgery, University of Rome Tor Vergata, Rome 00133, Italy

**Roberta Angelico, Domiziana Pedini, Marco Spada,** Division of Abdominal Transplantation and HPB Surgery, Bambino Gesù Children's Hospital IRCCS, Rome 00165, Italy

**Carlo Gazia, Oludamilola T Ademoyero,** Wake Forest Institute for Regenerative Medicine, Winston-Salem, NC 27101, United States

**Ilaria Lenci, Martina Milana, Leonardo Baiocchi,** Hepatology and Liver Transplant Unit, University of Tor Vergata, Rome 00133, Italy

**Corresponding author:** Tommaso Maria Manzia, MD, PhD, Assistant Professor, HPB and Transplant Unit, Department of Surgery, University of Rome Tor Vergata, Viale Oxford, 81, Rome 00133, Italy. tomanzia@libero.it
**Telephone:** +39-6-20902498

## Abstract

### *BACKGROUND*

Immunosuppression has undoubtedly raised the overall positive outcomes in the post-operative management of solid organ transplantation. However, long-term exposure to immunosuppression is associated with critical systemic morbidities. *De novo* malignancies following orthotopic liver transplants (OLTs) are a serious threat in pediatric and adult transplant individuals. Data from different experiences were reported and compared to assess the connection between immunosuppression and *de novo* malignancies in liver transplant patients.

### *AIM*

To study the role of immunosuppression on the incidence of *de novo* malignancies in liver transplant recipients.

### *METHODS*

A systematic literature examination about *de novo* malignancies and immunosuppression weaning in adult and pediatric OLT recipients was described in the present review. Worldwide data were collected from highly qualified institutions performing OLTs. Patient follow-up, immunosuppression discontinuation and incidence of *de novo* malignancies were reported. Likewise, the review assesses the differences in adult and pediatric recipients by describing the adopted immunosuppression regimens and the different type of diagnosed solid and blood malignancy.

**Manuscript source**: Invited manuscript

**Received:** May 2, 2019
**Peer-review started:** May 4, 2019
**First decision:** May 30, 2019
**Revised:** August 8, 2019
**Accepted:** August 24, 2019
**Article in press:** August 24, 2019
**Published online:** September 21, 2019

**P-Reviewer:** Alexopoulou A, Bhatti ABH, Ding JX, Ho CM, Mikulic D, Ramsay MA, Sipahi AM, Zheng H
**S-Editor:** Yan JP
**L-Editor:** Filipodia
**E-Editor:** Ma YJ

***RESULTS***
Emerging evidence suggests that the liver is an immunologically privileged organ able to support immunosuppression discontinuation in carefully selected recipients. Malignancies are often detected in liver transplant patients undergoing daily immunosuppression regimens. Post-transplant lymphoproliferative diseases and skin tumors are the most detected *de novo* malignancies in the pediatric and adult OLT population, respectively. To date, immunosuppression withdrawal has been achieved in up to 40% and 60% of well-selected adult and pediatric recipients, respectively. In both populations, a clear benefit of immunosuppression weaning protocols on *de novo* malignancies is difficult to ascertain because data have not been specified in most of the clinical experiences.

***CONCLUSION***
The selected populations of tolerant pediatric and adult liver transplant recipients greatly benefit from immunosuppression weaning. There is still no strong clinical evidence on the usefulness of immunosuppression withdrawal in OLT recipients on malignancies. An interesting focus is represented by the complete reconstitution of the immunological pathways that could help in decreasing the incidence of *de novo* malignancies and may also help in treating liver transplant patients suffering from cancer.

**Key words:** Pediatric liver transplant; Immunosuppression weaning; Clinical operational tolerance; Adult liver transplant; Graft rejection; Immune system; *De novo* malignancies; Immunosuppression minimization; Cancer



**Core tip:** A systematic literature examination about *de novo* malignancies and immunosuppression weaning both in adult and pediatric orthotopic liver transplant recipients was described in the present review. Even though conclusive evidence on immunosuppression withdrawal in orthotopic liver transplant recipients with regard to malignancies are lacking, we can argue that the reconstitution of the immunological pathway could decrease the incidence of *de novo* malignancies and may also help in treating liver transplant patients suffering from cancers.

**Citation:** Manzia TM, Angelico R, Gazia C, Lenci I, Milana M, Ademoyero OT, Pedini D, Toti L, Spada M, Tisone G, Baiocchi L. *De novo* malignancies after liver transplantation: The effect of immunosuppression-personal data and review of literature. *World J Gastroenterol* 2019; 25(35): 5356-5375
**URL**: https://www.wjgnet.com/1007-9327/full/v25/i35/5356.htm
**DOI**: https://dx.doi.org/10.3748/wjg.v25.i35.5356

## INTRODUCTION

It has been shown that progress in surgical techniques and enhanced standards in patient selection, standard of care, peri-operative management, survival rates and quality of life after orthotopic liver transplant (OLT) has remarkably improved over the last three decades. This has led to OLT being the treatment of choice for end-stage acute and chronic liver failure. However, the life-long immunosuppression (IS) regimens following transplantation still burden OLT recipients. In fact, major risks include infections, oncogenic viruses and renal, cardiovascular and metabolic complications along with a worrisome time-dependent susceptibility to *de novo* malignancies (DNMs)[1]. The incidence of DNMs among transplant patients is two to four times higher than in the healthy population[2]. These numbers increase to greater than 19 times in the pediatric counterpart[3], and DNM-related mortality is becoming the most prevalent cause of death amongst transplant subjects[4-6]. Beyond the therapeutic strategies for DNMs after OLT, IS drug minimization or withdrawal has been proposed.

Several studies have demonstrated the tolerogenic potential of the liver[7,8]. Because

of its unique anatomy, several cell types in the liver have the capacity to act as antigen-presenting cells. In fact, dendritic cells, Kupffer cells and hepatocytes are capable of presenting antigens that activate $CD8^+$ T cells[7]. These mechanisms are believed to play a role in allowing IS discontinuation and a permanent IS-free state (IFS) in up to 30%-40% of adult OLT recipients and in up to 60% of the pediatric population[9,10]. The present review aimed to detect the role of IS and its minimization or withdrawal in OLT adult and pediatric recipients on DNMs.

The primary goal of the current review was to assess the incidence and the characteristics of the diagnosed DNMs after an OLT in adult and pediatric populations in comparison with the non-transplanted immunocompetent population. The secondary goals were to determine: the incidence and outcome of those recipients that were successfully weaned off IS; and to address whether the maintenance of an IFS decreases the incidence of DNMs in LT recipients.

## MATERIALS AND METHODS

### Search strategy

A literature review was conducted in February 2019 through MEDLINE databases (*via* PubMed) and Google Scholar to find studies pertaining to OLTs, DNMs, IS regimens and the clinical operational tolerance (COT) threshold. Articles published in languages other than English were excluded. All texts were full text accessible. Multiple keywords were used: "*de novo* tumor", "adult", "pediatric", "liver transplantation", "malignancy", "review" and "operational tolerance". The combination of words was used to maximize the results and achieve the highest possibility of articles related to the field of the present review. A flow chart of the article selection is provided in Figure 1.

### Inclusion and exclusion criteria

Studies published in journals describing DNMs and risk factors for their development were searched for both adult and pediatric OLT recipients including experiences from article bibliographies. Records on post-transplant lymphoproliferative diseases (PTLDs), skin, head, neck, breast, lung, prostate, kidney, colorectal and other DNMs were collected and discussed from systematic reviews, randomized clinical trials, observational studies and case-control studies. IS regimens included calcineurin inhibitors (CNIs), corticosteroids, azathioprine, mammalian target of rapamycin inhibitors (mTORi) and antibody-mediated induction therapies. No time limits were applied to provide the closest results to the effective impact of DNMs on OLT patients. Non-English articles and cohorts of patients who underwent allografts other than liver were excluded from this review.

### Data extraction

Information extracted from each selected article was first author name, year of publication, number of patients, follow-up period, characteristics of the detected malignancies, number of tolerant patients and study outcomes.

## RESULTS

### De novo malignancies in the OLT population

Recurrence and DNMs are the most frequent cause of mortality in adult OLT recipients[11] with an incidence up to 26%[12]. Conversely to cardiovascular complications, mortality from DNMs is increasing fast[13]: OLT recipients experience the highest onset rate of lymphomas (57%), and both PTLDs and non-PTLD tumors appear to develop after a shorter time in OLT recipients than other solid organ transplant patients[14]. Moreover, liver-localized PTLDs may originate from the donor and their treatment effect is very different. According to the donor/host origin of PTLDs, the prognostic significance might significantly change: Donor originated PTLDs might have different clinical and pathological features compared with the case of host originated PTLDs[15].

The probability of developing non-skin malignancies is higher in patients who underwent OLT for primary sclerosing cholangitis (PSC) (22% at 10 years) or alcoholic liver disease (ALD) (18% at 10 years)[16]. In particular, alcohol abuse[17] correlates with a three-fold increased risk of developing DNMs, and similar results are encountered in smokers of long duration due to the induced DNA damage[18,19] (Table 1). Overall, skin cancers are commonly diagnosed DNMs along with PTLDs after an OLT. The incidence of other malignancies is subject to a large variability due to the majority of

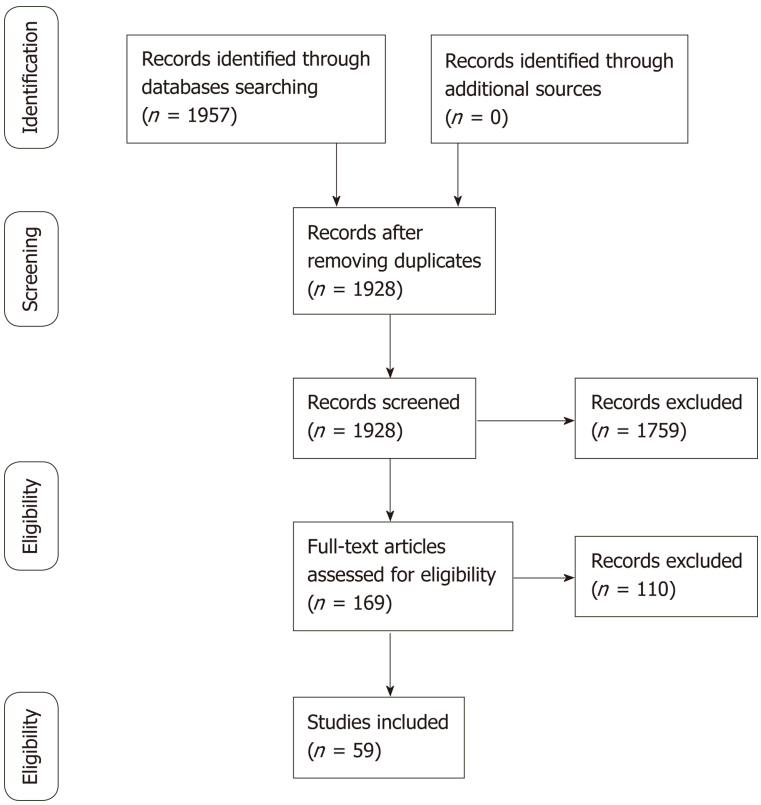


**Figure 1 Flow diagram of the article selection procedure.**

epidemiological data coming from registry databases or single-center retrospective studies.

### *Major* de novo *malignancy incidence in adult OLT recipients*

**PTLDs:** PTLDs are the second most diagnosed DNMs after an OLT accounting for around 35% of non-skin malignancies[20]. Most PTLDs are due to Epstein-Barr virus (EBV). Even if a clear cut-off range of EBV-DNA levels has not been well recognized, virus detection may be sufficient to reveal early PTLDs[2,21-24]. Although the mortality still remains high (up to 85% and 69% after 1 and 5 years, respectively), PTLDs are decreasing due to the PTLD type, prognosis and efficacy of the available treatments[23,25,26].

Certain types of IS regimens including anti-thymocyte globulin, cyclosporine (CsA) or muromonab-CD3 are more likely to determine the onset of PTLDs[27,28]. The survival rate was significantly better in patients undergoing tacrolimus regimens compared to CsA (81.2% *vs* 50% after 5 years from the PTLD diagnosis)[29]. Multidisciplinary approaches that include IS weaning, interferon, surgery, radiotherapy and chemotherapy were attempted to reduce the incidence or recurrence from PTLDs[30].

**Non-PTLDs:** The most represented malignancies in adult OLT recipients are skin cancers[31-33] despite their lower recurrence after other SOTs[33-35]. Non-melanoma skin cancer are the most represented, and OLT recipients express a much higher risk when compared to the healthy population[36]. The vast majority of non-melanoma skin cancer is represented by squamous cell carcinomas and basal cell carcinomas[18,35]. However, a recent report from Rademacher *et al*[37] described an inverted trend with a decline in the incidence of skin cancer in the OLT population. This suggests that the characteristics of the analyzed cohort and a more deliberate use of sun blockers, avoidance of direct UV radiation and the type of IS adopted may play a role[38,39].

Human papilloma virus infections, aging, pallor of skin, previous cutaneous malignancies, blue or hazelnut eyes, CD4 lymphocytopenia and history of actinic keratosis are associated to skin tumors after an OLT[18,35,40,41]. In addition, PSC (considered as an indication for transplant[42]), male phenotype, Caucasian ethnicity and monoclonal induction therapy[40] represent relevant assets. A longstanding clinical experience proved CsA to be the strongest predictor; in fact CsA-treated patients developed a skin malignancy in a shorter time than patients treated with tacrolimus, making CsA an independent and specific risk factor for skin cancer[43].

**Table 1 Incidence of *de novo* malignancies in adult orthotopic liver transplant patients**

| | | | | Number and % incidence of *de novo* malignancy types in all orthotopic liver transplant recipients | | | | | | | | | |
|---|---|---|---|---|---|---|---|---|---|---|---|---|---|
| Author | Yr | Number of patients | Number of DNM | PTLD | Skin and Kaposi | Head and Neck | Lung | Renal | Colon | Prosta-te | Breast | Gynecological | Others |
| Jonas *et al*[72] | 1997 | 458 | 33 | 7 (1.5) | 8 (1.7) | 2 (0.4) | 3 (0.7) | 0 | 0 | 0 | 3 (0.7) | 7 (1.5) | 3 (0.6) |
| Jain *et al*[134] | 1998 | 1000 | 57 | NA | 24 (2.4) | 7 (0.7) | 8 (0.8) | 2 (0.2) | 4 (0.4) | 3 (0.3) | 3 (0.3) | 0 | 6 (0.6) |
| Kelly *et al*[135] | 1998 | 888 | 31 | NA | 8 (0.9) | 6 (0.7) | 1 (0.1) | 0 | 3 (0.3) | 0 | 2 (0.2) | 1 (0.1) | 10 (1.1) |
| Jimenez *et al*[136] | 2002 | 505 | 62 | 13 (2.6) | 16 (3.2) | 10 (2.0) | 6 (1.2) | NA | NA | NA | NA | NA | 17 (3.3) |
| Saigal *et al*[73] | 2002 | 1140 | 30 | NA | 14 (1.2) | 3 (0.3) | 0 | 3 (0.3) | 1 (0.1) | 0 | 2 (0.2) | 1 (0.1) | 6 (0.5) |
| Sanchez *et al*[137] | 2002 | 1421 | 125 | 35 (2.5) | 42 (3.0) | 4 (0.3) | 11 (0.8) | 3 (0.2) | 9 (0.6) | 0 | 7 (0.5) | 2 (0.1) | 13 (0.8) |
| Benlloch *et al*[17] | 2004 | 772 | 41 | 10 (1.3) | NA | 9 (1.2) | 8 (1.0) | 3 (0.4) | 2 (0.3) | 1 (0.1) | 2 (0.3) | 2 (0.3) | 4 (0.5) |
| Oo *et al*[138] | 2005 | 1778 | 141 | 18 (1.0) | 51 (2.9) | NA | 14 (0.8) | NA | 18 (1.0) | NA | 11 (0.6) | 1 (0.06) | 28 (1.6) |
| Yao *et al*[12] | 2006 | 1043 | 53 | 9 (0.9) | 17 (0.6) | 3 (0.3) | 5 (0.5) | 2 (0.2) | 6 (0.6) | 0 | 4 (0.4) | 2 (0.2) | 5 (0.5) |
| Aberg *et al*[81] | 2008 | 540 | 39 | 9 (1.7) | 11 (2.0) | 2 (0.3) | NA | 2 (0.3) | 2 (0.3) | 2 (0.3) | 1 (0.1) | NA | 10 (1.8) |
| Jiang *et al*[20] | 2008 | 2034 | 113 | 44 (2.1) | NA | 3 (0.1) | 10 (0.5) | 4 (0.2) | 14 (0.7) | 5 (0.2) | 5 (0.2) | NA | 24 (1.2) |
| Baccarani *et al*[139] | 2010 | 417 | 43 | 9 (2.1) | 8 (1.9) | 8 (1.9) | 4 (0.9) | 0 | 2 (0.5) | 0 | 1 (0.2) | 3 (0.7) | 8 (1.9) |
| Engels *et al*[5] | 2011 | 37888 | 1563 | 365 (1.0) | NA | NA | 300 (0.8) | 67 (1.8) | NA | NA | NA | NA | 831 (2.2) |
| Chatrath *et al*[140] | 2013 | 534 | 80 | 16 (3.0) | 24 (4.5) | 9 (1.7) | 13 (2.4) | 1 (0.2) | 1 (0.2) | 1 (0.2) | NA | 1 (0.2) | 14 (2.6) |
| Schrem *et al*[141] | 2013 | 2000 | 120 | 23 (1.1) | NA | 11 (0.5) | 14 (0.7) | 7 (0.3) | 13 (0.6) | 5 (0.2) | 8 (0.4) | 10 (0.5) | 29 (1.4) |
| Krynitz *et al*[32] | 2013 | 1221 | 150 | 27 (2.2) | 58 (4.7) | 4 (0.3) | 6 (0.5) | 2 (0.1) | 6 (0.5) | 4 (0.3) | 7 (0.6) | 10 (0.8) | 26 (2.1) |
| Mouchli *et al*[62] | 2017 | 373 | 64 | 22 (5.9) | 5 (1.3) | NA | NA | 11 (2.9) | 11 (2.9) | 7 (1.9) | 5 (1.3) | 3 (0.8) | 0 |
| Egeli *et al*[142] | 2017 | 429 | 9 | NA | 1 (0.2) | 2 (0.4) | 5 (1.1) | NA | NA | NA | NA | NA | 1 (0.2) |
| Taborelli *et al*[143] | 2018 | 2832 | 266 | 37 (1.3) | 72 (2.5) | 34 (1.2) | 28 (1.0) | 4 (0.2) | 21 (0.7) | 2 (0.1) | 4 (0.2) | 3 (0.1) | 65 (2.1) |

NA: Not available; DNM: *De novo* malignancy; PTLD: Post-transplant lymphoproliferative disease.

A strong link between IS and DNM development is also found in the Kaposi sarcoma (KS), a multifocal angioproliferative muco-cutaneous tumor[27] that affects immunodeficient patients infected with human herpesvirus-8. However, in contrast with other DNMs[34,44,45], the KS incidence among the OLT population is constantly dropping. KS affects OLT patients around 500-fold more than the general population[27,44,46,47]. Thus, a tailored IS administration and a meticulous use of chemotherapy are crucial to avoid the outset of KS. Of note, a low blood viral concentration often limits the human herpesvirus-8 detection in most affected patients[34,48]. Typical KS diagnosis might also be missed by an inexperienced pathologist[49]. Even though there are ongoing trials on novel treatments for KS,

evidence suggests that switching the IS regimen from CsA/tacrolimus to mTORi represents the best option to reduce the growth of KS[44,49,50].

Head and neck cancer are less common, but they are still the most serious DNMs in the OLT population. Although no screening exam is approved to diagnose these malignancies[2,51], specific follow-up guidelines by the European Association for the Study of Liver highly recommended that smokers and former alcoholic OLT patients are screened[52]. A recent study by Piselli *et al*[53] on 2770 OLT recipients confirmed that these subjects are more prone to develop head and neck cancer especially in those with a previous history of smoking and alcoholic liver disease. The 5-year survival rate has been reported around 35% with a standardized incidence ratio (SIR) that increased to 11.2% in OLT subjects with alcoholic liver disease.

Tobacco seems to be involved in the development of pharyngeal and tongue cancer, whereas alcohol plays a predominant role in the onset of oropharyngeal and upper aerodigestive squamous tumors in OLT individuals[54,55]. Hence, regular screenings should be performed on ears, nose and throat especially if there is a prior history of smoking.

Lung cancer accounts about 26% of the total deaths related to post OLT DNMs[56]. In fact OLT recipients showed between two- and three-fold higher incidence than the general population[34]. Better outcomes in OLT subjects with no history of smoking were observed. Nevertheless, the survival rate in both OLT individuals and in the healthy population after being diagnosed with lung cancer was similar. Therefore, the major gamechanger is mainly represented by cigarette smoking[57].

OLT recipients have a high prevalence of colorectal malignancies usually diagnosed between the 1st and 4th year after OLT; the risk rises to 5.6% considering the PSC recipients[58]. Although the information about patients suffering from both PSC and inflammatory bowel disease are still scarce, the higher risk in developing colorectal malignancies has been well recognized[59,60] and a special surveillance in these patients is currently strongly recommended[61]. Moreover, after 5 years the risk goes up to 15%, and a closer follow up must be mandatory in order to early detect any tumour development[58,62,63]. Despite being identified at earlier stages, the prognosis of colorectal metastasis in OLT recipients is still worse than the general population mostly due to the IS regimens that reduce the immune cell activity[64,65].

OLT recipients did not show an overall increased risk of prostate cancer when compared to the general population[2,34,66,67]. Non-prostate genitourinary neoplasms are usually more lethal and develop earlier in OLT recipients. Renal malignancies after OLT have a SIR of 3.3, and annual ultrasound screenings after OLT are strongly encouraged[27,34].

Young OLT females under CsA-based IS are more likely to develop breast fibroadenomas compared to males[68,69]. In fact, CsA seems to: enhance the fibroblast activity; influence the hypothalamic-pituitary axis and interfere with the prolactin receptors on lymphocytes[34,70]. Furthermore, the capability of CsA to regulate the expression of pyruvate kinase M2 in different breast cancer cell lines is giving new insights about its role in cancer therapy[71]. A switch to tacrolimus is high advisable because the mass dimension seems to decrease in dimension after conversion[68,69]. Non-breast gynecological tumors are often more represented in the OLT patients than in the healthy population[27,72,73]. This might be explained by a pre-OLT stricter screening program towards breast cancer diagnosis that should also be more enforced in gynecological malignancies[27].

### *De novo malignancy in the pediatric OLT population*

DNMs account for 5%-16% of non-hepatic related deaths after pediatric OLT[74] and together with cardiovascular complications are becoming the major cause of late death after transplantation. In children, the risk of developing DNMs is 19-fold higher than adults, and tumors are more aggressive and less responsive to treatments[6]. Therefore, the early detection and prompt therapeutic management of DNMs in pediatric recipients is essential to achieve satisfactory results. As in adults, the major risk factors for DNMs after pediatric OLT include IS regimens as well as viral infections such as EBV, cytomegalovirus, human papilloma virus and human herpesvirus-8[75]. Due to the paucity of data in the pediatric population, data on DNMs after OLT in children are reported mainly in registry transplant studies including other solid organ (kidney, lung, heart)[76,77]. Therefore, records on the incidence and types of DNMs after pediatric OLT are limited to single case series and mainly related to PTLDs.

**PTLDs:** PTLDs are the most frequent DNMs after pediatric OLT with an incidence of 5%-20%. In 90%-95% of cases, PTLDs are related to EBV and cytomegalovirus infections[78]. The risk of developing PTLDs from EBV primary infections increases to 7-fold compared to the reactivation of a pre-existing infection[79,80]. Worldwide,

different series confirmed that EBV-related PTLDs were the most common DNM, ranging between 35% and 80% of all neoplasms either in liver and in kidney pediatric transplant recipients[76].

The subtypes of PTLDs might vary from benign polymorphic conditions to aggressive monomorphic states such as lymphomas. From a large registry analysis of DNMs after pediatric OLTs, non-Hodgkin's lymphoma is the most frequent (71%) type of PTLD, out of which nodal diffuse large-B cell lymphoma and Burkitt's lymphoma are the most detected, while Hodgkin's lymphoma and leukemia account for 8% and 4%, respectively[3]. Non-Hodgkin's lymphoma occurs mainly in younger patients: Estimated SIR is 123 (95% confidence interval 3.12-686) for children aged < 17 years old, 55.7 (95% confidence interval 6.74-201) for recipients aged between 17 and 39 years old and 9.42 (95% confidence interval 3.06-22.0) for patients ≥ 40 years old[81]. Several series suggest that donor-derived PTLD might be more likely to relapse in transplanted organs when compared with recipient-derived PTLD. In addition, donor-derived PTLD seems to appear earlier in the post-transplant period and present a more positive 5-year prognosis than the ones arising from recipients[81].

**Non-PTLD:** Non-PTLD neoplasms are rare in pediatric OLT recipients, so that, the incidence of non-PTLD malignancy is unclear due to paucity of data (Figure 2). Non-melanoma skin cancer is the most common non-PTLD DNMs represented mainly by squamous cell carcinomas[78]. Cases of melanomas have also been reported with a higher incidence than in adults. Other non-PTLDs include gynecologic neoplasms, KS, papillary thyroid tumors, sarcomas, brain tumors, renal cell carcinoma, liver tumors, testis neoplasms and bladder cancer.

The incidence of PTLD versus non-PTLD malignancies differs among age groups. Data from the Israel Penn International Transplant Tumor Registry[78] reported that children with post-transplant non-PTLD DNMs are older than recipients developing PTLD malignancies (13.2 *vs* 7.9 years of age, $P < 0.0001$). Moreover, from the time of transplantation, non-PTLD tumors are diagnosed within 99.2 months ($P < 0.0001$) while PTLD malignancies are detected within 60.2 months ($P < 0.0001$), and the latest to onset are usually vulvar and perineal cancer (113 mo)[78].

### *Modulation of risk: Immunosuppression features*

The Consensus on Managing Modifiable Risk in Transplantation group extensively described the main risk factors for graft loss in kidney and OLT recipients and provided useful recommendations to extend the long-term graft survival and to decrease the chances of DNMs onset[82]. IS drugs activate different pathways in the immune system and need to be carefully selected[83]. The primary disease needs to be considered in order to prescribe the most appropriate IS treatment. Of interest, mTORi might play a slight protective role reducing the incidence of DNMs especially within the 1st year of the transplant[84-86]. Similar data were described for mycophenolate mofetil[87]. The use of mTORi, mycophenolate mofetil, and tacrolimus represents the first choice when cancer develops in transplant recipients. There are no reports of such use of mTORi in the pediatric population. On the other hand, CNIs seem to have a cancer-promoting influence that might be related to their blood level concentration. Antilymphocyte medications also influence the onset of DNMs in long-lasting IS, while corticosteroids do not directly affect the risk of developing DNMs unless they are associated with chronic IS[88,89]. The association of multiple agents in lifelong IS regimens might be responsible for a substantially higher risk of DNMs. For these reasons, the discontinuation of IS (especially carcinogenic IS) should always be considered in transplant patients[88]. The primary aim is to achieve a COT status defined as a condition of non-reactivity of the immune system with a good graft function and no rejection in the absence of IS[90,91].

On the other hand, the non-compliance to IS considerably reduced the mid- and long-term survival of transplanted organs. It is estimated that about 10% of deaths or graft loss in adult OLT individuals were due to a poor compliance to the IS regimen[92,93]. Therefore, patients unintentionally or surreptitiously do not comply with IS regimens[94-96] due to the most disparate reasons are more likely to lose the graft. The cost and necessity of IS along with the prescribed dosage and the size of daily pills represents irresponsible behaviors that might compromise the patient compliance. Physicians should always be alerted for the possibility of these situations. For these reasons, it is important to establish a positive connection between the recipient and the healthcare provider[82,97].

Therefore, the spectrum of DNMs can also be reduced with a deeper understanding of the reasons for negligent conduct. Earlier studies demonstrated that patients already benefited from reminders of the importance of IS medication combined with counseling and psychological interventions[82,95,96]. Likewise, OLT individuals who do not regularly take daily medications face higher risks of graft rejection and elevated

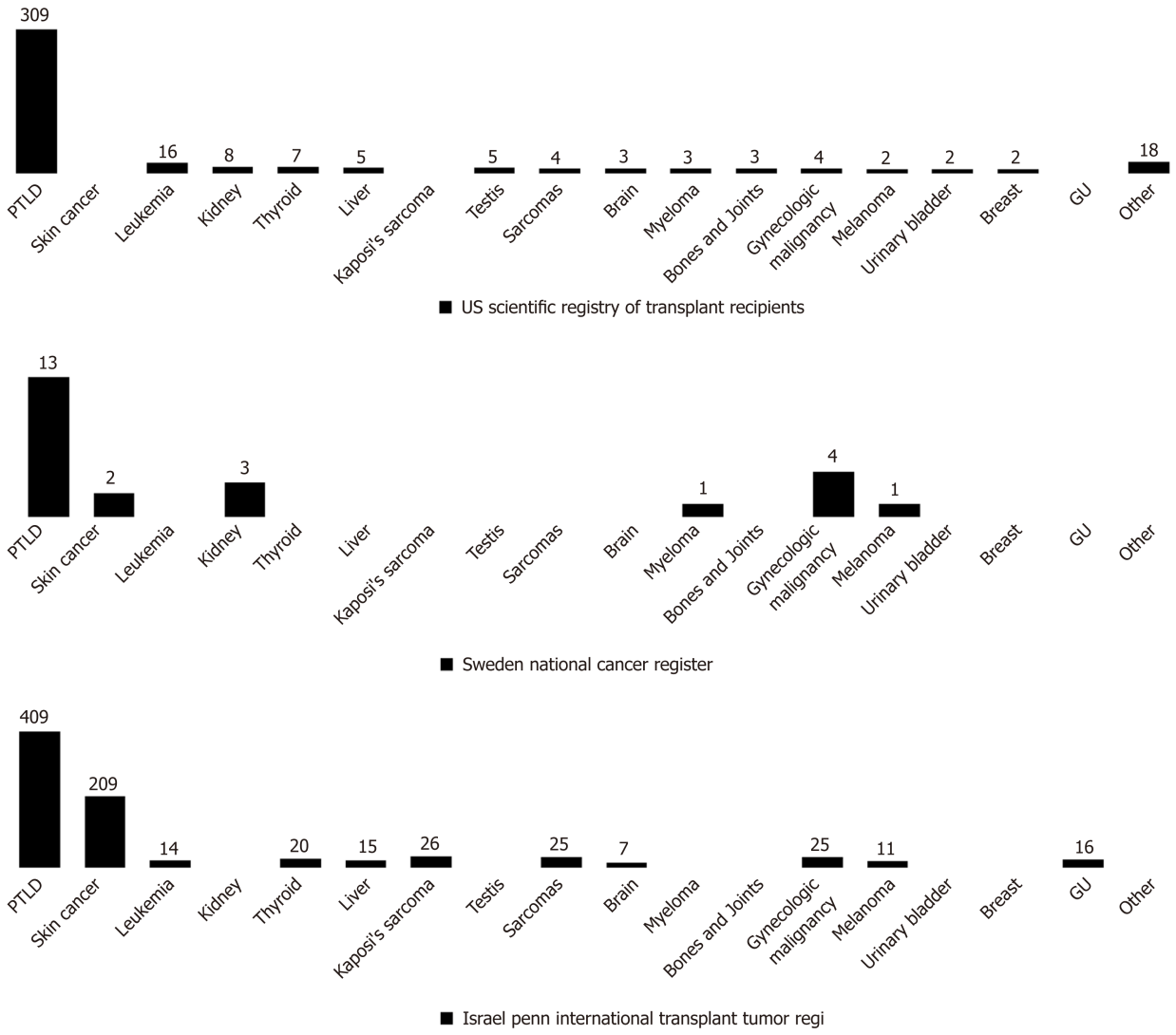


**Figure 2** ***De novo*** **malignancy distribution in three main cancer registries.**

chances of developing DNMs. Consequently, the IS withdrawal must be physician-driven and always under close clinical surveillance.

### *Role of immunosuppression minimization and withdrawal in liver transplant patients*

The "Holy Grail" of transplantation is the achievement of an IFS. As mentioned above, long-lasting IS exposes patients to multiple adverse effects such as infections, tumors and target organ damage. The paramount importance of COT in LT can be achieved in selected recipients starting from a cautious IS minimization and constantly monitoring the liver function tests (LFTs)[9,98]. Unfortunately, as shown in most series only 30% of well-selected LT recipients can be safely weaned from IS[9,98-101] (Table 2).

The molecular mechanisms responsible for graft acceptance still need to be fully understood, but the liver seems less likely to cause rejection in their hosts than other organs. Multiple theories were hypothesized: (1) The production of higher levels of major histocompatibility complex might affect the recipient immune response[102]; (2) An OLT donor leukocytes migrating in the recipient blood stream could influence the graft tolerance because their irradiation causes organ rejection[103]; and (3) Donor hematopoietic stem cells might determine a chimeric effect in the recipient[104]. Moreover, the huge amount of blood that is constantly flowing in the liver exposes it to plenty of bacteria and antigens that could enhance a COT status[90].

New insights on human leukocyte antigen donor-specific antibody/antibodies (DSA) are emerging in OLT recipients. A recent study described how the IS management and IS withdrawal protocols might affect the onset of *de novo* DSA (dnDSA) after OLT especially during the transition to IS monotherapy in the 1st year after the OLT[105]. Interestingly, a higher dnDSA prevalence was found in patients

**Table 2 Clinical operational tolerance literature and clinical trials in adult orthotopic liver transplant recipients[9,90]**

| First authors | Yr/Trial start | Number of patients | Complete IS weaning, % | Median follow-up mo from IS withdrawal | Rejection rate, for acute, % | Weaned patients due to DNM diagnosis |
|---|---|---|---|---|---|---|
| Ramos *et al*[110] | 1995 | 39 | 41 | 15 | 38.4 | None |
| Devlin *et al*[144] | 1998 | 18 | 27.8 | > 36 | 44.4 | None |
| Eason *et al*[145] | 2005 | 18 | 5.5 | 9 | 61.1 | None |
| Girlanda *et al*[146] | 2005 | 18 | 11 | 84 | 5.5 | None |
| Tisone *et al*[109] | 2006 | 34 | 23.4 | 45.5 ± 5.8 | 21.0 | None |
| Assy *et al*[147] | 2007 | 26 | 42 | 6 | 58.0 | None |
| Pons *et al*[148] | 2008 | 12 | 38.0 | 10-30 | 58.0 | None |
| Tryphonopoulos *et al*[149] | 2010 | 23 | 22.0 | 87 ± 3.0 | 5.0 | None |
| Manzia *et al*[106] | 2013 | 28 | 21.4 | 113 ± 20.0 | 21.0 | None |
| **De la Garza *et al*[150]** | 2013 | 24 | 62.5 | 14.0 | 37.5 | None |
| Benitez *et al*[151] | 2014 | 102 | 40.2 | 48.9 | 59.8 | None |
| Bohne *et al*[152] | 2014 | 34 | 50 | 12 | 44.1 | None |
| Todo *et al*[153] | 2016 | 10 | 70 | NA | 30.0 | None |
| Manzia *et al*[107] | 2018 | 75 | 42.6 | 78.5 | 0 | None |
| Shaked[154] | 2005 (clinical trial) | 275 | 20.3 | NA | 5.5 | None |
| Markman[155] | 2016 (ongoing trial) | 60 | NA | NA | NA | NA |
| Markman *et al*[156] | 2019 (ongoing trial) | NA | NA | NA | NA | NA |

NA: Not available; IS: Immunosuppression: DNM: *De novo* malignancy.

undergoing IS minimization (51.7%) and IS-free patients (66.7%). These findings suggest that monitoring dnDSA is high advisable and the IS minimization or withdrawal should be taken in consideration after at least 1 year from OLT in order to prevent negative consequences on the graft.

**The Tor Vergata experience:** In the last decade, our Liver Unit from Tor Vergata Institute described multiple trials attempting IS minimization and IS withdrawal after OLTs[9,10,90,106-109]. The first purpose was to minimize the uptake of IS drugs in the first years post-OLT. Afterwards, patients with stable LFTs, no rejection or autoimmune disease who underwent IS minimization were discontinued from IS. Initially, LFTs are monitored every week and then monthly within the 1st year during the IS withdrawal process[90]. IS was resumed in patients who had double the normal LFT levels during follow-up or when a liver biopsy showed features of acute rejection[90].

From April 1998 to December 2014, in the HPB and Transplant Unit, 299 OLT were performed. Of these, 65 (21.7%) patients with a mean follow-up of 81 months were considered for weaning protocol while 234 (78.2%, mean follow-up of 125.6 months) were under CNIs or mTORi and mycophenolate mofetil IS regimens. In unpublished series, data on DNMs were compared in order to address the differences in DNM incidence during a median follow-up of 4 years (Table 3).

Among the 65 recruited patients enrolled in local IS withdrawal protocol[106,108,109], 22 (33.8%) were successfully weaned from IS (tolerant; Tol), while 43 (66.2%) were non-tolerant (Non-Tol) and needed IS resumption after an observed upsurge of the LFTs or biopsy-proven acute rejection. In the Tol group, none experienced DNMs *versus* two (4.6%) in the Non-Tol group and thirty-two (13%) in the standard immunosuppressed recipients (Table 4). LT recipients under daily IS showed an increased relative risk of 4.45 of developing DNMs *versus* Tol and Non-Tol recipients and a SIR of 1.5 when compared to the general population.

**Role of immunosuppression minimization and withdrawal in pediatric OLT recipients:** Because chronic IS significantly affects the long-term outcomes of pediatric OLT recipients, children were the primary OLT population who experienced IS minimization and withdrawal protocols (Table 4).

Ramos *et al*[110] reported the first clinical trial of IS weaning where 20 pediatric patients underwent drug discontinuation for long-term IS complications (in two cases for *de novo* squamous cell carcinomas) reaching COT in 16 patients (27.1%). Takatsuki *et al*[111] reported the result of a prospective trial where a COT status was reached in 24

**Table 3 *De novo* malignancy features in orthotopic liver transplant recipients: The Tor Vergata experience between April 1998 and December 2014**

| | Patients under standard IS, *n* = 234Median age: 53.6 ± 7.1 yr | Tolerant patients, *n* = 22Median age: 52.3 ± 6.0 yr | Non-tolerant patients, *n* = 43Median age: 51.5 ± 9.6 yr |
|---|---|---|---|
| Number of patients | 234 | 22 | 43 |
| Median follow-up time from OLT to IS weaning, mo | - | 112.9 | 59.8 |
| Median follow-up time from weaning start to IS withdrawal, mo | - | 6.0 | 4.9 |
| Median follow-up time with no IS, mo | - | 92.3 | 2.3 |
| Median follow-up time after IS resumption, mo | - | - | 149.1 |
| Patients who developed DNMs, % | 13.7 | 0 | 6.4 |
| Median time from OLT to DNM development, mo | 44.5 | - | 113.0 |
| Incidence and type of DNMs | (*n* = 32) Lung (7) Head and neck (5) Colon (4) Oral cavity (4) PTLD (4) Genito-urinary (3) Esophagus (2) Liver (1) Mesothelioma (1) KS (1) | None | Bladder (1) Larynx (1) Lung (1) |

DNM: *De novo* malignancy; OLT: Orthotopic liver transplant; IS: Immunosuppression; PTLD: Post-transplant lymphoproliferative diseases; KS: Kaposi's sarcoma.

(38%) out of 63 children after ≥ 2 years from the OLT, and this promising COT rate remained similar in the subsequent trials from the same study group[112-114]. All tolerant patients had normal LFTs after 1-year follow-up, and no rejection episodes were reported. However, almost 6% of selected COT patients showed signs of allograft fibrosis at histological finding, driving the introduction of a protocol liver biopsy for patients undergoing IS withdrawal[115].

Hurwitz *et al*[116] described the only report focusing on the effects of IS withdrawal on DNMs after pediatric OLTs. Thirty-eight pediatric OLT recipients affected by PTLDs (*n* = 19) or severe EBV infection (*n* = 19) after a mean time of 1.8 ± 2.3 years and 1.1 ± 1.1 years from OLT, respectively, attempted IS withdrawal in combination with antiviral drugs with or without chemotherapy. A complete IS withdrawal was achieved in eight (21%) patients for 4.2 ± 1.7 years with an overall 84% survival rate. Episodes of rejection that did occur after stopping IS were successfully treated with standard therapy with no graft loss. Although the results are tempered by the intrinsic limitations of retrospective studies, the authors state that the mortality risk from cancer well outweighs the risk of graft loss due to acute rejection from IS withdrawal. Also, Lee *et al*[117] reported in his COT series another case of a successful IS weaning in a child with a *de novo* PTLD with a 3-year follow-up.

Feng *et al*[118] published the results from a pilot prospective multi-centric trial aiming to withdraw IS in order to reduce drug-related complications: Out of 20 pediatric OLT recipients attempting COT, 12 (60%) children successfully discontinued (over a period at least of 36 wk) IS, while 8 patients experienced rejection resolved by IS resumption. Recently, the authors reported that after a 5-year follow-up all COT recipients have normal LFTs and no histological inflammation or fibrosis, despite some patients were found with DSA and modest increases in sinusoidal C4d staining[119]. These promising results suggested that in selected pediatric OLT recipients, COT was feasible; yet selection criteria (such as clinical and biomarkers criteria) are needed to identify the children who could successfully attempt IS withdrawal. High rates (40%-42%) of successful COT were also reported by other series[120,121]. Likewise, Waki *et al*[120] demonstrated that Non-tol patients were associated with post-transplant human leukocyte antigen antibodies. This could represent a future screening criterion to select children who could discontinue IS regimen.

## DISCUSSION

The outset of DNMs in LT recipients seems to be connected to the IS regimen. In fact, IS drugs downregulate different pathways both of the adaptive and the innate immune response leading to a higher risk of tumor relapse after OLT. Hepatocellular carcinoma represents one of the indications for OLT. Due to the nature of the

**Table 4 Clinical operational tolerance trials in pediatric orthotopic liver transplant recipients**

| First author | Yr | Type of study | Number of patients | DNM-Patients indicated to withdraw IS | Complete IS weaning, % | Time interval: OLT to withdrawal, mo/yr | Rejection rate, for acute, % |
|---|---|---|---|---|---|---|---|
| Ramos *et al*[110] | 1995 | Prospective | 20 (12-20 yr at entry) (59 total patients) | 2 | 27.10% | > 5 yr | 20.3% |
| Mazariegos *et al*[157] | 1997 | Historical cohort (self-weaned) and prospective cases | 31 (≤ 20 yr) (100 total patients) | 12 | Pediatric cohort: 29% | > 5 yr | 10% |
| Takatsuki *et al*[111] | 2001 | Prospective | 63 | NA | 38.1% | ≥ 2 yr | 25.4% |
| Oike *et al*[112] | 2002 | Prospective | 115 | NA | 42.6% | ≥ 2 yr | 20% |
| Koshiba *et al*[113] | 2007 | Retrospective | 581 | NA | 15% | ≥ 2 yr | 1.5% |
| Ohe *et al*[114] | 2012 | Historical cohort | 190 | NA | 44.2% | ≥ 2 yr | 26.3% |
| Hurwitz *et al*[116] | 2004 | Retrospective | 38 | 19 (PTLD) | 21% ($n$ = 4 PTLD; $n$ = 4 EBV) | Mean time to PTLD onset: 1.8 ± 2.3 yr; Mean time to EBV infection onset: 1.1 ± 1.1 yr | 55.2% |
| Lee *et al*[117] | 2009 | Prospective | 5 | 1 (PTLD) | 100% | 1.2-2 yr | 0% |
| Feng *et al*[118,158] (WISP-R trial) | 2012 | Prospective | 20 | NA | 60% | ≥ 4 yr | 35% |
| Feng *et al*[159] (iWITH trial, partial results, 2016) | 2012 | Prospective | 88 | NA | 60% | ≥ 4 yr | 40% |
| Waki *et al*[120] | 2013 | Retrospective | 52 | NA | 42.5% | > 2 yr | 57.5% |
| Lin *et al*[121] | 2015 | Prospective | 16 | NA | 40% | > 2 yr | 40% |

OLT: Orthotopic liver transplant; DNM: *De novo* malignancy; IS: Immunosuppression; PTLD: Post-transplant lymphoproliferative diseases; EBV: Epstein-Barr virus; NA: Not available.

transplant indication itself, it would be beneficial to quickly tailor or withdraw IS because these recipients face a higher risk of recurrent hepatocellular carcinoma[90,122]. Thus, immediately after OLT, CNIs should be discontinued to minimize this threat as they seem more likely to trigger DNMs[123,124]. Conversely, mTORi seems to reduce the impact of DNMs at least within 5 years post-OLT[125].

The IS non-adherence must be always avoided due to its dangerous effects often underestimated in the overall graft longevity[126]. Nowadays, COT can be achieved in almost 30% of adult OLT individuals after a meticulous selection, but it is hard to accomplish for other solid organ transplant subjects because COT is organ dependent[127]. Strict criteria from the studies cited in Table 3 include IS regimens and IS drug blood levels, stable allograft function, no history of rejection or autoimmune diseases and a similar human leukocyte antigen match between donors and recipients. All these conditions need to be met in order to attempt COT. The accomplishment of a complete IFS in pediatric OLT recipients proved to be suitable in carefully designated patients albeit the heterogeneous considered cohorts. In fact, up to 60% of the total recipients were successfully withdrawn from IS while preserving a normal graft function.

Histological findings are as important as biochemical assessments in the definition of COT, even if not all studies reported liver biopsies features after weaning off IS. OLT recipients with normal LFTs might hide relevant graft inflammation or fibrosis that offset the risk of organ injury. In addition, modern studies stressed the relevance of histological features when outlining future trials. Considerations on graft fibrosis, independent from IS maintenance or withdrawal, need further investigations to fully understand the etiopathogenetic pathways involved. To the best of our knowledge, no clinical experience has been reported so far on IS withdrawal due to DNMs occurrence. Therefore, we can only speculate that the reconstitution of the immunological pathways can counteract the tumor growing.

The main drawback of the present review is that most COT studies explored have been fitted in order to address the possibility to achieve COT status and not in those who experienced DNMs. In fact, the majority of studies on IS withdrawal is referred

to patients who demonstrated a stable clinical pathway with normal LFTs and no rejection post-OLT. An international registry including all adult and pediatric IS weaning experiences might represent an interesting approach to both gain knowledge about the entity of DNMs in OLT subjects and the final outcomes after IS withdrawal in such patients.

The minimization of IS dosages would provide multiple beneficial aspects that include: (1) Releasing from all IS burdens; (2) Remarkable savings in IS drugs[107]; and (3) Increased quality of life after the reduction of daily medications, which can positively influence compliance and graft outcomes in long-term treatments[9,128]. COT immunological biomarkers are constantly researched because their clinical predictor role would represent a game changer in the transplantation field. The blood stream represents the most used source of non-invasive liver tolerance biomarkers due to its potential never-ending amount[129,130]. Unfortunately, the lack of consistent assays and validated biomarkers that might predict graft failure currently represent an arduous issue. Patients are in desperate need of alternative treatments to lifelong IS, and until reliable biomarkers are available the gold standard for rejection diagnosis is still represented by liver biopsies[131].

### Conclusion and future prospects

In the last few decades, there have been multiple efforts to reach an IFS in OLT recipients. These attempts might lead to ethical concerns as they shift to a potential unsafe option, which could raise future complications. Patients demand the best long-term quality of life after such a tough experience of an organ transplantation. Researchers methodically commit to fulfill this urgency, and physicians struggle to prevent the recurrence of physical and psychological complications that mainly result from the IS itself or from the primary disease recurrence.

A COT status perfectly frames the overarching goal of transplantation, which aims to provide the best quality of life for transplant recipients who would not be burdened by the IS threats while providing economic benefits. From these perspectives an IFS remains the most enticing path to follow and considered worth it in spite of all the challenges to overcome. Likewise, the relatively recent field of regenerative medicine is constantly gaining ground through new outstanding findings. Specifically, the astonishing capabilities of the extracellular matrix capable of closely emulating the ideal milieu of native organs enhancing cell growth, migration and proliferation is promising to offer innovative hints for future research[132,133].

We are still far away from a translational side of these results, but the immense potential of regenerative medicine surely represents a hope for future therapies and IS avoidance. More than 60 years ago the transplantation era began after the first successful transplantation was performed among identical twins, and the first case of COT was described. Since that moment, tolerance continues to be a grueling problem albeit remarkable steps were taken over the past decades. In fact, when experienced hands were called to action, undeniable evidence proved that a stable IFS is achievable in carefully selected OLT recipients. Clues that COT is no longer intangible is becoming clearer, and the concept that considered IS weaning protocols as detrimental procedures should be now considered out-of-date. However, an in-depth knowledge is certainly required as many immunological pathways responsible for COT still remain arcane, and crucial challenges about tolerance need to be addressed with further investigations.

## ARTICLE HIGHLIGHTS

### Research background

Immunosuppression (IS) has undoubtedly raised the overall positive outcomes in the post-operative management of solid organ transplantation. However, long-term exposure to IS is associated with critical systemic morbidities. *De novo* malignancies (DNMs) following orthotopic liver transplants (OLTs) are a serious threat in pediatric and adult transplant individuals. Data from different experiences were reported and compared to assess the connection between IS and DNMs in liver transplant patients.

### Research motivation

DNMs represent a major threat in OLT children and adults. Multiple experiences were described to analyze the connection between IS and DNMs in liver transplant patients. Different pathways seem to be involved in the incidence of DNMs, but molecular mechanisms are still unknown. Giving an answer to this concern might lead to a solution for the complications related to the long-term use of IS.

### Research objectives

To study the role of IS on the incidence of DNMs in liver transplant recipients.

### Research methods

A systematic literature examination of DNMs and IS weaning in adult and pediatric OLT recipients was described in the present review. Data from worldwide clinical trials was collected from highly qualified institutions performing OLTs. Patient follow-up, IS discontinuation and incidence of DNMs were reported. Likewise, the review assesses the differences in adult and pediatric recipients by describing the adopted IS regimens and the type of diagnosed solid and blood malignancy.

### Research results

Emerging evidence suggests that the liver is an immunologically privileged organ able to support IS discontinuation in carefully selected recipients. Malignancies are often detected in liver transplant patients undergoing daily IS regimens. Post-transplant lymphoproliferative diseases and skin tumors are the most detected DNMs in pediatric and adult OLT patients, respectively. To date, IS withdrawal has been achieved in 40% and 60% of well-selected adult and pediatric recipients, respectively. In both populations, a clear benefit of IS weaning protocols on DNMs is difficult to ascertain because data have not been specified in most of the clinical experiences.

### Research conclusions

The selected populations of tolerant pediatric and adult liver transplant recipients greatly benefit from IS weaning. There is still no strong clinical evidence on the usefulness of IS withdrawal in OLT recipients on malignancies. An interesting focus is represented by the complete reconstitution of the immunological pathways that could help in decreasing the incidence of DNMs and may also help in treating liver transplanted patients suffering from cancer.

### Research perspectives

Most of the current studies on IS withdrawal describe patients with a stable clinical pathway with normal liver function test levels and no history of rejection post-OLT. In the future, an international registry including all IS weaning experiences in OLT patients would offer a promising database to explore the connections between DNMs and the final outcomes after IS withdrawal in such patients. Seriate graft biopsies should always be considered in future studies to take into account the risk of graft fibrosis. Fibrosis is independent from IS maintenance or withdrawal, and further investigations are strongly suggested to fully understand the etiopathogenetic pathways involved. The minimization of IS dosages may decrease all IS complications and induce remarkable savings in IS drugs. Moreover, the recipient's quality of life after the reduction of daily medications could significantly boost their compliance and graft outcomes in the long-term. IS withdrawal is still arduous to realize. However, it is possible, and it is supported by the described cases of clinical operational tolerance in OLT individuals. In-depth investigations are needed to study the possibilities of achieving a complete IS-free state and clinical operational tolerance in OLT patients affected by DNMs because few studies explore this possibility. Regenerative medicine and clinical operational tolerance biomarkers are new promising frontiers that could provide novel insights about tolerance mechanisms in order to replace liver biopsies as the currently recognized gold standard method for rejection diagnosis.

## REFERENCES


1 **Asfar S**, Metrakos P, Fryer J, Verran D, Ghent C, Grant D, Bloch M, Burns P, Wall W. An analysis of late deaths after liver transplantation. *Transplantation* 1996; **61**: 1377-1381 [PMID: 8629300 DOI: 10.1097/00007890-199605150-00016]

2 **Herrero JI**. Screening of de novo tumors after liver transplantation. *J Gastroenterol Hepatol* 2012; **27**: 1011-1016 [PMID: 22098062 DOI: 10.1111/j.1440-1746.2011.06981.x]

3 **Yanik EL**, Smith JM, Shiels MS, Clarke CA, Lynch CF, Kahn AR, Koch L, Pawlish KS, Engels EA. Cancer Risk After Pediatric Solid Organ Transplantation. *Pediatrics* 2017; **139**: pii: e20163893 [PMID: 28557749 DOI: 10.1542/peds.2016-3893]

4 **Adami J**, Gäbel H, Lindelöf B, Ekström K, Rydh B, Glimelius B, Ekbom A, Adami HO, Granath F. Cancer risk following organ transplantation: A nationwide cohort study in Sweden. *Br J Cancer* 2003; **89**: 1221-1227 [PMID: 14520450 DOI: 10.1038/sj.bjc.6601219]

5 **Engels EA**, Pfeiffer RM, Fraumeni JF, Kasiske BL, Israni AK, Snyder JJ, Wolfe RA, Goodrich NP, Bayakly AR, Clarke CA, Copeland G, Finch JL, Fleissner ML, Goodman MT, Kahn A, Koch L, Lynch CF, Madeleine MM, Pawlish K, Rao C, Williams MA, Castenson D, Curry M, Parsons R, Fant G, Lin M. Spectrum of cancer risk among US solid organ transplant recipients. *JAMA* 2011; **306**: 1891-1901 [PMID: 22045767 DOI: 10.1001/jama.2011.1592]

6 **Zhou J**, Hu Z, Zhang Q, Li Z, Xiang J, Yan S, Wu J, Zhang M, Zheng S. Spectrum of De Novo Cancers and Predictors in Liver Transplantation: Analysis of the Scientific Registry of Transplant Recipients Database. *PLoS One* 2016; **11**: e0155179 [PMID: 27171501 DOI: 10.1371/journal.pone.0155179]

7 **Moris D**, Lu L, Qian S. Mechanisms of liver-induced tolerance. *Curr Opin Organ Transplant* 2017; **22**: 71-78 [PMID: 27984276 DOI: 10.1097/MOT.0000000000000380]

8 **Levitsky J**, Feng S. Tolerance in clinical liver transplantation. *Hum Immunol* 2018; **79**: 283-287 [PMID: 29054397 DOI: 10.1016/j.humimm.2017.10.007]

9 **Manzia TM**, Angelico R, Ciano P, Mugweru J, Owusu K, Sforza D, Toti L, Tisone G. Impact of immunosuppression minimization and withdrawal in long-term hepatitis C virus liver transplant recipients. *World J Gastroenterol* 2014; **20**: 12217-12225 [PMID: 25232255 DOI: 10.3748/wjg.v20.i34.12217]

10 **Manzia TM**, Angelico R, Toti L, Lai Q, Ciano P, Angelico M, Tisone G. Hepatitis C virus recurrence and immunosuppression-free state after liver transplantation. *Expert Rev Clin Immunol* 2012; **8**: 635-644 [PMID: 23078061 DOI: 10.1586/eci.12.66]

11 **Fung JJ**, Jain A, Kwak EJ, Kusne S, Dvorchik I, Eghtesad B. De novo malignancies after liver transplantation: A major cause of late death. *Liver Transpl* 2001; **7**: S109-S118 [PMID: 11689783 DOI: 10.1053/jlts.2001.28645]

12 **Yao FY**, Gautam M, Palese C, Rebres R, Terrault N, Roberts JP, Peters MG. De novo malignancies following liver transplantation: A case-control study with long-term follow-up. *Clin Transplant* 2006; **20**: 617-623 [PMID: 16968488 DOI: 10.1111/j.1399-0012.2006.00527.x]

13 **Pruthi J**, Medkiff KA, Esrason KT, Donovan JA, Yoshida EM, Erb SR, Steinbrecher UP, Fong TL. Analysis of causes of death in liver transplant recipients who survived more than 3 years. *Liver Transpl* 2001; **7**: 811-815 [PMID: 11552217 DOI: 10.1053/jlts.2001.27084]

14 **Penn I**. Posttransplantation de novo tumors in liver allograft recipients. *Liver Transpl Surg* 1996; **2**: 52-59 [PMID: 9346628 DOI: 10.1002/lt.500020109]

15 **Nuckols JD**, Baron PW, Stenzel TT, Olatidoye BA, Tuttle-Newhall JE, Clavien PA, Howell DN. The pathology of liver-localized post-transplant lymphoproliferative disease: A report of three cases and a review of the literature. *Am J Surg Pathol* 2000; **24**: 733-741 [PMID: 10800993 DOI: 10.1097/00000478-200005000-00013]

16 **Watt KD**, Pedersen RA, Kremers WK, Heimbach JK, Sanchez W, Gores GJ. Long-term probability of and mortality from de novo malignancy after liver transplantation. *Gastroenterology* 2009; **137**: 2010-2017 [PMID: 19766646 DOI: 10.1053/j.gastro.2009.08.070]

17 **Benlloch S**, Berenguer M, Prieto M, Moreno R, San Juan F, Rayón M, Mir J, Segura A, Berenguer J. De novo internal neoplasms after liver transplantation: Increased risk and aggressive behavior in recent years? *Am J Transplant* 2004; **4**: 596-604 [PMID: 15023152 DOI: 10.1111/j.1600-6143.2004.00380.x]

18 **Herrero JI**, España A, Quiroga J, Sangro B, Pardo F, Alvárez-Cienfuegos J, Prieto J. Nonmelanoma skin cancer after liver transplantation. Study of risk factors. *Liver Transpl* 2005; **11**: 1100-1106 [PMID: 16123952 DOI: 10.1002/lt.20525]

19 **Das R**, Kundu S, Laskar S, Choudhury Y, Ghosh SK. Assessment of DNA repair susceptibility genes identified by whole exome sequencing in head and neck cancer. *DNA Repair (Amst)* 2018; **66-67**: 50-63 [PMID: 29747023 DOI: 10.1016/j.dnarep.2018.04.005]

20 **Jiang Y**, Villeneuve PJ, Fenton SS, Schaubel DE, Lilly L, Mao Y. Liver transplantation and subsequent risk of cancer: Findings from a Canadian cohort study. *Liver Transpl* 2008; **14**: 1588-1597 [PMID: 18975293 DOI: 10.1002/lt.21554]

21 **Bakker NA**, van Imhoff GW, Verschuuren EA, van Son WJ. Presentation and early detection of post-transplant lymphoproliferative disorder after solid organ transplantation. *Transpl Int* 2007; **20**: 207-218 [PMID: 17291214 DOI: 10.1111/j.1432-2277.2006.00416.x]

22 **Dierickx D**, Tousseyn T, De Wolf-Peeters C, Pirenne J, Verhoef G. Management of posttransplant lymphoproliferative disorders following solid organ transplant: An update. *Leuk Lymphoma* 2011; **52**: 950-961 [PMID: 21338285 DOI: 10.3109/10428194.2011.557453]

23 **Mizuno S**, Hayasaki A, Ito T, Fujii T, Iizawa Y, Kato H, Murata Y, Tanemura A, Kuriyama N, Azumi Y, Kishiwada M, Usui M, Sakurai H, Isaji S. De Novo Malignancy Following Adult-to-Adult Living Donor Liver Transplantation Focusing on Posttransplantation Lymphoproliferative Disorder. *Transplant Proc* 2018; **50**: 2699-2704 [PMID: 30401380 DOI: 10.1016/j.transproceed.2018.03.059]

24 **Shroff R**, Rees L. The post-transplant lymphoproliferative disorder-a literature review. *Pediatr Nephrol* 2004; **19**: 369-377 [PMID: 14986084 DOI: 10.1007/s00467-003-1392-x]

25 **Jain A**, Nalesnik M, Reyes J, Pokharna R, Mazariegos G, Green M, Eghtesad B, Marsh W, Cacciarelli T, Fontes P, Abu-Elmagd K, Sindhi R, Demetris J, Fung J. Posttransplant lymphoproliferative disorders in liver transplantation: A 20-year experience. *Ann Surg* 2002; **236**: 429-36; discussion 436-7 [PMID: 12368671 DOI: 10.1097/00000658-200210000-00005]

26 **Kremers WK**, Devarbhavi HC, Wiesner RH, Krom RA, Macon WR, Habermann TM. Post-transplant lymphoproliferative disorders following liver transplantation: Incidence, risk factors and survival. *Am J Transplant* 2006; **6**: 1017-1024 [PMID: 16611339 DOI: 10.1111/j.1600-6143.2006.01294.x]

27 **Burra P**, Rodriguez-Castro KI. Neoplastic disease after liver transplantation: Focus on de novo neoplasms. *World J Gastroenterol* 2015; **21**: 8753-8768 [PMID: 26269665 DOI: 10.3748/wjg.v21.i29.8753]

28 **Dantal J**, Soulillou JP. Immunosuppressive drugs and the risk of cancer after organ transplantation. *N Engl J Med* 2005; **352**: 1371-1373 [PMID: 15800234 DOI: 10.1056/NEJMe058018]

29 **Newell KA**, Alonso EM, Whitington PF, Bruce DS, Millis JM, Piper JB, Woodle ES, Kelly SM, Koeppen H, Hart J, Rubin CM, Thistlethwaite JR. Posttransplant lymphoproliferative disease in pediatric liver transplantation. Interplay between primary Epstein-Barr virus infection and immunosuppression. *Transplantation* 1996; **62**: 370-375 [PMID: 8779685 DOI: 10.1097/00007890-199608150-00012]

30 **Eshraghian A**, Imanieh MH, Dehghani SM, Nikeghbalian S, Shamsaeefar A, Barshans F, Kazemi K, Geramizadeh B, Malek-Hosseini SA. Post-transplant lymphoproliferative disorder after liver transplantation: Incidence, long-term survival and impact of serum tacrolimus level. *World J Gastroenterol* 2017; **23**: 1224-1232 [PMID: 28275302 DOI: 10.3748/wjg.v23.i7.1224]

31 **Ducroux E**, Boillot O, Ocampo MA, Decullier E, Roux A, Dumortier J, Kanitakis J, Jullien D, Euvrard S. Skin cancers after liver transplantation: Retrospective single-center study on 371 recipients. *Transplantation* 2014; **98**: 335-340 [PMID: 24621534 DOI: 10.1097/TP.0000000000000051]

32 **Krynitz B**, Edgren G, Lindelöf B, Baecklund E, Brattström C, Wilczek H, Smedby KE. Risk of skin cancer and other malignancies in kidney, liver, heart and lung transplant recipients 1970 to 2008--a Swedish population-based study. *Int J Cancer* 2013; **132**: 1429-1438 [PMID: 22886725 DOI: 10.1002/ijc.27765]

33 **Tran M**, Sander M, Ravani P, Mydlarski PR. Incidence of melanoma in organ transplant recipients in Alberta, Canada. *Clin Transplant* 2016; **30**: 1271-1275 [PMID: 27448204 DOI: 10.1111/ctr.12818]

34 **Burra P**, Shalaby S, Zanetto A. Long-term care of transplant recipients: De novo neoplasms after liver transplantation. *Curr Opin Organ Transplant* 2018; **23**: 187-195 [PMID: 29324517 DOI: 10.1097/MOT.0000000000000499]

35 **Herrero JI**, España A, D'Avola D, Pardo F, Iñarrairaegui M, Rotellar F, Sangro B, Quiroga J. Subsequent nonmelanoma skin cancer after liver transplantation. *Transplant Proc* 2012; **44**: 1568-1570 [PMID: 22841216 DOI: 10.1016/j.transproceed.2012.05.005]

36 **Euvrard S**, Kanitakis J, Claudy A. Skin cancers after organ transplantation. *N Engl J Med* 2003; **348**: 1681-1691 [PMID: 12711744 DOI: 10.1056/NEJMra022137]

37 **Rademacher S**, Seehofer D, Eurich D, Schoening W, Neuhaus R, Oellinger R, Denecke T, Pascher A, Schott E, Sinn M, Neuhaus P, Pratschke J. The 28-year incidence of de novo malignancies after liver

transplantation: A single-center analysis of risk factors and mortality in 1616 patients. *Liver Transpl* 2017; **23**: 1404-1414 [PMID: 28590598 DOI: 10.1002/lt.24795]
38 **Jiyad Z**, Olsen CM, Burke MT, Isbel NM, Green AC. Azathioprine and Risk of Skin Cancer in Organ Transplant Recipients: Systematic Review and Meta-Analysis. *Am J Transplant* 2016; **16**: 3490-3503 [PMID: 27163483 DOI: 10.1111/ajt.13863]
39 **Santana AL**, Felsen D, Carucci JA. Interleukin-22 and Cyclosporine in Aggressive Cutaneous Squamous Cell Carcinoma. *Dermatol Clin* 2017; **35**: 73-84 [PMID: 27890239 DOI: 10.1016/j.det.2016.07.003]
40 **Berg D**, Otley CC. Skin cancer in organ transplant recipients: Epidemiology, pathogenesis, and management. *J Am Acad Dermatol* 2002; **47**: 1-17; quiz 18-20 [PMID: 12077575 DOI: 10.1067/mjd.2002.125579]
41 **Carroll RP**, Ramsay HM, Fryer AA, Hawley CM, Nicol DL, Harden PN. Incidence and prediction of nonmelanoma skin cancer post-renal transplantation: A prospective study in Queensland, Australia. *Am J Kidney Dis* 2003; **41**: 676-683 [PMID: 12612993 DOI: 10.1053/ajkd.2003.50130]
42 **Otley CC**, Cherikh WS, Salasche SJ, McBride MA, Christenson LJ, Kauffman HM. Skin cancer in organ transplant recipients: Effect of pretransplant end-organ disease. *J Am Acad Dermatol* 2005; **53**: 783-790 [PMID: 16243126 DOI: 10.1016/j.jaad.2005.07.061]
43 **Mithoefer AB**, Supran S, Freeman RB. Risk factors associated with the development of skin cancer after liver transplantation. *Liver Transpl* 2002; **8**: 939-944 [PMID: 12360438 DOI: 10.1053/jlts.2002.35551]
44 **Piselli P**, Busnach G, Citterio F, Frigerio M, Arbustini E, Burra P, Pinna AD, Bresadola V, Ettorre GM, Baccarani U, Buda A, Lauro A, Zanus G, Cimaglia C, Spagnoletti G, Lenardon A, Agozzino M, Gambato M, Zanfi C, Miglioresi L, Di Gioia P, Mei L, Ippolito G, Serraino D; Immunosuppression and Cancer Study Group. Risk of Kaposi sarcoma after solid-organ transplantation: Multicenter study in 4,767 recipients in Italy, 1970-2006. *Transplant Proc* 2009; **41**: 1227-1230 [PMID: 19460525 DOI: 10.1016/j.transproceed.2009.03.009]
45 **Piselli P**, Taborelli M, Cimaglia C, Serraino D; Italian Transplant & Cancer Cohort Study. Decreased incidence of Kaposi sarcoma after kidney transplant in Italy and role of mTOR-inhibitors: 1997-2016. *Int J Cancer* 2019; **145**: 597-598 [PMID: 30613958 DOI: 10.1002/ijc.32098]
46 **Berber I**, Altaca G, Aydin C, Dural A, Kara VM, Yigit B, Turkmen A, Titiz MI. Kaposi's sarcoma in renal transplant patients: Predisposing factors and prognosis. *Transplant Proc* 2005; **37**: 967-968 [PMID: 15848593 DOI: 10.1016/j.transproceed.2004.12.034]
47 **Euvrard S**, Kanitakis J. Skin cancers after liver transplantation: What to do? *J Hepatol* 2006; **44**: 27-32 [PMID: 16290909 DOI: 10.1016/j.jhep.2005.10.010]
48 **Haq IU**, Dalla Pria A, Papanastasopoulos P, Stegmann K, Bradshaw D, Nelson M, Bower M. The clinical application of plasma Kaposi sarcoma herpesvirus viral load as a tumour biomarker: Results from 704 patients. *HIV Med* 2016; **17**: 56-61 [PMID: 26111246 DOI: 10.1111/hiv.12273]
49 **Schneider JW**, Dittmer DP. Diagnosis and Treatment of Kaposi Sarcoma. *Am J Clin Dermatol* 2017; **18**: 529-539 [PMID: 28324233 DOI: 10.1007/s40257-017-0270-4]
50 **Stallone G**, Schena A, Infante B, Di Paolo S, Loverre A, Maggio G, Ranieri E, Gesualdo L, Schena FP, Grandaliano G. Sirolimus for Kaposi's sarcoma in renal-transplant recipients. *N Engl J Med* 2005; **352**: 1317-1323 [PMID: 15800227 DOI: 10.1056/NEJMoa042831]
51 **Jain A**, Patil VP, Fung J. Incidence of de novo cancer and lymphoproliferative disorders after liver transplantation in relation to age and duration of follow-up. *Liver Transpl* 2008; **14**: 1406-1411 [PMID: 18825680 DOI: 10.1002/lt.21609]
52 **European Association for the Study of the Liver**. EASL Clinical Practice Guidelines: Liver transplantation. *J Hepatol* 2016; **64**: 433-485 [PMID: 26597456 DOI: 10.1016/j.jhep.2015.10.006]
53 **Piselli P**, Burra P, Lauro A, Baccarani U, Ettorre GM, Vizzini GB, Rendina M, Rossi M, Tisone G, Zamboni F, Bortoluzzi I, Pinna AD, Risaliti A, Galatioto L, Vennarecci G, Di Leo A, Nudo F, Sforza D, Fantola G, Cimaglia C, Verdirosi D, Virdone S, Serraino D; Italian Transplant and Cancer Cohort Study. Head and neck and esophageal cancers after liver transplant: Results from a multicenter cohort study. Italy, 1997-2010. *Transpl Int* 2015; **28**: 841-848 [PMID: 25778395 DOI: 10.1111/tri.12555]
54 **Bellamy CO**, DiMartini AM, Ruppert K, Jain A, Dodson F, Torbenson M, Starzl TE, Fung JJ, Demetris AJ. Liver transplantation for alcoholic cirrhosis: Long term follow-up and impact of disease recurrence. *Transplantation* 2001; **72**: 619-626 [PMID: 11544420 DOI: 10.1097/00007890-200108270-00010]
55 **Jain A**, DiMartini A, Kashyap R, Youk A, Rohal S, Fung J. Long-term follow-up after liver transplantation for alcoholic liver disease under tacrolimus. *Transplantation* 2000; **70**: 1335-1342 [PMID: 11087149 DOI: 10.1097/00007890-200011150-00012]
56 **Daniel KE**, Eickhoff J, Lucey MR. Why do patients die after a liver transplantation? *Clin Transplant* 2017; 31 [PMID: 28039946 DOI: 10.1111/ctr.12906]
57 **Kocher F**, Finkenstedt A, Fiegl M, Graziadei I, Gamerith G, Oberaigner W, Vogel W, Hilbe W. Liver Transplantation-Associated Lung Cancer: Comparison of Clinical Parameters and Outcomes. *Clin Lung Cancer* 2015; **16**: e75-e81 [PMID: 25783479 DOI: 10.1016/j.cllc.2015.02.003]
58 **Vera A**, Gunson BK, Ussatoff V, Nightingale P, Candinas D, Radley S, Mayer A, Buckels JA, McMaster P, Neuberger J, Mirza DF. Colorectal cancer in patients with inflammatory bowel disease after liver transplantation for primary sclerosing cholangitis. *Transplantation* 2003; **75**: 1983-1988 [PMID: 12829898 DOI: 10.1097/01.Tp.0000058744.34965.38]
59 **Brentnall TA**, Haggitt RC, Rabinovitch PS, Kimmey MB, Bronner MP, Levine DS, Kowdley KV, Stevens AC, Crispin DA, Emond M, Rubin CE. Risk and natural history of colonic neoplasia in patients with primary sclerosing cholangitis and ulcerative colitis. *Gastroenterology* 1996; **110**: 331-338 [PMID: 8566577 DOI: 10.1053/gast.1996.v110.pm8566577]
60 **Higashi H**, Yanaga K, Marsh JW, Tzakis A, Kakizoe S, Starzl TE. Development of colon cancer after liver transplantation for primary sclerosing cholangitis associated with ulcerative colitis. *Hepatology* 1990; **11**: 477-480 [PMID: 2312061 DOI: 10.1002/hep.1840110320]
61 **Lindor KD**, Kowdley KV, Harrison ME; American College of Gastroenterology. ACG Clinical Guideline: Primary Sclerosing Cholangitis. *Am J Gastroenterol* 2015; **110**: 646-59; quiz 660 [PMID: 25869391 DOI: 10.1038/ajg.2015.112]
62 **Mouchli MA**, Singh S, Loftus EV, Boardman L, Talwalkar J, Rosen CB, Heimbach JK, Wiesner RH, Hasan B, Poterucha JJ, Kymberly WD. Risk Factors and Outcomes of De Novo Cancers (Excluding Nonmelanoma Skin Cancer) After Liver Transplantation for Primary Sclerosing Cholangitis. *Transplantation* 2017; **101**: 1859-1866 [PMID: 28272287 DOI: 10.1097/TP.0000000000001725]
63 **Singh S**, Loftus EV, Talwalkar JA. Inflammatory bowel disease after liver transplantation for primary sclerosing cholangitis. *Am J Gastroenterol* 2013; **108**: 1417-1425 [PMID: 23896954 DOI:

10.1038/ajg.2013.163]
64 **Buell JF**, Papaconstantinou HT, Skalow B, Hanaway MJ, Alloway RR, Woodle ES. De novo colorectal cancer: Five-year survival is markedly lower in transplant recipients compared with the general population. *Transplant Proc* 2005; **37**: 960-961 [PMID: 15848590 DOI: 10.1016/j.transproceed.2004.12.122]
65 **Johnson EE**, Leverson GE, Pirsch JD, Heise CP. A 30-year analysis of colorectal adenocarcinoma in transplant recipients and proposal for altered screening. *J Gastrointest Surg* 2007; **11**: 272-279 [PMID: 17458597 DOI: 10.1007/s11605-007-0084-4]
66 **Carenco C**, Faure S, Herrero A, Assenat E, Duny Y, Danan G, Bismuth M, Chanques G, Ursic-Bedoya J, Jaber S, Larrey D, Navarro F, Pageaux GP. Incidence of solid organ cancers after liver transplantation: Comparison with regional cancer incidence rates and risk factors. *Liver Int* 2015; **35**: 1748-1755 [PMID: 25488375 DOI: 10.1111/liv.12758]
67 **Nordin A**, Åberg F, Pukkala E, Pedersen CR, Storm HH, Rasmussen A, Bennet W, Olausson M, Wilczek H, Ericzon BG, Tretli S, Line PD, Karlsen TH, Boberg KM, Isoniemi H. Decreasing incidence of cancer after liver transplantation-A Nordic population-based study over 3 decades. *Am J Transplant* 2018; **18**: 952-963 [PMID: 28925583 DOI: 10.1111/ajt.14507]
68 **Tanaka N**, Ueno T, Takama Y, Yamanaka H, Tazuke Y, Bessho K, Okuyama H. Fibroadenoma in adolescent females after living donor liver transplantation. *Pediatr Transplant* 2017; 21 [PMID: 28556594 DOI: 10.1111/petr.12947]
69 **Iaria G**, Pisani F, De Luca L, Sforza D, Manuelli M, Perrone L, Bellini I, Angelico R, Tisone G. Prospective study of switch from cyclosporine to tacrolimus for fibroadenomas of the breast in kidney transplantation. *Transplant Proc* 2010; **42**: 1169-1170 [PMID: 20534252 DOI: 10.1016/j.transproceed.2010.03.035]
70 **Foxwell BM**, Woerly G, Husi H, Mackie A, Quesniaux VF, Hiestand PC, Wenger RM, Ryffel B. Identification of several cyclosporine binding proteins in lymphoid and non-lymphoid cells in vivo. *Biochim Biophys Acta* 1992; **1138**: 115-121 [PMID: 1540657 DOI: 10.1016/0925-4439(92)90050-W]
71 **Jiang K**, He B, Lai L, Chen Q, Liu Y, Guo Q, Wang Q. Cyclosporine A inhibits breast cancer cell growth by downregulating the expression of pyruvate kinase subtype M2. *Int J Mol Med* 2012; **30**: 302-308 [PMID: 22580449 DOI: 10.3892/ijmm.2012.989]
72 **Jonas S**, Rayes N, Neumann U, Neuhaus R, Bechstein WO, Guckelberger O, Tullius SG, Serke S, Neuhaus P. De novo malignancies after liver transplantation using tacrolimus-based protocols or cyclosporine-based quadruple immunosuppression with an interleukin-2 receptor antibody or antithymocyte globulin. *Cancer* 1997; **80**: 1141-1150 [PMID: 9305716 DOI: 10.1002/(SICI)1097-0142(19970915)80:6<1141::AID-CNCR18>3.0.CO;2-8]
73 **Saigal S**, Norris S, Muiesan P, Rela M, Heaton N, O'Grady J. Evidence of differential risk for posttransplantation malignancy based on pretransplantation cause in patients undergoing liver transplantation. *Liver Transpl* 2002; **8**: 482-487 [PMID: 12004349 DOI: 10.1053/jlts.2002.32977]
74 **Soltys KA**, Mazariegos GV, Squires RH, Sindhi RK, Anand R; SPLIT Research Group. Late graft loss or death in pediatric liver transplantation: An analysis of the SPLIT database. *Am J Transplant* 2007; **7**: 2165-2171 [PMID: 17608834 DOI: 10.1111/j.1600-6143.2007.01893.x]
75 **Simard JF**, Baecklund E, Kinch A, Brattström C, Ingvar A, Molin D, Adami J, Fernberg P, Wilczek H, Ekbom A, Smedby KE. Pediatric organ transplantation and risk of premalignant and malignant tumors in Sweden. *Am J Transplant* 2011; **11**: 146-151 [PMID: 21199354 DOI: 10.1111/j.1600-6143.2010.03367.x]
76 **Debray D**, Baudouin V, Lacaille F, Charbit M, Rivet C, Harambat J, Iserin F, Di Filippo S, Guyot C; Pediatric Transplantation Working Group of the French Speaking Society of Transplantation. De novo malignancy after solid organ transplantation in children. *Transplant Proc* 2009; **41**: 674-675 [PMID: 19328954 DOI: 10.1016/j.transproceed.2008.12.020]
77 **Karakoyun M, Önen Ş, Baran M, Çakır M, Ömür Ecevit Ç, Kılıç M, Kantar M, Aksoylar S, Özgenç F, Aydoğdu S**. Post-transplant malignancies in pediatric liver transplant recipients: Experience of two centers in Turkey. *Turk J Gastroenterol* 2018; **29**: 89-93 [PMID: 29391313 DOI: 10.5152/tjg.2017.17089]
78 **Buell JF**, Gross TG, Thomas MJ, Neff G, Muthiah C, Alloway R, Ryckman FC, Tiao GM, Woodle ES. Malignancy in pediatric transplant recipients. *Semin Pediatr Surg* 2006; **15**: 179-187 [PMID: 16818139 DOI: 10.1053/j.sempedsurg.2006.03.005]
79 **Aucejo F**, Rofaiel G, Miller C. Who is at risk for post-transplant lymphoproliferative disorders (PTLD) after liver transplantation? *J Hepatol* 2006; **44**: 19-23 [PMID: 16298453 DOI: 10.1016/j.jhep.2005.10.008]
80 **Mynarek M**, Schober T, Behrends U, Maecker-Kolhoff B. Posttransplant lymphoproliferative disease after pediatric solid organ transplantation. *Clin Dev Immunol* 2013; **2013**: 814973 [PMID: 24174972 DOI: 10.1155/2013/814973]
81 **Aberg F**, Pukkala E, Höckerstedt K, Sankila R, Isoniemi H. Risk of malignant neoplasms after liver transplantation: A population-based study. *Liver Transpl* 2008; **14**: 1428-1436 [PMID: 18825704 DOI: 10.1002/lt.21475]
82 **Neuberger JM**, Bechstein WO, Kuypers DR, Burra P, Citterio F, De Geest S, Duvoux C, Jardine AG, Kamar N, Krämer BK, Metselaar HJ, Nevens F, Pirenne J, Rodríguez-Perálvarez ML, Samuel D, Schneeberger S, Serón D, Trunečka P, Tisone G, van Gelder T. Practical Recommendations for Long-term Management of Modifiable Risks in Kidney and Liver Transplant Recipients: A Guidance Report and Clinical Checklist by the Consensus on Managing Modifiable Risk in Transplantation (COMMIT) Group. *Transplantation* 2017; **101**: S1-S56 [PMID: 28328734 DOI: 10.1097/TP.0000000000001651]
83 **Rodríguez-Perálvarez M**, De la Mata M, Burroughs AK. Liver transplantation: Immunosuppression and oncology. *Curr Opin Organ Transplant* 2014; **19**: 253-260 [PMID: 24685671 DOI: 10.1097/MOT.0000000000000069]
84 **Alberú J**, Pascoe MD, Campistol JM, Schena FP, Rial Mdel C, Polinsky M, Neylan JF, Korth-Bradley J, Goldberg-Alberts R, Maller ES; Sirolimus CONVERT Trial Study Group. Lower malignancy rates in renal allograft recipients converted to sirolimus-based, calcineurin inhibitor-free immunotherapy: 24-month results from the CONVERT trial. *Transplantation* 2011; **92**: 303-310 [PMID: 21792049 DOI: 10.1097/TP.0b013e3182247ae2]
85 **Kauffman HM**, Cherikh WS, Cheng Y, Hanto DW, Kahan BD. Maintenance immunosuppression with target-of-rapamycin inhibitors is associated with a reduced incidence of de novo malignancies. *Transplantation* 2005; **80**: 883-889 [PMID: 16249734 DOI: 10.1097/01.TP.0000184006.43152.8D]
86 **Thimonier E**, Guillaud O, Walter T, Decullier E, Vallin M, Boillot O, Dumortier J. Conversion to everolimus dramatically improves the prognosis of de novo malignancies after liver transplantation for alcoholic liver disease. *Clin Transplant* 2014; **28**: 1339-1348 [PMID: 25081431 DOI: 10.1111/ctr.12430]
87 **Kaltenborn A**, Schrem H. Mycophenolate mofetil in liver transplantation: A review. *Ann Transplant*

2013; **18**: 685-696 [PMID: 24346057 DOI: 10.12659/AOT.889299]
88 **Bhat M**, Mara K, Dierkhising R, Watt KDS. Immunosuppression, Race, and Donor-Related Risk Factors Affect De novo Cancer Incidence Across Solid Organ Transplant Recipients. *Mayo Clin Proc* 2018; **93**: 1236-1246 [PMID: 30064826 DOI: 10.1016/j.mayocp.2018.04.025]
89 **Zhu H**, Sun Q, Tan C, Xu M, Dai Z, Wang Z, Fan J, Zhou J. Tacrolimus promotes hepatocellular carcinoma and enhances CXCR4/SDF1α expression in vivo. *Mol Med Rep* 2014; **10**: 585-592 [PMID: 24912495 DOI: 10.3892/mmr.2014.2302]
90 **Angelico R**, Parente A, Manzia TM. Using a weaning immunosuppression protocol in liver transplantation recipients with hepatocellular carcinoma: A compromise between the risk of recurrence and the risk of rejection? *Transl Gastroenterol Hepatol* 2017; **2**: 74 [PMID: 29034347 DOI: 10.21037/tgh.2017.08.07]
91 **Lerut J**, Sanchez-Fueyo A. An appraisal of tolerance in liver transplantation. *Am J Transplant* 2006; **6**: 1774-1780 [PMID: 16889539 DOI: 10.1111/j.1600-6143.2006.01396.x]
92 **De Geest S**, Burkhalter H, Bogert L, Berben L, Glass TR, Denhaerynck K; Psychosocial Interest Group; Swiss Transplant Cohort Study. Describing the evolution of medication nonadherence from pretransplant until 3 years post-transplant and determining pretransplant medication nonadherence as risk factor for post-transplant nonadherence to immunosuppressives: The Swiss Transplant Cohort Study. *Transpl Int* 2014; **27**: 657-666 [PMID: 24628915 DOI: 10.1111/tri.12312]
93 **O'Carroll RE**, McGregor LM, Swanson V, Masterton G, Hayes PC. Adherence to medication after liver transplantation in Scotland: A pilot study. *Liver Transpl* 2006; **12**: 1862-1868 [PMID: 16773637 DOI: 10.1002/lt.20828]
94 **Griva K**, Davenport A, Harrison M, Newman SP. Non-adherence to immunosuppressive medications in kidney transplantation: Intent vs. forgetfulness and clinical markers of medication intake. *Ann Behav Med* 2012; **44**: 85-93 [PMID: 22454221 DOI: 10.1007/s12160-012-9359-4]
95 **De Bleser L**, Dobbels F, Berben L, Vanhaecke J, Verleden G, Nevens F, De Geest S. The spectrum of nonadherence with medication in heart, liver, and lung transplant patients assessed in various ways. *Transpl Int* 2011; **24**: 882-891 [PMID: 21740471 DOI: 10.1111/j.1432-2277.2011.01296.x]
96 **Prendergast MB**, Gaston RS. Optimizing medication adherence: An ongoing opportunity to improve outcomes after kidney transplantation. *Clin J Am Soc Nephrol* 2010; **5**: 1305-1311 [PMID: 20448067 DOI: 10.2215/CJN.07241009]
97 **Tielen M**, van Exel J, Laging M, Beck DK, Khemai R, van Gelder T, Betjes MG, Weimar W, Massey EK. Attitudes to medication after kidney transplantation and their association with medication adherence and graft survival: A 2-year follow-up study. *J Transplant* 2014; **2014**: 675301 [PMID: 24868449 DOI: 10.1155/2014/675301]
98 **Orlando G**, Soker S, Wood K. Operational tolerance after liver transplantation. *J Hepatol* 2009; **50**: 1247-1257 [PMID: 19394103 DOI: 10.1016/j.jhep.2009.03.006]
99 **Orlando G**. Finding the right time for weaning off immunosuppression in solid organ transplant recipients. *Expert Rev Clin Immunol* 2010; **6**: 879-892 [PMID: 20979553 DOI: 10.1586/eci.10.71]
100 **Sánchez-Fueyo A**. Identification of tolerant recipients following liver transplantation. *Int Immunopharmacol* 2010; **10**: 1501-1504 [PMID: 20601182 DOI: 10.1016/j.intimp.2010.06.011]
101 **Sánchez-Fueyo A**. Hot-topic debate on tolerance: Immunosuppression withdrawal. *Liver Transpl* 2011; **17** Suppl 3: S69-S73 [PMID: 21850680 DOI: 10.1002/lt.22421]
102 **Sumimoto R**, Kamada N. Specific suppression of allograft rejection by soluble class I antigen and complexes with monoclonal antibody. *Transplantation* 1990; **50**: 678-682 [PMID: 2219291 DOI: 10.1097/00007890-199010000-00029]
103 **Sriwatanawongsa V**, Davies HS, Calne RY. The essential roles of parenchymal tissues and passenger leukocytes in the tolerance induced by liver grafting in rats. *Nat Med* 1995; **1**: 428-432 [PMID: 7585089 DOI: 10.1038/nm0595-428]
104 **Qian S**, Demetris AJ, Murase N, Rao AS, Fung JJ, Starzl TE. Murine liver allograft transplantation: Tolerance and donor cell chimerism. *Hepatology* 1994; **19**: 916-924 [PMID: 8138266 DOI: 10.1002/hep.1840190418]
105 **Jucaud V**, Shaked A, DesMarais M, Sayre P, Feng S, Levitsky J, Everly MJ. Prevalence and Impact of De Novo Donor-Specific Antibodies During a Multicenter Immunosuppression Withdrawal Trial in Adult Liver Transplant Recipients. *Hepatology* 2019; **69**: 1273-1286 [PMID: 30229989 DOI: 10.1002/hep.30281]
106 **Manzia TM**, Angelico R, Baiocchi L, Toti L, Ciano P, Palmieri G, Angelico M, Orlando G, Tisone G. The Tor Vergata weaning of immunosuppression protocols in stable hepatitis C virus liver transplant patients: The 10-year follow-up. *Transpl Int* 2013; **26**: 259-266 [PMID: 23278973 DOI: 10.1111/tri.12023]
107 **Manzia TM**, Angelico R, Toti L, Angelico C, Quaranta C, Parente A, Blasi F, Iesari S, Sforza D, Baiocchi L, Lerut J, Tisone G. Longterm Survival and Cost-Effectiveness of Immunosuppression Withdrawal After Liver Transplantation. *Liver Transpl* 2018; **24**: 1199-1208 [PMID: 30129171 DOI: 10.1002/lt.25293]
108 **Orlando G**, Manzia T, Baiocchi L, Sanchez-Fueyo A, Angelico M, Tisone G. The Tor Vergata weaning off immunosuppression protocol in stable HCV liver transplant patients: The updated follow up at 78 months. *Transpl Immunol* 2008; **20**: 43-47 [PMID: 18773958 DOI: 10.1016/j.trim.2008.08.007]
109 **Tisone G**, Orlando G, Cardillo A, Palmieri G, Manzia TM, Baiocchi L, Lionetti R, Anselmo A, Toti L, Angelico M. Complete weaning off immunosuppression in HCV liver transplant recipients is feasible and favourably impacts on the progression of disease recurrence. *J Hepatol* 2006; **44**: 702-709 [PMID: 16473433 DOI: 10.1016/j.jhep.2005.11.047]
110 **Ramos HC**, Reyes J, Abu-Elmagd K, Zeevi A, Reinsmoen N, Tzakis A, Demetris AJ, Fung JJ, Flynn B, McMichael J. Weaning of immunosuppression in long-term liver transplant recipients. *Transplantation* 1995; **59**: 212-217 [PMID: 7839442 DOI: 10.1097/00007890-199501000-00010]
111 **Takatsuki M**, Uemoto S, Inomata Y, Egawa H, Kiuchi T, Fujita S, Hayashi M, Kanematsu T, Tanaka K. Weaning of immunosuppression in living donor liver transplant recipients. *Transplantation* 2001; **72**: 449-454 [PMID: 11502975 DOI: 10.1097/00007890-200108150-00016]
112 **Oike F**, Yokoi A, Nishimura E, Ogura Y, Fujimoto Y, Kasahara M, Kaihara S, Kiuchi T, Egawa H, Uemoto S, Tanaka K. Complete withdrawal of immunosuppression in living donor liver transplantation. *Transplant Proc* 2002; **34**: 1521 [PMID: 12176465 DOI: 10.1016/S0041-1345(02)02980-9]
113 **Koshiba T**, Li Y, Takemura M, Wu Y, Sakaguchi S, Minato N, Wood KJ, Haga H, Ueda M, Uemoto S. Clinical, immunological, and pathological aspects of operational tolerance after pediatric living-donor liver transplantation. *Transpl Immunol* 2007; **17**: 94-97 [PMID: 17306739 DOI: 10.1016/j.trim.2006.10.004]
114 **Ohe H**, Waki K, Yoshitomi M, Morimoto T, Nafady-Hego H, Satoda N, Li Y, Zhao X, Sakaguchi S, Uemoto S, Bishop GA, Koshiba T. Factors affecting operational tolerance after pediatric living-donor liver

transplantation: Impact of early post-transplant events and HLA match. *Transpl Int* 2012; **25**: 97-106 [PMID: 22117557 DOI: 10.1111/j.1432-2277.2011.01389.x]

115 **Yoshitomi M**, Koshiba T, Haga H, Li Y, Zhao X, Cheng D, Miyagawa A, Sakashita H, Tsuruyama T, Ohe H, Ueda M, Okamoto S, Egawa H, Wood K, Sakaguchi S, Manabe T, Tanaka K, Uemoto S. Requirement of protocol biopsy before and after complete cessation of immunosuppression after liver transplantation. *Transplantation* 2009; **87**: 606-614 [PMID: 19307800 DOI: 10.1097/TP.0b013e318195a7cb]

116 **Hurwitz M**, Desai DM, Cox KL, Berquist WE, Esquivel CO, Millan MT. Complete immunosuppressive withdrawal as a uniform approach to post-transplant lymphoproliferative disease in pediatric liver transplantation. *Pediatr Transplant* 2004; **8**: 267-272 [PMID: 15176965 DOI: 10.1111/j.1399-3046.2004.00129.x]

117 **Lee JH**, Lee SK, Lee HJ, Seo JM, Joh JW, Kim SJ, Kwon CH, Choe YH. Withdrawal of immunosuppression in pediatric liver transplant recipients in Korea. *Yonsei Med J* 2009; **50**: 784-788 [PMID: 20046418 DOI: 10.3349/ymj.2009.50.6.784]

118 **Feng S**, Ekong UD, Lobritto SJ, Demetris AJ, Roberts JP, Rosenthal P, Alonso EM, Philogene MC, Ikle D, Poole KM, Bridges ND, Turka LA, Tchao NK. Complete immunosuppression withdrawal and subsequent allograft function among pediatric recipients of parental living donor liver transplants. *JAMA* 2012; **307**: 283-293 [PMID: 22253395 DOI: 10.1001/jama.2011.2014]

119 **Feng S**, Demetris AJ, Spain KM, Kanaparthi S, Burrell BE, Ekong UD, Alonso EM, Rosenthal P, Turka LA, Ikle D, Tchao NK. Five-year histological and serological follow-up of operationally tolerant pediatric liver transplant recipients enrolled in WISP-R. *Hepatology* 2017; **65**: 647-660 [PMID: 27302659 DOI: 10.1002/hep.28681]

120 **Waki K**, Sugawara Y, Mizuta K, Taniguchi M, Ozawa M, Hirata M, Nozawa M, Kaneko J, Takahashi K, Kadowaki T, Terasaki PI, Kokudo N. Predicting operational tolerance in pediatric living-donor liver transplantation by absence of HLA antibodies. *Transplantation* 2013; **95**: 177-183 [PMID: 23232368 DOI: 10.1097/TP.0b013e3182782fef]

121 **Lin NC**, Wang HK, Yeh YC, Liu CP, Loong CC, Tsai HL, Chen CY, Chin T, Liu C. Minimization or withdrawal of immunosuppressants in pediatric liver transplant recipients. *J Pediatr Surg* 2015; **50**: 2128-2133 [PMID: 26377868 DOI: 10.1016/j.jpedsurg.2015.08.043]

122 **Santopaolo F**, Lenci I, Milana M, Manzia TM, Baiocchi L. Liver transplantation for hepatocellular carcinoma: Where do we stand? *World J Gastroenterol* 2019; **25**: 2591-2602 [PMID: 31210712 DOI: 10.3748/wjg.v25.i21.2591]

123 **Cholongitas E**, Mamou C, Rodríguez-Castro KI, Burra P. Mammalian target of rapamycin inhibitors are associated with lower rates of hepatocellular carcinoma recurrence after liver transplantation: A systematic review. *Transpl Int* 2014; **27**: 1039-1049 [PMID: 24943720 DOI: 10.1111/tri.12372]

124 **Rodríguez-Perálvarez M**, Tsochatzis E, Naveas MC, Pieri G, García-Caparrós C, O'Beirne J, Poyato-González A, Ferrín-Sánchez G, Montero-Álvarez JL, Patch D, Thorburn D, Briceño J, De la Mata M, Burroughs AK. Reduced exposure to calcineurin inhibitors early after liver transplantation prevents recurrence of hepatocellular carcinoma. *J Hepatol* 2013; **59**: 1193-1199 [PMID: 23867318 DOI: 10.1016/j.jhep.2013.07.012]

125 **Geissler EK**, Schnitzbauer AA, Zülke C, Lamby PE, Proneth A, Duvoux C, Burra P, Jauch KW, Rentsch M, Ganten TM, Schmidt J, Settmacher U, Heise M, Rossi G, Cillo U, Kneteman N, Adam R, van Hoek B, Bachellier P, Wolf P, Rostaing L, Bechstein WO, Rizell M, Powell J, Hidalgo E, Gugenheim J, Wolters H, Brockmann J, Roy A, Mutzbauer I, Schlitt A, Beckebaum S, Graeb C, Nadalin S, Valente U, Turrión VS, Jamieson N, Scholz T, Colledan M, Fändrich F, Becker T, Söderdahl G, Chazouillères O, Mäkisalo H, Pageaux GP, Steininger R, Soliman T, de Jong KP, Pirenne J, Margreiter R, Pratschke J, Pinna AD, Hauss J, Schreiber S, Strasser S, Klempnauer J, Troisi RI, Bhoori S, Lerut J, Bilbao I, Klein CG, Königsrainer A, Mirza DF, Otto G, Mazzaferro V, Neuhaus P, Schlitt HJ. Sirolimus Use in Liver Transplant Recipients With Hepatocellular Carcinoma: A Randomized, Multicenter, Open-Label Phase 3 Trial. *Transplantation* 2016; **100**: 116-125 [PMID: 26555945 DOI: 10.1097/TP.0000000000000965]

126 **Adams DH**, Sanchez-Fueyo A, Samuel D. From immunosuppression to tolerance. *J Hepatol* 2015; **62**: S170-S185 [PMID: 25920086 DOI: 10.1016/j.jhep.2015.02.042]

127 **Orlando G**, Hematti P, Stratta RJ, Burke GW, Di Cocco P, Pisani F, Soker S, Wood K. Clinical operational tolerance after renal transplantation: Current status and future challenges. *Ann Surg* 2010; **252**: 915-928 [PMID: 21107102 DOI: 10.1097/SLA.0b013e3181f3efb0]

128 **Karam VH**, Gasquet I, Delvart V, Hiesse C, Dorent R, Danet C, Samuel D, Charpentier B, Gandjbakhch I, Bismuth H, Castaing D. Quality of life in adult survivors beyond 10 years after liver, kidney, and heart transplantation. *Transplantation* 2003; **76**: 1699-1704 [PMID: 14688519 DOI: 10.1097/01.Tp.0000092955.28529.1e]

129 **Biomarkers Definitions Working Group**. Biomarkers and surrogate endpoints: Preferred definitions and conceptual framework. *Clin Pharmacol Ther* 2001; **69**: 89-95 [PMID: 11240971 DOI: 10.1067/mcp.2001.113989]

130 **Londoño MC**, Danger R, Giral M, Soulillou JP, Sánchez-Fueyo A, Brouard S. A need for biomarkers of operational tolerance in liver and kidney transplantation. *Am J Transplant* 2012; **12**: 1370-1377 [PMID: 22486792 DOI: 10.1111/j.1600-6143.2012.04035.x]

131 **Feng S**, Bucuvalas J. Tolerance after liver transplantation: Where are we? *Liver Transpl* 2017; **23**: 1601-1614 [PMID: 28834221 DOI: 10.1002/lt.24845]

132 **Park KM**, Hussein KH, Hong SH, Ahn C, Yang SR, Park SM, Kweon OK, Kim BM, Woo HM. Decellularized Liver Extracellular Matrix as Promising Tools for Transplantable Bioengineered Liver Promotes Hepatic Lineage Commitments of Induced Pluripotent Stem Cells. *Tissue Eng Part A* 2016; **22**: 449-460 [PMID: 26801816 DOI: 10.1089/ten.TEA.2015.0313]

133 **Edgar L**, Altamimi A, García Sánchez M, Tamburrinia R, Asthana A, Gazia C, Orlando G. Utility of extracellular matrix powders in tissue engineering. *Organogenesis* 2018; **14**: 172-186 [PMID: 30183489 DOI: 10.1080/15476278.2018.1503771]

134 **Jain AB**, Yee LD, Nalesnik MA, Youk A, Marsh G, Reyes J, Zak M, Rakela J, Irish W, Fung JJ. Comparative incidence of de novo nonlymphoid malignancies after liver transplantation under tacrolimus using surveillance epidemiologic end result data. *Transplantation* 1998; **66**: 1193-1200 [PMID: 9825817 DOI: 10.1097/00007890-199811150-00014]

135 **Kelly DM**, Emre S, Guy SR, Miller CM, Schwartz ME, Sheiner PA. Liver transplant recipients are not at increased risk for nonlymphoid solid organ tumors. *Cancer* 1998; **83**: 1237-1243 [PMID: 9740091 DOI: 10.1002/(SICI)1097-0142(19980915)83:6<1237::AID-CNCR25>3.3.CO;2-K]

136 **Jiménez C**, Rodríguez D, Marqués E, Loinaz C, Alonso O, Hernández-Vallejo G, Marín L, Rodríguez F,

García I, Moreno E. De novo tumors after orthotopic liver transplantation. *Transplant Proc* 2002; **34**: 297-298 [PMID: 11959293 DOI: 10.1016/S0041-1345(01)02770-1]

137 **Sanchez EQ**, Marubashi S, Jung G, Levy MF, Goldstein RM, Molmenti EP, Fasola CG, Gonwa TA, Jennings LW, Brooks BK, Klintmalm GB. De novo tumors after liver transplantation: A single-institution experience. *Liver Transpl* 2002; **8**: 285-291 [PMID: 11910575 DOI: 10.1053/jlts.2002.29350]

138 **Oo YH**, Gunson BK, Lancashire RJ, Cheng KK, Neuberger JM. Incidence of cancers following orthotopic liver transplantation in a single center: Comparison with national cancer incidence rates for England and Wales. *Transplantation* 2005; **80**: 759-764 [PMID: 16210962 DOI: 10.1097/01.TP.0000173775.16579.18]

139 **Baccarani U**, Piselli P, Serraino D, Adani GL, Lorenzin D, Gambato M, Buda A, Zanus G, Vitale A, De Paoli A, Cimaglia C, Bresadola V, Toniutto P, Risaliti A, Cillo U, Bresadola F, Burra P. Comparison of de novo tumours after liver transplantation with incidence rates from Italian cancer registries. *Dig Liver Dis* 2010; **42**: 55-60 [PMID: 19497797 DOI: 10.1016/j.dld.2009.04.017]

140 **Chatrath H**, Berman K, Vuppalanchi R, Slaven J, Kwo P, Tector AJ, Chalasani N, Ghabril M. De novo malignancy post-liver transplantation: A single center, population controlled study. *Clin Transplant* 2013; **27**: 582-590 [PMID: 23808800 DOI: 10.1111/ctr.12171]

141 **Schrem H**, Kurok M, Kaltenborn A, Vogel A, Walter U, Zachau L, Manns MP, Klempnauer J, Kleine M. Incidence and long-term risk of de novo malignancies after liver transplantation with implications for prevention and detection. *Liver Transpl* 2013; **19**: 1252-1261 [PMID: 24106037 DOI: 10.1002/lt.23722]

142 **Egeli T**, Unek T, Ozbilgin M, Agalar C, Derici S, Akarsu M, Unek IT, Aysin M, Bacakoglu A, Astarcıoglu I. De Novo Malignancies After Liver Transplantation: A Single Institution Experience. *Exp Clin Transplant* 2019; **17**: 74-78 [PMID: 29237362 DOI: 10.6002/ect.2017.0111]

143 **Taborelli M**, Piselli P, Ettorre GM, Lauro A, Galatioto L, Baccarani U, Rendina M, Shalaby S, Petrara R, Nudo F, Toti L, Sforza D, Fantola G, Cimaglia C, Agresta A, Vennarecci G, Pinna AD, Gruttadauria S, Risaliti A, Di Leo A, Burra P, Rossi M, Tisone G, Zamboni F, Serraino D; Italian Transplant & Cancer Cohort Study. Risk of virus and non-virus related malignancies following immunosuppression in a cohort of liver transplant recipients. Italy, 1985-2014. *Int J Cancer* 2018 [PMID: 29693248 DOI: 10.1002/ijc.31552]

144 **Devlin J**, Doherty D, Thomson L, Wong T, Donaldson P, Portmann B, Williams R. Defining the outcome of immunosuppression withdrawal after liver transplantation. *Hepatology* 1998; **27**: 926-933 [PMID: 9537430 DOI: 10.1002/hep.510270406]

145 **Eason JD**, Cohen AJ, Nair S, Alcantera T, Loss GE. Tolerance: Is it worth the risk? *Transplantation* 2005; **79**: 1157-1159 [PMID: 15880061 DOI: 10.1097/01.TP.0000162084.46555.10]

146 **Girlanda R**, Rela M, Williams R, O'Grady JG, Heaton ND. Long-term outcome of immunosuppression withdrawal after liver transplantation. *Transplant Proc* 2005; **37**: 1708-1709 [PMID: 15919439 DOI: 10.1016/j.transproceed.2005.03.070]

147 **Assy N**, Adams PC, Myers P, Simon V, Minuk GY, Wall W, Ghent CN. Randomized controlled trial of total immunosuppression withdrawal in liver transplant recipients: Role of ursodeoxycholic acid. *Transplantation* 2007; **83**: 1571-1576 [PMID: 17589339 DOI: 10.1097/01.tp.0000266678.32250.76]

148 **Pons JA**, Revilla-Nuin B, Baroja-Mazo A, Ramírez P, Martínez-Alarcón L, Sánchez-Bueno F, Robles R, Rios A, Aparicio P, Parrilla P. FoxP3 in peripheral blood is associated with operational tolerance in liver transplant patients during immunosuppression withdrawal. *Transplantation* 2008; **86**: 1370-1378 [PMID: 19034005 DOI: 10.1097/TP.0b013e318188d3e6]

149 **Tryphonopoulos P**, Ruiz P, Weppler D, Nishida S, Levi DM, Moon J, Tekin A, Velez M, Neuman DR, Island E, Selvaggi G, Tzakis AG. Long-term follow-up of 23 operational tolerant liver transplant recipients. *Transplantation* 2010; **90**: 1556-1561 [PMID: 21085060 DOI: 10.1097/TP.0b013e3182003db7]

150 **de la Garza RG**, Sarobe P, Merino J, Lasarte JJ, D'Avola D, Belsue V, Delgado JA, Silva L, Iñarrairaegui M, Sangro B, Sola JJ, Pardo F, Quiroga J, Herrero JI. Trial of complete weaning from immunosuppression for liver transplant recipients: Factors predictive of tolerance. *Liver Transpl* 2013; **19**: 937-944 [PMID: 23784747 DOI: 10.1002/lt.23686]

151 **Benítez C**, Londoño MC, Miquel R, Manzia TM, Abraldes JG, Lozano JJ, Martínez-Llordella M, López M, Angelico R, Bohne F, Sese P, Daoud F, Larcier P, Roelen DL, Claas F, Whitehouse G, Lerut J, Pirenne J, Rimola A, Tisone G, Sánchez-Fueyo A. Prospective multicenter clinical trial of immunosuppressive drug withdrawal in stable adult liver transplant recipients. *Hepatology* 2013; **58**: 1824-1835 [PMID: 23532679 DOI: 10.1002/hep.26426]

152 **Bohne F**, Londoño MC, Benítez C, Miquel R, Martínez-Llordella M, Russo C, Ortiz C, Bonaccorsi-Riani E, Brander C, Bauer T, Protzer U, Jaeckel E, Taubert R, Forns X, Navasa M, Berenguer M, Rimola A, Lozano JJ, Sánchez-Fueyo A. HCV-induced immune responses influence the development of operational tolerance after liver transplantation in humans. *Sci Transl Med* 2014; **6**: 242ra81 [PMID: 24964989 DOI: 10.1126/scitranslmed.3008793]

153 **Todo S**, Yamashita K, Goto R, Zaitsu M, Nagatsu A, Oura T, Watanabe M, Aoyagi T, Suzuki T, Shimamura T, Kamiyama T, Sato N, Sugita J, Hatanaka K, Bashuda H, Habu S, Demetris AJ, Okumura K. A pilot study of operational tolerance with a regulatory T-cell-based cell therapy in living donor liver transplantation. *Hepatology* 2016; **64**: 632-643 [PMID: 26773713 DOI: 10.1002/hep.28459]

154 **Shaked A**. Gradual Withdrawal of Immune System Suppressing Drugs in Patients Receiving a Liver Transplant. [accessed]. 2019; ClinicalTrials.gov [Internet]. Bethesda (MD): U.S. National Library of Medicine Available from: https://ClinicalTrials.gov/show/NCT00135694 ClinicalTrials.gov Identifier: NCT00135694

155 **Markman JF**. Evaluation of Donor Specific Immune Senescence and Exhaustion as Biomarkers of Tolerance Post Liver Transplantation. [accessed]. 2019; ClinicalTrials.gov [Internet]. Bethesda (MD): U.S. National Library of Medicine Available from: https://ClinicalTrials.gov/show/NCT02533180 ClinicalTrials.gov Identifier: NCT02533180

156 **Markman JF**, Feng S. Liver Transplantation With Tregs at MGH. [accessed]. 2019; ClinicalTrials.gov [Internet]. Bethesda (MD): U.S. National Library of Medicine Available from: https://ClinicalTrials.gov/show/NCT03577431 ClinicalTrials.gov Identifier: NCT03577431

157 **Mazariegos GV**, Reyes J, Marino IR, Demetris AJ, Flynn B, Irish W, McMichael J, Fung JJ, Starzl TE. Weaning of immunosuppression in liver transplant recipients. *Transplantation* 1997; **63**: 243-249 [PMID: 9020325 DOI: 10.1097/00007890-199701270-00012]

158 **Feng S**. Withdrawal of Immunosuppression in Pediatric Liver Transplant Recipients. [accessed]. 2019; ClinicalTrials.gov [Internet]. Bethesda (MD): U.S. National Library of Medicine. Available from: https://ClinicalTrials.gov/show/NCT00320606 ClinicalTrials.gov Identifier: NCT00320606

159 **Feng S**, Bucuvalas J, Demetris A, Spain K, Kanaparthi S, Magee J, Mazariegos G. The iWITH

Investigators Primary Outcome of iWITH: A Multi-Center Clinical Trial of Complete Immunosuppression Withdrawal (ISW) in Stable Pediatric Liver Transplant (LT) Recipients. *Am J Transplant* 2016; **16**: 2016

World Journal of Gastroenterology

Submit a Manuscript: https://www.f6publishing.com

*World J Gastroenterol* 2019 September 21; 25(35): 5376-5387

DOI: 10.3748/wjg.v25.i35.5376

ISSN 1007-9327 (print) ISSN 2219-2840 (online)

*META-ANALYSIS*

# Gastric neuroendocrine neoplasms type 1: A systematic review and meta-analysis

Apostolos V Tsolakis, Athanasia Ragkousi, Miroslav Vujasinovic, Gregory Kaltsas, Kosmas Daskalakis

**ORCID number:** Apostolos V Tsolakis (0000-0002-6784-5572); Athanasia Ragkousi (0000-0003-0965-8119); Miroslav Vujasinovic (0000-0002-6496-295X); Gregory Kaltsas (0000-0002-5876-7883); Kosmas Daskalakis (0000-0003-4224-8912).

**Author contributions:** Tsolakis AV contributed to conception and design of the study, selection and assessment of the quality of the eligible studies, analysis and interpretation of data, drafting of the manuscript and final approval of the manuscript; Ragkousi A contributed to statistical consultation, analysis and interpretation of data and final approval of the manuscript; Vujasinovic M contributed to drafting of the manuscript, final approval of the manuscript; Kaltsas G contributed to analysis and interpretation of the data, drafting of the manuscript, final approval of the manuscript; Daskalakis K contributed to conception and design of the study, acquisition of studies, selection and assessment of the quality of the eligible studies, analysis and interpretation of data, writing and drafting the manuscript, study supervision and final approval of manuscript.

**Supported by** Swedish Society of Medicine Post Doctoral Scholarship, No. SLS-785911; the Lennander Scholarship.

**PRISMA 2009 Checklist statement:** The authors have read the PRISMA 2009 Checklist, and the manuscript was prepared and revised according to the PRISMA 2009

**Apostolos V Tsolakis,** Department of Oncology and Pathology, Karolinska Institute, Stockholm 17177, Sweden

**Apostolos V Tsolakis,** Cancer Centre Karolinska, CCK, Karolinska University Hospital, Stockholm 17176, Sweden

**Athanasia Ragkousi, Gregory Kaltsas, Kosmas Daskalakis,** 1st Department of Propaupedic Internal Medicine, Endocrine Oncology Unit, Laiko Hospital, National and Kapodistrian University of Athens, Athens 11527, Greece

**Miroslav Vujasinovic,** Department of Digestive Diseases, Karolinska University Hospital, Stockholm 14186, Sweden

**Kosmas Daskalakis,** Department of Surgical Sciences, Uppsala University, Uppsala 75185, Sweden

**Corresponding author:** Apostolos V Tsolakis, MD, PhD, Doctor, Department of Oncology and Pathology, Karolinska Institute, Solna R8:04, Stockholm 17177, Sweden.
apobtsol@hotmail.com
**Telephone:** +46-8-58580000

## Abstract

### *BACKGROUND*

To date, the histopathological parameters predicting the risk of lymph node (LN) metastases and local recurrence, associated mortality and appropriateness of endoscopic or surgical resection in patients with gastric neuroendocrine neoplasms type 1 (GNENs1) have not been fully elucidated.

### *AIM*

To determine the rate of LN metastases and its impact in survival in patients with GNEN1 in relation to certain clinico-pathological parameters.

### *METHODS*

The PubMed, EMBASE, Cochrane Library, Web of Science and Scopus databases were searched through January 2019. The quality of the included studies and risk of bias were assessed using the Newcastle-Ottawa Scale (NOS) in accordance with the Cochrane guidelines. A random effects model and pooled odds ratios (OR) with 95%CI were applied for the quantitative meta-analysis.

### *RESULTS*

We screened 2933 articles. Thirteen studies with 769 unique patients with GNEN1 were included. Overall, the rate of metastasis to locoregional LNs was

**Manuscript source**: Invited manuscript

**Received:** April 30, 2019
**Peer-review started:** April 30, 2019
**First decision:** June 6, 2019
**Revised:** June 12, 2019
**Accepted:** July 19, 2019
**Article in press:** June 6, 2019
**Published online:** September 21, 2019

**P-Reviewer:** Krishna SG, Sato Y, Voutsadakis IA
**S-Editor:** Cui LJ
**L-Editor:** A
**E-Editor:** Ma YJ

3.3% (25/769). The rate of LN metastases with a cut-off size of 10 mm was 15.3% for lesions > 10 mm (*vs* 0.8% for lesions < 10 mm) with a random-effects OR of 10.5 (95%CI: 1.4 -80.8; heterogeneity: $P$ = 0.126; $I^2$ = 47.5%). Invasion of the muscularis propria was identified as a predictor for LN metastases (OR: 17.2; 95%CI: 1.8-161.1; heterogeneity: $P$ = 0.165; $I^2$ = 44.5%), whereas grade was not clearly associated with LN metastases (OR: 2; 95%CI: 0.3-11.6; heterogeneity: $P$ = 0.304; $I^2$ = 17.4%). With regard to GNEN1 local recurrence, scarce data were available. The 5-year disease-specific survival for patients with and without LN metastases was 100% in most available studies irrespective of the type of intervention. Surgical resection was linked to a lower risk of recurrence (OR: 0.3; 95%CI: 0.1-1.1; heterogeneity: $P$ = 0.173; $I^2$ = 31.9%). The reported complication rates of endoscopic and surgical intervention were 0.6 and 3.8%, respectively.

### *CONCLUSION*

This meta-analysis confirms that tumor size ≥ 10 mm and invasion of the muscularis propria are linked to a higher risk of LN metastases in patients with GNEN1. Overall, the metastatic propensity of GNEN1 is low with favorable 5-year disease-specific survival rates reported; hence, no clear evidence of the prognostic value of LN positivity is available. Additionally, there is a lack of evidence supporting the prediction of local recurrence in GNEN1, even if surgery was more often a definitive treatment.

**Key words:** Gastric neuroendocrine neoplasms type 1; Meta-analysis; Lymph node metastasis; Tumor size; Invasion; Endoscopy; Surgery



**Core tip:** Hitherto, risk parameters predicting metastatic disease and the appropriateness of endoscopic *vs* surgical management of patients with gastric neuroendocrine neoplasms type 1 (GNENs1) have not been thoroughly investigated. The present systematic review and meta-analysis prove that locoregional lymph node (LN) metastases in GNENs1 are relatively rare (3.3%). Furthermore, tumour size ≥ 10 mm and the presence of the muscularis propria invasion are associated with an increased risk for LN metastasis. The latter finding suggests that endoscopic ultrasound investigation is very valuable in the work up of these lesions. Finally, surgical resection is linked to a lower risk for recurrence.

**Citation:** Tsolakis AV, Ragkousi A, Vujasinovic M, Kaltsas G, Daskalakis K. Gastric neuroendocrine neoplasms type 1: A systematic review and meta-analysis. *World J Gastroenterol* 2019; 25(35): 5376-5387
**URL**: https://www.wjgnet.com/1007-9327/full/v25/i35/5376.htm
**DOI**: https://dx.doi.org/10.3748/wjg.v25.i35.5376

## INTRODUCTION

Gastric neuroendocrine neoplasms (GNENs) are rare and account for approximately 3% of all gastrointestinal neuroendocrine tumors and 0,3% of all gastric malignancies[1]. GNENs are divided into well-differentiated (WD) GNENs and neuroendocrine carcinomas (NECs). WD GNENs are mainly of enterochromaffin-like (ECL) cell origin, and three types are recognized[2-6]. Types 1 and 2 (GNEN1 and 2) are associated with hypergastrinaemia, the former because of autoimmune chronic atrophic gastritis and the latter due to Zollinger-Ellison syndrome in the context of multiple endocrine neoplasia type 1. Patients with type 3 GNENs have normal gastrin concentrations and a more aggressive clinical behavior mimicking that of gastric adenocarcinoma[7]. Finally, NECs are poorly-differentiated tumors that show a certain degree of neuroendocrine differentiation and the affected patients have normal circulating gastrin concentrations and a poor prognosis.

GNEN1s commonly exhibit a generally benign clinical course with a minority developing locoregional lymph node (LN) metastases and only a few cases of distant metastases have been reported[8]. In terms of the long-term disease-specific mortality,

reports differ regarding its association with the presence of metastases in locoregional LNs and the selection of the type and the extent of intervention undertaken. This is mainly because in the majority of published GNEN series and existing NEN registries, GNEN1s are reported together with other types of GNENs. Importantly, compared with other types of GNENs, GNEN1s have distinct differences in tumour biology and patient outcomes. However, informative clinico-pathological features (size, grade, depth of invasion) are currently used indistinguishably for most GNEN types, even if GNEN are a heterogeneous group and the prognostic impact of such parameters may differ considerably among the types.

Due to the indolent course of GNEN1, endoscopic resection is considered the mainstay of treatment for these tumours ranging from simple polypectomy and endoscopic mucosal resection (EMR) to endoscopic submucosal resection (ESMR) and endoscopic submucosal dissection (ESD). Surgery has been considered for tumours not amenable to endoscopic treatment, *i.e.*, locally advanced lesions > 10 mm invading deeper layers of the gastric wall. This approach in GNEN1 management is also in accordance with the current European Neuroendocrine Tumour Society guidelines[9]. However, risk stratification based on patient-related parameters to determine the risk of LN metastases and disease-specific mortality in patients with larger and more locally advanced GNEN1 remains to be defined. Therefore, there is a great need of a summary of the evidence regarding the risk of LN metastases and local recurrence in GNEN1s, as well as the appropriateness and safety of endoscopic versus surgical resection of larger lesions.

The aim of this systematic review and meta-analysis was to compare the rate of LN metastases and associated mortality, and recurrence in patients with GNEN1s undergoing endoscopic or surgical resection with respect to their clinico-pathological parameters, such as the size, grade and depth of invasion and to assess the rate of complications associated with the aforementioned interventions. Our hypothesis was that patients with particular clinico-pathological characteristics, *i.e.*, larger lesions, grade 2 tumours and deeper invasion of the gastric wall, may be at a higher risk for locoregional LN metastases and/or local recurrence; thus, necessitating the implementation of a more patient-tailored management of GNEN1.

## MATERIALS AND METHODS

### Study selection

Retrospective cohort studies with GNEN and GNEN1 patients undergoing endoscopic or surgical resection were included in this systematic review and meta-analysis. The outcomes that were required for study selection included two or more of the following terms: tumour size, grade, depth of invasion, vascular invasion, LN metastases, local recurrence, disease-specific and overall survival and complications. For potentially eligible studies a sample size of at least ten patients with GNEN1 was required; hence case reports and small case series were excluded. Studies reporting data on GNEN type 2, type 3 and GNEC altogether with GNEN1 were also excluded. In particular, GNEN1 diagnosis was based on histopathological and biochemical criteria reported in the methods section of the included studies. Registry and institutional studies reporting data without specifying the diagnostic criteria of GNEN1 (histopathologic confirmation and hypergastrinaemia) were excluded from the present study. Among multiple reports from the same institution, only the latest eligible study was included. A study protocol for this meta-analysis was not registered before the study initiation. Preferred Reporting Items for Systematic Reviews and Meta-Analyses (PRISMA) guidelines were followed[10].

### Search strategy

We conducted a systematic search to identify all potentially eligible studies in the PubMed, EMBASE, Cochrane Library, Web of Science and SCOPUS databases. Search terms included “Gastric Carcinoid”, “ECL cell carcinoid”, “Gastric Neuroendocrine Tumor”, ”Gastric Neuroendocrine Neoplasm”, “Neuroendocrine Tumor of the Stomach”, “Endoscopy”, "endoscopic resection”, “endoscopic mucosal resection”, “endoscopic submucosal dissection”, “polypectomy”, “polyp resection”, “mucosectomy”, “gastric resection”, “antrectomy”, “surgery”, “ surgical resection”, “partial resection”, “partial gastrectomy” and “gastrectomy”, and all the terms were used in combination with the Boolean operators AND OR. The search terms were input as free text. Two of the authors independently examined all potentially eligible titles and abstracts. Full articles were obtained for preliminary selected studies to finalize eligibility (Supplementary Table 1).

### Data extraction

The hypothesis of the study was formulated prior to the data collection and extraction. Two reviewers independently extracted all available data. We defined the primary outcome as the rate of LN metastases after using different clinico-pathological data to stratify the patients. The secondary outcomes were recurrence rate, disease-specific mortality rate associated with LN metastases and type of intervention, and the complication rate in GNEN1 patients undergoing endoscopic and surgical resection. Potentially eligible studies with double zero cells in all strata and the investigated outcomes were excluded at the final stage of data extraction. Disagreements between the two reviewers were resolved by consensus.

Patients with distant stage disease were not included in the present meta-analysis. The staging methods applied in the included studies and according to the TNM classification varied greatly and was primarily based on available histopathology in all patients subjected to resective surgery. However, in patients subjected to endoscopic resection staging criteria were applied to data extracted from endoscopy and corresponding histopathology regarding T stage and endoscopic ultrasonography, as well as cross-sectional imaging regarding the presence of locoregional LN metastases (N stage).

### Quality/risk for bias assessment

The classification of observational studies described by Mathes *et al*[11] was applied in this meta-analysis. The quality of the included studies was measured by the Newcastle-Ottawa Scale (NOS) and independently assessed in accordance with the Cochrane guidelines by two reviewers The total NOS scores ranged from 0 to 9 for cohort studies; a score of 6 or higher indicated high quality[12].

### Statistical analysis

Statistical analyses were conducted with STATA 14.0 software (StataCorp. 2015. Stata Statistical Software: Release 14. College Station, TX: StataCorp LP). A random-effects model was adopted for summary statistics. Pooled odds ratios (OR) were reported for all investigated outcomes. Automatic correction set at 0.5 by default in the "metan" application of STATA in eligible data with single zero cells was applied as appropriate. Statistical heterogeneity was evaluated by the $I^2$ method and the $\chi^2$ test was employed to provide *P*-values; $I^2$ values > 50% indicated a high degree of heterogeneity. Small study effects and the presence of publication bias were evaluated by Galbraith and funnel plots, respectively. The results were reported as OR with 95%CI and *P*-values. The level of statistical significance was set at 5% ($P < 0.05$).

## RESULTS

### Characteristics of the Included Studies

We screened 2933 potentially eligible articles. The 13 included studies had 769 unique patients with GNEN1. The results of the systematic literature search and the study selection process are shown in the PRISMA flow diagram (Figure 1). Table 1 summarizes the characteristics of the included studies.

### Quality/risk of bias assessment

The quality assessment of all the included studies is presented in Table 2 (NOS template). All studies were retrospective cohort studies based on the analysis of institutional multi- or single-centre data. We did not identify any controlled randomized trials or national registry studies eligible for inclusion in the meta-analysis. General factors accounting for poor quality were the lack of clarity regarding the diagnostic criteria of GNEN1, short duration of follow-up, ambiguity regarding the criteria for endoscopic or surgical intervention and failure to report the rate of complications for patients who underwent endoscopic or surgical treatment.

Reporting bias was visually assessed in funnel plots for each of the investigated parameters (Supplementary Figures 1A-4A). Complementary tests did not reveal small size effects (Supplementary Figures 1B-4B). The observed funnel plot asymmetry could be due to the few studies included in the analysis (< 10 studies in all meta-analyses performed) and also publication bias. Between studies heterogeneity was less than 50%, *i.e.*, acceptable for all the meta-analyses in this study.

### Pooled results for clinico-pathological parameters with respect to LN metastases

Overall, the rate of metastases to locoregional LNs was 3.3% (25/769). We identified four studies reporting LN status for primary tumours with a size cut-off of 10 mm[13-16]. The rate of LN metastases for a cut-off size of 10 mm were 15.3% *vs* 0.8% for lesions ≥

**Table 1 Characteristics of the included studies**

| Included studies | Study design | No. of patients | Outcomes | | Funding and conflict of interest statement |
|---|---|---|---|---|---|
| | | | Primary (positive LN status) | Secondary (R, DSS, complications) | |
| Ahlman *et al*[13], 1994 | Single-center restrospective cohort study | 11 | 2/11 (data available at the individual level) | Median follow-up 5 yr; 100% 5-yr DSS | Funding: Swedish Mekong River Commission, Swedish Cancer Society, Jubileumsklinikens Cancer Research Fund, Sahlgrenska Hospital Research Foundation, Göteborg Medical Society, Assar Gabrielsson Research Foundation, Östergötland County Council and AB Hässle. |
| Borch *et al*[19], 2005 | Multi-center prospective cohort study | 51 | 4/51 (data not available at the individual level) | 5-yr DSS reported for LN status and type of intervention strata. R also reported for different strata. | No funding or conflict of interest reported. |
| Chen *et al*[18], 2013 | Single-center retrospective cohort study | 56 | 2/56 (data not available at the individual level) | 100% 5- and 10 yr DSS reported. | Funding: National Center for Advancing Translational Studies. The authors report no conflicts of interest. |
| Kim *et al*[25], 2010 | Single-center retrospective cohort study | 22 | 1/22 (data not available at the individual level) | Mean follow-up 68months for GC cohort; 5-yr DSS 100%. R: 15/22 | No funding or conflict of interest reported |
| Louthan *et al*[24], 2014 | Single-center retrospective cohort study | 18 | 0/18 (data not available at the individual level) | Mean follow-up 47 months for GC cohort; 100% 5-yr DSS for type of intervention strata. | Funding: RVO VFN64165 and PRVOUK-P25/LF1/2. |
| Rappel *et al*[22], 1995 | Single-center retrospective cohort study | 88 | 0/88 (data not available at the individual level) | Median follow-up 72.2 mo; 100% 5-yr DSS; R: 26/54 | No funding or conflict of interest information mentioned in the article. |
| Rindi *et al*[14], 1996 | Multi-center retrospective cohort study | 152 | 2/152 (data not available at the individual level) | Mean follow up 58months; 5-yr DSS 100%; R: 77/119 | No funding or conflict of interest information mentioned in the article. |
| Safatle-Ribeiro *et al*[15], 2006 | Single-center restrospective cohort study | 13 | 1/13 (data available at the individual level) | Median follow-up 72.2 mo | No funding or conflict of interest information mentioned in the article. |
| Sagatun *et al*[17], 2016 | Single-center restrospective cohort study | 26 | 5/26 (data not available at the individual level) | Median follow-up not reported; 5-yr DSS not properly reported | No funding or conflict of interest reported. |
| Sato *et al*[20], 2014 | Multi-center retrospective cohort study | 82 | 0/82 (data not available at the individual level) | Median follow-up reported for different strata. 5-yr DSS not reported; R: 2/82. | No funding or conflict of interest reported. |
| Schindl *et al*[21], 2001 | Single-center retrospective cohort study | 16 | 0/16 (data not available at the individual level) | Median follow-up 70.3 mo; 5-yr DSS 100%. | No funding or conflict of interest information mentioned in article. |
| Thomas *et al*[23], 2013 | Multi-center retrospective cohort study | 111 | 2/111 (data not available at the individual level for all cases). | Mean follow up 76 mo; DSS not reported. R:8/111 | Funding: Selander foundation. No conflict of interest reported. |
| Vanoli *et al*[16], 2018 | Multi-center retrospective cohort study | 123 | 6/123 (data not available at the individual level) | Median follow up 87 mo. 5-yr DSS reported for different strata. | Funding: Internal university grants and the Associazione Italiana Ricerca sul Cancro; Fellowship from San Matteo Hospital Foundation. Conflict of interest: Novartis Pharma and Ipsen Pharma. |

DSS: Disease-specific survival; LN: Lymph node; R: Recurrence.

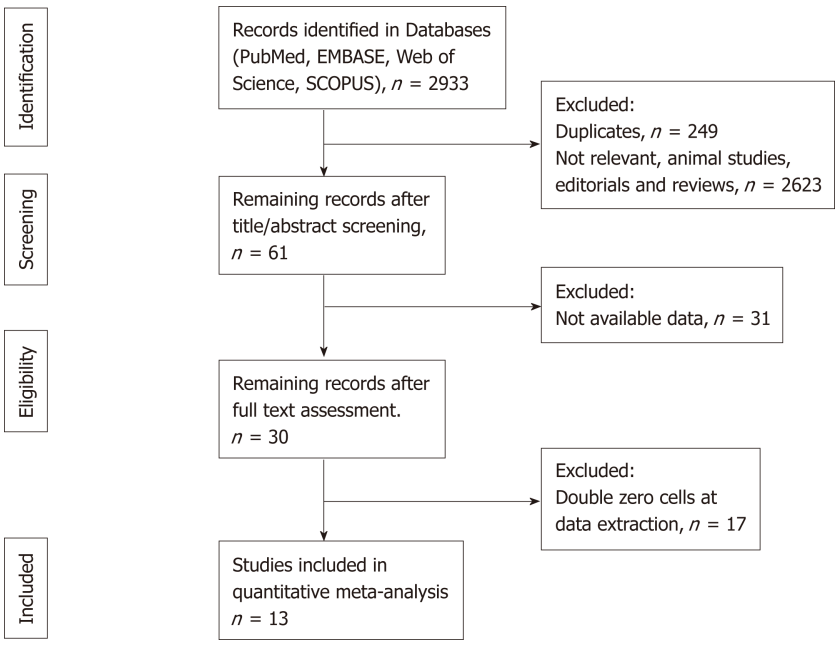


**Figure 1 PRISMA flow diagram of the quantitative meta-analysis.**

10 mm and < 10 mm, respectively with a random-effects OR of 10.5 (95%CI: 1.4-80.8; heterogeneity: $P$ = 0.126; $I^2$ = 47.5%, Figure 2).

Four studies reporting LN status in connection to GNEN1 grade [Grade 1 (G1) *vs* Grade 2 (G1)] were included in this analysis[15-18]. The rates of LN metastases in G1 GNEN1 were 6.7% *vs* 10% for G2 lesions with a random-effects OR of 2(95%CI: 0.3 - 11.6; heterogeneity, $P$ = 0.304; $I^2$ = 17.4%, Figure 3).

Three studies reported LN status in connection to muscularis propria invasion of the primary tumour and were included in the analysis[14,16,19]. The rates of LN metastases in patients demonstrating muscularis propria invasion were 29.4% *vs* 3.1% in patients without invasion with a random-effects OR of 17.2(95%CI: 1.8 -161.1; heterogeneity, $P$ = 0.165; $I^2$ = 44.5%, Figure 4).

### Pooled results for local recurrence

Eight studies reporting local recurrence ($n$ = 75/422) in connection to the type of intervention were included[16,19-25]. The rates of local recurrence in patients undergoing endoscopic resection were 22% ($n$ = 72/328) *vs* 3.2% ($n$ = 3/94) in patients subjected to surgical resection with a random-effects OR of 0.32 (95%CI: 0.1-1.1; heterogeneity, $P$ = 0.173; $I^2$ = 31.9%, Figure 5).

### Pooled results for disease-specific survival and complications

In seven studies, the reported 5-year disease-specific survival (DSS) rate was 100% in patients with ($n$ = 17) and without locoregional LN metastases ($n$ = 479)[13,14,18,23,26-28]. Only two studies reported 5-year DSS less than 100% stratified by LN status [5-year DSS: 80% ($n$ = 8/10) *vs* 100% ($n$ = 164/164)]; random-effects OR: 0.02; 95%CI: 0-0.21; heterogeneity: $P$ = 0.850; $I^2$ = 0%)[16,19].

In thirteen studies reporting 5-year DSS rates following endoscopic *vs* surgical resection, 100% 5-year DSS was evident in both arms [$n$ = 456 (endoscopic intervention)and $n$=162 (surgical intervention)], irrespective of the type of intervention that was undertaken[13,18,20-27,29]. Two additional studies reported 5-year DSS rates less than 100% stratified by the type of intervention (5-year DSS: 99% for endoscopic *vs* 98% for surgical intervention; random-effects OR of 0.64; 95%CI: 0.1-8.5; heterogeneity: $P$ = 0.270, $I^2$ = 17.7%;)[15,16].

The complication rates attributed to endoscopic and surgical intervention were reported in six studies and were as low as 0.6% for the former and 3.8% for the latter[16,18,30-32]. The severity of complications ranged from mild to severe and even death in one operative case. However, the data were not sufficient to provide a more comprehensive classification of patients who underwent surgery (*i.e.*, according to the Clavien-Dindo classification system).

Finally, scarce data were available or appropriately reported with respect to recurrence rates in relation to tumour size, grade and depth of invasion. In particular, one study only reported tumour size as a predictor of recurrence (OR: 1.7, 95%CI:

**Table 2 Newcastle-Ottawa scale cohort star template**

| Included studies | Selection | Comparability | Outcome |
|---|---|---|---|
| Ahlman *et al*[13], 1994 | *** | * | ** |
| Borch *et al*[19], 2005 | **** | ** | ** |
| Chen *et al*[18], 2015 | *** | * | ** |
| Kiim *et al*[25], 2010 | *** | * | ** |
| Louthan *et al*[24], 2014 | *** | * | ** |
| Rappel *et al*[22], 1995 | *** | * | ** |
| Rindi *et al*[14], 1996 | *** | ** | ** |
| Safatle-Ribeiro *et al*[15], 2006 | *** | ** | ** |
| Sagatun *et al*[17], 2016 | *** | * | * |
| Sato *et al*[20], 2014 | *** | * | * |
| Schindl *et al*[21], 2001 | *** | * | ** |
| Thomas *et al*[23], 2013 | *** | * | ** |
| Vanoli *et al*[16], 2018 | *** | ** | ** |

The total Newcastle-Ottawa scale scores ranged from 0 (worst) to 9 (best) for the included cohort studies, with a score of at least 6 indicating high quality.

0.13-22)[32]. Similarly, another study addressed grade (OR: 0.2; 95%CI: 0.01-4.6)[33], and one study discussed depth of invasion (OR: 33 95%CI: 0.9-1220)[25].

## DISCUSSION

Our systematic review and meta-analysis demonstrate that although the metastatic propensity of GNEN1 is low (3.3%), tumour size ≥ 10 mm and invasion of the muscularis propria in the gastric wall may be potential predictors of LN metastases in these patients. Foremost, the negative predictive value of tumour size for lesions < 10 mm and that of the absence of muscularis propria invasion with respect to the presence of locoregional LN metastases were as high as 99.2% and 96.9% respectively. Primary tumour grade was not clearly associated with the risk of LN metastases in GNEN1. Additionally, the disease course is indolent, and the overall prognosis is excellent, with a 5-year DSS of 100% in most studies, with only two patients reported with locoregional LN metastases who died within 5-years of diagnosis. Therefore, the presence of LN metastases does not seem to clearly affect survival in GNEN1 patients. Moreover, most studies reported 98%-100% 5-year DSS, irrespective of the type of intervention that was undertaken. However, studies reporting adequate follow-up *i.e.*, of 10 years are lacking; hence, we were not able to provide evidence that prophylactic surgical resection exerts a survival benefit in the long-term. The complication rates of endoscopic *vs* surgical resection in the few studies reporting this information were 0.6 and 3.8%, respectively. Finally, scarce data were available with regard to GNEN1 local recurrence after endoscopic or surgical intervention; although the latter was associated with a lower recurrence rate [OR: 0.32 (95%CI: 0.1-1.1). Recurrence prediction stratified by patient-related parameters was not feasible in our study.

Larger sizes and the cut-off of 20 mm may be of particular interest in predicting metastatic disease to locoregional LN. Therefore, we scrutinized all available studies for this information, but a lack of data on larger sizes with double zero cells in the tables of the extracted data was evident in most studies; hence, meta-analysis at 20 mm size cut-off was not feasible. Regarding the presence of distant metastases in contemporary literature, GNEN1 is indeed a generally benign disease with very few metastatic cases reported, thus there was no sufficient material for a meta-analysis.

NOS-based quality assessment was undertaken and the included studies were generally assessed as being of moderate to high quality. Significant heterogeneity was not observed in the meta-analyses of clinico-pathological parameters investigated here, nor were small study effects. To avoid reporting bias, we also assessed and included non-English language studies, as well as unpublished data from conference papers. Various observational studies on GNEN1 have exhibited contradictory results regarding the association of certain clinico-pathological parameters with the risk of LN metastases, *e.g.*, that of the Ki67 labeling index. This observation may be due to the inclusion of other GNEN types and GNECs, which are known for a more aggressive biological behavior compared to that of WD GNEN1[14,16]. Therefore, to control biases

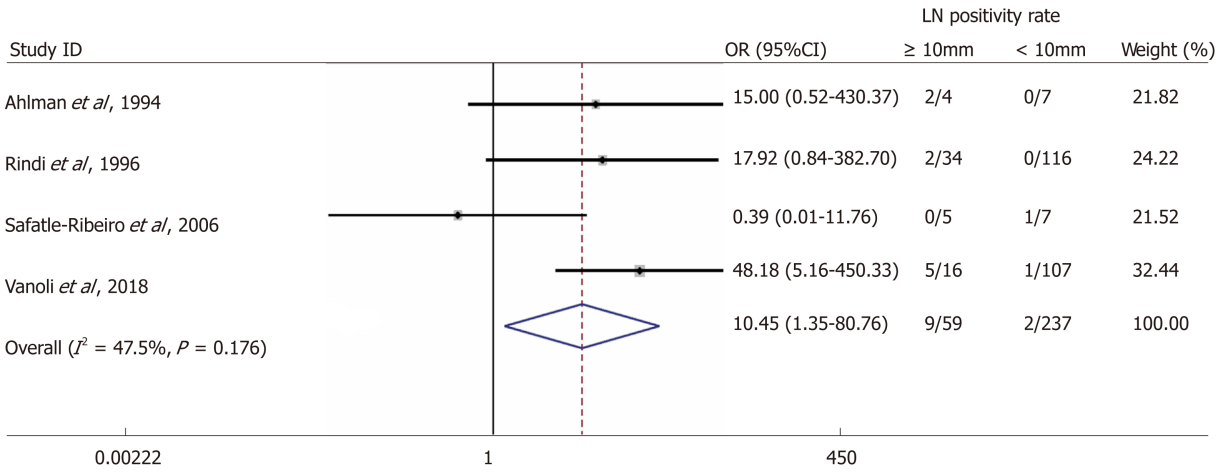


**Figure 2 Forest plot comparing the rate of lymph node metastases at a 10 mm size cut-off, *i.e.*, in tumour size ≥ 10 mm *vs* tumour size < 10 mm.** Meta-analysis of all studies carried out using a random-effects model; Odds ratios are shown with 95%CI.

attributed to tumour heterogeneity, registry and institutional studies reporting data on all types of GNEN and GNECs together with GNEN1 were excluded from our study.

In the modern management of GNEN1, endoscopic ultrasonography is an important complementary diagnostic tool that can be utilized in the assessment of lesions that are potentially invading deeper layers of the gastric wall. Endoscopic ultrasonography helps to determine the feasibility of endoscopic resection and the possible presence of locoregional LN metastases.

The majority of GNEN1 lesions are small and have traditionally been treated endoscopically; thus, the presence of locoregional LN metastases may have been underestimated. This was evident in our meta-analysis as lesions < 10 mm accounted for the majority in studies reporting size in connection to patient outcomes [237/296 (80%) lesions < 10 mm; Figure 2]. Nevertheless, cross-sectional and functional imaging were not performed or reported in all patients in the included studies, as the sensitivity of these modalities for detecting LN metastases is low and their overall impact on GNEN1 management and clinical decision-making is rather limited[23]. This should of course be taken into consideration when interpreting the findings of this meta-analysis. Additionally, a few studies only reported patient data at the individual level and in most series, ambiguity regarding the criteria for surgical resection was noted. Thus, the rates and ORs of LN metastases in GNEN1s < 10 mm and ≥ 10 mm, has to be interpreted in light of this knowledge. Finally, patients subjected to endoscopic surveillance alone without any intervention, with or without somatostatin analogues treatment, were not included in the scope of the present systematic review and meta-analysis.

The prognostic significance of tumour grade was not confirmed in our meta-analysis, as no clear association with the presence of LN metastases was evident. This is indeed an important finding that contrasts with the existing evidence in GNEN3 and GNEC, in which Ki67 is of paramount importance in disease prognostication and patient management; thus, the implication is that the GNEN type may be the most significant factor affecting patient outcomes and that this factor should be separately addressed in future studies and national registry data. Another possible explanation is that the span of Ki67 in G2 tumours is wide (3-20) and cases with a higher level of Ki67 within G2 tumours may have a substantially different course. In particular, there are studies postulating that a higher Ki67 cut-off should be considered in the clinical praxis of NEN when G2 is determined[34-36]. Additionally, we cannot exclude the possibility that additive effects of other clinico-pathological parameters combined with the concomitant G2 status may trigger metastasis. Importantly, the GNEN1 clinical course seems to be mainly benign as most studies report a 5-year DSS of 100% in patients who had undergone resection, whether endoscopic or surgical. Thus, the tumour biology, the insufficient length of follow-up and the scarcity of LN metastases in these indolent neoplasms may be the reasons the present meta-analysis could not confirm a survival difference associated with the presence of LN metastases or the type of intervention in GNEN1 patients.

Our study has some limitations. Importantly, it represents an analysis of clinico-pathological parameters extracted from multiple retrospective studies on GNEN, particularly GNEN1; hence, the included studies lacked sufficient power and were

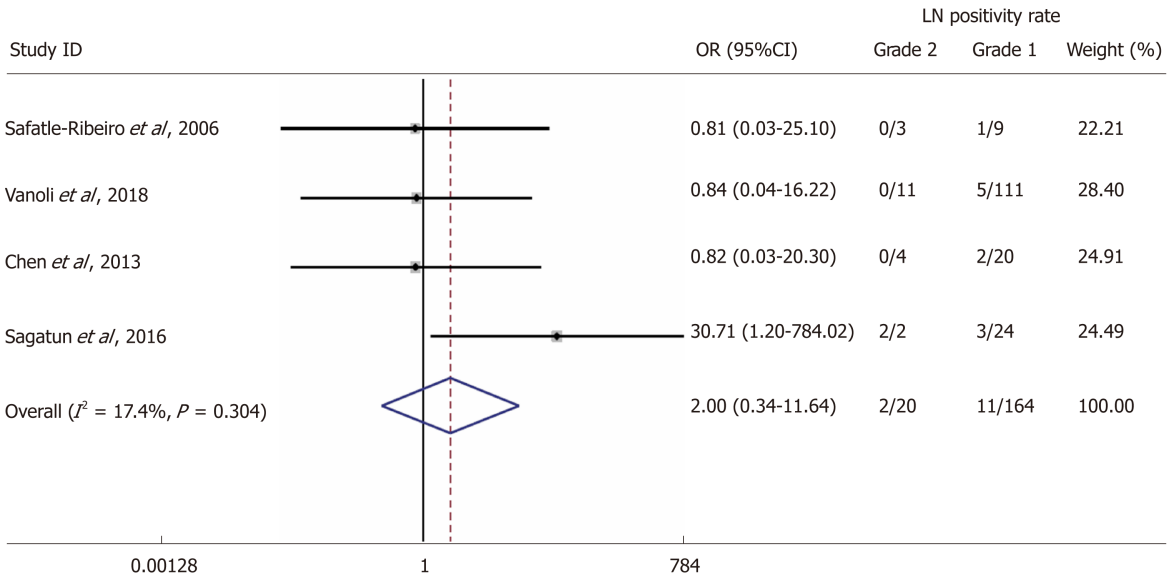


**Figure 3 Forest plot comparing the rate of lymph node metastases in patients with grade 1 *vs* grade 2 gastric neuroendocrine neoplasms type 1.** Meta-analysis of all studies carried out using a random-effects model; Odds ratios are shown with 95%CI.

often not designed to evaluate the end-points investigated in our meta-analysis. Further limitations include a diagnostic GNEN increment of more indolent lesions over time along with the wide-spread application of endoscopic screening and the clinical implementation of modern diagnostic and therapeutic modalities, such as endoscopic ultrasonography, EMR/ESMR and ESD, which may have confounded our results because different diagnostic and interventional techniques may have been potentially applied in the included studies. Additionally, a lack of data regarding larger primary tumour size cut-off values and the lack of a centralized pathology review may have caused the loss of valuable information and introduced certain biases. Another limitation was the lack of data on GNEN1 local recurrence and the lack of data at the individual level to evaluate potential additive effects of the investigated factors. Finally, heterogeneity of the included studies and the broad CIs of ORs encountered in the pooled analysis of the study estimates may be an important limitation, highlighting the need for further research in the field of GNEN1 to assess the outcomes investigated in our meta-analysis.

In, conclusion, our results have important implications for clinicians and researchers. The present study provides a systematic review and meta-analysis of GNEN1 confirming the indolent course of this neoplasm and providing patient-tailored parameters for disease prognostication and suggestions for future research. We demonstrated that locoregional LN metastases in GNEN1 are relatively rare (3.3%) and that tumour size and depth of invasion may be important predictive factors that can be used to assess the disease metastatic propensity. Generally, GNEN1 seems to have an overall excellent prognosis with very low disease-specific mortality rates reported. Additionally, survival does not seem to be negatively affected by either endoscopic or surgical resection. However, studies with long-term follow-up are scarce, and the true prognostic impacts of LN status and the type of intervention remain to be determined. Based on the findings of this meta-analysis, paying special attention to GNEN1 size and the depth of invasion and making use of diagnostic modalities such as endoscopic ultrasonography seem reasonable in clinical practice, and in future studies in the field of GNEN.

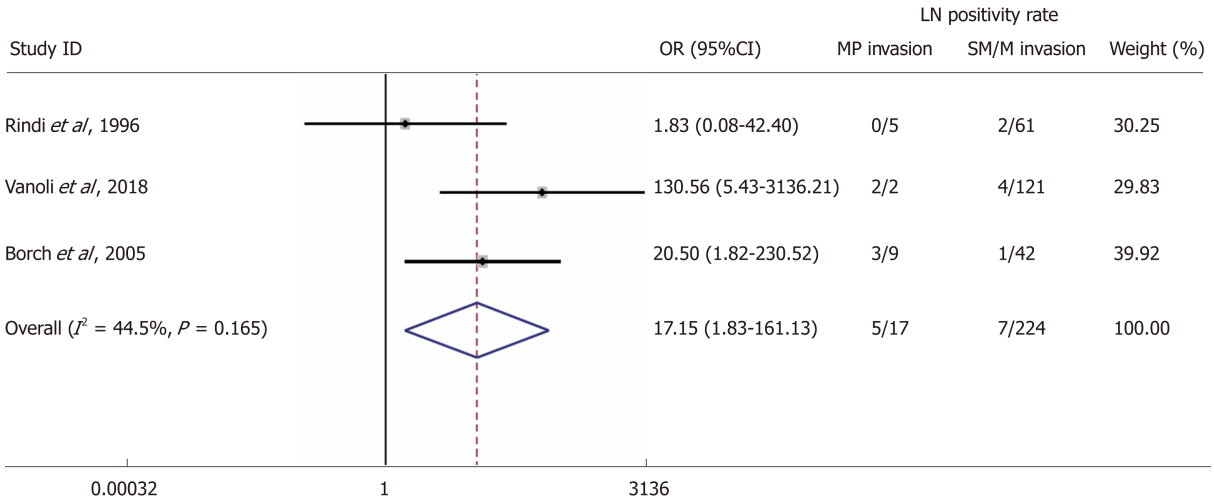


**Figure 4 Forest plot comparing the rate of lymph node metastases in tumours with mucosal/submucosal invasion *vs* tumours with invasion of the muscularis propria.** Meta-analysis of all studies carried out using a random-effects model; Odds ratios are shown with 95%CI.

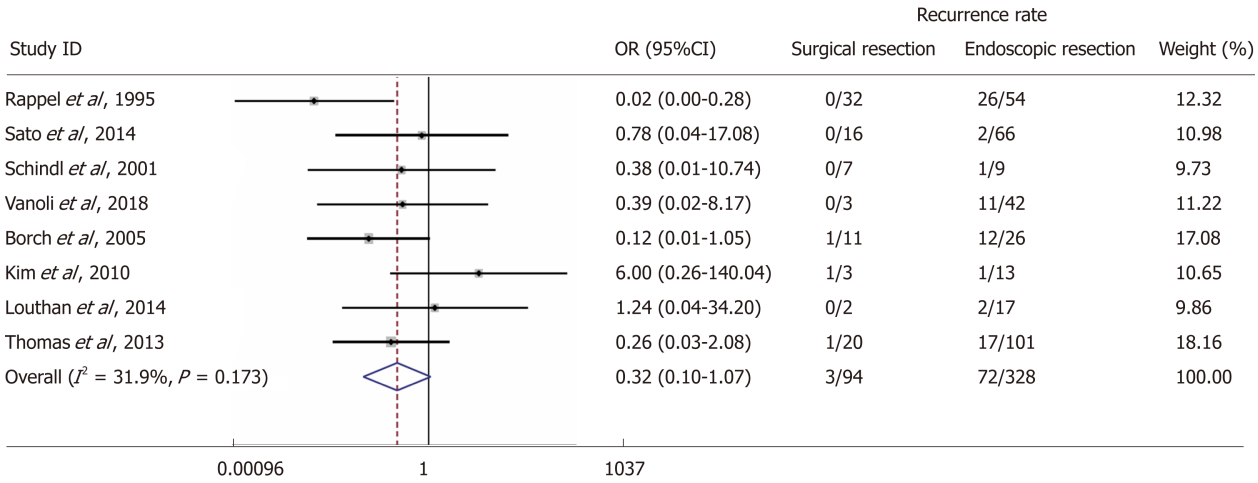


**Figure 5 Forest plot comparing the rate of local recurrence in patients with gastric neuroendocrine neoplasms type 1 undergoing endoscopic resection *vs* surgical resection.** Meta-analysis of all studies carried out using a random-effects model; Odds ratios are shown with 95%CI.

## ARTICLE HIGHLIGHTS

### *Research background*

Gastric neuroendocrine neoplasms type 1 (GNENs1) exhibit a generally benign clinical course and have distinct differences in tumour biology and patient outcomes, as compared to other types of GNENs.

### *Research motivation*

Informative clinico-pathological features (size, grade, depth of invasion) are currently used indistinguishably for most GNEN types and remain to be elucidated for GNEN1s in particular in order to determine the risk of lymph node (LN) metastases, disease-specific survival and local recurrence; and guide a more patient-tailored management.

### *Research objectives*

The aim of our study was to compare the rate of LN metastases, disease-specific mortality, and recurrence rates post intervention in patients with GNEN1s undergoing endoscopic or surgical resection with respect to the aforementioned clinico-pathological parameters (size, grade and depth of invasion). Additionally, we aimed to evaluate the rate of procedural complications associated with endoscopic and surgical interventions.

### *Research methods*

The PubMed, EMBASE, Cochrane Library, Web of Science and SCOPUS databases were searched through January 2019. The quality of the included studies and risk of bias were assessed using the Newcastle-Ottawa Scale and in accordance with the Cochrane guidelines. A

random effects model and pooled odds ratios with 95%CI were applied for the quantitative meta-analysis.

### Research results

Although the metastatic propensity of GNEN1 is low (3.3%), tumour size ≥ 10 mm and invasion of the muscularis propria in the gastric wall may be utilized to predict the presence LN. The negative predictive value of tumour size for lesions < 10 mm and that of the absence of muscularis propria invasion with respect to the presence of locoregional LN metastases were as high as 99.2% and 96.9% respectively. Contrary to other GNEN types, tumour grade was not clearly associated with the risk of LN metastases in GNEN1. The disease prognosis is excellent, with a 5-year DSS of 100% in most studies; thus, the presence of LN metastases does not seem to clearly affect survival in GNEN1 patients. Moreover, most studies reported 98-100% 5-year DSS, irrespective of the type of intervention that was undertaken. However, studies reporting long-term follow-up (*i.e.*, >10 years post-treatment surveillance) are lacking; hence, we were not able to provide evidence that prophylactic surgical resection exerts a survival benefit. The complication rates of endoscopic *vs* surgical resection in the few studies reporting this information were 0.6 and 3.8%, respectively. Finally, scarce data were available with regard to GNEN1 local recurrence after endoscopic or surgical intervention. Although surgery was associated with a lower recurrence rate, recurrence prediction stratified by patient-related parameters was not feasible in our study.

### Research conclusions

Herein, we have thoroughly investigated patient-related clinico-pathological risk parameters potentially predicting metastatic disease, recurrence following endoscopic or surgical management and disease-specific mortality rates. We confirmed that LN metastases in GNENs1 are relatively rare and that tumour size ≥ 10 mm, as well as the presence of the muscularis propria invasion are associated with an increased risk for LN metastasis. The latter finding suggests that endoscopic ultrasound investigation is very valuable in the work up of these lesions. Finally, surgical resection is linked to a lower risk for local recurrence.

### Research perspectives

The present study provides a systematic review and meta-analysis of GNEN1 confirming the indolent course of this neoplasm and providing suggestions for future research towards a stratified approach based on patient-tailored parameters in the era of personalized medicine. Foremost, based on our findings, special attention to GNEN1 size and the depth of invasion and making use of diagnostic modalities, such as endoscopic ultrasonography, seem reasonable in clinical practice, and in future studies with long-term follow up in the field of GNEN1.

## REFERENCES


1 **Grozinsky-Glasberg S**, Alexandraki KI, Angelousi A, Chatzellis E, Sougioultzis S, Kaltsas G. Gastric Carcinoids. *Endocrinol Metab Clin North Am* 2018; **47**: 645-660 [PMID: 30098721 DOI: 10.1016/j.ecl.2018.04.013]

2 **Tsolakis AV**, Portela-Gomes GM, Stridsberg M, Grimelius L, Sundin A, Eriksson BK, Oberg KE, Janson ET. Malignant gastric ghrelinoma with hyperghrelinemia. *J Clin Endocrinol Metab* 2004; **89**: 3739-3744 [PMID: 15292299 DOI: 10.1210/jc.2003-032118]

3 **Tsolakis AV**, Stridsberg M, Grimelius L, Portela-Gomes GM, Falkmer SE, Waldum HL, Janson ET. Ghrelin immunoreactive cells in gastric endocrine tumors and their relation to plasma ghrelin concentration. *J Clin Gastroenterol* 2008; **42**: 381-388 [PMID: 18277901 DOI: 10.1097/MCG.0b013e318032338c]

4 **Tsolakis AV**, Grimelius L, Stridsberg M, Falkmer SE, Waldum HL, Saras J, Janson ET. Obestatin/ghrelin cells in normal mucosa and endocrine tumours of the stomach. *Eur J Endocrinol* 2009; **160**: 941-949 [PMID: 19289536 DOI: 10.1530/EJE-09-0001]

5 **Tsolakis AV**, Grimelius L, Granerus G, Stridsberg M, Falkmer SE, Janson ET. Histidine decarboxylase and urinary methylimidazoleacetic acid in gastric neuroendocrine cells and tumours. *World J Gastroenterol* 2015; **21**: 13240-13249 [PMID: 26715806 DOI: 10.3748/wjg.v21.i47.13240]

6 **Solcia E**, Arnold R, Capella C, Klimstra DS, Klöppel G, Komminoth P, Rindi G. *Neuroendocrine neoplasms of the stomach*. In: Bosman FT, Carneiro F, Hruban RH, Theise ND, editors. WHO Classification of Tumours of the Digestive System. 4th ed. Lyon World Health Organization 2010; 64-68

7 **Modlin IM**, Lye KD, Kidd M. A 50-year analysis of 562 gastric carcinoids: small tumor or larger problem? *Am J Gastroenterol* 2004; **99**: 23-32 [PMID: 14687136]

8 **Spampatti MP**, Massironi S, Rossi RE, Conte D, Sciola V, Ciafardini C, Ferrero S, Lodi L, Peracchi M. Unusually aggressive type 1 gastric carcinoid: a case report with a review of the literature. *Eur J Gastroenterol Hepatol* 2012; **24**: 589-593 [PMID: 22465973 DOI: 10.1097/MEG.0b013e328350fae8]

9 **Delle Fave G**, O'Toole D, Sundin A, Taal B, Ferolla P, Ramage JK, Ferone D, Ito T, Weber W, Zheng-Pei Z, De Herder WW, Pascher A, Ruszniewski P; Vienna Consensus Conference participants. ENETS Consensus Guidelines Update for Gastroduodenal Neuroendocrine Neoplasms. *Neuroendocrinology* 2016; **103**: 119-124 [PMID: 26784901 DOI: 10.1159/000443168]

10 **Moher D**, Liberati A, Tetzlaff J, Altman DG; PRISMA Group. Preferred reporting items for systematic reviews and meta-analyses: the PRISMA statement. *Ann Intern Med* 2009; **151**: 264-269, W64 [PMID: 19622511 DOI: 10.7326/0003-4819-151-4-200908180-00135]

11 **Mathes T**, Pieper D. Study design classification of registry-based studies in systematic reviews. *J Clin Epidemiol* 2018; **93**: 84-87 [PMID: 28951107 DOI: 10.1016/j.jclinepi.2017.09.016]

12 **Stang A**. Critical evaluation of the Newcastle-Ottawa scale for the assessment of the quality of nonrandomized studies in meta-analyses. *Eur J Epidemiol* 2010; **25**: 603-605 [PMID: 20652370 DOI: 10.1007/s10654-010-9491-z]

13 **Ahlman H**, Kölby L, Lundell L, Olbe L, Wängberg B, Granérus G, Grimelius L, Nilsson O. Clinical management of gastric carcinoid tumors. *Digestion* 1994; **55** Suppl 3: 77-85 [PMID: 7698542 DOI: 10.1159/000201206]

14 **Rindi G**, Bordi C, Rappel S, LaRosa S, Stolte M, Solcia E. Gastric carcinoids and neuroendocrine carcinomas: Pathogenesis, pathology, and behavior. I1996; 20: 168-172. [PMID: 8661813]

15 **Safatle-Ribeiro AV**, Ribeiro U, Corbett CE, Iriya K, Kobata CH, Sakai P, Yagi OK, Pinto PE, Zilberstein B, Gama-Rodrigues J. Prognostic value of immunohistochemistry in gastric neuroendocrine (carcinoid) tumors. *Eur J Gastroenterol Hepatol* 2007; **19**: 21-28 [PMID: 17206073 DOI: 10.1097/01.meg.0000250582.30737.bd]

16 **Vanoli A**, La Rosa S, Miceli E, Klersy C, Maragliano R, Capuano F, Persichella A, Martino M, Inzani F, Luinetti O, Di Sabatino A, Sessa F, Paulli M, Corazza GR, Rindi G, Bordi C, Capella C, Solcia E. Prognostic Evaluations Tailored to Specific Gastric Neuroendocrine Neoplasms: Analysis Of 200 Cases with Extended Follow-Up. *Neuroendocrinology* 2018; **107**: 114-126 [PMID: 29895024 DOI: 10.1159/000489902]

17 **Sagatun L**, Fossmark R, Jianu CS, Qvigstad G, Nordrum IS, Mjønes P, Waldum HL. Follow-up of patients with ECL cell-derived tumours. *Scand J Gastroenterol* 2016; **51**: 1398-1405 [PMID: 27309188 DOI: 10.3109/00365521.2016.1169588]

18 **Chen WC**, Warner RRP, Harpaz N, Zhu H, Roayaie S, Kim MK. Gastric Neuroendocrine Tumor and Duodenal Gastrinoma With Chronic Autoimmune Atrophic Gastritis. *Pancreas* 2019; **48**: 131-134 [PMID: 30531243 DOI: 10.1097/MPA.0000000000001204]

19 **Borch K**, Ahrén B, Ahlman H, Falkmer S, Granérus G, Grimelius L. Gastric carcinoids: biologic behavior and prognosis after differentiated treatment in relation to type. *Ann Surg* 2005; **242**: 64-73 [PMID: 15973103 DOI: 10.1097/01.sla.0000167862.52309.7d]

20 **Sato Y**, Imamura H, Kaizaki Y, Koizumi W, Ishido K, Kurahara K, Suzuki H, Fujisaki J, Hirakawa K, Hosokawa O, Ito M, Kaminishi M, Furuta T, Chiba T, Haruma K. Management and clinical outcomes of type I gastric carcinoid patients: retrospective, multicenter study in Japan. *Dig Endosc* 2014; **26**: 377-384 [PMID: 24188531 DOI: 10.1111/den.12197]

21 **Schindl M**, Kaserer K, Niederle B. Treatment of gastric neuroendocrine tumors - The necessity of a type-adapted treatment. *Arch Surg* 2001; **136**: 49-54 [PMID: 11146777 DOI: 10.1001/archsurg.136.1.49]

22 **Rappel S**, Altendorf-Hofmann A, Stolte M. Prognosis of gastric carcinoid tumours. *Digestion* 1995; **56**: 455-462 [PMID: 8536814 DOI: 10.1159/000201276]

23 **Thomas D**, Tsolakis AV, Grozinsky-Glasberg S, Fraenkel M, Alexandraki K, Sougioultzis S, Gross DJ, Kaltsas G. Long-term follow-up of a large series of patients with type 1 gastric carcinoid tumors: data from a multicenter study. *Eur J Endocrinol* 2013; **168**: 185-193 [PMID: 23132699 DOI: 10.1530/EJE-12-0836]

24 **Louthan O**. Neuroendocrine neoplasms of the stomach. *Biomed Pap Med Fac Univ Palacky Olomouc Czech Repub* 2014; **158**: 455-460 [PMID: 23817299 DOI: 10.5507/bp.2013.045]

25 **Kim BS**, Oh ST, Yook JH, Kim KC, Kim MG, Jeong JW, Kim BS. Typical carcinoids and neuroendocrine carcinomas of the stomach: differing clinical courses and prognoses. *Am J Surg* 2010; **200**: 328-333 [PMID: 20385369 DOI: 10.1016/j.amjsurg.2009.10.028]

26 **Manfredi S**, Walter T, Baudin E, Coriat R, Ruszniewski P, Lecomte T, Laurenty AP, Goichot B, Rohmer V, Roquin G, Cojocarasu OZ, Lombard-Bohas C, Lepage C, Morcet J, Cadiot G. Management of gastric neuro-endocrine tumours in a large French national cohort (GTE). *Endocrine* 2017; **57**: 504-511 [PMID: 28664309 DOI: 10.1007/s12020-017-1355-9]

27 **Gladdy RA**, Strong VE, Coit D, Allen PJ, Gerdes H, Shia J, Klimstra DS, Brennan MF, Tang LH. Defining surgical indications for type I gastric carcinoid tumor. *Ann Surg Oncol* 2009; **16**: 3154-3160 [PMID: 19727959 DOI: 10.1245/s10434-009-0687-y]

28 **Lee HE**, Mounajjed T, Erickson LA, Wu TT. Sporadic Gastric Well-Differentiated Neuroendocrine Tumors Have a Higher Ki-67 Proliferative Index. *Endocr Pathol* 2016; **27**: 259-267 [PMID: 27306997 DOI: 10.1007/s12022-016-9443-6]

29 **Grozinsky-Glasberg S**, Thomas D, Strosberg JR, Pape UF, Felder S, Tsolakis AV, Alexandraki KI, Fraenkel M, Saiegh L, Reissman P, Kaltsas G, Gross DJ. Metastatic type 1 gastric carcinoid: a real threat or just a myth? *World J Gastroenterol* 2013; **19**: 8687-8695 [PMID: 24379587 DOI: 10.3748/wjg.v19.i46.8687]

30 **Li QL**, Zhang YQ, Chen WF, Xu MD, Zhong YS, Ma LL, Qin WZ, Hu JW, Cai MY, Yao LQ, Zhou PH. Endoscopic submucosal dissection for foregut neuroendocrine tumors: an initial study. *World J Gastroenterol* 2012; **18**: 5799-5806 [PMID: 23155323 DOI: 10.3748/wjg.v18.i40.5799]

31 **Merola E**, Sbrozzi-Vanni A, Panzuto F, D'Ambra G, Di Giulio E, Pilozzi E, Capurso G, Lahner E, Bordi C, Annibale B, Delle Fave G. Type I Gastric Carcinoids: A Prospective Study on Endoscopic Management and Recurrence Rate. *Neuroendocrinology* 2012; **95**: 207-213 [PMID: 21811050 DOI: 10.1159/000329043]

32 **Postlewait LM**, Baptiste GG, Ethun CG, Le N, Cardona K, Russell MC, Willingham FF, Kooby DA, Staley CA, Maithel SK. A 15-year experience with gastric neuroendocrine tumors: Does type make a difference? *J Surg Oncol* 2016; **114**: 576-580 [PMID: 27393718 DOI: 10.1002/jso.24369]

33 **Uygun A**, Kadayifci A, Polat Z, Yilmaz K, Gunal A, Demir H, Bagci S. Long-term results of endoscopic resection for type I gastric neuroendocrine tumors. *J Surg Oncol* 2014; **109**: 71-74 [PMID: 24165913 DOI: 10.1002/jso.23477]

34 **Campana D**, Ravizza D, Ferolla P, Faggiano A, Grimaldi F, Albertelli M, Ricci C, Santini D, Brighi N, Fazio N, Colao A, Ferone D, Tomassetti P. Risk factors of type 1 gastric neuroendocrine neoplasia in patients with chronic atrophic gastritis. A retrospective, multicentre study. *Endocrine* 2017; **56**: 633-638 [PMID: 27592118 DOI: 10.1007/s12020-016-1099-y]

35 **Klöppel G**, La Rosa S. Ki67 labeling index: assessment and prognostic role in gastroenteropancreatic neuroendocrine neoplasms. *Virchows Arch* 2018; **472**: 341-349 [PMID: 29134440 DOI: 10.1007/s00428-017-2258-0]

36 **Hauck L**, Bitzer M, Malek N, Plentz RR. Subgroup analysis of patients with G2 gastroenteropancreatic neuroendocrine tumors. *Scand J Gastroenterol* 2016; **51**: 55-59 [PMID: 26137871 DOI: 10.3109/00365521.2015.1064994]

World Journal of Gastroenterology

Submit a Manuscript: https://www.f6publishing.com

World J Gastroenterol 2019 September 21; 25(35): 5388-5402

DOI: 10.3748/wjg.v25.i35.5388

ISSN 1007-9327 (print) ISSN 2219-2840 (online)

CASE REPORT

# Autoimmune hepatitis in human immunodeficiency virus-infected patients: A case series and review of the literature

Roongruedee Chaiteerakij, Anapat Sanpawat, Anchalee Avihingsanon, Sombat Treeprasertsuk

**ORCID number:** Roongruedee Chaiteerakij (0000-0002-7191-3881); Anapat Sanpawat (0000-0002-6425-3379); Anchalee Avihingsanon (0000-0003-3222-9611); Sombat Treeprasertsuk (0000-0001-6459-8329).

**Author contributions:** Chaiteerakij R was the patients' hepatologist, reviewed the literature and contributed to manuscript drafting; Sanpawat A performed the pathological diagnosis and contributed to manuscript drafting; Avihingsanon A performed the HIV disease consultation and contributed to manuscript drafting; Treeprasertsuk S were the patients' hepatologist, reviewed the literature and contributed to manuscript drafting. Chaiteerakij R and Treeprasertsuk S were responsible for the revision of the manuscript for important intellectual content; all authors issued final approval for the version to be submitted.

**Informed consent statement:** Informed written consent was obtained from the patient for publication of this report and any accompanying images.

**Conflict-of-interest statement:** The authors declare that they have no conflict of interest.

**CARE Checklist (2016) statement:** The authors have read the CARE Checklist (2016), and the manuscript was prepared and revised according to the CARE Checklist (2016).



**Roongruedee Chaiteerakij, Sombat Treeprasertsuk,** Department of Medicine, Chulalongkorn University and King Chulalongkorn Memorial Hospital, Bangkok 10330, Thailand

**Anapat Sanpawat,** Department of Pathology, Chulalongkorn University and King Chulalongkorn Memorial Hospital, Bangkok 10330, Thailand

**Anchalee Avihingsanon,** Medical Department, The HIV Netherlands Australia Thailand Research Collaboration, Bangkok 10330, Thailand

**Corresponding author:** Sombat Treeprasertsuk, MD, PhD, Professor of Internal Medicine, Division of Gastroenterology, Department of Medicine, Chulalongkorn University and King Chulalongkorn Memorial Hospital, 1873 Rama IV Road, Patumwan, Bangkok 10330, Thailand. apobtsol@hotmail.com.
**Telephone:** +66-2-2564265
**Fax:** +66-2-6524129

## Abstract

*BACKGROUND*

Abnormal liver chemistry is a common problem in human immunodeficiency virus (HIV)-infected patients. Common causes of abnormal liver enzymes in this population include viral hepatitis B/C or opportunistic infection, drug toxicity, and neoplasm. Autoimmune hepatitis is a rare cause of hepatitis in HIV-infected individuals; however, this condition has been increasingly reported over the past few years.

*CASE SUMMARY*

We present 13 HIV-infected patients (5 males and 8 females) who developed autoimmune hepatitis (AIH) after their immune status was restored, i.e. all patients had stable viral suppression with undetectable HIV viral loads, and median CD4+ counts of 557 cells/× $10^6$ L. Eleven patients presented with chronic persistent elevation of aminotransferase enzyme levels. One patient presented with acute hepatitis and the other patient presented with jaundice. The median levels of aspartate aminotransferase and alanine aminotransferase enzymes were 178 and 177 U/mL, respectively. Elevation of immunoglobulin G levels was present in 11 (85%) patients. Antinuclear antibody and anti-smooth muscle antibody were positive in 11 (85%) and 5 (38%) patients. Liver biopsy was performed in all patients. They had histopathological findings compatible with AIH. The patients were started on prednisolone for remission induction, with good response. After improvement of the liver chemistry, the dose of prednisolone was tapered, and azathioprine was added as life-long maintenance therapy. At the last follow-up visit, all were doing well, without HIV viral

**Manuscript source**: Invited manuscript

**Received:** June 22, 2019
**Peer-review started:** June 25, 2019
**First decision:** July 22, 2019
**Revised:** August 14, 2019
**Accepted:** August 24, 2019
**Article in press:** July 22, 2019
**Published online:** September 21, 2019

**P-Reviewer:** Invernizzi P, Kreisel W
**S-Editor:** Gong ZM
**L-Editor:** A
**E-Editor:** Ma YJ

rebound or infectious complications.

*CONCLUSION*
This report underscores the emergence of autoimmune hepatitis in the context of HIV infection.

**Key words:** Autoimmune hepatitis; Human immunodeficiency virus; Liver biopsy; Immunosuppression; Autoimmunity; Antiretroviral therapy; Case report



**Core tip:** Elevated liver enzymes are a common problem in human immunodeficiency virus (HIV)-infected patients. Clinical manifestations of autoimmune hepatitis (AIH) range from no symptoms to mild chronic hepatitis to acute severe hepatitis leading to fulminant hepatic failure or cirrhosis. The diagnosis of AIH requires thorough investigation. It is crucial to perform liver biopsy to confirm the diagnosis. Although rare, AIH should be considered a differential diagnosis in HIV-infected patients presenting with elevated aminotransferase enzyme levels after the exclusion of other common causes of hepatitis. It is believed that this condition occurs due to immune reconstitution inflammatory syndrome (IRIS). Immunosuppressive drugs are the mainstay of treatment and can be used safely in HIV-infected patients.

**Citation:** Chaiteerakij R, Sanpawat A, Avihingsanon A, Treeprasertsuk S. Autoimmune hepatitis in human immunodeficiency virus-infected patients: A case series and review of the literature. *World J Gastroenterol* 2019; 25(35): 5388-5402
**URL**: https://www.wjgnet.com/1007-9327/full/v25/i35/5388.htm
**DOI**: https://dx.doi.org/10.3748/wjg.v25.i35.5388

## INTRODUCTION

Autoimmune hepatitis (AIH) is considered to be a relatively rare chronic liver disease. Its incidence, prevalence and clinical phenotype vary considerably by geographical area. The annual incidence of AIH ranges from 0.5-2.2 per 100000 individuals[1]. During the past 2 decades, the incidence of AIH has remained stable in Sweden and Finland[2,3] but has increased in certain countries, such as Denmark, Netherlands and Spain[4-6]. The prevalence of AIH in the Asia-Pacific region is lower than that reported in Europe and America (Table 1)[2-17]. Within the Asia-Pacific region, India has the lowest prevalence per 100,000 individuals of 1.5, while Japan and New Zealand have the highest prevalence of 23.4 and 24.5, respectively[8,14,15]. Among Western countries, Finland has the lowest prevalence per 100000 individuals of 14.3, while Alaska has the highest prevalence of 42.9[3,17]. Variations in disease occurrence across different countries suggest that some environmental factors may play a role in AIH development.

AIH is a chronic liver disease with progressive liver parenchymal inflammation and damage caused by regulatory T-cell dysfunction-induced hyperreactive responses. The disease is characterized by hypergammaglobulinemia, the presence of circulating autoantibodies, and typical histologic features including interface hepatitis, lymphoplasmacytic cell infiltration, liver cell rosette formation, emperipolesis and response to immunosuppressive therapy[18]. It has been suggested that a genetic predisposition, molecular mimicry and environmental factors are associated with the development of AIH[19].

The diagnosis of AIH relies on criteria comprising clinical, serological, and histological features. Clinical presentation is heterogeneous, ranging from no symptoms to acute or chronic hepatitis to acute liver failure or cirrhosis. Initial laboratory tests show elevation of aminotransaminase enzymes. Although abnormal liver chemistry commonly occurs in HIV-affected individuals (approximately 27%), AIH is rarely suspected at presentation. The most common cause of liver enzyme elevation in patients with HIV infection is nonalcoholic fatty liver disease, followed by alcohol intake, and viral hepatitis B and C infection[20]. Despite the rarity of this disease, the number of reports of AIH in HIV-infected individuals has increased in recent years[21-39]. Here, we present 13 HIV-infected patients who developed AIH after

**Table 1 Prevalence and incidence of autoimmune hepatitis among different countries in the world[1]**

| Country | Prevalence | Incidence | Study period |
|---|---|---|---|
| *Asia-Pacific* | | | |
| Taiwan[7] | NA | 0.5 | 2000 -2004 |
| India[8] | 1.5 | NA | 1999 -2002 |
| Singapore[9] | 4.0 | NA | 1990 -1996 |
| South Korea[10] | 4.8 | 1.1 | 2009 -2013 |
| Brunei Darussalam[11] | 5.6 | NA | NA |
| Australia[12] | 8.0 | NA | NA |
| Israel[13] | 11.0 | 0.7 | 1995 -2010 |
| Japan[14] | 23.4 | 2.2 | 2004 -2014 |
| New Zealand[15] | 24.5 | 2.0 | 2001 -2008 |
| *Europe and America* | | | |
| Spain[6] | NA | 1.1 | 2003 |
| Finland[3] | 14.3 | 1.1 | 1995 -2015 |
| Norway[16] | 16.9 | 1.9 | 1986 -1995 |
| Sweden[2] | 17.3 | 1.2 | 1989 -2011 |
| Netherlands[5] | 18.3 | 1.1 | 1967 -2011 |
| Denmark[4] | 23.9 | 1.7 | 1994 -2012 |
| United States (Alaska)[17] | 42.9 | NA | 1984 -2000 |

[1]Unit of prevalence and incidence: per 100000 population. NA: Not available.

treatment with antiretroviral therapy. The characteristics of previously reported HIV-infected patients with AIH are also summarized.

## CASE PRESENTATION

### *Chief complaints*

We identified a total of 13 patients with coexisting HIV infection and AIH. All were Asians. There were 5 (38%) males and 8 (62%) females, with a median age of 40 years at AIH diagnosis (range: 26–61 years). The patients were referred to our liver clinic for evaluation of abnormal liver functions.

### *History of present illness*

Most patients (11/13, 84.6%) presented with chronic persistent elevation of aminotransferase enzyme levels for a median duration of 10 mo (range: 4–31 mo). One patient presented with acute hepatitis for 2 mo, and the other patient presented with jaundice for a month.

### *History of past illness*

The median duration of HIV infection before AIH diagnosis was 6 years (range: 1–24 years). Eleven patients received antiretroviral therapy once HIV infection was diagnosed. Only 2 patients were started on antiretroviral drugs 13 and 4 years after HIV diagnosis, respectively. Eight (62%) patients received only one antiretroviral regimen and had never been switched to other regimens until the time of AIH presentation: 6 and 2 patients received tenofovir/emtricitabine/efavirenz (TDF/FTC/EFV) and tenofovir/lamivudine/efavirenz (TDF/3TC/EFV), respectively. Another 5 (38%) patients were treated with multiple antiretroviral regimens prior to AIH diagnosis. The first patient who had HIV infection for 10 years received zidovudine/3TC/EFV for 2 years and was subsequently switched to TDF/3TC/EFV for 1 year and TDF/FTC/EFV since then. The second patient with HIV infection for 2 years was put on TDF/FTC/EFV for a brief period and switched to abacavir (ABC)/3TC/rilpivirine (RPV). The third patient with HIV infection for 1 year was initially on stavudine (d4T)/3TC/EFV but developed peripheral neuropathy at the second month; therefore, he was switched to TDF/3TC/EFV. The fourth patient who had HIV for 13 years was initially treated with TDF/3TC/EFV and switched to TDF/FTC/EFV. The last patient had HIV infection for 24 years; 13 years after

diagnosis, she was started on d4T/3TC/nevirapine (NVP) for 4 years, followed by TDF/3TC/NVP for 3 years, and TDF/3TC/EFV since then. All patients had undetectable HIV viral loads at AIH presentation, with median CD4+ cell counts of 557 cells/x$10^6$ L (range: 82–963 cells/× $10^6$ L).

### Physical examination

Of the 13 patients, one (7.7%) had cirrhosis at the time of AIH presentation. She had signs of chronic liver diseases on examination and radiologic features of cirrhosis.

### Laboratory examinations

Table 2 summarizes the baseline characteristics and laboratory data of the 13 patients at the time of AIH diagnosis. The median (range) levels of aspartate aminotransferase (AST) and alanine aminotransferase (ALT) enzymes were 178 (63–393) and 177 (49–353) U/mL, respectively (normal AST and ALT levels are < 35 and < 40 U/mL, respectively). Twelve patients had normal bilirubin levels, and one patient had elevated total bilirubin levels of 6.3 mg/dL. Notably, elevated globulin levels were observed in all patients (normal range: 2.0-3.3 g/dL).

Because viral hepatitis infection, including viral hepatitis A, B, C and E (HAV, HBV, HCV and HEV), is one of the common causes of abnormal liver chemistry, blood tests for hepatitis B surface antigen (HBsAg), antibody to HAV, HCV and HEV were performed. All 13 patients were tested for HBsAg and anti-HCV antibody. One patient was positive for HBsAg and another patient was positive for Anti-HCV antibody, however, both patients had undetectable HBV DNA and HCV RNA viral load at AIH presentation. There were 7 (54%) and 7 (54%) of patients who were tested for anti-HAV IgM and anti-HEV IgM antibody. All were negative for the tests.

Other blood tests to investigate the possible causes of abnormal liver chemistry included thyroid function test ($n$ = 5), iron studies ($n$ = 5), ceruloplasmin level ($n$ = 1) and controlled attenuation parameter by FibroScan® ($n$ = 7). The results were all negative.

### Further diagnostic work-up

History of alcohol consumption as well as medication and herbal use was thoroughly reviewed to exclude alcoholic hepatitis and drug-induced liver injury as possible causes of abnormal liver chemistry. Further investigation revealed an elevation of immunoglobulin G (IgG) levels in 11 (85%) patients, with a median of 2,250 mg/dL (normal range: 7548–1768 mg/dL). Antinuclear antibody (ANA) was positive in 11 (85%) patients; however, anti-smooth muscle antibody (ASMA) was positive in only 5 (38%) patients.

### Pathological examinations

Liver biopsy was performed in all patients. They had histopathological findings compatible with AIH, *i.e.*, lymphoplasmacytic cell infiltration and interface hepatitis (Figures 1 and 2). Three (23%) patients revealed cirrhosis on histopathological examination.

## FINAL DIAGNOSIS

The final diagnosis of the presented cases was autoimmune hepatitis.

## TREATMENT

After the diagnosis of AIH was made, 2 patients were referred back to the primary hospital for treatment initiation and long-term follow up, and 11 patients received treatment and were followed at our hospital. Ten of the 11 patients were started on prednisolone monotherapy for remission induction at daily doses of 40, 30 and 20 mg in 1, 5 and 3 patients, respectively. One patient who had Child-Pugh class A cirrhosis at presentation was put on a combination of low-dose prednisolone (15 mg/d) and azathioprine (25 mg/d).

## OUTCOME AND FOLLOW-UP

Liver chemistry was monitored every 2 wk during the first month after treatment initiation and every 1-4 mo afterwards depending on clinical outcome and the primary physician's judgement. None of patients performed repeat liver biopsy. After

**Table 2 Baseline characteristics of 13 human immunodeficiency virus-infected patients at the time of autoimmune hepatitis diagnosis**

| Case | Sex | Age | HIV status | | | | Presentation, duration (mo) | Lab values[1] | | | | | | | | | AIH score |
|---|---|---|---|---|---|---|---|---|---|---|---|---|---|---|---|---|---|
| | | | Duration (yr) | Current ART regimen, duration (year or month) | Viral load, duration (year or month) | CD4+ count in 2 and 1 years ago and at AIH presentation | | AST | ALT | ALP | TB | Albumin | Globulin | ANA titer | ASMA | IgG | |
| 1 | M | 47 | 7 | TDF/FTC/EFV, 4 yr | < 40, 3 yr | 761, 885, 963 | Rising ALT, 10 mo | 121 | 263 | 145 | 0.8 | 4.4 | 4.8 | 0.0972222222 | + | 2930 | 7 |
| 2 | M | 44 | 21 | TDF/FTC/EFV, 1 yr | < 40, 5 yr | 588, 669, 798 | Rising ALT, 2 mo | 130 | 172 | 172 | 0.4 | 4.5 | 4 | 0.0972222222 | - | 1310 | 5 |
| 3 | M | 61 | 10 | TDF/FTC/EFV, 8 yr | < 40, 6 yr | 496, -, 646 | Rising ALT, 31 mo | 168 | 177 | 189 | 0.8 | 4 | 4.8 | > 1280 | - | 1890 | 6 |
| 4 | M | 26 | 1 | TDF/3TC/EFV, 6 mo | < 40, 1 mo | -, -, 82 | Rising ALT, 7 mo | 199 | 197 | 106 | 0.8 | 4.6 | 4.6 | < 1:40 | - | 1920 | 5 |
| 5 | F | 30 | 7 | TDF/3TC/EFV, 6 yr | < 40, - | -, -, 772 | Rising ALT, 9 mo | 236 | 157 | 191 | 0.4 | 3.6 | 5.9 | > 1:1280 | - | 4100 | 7 |
| 6 | F | 29 | 6 | TDF/FTC/EFV, 6 yr | < 40, - | -, -, 731 | Rising ALT, 10 mo | 108 | 133 | 125 | 1 | 4.1 | 3.7 | 0.2638888889 | - | 1710 | 5 |
| 7 | F | 57 | 25 | TDF/3TC/EFV, 8 yr | < 40, 7 yr | 583, 477, 384 | Rising ALT, 24 mo | 106 | 49 | 357 | 0.6 | 3.7 | 6.5 | 1.8194444444 | - | 2333 | 7 |
| 8 | F | 40 | 10 | TDF/3TC/EFV, 6 yr | < 40, 5 yr | -, 415, 480 | Rising ALT, 4 mo | 269 | 353 | 237 | 0.7 | 4.1 | 3.9 | < 1:40 | + | 1860 | 5 |
| 9 | F | 46 | 6 | TDF/FTC/EFV, 3 yr | < 40, - | -, -, 451 | Rising ALT, 20 mo | 178 | 230 | 262 | 1.4 | 3.8 | 4.2 | > 1:1280 | + | 2050 | 7 |
| 10 | F | 34 | 2 | TDF/FTC/EFV, 1 yr | < 40, 10 mo | -, 377, 557 | Rising ALT, 11 mo | 191 | 205 | 112 | 1.3 | 3.8 | 4.1 | 0.2638888889 | + | 2580 | 7 |
| 11 | F | 31 | 2 | TDF/FTC/EFV, 6 mo | < 40, 1 mo | -, -, 563 | Jaundice, 1 mo | 393 | 266 | 133 | 6.3 | 3.1 | 5.1 | 0.2638888889 | + | 3710 | 7 |
| 12 | F | 40 | 13 | TDF/FTC/EFV, 3 yr | < 40, 3 yr | 320, 298, 216 | Rising ALT, 6 mo | 314 | 150 | 304 | 2 | 3.3 | 6.8 | > 1:2560 | - | 5050 | 7 |
| 13 | M | 39 | 4 | ABC/RPV/3TC, 1 yr | < 40, 2 yr | -, 52, 310 | Rising ALT, 23 mo | 63 | 124 | 100 | 0.7 | 4.1 | 4.4 | 0.0972222222 | - | 2250 | 7 |

[1]Unit of labs: AST, ALT, and ALP – U/L, TB and IgG – mg/dL, albumin and globulin – g/dL. 3TC: Lamivudine; ABC: Abacavir; EFV: Efavirenz; RPV: Rilpivirine; TDF: Tenofovir; AIH: Autoimmune hepatitis; HIV: Human immunodeficiency virus.

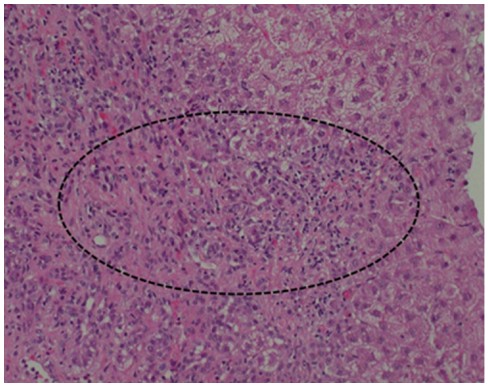

**Figure 1 Portal inflammation.** A mononuclear cell inflammatory infiltrate in portal tracts (circle).

1 mo of therapy, all 11 patients showed improvement in liver chemistry. All 10 patients experienced liver enzyme normalization at a median time of 6 mo after immunosuppressive therapy initiation. The last patient who had received treatment for 4 mo had ALT improvement, but the ALT level remained slightly above the upper limit of normal at the time of writing this manuscript. After improvement of the liver chemistry, the dose of prednisolone was tapered, and azathioprine was added as life-long maintenance therapy. One patient developed cytopenia from azathioprine, and was therefore placed on mycophenolate mofetil with a good response.

All 11 patients who received treatment at our hospital underwent regular follow-up visits. The median time to follow-up was 23 mo (range: 5–43 mo). During the follow-up period, one patient experienced a minor flare when the dose of steroid was tapered. At the time of AIH diagnosis, AST and ALT levels were 121 and 263 U/L, respectively, with IgG level of 2930 mg/dL. He was initially treated with prednisolone 30 mg/d for 2 wk, followed by 20 mg/d for 4 wk and 15 mg/d for 6 wk. Three months after treatment initiation, AST and ALT levels decreased to 50 and 93 U/L, respectively, with a declined level of IgG to 2130 mg/dL. Azathioprine 50 mg daily was therefore added with gradual reduction of prednisolone dosage to 10 mg, 5 and 2.5 mg/d during the next 7 mo period. At month 16 after therapy, AST and ALT levels increased to 71 and 100 U/L, respectively, with rising IgG of 2254 mg/dL. Prednisolone was therefore increased to 15 mg/d for 2 wk, followed by 10 mg/d for 10 wk, while the dose of azathioprine remained at 50 mg daily. Three months later, AST and ALT levels declined to normal limits (22 and 33 U/L) as well as IgG returned to normal level (1540 mg/dL). The patient was therefore prescribed a low dose prednisolone (5 mg daily) and azathioprine (50 mg daily) as a maintenance therapy to prevent relapse.

The immunosuppressive drugs had never been discontinued in all patients, thus, none of the patients had disease relapse, defined as ALT increases > 3 times the upper limit of normal. At the last follow-up visit, 10 patients were doing well with normalized ALT levels, and 1 patient remained in the induction phase. None experienced HIV viral rebound or infectious complications during treatment with immunosuppressive drugs. Table 3 displays the treatments and outcomes for each patient.

## DISCUSSION

In this review, we present 13 cases with coexisting HIV infection and AIH. The diagnosis of AIH in HIV-infected patients is challenging and complex for a number of reasons. First, hepatitis in HIV-infected patients more commonly has other etiologies, particularly viral hepatitis B and C, adverse effects from antiretroviral or other drugs, opportunistic infection, and non-alcoholic steatohepatitis. Second, the disease has a wide spectrum of clinical presentation, ranging from asymptomatic, hepatitis, cirrhosis to acute liver failure. Third, the natural history of AIH is dynamic. Transaminase enzyme levels are not always persistently elevated. Spontaneous remission or intermittent flares can occur, resulting in fluctuations of liver enzymes. Last, elevation of IgG and positivity of autoantibodies is a common phenomenon in HIV-infected individuals. HIV itself can cause elevation of IgG levels due to polyclonal stimulation of B cells[40-42]. The presence of autoantibodies has been reported in 45% of HIV-infected patients in the era of highly active antiretroviral therapy[41]. Given the difficulties in diagnosis, AIH in the setting of HIV infection is

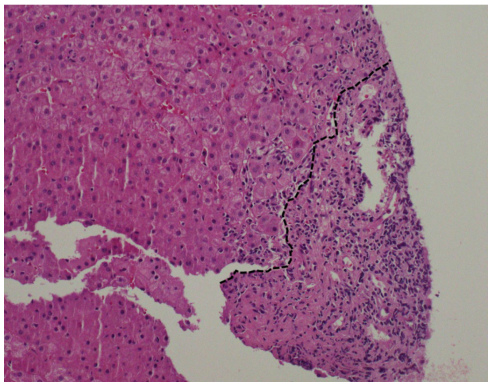

**Figure 2 Interface hepatitis.** Portal lymphoplasmacytic infiltrate extending into the lobule (dashed line).

not a well-recognized condition and may be underdiagnosed, with only 38 cases reported in the literature (Table 4)[21-39].

Due to the impaired immune status in HIV infection, autoimmune diseases in this context are counterintuitive. Nonetheless, accumulating evidence illustrates that autoimmune diseases can develop after HIV diagnosis. Two recent large epidemiologic studies described a list of autoimmune diseases that occurred in HIV-infected patients. A study of 5186 HIV-infected patients in France reported that 36 patients had coexisting autoimmune diseases, accounting for a prevalence of 0.69%. The most common autoimmune disease was immune thrombocytopenic purpura ($n$ = 15), followed by inflammatory myositis, sarcoidosis and Guillain-Barré syndrome ($n$ = 4 each). Autoimmune hepatitis was present in only 1 patient, accounting for the prevalence of AIH in HIV infection of 0.02%[35]. Another nationwide study of 20444 Taiwanese patients with HIV infection found that the most common autoimmune diseases were uveitis, psoriasis and inflammatory bowel diseases, with incidence rates per 100000 person-years of 104, 102 and 92, respectively[43]. Other autoimmune diseases frequently occurring in HIV-infected individuals include Sjögren syndrome, rheumatoid arthritis, ankylosing spondyloarthritis, and autoimmune hemolytic anemia. The study did not find any HIV-infected patients with AIH.

The pathogenesis of AIH includes genetic predisposition, with a loss of tolerance against self-antigens, hyperreactivity of cytotoxic T cells and production of autoantibodies against liver antigens, leading to hepatocellular toxicity and damage[44]. Human leukocyte antigens have been identified as genetic risk factors of AIH. HLA-DR3 and HLA-DR4 are known to be susceptible genes in Caucasian and Japanese populations, respectively[18]. However, genetic polymorphisms as risk factors for AIH specifically for HIV populations haven't yet been identified. Mechanisms by which AIH emerges in HIV infection remain poorly understood. In HIV infection, CD4 T-cells are affected and may lead to autoimmune diseases[45]. Another possible mechanism is B-cell dysfunction induced by chronic persistent HIV viremia[42].

In this report, 12 of 13 (92%) patients had CD4 counts over 300 cells/mm$^3$, while only 1 patient had CD4 counts of 82 at the time of AIH diagnosis. This is in-line with the previous reports of 38 HIV cases with AIH showing a CD4 count over 250 cells/mm$^3$ in 89% of cases (Table 4). These findings suggest that AIH in the context of HIV infection more frequently occurs when the immune status has been restored.

The demographic characteristics of AIH patients who have underlying HIV infection are slightly different from those of patients without HIV infection. In the non-HIV-infected population, AIH affects both sexes regardless of age and ethnicity. AIH more frequently occurs in females than in males. The proportion of affected females ranges from 70%–95% in both the Asia-Pacific region and Europe and America (Table 5)[2-17,46-48]. In patients with HIV infection and AIH, female predominance remains true but is less pronounced. The proportion of female patients was only 62% in the present study and was 71% in 38 previous reports (Table 4). In patients without HIV infection, AIH typically occurs in middle-aged populations, with an average peak onset from 50–70 years (Table 5)[2-17,46-48]. However, HIV-infected patients develop AIH at a younger age. The median age of our cohort was 40 years, with 46% and 85% developing AIH at an age less than 40 and 50 years, respectively. Similarly, for the 38 previously reported HIV-AIH patients, the median age was 43 years (range 21–70 years), among whom 38% and 75% younger than 40 and 50 years, respectively (Table 5).

Presentations of AIH vary greatly in both HIV- and non-HIV-infected patients. In non-HIV-infected patients with AIH, approximately 40% experience an acute onset,

**Table 3 Treatment and outcome of autoimmune hepatitis in human immunodeficiency virus-infected patients**

| | Induction regimen | | Time to ALT normalization (mo) | Maintenance regimen | | Outcome | Follow up duration (mo) | Last $CD_4$ count | Last HIV VL (copies/mL) |
|---|---|---|---|---|---|---|---|---|---|
| | Prednisolone (mg/d) | Azathioprine (mg/d) | | Prednisolone (mg/d) | Azathioprine (mg/d) | | | | |
| 1 | 30 | 0 | 9.5 | 5 | 50 | Minor flare | 43.4 | 775 | < 40 |
| 2 | 20 | 0 | 7.6 | 15 | 100 | No relapse | 12.8 | 799 | < 40 |
| 3 | 30 | 0 | 8.2 | 0 | 50 | No relapse | 35.4 | 451 | < 40 |
| 4[1] | - | - | - | - | - | - | - | - | - |
| 5 | 40 | 0 | 1.0 | 2.5 | 0 | No relapse | 10.3 | 772 | < 40 |
| 6 | 30 | 0 | 2.6 | 10 | 100 | No relapse | 5.4 | 1841 | < 40 |
| 7 | 15 | 25 | 0.9 | 0 | MMF 1000 mg/day | No relapse | 30.2 | 444 | < 40 |
| 8 | 30 | 50 | 2.3 | 0 | 50 | No relapse | 65.8 | 513 | < 40 |
| 9* | - | - | - | - | - | - | - | - | - |
| 10 | 20 | 0 | 1.4 | 0 | 50 | No relapse | 22.6 | 632 | < 40 |
| 11 | 30 | 0 | 7.6 | 0 | 50 | No relapse | 24.9 | 630 | < 40 |
| 12 | 20 | 0 | 3.0 | 5 | 75 | No relapse | 19.7 | 176 | < 40 |
| 13 | 30 | 0 | Remain in the induction phase | | | - | 4.9 | - | - |

[1]Patients were initiated treatment at their primary hospitals. MMF: Mycophenolate mofetil.

presenting with acute hepatitis or infrequently with jaundice. Approximately 30%-60% experience insidious onset or are asymptomatic (Table 5). Cirrhosis at AIH diagnosis is present in up to 40% of patients. HIV-infected patients who develop AIH have similar presentations to patients without HIV infection. Most patients (85%) in this case series had long-standing hepatitis, while only 15% experienced acute onset of the disease. Cirrhosis at the time of AIH diagnosis was present in 23% of our patients and 16% of the 38 previously reported cases.

The diagnosis of AIH is established by criteria comprising clinical, laboratory and immunoserological parameters, liver histopathology, and exclusion of other causes of hepatitis. A diagnostic scoring system was first developed by the International Autoimmune Hepatitis Group (IAIHG) in 1993 and subsequently revised in 1999. Both scoring systems are complex and not easy to use in real-world practice. Simplified diagnostic criteria were therefore proposed in 2008 and are now widely used (Table 6). With a cutoff of ≥ 6, the simplified scoring system has a sensitivity and specificity of 88% and 97% for the diagnosis of AIH. The specificity increases to 99%, with a decreased sensitivity to 81%, when a cutoff of ≥ 7 is used[49].

AIH is suspected in patients whose liver tests show transaminitis with elevated serum globulin levels. As shown in our HIV cohort, all patients have elevated globulin levels. Further investigation to support the diagnosis of AIH includes elevated serum IgG levels and the presence of circulating autoantibodies. Elevated IgG levels above the upper normal limit are observed in 70%-80% of non-HIV-infected cohorts (Table 6). Likewise, 11/13 (85%) of our HIV-infected patients with AIH had elevated IgG levels.

The presence of autoantibodies, including ANA, ASMA and anti-liver kidney microsome (LKM)-1, is a key laboratory feature of AIH. ANA is the most common autoantibody detected in AIH, with a prevalence of 80%-100% in most studies (Table 6). Among HIV-infected patients with AIH, the frequencies of ANA positivity were similar to those among non-HIV-infected patients, *i.e.*, 11/13 (85%) and 27/38 (71%), in our cohort and in previously reported cases, respectively. It is important to note that ANA is not a specific autoantibody to AIH and can be found in other diseases, including nonalcoholic fatty liver disease, and in healthy individuals[50-52]. Recent studies have reported that the prevalence of ANA positivity is 16% and 26% in patients with nonalcoholic fatty liver disease and in healthy individuals, respectively[50,52]. Anti-smooth muscle antibody (ASMA) is another common autoantibody detected in AIH. Although its prevalence is less than that of ANA, it is more specific to AIH[53]. The prevalence of ASMA positivity in AIH patients without HIV infection varies considerably, ranging from 18 to 66% (Table 5). The prevalence of ASMA positivity was relatively low in our HIV cohort, *i.e.*, 5/13 (38%). This number was lower than that in the 38 previously reported patients with AIH and HIV, *i.e.*, 24/35 (69%) (3 had missing data for ASMA). Although the presence of autoantibodies

**Table 4 Baseline characteristics at autoimmune hepatitis presentation of previously reported human immunodeficiency virus cases**

| No. | Sex, age (yr) | HIV status | | | | Presenta-tion | ANA titer | ASMA titer | Treatment | Outcome |
|---|---|---|---|---|---|---|---|---|---|---|
| | | HIV Duration | ART duration | Viral load | $CD_4$ | | | | | |
| 1[21] | NA | NA | NA | < 48 | 1011 | NA | 1:640 | 1:40 | P+ Z | Remission |
| 2[21] | NA | NA | NA | < 48 | 456 | NA | Neg | 1:20 | P+ Z | Remission |
| 3[21] | NA | NA | NA | < 48 | 783 | NA | 1:40 | 1:320 | P+ Z | Remission |
| 4[21] | NA | NA | NA | < 48 | 688 | Acute liver failure | 1:640 | 1:160 | LT | Relapse at 4 yr after LT |
| 5[21] | NA | NA | NA | < 48 | 653 | n/a | 1:1280 | 1:20 | P+ Z | Remission |
| 6[22] | M, 54 | NA | 3 yr | 5104 | 357 | ↑ ALT* | 1:40 | 1:640 | P+ Z | Remission |
| 7[22] | F, 55 | NA | NA | < 50 | 174 | ↑ ALT | Neg | 1:40 | P+ Z | Relapse |
| 8[22] | F, 49 | NA | NA | 69318 | 286 | ↑ ALT | Neg | Neg | P+ Z | Died |
| 9[22] | F, 56 | NA | NA | 232734 | 331 | ↑ ALT | 1:40 | 1:20 | P | Died |
| 10[23] | M, 21 | Newly diagnosed | 0 | 7900 | 753 | Jaundice | Neg | Neg | P | Relapse |
| 11[23] | F, 59 | n/a | 7 mo | - | 504 | ↑ ALT | Pos | Pos | P+ Z | Remission |
| 12[24] | M, 26 | 3 yr | 1 yr | - | NA | Jaundice | 1:160 | Neg | P+ Z | Relapse |
| 13[25] | M, 40 | 8 yr | 8 yr | ND | 832 | ↑ ALT | Neg | 1:60 | P+ Z | Relapse |
| 14[25] | F, 44 | 20 yr | 7 yr | ND | 823 | Acute hepatitis* | 1:640 | 1:180 | P | Remission |
| 15[26] | M, 52 | 7 yr | 7 | ND | 641 | ↑ ALT | 1:2560 | NA | P | Remission |
| 16[27] | F, 44 | 9 mo | 9 mo | ND | 526 | ↑ ALT | 1:160 | 1:160 | P+ Z | Minor flare during taper steroid |
| 17[28] | M, 29 | Newly diagnosed | 0 | 7122 | 259 | ↑ ALT | Neg | Neg | none | Resolved spontaneous-ly |
| 18[28] | F, 45 | 2 yr | 7 mo | ND | 297 | ↑ ALT | 1:640 | Neg | P+Z | Remission |
| 19[28] | F, 65 | 10 yr | n/a | ND | 922 | ↑ ALT | 1:160 | 1:320 | P+Z → MMF | Flare |
| 20[29] | M, 38 | 2 yr after AIH diagnosed | 0 | 81000 | 216 | ↑ ALT | 1:320 | 1:40 | ART | ALT improved after ART initiaion |
| 21[30] | F, - | 15 yr | 12 yr | ND | 634 | Acute hepatitis | 1:20000 | Neg | P | Remission |
| 22[31] | F, 48 | 20 yr | NA | ND | > 250 | Acute hepatitis | 1:80 | 1:300 | P | Died |
| 23[32] | F, 23 | NA | 8 mo | ND | 523 | ↑ Jaundice and ALT* | Pos | Neg | P ± Z | Remission |
| 24[32] | F, 31 | NA | 7 mo | < 40 | 277 | | Pos | Neg | | |
| 25[32] | F, 42 | NA | 10 mo | - | 593 | | Pos | Pos | | |
| 26[32] | F, 45 | NA | 6 mo | < 40 | 253 | | Neg | Pos | | |
| 27[32] | F, 35 | NA | 41 mo | ND | 339 | | Neg | Pos | | |
| 28[32] | M, 39 | NA | 77 mo | ND | 416 | | Neg | Pos | | |
| 29[32] | F, 39 | NA | 4 mo | ND | 357 | | Neg | Pos | | |
| 30[32] | F, 43 | NA | 4 mo | ND | 876 | | Pos | Neg | | |
| 31[32] | F, 36 | NA | 17 mo | ND | 693 | | Neg | Pos | | |
| 32[33] | F, 42 | 20 yr | NA | ND | 232 | Acute hepatitis | 1:1280 | Neg | P | Remission |
| 33[34] | F, 51 | NA | 11 mo | 94 | 417 | Acute liver failure | 1:256 | 1:80 | P | Died |
| 34[35] | F, 38 | 13 yr | NA | 6392 | 436 | NA | 1:400 | Pos | B | Remission |
| 35[36] | M, 38 | 2 yr | 0 | 8072 | 762 | Acute hepatitis | 1:640 | 1:160 | P+Z | Remission |
| 36[37] | F, 70 | 32 yr | 24 yr | < 50 | 938 | Decompensated cirrhosis* | 1:640 | NA | P | Remission |
| 37[38] | M, 43 | 13 yr | 2 yr | ND | 900 | ↑ ALT | 1:160 | NA | P | Remission |

| | | | | | | | | | | |
|---|---|---|---|---|---|---|---|---|---|---|
| 38[39] | F, 43 | 4 yr | 18 mo | ND | 425 | Acute hepatitis | 1:8000 | Neg | P+Z | Flare during tapering steroid |

ART: Antiretroviral therapy; B: Budesonide; M: Mycophenolate mofetil, P: Prednisolone; Z: Azathioprine; LT: Liver transplantation; NA: Not available.

is a diagnostic criterion, up to 17% of AIH patients are negative for ANA, ASMA and anti-LKM and are considered to have so-called "autoantibody-negative AIH"[54].

Liver biopsy is essential to confirm the diagnosis and assess the severity of AIH. Interface hepatitis (plasma cell and lymphocyte infiltration at the interface of hepatic parenchyma and portal tract), emperipolesis and hepatic rosette formation are classic histopathological features, although not pathognomonic of AIH. Figures 1-4 display the histopathology of AIH in our HIV-infected patients. Although interface hepatitis is a common histological finding of AIH and is present in up to 87% of cases, it can be found in patients with viral hepatitis A/B/C/E infection and drug-induced hepatitis[55,56]. Emperipolesis and rosette formation are more specific features than interface hepatitis for the diagnosis of AIH and can be detected in 78% and 49% of AIH patients, respectively[55].

There are no treatment guidelines specifically for HIV-infected patients. Based on evidence from previous and the currently reported cases, HIV-infected patients with AIH can be treated in a similar fashion to non-HIV-infected patients. Immunosuppressive drugs are the mainstay of treatment. To prevent further hepatocellular damage and cirrhosis development, complete biochemical remission (normalization of serum aminotransferase and IgG levels) and histological remission must be achieved. Prednisolone monotherapy or combination therapy with azathioprine is the first-line treatment for the induction of disease remission, followed by maintenance therapy with azathioprine as a steroid-sparing medication. Prednisolone at the dose of 0.5-1 mg/kg/d, with the maximum dose of 60 mg/d, can be initially used as a single agent, followed by the addition of azathioprine 1-2 mg/kg/d when the liver chemistry shows improvement, with a decrease in prednisolone slowly until discontinued. A combination of prednisolone, at a maximum dose of 30 mg/d, and azathioprine at 1-2 mg/kg/d can also be used as induction therapy. Approximately 80%-90% of patients shortly experience improvement in symptoms and liver tests, usually within 2 wk, after treatment initiation. As suggested by a recent multicenter study in the Netherlands[57], life-long azathioprine is usually required for maintaining sustained remission and preventing disease relapse. In this study, the outcomes of 131 patients for whom immunosuppressive therapy was tapered after disease remission for at least 2 years were determined. It was found that after immunosuppressive drug was discontinued, 47% of patients experienced disease relapse (*i.e.*, elevation in ALT levels three times above the upper limit of normal), and 42% had a loss of remission (*i.e.*, elevation in ALT levels that required retreatment). Retreatment was needed in approximately 60%, 70% and 80% of cases at 1, 2 and 3 years after drug withdrawal, respectively[57].

Treatment with immunosuppressive drugs improves the survival of AIH patients and decreases the 2-year mortality from 34% to 14%[58]. With proper treatment, AIH patients who do not have cirrhosis display comparable survival to the general population, while patients with cirrhosis have a higher mortality than the general population[59]. Frequent relapse or lack of disease remission increases liver-related mortality and liver transplantation[59].

## CONCLUSION

In summary, this review highlights the fact that AIH should be included in the differential diagnosis of hepatitis in patients with HIV infection. To avoid delay in the diagnosis of AIH, elevation in IgG and presence of autoantibodies should be tested once common causes of hepatitis, particularly viral hepatitis, drug-induced liver injury and non-alcoholic steatohepatitis, are ruled out. Liver biopsy should be further performed to confirm the diagnosis. Immunosuppressive therapy is safe and provides good outcomes in HIV-infected patients. After treatment, most patients experience rapid improvements in liver chemistry, followed by disease remission. However, long-term maintenance with low-dose immunosuppressive drugs is generally required to prevent disease relapse.

**Table 5 Demographics of non-human immunodeficiency virus infected patients with autoimmune hepatitis**

| Country | *n* | Female (%) | Age at onset | Cirrhosis[1] | Disease onset | ANA+ | ASMA+ | IgG > ULN |
|---|---|---|---|---|---|---|---|---|
| *Asia-Pacific* | | | | | | | | |
| South Korea[10] | 4085 | 86 | 60-69 | 32.3% | - | - | - | - |
| Japan[46] | 1682 | 87 | 60-69 | 6.7% (P) | 11.7% acute hepatitis 79.6% chronic hepatitis | 90.7% | 40.9% | n/a |
| South Korea[47] | 343 | - | - | 23% | 46.4% acute onset 30.6% asymptomatic | 94.2% | 23.0% | 78.2% |
| New Zealand[15] | 138 | 71 | 50-59 | 36% (P, R) | - | 56% | 57% | 97% |
| Israel[13] | 100 | 95 | 48 | 22.3% (P) | 35% asymptomatic | 91% | 55% | n/a |
| Taiwan[7] | 48 | 77 | 58 | 35.4% (P) | 12.5% asymptomatic 41.7% acute onset 45.8% insidious onset | 97.8% | 18.2% | 72.9% |
| Japan[14] | 48 | - | - | 8.3% (C+R) | 68.8% acute onset 31.2% chronic onset | 100% | 22.9% | 79.2% |
| Australia[12] | 42 | 74 | 53 | 24% (P) | - | n/a | 65.8% | n/a |
| India[8] | 38 | 89 | 30 | 34.2% (C±P) | 13.1% acute hepatitis 39.4% acute onset 50% chronic onset | 39.4% | 63.1% | n/a |
| Singapore[9] | 24 | 92 | 63 | 42% (C) | 2/3 insidious onset | 79.2% | 20.8% | n/a |
| Brunei Darussalam[11] | 19 | 79 | 52 | 21.1% (P) | 53% asymptomatic | 100% | 47.4% | n/a |
| *Europe and America* | | | | | | | | |
| Denmark[4] | 1721 | 72 | 70 | 28.3% (P) | - | - | - | - |
| Netherlands[5] | 1313 | 78 | Middle age | 12% (P) | - | 49% | 58% | 83% |
| Finland[3] | 887 | 76 | 55-64 | - | - | - | - | - |
| Sweden[2] | 634 | 73 | 50-60 | 28.1% | - | - | - | - |
| Alaska[48] | 71 | - | - | - | - | 79.1% | 60% | 66% |
| United States (Alaska)[17] | 49 | 92 | 52 | 0% | 34.7% acute hepatitis 65.3% asymptomatic | - | - | - |
| Norway[16] | 25 | 80 | 68 | 28% (P) | - | 68% | 40% | n/a |
| Spain[6] | 19 | 95 | 45-54 | - | - | - | - | - |

[1](P, C, R) – Diagnosis of cirrhosis at AIH presentation was made by pathological, clinical or radiological features, respectively.

**Table 6 Simplified diagnostic scoring system of autoimmune hepatitis**

| Parameters | | Score |
|---|---|---|
| I Seroimmunological test (maximum 2 points) | | |
| ANA or SMA + | ≥ 1:40 | +1 |
| ANA or SMA + | ≥ 1:80 | +2 |
| LKM + | ≥ 1:40 | +2 |
| SLA + | Any titer | +2 |
| II IgG or immunoglobulin level | > ULN | +1 |
| | > 1.1 × ULN | +2 |
| III Histological finding | Compatible | +1 |
| | Typical | +2 |
| IV Absence of viral hepatitis | No | 0 |
| | Yes | +2 |

≥ 6 points - probable AIH; ≥ 7 points - definite AIH. AIH: autoimmune hepatitis; ANA: Antinuclear antibody; LKM: Liver kidney microsomal antibody; SLA: Soluble liver antigen.

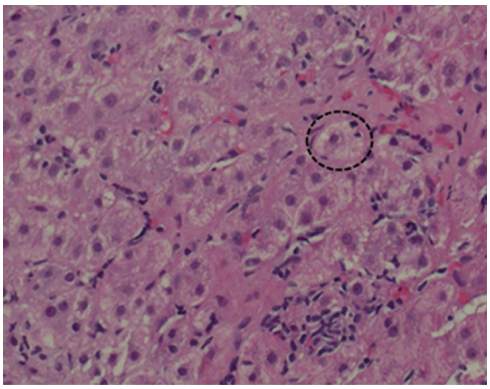

**Figure 3 Shows lymphoplasmacytic infiltrate in hepatic lobule, *i.e.*, lobular inflammation, and emperipolesis (circle).**

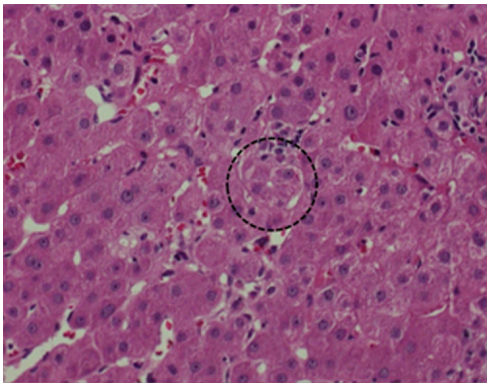

**Figure 4 Hepatocellular rosette formation (circle).**

## REFERENCES


1 **Wang Q**, Yang F, Miao Q, Krawitt EL, Gershwin ME, Ma X. The clinical phenotypes of autoimmune hepatitis: A comprehensive review. *J Autoimmun* 2016; **66**: 98-107 [PMID: 26614611 DOI: 10.1016/j.jaut.2015.10.006]

2 **Danielsson Borssén Å**, Marschall HU, Bergquist A, Rorsman F, Weiland O, Kechagias S, Nyhlin N, Verbaan H, Nilsson E, Werner M. Epidemiology and causes of death in a Swedish cohort of patients with autoimmune hepatitis. *Scand J Gastroenterol* 2017; **52**: 1022-1028 [PMID: 28562110 DOI: 10.1080/00365521.2017.1335772]

3 **Puustinen L**, Barner-Rasmussen N, Pukkala E, Färkkilä M. Incidence, prevalence, and causes of death of

patients with autoimmune hepatitis: A nationwide register-based cohort study in Finland. *Dig Liver Dis* 2019; Epub ahead of print [PMID: 30850346 DOI: 10.1016/j.dld.2019.01.015]
4 **Grønbæk L**, Vilstrup H, Jepsen P. Autoimmune hepatitis in Denmark: incidence, prevalence, prognosis, and causes of death. A nationwide registry-based cohort study. *J Hepatol* 2014; **60**: 612-617 [PMID: 24326217 DOI: 10.1016/j.jhep.2013.10.020]
5 **van Gerven NM**, Verwer BJ, Witte BI, van Erpecum KJ, van Buuren HR, Maijers I, Visscher AP, Verschuren EC, van Hoek B, Coenraad MJ, Beuers UH, de Man RA, Drenth JP, den Ouden JW, Verdonk RC, Koek GH, Brouwer JT, Guichelaar MM, Vrolijk JM, Mulder CJ, van Nieuwkerk CM, Bouma G; Dutch Autoimmune hepatitis STUDY group. Epidemiology and clinical characteristics of autoimmune hepatitis in the Netherlands. *Scand J Gastroenterol* 2014; **49**: 1245-1254 [PMID: 25123213 DOI: 10.3109/00365521.2014.946083]
6 **Primo J**, Maroto N, Martínez M, Antón MD, Zaragoza A, Giner R, Devesa F, Merino C, del Olmo JA. Incidence of adult form of autoimmune hepatitis in Valencia (Spain). *Acta Gastroenterol Belg* 2009; **72**: 402-406 [PMID: 20163033]
7 **Koay LB**, Lin CY, Tsai SL, Lee C, Lin CN, Sheu MJ, Kuo HT, Sun CS. Type 1 autoimmune hepatitis in Taiwan: diagnosis using the revised criteria of the International Autoimmune Hepatitis Group. *Dig Dis Sci* 2006; **51**: 1978-1984 [PMID: 17053960 DOI: 10.1007/s10620-005-9068-y]
8 **Choudhuri G**, Somani SK, Baba CS, Alexander G. Autoimmune hepatitis in India: profile of an uncommon disease. *BMC Gastroenterol* 2005; **5**: 27 [PMID: 16098234 DOI: 10.1186/1471-230X-5-27]
9 **Lee YM**, Teo EK, Ng TM, Khor C, Fock KM. Autoimmune hepatitis in Singapore: a rare syndrome affecting middle-aged women. *J Gastroenterol Hepatol* 2001; **16**: 1384-1389 [PMID: 11851837]
10 **Kim BH**, Choi HY, Ki M, Kim KA, Jang ES, Jeong SH. Population-based prevalence, incidence, and disease burden of autoimmune hepatitis in South Korea. *PLoS One* 2017; **12**: e0182391 [PMID: 28771543 DOI: 10.1371/journal.pone.0182391]
11 **Jalihal A**, Telisinghe PU, Chong VH. Profiles of autoimmune hepatitis in Brunei Darussalam. *Hepatobiliary Pancreat Dis Int* 2009; **8**: 602-607 [PMID: 20007077]
12 **Haider AS**, Kaye G, Thomson A. Autoimmune hepatitis in a demographically isolated area of Australia. *Intern Med J* 2010; **40**: 281-285 [PMID: 19712202 DOI: 10.1111/j.1445-5994.2009.02041.x]
13 **Delgado JS**, Vodonos A, Malnick S, Kriger O, Wilkof-Segev R, Delgado B, Novack V, Rosenthal A, Menachem Y, Melzer E, Fich A. Autoimmune hepatitis in southern Israel: a 15-year multicenter study. *J Dig Dis* 2013; **14**: 611-618 [PMID: 23815477 DOI: 10.1111/1751-2980.12085]
14 **Yoshizawa K**, Joshita S, Matsumoto A, Umemura T, Tanaka E, Morita S, Maejima T, Ota M. Incidence and prevalence of autoimmune hepatitis in the Ueda area, Japan. *Hepatol Res* 2016; **46**: 878-883 [PMID: 26670542 DOI: 10.1111/hepr.12639]
15 **Ngu JH**, Bechly K, Chapman BA, Burt MJ, Barclay ML, Gearry RB, Stedman CA. Population-based epidemiology study of autoimmune hepatitis: a disease of older women? *J Gastroenterol Hepatol* 2010; **25**: 1681-1686 [PMID: 20880179 DOI: 10.1111/j.1440-1746.2010.06384.x]
16 **Boberg KM**, Aadland E, Jahnsen J, Raknerud N, Stiris M, Bell H. Incidence and prevalence of primary biliary cirrhosis, primary sclerosing cholangitis, and autoimmune hepatitis in a Norwegian population. *Scand J Gastroenterol* 1998; **33**: 99-103 [PMID: 9489916]
17 **Hurlburt KJ**, McMahon BJ, Deubner H, Hsu-Trawinski B, Williams JL, Kowdley KV. Prevalence of autoimmune liver disease in Alaska Natives. *Am J Gastroenterol* 2002; **97**: 2402-2407 [PMID: 12358264 DOI: 10.1111/j.1572-0241.2002.06019.x]
18 **European Association for the Study of the Liver**. EASL Clinical Practice Guidelines: Autoimmune hepatitis. *J Hepatol* 2015; **63**: 971-1004 [PMID: 26341719 DOI: 10.1016/j.jhep.2015.06.030]
19 **Aizawa Y**, Hokari A. Autoimmune hepatitis: current challenges and future prospects. *Clin Exp Gastroenterol* 2017; **10**: 9-18 [PMID: 28176894 DOI: 10.2147/CEG.S101440]
20 **Crum-Cianflone N**, Collins G, Medina S, Asher D, Campin R, Bavaro M, Hale B, Hames C. Prevalence and factors associated with liver test abnormalities among human immunodeficiency virus-infected persons. *Clin Gastroenterol Hepatol* 2010; **8**: 183-191 [PMID: 19800985 DOI: 10.1016/j.cgh.2009.09.025]
21 **Kia L**, Beattie A, Green RM. Autoimmune hepatitis in patients with human immunodeficiency virus (HIV): Case reports of a rare, but important diagnosis with therapeutic implications. *Medicine (Baltimore)* 2017; **96**: e6011 [PMID: 28207511 DOI: 10.1097/MD.0000000000006011]
22 **Wan DW**, Marks K, Yantiss RK, Talal AH. Autoimmune hepatitis in the HIV-infected patient: a therapeutic dilemma. *AIDS Patient Care STDS* 2009; **23**: 407-413 [PMID: 19405870 DOI: 10.1089/apc.2008.0149]
23 **Parekh S**, Spiritos Z, Reynolds P, Perricone A, Quigley B. HIV and Autoimmune Hepatitis: A Case Series and Literature Review. *J Biomedical Sci* 2017; **6**: 1-4 [DOI: 10.4172/2254-609X.100057]
24 **Noreña I**, Morantes-Caballero JA, Garcés A, Gómez BJ, Rodríguez G, Saavedra C, Otero W. Autoimmune hepatitis in human immunodeficiency virus infection: Case report and literature review. *World J Clin Infect Dis* 2017; **7**: 50-57 [DOI: 10.5495/wjcid.v7.i4.50]
25 **Ofori E**, Ramai D, Ona MA, Reddy M. Autoimmune hepatitis in the setting of human immunodeficiency virus infection: A case series. *World J Hepatol* 2017; **9**: 1367-1371 [PMID: 29359021 DOI: 10.4254/wjh.v9.i36.1367]
26 **Hagel S**, Bruns T, Herrmann A, Tannapfel A, Stallmach A. Autoimmune hepatitis in an HIV-infected patient: an intriguing association. *Int J STD AIDS* 2012; **23**: 448-450 [PMID: 22807544 DOI: 10.1258/ijsa.2009.009337]
27 **O'Leary JG**, Zachary K, Misdraji J, Chung RT. De novo autoimmune hepatitis during immune reconstitution in an HIV-infected patient receiving highly active antiretroviral therapy. *Clin Infect Dis* 2008; **46**: e12-e14 [PMID: 18171203 DOI: 10.1086/524082]
28 **Puius YA**, Dove LM, Brust DG, Shah DP, Lefkowitch JH. Three cases of autoimmune hepatitis in HIV-infected patients. *J Clin Gastroenterol* 2008; **42**: 425-429 [PMID: 18277893 DOI: 10.1097/01.mcg.0000225591.08825.3e]
29 **German V**, Vassiloyanakopoulos A, Sampaziotis D, Giannakos G. Autoimmune hepatitis in an HIV infected patient that responded to antiretroviral therapy. *Scand J Infect Dis* 2005; **37**: 148-151 [PMID: 15764206 DOI: 10.1080/00365540510026841]
30 **Vispo E**, Maida I, Moreno A, Barreiro P, Soriano V. Autoimmune hepatitis induced by pegylated interferon in an HIV-infected patient with chronic hepatitis C. *J Antimicrob Chemother* 2008; **62**: 1470-1472 [PMID: 18835807 DOI: 10.1093/jac/dkn416]
31 **Coriat R**, Podevin P. Fulminant autoimmune hepatitis after successful interferon treatment in an HIV-

HCV co-infected patient. *Int J STD AIDS* 2008; **19**: 208-210 [PMID: 18397566 DOI: 10.1258/ijsa.2007.007185]
32 **Murunga E**, Andersson M, Rensburg Cv. Autoimmune hepatitis: a manifestation of immune reconstitution inflammatory syndrome in HIV infected patients? *Scand J Gastroenterol* 2016; **51**: 814-818 [PMID: 27000683 DOI: 10.3109/00365521.2016.1157888]
33 **Daas H**, Khatib R, Nasser H, Kamran F, Higgins M, Saravolatz L. Human immunodeficiency virus infection and autoimmune hepatitis during highly active anti-retroviral treatment: a case report and review of the literature. *J Med Case Rep* 2011; **5**: 233 [PMID: 21702972 DOI: 10.1186/1752-1947-5-233]
34 **Rodrigues EM Filho**, Fernandes R, Susin R, Fior B. Immune reconstitution inflammatory syndrome as a cause of autoimmune hepatitis and acute liver failure. *Rev Bras Ter Intensiva* 2017; **29**: 382-385 [PMID: 29044307 DOI: 10.5935/0103-507x.20170053]
35 **Virot E**, Duclos A, Adelaide L, Miailhes P, Hot A, Ferry T, Seve P. Autoimmune diseases and HIV infection: A cross-sectional study. *Medicine (Baltimore)* 2017; **96**: e5769 [PMID: 28121924 DOI: 10.1097/MD.0000000000005769]
36 **Iordache L**, Launay O, Bouchaud O, Jeantils V, Goujard C, Boue F, Cacoub P, Hanslik T, Mahr A, Lambotte O, Fain O; Associated authors. Autoimmune diseases in HIV-infected patients: 52 cases and literature review. *Autoimmun Rev* 2014; **13**: 850-857 [PMID: 24747058 DOI: 10.1016/j.autrev.2014.04.005]
37 **Zoboli F**, Ripamonti D, Benatti SV, Comi L, Rizzi M. Autoimmune hepatitis and HIV infection: two case reports and review of the literature. *AIDS* 2017; **31**: 2172-2175 [PMID: 28906281 DOI: 10.1097/QAD.0000000000001608]
38 **Kaku Y**, Kodama S, Higuchi M, Nakamura A, Nakamura M, Kaieda T, Takahama S, Minami R, Miyamura T, Suematsu E, Yamamoto M. Corticoid therapy for overlapping syndromes in an HIV-positive patient. *Intern Med* 2015; **54**: 223-230 [PMID: 25743017 DOI: 10.2169/internalmedicine.54.3094]
39 **Cazanave C**, Rakotondravelo S, Morlat P, Blanco P, Bonnet F, Beylot J. [Autoimmune hepatitis in a HIV-HCV co-infected patient: diagnostic ant therapeutic difficulties]. *Rev Med Interne* 2006; **27**: 414-419 [PMID: 16545501 DOI: 10.1016/j.revmed.2006.01.016]
40 **De Milito A**, Nilsson A, Titanji K, Thorstensson R, Reizenstein E, Narita M, Grutzmeier S, Sönnerborg A, Chiodi F. Mechanisms of hypergammaglobulinemia and impaired antigen-specific humoral immunity in HIV-1 infection. *Blood* 2004; **103**: 2180-2186 [PMID: 14604962 DOI: 10.1182/blood-2003-07-2375]
41 **Iordache L**, Bengoufa D, Taulera O, Rami A, Lascoux-Combe C, Day N, Parrinello M, Sellier PO, Molina JM, Mahr A. Nonorgan-specific autoantibodies in HIV-infected patients in the HAART era. *Medicine (Baltimore)* 2017; **96**: e6230 [PMID: 28272216 DOI: 10.1097/MD.0000000000006230]
42 **Moir S**, Fauci AS. B cells in HIV infection and disease. *Nat Rev Immunol* 2009; **9**: 235-245 [PMID: 19319142 DOI: 10.1038/nri2524]
43 **Yen YF**, Chuang PH, Jen IA, Chen M, Lan YC, Liu YL, Lee Y, Chen YH, Chen YA. Incidence of autoimmune diseases in a nationwide HIV/AIDS patient cohort in Taiwan, 2000-2012. *Ann Rheum Dis* 2017; **76**: 661-665 [PMID: 27590658 DOI: 10.1136/annrheumdis-2016-209815]
44 **Diamantis I**, Boumpas DT. Autoimmune hepatitis: evolving concepts. *Autoimmun Rev* 2004; **3**: 207-214 [PMID: 15110233 DOI: 10.1016/j.autrev.2003.09.003]
45 **Zandman-Goddard G**, Shoenfeld Y. HIV and autoimmunity. *Autoimmun Rev* 2002; **1**: 329-337 [PMID: 12848988]
46 **Takahashi A**, Arinaga-Hino T, Ohira H, Torimura T, Zeniya M, Abe M, Yoshizawa K, Takaki A, Suzuki Y, Kang JH, Nakamoto N, Fujisawa T, Yonemoto K, Tanaka A, Takikawa H; Autoimmune Hepatitis Study Group-Subgroup of the Intractable Hepato-Biliary Disease Study Group in Japan. Autoimmune hepatitis in Japan: trends in a nationwide survey. *J Gastroenterol* 2017; **52**: 631-640 [PMID: 27722997 DOI: 10.1007/s00535-016-1267-0]
47 **Kim BH**, Kim YJ, Jeong SH, Tak WY, Ahn SH, Lee YJ, Jung EU, Lee JI, Yeon JE, Hwang JS, Um SH, Seo YS, Kim YS, Song BC, Kim JH, Jung YK, Park CK, Kim KA, Min HJ, Cho EY, Lee ES, Kwon SY, Chae HB, Kim DJ, Shin SR. Clinical features of autoimmune hepatitis and comparison of two diagnostic criteria in Korea: a nationwide, multicenter study. *J Gastroenterol Hepatol* 2013; **28**: 128-134 [PMID: 23033899 DOI: 10.1111/j.1440-1746.2012.07292.x]
48 **Ferucci ED**, Choromanski TL, Hurlburt KJ, Livingston S, Plotnik J, Manns MP, McMahon BJ, James JA. Autoimmune hepatitis in the Alaska Native population: autoantibody profile and HLA associations. *Liver Int* 2014; **34**: 1241-1249 [PMID: 24939565 DOI: 10.1111/liv.12372]
49 **Hennes EM**, Zeniya M, Czaja AJ, Parés A, Dalekos GN, Krawitt EL, Bittencourt PL, Porta G, Boberg KM, Hofer H, Bianchi FB, Shibata M, Schramm C, Eisenmann de Torres B, Galle PR, McFarlane I, Dienes HP, Lohse AW; International Autoimmune Hepatitis Group. Simplified criteria for the diagnosis of autoimmune hepatitis. *Hepatology* 2008; **48**: 169-176 [PMID: 18537184 DOI: 10.1002/hep.22322]
50 **Ravi S**, Shoreibah M, Raff E, Bloomer J, Kakati D, Rasheed K, Singal AK. Autoimmune Markers Do Not Impact Clinical Presentation or Natural History of Steatohepatitis-Related Liver Disease. *Dig Dis Sci* 2015; **60**: 3788-3793 [PMID: 26173506 DOI: 10.1007/s10620-015-3795-5]
51 **Vuppalanchi R**, Gould RJ, Wilson LA, Unalp-Arida A, Cummings OW, Chalasani N, Kowdley KV; Nonalcoholic Steatohepatitis Clinical Research Network (NASH CRN). Clinical significance of serum autoantibodies in patients with NAFLD: results from the nonalcoholic steatohepatitis clinical research network. *Hepatol Int* 2012; **6**: 379-385 [PMID: 21557024 DOI: 10.1007/s12072-011-9277-8]
52 **Racoubian E**, Zubaid RM, Shareef MA, Almawi WY. Prevalence of antinuclear antibodies in healthy Lebanese subjects, 2008-2015: a cross-sectional study involving 10,814 subjects. *Rheumatol Int* 2016; **36**: 1231-1236 [PMID: 27432022 DOI: 10.1007/s00296-016-3533-0]
53 **Czaja AJ**, Cassani F, Cataleta M, Valentini P, Bianchi FB. Frequency and significance of antibodies to actin in type 1 autoimmune hepatitis. *Hepatology* 1996; **24**: 1068-1073 [PMID: 8903377 DOI: 10.1002/hep.510240515]
54 **Gassert DJ**, Garcia H, Tanaka K, Reinus JF. Corticosteroid-responsive cryptogenic chronic hepatitis: evidence for seronegative autoimmune hepatitis. *Dig Dis Sci* 2007; **52**: 2433-2437 [PMID: 17429719 DOI: 10.1007/s10620-006-9665-4]
55 **de Boer YS**, van Nieuwkerk CM, Witte BI, Mulder CJ, Bouma G, Bloemena E. Assessment of the histopathological key features in autoimmune hepatitis. *Histopathology* 2015; **66**: 351-362 [PMID: 25257662 DOI: 10.1111/his.12558]
56 **Tiniakos DG**, Brain JG, Bury YA. Role of Histopathology in Autoimmune Hepatitis. *Dig Dis* 2015; **33** Suppl 2: 53-64 [PMID: 26642062 DOI: 10.1159/000440747]
57 **van Gerven NM**, Verwer BJ, Witte BI, van Hoek B, Coenraad MJ, van Erpecum KJ, Beuers U, van

Buuren HR, de Man RA, Drenth JP, den Ouden JW, Verdonk RC, Koek GH, Brouwer JT, Guichelaar MM, Mulder CJ, van Nieuwkerk KM, Bouma G; Dutch Autoimmune Hepatitis Working Group. Relapse is almost universal after withdrawal of immunosuppressive medication in patients with autoimmune hepatitis in remission. *J Hepatol* 2013; **58**: 141-147 [PMID: 22989569 DOI: 10.1016/j.jhep.2012.09.009]

58 **Cook GC**, Mulligan R, Sherlock S. Controlled prospective trial of corticosteroid therapy in active chronic hepatitis. *Q J Med* 1971; **40**: 159-185 [PMID: 4933363]

59 **van den Brand FF**, van der Veen KS, de Boer YS, van Gerven NM, Lissenberg-Witte BI, Beuers U, van Erpecum KJ, van Buuren HR, den Ouden JW, Brouwer JT, Vrolijk JM, Verdonk RC, van Hoek B, Koek GH, Drenth JPH, Guichelaar MMJ, Mulder CJJ, Bloemena E, van Nieuwkerk CMJ, Bouma G; Dutch Autoimmune Hepatitis Study Group. Increased Mortality Among Patients With vs Without Cirrhosis and Autoimmune Hepatitis. *Clin Gastroenterol Hepatol* 2019; **17**: 940-947.e2 [PMID: 30291909 DOI: 10.1016/j.cgh.2018.09.046]

Published By Baishideng Publishing Group Inc
7041 Koll Center Parkway, Suite 160, Pleasanton, CA 94566, USA
Telephone: +1-925-2238242
E-mail: bpgoffice@wjgnet.com
Help Desk:http://www.f6publishing.com/helpdesk
http://www.wjgnet.com